Development of novel nucleic acid technologies for tackling neurological diseases

Madhuri Chakravarthy

Bachelor of Biomedical Science

This thesis is presented for the Doctor of Philosophy at Murdoch University

School of Veterinary and Life Sciences

Molecular and Medical Sciences

2019

Thesis Declaration

I, Madhuri Chakravarthy, declare that this thesis is my own account of my research and contains as its main content work that has not previously been submitted for a degree at any tertiary education institution.

This thesis does not contain any material previously published or written by another person, except where due reference has been made in the text.

This work (s) are not in any way a violation or infringement of any copyright, trademark, patent or other rights whatsoever of any person.

This thesis contains published work, some of which has been co-authored.

Signature: Madhuri Chakravarthy

Date: 11 November 2019

Abstract

Nucleic acid technologies such as antisense oligonucleotides (AOs) and DNAzymes can bind specifically to target messenger RNA and modulate gene expression by different mechanisms of actions. Recent approval of Nusinersen (Spinraza), by the United States Food and Drug Administration for the treatment of spinal muscular atrophy has demonstrated the potential of nucleic acid technologies in treatment of neuromuscular diseases. This thesis explores the potential of AOs and DNAzymes for tackling neurological diseases, particularly multiple sclerosis and Alzheimer's disease. Chapter 1 provides a broad overview of the various nucleic acid technologies including the importance of chemical modifications and delivery of the nucleic acid molecules for clinical applications. Chapter 2 focused on developing DNAzymes targeting integrin subunit alpha 4 (ITGA4), a validated therapeutic target in multiple sclerosis. A DNAzyme candidate, RNV143, was identified to efficiently cleave exon 9 of *ITGA4* RNA. This chapter also briefly explored the use of chemical modifications for nuclease resistance. Towards this, the DNAzyme, RNV143 was chemically modified and further evaluated for its nuclease resistance and cleavage activity. The focus of Chapter 3 was to develop DNAzyme and splice modulating AOs for tackling Alzheimer's Disease by targeting amyloid precursor protein (APP), beta-site amyloid precursor protein cleaving enzyme (BACE1), and microtubule-associated protein tau (MAPT). Splice modulating AOs targeting APP, BACE1, and MAPT were developed and evaluated at the RNA and protein levels. DNAzymes targeting MAPT were also developed and its efficacy was evaluated *in vitro*. The results presented here highlight the scope of DNAzymes and splice modulating AOs for tackling multiple sclerosis and Alzheimer's disease.

Table of Contents

List of Figures

List of Tables

Acknowledgements

There are a huge number of people who have supported me from the beginning to the end of my thesis.

First and foremost, I would like to express my deepest gratitude to my Principle supervisor, Rakesh and my co-supervisors Steve and Sue, who have supported me, given encouragement and provided feedback to continuously grow and improve. Rakesh, you have taught me a lot and I am grateful for the enthusiasm and the drive to publish papers that you have instilled in me. You have given me the opportunity to publish papers, attend conferences and take other opportunities to advance my career. You have taught me how to push myself and made me into the scientist I am today. I have learnt a lot from our discussions, the feedback and the open door you have always had for us.

Steve and Sue, you guys have inspired me both scientifically and personally. Your passion in the work you do and your success has been an inspiration and motivational.

I would also like to acknowledge and thank the generous financial support from Greg and Dale Higham who provided me with the funding for my PhD through Perron Institute for Neurological and Translational Science without whom this PhD would not have been possible. Greg and Dale, I am grateful for your generosity, it has truly been life changing.

I am grateful for all the good friends that I have made in the past 3.5 years. Bao, you were the first person in our lab and have supported me throughout by teaching me everything you know, making the time for discussions, troubleshooting and supporting me through the stressful times I have had. John, you have been my PhD buddy in this PhD journey. We have helped each other through every

part of the PhD. We have had a lot of fun times and laughs along the way that has made this journey memorable. Without the two of you I could not have achieved this.

I am also grateful for the friendship of Milena, Prithi and Akila. You guys have come in at different stages of my PhD and even though you have been there for a small part of my PhD you guys have made a big impact. Thank you for all the time you have given me, your friendship, the coffees, the dinners, the long chats and vents. You guys have shared in my successes and my failures. I am grateful that this PhD journey has allowed me to make such lifelong friends.

A big thank you to all of the RNV group, past and present, Kamal, Tamer, Tao, and Leon. Kamal and Prithi, some of my best times have been our afternoon coffee on the bean bags.

A big thank you especially to May, Kristin and Loren from MTL. The time you have taken out of your own busy schedules to always help guide me, give me advice, troubleshoot and teach me has been invaluable.

A big thankyou to Jodie, Janelle, Russell, Abbie, Kane and Danielle who have helped me a lot over the past 3.5 years and have made this journey so much easier. Jodie and Janelle, thank you for all your help dealing with the administrative tasks that has made this journey easier. A big thankyou to all of the MTL lab members.

I thank my best friend, Bindu, who has been there through the many phases of my life for the past 17 years. You have been there during the fun times and the tough times. Thank you for all the memorable dinners, brunches, the swimming, the walks, the long talks and the travels, you were my friend that took my mind off the PhD. Thank you even more for your support and help with the thesis. I am so grateful to have you as a friend.

To one of my greatest supporters, my family, thank you for your unconditional love and support. Dad, you have pushed when I needed to be pushed and always encouraged hard work and honesty in my life. You have pushed me to persevere through the tough times and grounded me in reality. To mum, your faith in me and life, your support in all my decisions and your calm presence has been equally important through the tough times. To my brother Murali, in spite of all our fights you stick by me and are there through all the adventures of my life. I am grateful for all the dinners, the movies, the travel, looking after Zuko and training him and all the other adventures we have been on together. To Zuko, my dog, you are my best friend and have given me your unconditional loyalty. You are the calming presence in my life and its in your company that I feel calmest even through the worst times.

And finally, to the other greatest support of my life, my husband Vikram, without whom this journey would not have been possible. Vikram, you have supported all my crazy ideas and dreams and given me your unconditional love and support through it all. You have been the person I have most vented to, you have listened patiently and have been on my side always. You have shown incredible patience and have put up with the exhausting flight travel so I wouldn't have to. Even living on the opposite sides of the country, you have managed to support me and make my life easier any way you can. Thank you for being there for me and believing in me. I could not have done this without you.

Authorship Declaration: Co-Authored Publications

This thesis contains some work that has been published while one section is in draft form and is being developed to be published.

Details of the work: Part of Chapter 2 of this thesis has been published in a co-authored paper, "Novel Chemically-modified DNAzyme targeting Integrin alpha-4 RNA transcript as a potential molecule to reduce inflammation in multiple sclerosis"

Location in thesis: Chapter 2

Student contribution to work: Madhuri Chakravarthy wrote the Methods, Results and Discussion section of this paper, and did some of the experimental work. Some of the experiments were performed by co-authors May T. Aung-Htut and Bao T. Le.

Details of the work: Part of Chapter 3 introduction of this thesis has been published in a co-authored review paper: "Nucleic Acid-Based Theranostics for Tackling Alzheimer's Disease."

Location in thesis: Chapter 3

Student contribution to work: Madhuri Chakravarthy wrote all sections of the paper. The figures were drawn by co-author Suxiang Chen.

Details of the work: Chapter 5 of this thesis has been published in a paper: "BACE1 inhibition using 2'-OMePS steric blocking antisense oligonucleotides"

Location in thesis: Chapter 5
Student Contribution to work: Madhuri Chakravarthy co-wrote the paper and performed all the experiments.
Details of the work: Chapter 6 of this thesis is published in a paper: "Development of Novel Chemically-Modified Nucleic Acid Molecules for Efficient Inhibition of Human MAPT Gene Expression"
Location in thesis: Chapter 6
Student Contribution to work: Madhuri Chakravarthy has co-written the paper and has performed 90% of all the experiments.
Details of the work: The third-author paper titled: "Systematic evaluation of 2′-Fluoro modified chimeric antisense oligonucleotide-mediated exon skipping in vitro" was not included in this thesis due to lack of significant contribution to the paper by Madhuri Chakravarthy.
Student Contribution to work: Madhuri Chakravarthy has performed one of the experiments that was presented in the paper.
Details of the work: The first-author paper titled: "Development of DNA aptamers targeting low-molecular-weight amyloid-β peptide aggregates in vitro" was not included in this thesis due to lack of significant contribution to all sections of the paper by Madhuri Chakravarthy.
Student Contribution to work: Madhuri Chakravarthy has co-written the western blot section of the paper both in the methods, results and discussion section as well as co-written the methods, results and discussion section for the ELISA assay presented in the paper.

Details of the work: The fourth-author paper titled: "Development of cell-specific aptamers: recent advances and insight into the selection procedures" was not included in this thesis due to lack of significant contribution to all sections of the paper by Madhuri Chakravarthy and due to its lack of relevance to the projects presented in this thesis.

Student Contribution to work: Madhuri Chakravarthy has co-written small sections of the paper and has co-edited the paper.

Details of the work: The third-author publication paper titled: "In vitro evolution of chemically-modified nucleic acid aptamers: Pros and cons, and comprehensive selection strategies" was not included in this thesis due to the review not having a relevance to the work presented in this thesis.

Student Contribution to work: Madhuri Chakravarthy has co-written the paper majorly edited the paper.

Authorship Declaration: Co-Authored Publications

This thesis contains some work that has been published.

Chapter 2:

Title: Novel Chemically-modified DNAzyme targeting Integrin alpha-4 RNA transcript as a potential molecule to reduce inflammation in multiple sclerosis

Name	Design	Data Collection	Data Analysis	Interpretation	Manuscript Development
Madhuri Chakravarthy	0	40	30	30	70
May T. Aung-Htut	50	40	30	30	10
Bao T. Le	0	20	15	10	5
Rakesh Veedu (Supervisor and Corresponding author)	50	0	25	30	15

Confirmation of contribution

As a contributor to this Chapter, I confirm that the level of contribution attributed to me is correct.

Madhuri Chakravarthy

May T. Aung-Htut

Bao T. Le

Rakesh Veedu

Chapter 3 (Introduction): Nucleic Acid-Based Theranostics for Tackling Alzheimer's Disease.

Name	Design	Data Collection	Data Analysis	Interpretation	Manuscript Development
Madhuri Chakravarthy	NA	NA	NA	NA	65%
Suxiang Chen	NA	NA	NA	NA	15%
Peter Dodd	NA	NA	NA	NA	5%
Rakesh Veedu (Supervisor and Corresponding author)	NA	NA	NA	NA	15%

Confirmation of contribution

As a contributor to this Chapter, I confirm that the level of contribution attributed to me is correct.

Madhuri Chakravarthy

Suxiang Chen

Peter Dodd

Rakesh Veedu

Chapter 3 (Part B: BACE1): BACE1 inhibition using 2'-OMePS steric blocking antisense oligonucleotides.

Name	Design	Data Collection	Data Analysis	Interpretation	Manuscript Development
Madhuri Chakravarthy	50%	100%	80%	50%	75%
Rakesh Veedu (Supervisor and Corresponding author)	50%	0%	20%	50%	25%

Confirmation of contribution

As a contributor to this Chapter, I confirm that the level of contribution attributed to me is correct.

Madhuri Chakravarthy

Rakesh Veedu

Abbreviations

mRNA	messenger RNA
SELEX	Systematic Evolution of Ligands by EXponential enrichment
ss	single-stranded
RNAi	RNA interference
ds	double-stranded
US	United States of America
FDA	Food and Drug Administration
EMEA	European Agency for the Evaluation of Medicinal Products
AO	antisense oligonucleotide
AMD	age-related macular degeneration
VEGF	vascular endothelial growth factor
DMD	Duchene muscular dystrophy
SMA	spinal muscular atrophy
siRNA	short interfering RNA
miRNA	micro RNA
PS	phosphorothioate
2'-OMe	2'-O-methyl

2'-MOE	2'-O-methoxyethyl
PMO	phosphoramidite Morpholino oligomer
SMN	survival of motor neuron
PPMO	cell-penetrating peptide-conjugated PMO
RISC	RNA-induced silencing complex
RT- PCR	Reverse transcription- Polymerase chain reaction page
miR	micro RNA
LNA	locked nucleic acid
2'F	2'-fluoro
2'NH$_2$	2'-amino
FANA	fluoroarabinonucleotide
TNA	threose nucleic acid
PNA	peptide nucleic acid
MNA	morpholino nucleic acid
HNA	hexitol nucleic acid
CeNA	Cyclohexenyl nucleic acid
ANA	anhydrohexitol nucleic acid
BBB	blood-brain barrier
CPP	cell-penetrating peptide

IV	intravenous
SC	subcutaneous
CNS	central nervous system
PEG	polyethylene glycol
CSF	cerebrospinal fluid
GalNAc	N-Acetylgalactosamine
MS	multiple sclerosis
MRI	magnetic resonance imaging
UV	ultra violet
HLA	human leukocyte antigen
EBV	Epstein Barr virus
EAE	Experimental autoimmune encephalomyelitis
GWAS	Genome-wide association studies
Th	T helper
IL	Interleukin
IFN	Interferon
TNF	tumor necrosis factor
ICAM-1	intracellular cell adhesion molecule-1
VCAM1	vascular adhesion molecule 1

ITGA4	Integrin alpha-4
MHC	major histocompatibility complex
SCR	scramble
PECAM-1	Platelet and endothelial cell adhesion molecule-1
PLP	myelin proteolipid protein
LMP1	Latent membrane protein1
IDT	Integrated DNA Technologies
ABI	Applied Biosystems
DMEM	Dulbecco's modified Eagle's medium
FBS	fetal bovine serum
CYCD	cyclin D
UT	Untreated
FAM	fluorescein amidites
FL	full-length
dT	inverted thymidine
NMDA	N-methyl-D-aspartate receptor
$A\beta$	amyloid-β
AD	Alzheimer's Disease
FAD	familial Alzheimer's disease

APP	Amyloid precursor protein
PSEN1	Presenillin 1
PSEN2	Presenillin 2
APOE	Apoliprotein E
BACE1	β-site APP cleaving enzyme 1
SAMP8	senescence-accelerated mouse-prone 8
PNA	Peptide nucleic acid
GSK-β	Glycogen synthase kinase 3 beta
Ache	Acetylcholinesterase
ApoER2	Apolipoprotein E receptor 2
Pre-miRNA	precursor miRNAs
ELISA	Enzyme-linked immunosorbent assay
EDTA	Ethylenediaminetetraacetic acid
HCl	Hydrochloric acid
SDS	Sodium dodecyl sulfate
GAPDH	Glyceraldehyde 3-phosphate dehydrogenase
HRP	Horse radish peroxidase
FL	Full-length
HEK	Human kidney embryonic

HPLC   High-performance liquid chromatography

UTR   untranslated region

MAPT   microtubule-associated protein tau

Chapter 1 Nucleic acid technologies

1.1 Introduction

The central dogma of biology introduced by Francis Crick in 1970 is the notion that genes encode protein (Figure 1.1); DNA is transcribed to messenger RNA (mRNA) that is translated to protein except for some genes that encode structural RNAs including ribosomal RNAs, transfer RNAs, small nucleolar RNAs, and spliceosomal RNAs to name a few (1). However, we now know that the central dogma is an overly simplified concept and has been challenged by the discovery of the importance of non-coding RNA (Figure 1.1).

Furthermore, we now know that introns make up 95% of the pre-mRNA, and 97-98% of all pre-mRNA transcripts are non-coding RNAs and only 1.5% of the total RNA codes for proteins (2). These non-coding RNA, although not extensively studied, have a significant role in cell and developmental biology (2). Multiple studies have shown that long non-coding RNAs are regulated during development and are expressed in specific cell types; they are localised to specific subcellular compartments and are implicated in many diseases (3, 4). RNAs have a role in epigenetic regulation, chromatin modification, transcriptional regulation, alternative splicing and post-transcriptional modification (2, 4-7). Non-coding RNAs can affect mRNA stability and translation and can interact with proteins to influence signalling (2). The non-protein coding DNA and RNA that was once considered junk is now seen to have an important role in developmental programming, regulation of many processes and regulation of proteins. The role of protein in diseases is well understood while the importance of RNA and in particular non-coding RNA in

diseases is now being explored. Nucleic acid technologies can be used to manipulate RNA and protein expression as research, diagnostic and therapeutic tools for various diseases.
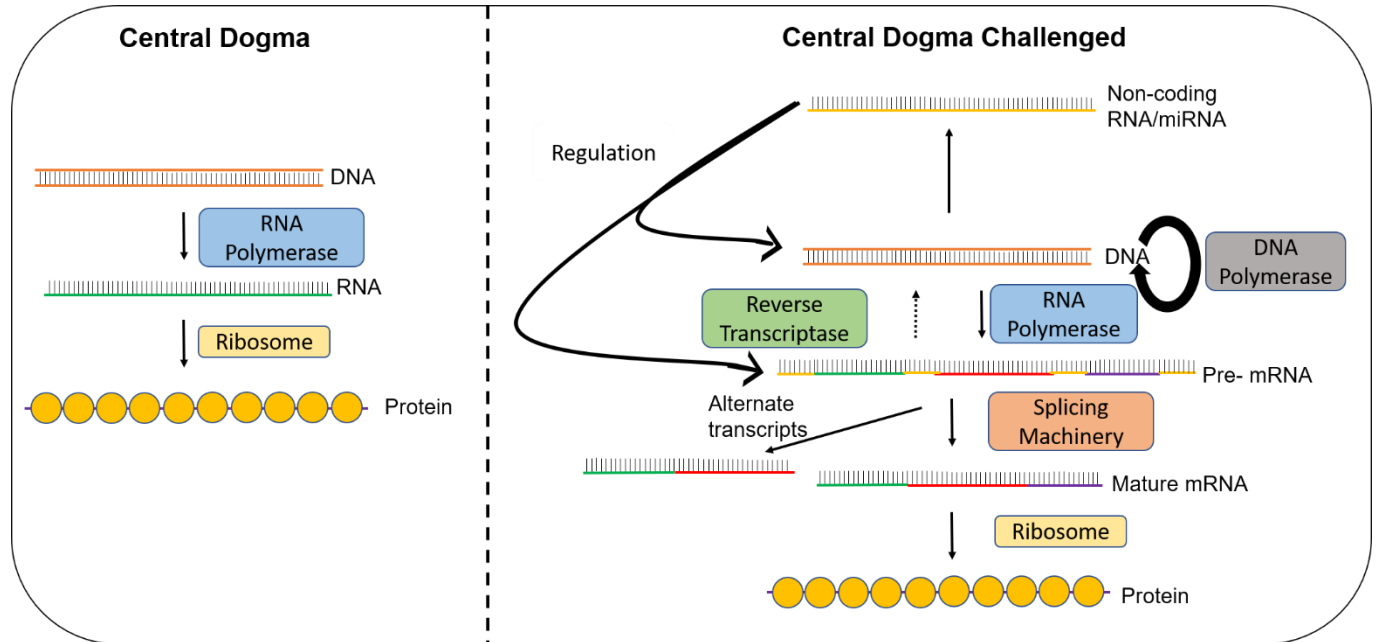
Figure 1.1   A schematic illustration of the central dogma (left) and the reinterpretation of the central dogma showing increased complexity in line with current knowledge (right). miRNA: micro RNA; mRNA: messenger RNA

1.2 Brief history of nucleic acid technologies

Interestingly, the natural roles of RNA have been exploited to develop nucleic acid technology that can mimic or manipulate the RNA in the body to regulate gene expression for drug and diagnostic development and increase our understanding of unknown genes. Zamecnik and Stephenson (1978) were the first to use antisense DNA to target and inhibit Rous sarcoma virus 35s RNA, that resulted in the inhibition of virus production (8). Cech and Altman (1990) showed that RNAs can act as catalysts to excise themselves from larger RNAs, and can with the help of proteins cut leader sequences off all transfer RNAs (9, 10). This discovery was contrary to the central dogma of molecular biology that RNA provides the intermediate information storage between DNA and proteins and has no other function. In 2004, both Tuerk and Gold first described

the systematic evolution of ligands by exponential enrichment (SELEX) process for generating single-stranded (ss) DNA or RNAs from random oligonucleotide libraries that can form a 3D structure called aptamers (11). Following the discovery of ribozymes, Breaker and Joyce (1994) generated DNA that similar to ribozymes could act as catalysts to cleave RNA through an *in vitro* procedure called DNAzymes although no such DNA enzymes have been found in nature (12). The RNA interference (RNAi) was then discovered in 1998 by Fire *et al*. who showed that injection of a double-stranded (ds) RNA into *Caenorhabditis elegans* reduced the expression of a specific endogenous transcript and the resultant protein (13). Till date, these nucleic acid technologies have been used to manipulate gene expression for therapeutic purposes and to investigate gene function.

The potential of nucleic acid technologies to be used as therapeutics was first realised in 1998 with the first United States of America (US) Food and Drug Administration (FDA) approval and the European Agency for the Evaluation of Medicinal Products (EMEA) for an antisense oligonucleotide (AO) Vitravene or fomivirsen to treat cytomegalovirus retinitis (14, 15). Following the first FDA approval of Vitravene in 2015, there was one aptamer and one other AO that received FDA approval. The first clinical aptamer approved by the FDA (2004) was Macugen or pegaptanib, an anti-vascular endothelial growth factor (VEGF) aptamer, to treat age-related macular degeneration (AMD) (11, 12, 15). Kynamro or mipomersen was the second AO to be approved by the FDA and was approved in 2013, 15 years after the first FDA approved AO. (15, 16). Importantly, from 2016-2019, six nucleic acid drugs were approved by the FDA, of which, four were AOs, including Exondys51 or eteplirsen for the treatment of Duchene muscular dystrophy (DMD), Spinraza or nusinersen for spinal muscular atrophy (SMA), Tegsedi or inotersen for familial amyloidotic polyneuropathy, volanesorsen or Waylivra for treatment of familial chylomicronemia syndrome, one short interfering RNA (siRNA) drug called Onpattro or

patisiran, again for familial amyloidotic polyneuropathy, and a GalNac siRNA called Givosiran for the treatment of acute hepatic porphyria (15, 17-19). The recent clinical success of the nucleic acid technologies has demonstrated the immense potential of various nucleic acid technologies as a viable class of therapeutics. This chapter describes nucleic acid technologies including RNase H mediated inhibition and steric block, DNAzymes/ Ribozymes, anti-micro RNA (miRNA)/ miRNA mimics, aptamers and RNA interference technologies, including siRNA.

1.3 Types of Nucleic Acid Technologies

1.3.1 Antisense oligonucleotides (AOs)

Synthetic AOs are short DNA or RNA analogue sequences around 13-25 nucleotides long that can be used as therapeutic agents or as tools to study gene function. These short sequences bind to the target mRNA by complementary Watson-Crick base pairing and regulate the expression by cleaving the target mRNA, modulating splicing of the target RNA or by acting as a steric block (Figure 1.2).
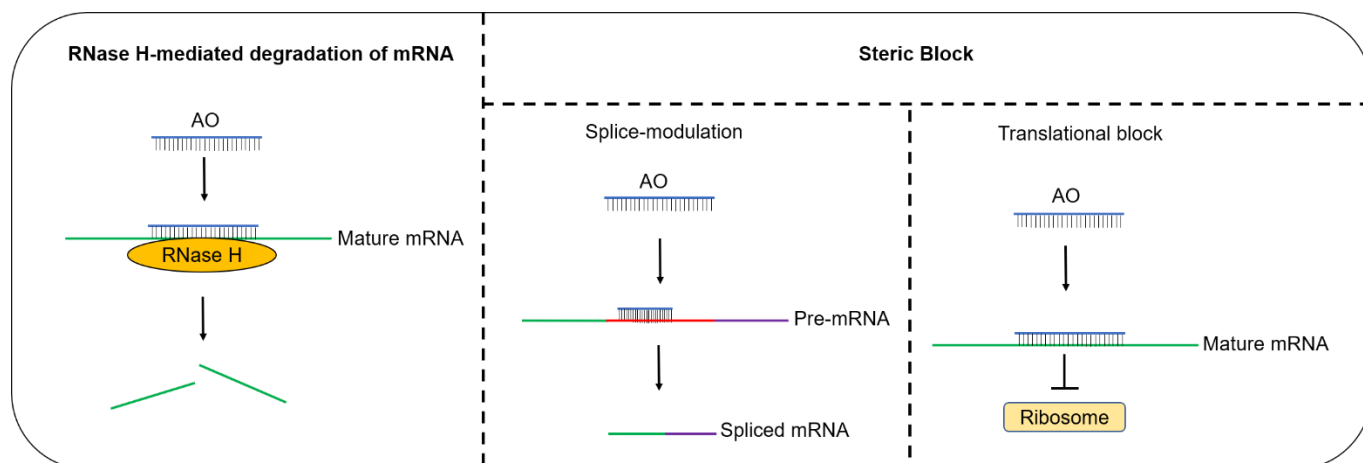
Figure 1.2   Simplified schematic demonstrating the mechanism of action of AOs including RNase H-mediated degradation of mRNA and steric blocking AOs. AO: antisense oligonucleotide; mRNA: messenger RNA

1.3.1.1 RNase H-mediated degradation dependent AOs

Antisense oligonucleotides (AOs) can modulate gene expression by inducing RNase H-mediated degradation of the target mRNA and therefore have potential as therapeutic molecules to tackle diseases by downregulating gene expression, for example, oncogenes as cancer therapies (20). The AO binds to its target mRNA through Watson-Crick base pairing, and this DNA-RNA heteroduplex recruits RNase H1, a mammalian cellular enzyme that then cleaves the RNA strand (Figure 1.2) (21). The cleaved mRNA fragments are then degraded by RNA degradation pathways (21). As the AO needs to be recognised by RNase H, we are restricted as to how much the AOs can be chemically modified, which limits its pharmacological abilities. However, the most common chemical modification is the phosphorothioate (PS) internucleotide linkages and the addition of 2'-sugar- modified analogues (2'-O-methyl (2'-OMe) or 2'-O-methoxyethyl (2'-MOE)) at the 3'and 5' ends. These modifications protect the AOs against degradation by nucleases, and increases the stability in cell culture and *in vivo,* without compromising its recognition by RNase H, also known as a 'gapmer' design (22). In the 'gapmer' design, typically a 20-nucleotide long sequence has a central phosphorothioate (PS) DNA core, and approximately five nucleotides at each ends containing 2'-sugar-modified nucleotides that protect the AOs against degradation by nucleases. The DNA nucleotide phosphorothioate (PS) gap in the centre allows the cleavage of targeted mRNA by RNase H (20, 23). A minimum of five phosphorothioate (PS) DNA nucleotides in the centre is sufficient for recruitment of RNase H (22, 23). A disadvantage of the PS backbone is its toxicity that varies according to sequences (24). Toxic effects include increased coagulation time, pro-inflammatory effects and activation of the complement pathway (23, 24). At higher concentrations, PS AOs lead to renal tubular changes and thrombocytopenia (24). Certain sequences on a PS backbone induce a strong immunostimulatory response through their

interactions with Toll-like receptors or bind directly to proteins, leading to unexpected effects (23, 24). The FDA approval of fomivirsen, mipomersen and inotersen have made RNase H-based AOs an effective class of therapeutic molecules, however, the admission of these drugs results in adverse events and therefore requires careful monitoring.

1.3.1.2 Steric Blocking AOs

Oligonucleotides can be designed to bind to RNA and block the access of cellular machinery to pre-RNA and mRNA, and can, thereby, modulate splicing, repair defective RNA, restore protein production or downregulate gene expression without degrading the RNA (Figure 1.2) (20, 23-25). As steric block oligonucleotides do not exploit cellular enzymes, to exert an effect, these oligonucleotides can be chemically modified more extensively to improve their pharmacological properties (25). The 2'-sugar modified oligonucleotides and phosphorodiamidate Morpholino oligomer (PMO) have been used extensively for this purpose, including in clinical trials.

Splice-modulating oligonucleotides are steric blockers, that may be applicable as therapeutics for a broad range of diseases, caused by particular protein isoforms or by mutations in particular regions of the gene (23). Splice-modulating oligonucleotides bind to the target RNA and block interaction of the pre-mRNA with splicing factors such as RNA-binding proteins, small nuclear RNAs and other components of the spliceosome (26). Eteplirsen and nusinersen were approved by the FDA (2016) to treat DMD and SMA respectively and show that splice-modulation AOs may be a good treatment strategy for various genetic diseases.

1.3.1.2.1 Splice-modulating AOs for Duchene muscular dystrophy (DMD)

Duchene muscular dystrophy (DMD) is a severe muscle wasting genetic disorder that affects 1 in 3500-5000 newborn males, leading to loss of mobility by 10-12 years of age and death in their mid-20s due to respiratory and cardiac function failure and is caused primarily by exon deletions

in the dystrophin gene (25, 27, 28). Dystrophin is required to connect the actin cytoskeleton to the sarcolemma and is essential for the maintenance of membrane integrity (25, 27, 28). Therefore, the lack of dystrophin leads to the disintegration of muscle fibres, that cannot be replaced indefinitely by muscle regeneration mechanisms (25, 27, 28). The disease causing deletions in the dystrophin gene disrupt the translational reading frame and prevent or greatly reduce production of dystrophin (25, 27, 28). In Becker muscular dystrophy, the deletions in the dystrophin gene do not generally disrupt the reading frame and therefore results in a truncated dystrophin isoform that retain partial function and lead to variable, milder forms of muscular dystrophy (25, 27, 28). The understanding of the molecular basis of Duchenne and Becker dystrophies provided the basis for development of splice-modulation as a strategy to reduce the severity of DMD. AOs that bind to and prevent selection of an exon adjacent to the frame-shifting deletion can restore the open reading frame and lead to a translation of a partially truncated but functional protein (25, 27, 28). Eteplirsen also known as Exondys51 is a splice-modulating PMO that has been approved by the US FDA for the treatment of DMD-causing deletions that flank exon 51 (27, 29).

1.3.1.2.2 *Splice-modulating AOs for spinal muscular atrophy (SMA)*

Spinal muscular atrophy (SMA) is a neuromuscular disease caused predominantly by homozygous deletion of the survival of motor neuron 1 (*SMN1*) gene that is critical for motor neuron development and function. The closely related variant *SMN2* encodes an identical protein but is inefficiently spliced and therefore cannot fully compensate for the loss of *SMN1* (25, 30, 31). The low protein activity of *SMN2* is due to a C>T change in exon 7 that results in the exclusion of exon 7 during splicing (25, 30, 31). Splice-modulating AOs that target exonic and intronic splicing silencer elements to promote the inclusion of exon 7 were screened and identified an AO sequence that led to splice-switching 2'-OMOE oligonucleotide, nusinersen, which has now been approved

by the US FDA for the treatment of selected SMA patients (25, 30, 31). The target tissue in SMA is the spinal cord. However, a key challenge for the use of oligonucleotide therapeutics in treating neurological diseases is the inability of the oligonucleotides to cross the blood-brain barrier (BBB). To bypass the BBB, oligonucleotides need to be delivered directly to the target tissue, that is the brain and/or spinal cord by intracerebroventricular or intrathecal injections (25, 31).

1.3.1.3 Other steric block AOs

Steric blocking AOs can also downregulate protein production by excluding exons that are out of frame or by inclusion of certain introns and therefore disrupt the reading frame, resulting in the mRNA being degraded by nonsense-mediated decay, preventing the production of protein (32). The AOs can also prevent protein translation by blocking the interaction of the translation machinery with the mRNA at the translational start site. Another mechanism through which steric blocking oligonucleotides can downregulate protein production is by the generation of external guide sequences (25, 33). External guide sequences are short RNAs that bind to the target mRNA and form a three-dimensional structure similar to a transfer RNA and guide the transfer RNA-processing ribozyme RNase P to cleave the targeted mRNA (25, 33). The targeted mRNA is cleaved at the first base pair of the duplex formed by the oligonucleotide and the targeted mRNA (25, 33). These steric-blocking AOs have been developed for antibacterial and antiviral treatments (25, 33). An 11-mer PMO can enter through the bacterial cell wall, unlike other types of oligonucleotides (34). Other oligonucleotides that can penetrate the bacterial cell wall are the PMOs conjugated to cell-penetrating peptides (PPMOs), and positively charged PMOs (35, 36).

1.3.2 RNA interference (RNAi)

RNA interference (RNAi) was first demonstrated in *Caenorhabditis elegans* where delivery of a long, dsRNA resulted in silencing of the expression of a gene that encoded a myofilament protein

(13). The mechanism of the silencing involved, degradation of the target mRNA mediated by siRNAs, small dsRNAs, 21-22 nucleotides long, that interacted with an RNA-induced silencing complex (RISC) (37). In this multi-complex, the siRNA is unwound, the sense strand discarded, and the antisense or guide strand binds to the target mRNA resulting in the cleavage of the mRNA at a particular site by the endonuclease Argonaute 2, a component of the RISC (Figure 1.3) (27). Although the dicers found in mammalian cells cannot process dsRNA to generate siRNA, synthetic siRNAs can enter the RISC and degrade the target mRNAs (38, 39). Unmodified siRNA is rapidly degraded by nucleases in the bloodstream, and its uptake into target organs is poor, although there has been some success in siRNA delivery to the liver (31). Although chemical modifications may help overcome these challenges, chemical modifications need to be compatible with maintaining RISC function (31). Inclusion of PS internucleotide linkages at the 3' end and 2'-OMe nucleotide substitution in one or two internal nucleotides in the antisense strand are tolerated and improve the siRNA nuclease resistance (31). In the sense strand, additional internal nucleotides can be substituted with 2'-OMe nucleotides (31). Alternative siRNA designs such as asymmetrical siRNA designs can increase the potency of the siRNA. For example, a divalent siRNA composed of two fully chemically modified phosphorothioate-containing siRNAs joined by a linked resulted in the siRNA reducing its target mRNA protein in mice brains for six months (40). Due to challenges to intracellular delivery, the siRNA is locally administered (31). An additional problem associated with RNAi technology are the off-target effects of siRNAs (30, 41, 42). Synthetic siRNAs can bind to mRNA with mismatched base pairs, acting as miRNAs and can therefore, also cleave untargeted mRNA, leading to off-target gene silencing (30, 41, 42).
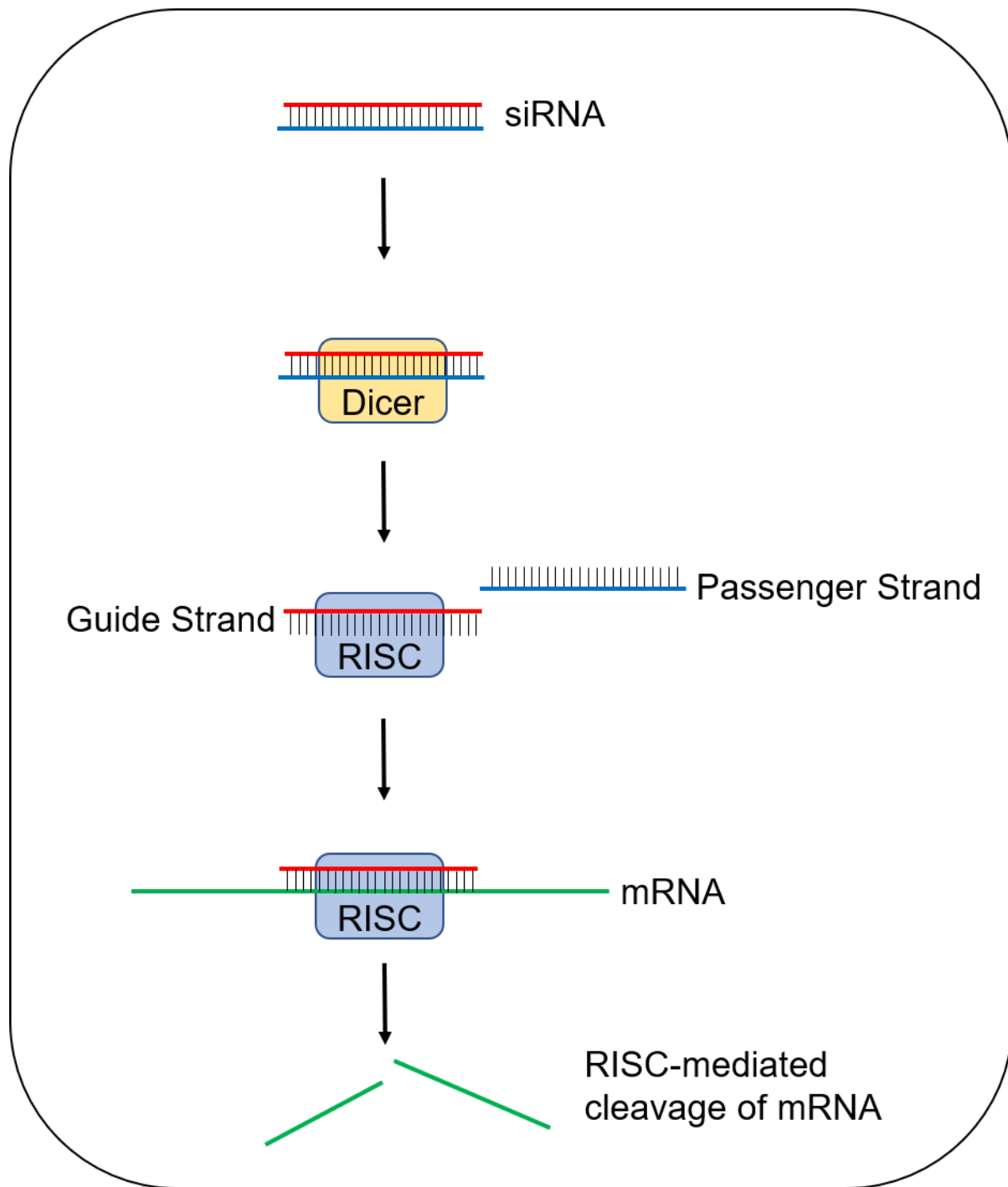
Figure 1.3   Basic schematic demonstrating the mechanism of action of siRNA. Dicer is an enzyme that cleaves double-stranded RNA into short double-stranded RNA fragments and activates the RISC complex. RISC is a multiprotein complex that recruits a single strand of the siRNA to recognize its complementary mRNA. Once the mRNA has been incorporated, the Argonaute protein which is part of the RISC complex cleaves the mRNA. siRNA: small interfering RNA; RISC: RNA-induced silencing complex; mRNA: messenger RNA

1.3.3 DNAzymes

DNAzymes are catalytic oligonucleotides that can target and cleave mRNA with high specificity (Figure 1.4) (12, 43-53). DNAzymes can catalyse RNA/ DNA cleavage, ligation, phosphorylation and other reactions (12, 43-53). By modifying the DNAzymes with fluorescent or signalling molecules, they can also act as a diagnostic marker or as a biosensor (54-56). DNAzymes are not found in nature as they are single-stranded, while most DNAs in cells are double-stranded (56). DNAzymes are selected by an *in vitro* selection method through the use of a ~ 10^{14} random oligonucleotides library and a synthetic target ribonucleotide/ RNA sequence to select for specific cleavage of the target that may be an RNA/ DNA chimeric substrate, or mRNA cleavage respectively (56). The selection can occur at physiological conditions or in biological fluids to optimise for activity *in vivo* (56). DNAzymes can cleave specific target RNA by binding to their target through complementary Watson-Crick base pairing of their arms (56). DNAzymes cleave specific sites through the catalytic loop (56) and show great potential as theranostic molecules, for diagnosis or as biosensors, as well as for therapeutics, and can overcome the challenges faced when the biodistribution of the diagnostic and therapeutic molecules differ (56). DNAzymes are useful as therapeutics since they can be reused within the cell and therefore can be potent at lower dosages (56). Using DNAzymes instead of exogenous protein enzymes overcomes the potential for immunological responses that may be elicited, and the high cost of producing recombinant enzymes (56). Other advantages of DNAzymes as therapeutics include the ease of production of different DNAzymes to target different RNA targets, modification of DNAzymes with low immunogenicity and the easy conjugation of the DNAzymes to other molecules for signalling and delivery (56). DNAzymes are preferred over ribozymes due to their increased stability and cost-effectiveness. DNAzymes require metal ions as cofactors for catalysis; therefore, it is

advantageous if the effective cofactors are Na^+, K^+, Mg^{2+} or Ca^{2+} as these are found at high concentrations in the blood and cells. DNAzymes with all-natural nucleotides are less costly to synthesise than DNAzymes with modified nucleotides, although DNAzymes selected from chemically modified libraries may have enhanced cleavage rates. Santoro and Joyce (1997) first reported a DNAzyme that when bound to target RNA through complementary base pairing with its binding arm has a catalytic loop that could cleave almost any targeted RNA (32). This ensures that *in vitro* selection procedures do not need to be carried out specifically for each RNA target which is both time consuming and can be expensive (32). Santoro and Joyce reported 10-23 and 8-17 DNAzymes, DNAzymes with a stem-loop or a hammerhead design that cleaved RNA substrates in the presence of Mg^{2+} (32). The 10-23 DNAzymes have high catalytic efficiency for cleavage, can cleave all purine-pyrimidine junctions and therefore can be designed to target any RNA sequence. The 10-23 DNAzymes' catalytic loop has now been exploited and used to synthesise many different DNAzymes (32). The 8-17 DNAzymes can only cleave sites next to the G·T wobble pair, which limits the RNA sequences that can be targeted (32). However, the 8-17 DNAzymes have shown high activity and high tolerance to mutations.

Although DNAzymes show potential *in vitro*, they have not achieved clinical or commercial successes yet. However, there are three DNAzymes currently in clinical trials for the treatment of allergic bronchial asthma (57, 58), basal cell carcinoma (59) and nasopharyngeal carcinoma indicating their potential as therapeutics. One of the limitations of DNAzymes is that although they can achieve high activity *in vitro*, they achieve this with a metal ion concentration higher than that is available in the cells (56). Other studies have claimed that the gene silencing seen due to DNAzymes may be an antisense effect rather than a cleavage effect (33). A study that compared the antisense effect and the cleavage effect of the DNAzyme 8-17 showed that in the presence of

Mg^{2+}, the antisense effect predominates while in the presence of Zn^{2+}, the cleavage activity was predominant (33).

1.3.4 Ribozymes

Natural ribozymes were discovered in the early 1980s in *Tetrahymena thermophila* and *Escherichia coli* (9, 10) and provided the first demonstration that nucleic acids could also have catalytic activity. Ribozymes like DNAzymes catalyse RNA cleavage and ligation reactions (Figure 1.4). The most common types of ribozymes used for therapeutics are the "hammerhead" or "hairpin motifs". The hammerhead ribozyme, similar to DNAzymes, contains a catalytic core that cleaves the target RNA and three hybridizing helices, where two helices flank the catalytic core and bind the target RNA through Watson-Crick base pairing (52). The hammerhead ribozyme cleaves its target RNA adjacent to the 3' of uracil and an A, C, or U base resulting in two shorter RNA that are unstable and rapidly degraded, resulting in decreased protein production (52). The ribozymes similar to DNAzymes can also have an antisense effect.

The first synthetic ribozyme tested in clinical trials was Angiozyme that targeted the mRNA of the vascular endothelial growth factor receptor-1 to block angiogenesis and tumour growth (44). Although angiozyme showed promising results in preclinical studies and Phase I clinical trials, in Phase II clinical trials, the drug did not show any significant positive clinical outcomes although it was safe (44). Angiozyme was discontinued and not further pursued (44). Another ribozyme, Herzyme was developed to treat cancer, and targeted the mRNA of the human epidermal growth factor type II oncogene (*HER2*), overexpressed in breast cancers (44). Herzyme was tested in Phase I clinical trials on *HER2*- overexpressing patients with metastatic breast cancer (44). Herzyme was well tolerated and showed stabilisation of disease in four patients, however, there were no partial or complete responses, and Herzyme like Angiozyme was not pursued further (44, 51).

Ribozymes have also been developed as anti-viral therapeutics. The ribozyme, Heptazyme targets the 5'untranslated region of the hepatitis C viral RNA (51). However, in animal studies, one mouse lost its eyesight resulting in the experiments being terminated (51). Similarly, the ribozyme HerBzyme is a ribozyme that targets the hepatitis B virus transcript, as well as hepatitis B virus pre-genomic RNA (51). HerBzyme was investigated in phase I/II clinical trials, but was also discontinued in 2003 (51).
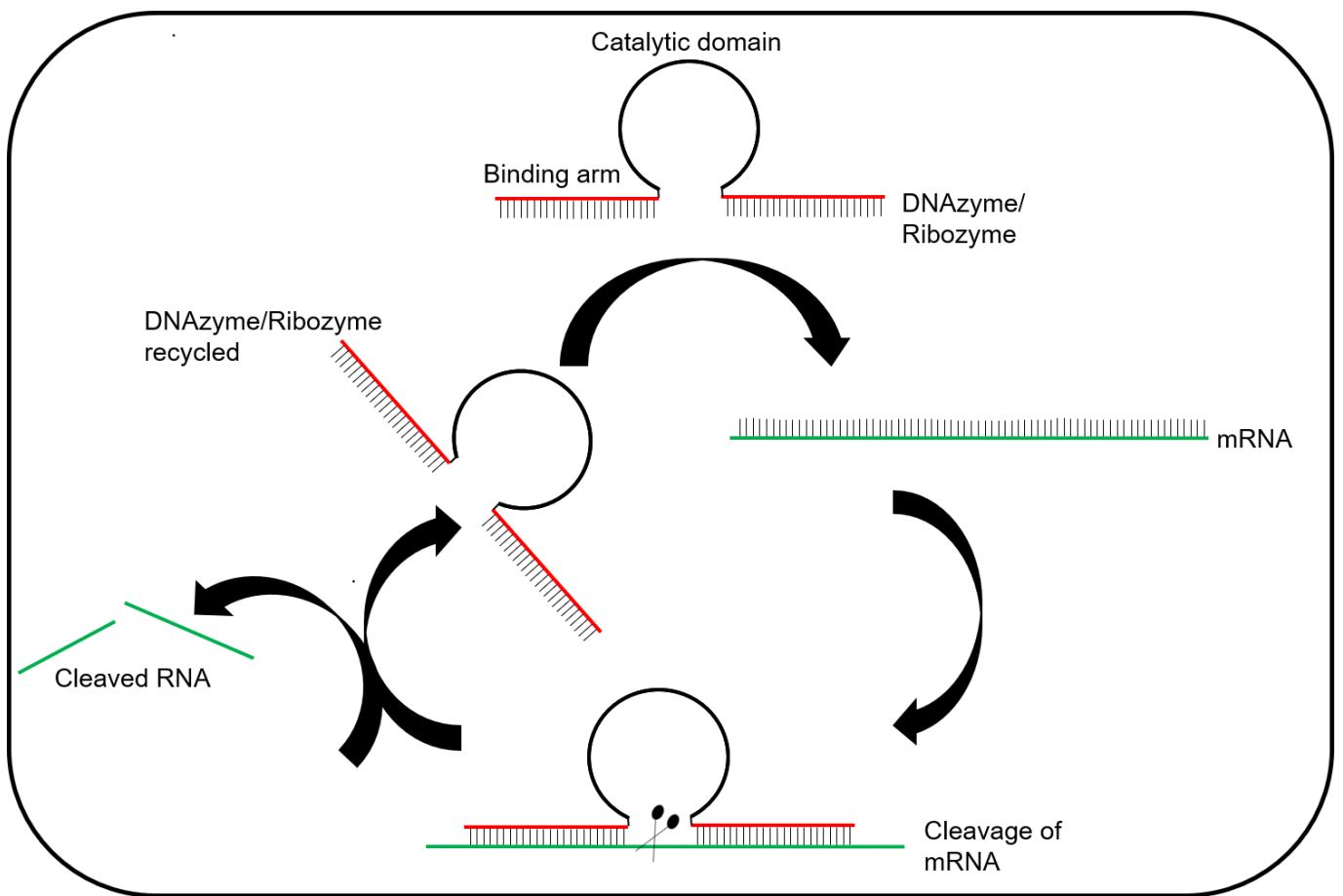
Figure 1.4   Schematic demonstrating the mechanism of action of a DNAzyme/Ribozyme. mRNA: messenger RNA

1.3.5 Nucleic acid aptamers

Aptamers are short single-stranded (ss) DNA or RNA sequences that can form a unique three-dimensional shape and bind to various targets, including proteins and whole cells. Aptamers are

isolated thorough systematic evolution of ligands by exponential enrichment (SELEX). The ability of DNA or RNA sequences to bind to proteins was first discovered in studies on human immunodeficiency virus, where a short RNA sequence called 'trans-activation response', binds to viral proteins T1 and Tat, that control gene expression and viral replication (60, 61). In 1990, two studies demonstrated that, RNA sequences that bound to target proteins with high affinity by folding into a specific three-dimensional conformation could be isolated from a library using SELEX (62, 63). This process could be performed similarly using a DNA library to isolate DNA sequences against specific protein targets (64, 65).

SELEX is an iterative process. In SELEX, a large DNA or RNA library that contains a randomised region of around 40 nucleotides and fixed flanking regions on both ends that allow reverse transcription-polymerase chain reaction (RT-PCR) to be used (66). The library is incubated with a target protein, and the nucleic acid molecules that bind to the target are separated and isolated (66). The bound nucleic acid molecules are amplified by RT-PCR, and the resulting nucleic acid molecules are used for another round of selection (66). The process is repeated 8-12 times until a high-affinity pool of aptamers is isolated (66). This pool is then sequenced and analysed to identify the aptamers with the highest affinity and specificity for the target (66). Aptamers can bind to their target with affinity in the nanomolar to picomolar range (66, 67). Aptamers can also be chemically modified to improve their pharmacological properties, which can be done either after selection or by using a chemically modified library to isolate the aptamers (68). Aptamers have several advantages over antibodies (67, 69). *In vitro* selection of aptamers means that aptamers for any target protein in a variety of conditions can be isolated (67, 69), and aptamers have low or no immunogenicity, unlike antibodies that often provoke immunogenic responses (67, 69). Besides,

other advantages include no batch to batch variation, low production costs, and the possibility to improve the pharmacological properties by chemical modifications (67, 69).

Since isolation of the first aptamer nearly 28 years ago, one aptamer, Macugen, has been approved by the US FDA for the treatment of age-related macular degeneration (AMD) (70). Macugen or pegaptanib is an RNA aptamer against VEGF$_{165,}$ that is upregulated in AMD (12). Macugen was approved in 2004 but has since been replaced by ranibizumab, an antibody-based therapy that recognises more of the VEGF isoforms (67). There have been two other aptamers to treat AMD that were tested in clinical trials, in combination with ranibizumab (67). Pegpleranib, a platelet-derived growth factor DNA aptamer showed positive outcomes in Phase II clinical trials, and Avacinacaptad pegol, a modified RNA aptamer targeting complement component C5, showed positive outcomes in open-label Phase IIa clinical trials (67). Aptamers have also been developed for the treatment of thrombosis, vascular disease and cancer and are currently being investigated in clinical trials (67, 71).

1.3.6 miRNA

Micro RNAs (miRNAs) were first discovered in 1993 by Victor Ambros and Gary Ruvkun in *Caenorhabditis elegans* where a small RNA encoded by the lin-4 locus was shown to be important in the developmental timing in the nematode (72, 73). The miRNAs are small non-coding single-stranded (ss) RNAs, 21-23 nucleotides long, and are crucial negative regulators of many processes in the body, and their dysregulation is implicated in a wide variety of diseases (74). Furthermore, a single miRNA can regulate the expression of multiple genes (74). Therefore, modulation of miRNA expression is an important therapeutic strategy that is now being explored. The two strategies used to regulate miRNAs include the use of AOs to block miRNA function, called anti-

micro RNA (anti-miRs) and the use of synthetic RNAs called miRNA mimics that can mimic the action of a miRNA and increase its function (74).

The long RNA precursors called pri-miRNAs are transcribed by RNA polymerase II in the nucleus and then processed by Drosha, a nuclear RNAse III enzyme, resulting in a 60-70 nucleotide pre-miRNA with a hairpin structure (75). The pre-miRNAs are then exported from the nuclease by exportin 5 and further processed by a second RNase III enzyme, Dicer, which recognises and cleaves the dsRNA to form single-stranded (ss) miRNA known as the guide strand (75). The miRNAs (guide strands) are then loaded into the RISC complex, similar to siRNAs, and can bind to their target mRNA and regulate gene expression (75). The miRNA inhibits its target mRNA through complementary base pairing of the nucleotides 2-7 at its 5' end and recruiting RISC (formed by the argonaute protein and Dicer) to the mRNA (75). The recruitment of the RISC complex to the mRNA results in degradation of the mRNA or inhibition of translation, and thereby regulates gene expression (75).

The most successful anti-miR reported to date is miravirsen, a β-D-oxy-locked nucleic acid (LNA)-modified PS AO targeting miR-122 that has shown promise in Phase II clinical trials on hepatitis C (76). Another miRNA antagonist RG-101 is also being investigated in Phase II clinical trials as a treatment strategy for hepatitis C (77) and a miRNA mimic targeting miR-34 as a treatment strategy for hepatocellular carcinoma is in Phase I clinical trials (78).

1.4 Chemical modifications

Unmodified RNA and DNA are unsuitable for clinical use as they are easily degraded by nucleases, have poor cellular uptake, have unfavourable biodistribution and pharmacokinetic properties and have lower binding affinity than needed (48). Furthermore, the degradation products of

phosphodiester oligonucleotides may be cytotoxic and have anti-proliferative effects. Chemical modifications can overcome the disadvantages of unmodified phosphodiester oligonucleotides and improve their pharmacological properties; including increasing stability against nucleases, making their use as therapeutics potentially more viable. Some of the chemical modifications that have been effective to date include changes to the backbone, sugar, or base that may increase target affinity and specificity while increasing resistance against nuclease degradation and improving pharmacokinetics. Some of the chemical modifications available are shown in Figure 1.5.
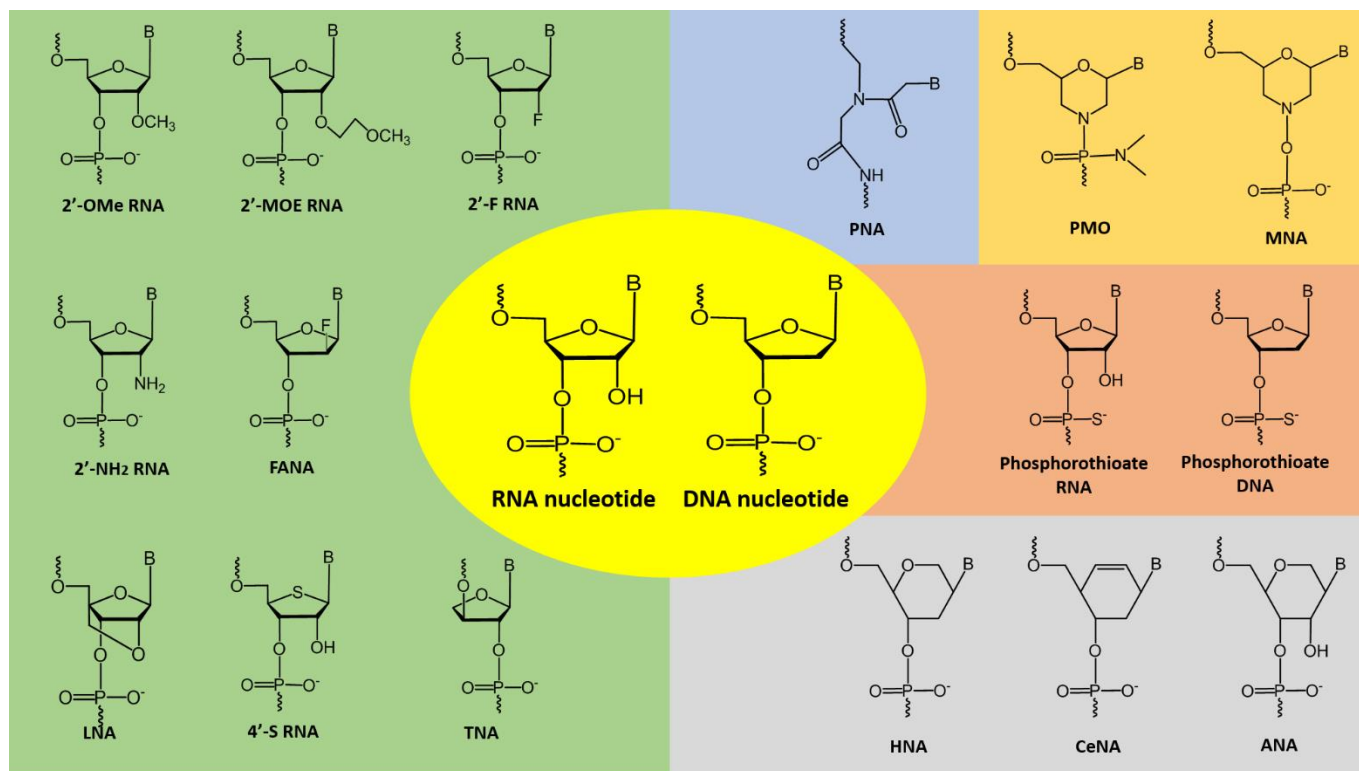
Figure 1.5   Examples of chemically-modified nucleotide analogues. 2'-OMe: 2'-O-methyl; 2'-MOE:2'-O-methoxyethyl; 2'-F: 2'-fluoro; 2'-NH2: 2'-amino; FANA: fluoroarabinonucleotide; LNA: locked nucleic acid; TNA: threose nucleic acid; PNA: peptide nucleic acid; PMO: phosphorodiamidate morpholino oligomer; MNA: morpholino nucleic acid; HNA: hexitol nucleic acid; CeNA: cyclohexenyl nucleic acid; ANA: anhydrohexitol nucleic acid (79)

One of the earliest chemical modifications reported was the PS backbone that provides stability against nucleases while still allowing the AOs to be recognised by RNase H and reducing renal clearance of the oligonucleotide (47, 48, 50). However, PS backbone modification results in

decreased AO binding affinity to target (47, 50). The PS backbone modification also results in the AOs suppressing immune responses by downregulation of TLR-induced immune activation (80). Other backbone modifications include methylphosphonate, N3'-P5' phosphoramidites and thiophosphoroamidites, amides, methylene(methylamino), fromacetal and thioformacetal, morpholino phosphorodiamidate (PMO) and peptide nucleic acids (49). In a PMO, the riobofuranose ring is replaced with a morpholino ring, and the phosphodiester backbone is replaced with a phosphorodiamidate linkage (49). PMOs are neutral in charge, have a similar affinity as in a DNA: DNA duplex, are nuclease resistant but cross the cell membrane poorly (49). PMOs do not support RNase H activity but are used as steric blockers as they have an excellent safety profile as shown by eteplirsen, an FDA approved splice-modulating PMO (49).

Chemical modifications that can increase the binding affinity as well as provide nuclease resistance are 2'-ribose modifications including 2'-OMe, 2'-MOE and 2'-fluoro (2'-F) modification of the RNA (48, 50). The 2' modifications result in the oligonucleotide adopting the most energy-favourable RNA conformation, an RNA-like C3'-endo sugar pucker that increases its binding affinity and improves its nuclease resistance. The nuclease resistance is also improved by the inability of the nucleases to recognise the chemical modifications. Clinically most oligonucleotide drugs including mipomersen, nusinersen and inotersen carry 2'-MOE modifications (50). The 2'-F modification can also enhance drug-like properties of siRNA and has been used for many nucleic acid technologies including ribozymes, RNase H competent AO gapmers, steric block AOs, siRNA duplexes, miRNA antagonists and aptamers (49). Macugen, an FDA approved aptamer is a partially 2'-F RNA (49). As these modifications are 'RNA-like', the duplex formed by binding of these modified AOS to the target mRNA cannot be recognised by RNase H (48). Therefore fully modified 2'- ribose modifications are used for steric blocking AOs while a gapmer design

(chemical modifications flank the central eight to ten base DNA 'gap' that can be recognised by RNase H) is exploited for RNase H competent AOs (48). The binding affinity of the oligonucleotides to their target RNA can be further improved by reducing conformational flexibility of the nucleotides by introducing locked nucleic acid (LNA) modifications that link the 2' oxygen and 4' carbon of the ribose sugar (50). The 2'-OMe and 2'-MOE modifications have lower binding affinity than LNA modified nucleotides but can be used to make fully modified oligonucleotides. However, although LNA modifications have higher binding affinity, fully LNA modified oligonucleotides tend to aggregate and therefore chimeric (RNase H competent AOs) or 'mixmer' (steric block AOs) oligonucleotide design incorporating LNAs is used (50). LNA modified gapmers have shown an increased risk of hepatotoxicity that is AO sequence dependent and may be overcome by a constrained ethyl modification (49).

There are many other bridged nucleic acids similar to LNA, and analogues that are being investigated include six-membered ring analogues, bicyclo and tricyclo DNA modifications and constrained nucleic acids (49). In addition, nucleobase modifications such as 5-methyl pyrimidines, 5-substituted pyrimidine analogues, 2-thio-thymine and purine modifications can be used (49). The chemical modifications, 2'-thiothymidine; 3'-fluorohexitol nucleic acid; 5'-modified pyrimidine base; and α,β constrained nucleic acid can be incorporated into gapmers to improve specificity, including replacing DNA within the gap-region of the RNase H AOs that are specific for single-nucleotide polymorphisms (49, 50). The 2'-fluroarabinonucleic acid modifications of the DNA can improve affinity and stability without affecting RNase H compatibility (50). Another unique class of nucleic acids are called spiegelmers that are enantiomers of the natural RNA and are used to create nuclease-resistant aptamers.

1.5 Delivery challenges and strategies

Oligonucleotides are commonly administered by intravenous (IV) infusion or subcutaneous (SC) injection, and the AOs can take minutes to hours to transfer from the blood into the tissues (81). The administration of the oligonucleotide by IV and SC injection results in the distribution of the oligonucleotides in numerous tissues, except for the central nervous system (CNS), although, the highest concentrations of the oligonucleotides are expected in the liver and kidney (81). The rapid uptake by cells is facilitated by endocytosis, and once the oligonucleotides have entered the cells, the oligonucleotides can exhibit long half-lives and prolonged antisense activity (81). Phosphorothioate (PS)-modified oligonucleotides show delayed renal filtration, as they bind to plasma proteins (81, 82). In contrast, oligonucleotides such as the peptide nucleic acids, and PMOs that are neutrally charged, and unmodified siRNAs are cleared more rapidly from the blood as they bind weakly to plasma proteins resulting in much lower tissue uptake (81, 82). Although chemical modifications to AO drugs can improve the target binding affinity and nuclease resistance, other major clinical challenges for nucleic acid therapeutics include poor delivery efficiency, tissue targeting and specificity, off-target effects and the stimulation of an immune response (82). Many drugs that are effective at the pre-clinical stages of testing and show good efficiency and specificity in animal studies fail in clinical trials. For example, naked siRNAs and aptamers that are typically used in lung, eye and skin applications may generate an inflammatory response due to the activation of the Toll-like receptors and result in poor cellular uptake, and siRNAs are degraded by nucleases (83). A major challenge to the use of AOs, RNAi and steric blocking oligonucleotides as therapeutics is the poor intracellular uptake. Most of the chemically modified nucleic acid therapeutics show limited tissue distribution and therefore need to be administered locally. Furthermore, once administered, the drugs become accumulated in the liver and kidney, are rapidly

excreted and therefore, require repeated administration. The concentration of the drugs required for a clinically effect is often high, which increases the risk of off-target effects.

1.5.1 Conjugation strategies

Antisense oligonucleotides (AOs) or siRNAs can be conjugated to ligands that are recognised by specific receptors, highly expressed in the target cells, to mediate cell type-specific intracellular delivery. Single-stranded (ss) AOs or siRNAs conjugated to triantennary N-Acetylgalactosamine (GalNAc) show increased delivery to hepatocytes where the GalNAc is recognised by the highly expressed asialoglycoprotein receptors (20, 81, 82). The siRNAs can be conjugated to cholesterol and incorporated into high-density lipoproteins for targeted delivery to the liver, gut, kidney and steroidogenic organs while incorporating them into low-density lipoprotein can specifically target the delivery of the siRNAs to the liver (84, 85). Conjugation of α-tocopherol with siRNAs also targets the siRNAs for delivery to the liver (86) and linking folic acid to liposome or nanoparticle encapsulated AOs or siRNAs can target the AOs or siRNAs to folate receptor-overexpressing cells, which is especially useful in cancers where folate receptors are overexpressed (85). Similarly, transferrin receptor is also overexpressed in many cancer cells and therefore, transferrin conjugated nanoparticle or liposome-encapsulated AOs or siRNAs can target transferrin mediated delivery to many cancers, endothelial cells and the brain (85). Previous studies show that peptide conjugated PMO (PPMO), phosphorothioated (PS) tricyclo DNA or 2'-OMePS modifications of splice modulating AOs can improve uptake by cells that express the scavenger receptor SCARA1, similar to GalNAc-conjugated oligonucleotides that also use a specific receptor (87).

1.5.1.1 Liposome-based delivery methods

Liposomes are vesicles with a phospholipid bilayer that can be used to carry oligonucleotides across the cell membrane (88). Liposomes come in a variety of sizes (as small as 20 nm to larger

than 1 µm) and the composition can be altered for different purposes (88). Conventional liposomes are composed of neutral or negatively charged phospholipids and cholesterol, and are quickly absorbed by the reticuloendothelial system (88). Liposomes need to be composed of cationic phospholipids to allow them to carry negatively charged oligonucleotides but can also be made pH-sensitive or induced to have long circulation time in the blood or be made cell-specific by changing the composition of the liposomes (88). Negatively charged siRNAs can be assembled into cationic liposomes through the formation of self-assembled nanoparticles or polyethylene glycol (PEG)-ylated liposomes (88). PEGylated liposomes have reduced clearance by the reticular-endothelial system and therefore have increased plasma half-life although they are less effective than non-PEGylated liposomes (88). The most successful liposome-based delivery system in the clinic is the stable nucleic acid-lipid particle produced by Tekmira Pharmaceuticals that has been used to administer many siRNA in guinea pigs, non-human primates and in human clinical trials (88). The siRNA patisiran, approved by the FDA recently, is encapsulated in a second-generation stable nucleic acid-lipid particle or lipid nanoparticle carrier that is a cationic lipid nanoparticle designed to deliver the siRNA to the target tissue (i.e. liver) by IV injection (83, 88, 89).

1.5.1.2 Nanoparticle (polymer)-based delivery methods

Polymeric nanoparticles with sizes between 10 nm and 100 nm are considered to be optimal for the delivery of siRNAs and-miRs. There are several types of nanoparticles similar to liposomes, into which, positively charged moieties such as polyethyleneimine can be incorporated to allow them to carry negatively charged AOs or siRNAs (90). Other ligands can also be incorporated including lipids, polyethyleneimine, cell-penetrating peptides, folates, antibodies and aptamers to ensure cell-specific delivery (90). Cyclo-dextrin nanoparticles complexed with siRNA and coated with polyethyleneimine were used to deliver siRNA into tumour cells in mice (91). Nanoparticles

composed of a lysine-based amino acid backbone with lipid functional groups have also been reported to deliver siRNAs *in vitro* and *in vivo* (92, 93). More recently, a nucleic acid nanoparticle that can self-assemble into particles of well-defined sizes was reported to deliver siRNAs to the target tumours with high specificity (94).

1.5.1.3 Antibody-based delivery methods

Antibodies can be used to direct the delivery of AOs or siRNAs to specific cell types (85). Antibodies are used as delivery vehicles by linking the fragment antigen binding or single-chain variable fragments isolated from the cell- or tissue- targeting antibody to the nanoparticles encapsulating the siRNA or AOs (85). However, the use of receptor-specific antibodies to deliver AOs or siRNA to target tissue may result in an immunogenic response (85, 95).

1.5.1.4 Cell-penetrating peptides (CPP)

Cell-penetrating peptides (CPP) are short positively charged peptide sequences that can cross the cell membrane (85, 96, 97). Cell-penetrating peptides (CPP) can be conjugated to the AOs or siRNAs directly or with the other delivery systems including liposomes or nanoparticles encapsulating siRNAs or AOs to deliver the AOs or siRNAs into the cell (85, 96, 97). Conjugation of CPPs directs oligonucleotides to Toll-like receptor 9 expressing cells (87). A skin-penetrating peptide conjugated to siRNAs was reported to deliver the siRNAs to keratinocytes, skin fibroblasts and endothelial cells after topical application in mice (98). Polyethylene glycol (PEG)-conjugated nanoparticles were conjugated with integrin-binding Arginylglycylaspartic acid peptides to form polyplexes for the successful delivery of siRNAs into tumours (84, 91).

1.5.1.5 Aptamer-based delivery methods

Aptamers similar to antibodies can be conjugated with other AOs or siRNAs to serve as a delivery vehicle. Aptamers, unlike peptides and antibodies, have low immunogenicity and are cheap to

produce. Aptamers can also be chemically modified to overcome degradation issues and are smaller than antibodies. For example, a nucleolin-specific aptamer can mediate delivery of AOs to cancer cells (87) and a prostate membrane-specific antigen targeting aptamer increased cellular uptake of siRNA *in vitro* in cancer cells that overexpress prostate-specific membrane antigens (99).

1.5.2 Crossing the blood-brain barrier (BBB)

A major challenge in developing therapeutics for neurological diseases is the inability of the oligonucleotides to cross the intact BBB. However, the oligonucleotides can be delivered to the cerebrospinal fluid (CSF) by intrathecal administration that results in the distribution of the oligonucleotides into the spinal cord and brain tissue (81). An FDA approved AO drug, Spinraza, has been delivered to ~7000 spinal muscular atrophy (SMA) patients through intrathecal administration (81); however AOs can also be delivered to the nervous system using other strategies.

1.5.2.1 Peripheral delivery

Peripheral delivery involves the administration of the oligonucleotides systemically and the uptake of these oligonucleotides into the nervous system (23). When AOs are administered systemically, a fraction of the oligonucleotides bind to plasma proteins while a fraction does not (23). The oligonucleotides that bind to the plasma proteins constitute the pharmacologically relevant fraction, that with the right properties will be able to cross the BBB (23). The fraction that does not bind to the plasma proteins is excreted (23). The bound fraction can cross the BBB by simple diffusion, if they are small lipophilic substances (23), however, AOs are too large (approximately around 6000 to 10000 Da) to cross the BBB (23).

The AOs can cross the BBB via receptor-mediated endocytosis that allows macromolecules, for example, insulin and transferrin to cross the barrier (23). The transferrin transport pathway has been used to transport AOs as well as nanoparticles carrying AOs into the brain parenchyma (23). Cell-penetrating peptide (CPP) delivery systems have also been successful in delivering AOs across the BBB (23). In particular, systemically delivered AOs tagged with arginine-rich CPPs were able to cross the BBB in mice (23). However, not all AO modifications can be coupled successfully with the CPPs (23).

1.5.2.2 Direct delivery into the nervous system

The AOs can be delivered directly into the cerebrospinal fluid by intracerebroventricular infusion (23), however, the oligonucleotide will then have to cross the ependymal cell layer to enter the parenchyma (23). Oligonucleotides can also be delivered intrathecally into the subarachnoid space of the spinal cord but will have to pass the pia mater to enter the parenchyma (23). Although both intracerebroventricular infusion and intrathecal infusions have been tested in animal models, intrathecal infusions of AOs has been used in humans and shows no major adverse effects (23).

1.5.2.3 Intranasal delivery

Intranasal delivery, if successful, could overcome challenges faced with invasive delivery strategies as well as being permissive to crossing the BBB (23). Intranasal administration of molecules transports the molecules along the olfactory and trigeminal nerve pathway and has been successfully used in clinical trials to deliver insulin to Alzheimer disease (AD) patients as well as CPP-conjugated siRNAs targeting intracerebral tumours (23).

Table 1.1   Different delivery strategies sfor nucleic acid technologies and their pros and cons

Delivery Strategy	Pros	Cons
Unmodified naked siRNAs/ AOs		

Delivery Strategy	Pros	Cons
Intravenous injection/ Subcutaneous injection	• Minutes to hours to transfer from the blood into the tissues • Distribution of AOs to numerous tissues	• Cannot enter the central nervous system • Highest concentration in the liver and kidney and is rapidly excreted out.
Modified naked siRNAs/ AOs		
Intravenous injection/ Subcutaneous injection	• PS- modified AOs have delayed renal filtration • PPMO, PS tricyclo DNA or 2'-OMePS modified AOs improve uptake of cells that express scavenger receptor SCARA1	• Have lower tissue uptake. • Poor delivery efficiency • Poor tissue targeting and specificity • Off-target effects • Stimulation of an immune response • Limited tissue distribution • Need to be administered locally • Accumulated in the liver and kidneys and rapidly excreted and require repeated administration.
Conjugation strategies		
GalNAc conjugation	• Increased delivery to hepatocytes where GalNAc is recognized by asialoglycoprotein receptors	• Delivery to only those cells that express asialoglycoprotein receptors
Cholesterol conjugation and incorporation into high or low-density lipoproteins	• Targeted delivery to liver, gut, kidney and steroidognic organs when incorporated into high-density lipoproteins • Targeted delivery to liver when incorporated into low-density lipoprotein	
α- tocopherol conjugation	• Targeted delivery to the liver	
Folic acid to liposome or nanoparticle encapsulated AOs or siRNAs	• Target AOs or siRNAs to folate receptor-overexpression cells- Useful for cancers where folate receptors are overexpressed	
Transferrin conjugated nanoparticle or liposome-encapsulated AOs or siRNAs	• Transferrin mediated delivery to transferrin receptor overexpressing cells- in cancers, endothelial cells and the brain	
Liposome-based delivery methods	• Liposome composition can be changed to make them pH-sensitive, induced to have long circulation time in the blood and made cell-specific	• Quickly absorbed by the reticuloendothelial system.

Delivery Strategy	Pros	Cons
	• PEGylated liposomes have reduced clearance by the reticular-endothelial system- increased plasma half-life but less effective than non-PEGylated liposomes • Stable nucleic acid-lipid particle- cationic lipid nanoparticle- delivers siRNA to target tissue by IV injection. FDA approved siRNA patisiran is delivered using this method.	• Unless composed of cationic phospholipids, cannot carry negatively charged oligonucleotides
Polymeric nanoparticles	• For delivery of siRNAs and miRNAs • Ligands incorporated into nanoparticles include lipids, polyethyleneimine, cell-penetrating peptides, folates, antibodies and aptamers for cell-specific delivery. • E.g. Cyclo-dextrin nanoparticles complexed with siRNA and coated with polyethyleneimine were used to deliver siRNAs into tumour cells.	
Antibody-based delivery	• Link the fragment antigen binding or single-chain variable fragments isolated from cell- or tissue-targeting antibody to nanoparticles encapsulating siRNA or AOs.	• May result in immunogenic response.
Cell-penetrating peptides	• Short positively charged peptide sequences that can cross the cell membranes. • Can be conjugated to siRNAs or AOs directly and directs AOs to Toll-like receptor 9 expressing cells. • Can be conjugated to other delivery systems including liposomes or nanoparticles encapsulating siRNAs or AOs.	• Not all AO modifications can be coupled successfully with the cell-penetrating peptides.
Aptamer-based delivery methods	• Like antibodies, can be conjugated with other AOs or siRNAs to serve as a delivery vehicle. • Low immunogenicity and are cheap to produce • Can be chemically-modified to overcome degradation issues and smaller than antibodies	
Delivery strategies for crossing the blood-brain barrier		
Peripheral delivery	• Only a fraction of the oligonucleotides bind to plasma proteins and will be able to cross the BBB. • Bound fraction can cross the BBB via receptor-mediated endocytosis that allows macromolecules to cross the barrier.	• The fraction that does not bind to plasma proteins is excreted. • AOs are too large to cross the BBB by simple diffusion.
Direct delivery into the nervous system	• By intracerebroventricular infusion. • Delivered intrathecally into subarachnoid space of the spinal cord. • Intrathecal infusions of AOs has been used in humans and shows no major adverse effects.	• Intracerebroventricular infusion of AOs need to cross ependymal cell layer to enter parenchyma. • Intrathecal infusion of AOs need to pass the pia mater to enter the parenchyma.

Delivery Strategy	Pros	Cons
Intranasal delivery	• Less invasive than other delivery methods. • Permissive to crossing the BBB • Transports molecules along olfactory and trigeminal nerve pathway • Used successfully in clinical trials to delivery insulin to AD patients as well as CPP-conjugated siRNAs targeting intracerebral tumours.	

1.6 Conclusion and Overall Aims

Nucleic acid molecules have shown great potential and have been approved by the United States Food and drug administration for the treatment of many diseases in recent years including an AO which was approved for the treatment of spinal muscular atrophy. Nucleic acid technologies have many advantages as therapeutics over antibodies, the traditional therapeutics used as treatment for many diseases, including the vast number of chemical modifications and delivery agents that can be conjugated. Chemical modifications and delivery strategies can be used to increase efficiency and specificity while decreasing nuclease degradation and renal clearance of the nucleic acid technologies. This thesis aims to develop novel nucleic acid technologies against ITGA4 for treatment of multiple sclerosis and against various targets including BACE1, APP and MAPT for Alzheimer's disease.

Aim 1: Developing DNAzymes against ITGA4 for tackling Multiple Sclerosis.

Aim 2: To develop splice-modulating antisense oligonucleotides to induce exon 16 and exon 17 skipping.

Aim 3: To develop splice-modulating antisense oligonucleotides to downregulate BACE1.

Aim 4: To develop DNAzymes and splice-modulating antisense oligonucleotides to downregulate MAPT.

1.7 References

1.   Crick F. Central Dogma of Molecular Biology. Nature. 1970;227(5258):561-3.

2.   Mattick JS. Challenging the dogma: the hidden layer of non-protein-coding RNAs in complex organisms. 2003;25(10):930-9.

3.   Wilusz JE, Sunwoo H, Spector DL. Long noncoding RNAs: functional surprises from the RNA world. Genes & Development. 2009;23(13):1494-504.

4.   Qureshi IA, Mehler MF. Emerging roles of non-coding RNAs in brain evolution, development, plasticity and disease. Nature Reviews Neuroscience. 2012;13(8):528-41.

5.   Mercer TR, Dinger ME, Mattick JS. Long non-coding RNAs: insights into functions. 2009;10(3):155-9.

6.   Shi X, Sun M, Liu H, Yao Y, Song Y. Long non-coding RNAs: A new frontier in the study of human diseases. Cancer Lett. 2013;339(2):159-66.

7.   Esteller M. Non-coding RNAs in human disease. Nature Reviews Genetics. 2011;12(12):861-74.

8.   Zamecnik PC, Stephenson ML. Inhibition of Rous sarcoma virus replication and cell transformation by a specific oligodeoxynucleotide. Proc Natl Acad Sci. 1978;75(1):280-4.

9.   Cech TR. Self-splicing and Enzymatic Activity of an Intervening Sequence RNA from Tetrahymena (Nobel Lecture). Angewandte Chemie International Edition in English. 1990;29(7):759-68.

10.   Altman S. Enzymatic cleavage of RNA by RNA. Bioscience reports. 1990;10(4):317-37.

11.	Gragoudas E. VEGF Inhibition Study in Ocular Neovascularization–1 (VISION–1): Efficacy Results From Phase II/III MacugenTM (Pegaptanib Sodium) Clinical Trials. Investigative Ophthalmology & Visual Science. 2004;45(13):2364-.

12.	Schwartz S. Anti-VEGF: Eyetech-Macugen. Data taken from presentation at. 2004.

13.	Fire A, Xu S, Montgomery MK, Kostas SA, Driver SE, Mello CC. Potent and specific genetic interference by double-stranded RNA in Caenorhabditis elegans. Nature. 1998;391(6669):806-11.

14.	Roehr B. Fomivirsen approved for CMV retinitis. Journal of the International Association of Physicians in AIDS Care. 1998;4(10):14.

15.	Stein CA, Castanotto D. FDA-Approved Oligonucleotide Therapies in 2017. Mol Ther. 2017;25(5):1069-75.

16.	Crooke ST, Geary RS. Clinical pharmacological properties of mipomersen (Kynamro), a second generation antisense inhibitor of apolipoprotein B. Br J Clin Pharmacol. 2013;76(2):269–76.

17.	Gales L. Tegsedi (Inotersen): An Antisense Oligonucleotide Approved for the Treatment of Adult Patients with Hereditary Transthyretin Amyloidosis. Pharmaceuticals. 2019;12(2):78.

18.	Garber K. Alnylam launches era of RNAi drugs. Nature Publishing Group; 2018.

19.	Scott LJ. Givosiran: First Approval. Drugs. 2020;80(3):335-9.

20.	Yin W, Rogge M. Targeting RNA: A Transformative Therapeutic Strategy. Clinical and Translational Science. 2019.

21.   Crooke ST. Molecular Mechanisms of Antisense Oligonucleotides. Nucleic Acid Ther. 2017;27(2):70-7.

22.   Rinaldi C, Wood MJA. Antisense oligonucleotides: the next frontier for treatment of neurological disorders. Nat Rev Neurol. 2018;14(1):9-21.

23.   Evers MM, Toonen LJA, Van Roon-Mom WMC. Antisense oligonucleotides in therapy for neurodegenerative disorders. Advanced Drug Delivery Reviews. 2015;87:90-103.

24.   Schoch KM, Miller TM. Antisense Oligonucleotides: Translation from Mouse Models to Human Neurodegenerative Diseases. Neuron. 2017;94(6):1056-70.

25.   Kole R, Krainer AR, Altman S. RNA therapeutics: beyond RNA interference and antisense oligonucleotides. Nat Rev Drug Discov. 2012;11(2):125–40.

26.   Havens MA, Hastings ML. Splice-switching antisense oligonucleotides as therapeutic drugs. Nucleic Acids Res. 2016;44(14):6549-63.

27.   Rand TA, Petersen S, Du F, Wang X. Argonaute2 Cleaves the Anti-Guide Strand of siRNA during RISC Activation. 2005;123(4):621-9.

28.   Kole R, Krieg AM. Exon skipping therapy for Duchenne muscular dystrophy. Advanced Drug Delivery Reviews. 2015;87:104–7.

29.   Mendell JR, Goemans N, Lowes LP, Alfano LN, Berry K, Shao J, et al. Longitudinal effect of eteplirsen versus historical control on ambulation in Duchenne muscular dystrophy. Ann Neurol. 2016;79(2):257–71.

30.   Jackson AL. Widespread siRNA "off-target" transcript silencing mediated by seed region sequence complementarity. RNA. 2006;12(7):1179-87.

31.   Watts J, Deleavey G, Damha M. Chemically modified siRNA: tools and applications. 2008;13(19-20):842-55.

32.   Santoro SW, Joyce GF. A general purpose RNA-cleaving DNA enzyme. Proc Natl Acad Sci. 1997;94(9):4262-6.

33.   Young DD, Lively MO, Deiters A. Activation and deactivation of DNAzyme and antisense function with light for the photochemical regulation of gene expression in mammalian cells. J Am Chem Soc. 2010;132(17):6183-93.

34.   Young DD, Lively MO, Deiters A. Activation and Deactivation of DNAzyme and Antisense Function with Light for the Photochemical Regulation of Gene Expression in Mammalian Cells. 2010;132(17):6183-93.

35.   Jimenez RM, Polanco JA, Lupták A. Chemistry and Biology of Self-Cleaving Ribozymes. 2015;40(11):648-61.

36.   Müller S. Special Issue: Ribozymes and RNA Catalysis. Molecules. 2017;22(5):789.

37.   Mello CC, Conte D. Revealing the world of RNA interference. Nature. 2004;431(7006):338-42.

38.   Elbashir SM, Harborth J, Lendeckel W, Yalcin A, Weber K, Tuschl T. Duplexes of 21-nucleotide RNAs mediate RNA interference in cultured mammalian cells. Nature. 2001;411(6836):494-8.

39.   Gantier MP. Processing of double-stranded RNA in mammalian cells: a direct antiviral role? Journal of Interferon & Cytokine Research. 2014;34(6):469-77.

40. Alterman JF, Godinho BM, Hassler MR, Ferguson CM, Echeverria D, Sapp E, et al. A divalent siRNA chemical scaffold for potent and sustained modulation of gene expression throughout the central nervous system. Nature Biotechnol. 2019;37(8):884-94.

41. Jackson AL, Bartz SR, Schelter J, Kobayashi SV, Burchard J, Mao M, et al. Expression profiling reveals off-target gene regulation by RNAi. 2003;21(6):635-7.

42. Birmingham A, Anderson EM, Reynolds A, Ilsley-Tyree D, Leake D, Fedorov Y, et al. 3′ UTR seed matches, but not overall identity, are associated with RNAi off-targets. 2006;3(3):199-204.

43. Doherty EA, Doudna JA. Ribozyme Structures and Mechanisms. 2001;30(1):457-75.

44. Kashani-Sabet M. Non-viral delivery of ribozymes for cancer gene therapy. 2004;4(11):1749-55.

45. Geary RS, Norris D, Yu R, Bennett CF. Pharmacokinetics, biodistribution and cell uptake of antisense oligonucleotides. Advanced Drug Delivery Reviews. 2015;87:46-51.

46. Li Y, Breaker RR. Phosphorylating DNA with DNA. 1999;96(6):2746-51.

47. Eckstein F. Phosphorothioates, essential components of therapeutic oligonucleotides. Nucleic Acid Ther. 2014;24(6):374-87.

48. Shen X, Corey DR. Chemistry, mechanism and clinical status of antisense oligonucleotides and duplex RNAs. Nucleic Acids Res. 2018;46(4):1584-600.

49. Wan WB, Seth PP. The medicinal chemistry of therapeutic oligonucleotides. J Med Chem. 2016;59(21):9645-67.

50.   Khvorova A, Watts JK. The chemical evolution of oligonucleotide therapies of clinical utility. Nature Biotechnol. 2017;35(3):238-48.

51.   Balke D, Müller S. Therapeutic Potential of Ribozymes. Advances in Nucleic Acid Therapeutics. 2019;68:434.

52.   Kashani-Sabet M. Ribozyme Therapeutics. 2002;7(1):76-8.

53.   Li Y, Liu Y, Breaker RR. Capping DNA with DNA. Biochemistry-Us. 2000;39(11):3106-14.

54.   Li J, Lu Y. A Highly Sensitive and Selective Catalytic DNA Biosensor for Lead Ions. J Am Chem Soc. 2000;122(42):10466-7.

55.   Tram K, Kanda P, Li Y. Lighting Up RNA-Cleaving DNAzymes for Biosensing. 2012;2012:1-8.

56.   Zhou W, Ding J, Liu J. Theranostic dnazymes. Theranostics. 2017;7(4):1010.

57.   Garn H, Renz H. GATA-3-specific DNAzyme - A novel approach for stratified asthma therapy. 2016.

58.   Krug N, Hohlfeld JM, Kirsten A-M, Kornmann O, Beeh KM, Kappeler D, et al. Allergen-Induced Asthmatic Responses Modified by a GATA3-Specific DNAzyme. N Engl J Med. 2015;372(21):1987-95.

59.   Cho E-A, Moloney FJ, Cai H, Au-Yeung A, China C, Scolyer RA, et al. Safety and tolerability of an intratumorally injected DNAzyme, Dz13, in patients with nodular basal-cell carcinoma: a phase 1 first-in-human trial (DISCOVER). 2013;381(9880):1835-43.

60.   Dingwall C, Ernberg I, Gait MJ, Green SM, Heaphy S, Karn J, et al. Human immunodeficiency virus 1 tat protein binds trans-activation-responsive region (TAR) RNA in vitro. Proc Natl Acad Sci. 1989;86(18):6925-9.

61.   Sullenger BA, Gallardo HF, Ungers GE, Gilboa E. Overexpression of TAR sequences renders cells resistant to human immunodeficiency virus replication. Cell. 1990;63(3):601-8.

62.   Ellington AD, Szostak JW. In vitro selection of RNA molecules that bind specific ligands. Nature. 1990;346(6287):818-22.

63.   Tuerk C, Gold L. Systematic evolution of ligands by exponential enrichment: RNA ligands to bacteriophage T4 DNA polymerase. science. 1990;249(4968):505-10.

64.   Ellington AD, Szostak JW. Selection in vitro of single-stranded DNA molecules that fold into specific ligand-binding structures. 1992;355(6363):850-2.

65.   Bock LC, Griffin LC, Latham JA, Vermaas EH, Toole JJ. Selection of single-stranded DNA molecules that bind and inhibit human thrombin. Nature. 1992;355(6360):564.

66.   Darmostuk M, Rimpelova S, Gbelcova H, Ruml T. Current approaches in SELEX: An update to aptamer selection technology. Biotechnology Advances. 2015;33(6):1141-61.

67.   Nimjee SM, White RR, Becker RC, Sullenger BA. Aptamers as Therapeutics. Annu Rev Pharmacol Toxicol. 2017;57(1):61-79.

68.   Lipi F, Chen S, Chakravarthy M, Rakesh S, Veedu RN. *In vitro* evolution of chemically-modified nucleic acid aptamers: pros and cons, and comprehensive selection strategies. RNA Biol. 2016;13(12):1232-45.

69.   Song K-M, Lee S, Ban C. Aptamers and Their Biological Applications. Sensors. 2012;12(1):612-31.

70.   Macugen Diabetic Retinopathy Study Group. Changes in retinal neovascularization after pegaptanib (Macugen) therapy in diabetic individuals. Ophthalmology. 2006;113(1):23–8.

71.   Kaur H, Bruno JG, Kumar A, Sharma TK. Aptamers in the therapeutics and diagnostics pipelines. Theranostics. 2018;8(15):4016.

72.   Wightman B, Ha I, Ruvkun G. Posttranscriptional regulation of the heterochronic gene lin-14 by lin-4 mediates temporal pattern formation in C. elegans. Cell. 1993;75(5):855-62.

73.   Lee RC, Feinbaum RL, Ambros V. The C. elegans heterochronic gene lin-4 encodes small RNAs with antisense complementarity to lin-14. Cell. 1993;75(5):843-54.

74.   Sridharan K, Gogtay NJ. Therapeutic nucleic acids: current clinical status. Br J Clin Pharmacol. 2016;82(3):659-72.

75.   Krützfeldt J. Strategies to use microRNAs as therapeutic targets. Best Practice & Research Clinical Endocrinology & Metabolism. 2016;30(5):551-61.

76.   Van Der Ree MH, Van Der Meer AJ, Van Nuenen AC, De Bruijne J, Ottosen S, Janssen HL, et al. Miravirsen dosing in chronic hepatitis C patients results in decreased microRNA-122 levels without affecting other microRNAs in plasma. 2016;43(1):102-13.

77.   Van Der Ree MH, De Vree JM, Stelma F, Willemse S, Van Der Valk M, Rietdijk S, et al. Safety, tolerability, and antiviral effect of RG-101 in patients with chronic hepatitis C: a phase 1B, double-blind, randomised controlled trial. 2017.

78.   Beg MS, Brenner AJ, Sachdev J, Borad M, Kang Y-K, Stoudemire J, et al. Phase I study of MRX34, a liposomal miR-34a mimic, administered twice weekly in patients with advanced solid tumors. Investigational new drugs. 2017;35(2):180-8.

79. Chakravarthy M, Chen S, Dodd PR, Veedu RN. Nucleic acid-based theranostics for tackling Alzheimer's Disease. Theranostics. 2017;7(16):3933.

80. Bayik D, Gursel I, Klinman DM. Structure, mechanism and therapeutic utility of immunosuppressive oligonucleotides. Pharmacological research. 2016;105:216-25.

81. Geary RS, Norris D, Yu R, Bennett CF. Pharmacokinetics, biodistribution and cell uptake of antisense oligonucleotides. 2015;87:46-51.

82. Smith CIE, Zain R. Therapeutic Oligonucleotides: State of the Art. Annu Rev Pharmacol Toxicol. 2019;59(1):605-30.

83. John, John. RNA-Based Therapeutics: Current Progress and Future Prospects. Chemistry & Biology. 2012;19(1):60-71.

84. Wolfrum C, Shi S, Jayaprakash KN, Jayaraman M, Wang G, Pandey RK, et al. Mechanisms and optimization of in vivo delivery of lipophilic siRNAs. 2007;25(10):1149-57.

85. Yu B, Zhao X, Lee LJ, Lee RJ. Targeted Delivery Systems for Oligonucleotide Therapeutics. 2009;11(1):195-203.

86. Nishina T, Numata J, Nishina K, Yoshida-Tanaka K, Nitta K, Piao W, et al. Chimeric Antisense Oligonucleotide Conjugated to α-Tocopherol. 2015;4(1):e220.

87. Crooke ST, Wang S, Vickers TA, Shen W, Liang X-H. Cellular uptake and trafficking of antisense oligonucleotides. Nature Biotechnol. 2017;35(3):230-7.

88. Bochicchio S, Dalmoro A, Angela Barba A, Grassi G, Lamberti G. Liposomes as siRNA delivery vectors. Current drug metabolism. 2014;15(9):882-92.

89. Hoy SM. Patisiran: first global approval. Drugs. 2018;78(15):1625-31.

90.   Juliano RL. The delivery of therapeutic oligonucleotides. Nucleic Acids Res. 2016;44(14):6518-48.

91.   Schiffelers RM, Ansari A, Xu J, Zhou Q, Tang Q, Storm G, et al. Cancer siRNA therapy by tumor selective delivery with ligand-targeted sterically stabilized nanoparticle. Nucleic Acids Res. 2004;32(19):e149-e.

92.   Dong Y, Love KT, Dorkin JR, Sirirungruang S, Zhang Y, Chen D, et al. Lipopeptide nanoparticles for potent and selective siRNA delivery in rodents and nonhuman primates. Proc Natl Acad Sci. 2014;111(11):3955-60.

93.   Leonetti JP, Degols G, Lebleu B. Biological activity of oligonucleotide-poly (L-lysine) conjugates: mechanism of cell uptake. Bioconjugate chemistry. 1990;1(2):149-53.

94.   Lee H, Lytton-Jean AK, Chen Y, Love KT, Park AI, Karagiannis ED, et al. Molecularly self-assembled nucleic acid nanoparticles for targeted in vivo siRNA delivery. Nature nanotechnology. 2012;7(6):389.

95.   Harding JA, Engbers CM, Newman MS, Goldstein NI, Zalipsky S. Immunogenicity and pharmacokinetic attributes of poly (ethylene glycol)-grafted immunoliposomes. Biochim Biophys Acta. 1997;1327(2):181-92.

96.   Lee SH, Castagner B, Leroux J-C. Is there a future for cell-penetrating peptides in oligonucleotide delivery? 2013;85(1):5-11.

97.   Margus H, Padari K, Pooga M. Cell-penetrating Peptides as Versatile Vehicles for Oligonucleotide Delivery. 2012;20(3):525-33.

98.   Chen M, Zakrewsky M, Gupta V, Anselmo AC, Slee DH, Muraski JA, et al. Topical delivery of siRNA into skin using SPACE-peptide carriers. 2014;179:33-41.

99.	McNamara II JO, Andrechek ER, Wang Y, Viles KD, Rempel RE, Gilboa E, et al. Cell type–specific delivery of siRNAs with aptamer-siRNA chimeras. Nature Biotechnol. 2006;24(8):1005.

Chapter 2 Developing novel DNAzymes targeting Integrin alpha-4 RNA transcript as a potential molecule to reduce inflammation in multiple sclerosis

2.1 Introduction

Multiple sclerosis (MS) is a chronic inflammatory neurological disease that results in demyelination of the axons in the central nervous system (CNS). Multiple sclerosis (MS) affects over 25000 Australians and more than 2 million people worldwide. Multiple sclerosis (MS) is three times more prevalent in women than men. Multiple Sclerosis (MS) mostly affects people between the ages of 20-40 years and is the leading cause of disability in young adults. As MS predominantly affects young adults at the peak of their active life, this condition places an enormous psychological, physical and financial burden on the patients and their families and reduces life expectancy by around seven years.

There is no single test to diagnose MS that is often made after a combination of clinical tests including an magnetic resonance imaging (MRI) scan to observe areas of scarring, inflammation in the brain and spinal cord, and a clinical exam to look for characteristic symptoms. Multiple sclerosis (MS) patients exhibit different clinical symptoms such as: motor symptoms (muscular spasms, limb weakness and problems with balance, coordination and mobility); fatigue and heat

sensitivity; other neurological symptoms (loss of vision or vision disturbances, vertigo, sensory changes including pins and needles, tingling and numbness, neuralgia and cognitive dysfunction); continence problems (lack of bladder control and constipation); and neuropsychological symptoms (anxiety, depression and difficulties sleeping, cognitive difficulties, impaired memory and concentration, changes in processing speed and ability, impaired cognitive function and memory loss) (1). Diagnosis is confirmed when there have been two or more attacks each lasting a minimum of 24 hours at least one month apart. In addition, diagnosis requires MRI or electrophysiological testing showing central nervous system (CNS) damage in more than one area. Currently, there is no cure for MS, however, United States of America (US) Food and Drug Administration (FDA) have approved several treatments that slow the disease progression and help manage disease symptoms that are discussed later.

The course of MS differs widely between each individual, however, it tends to take one of the following three courses: relapsing-remitting MS, secondary progressive MS, and primary progressive MS. Relapsing-remitting is the most common form of MS affecting 70-75% of diagnosed patients initially and is characterised by partial or total recovery after attacks. More than 50% of people with relapsing-remitting MS go on to develop the secondary progressive form within 10 years and 90% within 25 years. The secondary progressive form is characterised by continual attacks, partial recoveries and a steady increase in permanent neurological disability. The primary progressive form affects 15% of people diagnosed with MS and is characterised by no recovery from the attacks and steady neurological function decline from onset without recovery. Primary progressive MS is diagnosed when a person has been living with MS for a long period of time and shows progressive disability rather than acute attacks.

2.1.1 Pathobiology of MS

There is no known cause for the disease, although a combination of environmental and genetic factors have been identified to increase or decrease the risk of disease. The role of environmental and genetic factors in MS has been discussed in detail in many reviews and therefore will only be briefly mentioned here.

Environmental exposures before adolescence may have a role in determining your risk of developing MS later on in life. Some of the environmental factors that have been shown to have a protective role in MS include lower latitudes, increased UV exposure and Vitamin D (2). Furthermore, evidence suggesting that exposure to pathogens early in life can also be protective against developing immune-mediated diseases such as MS gave rise to the 'hygiene hypothesis' (3, 4). The type of gut microbiota and its distribution may also affect the risk and course of MS (2). Lastly, increase in smoking, obesity and shift work has been linked to increased MS risk during adolescence (2).

The relative risk of a sibling with MS is increased by 7 fold, indicating the importance of genetic factors in MS (2). Genetic variations in the HLA complex code for immunoregulatory gene products, can confer risk or have a protective role in MS (2). Genome-wide association studies (GWAS) have identified 110 non-HLA single nucleotide polymorphisms that confer a risk for MS (2). For example, polymorphisms close to a central vitamin D metabolism gene *CYP27B1*, is associated with increased MS risk (2).

The presence of the environmental and genetic risk factors discusses above may confer risk alone, however, the interaction of the environmental and genetic risk factors confer a greater risk for MS. For example, the presence of HLA variant *HLA-DRB1*15:01* increases the MS risk by three times, the lack of HLA variant *HLA-A*02* increases the risk by 1.8 times, however, having the first HLA

variant and not the second HLA variant increases the risk by five times in non-smokers (2). Smoking increases MS risk further by 14 times (2). Similarly, obese individuals that have HLA variant *HLA-DRB1*15:01* and lack variant *HLA-A*02* also have 14 times increased MS risk (2). The interaction between smoking and a non-HLA gene variant *NAT1* has also been observed (2).

2.1.2 Pathobiology

Multiple sclerosis (MS) is a complex disease that may be caused by the accumulation of multiple risk factors, although the cause is unknown, the pathobiology is well understood. The pathobiology of MS has been largely attributed to immune system dysregulation or dysfunction and compromised blood-brain barrier (BBB).

In MS, dendritic cells and other antigen-presenting cells are activated by the recognition of self- or myelin antigens. The dendritic cells release various cytokines to communicate with the naïve CD4+ T cells, polarising the memory T cells into differentiated T helper 1 (Th1) and Th17 cells (5). CD4+ T cells differentiate into interferon-γ secreting Th1 cells in the presence of interleukin (IL)-12, while they differentiate into IL-17 secreting Th-17 cells in the presence of IL-23 (5). Under normal physiological conditions, the Th1 cells and Th17 cells are defence mechanisms against intracellular pathogens and fungal infections respectively, however, these pro-inflammatory cytokines have a deleterious effect in autoimmune diseases like MS (5). In MS, the myelin antigens activate the T lymphocytes in the lymph node, that produce pro-inflammatory cytokines to mediate their toxic effects by producing matrix metalloproteinases and radical oxygen species, increasing the blood-brain barrier (BBB) permeability for T lymphocytes into the CNS (5, 6).

Myelin peptide mimics can compete with the native peptide to protect against induction of experimental autoimmune encephalomyelitis (EAE) in mouse models (6). In MS patients, myelin-

specific T cells are active and show increased production of pro-inflammatory cytokines, including IL-2, IFN-γ and tumor necrosis factor (TNF) (6). Injection of an altered myelin peptide in clinical trials, resulted in increased Th1 responses and new inflammatory lesions in the CNS, causing relapses (6). Reducing the expression or knocking down IL-23 and IL-17 results in suppressed disease activity in animal models of MS supporting the role of Th17 cells (5). Furthermore, increased Th17 cells were observed in the peripheral blood of MS patients (5).

The activated memory T cells cross the BBB and penetrate the CNS, where they are reactivated by myelin presenting antigen-presenting cells, including macrophages, microglia, dendritic and B cells, thereby inducing an inflammatory response (5, 6). The reactivated T-cells, and activated macrophages and microglia release pro-inflammatory factors, and produce oxygen and nitric oxide radicals, leading to demyelination and axonal loss (5, 6).

Studies show that the other immune cells also have a role in MS including microglia, astrocytes, natural killer cells and B cells. The exact role of microglia and its interaction with T cells are not well understood, however, increased levels of activated microglia in MS lesions and in CNS of MS patients has been observed (6). Furthermore, in EAE models, the increased levels of activated microglia precedes infiltration of macrophages and T cells into the CNS (6). Microglia can also activate the naïve T cells by secretion of specific cytokines to enable their differentiation into Th1 or Th17 subsets (6). The crosstalk between the microglia and T cells can be beneficial by the promotion of an anti-inflammatory response or deleterious by sustaining an inflammatory response (6).

The B cells also have a role in MS, where B cells produce antibodies and autoantibodies against antigens resulting in demyelination and axonal damage in MS (5). B cells can be reactivated in the CNS and contribute to myelin damage by inducing complement-mediated damage to myelin and

reactivating the T cells (5). B cells can also activate the microglia, causing damage to neurons and loss of dendrite density (5). B cells, can both be beneficial or deleterious depending on the cytokines produced, by either increasing activation of macrophages and T cells or producing cytokines that may be protective (5).

Astrocytes can produce and secrete cytokines and chemokines, which can alter T cell responses and contribute to CNS inflammation and neurodegeneration (6). Astrocytes can also control the infiltration of the pro-inflammatory leukocytes into the CNS and regulate the activation of microglia, oligodendrocytes and other cells from the adaptive immune system (5). Natural killer cells could have a role in MS by stimulating antigen-presenting cell maturation and cytokine production (5).

2.1.3 Blood-brain barrier (BBB) and its role in MS

The BBB plays an important role in MS by restricting migration of cells from the periphery to the CNS under normal physiological conditions (6). However, in MS there is a huge infiltration of the pro-inflammatory leukocytes early in the disease (6). The migration of the immune cells from the periphery to the CNS is called extravasation, that involves key steps including capture/rolling, activation, firm adhesion, crawling and diapedesis/transmigration (6). Activated T cells have the ability to cross the BBB and increase its permeability due to the expression of key molecules such as chemokine receptors, adhesion molecules, integrins, cytokines, matrix metalloproteinases and reactive oxygen species (6). The transmigration of the leukocytes across the BBB invovels interaction between adhesion molecules expressed by the endothelial cells of the BBB and their ligands expressed by the activated leukocytes (6). The cytokines increase the expression of the adhesion molecules such as the intracellular cell adhesion molecule-1 (ICAM-1), vascular adhesion molecule-1 (VCAM1)/ Integrin alpha-4 (ITGA4), activated leukocyte cell adhesion

molecule and melanoma cell adhesion molecule (6). Two treatments for MS, Natalizumab and Efalizumab (discussed further in section 2.1.4) prevent migration of the immune cells into the CNS by blocking the cell adhesion molecules on the endothelial cells of the BBB, thereby preventing myelin degeneration and axonal damage (Figure 2.1) (6). The BBB and the migration of cells across the BBB have an important role in the treatment strategies for MS (6). Chemokines produced by the CNS derived cells can also influence the migration of cells across the BBB including activated T cells (6).
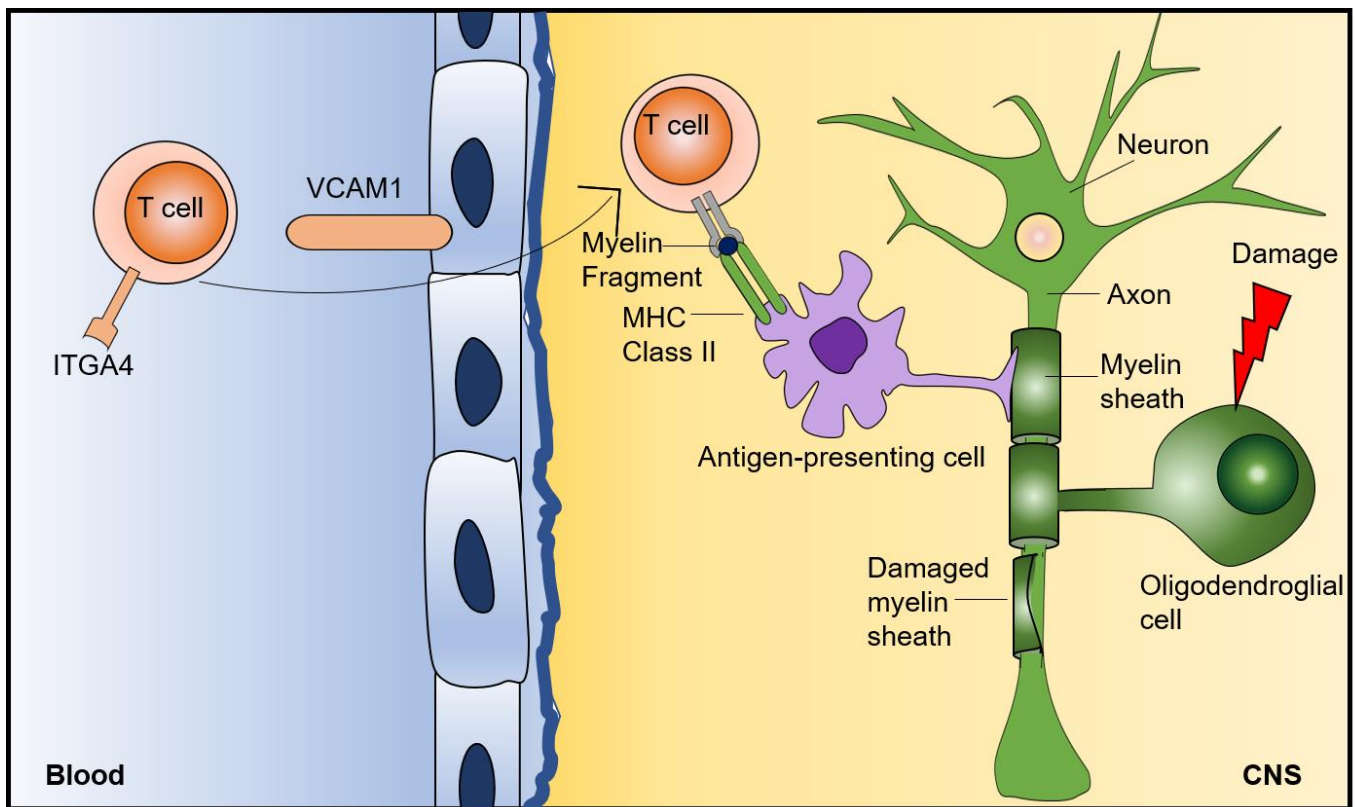
Figure 2.1   Schematic representing the migration of T cells across the BBB resulting in degradation of the myelin sheath. Adapted from Noseworthy et al (2005) (7). ITGA4: Integrin alpha-4; VCAM1: Vascular cell adhesion molecule; MHC: major histocompatibility complex; CNS: central nervous system; BBB: blood-brain barrier

2.1.4 Current treatments for MS

Treatments for MS can be categorised into relapse treatments, treatments that slow down disease progression, and treatments that help manage symptoms. There are many treatments that slow

progression of the relapsing-remitting MS and occasionally secondary progressive MS but no drug has been approved for the treatment of primary progressive MS. Treatments that slow progression of the relapsing-remitting MS can be categorised into two approaches, induction therapy and escalation therapy. In induction therapy, immunosuppressant drugs are used as first line of therapy and are followed by use of immunomodulatory agents for long-term maintenance of treatment (8). The escalation therapy approach uses disease modifying drugs like beta interferon, glatiramer acetate, teriflunomide and dimethyl fumarate as first life of treatment and if these disease modifying drugs are ineffective or only partially effective, a second line of more aggressive drugs like mitoxantrone, natalizumab and fingolimod are used (8).

Multiple sclerosis (MS) patients are initially treated with basic therapeutics; including immunomodulators, interferon beta (IFN-β) and glatiramer acetate, first approved in 1995, and are administered as injections (9). The immunomodulators reduce the annual relapse rate by 30% and do not cause any severe side effects, although in some patients, they cause reactions at the site of injection while some develop neutralising antibodies that tends to reduce or abolish the therapeutic effect of the drug (9). An anti-inflammatory response is induced by glatiramer acetate, a mixture of short polypeptides of varying lengths of four amino acids, by proliferation and activation of glatiramer acetate specific lymphocytes and IFN-β, a cytokine (9).

Alemtuzumab, is a humanised monoclonal antibody developed against CD52 that is found on the surface of lymphocytes and monocytes (9, 10). Treatment of Alemtuzumab, resulted in reduced B and T cells, reduced annual relapse rates and worsening of the disease than the IFN-β-1a treatment (9, 10). The most frequent adverse effects are infusion reactions, and in some patients, the development of herpetic and fungal infections (9, 10). There is a risk of developing autoimmune

disorders including thyroid disorders in 30% of the patients, immune thrombocytopenia in 1-3% of patients and glomerulonephritis in 0.3% of the patients (9, 10).

Teriflunomide is a dihydroorotate dehydrogenase inhibitor that suppresses the proliferation of autoreactive B and T cells causing a shift from a pro-inflammatory to an anti-inflammatory cytokine profile (9, 10). Teriflunomide reduces annual relapse rate and has a similar efficacy to IFN-β (9, 10). Adverse side effects include headache, diarrhea, hair thinning, increased liver enzymes, nausea and in rare cases, peripheral neuropathy (9, 10). The treatment should be constantly monitored due to the risk of hepatic failure, serum transaminase and bilirubin (9, 10).

Dimethyl fumarate has a dual anti-oxidant and anti-inflammatory effect through activation of transcription factor E2 related factor and inhibition of transcription factor nuclear factor κB respectively. Subsequently, there is a reduction in the release of inflammatory cytokines and migration of the inflammatory cells through the BBB (9, 10). The drug reduces the relapse rates and delays disease progression, but side effects are flushing and gastrointestinal symptoms, and development of multiple leukoencephalopathy in a few patients (9, 10).

When first-line of treatments fail, more aggressive therapies are administered, one of which is an immunomodulatory and immunosuppressive oral drug, Fingolimod (9, 10). Fingolimod binds to sphingosine-1-phosphate receptors and inhibits release of B and T cells from the lymph nodes, reducing the annual relapse rate by 54% compared to placebo and 52% compared to IFN-β-1a (9, 10). The side effects include transient cardiac arrhythmias at start of therapy, macular edema within six months of start of therapy and in some cases serious cardiac side effects (9, 10).

Another immunosuppressive therapeutic that may be used either as an induction or escalation therapeutic treatment is Mitoxantrone (9, 10). Mitoxantrone can be administered for worsening of

relapsing-remitting MS or secondary progressive MS (9, 10). However, this treatment does pose a risk of cardiac toxicity and side-effects includes risk of acute leukemia (9, 10).

Natalizumab, another escalation therapeutic, is a humanized monoclonal anti integrin alpha-4 (ITGA4) antibody, that is a component of the very late antigen-4 present on lymphocytes (9, 10). Natalizumab inhibits ITGA4's interaction with the VCAM found on the endothelial cells of the BBB, thereby preventing leukocytes from migrating across the BBB (9, 10). Natalizumab reduces the annual relapse rate by 68%; however, the treatment results in severe side effects including progressive multifocal leukoencephalopathy and the presence of neutralising antibodies was found in 6% of patients (9, 10).

Daclizumab, another monoclonal antibody, against IL2 decreases the annual relapse rate by 45% compared to IFN-β-1a, however did not slow down progression of MS (9, 10). Orelizumab, a humanised monoclonal antibody, developed against CD20, is in phase III clinical trials for treatment of remitting-relapsing MS patients (9, 10). Ocrelizumab reduces annual relapse rate by 46% and disease progression by 40% compared to IFN-β-1a (9, 10).

MS patients may also be treated symptomatically for other neurological symptoms, including fatigue, depression, spasticity, tremor, ataxia, seizures, pain and sleep disorders to name a few. Treatment and management of these symptoms can help improve the quality of life of MS patients (1).

Table 2.1   Summary of the treatment strategies for multiple sclerosis, the target of the treatment strategies, their outcomes and adverse effects.

Treatment Strategy	Target	Outcomes	Adverse Effects
Interferon beta/ Glatiramer acetate	• Proliferation and activation of interferon beta • Proliferation and activation of glatiramer	• Reduce annual relapse rate by 30%	• Cause reaction at site of injection • Some develop neutralizing antibodies that tends to reduce or

Treatment Strategy	Target	Outcomes	Adverse Effects
	acetate specific lymphocytes		abolish therapeutic effect of drug • Infusion reactions • Development herpetic and fungal infections in some patients
Alemtuzumab	• Monoclonal antibody against CD52 found on surface of lymphocytes and monocytes • Reduced B and T cells	• Reduced annual relapse rates • Reduced worsening of the disease	• Risk of developing thyroid disorders in 30% of patients, immune thrombocytopenia in 1-3% of patients and glomerulonephritis in 0.3% of the patients.
Teriflunomide	• Dihydroorotate dehydrogenase inhibitor • Suppresses proliferation of autoreactive B and T cells	• Reduces annual relapse rate similar to IFN-β	• Headache, diarrhea, hair thinning, increased liver enzymes, nausea and in rare cases peripheral neuropathy. • Risk of hepatic failure, serum transaminase and bilirubin.
Dimethyl fumarate	• Anti-oxidant and anti-inflammatory effect. Activates transcription factor E2 related factor • Inhibits transcription factor nuclear factor κB	• Reduction in release of inflammatory cytokines and migration of the inflammatory cells through the blood brain barrier • Reduces relapse rates • Delays disease progression	• Flushing • Gastrointestinal symptoms • Development of multiple leukoencephalopathy in a few patients.
Fingolimod	• Binds to sphingosine-1-phosphate receptors • Inhibits release of B and T cells from lymph nodes	• Reduces annual relapse rate by 54% compared to placebo and 52% compared to IFN-β	• Transient cardiac arrhythmias at start of therapy • Macular edema within six months of start of therapy • Serious cardiac side effects in some cases.
Mitoxantrone	• Immunosuppressive	• Recues worsening of relapsing-remitting MS or secondary progressive MS	• Poses a risk of cardiac toxicity • Risk of acute leukemia
Natalizumab	• Monoclonal anti ITGA4 antibody • Inhibits ITGA4's interaction with VCAM found on endothelial	• Reduces annual relapse rate by 68%	• Risk of progressive multiple leukoencephalopathy • Presence of neutralising antibodies in 6% of patients.

Treatment Strategy	Target	Outcomes	Adverse Effects
	cells of the blood-brain barrier		
	• Prevents leukocytes from migrating across the blood-brain barrier.		
Daclizumab	• Monoclonal antibody against IL2	• Decreases annual relapse rate by 45% compared to IFN-β-1a	• Did not slow down progression of MS
		• Reduces annual relapse rate by 46% compared to IFN-β-1a.	
Orelizumab	• Humanised monoclonal antibody against CD20	• Reduces disease progression by 40% compared to IFN-β-1a.	

2.1.5 Disadvantages of monoclonal antibodies as treatment strategies

Many humanised monoclonal antibodies are used as treatment strategies for MS, and a major disadvantages are their limits of targets (11). Antibodies can only be targeted against protein targets, but not miRNA, transcription factors and other junk DNA, that also have an important role in disease (11). Furthermore, antibodies can only target proteins expressed on the cell surface of the host cells or invading pathogens, although developing intrabodies or antibodies that can target the proteins inside the cells is now possible, its therapeutic potential is unknown (11).

Monoclonal antibodies are large (150 kDa), multimeric proteins containing numerous disulphide bonds and post-translational modifications such as glycosylation, therefore, producing the active form of the antibody requires sophisticated eukaryotic machinery. Furthermore, large amounts of antibodies are needed to achieve clinical efficacy that requires large cultures of mammalian cells and extensive purification steps, leading to high production costs, limiting their use to serious medical conditions (12). The large molecular size of the antibodies mean that they cannot easily penetrate tissue or tumours (only around 20% of the administered dose) to have a therapeutic effect

(12). Therefore, the limited efficacy of antibody-based therapy cannot justify the high production costs.

Antibodies are potentially immunogenic and occasionally result in producing an anti-drug antibody response, leading to a major safety issue and reducing the therapeutic benefit in patients (13). Furthermore, antibodies can cause rare but serious adverse events like multifocal leukoencephalopathy with the treatment of Natalizumab, which led to two deaths out of 5000 patients (11). Antibodies are also at risk of degradation during the manufacturing and storage stages, as well as *in vivo,* that cannot be controlled adequately (14). The degradation may affect antigen recognition, reduce its function and in severe cases, lead to immunogenic responses (14). Antibodies are denatured and/or proteolysed in the gut and are not orally bioavailable (13). Antibodies have a poor ability to penetrate the BBB and therefore, are poorly suited for the treatment of chronic neurodegenerative diseases or tumours that originate or have metastasised to the brain (13).

2.1.6 Nucleic Acid Technologies as Treatment Strategies

The major advantage of nucleic acid technologies as therapeutics over antibodies, is their ability to selectively target the undruggable human and viral genomes, upregulate or downregulate gene expression, alter mRNA splicing, target trinucleotide repeats disorders and target non-coding RNAs, to modulate gene expression. RNA based therapeutics can also evolve with cancer or pandemic influenza, (15). With the FDA approval of many nucleic acid therapeutics in recent years, nucleic acids are becoming attractive therapeutic strategies.

2.1.6.1 Nucleic Acid technology for the treatment of MS

Myers *et al*. (2005) reported a 20-mer PS oligonucleotide gapmer containing 2'-OMOE modifications (ISIS 17044) that binds at the 3' end of the translation initiation codon of mouse

Itga4 mRNA (16). ISIS 17044 reduced the *Itga4* mRNA expression as well as the cell surface expression of ITGA4 in bEND.3 cells dose-dependently (16). At a concentration of 100 nM, ISIS 17044 reduced the mRNA expression by 98% and cell surface expression by 75% compared to the scrambled (SCR) control (16). Furthermore, with the reduction in ITGA4 expression, there were no alterations in the expression of other cell adhesion molecules expressed by bEND.3 cells, including platelet and endothelial cell adhesion molecule (PECAM-1), and TNF-induced decreases in ICAM-1 or VCAM-1 (16). ISIS 17044 had similar inhibitory effects on the *Itga4* mRNA in IC-21 cells, a macrophage-like cell line with an IC-50 of 2 nM (16). In primary CSJLF1 mouse lymph node cells and splenocytes from DBA mice, a dose-dependent reduction in ITGA4 levels were seen by flow cytometry in both the unfractionated lymph node cells and in T cell subpopulations (16). In an experimental autoimmune encephalomyelitis (EAE) mouse model, treatment of ISIS 17044 prevented or ameliorated paralysis when given as a prophylactic and reduced disease severity when given as a therapeutic drug (16). Immunohistochemical staining of the spinal cord tissue from these mice indicated reduced T cell and macrophage trafficking and reduced ITGA4 expressing cells (16). The oligonucleotides were present in the CNS white matter, even though it has been previously shown that the AOs do not cross the BBB in healthy mice,and this may be due to the disruption of the BBB in the EAE mouse model (16). However, the AOs that reduce ITGA4 levels and prevent the immune cells from migrating to the CNS do not need to enter the BBB to modulate disease (16).

Recently, a splice modulating AO has been reported by Aung-Htut *et al.* (2019) to downregulate ITGA4 in human dermal fibroblasts and Jurkat cells (17). AOs with a 2'-OMePS and a PMO chemistry were effective in inducing exon-skipping of the *ITGA4* transcript and resulted in downregulation of the ITGA4 protein in human dermal fibroblasts and Jurkat cells (17). The most

efficient AO targeted exon 4 and was tested in an EAE mouse model using peptide conjugated PMO (PPMO) chemistry, resulting in delaying disease progression (17).

Nerve growth factor levels were increased in stress and inflammation in the cerebrospinal fluid (CSF) of MS patients (18). Nerve growth factor signalling transduction pathways control the activation of integrins on the leukocytes and subsequent transmigration of the inflammatory cells into the brain through the TrkA/p75 heterodimer (18).A growth factor receptor, p75, that binds to the nerve growth factor, had increased expression on endothelial and perivascular cells in the CNS of EAE. Soilu-Hanninen *et al.* (2000) induced EAE in mice using myelin proteolipid protein (PLP)-peptide, resulting in upregulation of p75 in the CNS (18). A PS AO against p75 resulted in downregulating *p75* mRNA and protein levels by 30% and attenuation of EAE (18). The AO treatment did not induce a nonspecific immunostimulatory response, however, there were two cases of liver abscesses that were only in the AO treated mice (18).

IL-23 is a heterodimeric cytokine comprising of a p19 subunit that associates with the IL-12/23p40 subunit expressed in activated dendritic cells and phagocytic cells (19). Functional IL-23 is required for inducing EAE in mice; and dendritic cells from MS patients had increased levels of *IL-23* and *IL-23p19* mRNA (19). Inhibition of the *IL-23p19* mRNA by AOs resulted in decreased levels of IL-23, IL-12 and TNF-α production (19). Decreased IL-23 expression increased IL-10 production, which may inhibit T cell proliferation or decrease IL-12 (19). In secondary progressive MS patients, IL-12 levels are increased and reduced IL-10 production is associated with increased severity of MS (19).

The dysregulated inflammatory response in MS is mediated by TNF- α and associated neuronal apoptosis (20). Kim *et al.* (2010) developed a siRNA to reduce TNF-α expression by targeted delivery of the siRNAs to TNF-α expressing macrophages and microglial cell (20). Targeted

delivery was achieved by conjugating an acetylcholine receptor binding peptide fused to non-D-arginine residues, that can bind to and deliver siRNAs to macrophage and microglial cells (20). The siRNA silenced the expression of liposaccharide-induced TNF-α expression *in vitro* and *in vivo* accompanied by reduced neuronal apoptosis (20).

2.1.6.2 DNAzymes as a therapeutic strategy

The advantage of DNAzymes over other nucleic acid technologies, including RNAi technology and AOs is their ability to turn over, capability to cleave mRNA independently of endogenous nucleases and cellular machinery unlike siRNAs and RNAse H AOs (Figure 1.4) (21). DNAzymes also have several advantages over natural protein-based enzymes. The production of foreign protein-based enzymes requires fermentation and high costs, the products are easily contaminated and can elicit immune responses (21). Proteins are difficult to label at specific sites making *in situ* production of signal quite challenging , however, DNAzymes are easily modified and can be labelled easily with very low immunogenicity (21). DNAzymes can be conjugated to various nanomaterials for signalling and delivery and are more stable and cost-effective than RNA and proteins (21).

2.1.6.3 DNAzymes in clinical trials:

The potential of DNAzymes as a therapeutic strategy has been realised through their pre-clinical success and positive results in clinical trials. SB010 is a DNAzyme that cleaves *GATA3* mRNA and has shown positive results in phase IIa clinical trials (22, 23). GATA3 is a transcription factor essential for Th2-cell differentiation and activation (22, 23). An Th2 driven immune response has been implicated in allergic bronchial asthma, an inflammatory disease of the airways, where there is dysregulation of the innate and adaptive immune system (22, 23). GATA3 is overexpressed in asthma patient bronchoalveolar lavage and lung biopsies, even those undergoing treatment,

emphasizing the need for better therapeutics (22, 23). In Phase IIa clinical trial, SB010 reduced both late and early asthmatic responses and Th2- regulated inflammatory responses to allergens in patients with allergic asthma (22, 23). Sterna Biologicals is now preparing for conducting Phase IIb clinical trials.

The DNAzyme Dz1 in phase I/II clinical trials, targeted Epstein-Barr virus (EBV) *LMP1* mRNA to treat nasopharyngeal carcinoma in combination with radiotherapy. Dz1 was given to 40 nasopharyngeal carcinoma patients and showed a higher tumour regression at week 12 and impacted tumour microvascular permeability as shown by molecular imaging analysis. The Dz1-treated group had a higher number of samples with an undetectable level of EBV DNA copies, and DZ1 was considered safe.

The two DNAzymes in clinical trials have demonstrated the impact of DNAzymes as potential therapeutic strategies. DNAzymes are unique and have distinct advantages over other protein-based enzymes, other nucleic acid technologies and antibodies. The use of the antibody Natalizumab against ITGA4 in treatment of MS has shown the importance of ITGA4 as a validated target for MS. However, Natalizumab, a monoclonal antibody has severe adverse effects and therefore there is need for better therapeutic strategies that minimise the adverse effects. DNAzymes targeting ITGA4 may be a good therapeutic strategy for tackling MS. DNAzymes, unlike antibodies will not induce production of neutralizing antibodies. Use of DNAzymes as therapeutics to target ITGA4 rather than antibodies like Natalizumab may result in patients not developing multifocal encephalopathy in those rare cases although this would have to be validated.

2.2 Aim

To develop novel chemically modified DNAzymes targeting *ITGA4* RNA transcript as a potential molecule to reduce inflammation in MS

2.3 Methods

2.3.1 DNAzyme design and synthesis

DNAzymes with either stem loop or hammer head conformation were designed for the selected exons (exon map shown in Figure 2.2) and the oligonucleotides (sequences given in Figure 2B) were ordered from Integrated DNA Technologies (IDT). The locked nucleic acid (LNA)-modified DNAzyme was made in-house by ABI Expedite™ 8909 (Applied Biosystems, Foster City, CA, USA) oligonucleotide synthesiser system in 1 µM scale. The synthesised oligonucleotides were deprotected by treatment with 1 mL Ammonium Hydroxide (Sigma; Cat# 221228-500Ml, Castle Hill, NSW, Australia overnight at 55 °C. The oligonucleotides were then purified and desalted using illustra NAP-10 columns (GE Healthcare; Cat# 45-000-153, Springfield, QLD, Australia) according to the manufacturer's protocol.
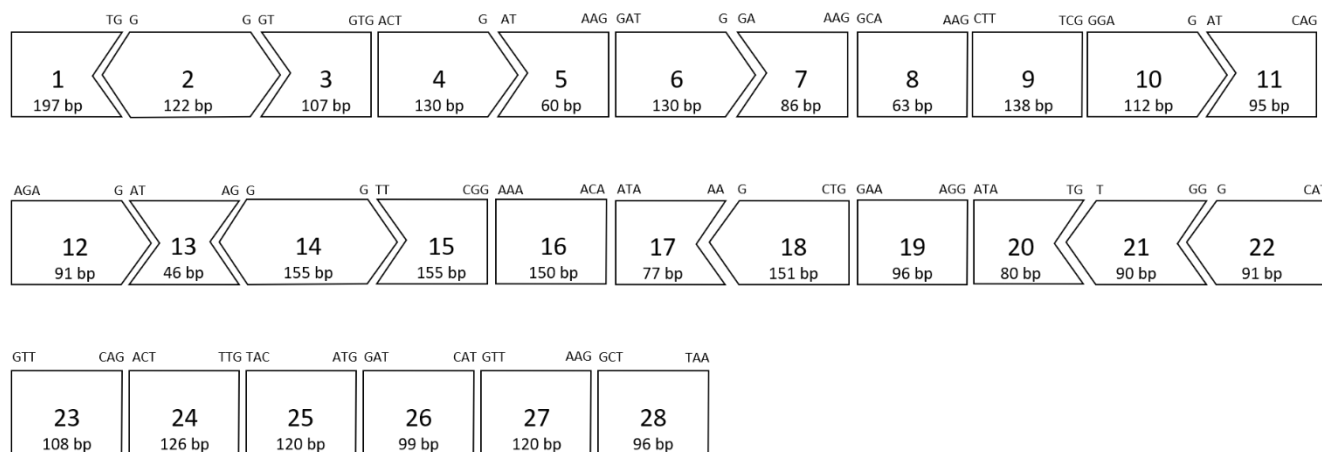
Figure 2.2   Exon map of ITGA4.

2.3.2 Cell propagation and transfection

Normal primary human fibroblasts from muscle biopsies were kindly provided by Prof. Sue Fletcher. Cell culture media and supplements were purchased from (Life technologies, Australia) unless specified. Normal human fibroblasts were propagated in Dulbecco's modified Eagle's medium (DMEM) (Thermofisher Scientific; Cat # 11995073) supplemented with GlutaMAX™ (Thermofisher Scientific; Cat #: 35050061) and 10% fetal bovine serum (FBS) (Serana; Cat # FBS-AU-015). Transfections were performed in 24 well-plate format with approximately 15,000 cells/well. The cells were seeded one day before transfecting with the DNAzymes complexed with Lipofectamine 3000® transfection reagent (Thermofisher Scientific; Cat # L3000015) per the manufacturer's protocol. Transfection was carried out for 24 hours before harvesting RNA for transcript analysis. RNA was extracted using Direct-zol RNA MiniPrep Kit (Zymo Research; Cat: R2051) following manufacturer's protocol.

2.3.3 RT-PCR assays

50 ng of total RNA was analysed using a Superscript III One-Step RT-PCR System (Thermofisher Scientific; Cat #: 12574026) and reaction conditions are as follows: 55°C for 30 min, 94°C for 2 min, 28 rounds of 94°C for 30 sec, 55°C for 30 sec and 68°C for 1 min 30 sec. Exon 1-10 was amplified using primer pair 1F (5'gagagcgcgctgctttaccagg3') and 10R (5'gccatcattgtcaatgtcgcca3'); exon 9-20 using primer pair 9F (5'ggatcgtactttggagcttctg3') and 20R (5'gcatgcactgtgatactgaggt3'). The products were analysed on 2% agarose gels in Tris-acetate-EDTA buffer, stained with Red Safe (iNtRON Biotechnology; Cat# 21141) and destained with water before being visualised with the Fusion Fx gel documentation system (Vilber Lourmat).

2.3.4 Image analysis of the gel from gel electrophoresis

Densitometry (measuring the band intensity) of the bands was performed using Image J Software (24). The band intensity of the *ITGA4* bands in different DNAzymes treated samples were measured and normalised to the band intensity of the corresponding *CYCD* bands before comparing to the band intensity of the untreated samples. The percentage of *ITGA4* transcript knockdown by DNAzymes in fibroblasts was expressed as activity of DNAzyme.

2.3.5 *In vitro* cleavage assay

4.4 µL of 20 µM DNAzyme was incubated with equal molar concentration of FAM-conjugated *ITGA4* RNA (5'-FAM-CUGUGCUGUGGACCUCAAUGCAGAUGGCUUCUCA-3') in 5 µL of buffer containing Mg^{2+} divalent cations (10 mM $MgCl_2$) at 37°C. The reaction was stopped by adding 10 µL of formamide to 10 µL of the reaction mixture at 0, 30 mins, 60 mins and 2 hours. Scrambled DNAzyme RNV174, RNV143-Mut1 (CATCTGCAGGCTAAATACAACGATGAG), RNV143-Mut2 (CATCTGCAAACTAGCTACAACGATGAG) and RNV143-Mut3 (CATCTGCAGGCTAGCAACAACGATGAG) were used as negative controls and the untreated samples did not have any DNAzyme. The red bases are the mutated bases and the two double mutants RNV143-Mut1 and RNV 143-Mut2 were designed based on a previous paper (25). The reaction mixtures were separated on a 15% polyacrylamide gel/ 7M urea for 50 mins at 13 W. The gel was visualised using the Fusion Fx gel documentation system (Vilber Lourmat).

2.3.6 Image Analysis of the gel from *in vitro* cleavage assay

Densitometry (measuring the band intensity) of the bands was performed using Image J Software.(24) The band intensity of the full length RNA bands for different time points were measured and normalised to the combined band intensity of both cleaved and full length RNA bands for different time points and plotted on excel as the % of uncleaved RNA. The same analysis

was repeated to calculate % of cleaved RNA. The slope of the curve was used to calculate the % cleaved per minute.

2.3.7 Phosphodiesterase assay

5 µM DNAzyme was incubated with 0.00001 U phosphodiesterase from *Crotalus adamanteurs* venom (Sigma Aldrich; Cat #: P3243-1VL) at 37°C. At different time points 0, 2 mins, 5 mins, 10 mins, 30 mins and 1 hour, 10 µL of formamide was added to equal volume of the reaction mixture to stop the reaction. The reaction mixture was separated on a 20% polyacrylamide/ 7 M urea gel. The gel was stained with ethidium bromide for 10 minutes and destained in water for 10 minutes before visualizing under UV light using ChemiDoc XRS Imaging System (Bio-Rad Molecular Imager).

2.3.8 Human serum degradation assay

5 µM DNAzyme was incubated in human serum at 37°C. At different time points 0, 30 mins, 60 mins, 2 hours, 4 hours and 6 hours, 10 µL of formamide was added to equal volume of the reaction mixture to stop the reaction. The reaction mixture was separated on a 15% polyacrylamide (BioRad; Cat #: 1610146)/ 7 M urea (Ajax Finechem; Cat #: AJA572) gel. The gel was stained with ethidium bromide for 10 minutes and destained in water for 10 minutes before visualizing under UV light using ChemiDoc XRS Imaging System (Bio-Rad Molecular Imager). The images are shown in Figure A.5 (Appendix A).

2.4 Results

2.4.1 Design and screening of first-generation DNAzymes targeting *ITGA4* mRNA

Two groups of non-modified DNAzymes, one with 10-23 catayltic motif (hammerhead) and the other with 8-17 catalytic motif (arm-loop) (Figure 2.3) were designed to target various exons of

the *ITGA4* transcript (first-generation DNAzymes). The sequences of the catalytic regions were pre-fixed according to previous reports(26, 27) and the arm regions were designed to be specific and complementary to the *ITGA4* mRNA sequences (Figure 2.3). The catalytic activities of these DNAzymes against *ITGA4* mRNA were screened in human primary fibroblasts by transfecting DNAzymes at different concentrations (600 nM, 400 nM, 200 nM, 100 nM and 50 nM) for 24 h. RNA was extracted from the cell lysate and the integrity of *ITGA4* transcript was assessed by performing RT-PCR. Scrambled sequence (SCR) was used as a negative control to account for the non-specific effects.

Dose-dependent reduction of the full-length *ITGA4* transcript was observed for all DNAzymes treated samples. The best *ITGA4* transcript knockdown was observed at 600 nM and therefore, the efficiency of each DNAzyme was calculated as a percentage of *ITGA4* transcript knockdown at 600 nM after normalising to the house keeping gene transcript cyclin D (*CYCD*) and described as the activity in fibroblasts (Figure 2.3). DNAzyme candidate RNV143 targeting the exon 9 of the *ITGA4* mRNA showed highest efficacy with 84% knockdown of *ITGA4* (gel shown in Figure 2.3) followed by RNV148 (71% although this was not statistically significant) and RNV145 (68%) (Figure 2.3).

A

10-23 catalytic motif

5'————————— G A C C U C A A U G C A G A U G ————— mRNA ——— 3'

3' C T G G A G T   A C G T C T A C   5' DNAzyme

(catalytic loop: A G C A A C A T C G A T C G G)

8-17 catalytic motif

5'————————— G U G G C C G U U U A A C G U U G A A U ————— mRNA ——— 3'

3' C A C C G G C A A A   T A C A A C T T A   5' DNAzyme

(catalytic loop: A G C T G C A G C C G C G A C G C G A)
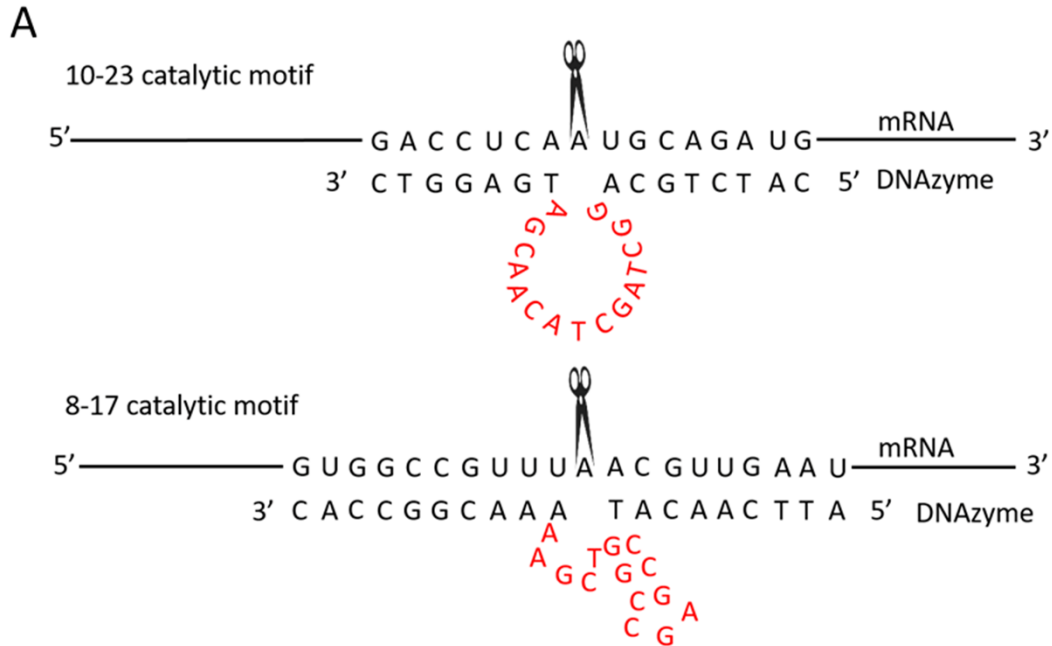
B

Type	Name	Sequences	Target	Activity in fibroblasts (%)	P-values
10-23 catalytic motif	140	AGAGCGGAGGCTAGCTACAACGACTGATGG	5' UTR	37±0.43	0.27
	141	CCAAGCCAGGCTAGCTACAACGAGCGCTCT	exon 1	40±0.34	0.18
	142	AGTGTCCAGGCTAGCTACAACGAGTTGTAG	exon 1	61±0.18*	0.026*
	143	CATCTGCAGGCTAGCTACAACGATGAGGTC	exon 9	85±0.05***	0.000071***
	144	TGAGCTCAGGCTAGCTACAACGAATCCAGG	exon 20	63±0.13*	0.013*
8-17 catalytic motif	145	ATTCAACATCCGAGCCGGTCGAAAAACGGCCAC	exon 1	68±0.08**	0.0042**
	146	ATTGATCATCCGAGCCGGTCGAAGAAGCGTTGG	exon 2	11±0.19	0.19
	147	AAACAAGTTCCGAGCCGGTCGAATTCCACAAGG	exon 3	17±0.48	0.61
	148	CAAACATATCCGAGCCGGTCGAATAACGATTTG	exon 12	71±0.10	0.064
	149	CATCCAAATCCGAGCCGGTCGAACATGTTATAA	exon 15	65±0.02*	0.022*
Scrambled	SCR	GACCTCATCGTTGTAGCTAGCCTGCAGATG	none	31±0.60	0.32

C
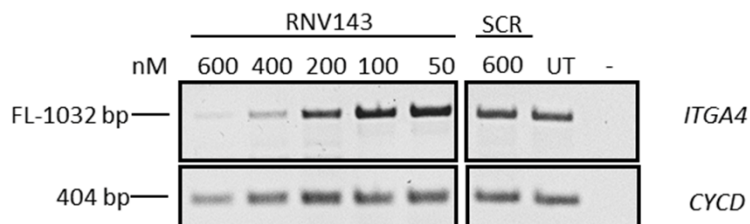
Figure 2.3 *(A) Schematic illustration of the 10-23 and 8-17 catalytic motifs of DNAzymes. (B) Table for the activities of first-generation DNAzymes targeting ITGA4 mRNA that is directly correlated with the percentages of ITGA4 mRNA knockdown (See Materials and Methods for detailed procedures); The catalytic motifs are shown in red, the arm regions are in black, and the sequences are from 5'→ 3'. p-values were calculated for the activity in fibroblasts which was normalised to the UT using student t-test and * indicates p-value<0.05, ** indicates p-*

value<0.005 and *** indicates p-value<0.0005. p-values have been rounded to 2 s.f. (C) Representative RT-PCR products (of three replicates) of the ITGA4 and CycD transcripts from normal human primary fibroblasts after treatment with DNAzyme at different concentrations. The RT-PCR products after treatment with RNV143 are shown here. FL, full-length; UT, untreated; SCR, scrambled sequence; CYCD was used as a loading control. The gel images were cropped to highlight the ITGA4 specific products and the corresponding house-keeping gene control CYCD. The original images are shown in Figure A.2 (Appendix A).

2.4.2 Design and screening of second-generation DNAzymes targeting *ITGA4* mRNA

Based on the initial screen, the best performing DNAzyme RNV143 was selected for further modifications. Many studies have shown that increasing the hybridisation arms on either side of the catalytic motif can increase the binding affinity and efficacy (28-30). In our study, the first generation of DNAzymes initially had 8 nucleotides on one arm and 7 on the other. Several studies showed that the optimal arm lengths vary from 7 to 10 nucleotides long (28-33). Therefore, the length of RNV143 was systematically increased at the end of both arms, and then the efficacy of the modified DNAzymes was verified. One, two and three nucleotides were added to both arms of RNV143 and named RNV182, RNV183 and RNV184 respectively (Figure 2.4). The catalytic activities of these second generation DNAzyme candidates were analysed in human primary fibroblasts as described above. The transfections were repeated at least twice. Notably, a decrease in activities were observed for RNV182 (57%) and RNV183 (74%) at 600 nM compared to the parent DNAzyme RNV143 (84%) (Figure 2.4). RNV184 with additional six nucleotides (three on each ends) was the only candidate that showed similar activity to the parent RNV143, with 89% knockdown of *ITGA4* mRNA. These results showed that increasing the arm length did not dramatically improve the efficacy of DNAzyme RNV143 in fibroblasts.

Next, we explored the improvement of nuclease stability of the DNAzymes since the natural nucleotide monomers are rapidly degraded *in vivo*. First, we introduced phosphorothioate (PS) linkages to the arm regions of RNV143 to improve nuclease resistance and named RNV143PS.

However, RNV143PS failed to cleave *ITGA4* RNA when transfected into the human fibroblasts. Only 10% of the *ITGA4* transcript was degraded when treated with RNV143PS while nearly 29% of the *ITGA4* transcript was non-specifically knocked down by the scrambled control (Figure 2.4). Then we introduced another chemical modification, an 'inverted dT' at the 3' end of RNV143, RNV183 and RNV184, the DNAzymes with high activities, and the new generation DNAzymes were named RNV143A, RNV183A and RNV184A respectively. RNV143A, RNV183A and RNV184A slightly improved the activities of DNAzymes (89%, 76% and 92% respectively; Figure 2.4).

We also investigated the potential of LNA nucleotides in DNAzymes. Two LNA nucleotides were incorporated to both arms of RNV183 at positions 2, 5 and 31, 35. However, RNV183 with 4 LNA modifications was not effective (did not cleave *ITGA4*) when tested in cells (data not shown). We believe that this may be due to the formation of secondary structures caused by LNAs within the arms of the DNAzymes that could potentially affect the catalytic motif (sequence of the LNA modified RNV183 and the mfold (34) predicted structures are shown in Appendix A, **Error! R eference source not found.**). To limit this secondary structure formation, we truncated the LNA modified RNV183 by four nucleotides from the 5' end to generate RNVLNA-3 (Figure 2.4) with one LNA nucleotide on the truncated arm and two LNA nucleotides on the other non-truncated arm. This truncation is predicted to limit the secondary structure formation and promote its ability to bind to the *ITGA4* mRNA. Transfection with RNVLNA-3 showed 58% knockdown of *ITGA4* transcript indicating that the truncation helped to improve the activity, although the efficacy of *ITGA4* knockdown was not efficient (Figure 2.4).

Name	Sequences	Activity in fibroblasts (%)
182	CCATCTGCAGGCTAGCTACAACGATGAGGTCC	57
183	GCCATCTGCAGGCTAGCTACAACGATGAGGTCCA	74
184	AGCCATCTGCAGGCTAGCTACAACGATGAGGTCCAC	89
143PS	CATCTGCAGGCTAGCTACAACGATGAGGTC	10
143A	CATCTGCAGGCTAGCTACAACGATGAGGTC/3InvdT/	89
183A	GCCATCTGCAGGCTAGCTACAACGATGAGGTCCA/3InvdT/	76
184A	AGCCATCTGCAGGCTAGCTACAACGATGAGGTCCAC/3InvdT/	92
LNA-3	TCTGCAGGCTAGCTACAACGATGAGGTCCA	58
SCR	GACCTCATCGTTGTAGCTAGCCTGCAGATG	31

Figure 2.4   Second-generation DNAzymes derived from RNV143, targeting the ITGA4 mRNA. The activity of DNAzymes directly correlated with the percentage of ITGA4 mRNA knockdown. Activities of DNAzymes were calculated as described in section 2.3.4. The catalytic motifs are shown in red, the arm regions are in black and the residues modified with LNA are in blue. The sequences are from 5'→ 3'.

2.4.3 *In vitro* cleavage of *ITGA4* RNA template

To further verify the catalytic activity of DNAzyme towards the target region of *ITGA4* transcript, we performed the cleavage efficacy *in vitro* using a synthetic fluorescein dye (FAM)-labelled RNA target composed of exon 9 region of the *ITGA4* transcript. The experiments were performed by incubating DNAzymes with FAM-labelled RNA template in the presence of divalent metal ions and the products were separated and analysed on polyacrylamide gels. Briefly, 1.76 µM oligonucleotides were incubated with 1.76 µM FAM-conjugated *ITGA4* RNA in the presence of Mg^{2+} divalent cations for 30 min, 60 min and 120 min at 37°C. The reactions were stopped by adding 10 µL of formamide solution. The products were then separated on a 15% denaturing polyacrylamide gel and visualised using Fusion FX Vilber Lourmat imager. The cleaved products of the 34mer full length FAM-conjugated RNA was expected to be 18 nucleotides. A scrambled (SCR) sequence and RNV143 mutants with different mutations within the catalytic region of RNV143 were used as negative controls in parallel and an untreated (UT) sample with no DNAzyme was also included.

Although variable efficiencies were observed for these DNAzymes in fibroblasts, RNV143, RNV182, RNV183 and RNV184 showed similar cleavage efficiency *in vitro* (around 0.7%/min) (Figure 2.5). In general, the *in vitro* cleavage rates of the modified DNAzymes were slower than that of their parent oligonucleotides. Notably, RNV143PS showed very low cleavage efficiency with small percentage of cleaved FAM-conjugated RNA appeared after 120 minutes of incubation. Similar results were observed for RNV143-Mut3 while the other mutant DNAzymes and the SCR sequence showed no cleavage (Figure 2.5).

Name	*In vitro* cleavage (% cleaved per minute)
RNV143	0.71
RNV182	0.77
RNV183	0.75
RNV184	0.71
RNV143PS	N/A
RNV143A	0.47
RNV183A	0.58
RNV184A	0.56
RNVLNA-3	0.63
SCR and all RNV143 mutants	N/A
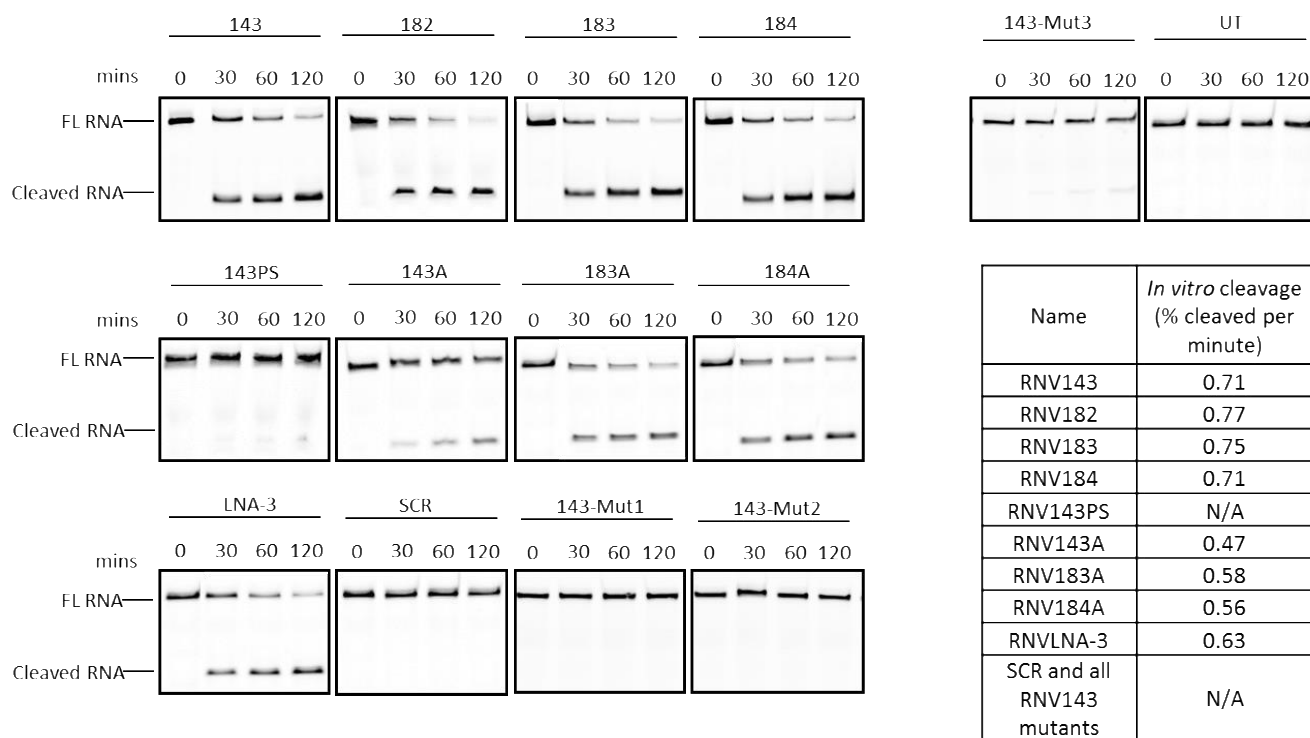
Figure 2.5   In vitro cleavage of the FAM-conjugated ITGA4 RNA template composed of exon 9 region (34 nucleotides) by RNV143 and its derivatives. FL RNA, full-length; FAM-conjugated RNA; cleaved RNA; the cleaved FAM-conjugated ITGA4 RNA (18 nucleotides long). The FAM- conjugated template RNA is a small region of the ITGA4 transcript complementary to the hybridisation arms of the DNAzymes of interest. The gel images were cropped for better overview. The original images are shown in Figure A.3 (Appendix A). The table shows the cleavage rate in %/min which was calculated as described in the Methods section (Section 2.3.)

2.4.4 Nuclease stability analysis of DNAzymes

High nuclease stability is paramount towards the clinical development of oligonucleotides. Towards this goal, we tested the stability of DNAzymes 143, 183, 184, RNVLNA-3, 143A, 183A, and 184A using snake venom phosphodiesterase, a harsh enzyme with very high 3'→5' exonuclease activity. DNAzyme candidates were incubated with the enzyme at 37°C and samples were collected at different time points (0, 30, 60 and 120 minutes) followed by the products analysis on 15% denaturing polyacrylamide gels. As expected the stability was increased by increasing the arm lengths of the DNAzymes and RNV184 (36 nt long) was found to be the most stable compared to RNV183 and RNV143 (Figure 2.6). RNVLNA-3 with LNA modifications (known for high nuclease stability(35, 36)) was more stable than RNV143, RNV183 and RNV183. A weak product band was visible even after 60 minutes of incubation. Remarkably, the DNAzymes with inverted dT nucleotide at 3'-end (RNV143A, RNV183A and RNV184A) showed highest stability with no significant degradation even after 1 hour incubation with phosphodiesterase (Figure 2.6).
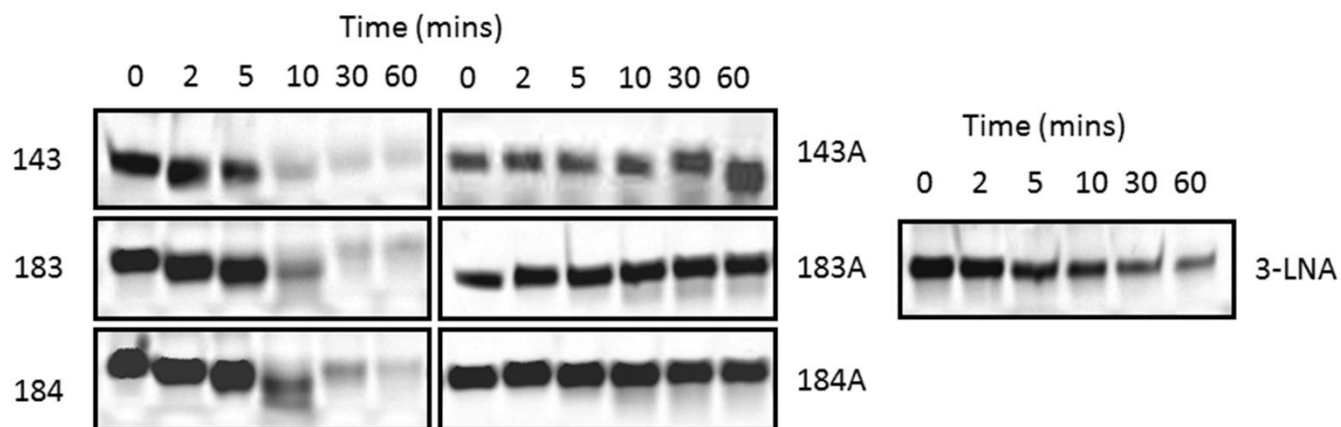
Figure 2.6   Phosphodiesterase degradation analysis of DNAzymes that showed high efficacy in the cleavage of ITGA4 RNA in vitro and knockdown of ITGA4 RNA in fibroblasts. The gel images were cropped for better overview. The original images are shown in Figure A.4(Appendix A).

2.5 Discussion

We have successfully identified a DNAzyme that cleaves the *ITGA4* transcript both *in vitro* and in human primary fibroblasts by screening different DNAzyme constructs with 10-23 catalytic motif and 8-17 catalytic motif targeting different sites of *ITGA4* mRNA. The DNAzyme was not only capable of downregulating the *ITGA4* transcript *in vitro* and in human primary fibroblasts but also showed high resistance to exonuclease degradation. Our study thus provides a novel approach for downregulating *ITGA4* transcript that may have therapeutic potential towards the treatment of MS where ITGA4 is a validated target for tackling inflammation.

Cleavage by first generation DNAzymes with either 10-23 or 8-17 catalytic motif targeting five different cleavage sites of the *ITGA4* transcript showed variable cleavage efficiencies (Figure 2.3). The best cleavage efficiency was achieved with the 10-23 catalytic motif DNAzymes designed to cleave a site located in exon 9 of the *ITGA4* transcript. The variable target-cleaving efficiencies observed for different first generation DNAzymes targeting different regions of the *ITGA4* transcript could be due to the structure variations that might affect the accessibility of target sequences. This is consistent with previous observations by Vester *et al.*(2006) (29, 33, 37) The cleavage efficiency of DNAzyme has been proposed to be dependent on the structural complexity of the RNA that is targeted (29, 38). In a comparison between different substrate structures, Vester *et al.* (2006)*,* targeted three different cleavage sites of either a short (17 nucleotides) unstructured RNAs; or longer (58 nucleotides) RNAs with stable secondary structures; or longer (2904 nucleotides) RNAs with both stable secondary and tertiary structures (29, 38). The results indicated that only one cleavage site out of three could be efficiently cleaved by the DNAzymes and the cleavage of the short unstructured RNAs were more efficient than the longer structured RNA (29, 38). This implies that the accessibility of the purine-pyrimidine sites differs in different regions of

the *ITGA4* (1032 bp long) transcript due to the formation of different secondary and tertiary structures in the transcript inside the cells, leading to differences in the ability of DNAzymes to cleave them.

The optimal arm length may vary for different DNAzymes and there is no evidence on whether the arms should be asymmetrical or symmetrical for optimal catalytic activity. In addition, the GC content may also have an effect on the catalytic efficiency (28, 30, 33, 39), but how it is affected is unclear (28, 30, 31). In parallel, increasing the DNAzyme binding arm length would increase DNAzyme- target affinity as it enhances the heteroduplex stability (40), but it could also result in slower product release that would inhibit or decrease the rate of multiple turnovers. Therefore, longer binding arms may not always produce higher catalytic efficiency (26, 41). Using the best candidate RNV143 from the first screen, we further tested the impact of DNAzyme arm lengths aiming for increased efficiency. However, the catalytic efficiency was decreased in most DNAzymes with longer arms. ENREF 26We speculate that increasing the arm length of the DNAzyme RNV143 could increase the binding affinity of DNAzymes to the target RNA but result in slower product release and turnover (38). For DNAzymes to have therapeutic potential, it is desirable to have high turnover.

Although we have identified a DNAzyme with high cleavage efficiency, one of the disadvantages of unmodified DNAzymes, similar to antisense oligonucleotides, is their vulnerability to nucleases *in vivo* and therefore, nuclease resistance is a critical characteristic of their physical property (42). The suitable solution to increase nuclease resistance is to introduce chemical modifications (42). Several modifications have been successfully introduced into the oligonucleotides including sugar modifications such as LNA,[21,22] and inverted thymidine and backbone modification such as PS (42). In line with this, we modified several of our efficient DNAzyme candidates, RNV143 and its

two derivatives RNV183 and 184 with PS, LNA and inverted-dT. When modified with PS modification (RNV143PS), RNV143 resulted in decreased cleavage efficiency both *in vitro* (Figure 2.5) and in human fibroblasts (Figure 2.4). PS modification typically enhances the stability of the oligonucleotide against nucleases, however, they compromise the affinity to their target in some cases which could result in decreased cleavage efficiency (42). Similar results were also observed in another study that further support our observation that PS modification may not be ideal for developing efficient DNAzymes (31). Although truncation and incorporation of LNA to the DNAzymes increased resistance to nuclease (Figure 2.6), the activity was decreased (Figure 2.4). The reduction in the activity may be due to a combination of reduced size and slower DNAzyme dissociation from the mRNA target based on the high affinity of LNA nucleotides (31). Among all modifications tested, incorporation of inverted dT (RNV143A, 183A and 184A) was found to be the best chemistry in this case, since it not only conferred nuclease resistance (Figure 2.6) but also achieved high activity (89%, 76% and 92% respectively) (Figure 2.4). The result is also consistent with a previous study performed by Schubert *et al* (2003) (31). Additionally, we have also performed a human serum degradation experiment to observe the stability of the DNAzymes in human serum (Figure A.5 in Appendix A). RNV143, 182, 183 and 184 showed similar stability (degradation observed after 2 hours incubation) in human serum and as expected their modified counterparts RNV143A, 183A and 184A showed better stability (˜26%-50% DNAzymes remained after 6h incubation). Interestingly, LNA-3 conferred the best stability in human serum, however as discussed above, its activity in cells was decreased (Figure 2.4).

We observed a discrepancy between the *ITGA4* knock down observed in fibroblasts and the *in vitro* cleavage for the same DNAzymes. Although variable efficiencies are observed for second generation DNAzymes in human primary fibroblasts (Figure 2.4), the *in vitro* data does not reflect

this (Figure 2.5). It is expected that *cell-free* conditions are incomparable to the crowded *cell-culture* environment and the mRNA folding and accessibility of the template may significantly influence the success of experiments within the cells. It is also expected that the *ITGA4* RNA expressed in fibroblasts (1032 base pairs long) is much longer and can adopt complex secondary and tertiary structures. However, the synthetic short single-stranded (ss) RNA (34 nucleotides long) used for the *in vitro* cleavage assay may not form any secondary or tertiary structures and therefore it is much easier for the DNAzyme to access and cleave. However, the DNAzymes that knocked down *ITGA4* transcript in fibroblasts also showed the ability to cleave the synthetic *ITGA4* transcript template *in vitro* and from this we may suggest that the *ITGA4* knock down observed in the fibroblast could be due to the DNAzymes-mediated cleavage of *ITGA4* transcript. Furthermore, we designed three RNV 143 mutants, RNV143-Mut1, RNV143-Mut2 and RNV143-Mut3 to investigate the possibility of antisense effect rather than DNAzyme cleavage. RNV143-Mut1 and RNV 143-Mut2 are double mutants designed based on the paper by Wang *et al*. (2015) that suggested that these double mutants were critical for activity in the hammerhead and the stem loop respectively (25). Both double mutants may be important for catalytic activity as they abolished the *in vitro* cleavage activity (Figure 2.5). However, RNV143-Mut3 showed very small cleavage activity indicating that the mutated nucleotide may not be crucial for catalytic activity, supporting the previous study by Wang et al.(2015) (25). These controls also suggest that the gene silencing effects seen in cells by RNV143 may be due to DNAzyme cleavage rather than the antisense effect. The cleavage rates of the DNAzymes observed here is about half of that reported by Schubert *et al* (2003) (31). However, we performed the *in vitro* cleavage reactions with equal molar ratio of the DNAzyme to substrate in the presence of 0.5 mM $MgCl_2$ while Schubert *et al*.

(2003), performed the reactions with 10-fold excess of DNAzyme to substrate in 10mM MgCl$_2$ (31).

2.6 Conclusion

In conclusion, we identified DNAzymes that are capable of cleaving the *ITGA4* transcript in human primary fibroblasts. The DNAzyme candidate RNV143 targeting exon 9 of the *ITGA4* transcript showed 92% knock down of the *ITGA4* transcript and the catalytic ability of the DNAzyme was verified by *in vitro* cleavage assay. Furthermore, introducing a chemical modification such as an inverted dT at the 3' end (RNV143A) significantly improved the stability while maintaining efficient catalytic activity. Although RNV143A needs further validations, based our current results, we firmly believe that the candidate could provide therapeutic benefits.

2.7 References

1.   Feinstein A, Freeman J, Lo AC. Treatment of progressive multiple sclerosis: what works, what does not, and what is needed. Lancet Neurol. 2015;14(2):194-207.

2.   Olsson T, Barcellos LF, Alfredsson L. Interactions between genetic, lifestyle and environmental risk factors for multiple sclerosis. Nat Rev Neurol. 2017;13(1):25-36.

3.   Wendel-Haga M, Celius EG. Is the hygiene hypothesis relevant for the risk of multiple sclerosis? Acta Neurol Scand. 2017;136.

4.   Ascherio A. Environmental factors in multiple sclerosis. Expert Rev Neurother. 2013;13(sup2):3-9.

5.   Grigoriadis N, Van Pesch V. A basic overview of multiple sclerosis immunopathology. European Journal of Neurology. 2015;22:3-13.

6.   Legroux L, Arbour N. Multiple Sclerosis and T Lymphocytes: An Entangled Story. Journal of Neuroimmune Pharmacology. 2015;10(4):528-46.

7.   Noseworthy JH, Kirkpatrick P. Natalizumab. Nat Rev Drug Discov. 2005;4(2):101-2.

8.   Fenu G, Lorefice L, Frau F, Coghe G, Marrosu M, Cocco E. Induction and escalation therapies in multiple sclerosis. Anti-Inflammatory & Anti-Allergy Agents in Medicinal Chemistry (Formerly Current Medicinal Chemistry-Anti-Inflammatory and Anti-Allergy Agents). 2015;14(1):26-34.

9.   Dargahi N, Katsara M, Tselios T, Androutsou M-E, De Courten M, Matsoukas J, et al. Multiple Sclerosis: Immunopathology and Treatment Update. Brain Sciences. 2017;7(12):78.

10.   Comi G, Radaelli M, Soelberg Sørensen P. Evolving concepts in the treatment of relapsing multiple sclerosis. The Lancet. 2017;389(10076):1347-56.

11.   Carter PJ. Potent antibody therapeutics by design. Nature Reviews Immunology. 2006;6(5):343-57.

12.   Chames P, Van Regenmortel M, Weiss E, Baty D. Therapeutic antibodies: successes, limitations and hopes for the future. 2009;157(2):220-33.

13.   Carter PJ. Introduction to current and future protein therapeutics: A protein engineering perspective. 2011;317(9):1261-9.

14.   Elgundi Z, Reslan M, Cruz E, Sifniotis V, Kayser V. The state-of-play and future of antibody therapeutics. Advanced Drug Delivery Reviews. 2017;122:2-19.

15. Dowdy SF. Overcoming cellular barriers for RNA therapeutics. Nature Biotechnol. 2017;35(3):222-9.

16. Myers KJ, Witchell DR, Graham MJ, Koo S, Butler M, Condon TP. Antisense oligonucleotide blockade of alpha 4 integrin prevents and reverses clinical symptoms in murine experimental autoimmune encephalomyelitis. 2005;160(1-2):12-24.

17. Aung-Htut MT, Comerford I, Johnsen R, Foyle K, Fletcher S, Wilton SD. Reduction of integrin alpha 4 activity through splice modulating antisense oligonucleotides. Sci Rep. 2019;9(1).

18. Soilu-Hänninen M, Epa R, Shipham K, Butzkueven H, Bucci T, Barrett G, et al. Treatment of experimental autoimmune encephalomyelitis with antisense oligonucleotides against the low affinity neurotrophin receptor. 2000;59(6):712.

19. Vaknin-Dembinsky A, Balashov K, Weiner HL. IL-23 Is Increased in Dendritic Cells in Multiple Sclerosis and Down-Regulation of IL-23 by Antisense Oligos Increases Dendritic Cell IL-10 Production. 2006;176(12):7768-74.

20. Kim S-S, Ye C, Kumar P, Chiu I, Subramanya S, Wu H, et al. Targeted Delivery of siRNA to Macrophages for Anti-inflammatory Treatment. 2010;18(5):993-1001.

21. Zhou W, Ding J, Liu J. Theranostic dnazymes. Theranostics. 2017;7(4):1010.

22. Krug N, Hohlfeld JM, Kirsten A-M, Kornmann O, Beeh KM, Kappeler D, et al. Allergen-Induced Asthmatic Responses Modified by a GATA3-Specific DNAzyme. N Engl J Med. 2015;372(21):1987-95.

23. Garn H, Renz H. GATA-3-specific DNAzyme - A novel approach for stratified asthma therapy. 2016.

24.   Schindelin J, Rueden CT, Hiner MC, Eliceiri KW. The ImageJ ecosystem: An open platform for biomedical image analysis. Mol Reprod Dev. 2015;82(7-8):518-29.

25.   Wang F, Saran R, Liu J. Tandem DNAzymes for mRNA cleavage: Choice of enzyme, metal ions and the antisense effect. Bioorganic Med Chem Lett. 2015;25(7):1460-3.

26.   Santoro SW, Joyce GF. A general purpose RNA-cleaving DNA enzyme. Proc Natl Acad Sci. 1997;94(9):4262-6.

27.   Haseloff J, Gerlach WL. Simple RNA enzymes with new and highly specific endoribonuclease activities. Nature. 1988;334:585-91.

28.   Ackermann JM, Kanugula S, Pegg AE. DNAzyme-mediated silencing of ornithine decarboxylase. Biochemistry-Us. 2005;44(6):2143-52.

29.   Vester B, Hansen LH, Lundberg LB, Babu BR, Sørensen MD, Wengel J, et al. Locked nucleoside analogues expand the potential of DNAzymes to cleave structured RNA targets. BMC molecular biology. 2006;7(1):1.

30.   Santoro SW, Joyce GF. Mechanism and utility of an RNA-cleaving DNA enzyme. Biochemistry-Us. 1998;37(38):13330-42.

31.   Schubert S, GuÈl DC, Grunert HP, Zeichhardt H, Erdmann VA, Kurreck J. RNA cleaving '10-23'DNAzymes with enhanced stability and activity. Nucleic Acids Res. 2003;31(20):5982-92.

32.   Sun L-Q, Cairns MJ, Gerlach WL, Witherington C, Wang L, King A. Suppression of smooth muscle cell proliferation by a c-myc RNA-cleaving deoxyribozyme. J Biol Chem. 1999;274(24):17236-41.

33.   Kurreck J, Bieber B, Jahnel R, Erdmann VA. Comparative study of DNA enzymes and ribozymes against the same full-length messenger RNA of the vanilloid receptor subtype I. J Biol Chem. 2002;277(9):7099-107.

34.   Zuker M. Mfold web server for nucleic acid folding and hybridization prediction. Nucleic Acids Res. 2003;31(13):3406-15.

35.   Veedu RN, Wengel J. Locked nucleic acids: promising nucleic acid analogs for therapeutic applications. Chem Biodivers. 2010;7(3):536-42.

36.   Veedu RN, Wengel J. Locked nucleic acid as a novel class of therapeutic agents. RNA Biol. 2009;6(3):321-3.

37.   Cairns MJ, Hopkins TM, Witherington C, Wang L, Sun L-Q. Target site selection for an RNA-cleaving catalytic DNA. Nature Biotechnol. 1999;17(5):480-6.

38.   Vester B, Lundberg LB, Sørensen M, Babu B, Douthwaite S, Wengel J. Improved RNA cleavage by LNAzyme derivatives of DNAzymes. Portland Press Limited; 2004.

39.   Cairns MJ, Hopkins TM, Witherington C, Sun L-Q. The influence of arm length asymmetry and base substitution on the activity of the 10-23 DNA enzyme. Antisense Nucleic Acid Drug Dev. 2000;10(5):323-32.

40.   Cairns M, Saravolac E, Sun L. Catalytic DNA: a novel tool for gene suppression. Current drug targets. 2002;3(3):269-79.

41.   Tsuchihashi Z, Khosla M, Herschlag D. Protein enhancement of hammerhead ribozyme catalysis. Science. 1993;262(5130):99-102.

42.   Chan C, Khachigian L. DNAzymes and their therapeutic possibilities. Internal medicine journal. 2009;39(4):249-51.

Chapter 3 Alzheimer's Disease

3.1 Introduction

Alzheimer's disease (AD) is the most common form of dementia; accounting for 70% of cases with a dementia diagnosis. Globally, there are ˃47 million current cases; with 7.7 million new cases added each year (1). Alzheimer's disease (AD) is characterised by a progressive loss of memory and cognitive function (2), patients eventually needing 24-hour care that places emotional and economic burdens on the community. There is no cure for AD nor any treatment that addresses the underlying molecular cause (1). Current treatments use cholinesterase inhibitors (3) and *N*-methyl-d-aspartate receptor (NMDA) antagonists (4) that improve cognitive function and reduce symptoms temporarily but do not stop the progression of the disease. The current approach to diagnosis relies on a combination of cognitive and clinical assessment, genetic profiling, and magnetic resonance imaging (MRI) to measure anatomical changes in the brain (5), but confirmation relies on post-mortem neuropathological assessment and misdiagnosis is common (2). The two hallmarks of the disease, the extracellular amyloid-β (Aβ) plaques (mainly an agglomeration of Aβ peptides) and intracellular neurofibrillary tangles (hyperphosphorylated tau peptides). This chapter explores the potential of nucleic acid therapeutic, diagnostic, and research strategies that target both Aβ and tau pathologies to treat AD and focuses on manipulating gene expression in both sporadic and familial forms of AD.

3.1.1 Types of AD

Alzheimer's disease (AD) can be classified into two types, early-onset AD is characterised by a clinical onset under 65 years of age while late-onset of AD is characterised by a clinical onset

above 65 years of age. Early-onset AD can then be further classified into two groups, sporadic and familial AD (FAD), while most late-onset AD is a sporadic form of AD. Early-onset AD affects around 10% of all AD patients, of which 10-15% are diagnosed with FAD. Sporadic AD is a multifactorial disease with a complex etiology, influenced by both genetic and environmental factors have a role, while genetics has a major role in early-onset AD patients.

3.1.1.1 Familial Alzheimer's Disease

Familial Alzheimer's disease (FAD) accounts for around less than 1% of all AD cases (6, 7) and has a strong genetic determinant, with increased risk of AD development in relatives as well as more severe clinical features (6, 7). Familial Alzheimer's disease (FAD) is an autosomal dominant disease, with 50% of the patients carrying mutations in one of the following three genes: *APP*, *PSEN1* and *PSEN2*. Mutations in the *APP*, *PSEN1* and *PSEN2* genes leads to aberrant cleavage of APP and aggregation of Aβ (detailed discussion in section 3.1.2.1) (8, 9). These patients present similar memory problems to those seen in sporadic AD patients (8).

3.1.1.2 Sporadic Alzheimer's Disease

Most late-onset AD and a large proportion of early-onset AD occur sporadically. However, many gene loci have been identified as risk factors for AD with the apolipoprotein E (*APOE*) locus being identified as the biggest risk factor for sporadic AD (10). Since then many susceptibility genes have been identified that are part of the Aβ pathway, tau pathway, immune system/ inflammation pathway, lipid transport and metabolism pathway, and synaptic cell functioning or endocytosis pathways have now been identified (10). This section will explore the pathways implicated in AD pathogenesis rather than the susceptibility genes themselves.

3.1.2 Pathogenesis of Alzheimer's Disease

3.1.2.1 Amyloid β (Aβ) hypothesis

The Aβ hypothesis states that there is an imbalance of toxic Aβ peptide production and clearance (11-13). The main Aβ species, $A\beta_{1-40}$ and $A\beta_{1-42}$, can aggregate to form fibrils and plaques (11-13). $A\beta_{1-40}$ and $A\beta_{1-42}$ are produced by the aberrant processing of the APP by β-site APP cleaving enzyme 1 (BACE1) and γ-secretase (Figure 3.1) (12-16). Mutations in the *APP* and Presenilin genes (*PSEN1* codes for the catalytic subunits of γ-secretase) increase $A\beta_{1-42}$ levels (11-13, 15, 17-19) and lead to early-onset familial AD. People with Down syndrome cases have an extra copy of chromosome 21, and hence of the *APP* gene, and develop Aβ plaques early in adulthood (20). Oligomers of Aβ promote synaptic loss, neuronal dysfunction, and cell death (21, 22). $A\beta_{1-42}$ inhibits the maintenance of long-term hippocampal potentiation, resulting in altered memory function (11, 23) and reduced synaptic neurotransmission through NMDA receptor-mediated signalling (11, 23, 24). Aβ toxicity has also been implicated in inflammation (12), oxidative stress (12, 25) and impaired cholinergic transmission (24), glucose metabolism(26, 27), and cholesterol metabolism (28).
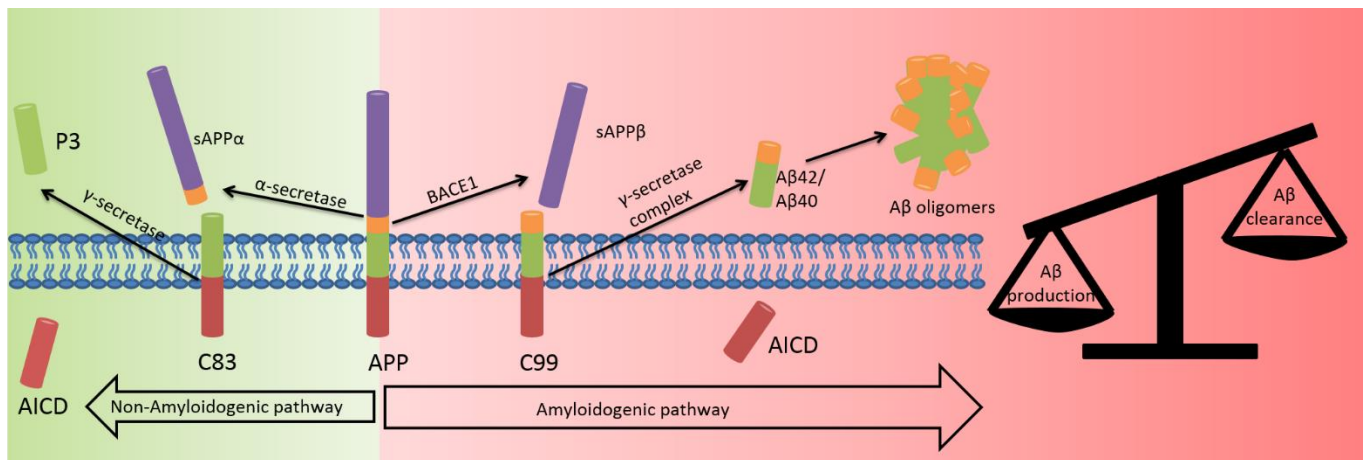
Figure 3.1   Non-amyloidogenic and amyloidogenic pathways in AD neurons. In the amyloidogenic pathway, the APP is aberrantly spliced by BACE1 and γ-secretase leading to accumulation of toxic Aβ species. AICD:

amyloid precursor protein intracellular domain; sAPP: soluble amyloid precursor protein; APP: amyloid precursor protein; BACE1: beta site amyloid precursor protein cleaving enzyme 1;Aβ: amyloid beta

3.1.2.2 Tau hypothesis

Microtubule-associated protein tau (tau), predominantly expressed in neuronal axons, is involved in microtubule assembly and stability. Tau is regulated by phosphorylation (29, 30); hyperphosphorylation decreases the ability of tau to bind to microtubules, leading to reduced trafficking, destabilisation of microtubules, and synaptic loss (30, 31) (Figure 3.2). Abnormal tau can aggregate into paired helical filaments to form neurofibrillary tangles (32) in the cytosol and sequester normal tau and inhibit microtubule assembly (30). Alternatively, tau aggregation may be a protective mechanism to prevent hyperphosphorylated tau sequestering normal tau and inhibit microtubule assembly (30). Tau hyperphosphorylation is detrimental in various neurodegenerative diseases termed "tauopathies" (29, 33) and correlates with neurodegeneration and cognitive decline (30, 33). Other post-translational modifications of tau, including abnormal glycosylation and reduced β-linked acylation of N-acetylglucosamine, increase hyperphosphorylation (30, 34). Inhibition of the ubiquitin-proteasome system may also increase the aggregation of hyperphosphorylated tau (32).
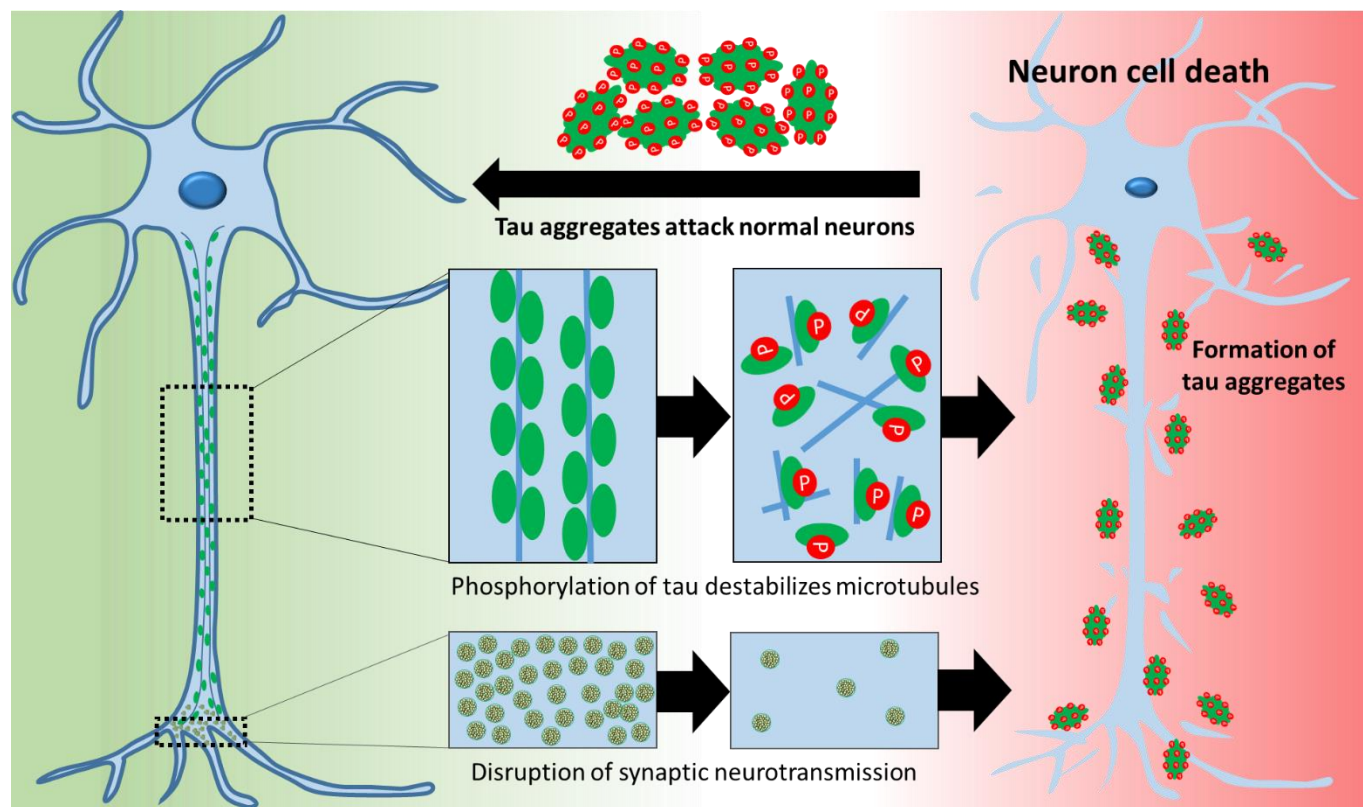
Figure 3.2   The roles of tau in healthy neurons and of hyperphosphorylated tau in AD neurons that leads to neuronal toxicity. Tau plays a role in stabilising microtubules in axons. Hyperphosphorylation of tau results in destabilisation of microtubules.

3.1.2.3 Other hypotheses of AD

Drugs currently approved by the FDA for the treatment of AD are Donepezil, Rivastigmine, Galantamine and Memantine (Table 3.1) (35-38). These agents enhance cholinergic and glutamatergic neurotransmission and improve cognitive function temporarily, these drugs, do not slow the progression of the disease. Oxidative stress (39), inflammation (40), insulin impairment (41, 42) and abnormal cholesterol metabolism (28) may also play roles (Table 3.1), but are not considered in-depth here.

3.1.3 Current therapeutic molecules and clinical trials for the treatment of AD

Many disease-modifying therapeutics show promising results in animal models but disappointing outcomes in clinical trials (for drug candidates and ongoing trials see Table 3.1). Poor outcomes

might have arisen because each agent targets a single pathway, whereas AD is a complex disease, and it may be important to address multiple targets (43, 44). Developing a suitable therapeutic approach is challenging because the pathogenesis of AD is unknown (45) and trials might be affected by factors such as genetics, metabolism, diet and environment (46), but there is a need to develop novel therapeutics for this disease. Current strategies under investigation have been comprehensively reviewed elsewhere (47).

Table 3.1   Therapeutic molecules in clinical trials, their targets, and trial outcomes.

Drug molecule	Role/ Target	Trial stage	Results	References
Donepezil (Pfizer)	Cholinesterase inhibitor	FDA approved- Although they improve the symptoms temporarily, these drugs do not stop the progression of the disease.		(172-175)
Rivastigmine (Novartis)	Cholinesterase inhibitor			
Galantamine (Jansen-Cilag)	Cholinesterase inhibitor			
Memantine (Lundbeck)	NMDA receptor antagonist			
Tramiprosate	Aβ aggregation inhibitor	Phase III	No significant benefit. May promote abnormal tau aggregation	(185-187)
Colostrinin	Aβ aggregation inhibitor	Phase III	Modest improvements not sustained	(188-190)
Scyllo-inositol	Stabilises Aβ aggregates and inhibits toxicity	Phase II	No statistically significant effect. Reduced Aβ in cerebrospinal fluid	(191)
Aβ vaccination	Aβ aggregation inhibitor	Phase II	Halted because patients developed meningoencephalitis	(192)
Bapineuzumab	Aβ aggregation inhibitor	Phase III	Endpoints not significantly different	(193)
Solanezumab	Aβ aggregation inhibitor	Phase III	Endpoints not significantly improved	(194)
Anti-amyloid Ab	Aβ aggregation inhibitor	Phase III	No positive primary outcome	(195)
Other mAbs	Aβ aggregation inhibitor	Various	No positive outcome	(184, 196, 197)
Tarenflurbil	γ-secretase inhibitor	Phase III	No significant improvement	(198-200)
LY450139 (Eli Lilly)	γ-secretase inhibitor	Phase III	Discontinued: no $A\beta_{40/42}$ reduction	(201)
BMS-708163 (B-M Squibb)	γ-secretase inhibitor	Phase II	Terminated due to lack of favourable pharmacodynamics	(184, 202)
Verubecestat	BACE1 inhibitor	Phase III	No positive outcome	(203)
Rosiglitazone	BACE1 inhibitor and Type 2 diabetes drug	Phase III	No positive outcome	(204)
Pioglitazone	BACE1 inhibitor and Type 2 diabetes drug	Phase III	No positive outcome	(204)
Methyl thionium chloride	Tau aggregation inhibitor	Phase II	Significantly improved cognitive function	(205, 206)
Tideglusib	GSK3β	Phase IIb	No positive outcome	(206, 207)

Drug molecule	Role/ Target	Trial stage	Results	References
Davunetide	Microtubule stabilizer	Phase III	No significant improvement	(168)
Antioxidants	ROS	Phase III	No positive outcome	(184, 208)
Anti-inflammatories	Inflammation	Phase III	No significant improvement	(163, 177, 197, 209-211)
Intranasal insulin	Insulin impairment	Pilot	Improvement in patients without APOE-ε4 allele	(178, 212)
Other anti-diabetics	Insulin impairment	Phase III	Currently running	
Statins	Cholesterol metabolism	Phase III	Preliminary results positive; mechanism unknown.	(165, 213)

3.1.4 Current animal models of AD

Most of the animal models for AD are based on the genetics of AD or are based on transgenic expression of genes that result in overproduction of proteins that are implicated in the pathology of AD (77). Some popular genetic mouse models include mouse models that express transgenic human APP, transgenic Aβ expression, transgenic double presenilin and human APP expression, and transgenic human APP and human tau expression to name a few (77). One of the most popular mouse model is the mouse model that expresses the Swedish double mutation that results in overexpression of APP and results in FAD, discovered in a Swedish family (77). No mouse model exhibits all clinical and pathological features of AD but exhibit different combinations of the clinical and pathological features to varying degrees (77). However, almost all mouse models exhibit amyloid plaques but very few mouse models exhibit neurofibrillary tangles and neuronal loss (77). Therefore, different mouse models are useful for studies that study the role of targets and drugs for particular mechanisms (77). For example, mouse models that express human tau and therefore the resulting neurofibrillary tangles, are used when testing drugs or studying targets and their effect against tau (77). Many drugs that showed improvement in mouse models were unsuccessful in clinical trials, possibly due to lack of mouse models that exhibit all clinical and pathological features of AD (77). Therefore, mouse models may be more useful for studying

therapeutic molecules against FAD than sporadic AD and may explain the discrepancy between

the success in animal testing but failure in human clinical trials.

3.2 Nucleic-acid molecules for tackling AD
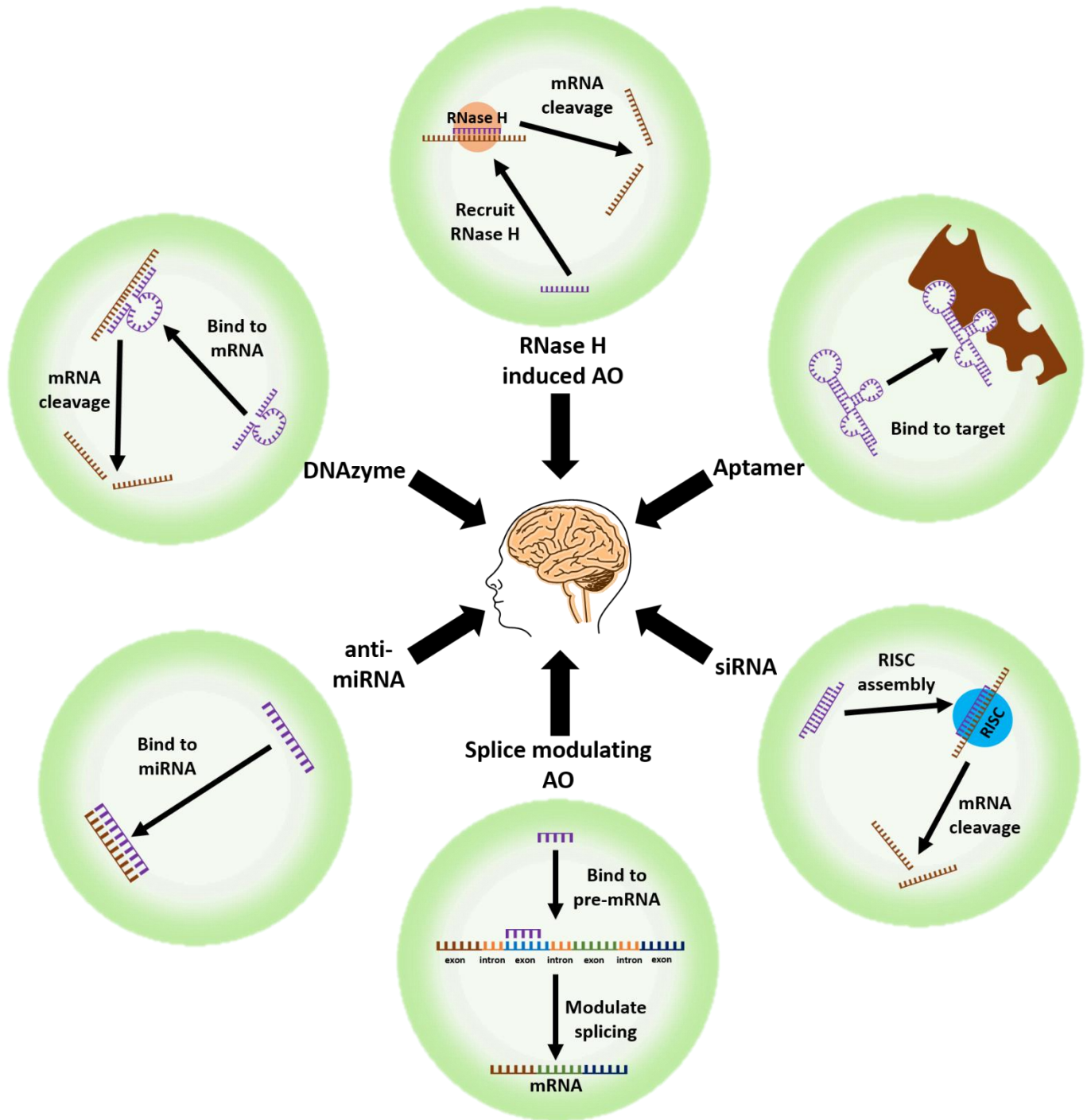
Figure 3.3   Nucleic acid therapeutic strategies. mRNA: messenger RNA; RNase H: ribonuclease H; siRNA: small interfering RNA; RISC: RNA induced silencing complex; AO: antisense oligonucleotide; antimiR: anti-microRNA; miRNA mimic: microRNA mimic

3.2.1 Antisense oligonucleotides

A classical nucleic acid approach to controlling the expression of proteins is to use AOs, short single-stranded (ss) synthetic oligonucleotides, that can precisely target an mRNA transcript to regulate expression of the encoded protein. Antisense mechanisms include RNase H recruitment and cleavage of mRNA, modulation of splicing in pre-mRNA, and steric blockade of either mature or pre-mRNAs (Figure 3.3). RNase H-mediated cleavage involves designing a short DNA oligonucleotide that binds to the target mRNA to form an RNA-DNA duplex (78). The duplex is recognised and cleaved by endogenous RNase H. Antisense oligonucleotides (AOs) that modulate pre-mRNA splicing can be used to repair defective RNA and eliminate disease-associated splice variants (79). Many pre-mRNA transcripts are alternatively spliced to produce different mRNA isoforms, and hence protein, variants (79).

3.2.1.1 APP

Many groups have designed AOs that target APP to reduce APP expression. An early study by Allinquant *et al*. (1995) (80) developed AOs that successfully blocked rat APP synthesis. Administration of the AOs showed that APP played a role in axonal and dendritic growth, and thus in neuronal differentiation (80). ISIS Pharmaceuticals (now Ionis Pharma) have patented (US 2003/0232435 A1) 78 gapmer AOs with 2'-MOE wings and a central DNA region. The AOs target various regions of APP mRNA and inhibit 39–82% of APP protein expression (81).

Kumar and colleagues (2000) (82) developed DNA PS AOs against sequences that correspond to the Aβ region of APP (17-42 amino acids). Administration of the AOs led to improved cognitive function in senescence-accelerated mouse-prone 8 (SAMP8) mice. SAMP8 mice have a natural mutation that leads to APP over-expression, impaired Aβ removal, and loss of memory with increasing age. The AOs that target the mid-Aβ region reduced APP levels by 43–68% in the

amygdala, septum and hippocampus (82). The mice showed improvement in acquisition and retention in the footshock avoidance paradigm, which reversed their deficits in learning and memory (82). The AOs that target sequences that correspond to the region of APP encoding the first 17–30 amino acids of Aβ were the subject of intellectual property protection (83). Banks and colleagues (2001) (84) showed that a radioactively tagged phosphorothioate DNA AO targeting the Aβ region of APP could transit the blood-brain barrier (BBB) of mice to enter the cerebrospinal fluid. When a 100-fold higher dose of the AO was injected into the brain by intracerebroventricular injection, it reversed the learning and memory deficits in SAMP8 mice, possibly through reduced oxidative stress. Poon *et al*. (2005) (85) used proteomics to show that lower Aβ levels result in reduced oxidative stress in brain.

Opazo *et al*. (2006) (86) transfected the AOs described by Kumar and colleagues (2000) (82) into the CTb cell line, a neuronal line from mice that overexpresses APP, and the CNh cell line from normal mice. The AOs resulted in APP knockdown in CTb cells by 36%, 40% and 50% compared with normal CNh cells after 24 h, 48 h and 72 h respectively (86). By 72 h after AO transfection, choline uptake was similar to that in CNh cells, and there was increased choline release in response to glutamate, nicotine and KCl depolarisation, that reached similar levels to those observed in CNh cells. The CTb cells were derived from a Down syndrome mouse model, that shows some learning deficits and cholinergic dysfunction, similar to those found in AD (87). Similarly, Rojas *et al*. (2008) (88) showed that APP overexpression reduced the expression and retrograde transport of nerve growth factor. This reduced nicotine-induced stimulation of $\alpha_3\beta_2$ nicotinic acetylcholine receptor and in consequence lowered intracellular Ca^{2+} responses in CTb cells. The effects of APP overexpression were restored close to normal by treatment with AOs targeting APP expression.

Chauhan and colleagues (2002) (89) designed gapmer AOs composed of 2'-OMe and DNA nucleotides on a PS backbone that targeted the β-secretase cleavage site of APP and found that they reduced brain $A\beta_{40}$ and $A\beta_{42}$ levels in a mouse model of AD. The AOs were delivered intracerebroventricularly and showed rapid uptake and retention for 30 minutes. They efficiently crossed cell membranes into the nuclear and cytoplasmic compartments of neuronal and non-neuronal cells. Chauhan and Siegel (2007) (90) designed two additional AOs targeting the β- and γ-secretase site of APP in the Tg2576 mouse model that expresses APP. The AO targeting the mutated β-secretase site increased soluble APPα by 43% and decreased soluble $A\beta_{40}$ and $A\beta_{42}$ levels by 39%, whereas the AO targeting the γ-secretase site had no effect. The AO targeting β-secretase also inhibited acetylcholinesterase activity, increasing acetylcholine by five-fold in cortex compared with controls.

Erickson *et al*. (2012) (91) peripherally administered an APP AO to SAMP8 mice, that resulted in a 30% decrease in APP levels but no change in soluble Aβ levels. The treated mice showed improved memory. They also showed (92) that AO-mediated APP knockdown in Tg2576 mouse brains reduced cytokine expression and improved learning and memory. Attenuating APP overexpression may improve learning and memory by reducing inflammation (also implicated in AD pathology).

3.2.1.2 BACE1

Yan *et al*. (1999) (93) developed two AOs that target β-secretase aspartyl protease and found that they reduced the release of $A\beta_{40}$ and $A\beta_{42}$ by 50–80%. Vassar and colleagues (1999) (94) also used AOs that target β-secretase to reduce $A\beta_{40}$ and $A\beta_{42}$ production by around 30%. These studies showed that β-secretase is important for the production of $A\beta_{40}$ and $A\beta_{42}$ and highlighted BACE1 as an important target for AD. Wolfe *et al*. (95) designed splice-modulating AOs to target *BACE1*

since alternatively spliced transcript variants at exons 2 and 3 do not show β-secretase activity. The AOs reduced Aβ production significantly in cells without altering total *BACE1* mRNA.

3.2.1.3 Presenilin 1 (PSEN1)

Refolo *et al.* (1999) (96) found that AOs targeting *PSEN1* in a human cell line reduced PSEN1 holoprotein by 80% 12 days after treatment and by 90 % after 14 days. The reduced PSEN1 holoprotein was correlated with a two-fold increase in $A\beta_{42}$ levels. Grilli *et al.* (2000) (97) found that primary hippocampal neurons overexpressing mutant PSEN1 were vulnerable to excitotoxic and hypoxia-hypoglycemic damage and increased cell death. They designed two phosphorothioates AOs targeting *Psen1* in wild type mice. In contrast to Refolo *et al.* (1999) (96) they found that lower PSEN1 expression reduced cell death and provided neuroprotection (97). Fiorini *et al*. (2013) (98) administered AOs targeting *Psen1* to aged SAMP8 mice that then showed reduced brain oxidative stress biomarkers. In the T-maze foot shock avoidance and novel object recognition tests the mice showed a reversal of learning and memory deficits.

3.2.1.4 Tau

Tau proteins come from alternative splicing of the *MAPT* gene transcript. Caceres *et al*. (1990) (99) targeted an AO to the 5' end of the *Mapt* gene, in the region before the start codon, and showed strong inhibition of neurite elongation in primary rat neurons. Immunoblotting revealed that the tau protein level was reduced in AO-treated mice but not in control mice. The effect of AO treatment on cognition remains to be assessed. DeVos *et al.* (2013) (100) screened 80 AOs targeting *Mapt* and selected the three that showed the best knockdown of *Mapt* to test *in vivo*. The latter reduced *Mapt* mRNA levels by more than 75%. The best AO was selected for further testing in mice; it lowered brain *Mapt* mRNA and protein significantly in a dose-dependent manner. Behavioural impacts and neurotoxicity were not measured. Alternate splicing of the *MAPT* mRNA

at exons 2,3, and 10 results in tau proteins containing three of four microtubule binding repeats and are referred to as Tau3R and Tau4R respectively (101). The ratio of Tau3R and Tau4R transcripts is one in the human adult brain (101). Mutations that disrupt the Tau3R and Tau4R transcript ratio result in destabilising microtubules and therefore result in tauopathies like frontotemporal dementia and parkinsonism (101). Kalbfuss *et al.* (2001) (102) developed splice-modulating AOs modified with 2'-OMe nucleotides to target the tau exon 10 splice junctions to reduce exon 10 exclusion. Exclusion of exon 10 increases the ratio of tau proteins lacking the microtubule-binding domain with the consequence, that the microtubule cytoskeleton becomes destabilised as occurs in frontotemporal dementia and parkinsonism.

Peacey *et al.* (2012) (103) designed bipartite AOs that bound to the hairpin structure at the boundary between exon 10 and intron 10 of tau to inhibit exon 10 splicing, reversing the effect of disease-causing mutations in cells. Liu *et al.* (2014) (104) developed a small-molecule (mitoxantrone) conjugated to a bipartite AO that binds to the *MAPT* RNA hairpin structure. The conjugate also inhibited exon 10 splicing in cell-free conditions more effectively than mitoxantrone or the bipartite AO alone, but induced cytotoxicity in cells. The same group used a PNA-modified bipartite AO conjugated to mitoxantrone that inhibited *MAPT* splicing but was also cytotoxic (95).

Sud *et al.* (2014) (105) developed PMOs to modulate the splicing of *MAPT* and tau expression. The AOs were designed to target sequences at the donor and acceptor splice sites, the splicing branch points, and splicing enhancers and inhibitors to induce exon skipping (105). Exons 0, 1, 4, 5, 7, 9 and 10 were targeted (105). Exons 1, 4, 5, 7 and 9 are found in all six isoforms of *MAPT* while exon 10 is present in only three of the six isoforms (105). Of the 31 AOs tested, AO E1.4 targeting the splice donor site at the exon 1 intron 1 junction reduced *MAPT* mRNA expression by

50% (105). The other AOs effective in this region were a combination of AOs that targeted the splice donor and acceptor sites and the start codon (105). AO E5.3 targeted the splice donor site at the exon 5 intron 5 junction and reduced total *MAPT* mRNA expression by 29–46% (105). It also reduced tau protein level by 58–62% (105). The resulting transcript was missing exons 4 to exon 7 using the normal splice sites. AO E7.7 targeted the exon 7 splice donor site; and it reduced *MAPT* mRNA expression by 30% and tau protein levels by 67% (105). E5.3 injected into mice *in vivo* produced lower *Mapt* mRNA levels than in non-injected regions (105).

3.2.1.5 GSK-β

Farr *et al*. (2014) (106) showed that a phosphorothioated AO that targets *GSK-3β* decreased GSK-3β protein levels in the cortex of SAMP8 mice. There were improvements in learning and memory, reduced oxidative stress, increased levels of the antioxidant transcription factor nuclear factor erythroid-2 related factor 2, and decreased tau phosphorylation.

3.2.1.6 Acetylcholinesterase (AChE)

Fu *et al.* (2005) (107) found that AOs targeted to human *AChE* mRNA reduced AChE activity in an AD mouse model after 8 h; the effect lasted till 42 h. The lower enzymic activity was accompanied by an improvement in behavioural tasks, that showed increased memory retention and improved water maze performance (shorter swimming time).

3.2.1.7 Apolipoprotein E receptor 2 (ApoER2)

Apolipoprotein E receptor 2 (ApoER2) may be a primary risk factor for late-onset AD (108, 109). Dysregulation of *ApoER2* splicing may result in impaired synaptic homeostasis. Cerebral injection of mice with AOs targeting the adjacent introns enhanced exon 19 inclusion, an effect that persisted for up to 6 months (109). The mice showed improvement in Aβ-induced cognitive defects. It was postulated that the AOs bind to the splicing factor SRF1 to reduce its expression and increase the

inclusion of exon 19, thereby increasing the level of the active form of ApoER2 to enhance NMDA receptor phosphorylation.

3.2.2 Small interfering RNA (siRNA)

These are short synthetic double-stranded (ds) RNA oligonucleotides that target complementary mRNA and silence gene expression through the assembly of the RNA-induced silencing complex (RISC) (Figure 3.3) (78, 110). Chemical modifications can be introduced into the siRNA to increase its stability against nucleases and increase its selectivity for the target (Figure 1.5).

3.2.2.1 APP

Miller and colleagues (2004) (111) found that siRNAs targeting the Swedish mutant in *APP* that causes a familial form of AD silenced the expression of mutant alleles in cells. The siRNAs were designed to ensure that they bound specifically to the mutant alleles and not the healthy allele. The mutation was placed in the central region of the siRNA duplex to achieve high silencing efficiency.

3.2.2.2 BACE1

McSwiggen and colleagues (2002) (112) patented 325 siRNAs that target *BACE* (NCBI ID: NM_012104). The patent covers sequences of various chemically modified siRNAs that include 2'-deoxy, 2'-F and 2'-OMe pyrimidine and purine nucleotides, phosphorothioate internucleotide linkages and inverted deoxy abasic caps. Four of the siRNAs reduced BACE1 expression by 40–90% at 25 nM concentration, but there was no data on whether this altered $A\beta_{40}$ and $A\beta_{42}$ expression. Basi *et al*. (2003) (113) made an siRNA that reduced the *BACE1* mRNA level by 50% and BACE protein by more than 90% and decreased the secretion of $A\beta$ peptide without affecting BACE2 expression, indicating specificity for BACE1. Kao *et al.* (2004) (114) also designed siRNAs, where two of the siRNAs reduced *BACE1* mRNA by more than 90% and $A\beta$ production

by 36–41%. Pretreatment of neurons with the siRNA increased neuroprotection against hydrogen peroxide-induced oxidative stress. Modarresi *et al.* (2011) (115) injected LNA-modified siRNAs targeting *Bace1* antisense transcripts into the third ventricle of Tg-19959 mice to downregulate *Bace1* and *Bace1* antisense transcripts, which led to lower BACE1 protein levels and lower Aβ production and aggregation in the brain. Notably, Cai *et al.* (2012) (116) ENREF_140showed that siRNAs targeting *Bace1* inhibited its expression in mice and increased choroidal neovascularisation: BACE1 is also expressed in the neural retina and in *in vitro* and *in vivo* angiogenesis. Although BACE1 inhibition may be therapeutically beneficial in AD, this strategy may contribute to retinal pathologies and exacerbate conditions such as age-related macular degeneration.

3.2.2.3 Heterogeneous nuclear ribonucleoprotein H

A G-rich region in exon 3 of *BACE1* may form a G-quadruplex structure and recruit a splicing regulator, heterogeneous nuclear ribonucleoprotein H, that regulates splicing to increase the generation of the BACE1 501 isoform (501 kDa protein). Fisette *et al.* (2012) (117) reported that siRNA and short hairpin RNA candidates that target heterogeneous nuclear ribonucleoprotein H reduced its expression and thereby decreased BACE1 501 isoform levels and Aβ production.

3.2.3 AntimiRs and miRNA mimics

miRNAs are short non-coding RNAs that regulate protein expression post-transcriptionally. miRNA mimics can modulate RNA and protein expression by acting in the same way as their endogenous miRNA counterparts. AntimiRs can modulate RNA and protein expression by inhibiting endogenous miRNA (Figure 3.3). Micro RNAs (miRNAs) generally silence gene expression by translational repression and/or mRNA degradation (118, 119). miRNAs are first transcribed by RNA polymerases II or III to form long primary miRNA with a 5' CAP and a

poly(A) tail (119-121). These are then processed in the nucleus into short 70-nucleotide hairpin structures called precursor miRNAs (pre-miRNA) by the microprocessor complex (119-121). The pre-miRNAs are exported to the cytoplasm by Exportin 5 and processed by Dicer into double-stranded miRNA duplexes, that are approximately 22 nucleotides long (119-121).

3.2.3.1 BACE1

An endogenous non-coding *BACE1* antisense transcript stabilises the BACE1 transcript and may upregulate BACE1 in AD. *BACE1* antisense binds to *BACE1* at the miR-485-5p binding site and suppresses BACE1 expression. Faghihi *et al.* (122) found that LNA-antimiRs that target miR-485-5p decreased miRNA-induced suppression of BACE1 and increased *BACE1* antisense expression. Hebért *et al.* (2008) (123) showed that miR-29a/b-1 cluster was significantly reduced in sporadic AD patients and correlated with increased BACE1 expression and Aβ generation, and therefore may be a potential target for miRNA mimics as a therapeutic strategy for AD.

3.2.3.2 Tau

MiR-34a reduces endogenous *MAPT*/tau expression at both the mRNA and protein level in M17D cells by binding to the 3' UTR region of *MAPT* (95), whereas miR-34c levels are elevated in the hippocampus of AD patients and mouse AD models (124). Wolfe *et al.* (2014) (95) used LNA antimiRs to inhibit miR-34a, -34b and -34c and found increased tau expression. Zovolis *et al.* (2011) (124) found that an antimiR that targets miR-34c rescued learning in mouse models.

3.2.3.3 Acetyl-CoA acyltransferase

Acetyl-CoA acyltransferase has a role in lipid metabolism and has been implicated in the pathogenesis of AD. Murphy *et al.* (125) inhibited Acetyl-CoA acyl transferase using an artificial miRNA to reduce Aβ plaque burden and improve cognition in a mouse model of AD. The miRNA also reduced full-length human APP levels.

3.2.3.4 Brain-derived neurotrophic factor:

Brain-derived neurotrophic factor regulates synaptic plasticity and memory and is decreased in AD brains (126-128), while miR-206 suppresses brain-derived neurotrophic factor levels and memory function in AD mice (129). Lee *et al.* (129) injected an anti-miR candidate AM-206 that targets miR-206 into the third ventricle of Tg2576 mice. It increased brain levels of brain-derived neurotrophic factor, enhanced hippocampal synaptic density, neurogenesis, and memory. Intranasally administered AM-206 also reached the brain and had similar effects to the injected AM-206.

3.2.4 DNAzymes/Ribozymes as therapeutic candidates for AD

DNAzymes and ribozymes have been previously discussed in Chapter 2.

3.2.4.1 BACE1

Nawrot *et al.* (130) designed RNA-cleaving hammerhead ribozymes that downregulated BACE1 mRNA expression by more than 90% in HEK293 and SH-SY5Y cells and reduced $A\beta_{40}$ and $A\beta_{42}$ production by more than 80%. They also showed that a DNAzyme with the 10–23 catalytic loop reduced BACE mRNA expression by 70%. However, whether the reduced BACE mRNA expression leads to reduced $A\beta$ production is unknown and requires validation.

3.2.5 Nucleic acid aptamers

Aptamers are short single-stranded RNA or DNA oligonucleotides with unique three-dimensional structure that bind to targets with high affinity and specificity. Aptamers can be developed against a variety of targets ranging from small molecules to complex proteins over whole cells. Aptamers can be used for therapeutic, diagnostic (biosensors and molecular imaging), and targeted drug delivery applications. They are typically selected from large DNA and RNA oligonucleotide

libraries through a process called Systematic Evolution of Ligands by EXponential enrichment (SELEX) (131, 132).

3.2.5.1 Aβ

Ylera *et al.* (133) were the first to report novel RNA aptamers that bound to $Aβ_{1-40}$ fibrils with high affinity (29–48 nM). Bunka *et al.* (134) made aptamers against amyloid-like fibrils from $β_2$-microglobulin that bound to the target with high affinity but also bound to other amyloid fibrils including, but not confined to, those found in dialysis-related amyloidosis patients. Rahimi *et al.* (135) also developed RNA aptamers against Aβ fibrils, and these similarly interacted with other amyloidogenic proteins by binding to a common β-sheet motif. They bound to fibrils with ≥15-fold higher sensitivity than thioflavin-T, suggesting that aptamers might be applicable as diagnostic tools for AD. Takahashi *et al.* (136) isolated two RNA aptamers, N2 and E2, that bound to monomeric $Aβ_{40}$ with dissociation constants of 21.6 and 10.9 µM respectively. Though the affinities were quite low for clinical use, enzyme-linked immunosorbent assay (ELISA) showed that they could inhibit Aβ aggregation efficiently. When conjugated to AuNP gold nanoparticles, N2 and E2 bound to both Aβ monomers and oligomers. Mathew *et al.* (137) showed that the N2 aptamer conjugated to curcumin-polymer nanoparticles enhanced binding to, and disaggregated, amyloid plaques, that were then cleared by phagocytosis. The study targeted peripheral amyloid as peripheral organs may also generate amyloid proteins, which have also been implicated in AD. Targeting peripheral amyloid is easier than targeting the CNS due to the challenges of brain delivery of aptamers.

Farrar *et al.* (138) developed a fluorescently tagged aptamer that bound to Aβ oligomers in both AD and transgenic mouse brain tissue. The aptamer may be useful for Aβ imaging, which has diagnostic implications. Similarly, Babu and colleagues (139) developed an aptamer complexed

with ruthenium that binds to and inhibits the formation of, Aβ oligomers. The aptamer-ruthenium interaction increases luminescence intensity, which is reduced when the aptamer binds to Aβ monomer or oligomers.

3.2.5.2 BACE1

Rentmeister *et al.* (140) made an RNA aptamer that binds to the short cytoplasmic tail of BACE1. The aptamer is a good research tool to investigate the biological function of the cytoplasmic tail without interfering with BACE1 transport and localisation. Liang *et al.* (141) developed two DNA aptamers, A1 and A4, that bind to the extracellular domain of BACE1 with high affinity (K_d 15–69 nM) and specificity, showing similar affinities to the anti-BACE1 antibody. *In vitro*, APP Swedish mutant cells treated with A1 showed lower $Aβ_{40}$ and $Aβ_{42}$ levels than control cells. Soluble APPβ expression decreased with A1 treatment compared with untreated controls.

3.2.5.3 Tau

Kim et al. (142) used recombinant his-tagged tau40 to select aptamers from an RNA library through SELEX. Twelve rounds of selection produced a tau-1 aptamer, which represented ~76% of identified aptamers, that reduced the levels of oligomeric tau (by ~94%) *in vitro* in a dose-dependent manner. However, it could not de-oligomerize pre-existing tau oligomers and had no effect on tau degradation. The aptamer bound to tau protein and inhibited its oligomerisation, unlike control aptamers. Primary neurons treated with tau-1 aptamer showed less cytotoxicity than controls but no difference in membrane integrity or viability; there was little effect on normal tau function. Primary rat cortical neurons administered tau oligomers and treated with tau-1 aptamers showed significantly less oligomeric tau phosphorylation at Ser199/202, but there was no effect on monomeric tau. Extracellular tau oligomers also stress neighbouring neurons. Tau-1 aptamers can prevent or reverse cytotoxicity mediated by tau oligomerisation both in a non-neuronal cell

line and in primary rat cortical neurons. Unfortunately, the tau-1 aptamers isolated by Kim et al. bound only to one of the six isoforms of tau. Therefore, the effects of tau-1 aptamers observed in mice may not translate clinically, because six isoforms are prone to aggregation and implicated in neurodegeneration. To be successful clinically, the aptamers must be able to cross the BBB and the neuronal cell membrane, and disaggregate the neurofibrillary tangles after binding (143). Kim et al. (144) reported a DNA aptamer-antibody sandwiched to the tau-381 isoform that detected tau in human plasma at femtomolar concentrations by surface plasmon resonance.

3.2.5.4 The ubiquitin-proteasome system

Lee *et al*. (145) developed an aptamer against USP14, an enzyme that delays protein degradation by the ubiquitin-proteasome system. Recombinant USP14 was incubated with a random RNA library for SELEX. Three aptamers, USP14-1, USP14-2 and USP-14-3, were identified, all of which bound to USP14 with high affinity. USP14-3 showed the strongest inhibition of deubiquitination, which may be due to its ability to bind both USP14 and UCH37. UCH37 is a protein that also slows protein degradation in the proteasome. The aptamers have yet to be tested in mice for their effect on tau oligomerisation and degeneration.

3.2.5.5 Prion protein:

Mashima *et al.* (146) isolated aptamers against bovine prion protein by SELEX that may have therapeutic potential in prion diseases and AD. The Aβ oligomers bind to the prion protein to block long-term potentiation and may mediate Aβ oligomer-induced synaptic dysfunction.

3.3 Conclusions and Future Perspectives

Nucleic acid approaches offer great promise for developing novel therapeutics for AD, a complex neurodegenerative disease with several pathological features. Confounding factors include genetic

factors, metabolic disorders including high cholesterol levels, insulin resistance due to impaired glucose metabolism, and dysfunction in various molecular pathways. Existing therapies only treat AD symptoms, not the underlying molecular causes. Although many drug molecules have shown success in cell and animal models, this effect often cannot be replicated in human trials. There is an unmet need for better theranostic strategies. The drug Nusinersen, recently approved by the FDA for spinal muscular atrophy, shows that nucleic acids have the potential for the treatment of neurological diseases, including AD. Their efficacy in targeting several pathways that underlie AD highlights their potential to be developed as novel therapeutics for AD.

3.4 References

1.   Prince M, Comas-Herrera A, Knapp M, Guerchet M, Karagiannidou M. World Alzheimer Report 2016: Improving healthcare for people living with dementia. London, UK: London School of Economics and Political Sciences; 2016 September 2016.

2.   Alzheimers Association Update. Alzheimers Dement (Amst). 2015;11(1):104–5.

3.   Birks JS. Cholinesterase inhibitors for Alzheimer's disease. Cochrane Database Syst Rev. 2006(1).

4.   Olivares D, Deshpande VK, Shi Y, Lahiri DK, Greig NH, Rogers JT, et al. *N*-methyl D-aspartate (NMDA) receptor antagonists and memantine treatment for Alzheimer's disease, vascular dementia and Parkinson's disease. Curr Alzheimer Res. 2012;9(6):746–58.

5.   Robinson SW, Fernandes M, Husi H. Current advances in systems and integrative biology. Comput Struct Biotechnol J. 2014;11(18):35–46.

6.   Shea Y-F, Chu L-W, Chan AO-K, Ha J, Li Y, Song Y-Q. A systematic review of familial Alzheimer's disease: Differences in presentation of clinical features among three mutated genes

and potential ethnic differences. Journal of the Formosan Medical Association. 2016;115(2):67-75.

7.   Wu L, Rosa-Neto P, Hsiung G-YR, Sadovnick AD, Masellis M, Black SE, et al. Early-Onset Familial Alzheimer's Disease (EOFAD). Canadian Journal of Neurological Sciences / Journal Canadien des Sciences Neurologiques. 2012;39(4):436-45.

8.   Weggen S, Beher D. Molecular consequences of amyloid precursor protein and presenilin mutations causing autosomal-dominant Alzheimer's disease. Alzheimer's Research & Therapy. 2012;4(2):9.

9.   O'Brien RJ, Wong PC. Amyloid Precursor Protein Processing and Alzheimer's Disease. Annu Rev Neurosci. 2011;34(1):185-204.

10.   Raghavan N, Tosto G. Genetics of Alzheimer's Disease: the Importance of Polygenic and Epistatic Components. Current Neurology and Neuroscience Reports. 2017;17(10).

11.   Haass C, Selkoe DJ. Soluble protein oligomers in neurodegeneration: lessons from the Alzheimer's amyloid β-peptide. Nat Rev Mol Cell Biol. 2007;8(2):101–12.

12.   Selkoe DJ. Alzheimer's disease: genes, proteins, and therapy. Physiol Rev. 2001;81(2):741–66.

13.   Blennow K, de Leon MJ, Zetterberg H. Alzheimer's disease. The Lancet. 2006;368(9533):387–403.

14.   Haass C, Selkoe DJ. Cellular processing of beta-amyloid precursor protein and the genesis of amyloid β-peptide. Cell. 1993;75(6):1039–42.

15.   Selkoe DJ. Translating cell biology into therapeutic advances in Alzheimer's disease. Nature. 1999;399:A23–A31.

16.   Wilquet V, De Strooper B. Amyloid-β precursor protein processing in neurodegeneration. Curr Opin Neurol. 2004;14(5):582–8.

17.   Selkoe DJ. Normal and abnormal biology of the β-amyloid precursor protein. Annu Rev Neurosci. 1994;17(1):489–517.

18.   Tanzi RE, Bertram L. Twenty years of the Alzheimer's disease amyloid hypothesis: a genetic perspective. Cell. 2005;120(4):545–55.

19.   Hardy JA, Higgins GA. Alzheimer's disease: the amyloid cascade hypothesis. Science. 1992;256(5054):184-5.

20.   Lahiri DK, Farlow MR, Greig NH, Sambamurti K. Current drug targets for Alzheimer's disease treatment. Drug Dev Res. 2002;56(3):267–81.

21.   Palop JJ, Mucke L. Amyloid-β-induced neuronal dysfunction in Alzheimer's disease: from synapses toward neural networks. Nat Neurosci. 2010;13(7):812–8.

22.   Sindi IA, Tannenberg RK, Dodd PR. Role for the neurexin-neuroligin complex in Alzheimer's disease. Neurobiol Aging. 2014;35(4):746–56.

23.   Ondrejcak T, Klyubin I, Hu N-W, Barry AE, Cullen WK, Rowan MJ. Alzheimer's disease amyloid β-protein and synaptic function. Neuromolecular Med. 2010;12(1):13–26.

24.   Danysz W, Parsons CG. Alzheimer's disease, β-amyloid, glutamate, NMDA receptors and memantine–searching for the connections. Br J Pharmacol. 2012;167(2):324–52.

25.   Schelterns P, Feldman H. Treatment of Alzheimer's disease; current status and new perspectives. Lancet Neurol. 2003;2(9):539–47.

26.   Ferreira ST, Clarke JR, Bomfim TR, De Felice FG. Inflammation, defective insulin signaling, and neuronal dysfunction in Alzheimer's disease. Alzheimers Dement (Amst). 2014;10(1):S76–S83.

27.   Hoyer S. Glucose metabolism and insulin receptor signal transduction in Alzheimer disease. Eur J Pharmacol. 2004;490(1):115–25.

28.   Maulik M, Westaway D, Jhamandas J, Kar S. Role of cholesterol in APP metabolism and its significance in Alzheimer's disease pathogenesis. Mol Neurobiol. 2013;47(1):37–63.

29.   Lee VM, Goedert M, Trojanowski JQ. Neurodegenerative tauopathies. Annu Rev Neurosci. 2001;24(1):1121–59.

30.   Iqbal K, Alonso AdC, Chen S, Chohan MO, El-Akkad E, Gong C-X, et al. Tau pathology in Alzheimer disease and other tauopathies. Biochim Biophys Acta Mol Bas Dis. 2005;1739(2):198–210.

31.   Medina M, Avila J. New perspectives on the role of tau in Alzheimer's disease. Implications for therapy. Biochem Pharmacol. 2014;88(4):540–7.

32.   Hernandez F, Avila J. Tauopathies. Cell Mol Life Sci. 2007;64(17):2219–33.

33.   Brandt R, Hundelt M, Shahani N. Tau alteration and neuronal degeneration in tauopathies: mechanisms and models. Biochim Biophys Acta Mol Bas Dis. 2005;1739(2):331–54.

34.   Hart GW, Slawson C, Ramirez-Correa G, Lagerlof O. Cross talk between *O*-GlcNAcylation and phosphorylation: roles in signaling, transcription, and chronic disease. Annu Rev Biochem. 2011;80:825–58.

35.   Feldman H, Gauthier S, Hecker J, Vellas B, Emir B, Mastey V, et al. Efficacy of donepezil on maintenance of activities of daily living in patients with moderate to severe Alzheimer's disease and the effect on caregiver burden. J Am Geriatr Soc. 2003;51(6):737–44.

36.   McKeith I, Del Ser T, Spano P, Emre M, Wesnes K, Anand R, et al. Efficacy of rivastigmine in dementia with Lewy bodies: a randomised, double-blind, placebo-controlled international study. The Lancet. 2000;356(9247):2031–6.

37.   Raskind M, Peskind E, Wessel T, Yuan W, Galantamine USA Study Group. Galantamine in AD A 6-month randomized, placebo-controlled trial with a 6-month extension. Neurology. 2000;54(12):2261–8.

38.   Tariot PN, Farlow MR, Grossberg GT, Graham SM, McDonald S, Gergel I, et al. Memantine treatment in patients with moderate to severe Alzheimer disease already receiving donepezil: a randomized controlled trial. JAMA. 2004;291(3):317–24.

39.   Wang X, Wang W, Li L, Perry G, Lee H-g, Zhu X. Oxidative stress and mitochondrial dysfunction in Alzheimer's disease. Biochim Biophys Acta Mol Bas Dis. 2014;1842(8):1240–7.

40.   Pimplikar SW. Neuroinflammation in Alzheimer's disease: from pathogenesis to a therapeutic target. J Clin Immunol. 2014;34(1):64–9.

41.   Freiherr J, Hallschmid M, Frey II WH, Brünner YF, Chapman CD, Hölscher C, et al. Intranasal insulin as a treatment for Alzheimer's disease: a review of basic research and clinical evidence. CNS Drugs. 2013;27(7):505–14.

42.   Ribarič S. The rationale for insulin therapy in Alzheimer's disease. Molecules. 2016;21(6):E689.

43.   Mangialasche F, Solomon A, Winblad B, Mecocci P, Kivipelto M. Alzheimer's disease: clinical trials and drug development. Lancet Neurol. 2010;9(7):702–16.

44.   Karran E. Current status of vaccination therapies in Alzheimer's disease. J Neurochem. 2012;123(5):647–51.

45.   St George-Hyslop PH, Morris JC. Will anti-amyloid therapies work for Alzheimer's disease? The Lancet. 2008;372(9634):180–2.

46.   Ballard C, Gauthier S, Corbett A, Brayne C, Aarsland D, Jones E. Alzheimer's disease. The Lancet. 2011;377(9770):1019–31.

47.   Galimberti D, Scarpini E. Progress in Alzheimer's disease. J Neurol. 2012;259(2):201–11.

48.   Santa-Maria I, Hernández F, Del Rio J, Moreno FJ, Avila J. Tramiprosate, a drug of potential interest for the treatment of Alzheimer's disease, promotes an abnormal aggregation of tau. Mol Neurodegener. 2007;2:17.

49.   Aisen PS, Saumier D, Briand R, Laurin J, Gervais F, Tremblay P, et al. A Phase II study targeting amyloid-beta with 3APS in mild-to-moderate Alzheimer disease. Neurology. 2006;67(10):1757–63.

50.   Gervais F, Chalifour R, Garceau D, Kong X, Laurin J, McLaughlin R, et al. Glycosaminoglycan mimetics: a therapeutic approach to cerebral amyloid angiopathy. Amyloid. 2001;8 Suppl 1:28–35.

51.   Bilikiewicz A, Gaus W. Colostrinin (a naturally occurring, proline-rich, polypeptide mixture) in the treatment of Alzheimer's disease. J Alzheimers Dis. 2004;6(1):17–26.

52.   Leszek J, Inglot AD, Janusz M, Lisowski J, Krukowska K, Georgiades JA. Colostrinin: a proline-rich polypeptide (PRP) complex isolated from ovine colostrum for treatment of

Alzheimer's disease. A double-blind, placebo-controlled study. Archivum Immunologiæ et Therapiæ Experimentalis. 1999;47(6):377–85.

53.   Popik P, Bobula B, Janusz M, Lisowski J, Vetulani J. Colostrinin, a polypeptide isolated from early milk, facilitates learning and memory in rats. Pharmacol Biochem Behav. 1999;64(1):183–9.

54.   Townsend KP, Praticò D. Novel therapeutic opportunities for Alzheimer's disease: focus on nonsteroidal anti-inflammatory drugs. FASEB J. 2005;19(12):1592–601.

55.   Gilman S, Koller M, Black RS, Jenkins L, Griffith SG, Fox NC, et al. Clinical effects of Aβ immunization (AN1792) in patients with AD in an interrupted trial. Neurology. 2005;64(9):1553–62.

56.   Salloway S, Sperling R, Fox NC, Blennow K, Klunk W, Raskind M, et al. Two phase 3 trials of bapineuzumab in mild-to-moderate Alzheimer's disease. N Engl J Med. 2014;370(4):322–33.

57.   Doody RS, Thomas RG, Farlow M, Iwatsubo T, Vellas B, Joffe S, et al. Phase 3 trials of solanezumab for mild-to-moderate Alzheimer's disease. N Engl J Med. 2014;370(4):311–21.

58.   Relkin N. Clinical trials of intravenous immunoglobulin for Alzheimer's disease. J Clin Immunol. 2014;34(1):74–9.

59.   Moreth J, Mavoungou C, Schindowski K. Passive anti-amyloid immunotherapy in Alzheimer's disease: What are the most promising targets? Immunity and Ageing. 2013;10(1):18.

60.   McGeer PL, McGeer EG. The amyloid cascade-inflammatory hypothesis of Alzheimer disease: implications for therapy. Acta Neuropathol. 2013;126(4):479–97.

61.   Kukar T, Prescott S, Eriksen JL, Holloway V, Murphy MP, Koo EH, et al. Chronic administration of R-flurbiprofen attenuates learning impairments in transgenic amyloid precursor protein mice. BMC Neurosci. 2007;8:54.

62.   Galasko DR, Graff-Radford N, May S, Hendrix S, Cottrell BA, Sagi SA, et al. Safety, tolerability, pharmacokinetics, and Aβ levels after short-term administration of R-flurbiprofen in healthy elderly individuals. Alzheimer Disease and Associated Disorders. 2007;21(4):292–9.

63.   Wilcock GK, Black SE, Hendrix SB, Zavitz KH, Swabb EA, Laughlin MA, et al. Efficacy and safety of tarenflurbil in mild to moderate Alzheimer's disease: a randomised phase II trial. The Lancet Neurology. 2008;7(6):483–93.

64.   Siemers ER, Quinn JF, Kaye J, Farlow MR, Porsteinsson A, Tariot P, et al. Effects of a γ-secretase inhibitor in a randomized study of patients with Alzheimer disease. Neurology. 2006;66(4):602–4.

65.   Coric V, Salloway S, van Dyck C, Kerselaers W, Kaplita S, Curtis C, et al. A phase II study of the γ-secretase inhibitor avagacestat (BMS-708163) in predementia Alzheimer's disease. Alzheimers Dement (Amst). 2013;9(4):P283.

66.   Kennedy ME, Stamford AW, Chen X, Cox K, Cumming JN, Dockendorf MF, et al. The BACE1 inhibitor verubecestat (MK-8931) reduces CNS β-amyloid in animal models and in Alzheimer's disease patients. Science Translational Medicine. 2016;8(363):363ra150.

67.   Miller BW, Willett KC, Desilets AR. Rosiglitazone and pioglitazone for the treatment of Alzheimer's disease. Ann Pharmacother. 2011;45(11):1416–24.

68.   Wischik CM, Edwards PC, Lai RY, Roth M, Harrington CR. Selective inhibition of Alzheimer disease-like tau aggregation by phenothiazines. Proc Natl Acad Sci USA. 1996;93(20):11213–8.

69.   Martinez A, Gil C, Perez DI. Glycogen synthase kinase 3 inhibitors in the next horizon for Alzheimer's disease treatment. Int J Alzheimers Dis. 2011;2011:280502.

70.   Lovestone S, Boada M, Dubois B, Hüll M, Rinne JO, Huppertz H-J, et al. A phase II trial of tideglusib in Alzheimer's disease. J Alzheimers Dis. 2015;45(1):75–88.

71.   Mecocci P, Polidori MC. Antioxidant clinical trials in mild cognitive impairment and Alzheimer's disease. Biochim Biophys Acta Mol Bas Dis. 2012;1822(5):631–8.

72.   Ray B, Lahiri DK. Neuroinflammation in Alzheimer's disease: different molecular targets and potential therapeutic agents including curcumin. Curr Opin Pharmacol. 2009;9(4):434–44.

73.   Wyss-Coray T. Inflammation in Alzheimer disease: driving force, bystander or beneficial response? Nat Med. 2006;12(9):1005–15.

74.   Heneka MT, Carson MJ, El Khoury J, Landreth GE, Brosseron F, Feinstein DL, et al. Neuroinflammation in Alzheimer's disease. Lancet Neurol. 2015;14(4):388–405.

75.   Yarchoan M, Arnold SE. Repurposing diabetes drugs for brain insulin resistance in Alzheimer disease. Diabetes. 2014;63(7):2253–61.

76.   Casserly I, Topol EJ. Convergence of atherosclerosis and Alzheimer's disease: inflammation, cholesterol, and misfolded proteins. The Lancet. 2004;363(9415):1139–46.

77.   Hall AM, Roberson ED. Mouse models of Alzheimer's disease. Brain research bulletin. 2012;88(1):3-12.

78.   Bennett CF, Swayze EE. RNA targeting therapeutics: molecular mechanisms of antisense oligonucleotides as a therapeutic platform. Annu Rev Pharmacol Toxicol. 2010;50:259–93.

79.   Kole R, Krainer AR, Altman S. RNA therapeutics: beyond RNA interference and antisense oligonucleotides. Nat Rev Drug Discov. 2012;11(2):125–40.

80.   Allinquant B, Hantraye P, Mailleux P, Moya K, Bouillot C, Prochiantz A. Downregulation of amyloid precursor protein inhibits neurite outgrowth *in vitro*. J Cell Biol. 1995;128(5):919–27.

81.   Dobie K, inventor; Scios Inc., Fremont, CA (US), assignee. Antisense modulation of amyloid β protein precursor expression. US2007.

82.   Kumar VB, Farr SA, Flood JF, Kamlesh V, Franko M, Banks WA, et al. Site-directed antisense oligonucleotide decreases the expression of amyloid precursor protein and reverses deficits in learning and memory in aged SAMP8 mice. Peptides. 2000;21(12):1769–75.

83.   Kumar VB, inventor; St. Louis University, St. Louis, MO (US), assignee. Antisense modulation of amyloid β protein expression. US2001.

84.   Banks WA, Farr SA, Butt W, Kumar VB, Franko MW, Morley JE. Delivery across the blood-brain barrier of antisense directed against amyloid β: reversal of learning and memory deficits in mice overexpressing amyloid precursor protein. J Pharmacol Exp Ther. 2001;297(3):1113–21.

85.   Poon HF, Farr SA, Banks WA, Pierce WM, Klein JB, Morley JE, et al. Proteomic identification of less oxidized brain proteins in aged senescence-accelerated mice following administration of antisense oligonucleotide directed at the Aβ region of amyloid precursor protein. Brain Res Mol Brain Res. 2005;138(1):8–16.

86.   Opazo P, Saud K, de Saint Pierre M, Cárdenas AM, Allen DD, Segura-Aguilar J, et al. Knockdown of amyloid precursor protein normalizes cholinergic function in a cell line derived from the cerebral cortex of a trisomy 16 mouse: an animal model of Down syndrome. J Neurosci Res. 2006;84(6):1303–10.

87.   Saud K, Arriagada C, Cárdenas AM, Shimahara T, Allen DD, Caviedes R, et al. Neuronal dysfunction in Down syndrome: contribution of neuronal models in cell culture. Journal of Physiology, Paris. 2006;99(2–3):201–10.

88.   Rojas G, Cárdenas AM, Fernández-Olivares P, Shimahara T, Segura-Aguilar J, Caviedes R, et al. Effect of the knockdown of amyloid precursor protein on intracellular calcium increases in a neuronal cell line derived from the cerebral cortex of a trisomy 16 mouse. Exp Neurol. 2008;209(1):234–42.

89.   Chauhan NB. Trafficking of intracerebroventricularly injected antisense oligonucleotides in the mouse brain. Antisense Nucleic Acid Drug Dev. 2002;12(5):353–7.

90.   Chauhan NB, Siegel GJ. Antisense inhibition at the β-secretase-site of β-amyloid precursor protein reduces cerebral amyloid and acetyl cholinesterase activity in Tg2576. Neuroscience. 2007;146(1):143–51.

91.   Erickson MA, Niehoff ML, Farr SA, Morley JE, Dillman LA, Lynch KM, et al. Peripheral administration of antisense oligonucleotides targeting the amyloid-β protein precursor reverses AβPP and LRP-1 overexpression in the aged SAMP8 mouse brain. J Alzheimers Dis. 2012;28(4):951–60.

92.   Erickson M, Farr S, Niehoff M, Morley J, Banks W. Antisense directed against the amyloid precursor protein reduces cytokine expression in the brain and improves learning and memory in the Tg2576 mouse model of Alzheimer's disease. Brain Behav Immun. 2012;26:S27.

93.   Yan R, Bienkowski MJ, Shuck ME, Miao H, Tory MC, Pauley AM, et al. Membrane-anchored aspartyl protease with Alzheimer's disease β-secretase activity. Nature. 1999;402(6761):533–7.

94.   Vassar R, Bennett BD, Babu-Khan S, Kahn S, Mendiaz EA, Denis P, et al. β-Secretase cleavage of Alzheimer's amyloid precursor protein by the transmembrane aspartic protease BACE. Science. 1999;286(5440):735–41.

95.   Wolfe MS. Targeting mRNA for Alzheimer's and related dementias. Scientifica. 2014;2014:1-13.

96.   Refolo LM, Eckman C, Prada CM, Yager D, Sambamurti K, Mehta N, et al. Antisense-induced reduction of Presenilin 1 expression selectively increases the production of amyloid β42 in transfected cells. J Neurochem. 1999;73(6):2383–8.

97.   Grilli M, Diodato E, Lozza G, Brusa R, Casarini M, Uberti D, et al. Presenilin-1 regulates the neuronal threshold to excitotoxicity both physiologically and pathologically. Proc Natl Acad Sci USA. 2000;97(23):12822–7.

98.   Fiorini A, Sultana R, Förster S, Perluigi M, Cenini G, Cini C, et al. Antisense directed against PS-1 gene decreases brain oxidative markers in aged senescence accelerated mice (SAMP8) and reverses learning and memory impairment: a proteomics study. Free Radic Biol Med. 2013;65:1–14.

99.   Caceres A, Kosik KS. Inhibition of neurite polarity by tau antisense oligonucleotides in primary cerebellar neurons. Nature. 1990;343(6257):461–3.

100.   DeVos SL, Goncharoff DK, Chen G, Kebodeaux CS, Yamada K, Stewart FR, et al. Antisense reduction of tau in adult mice protects against seizures. J Neurosci. 2013;33(31):12887–97.

101.   Kar A, Kuo D, He R, Zhou J, Wu JY. Tau alternative splicing and frontotemporal dementia. Alzheimer disease and associated disorders. 2005;19(Suppl 1):S29.

102.   Kalbfuss B, Mabon SA, Misteli T. Correction of alternative splicing of tau in frontotemporal dementia and parkinsonism linked to chromosome 17. J Biol Chem. 2001;276(46):42986–93.

103.   Peacey E, Rodriguez L, Liu Y, Wolfe MS. Targeting a pre-mRNA structure with bipartite antisense molecules modulates tau alternative splicing. Nucleic Acids Res. 2012;40:9836-49.

104.   Liu Y, Rodriguez L, Wolfe MS. Template-directed synthesis of a small molecule-antisense conjugate targeting an mRNA structure. Bioorg Chem. 2014;54:7–11.

105.   Sud R, Geller ET, Schellenberg GD. Antisense-mediated exon skipping decreases tau protein expression: a potential therapy for tauopathies. Mol Ther Nucleic Acids. 2014;3(7):e180.

106.   Farr SA, Ripley JL, Sultana R, Zhang Z, Niehoff ML, Platt TL, et al. Antisense oligonucleotide against GSK-3β in brain of SAMP8 mice improves learning and memory and decreases oxidative stress: Involvement of transcription factor Nrf2 and implications for Alzheimer disease. Free Radic Biol Med. 2014;67:387–95.

107.   Fu A-L, Zhang X-M, Sun M-J. Antisense inhibition of acetylcholinesterase gene expression for treating cognition deficit in Alzheimer's disease model mice. Brain Res. 2005;1066(1):10–5.

108.   Wasser CR, Herz J. Splicing therapeutics for Alzheimer's disease. EMBO Mol Med. 2016;8(4):308–10.

109.   Hinrich AJ, Jodelka FM, Chang JL, Brutman D, Bruno AM, Briggs CA, et al. Therapeutic correction of ApoER2 splicing in Alzheimer's disease mice using antisense oligonucleotides. EMBO Mol Med. 2016;8(4):328–45.

110.   Hannon GJ. RNA interference. Nature. 2002;418(6894):244–51.

111.   Miller VM, Gouvion CM, Davidson BL, Paulson HL. Targeting Alzheimer's disease genes with RNA interference: an efficient strategy for silencing mutant alleles. Nucleic Acids Res. 2004;32(2):661–8.

112.   McSwiggen J, inventor; Terpstra, Anita, J.; McDonnell Boehnen Hulbert & Berghoff, Suite 3200, 300 South Wacker Drive, Chicago, IL 60606 (US), assignee. RNA interference mediated treatment of Alzheimer's disease using short interfering RNA2002.

113.   Basi G, Frigon N, Barbour R, Doan T, Gordon G, McConlogue L, et al. Antagonistic effects of β-site amyloid precursor protein-cleaving enzymes 1 and 2 on β-amyloid peptide production in cells. J Biol Chem. 2003;278(34):31512–20.

114.   Kao S-C, Krichevsky AM, Kosik KS, Tsai L-H. BACE1 suppression by RNA interference in primary cortical neurons. J Biol Chem. 2004;279(3):1942–9.

115.   Modarresi F, Faghihi MA, Patel NS, Sahagan BG, Wahlestedt C, Lopez-Toledano MA. Knockdown of BACE1-AS nonprotein-coding transcript modulates β-amyloid-related hippocampal neurogenesis. Int J Alzheimers Dis. 2011;2011:929042.

116.   Cai J, Qi X, Kociok N, Skosyrski S, Emilio A, Ruan Q, et al. β-Secretase (BACE1) inhibition causes retinal pathology by vascular dysregulation and accumulation of age pigment. EMBO Mol Med. 2012;4(9):980–91.

117.   Fisette JF, Montagna DR, Mihailescu MR, Wolfe MS. AG-Rich element forms a G-quadruplex and regulates BACE1 mRNA alternative splicing. J Neurochem. 2012;121(5):763–73.

118.   Jonas S, Izaurralde E. Towards a molecular understanding of microRNA-mediated gene silencing. Nat Rev Genet. 2015;16(7):421-33.

119.   Ha M, Kim VN. Regulation of microRNA biogenesis. Nat Rev Mol Cell Biol. 2014;15(8):509-24.

120.   He L, Hannon GJ. MicroRNAs: small RNAs with a big role in gene regulation. Nat Rev Genet. 2004;5(8):522-31.

121.   Stenvang J, Petri A, Lindow M, Obad S, Kauppinen S. Inhibition of microRNA function by antimiR oligonucleotides. Silence. 2012;3(1):1.

122.   Faghihi MA, Zhang M, Huang J, Modarresi F, Van der Brug MP, Nalls MA, et al. Evidence for natural antisense transcript-mediated inhibition of microRNA function. Genome Biol. 2010;11(5):R56.

123.   Hébert SS, Horré K, Nicolaï L, Papadopoulou AS, Mandemakers W, Silahtaroglu AN, et al. Loss of microRNA cluster miR-29a/b-1 in sporadic Alzheimer's disease correlates with increased BACE1/β-secretase expression. Proc Natl Acad Sci. 2008;105(17):6415-20.

124.   Zovoilis A, Agbemenyah HY, Agis-Balboa RC, Stilling RM, Edbauer D, Rao P, et al. microRNA-34c is a novel target to treat dementias. EMBO J. 2011;30(20):4299–308.

125.   Murphy SR, Chang CC, Dogbevia G, Bryleva EY, Bowen Z, Hasan MT, et al. ACAT1 knockdown gene therapy decreases amyloid-β in a mouse model of Alzheimer's disease. Mol Ther. 2013;21(8):1497–506.

126.   Zuccato C, Cattaneo E. Brain-derived neurotrophic factor in neurodegenerative diseases. Nat Rev Neurol. 2009;5(6):311-22.

127.   Peng S, Wuu J, Mufson EJ, Fahnestock M. Precursor form of brain-derived neurotrophic factor and mature brain-derived neurotrophic factor are decreased in the pre-clinical stages of Alzheimer's disease. J Neurochem. 2005;93(6):1412–21.

128.   Phillips HS, Hains JM, Armanini M, Laramee GR, Johnson SA, Winslow JW. BDNF mRNA is decreased in the hippocampus of individuals with Alzheimer's disease. Neuron. 1991;7(5):695–702.

129.   Lee ST, Chu K, Jung KH, Kim JH, Huh JY, Yoon H, et al. miR-206 regulates brain-derived neurotrophic factor in Alzheimer disease model. Ann Neurol. 2012;72(2):269–77.

130.   Nawrot B. Targeting BACE with small inhibitory nucleic acids — a future for Alzheimer's disease therapy? Acta Biochim Pol. 2004;51:431–44.

131.   Gopinath SCB. Methods developed for SELEX. Anal Bioanal Chem. 2007;387(1):171–82.

132.   Stoltenburg R, Reinemann C, Strehlitz B. SELEX — a (r) evolutionary method to generate high-affinity nucleic acid ligands. Biomol Eng. 2007;24(4):381–403.

133.   Ylera F, Lurz R, Erdmann VA, Fürste JP. Selection of RNA aptamers to the Alzheimer's disease amyloid peptide. Biochem Biophys Res Commun. 2002;290(5):1583–8.

134. Bunka DH, Mantle BJ, Morten IJ, Tennent GA, Radford SE, Stockley PG. Production and characterization of RNA aptamers specific for amyloid fibril epitopes. J Biol Chem. 2007;282(47):34500–9.

135. Rahimi F, Murakami K, Summers JL, Chen C-HB, Bitan G. RNA aptamers generated against oligomeric Aβ40 recognize common amyloid aptatopes with low specificity but high sensitivity. PLoS One. 2009;4(11):e7694.

136. Takahashi T, Tada K, Mihara H. RNA aptamers selected against amyloid β-peptide (Aβ) inhibit the aggregation of Aβ. Mol Biosyst. 2009;5(9):986–91.

137. Mathew A, Aravind A, Brahatheeswaran D, Fukuda T, Nagaoka Y, Hasumura T, et al. Amyloid-binding aptamer conjugated curcumin–PLGA nanoparticle for potential use in Alzheimer's disease. Bionanoscience. 2012;2(2):83–93.

138. Farrar CT, William CM, Hudry E, Hashimoto T, Hyman BT. RNA aptamer probes as optical imaging agents for the detection of amyloid plaques. PLoS One. 2014;9(2):e89901.

139. Babu E, Mareeswaran PM, Sathish V, Singaravadivel S, Rajagopal S. Sensing and inhibition of amyloid-β based on the simple luminescent aptamer–ruthenium complex system. Talanta. 2015;134:348–53.

140. Rentmeister A, Bill A, Wahle T, Walter J, Famulok M. RNA aptamers selectively modulate protein recruitment to the cytoplasmic domain of β-secretase BACE1 in vitro. RNA. 2006;12(9):1650–60.

141. Liang H, Shi Y, Kou Z, Peng Y, Chen W, Li X, et al. Inhibition of BACE1 Activity by a DNA Aptamer in an Alzheimer's Disease Cell Model. PLoS One. 2015;10(10):e0140733.

142.   Kim JH, Kim E, Choi WH, Lee J, Lee JH, Lee H, et al. Inhibitory RNA aptamers of tau oligomerization and their neuroprotective roles against proteotoxic stress. Mol Pharm. 2016;13(6):2039–48.

143.   Tannenberg RK, Lauridsen LH, Kanwar JR, Dodd PR, Veedu RN. Nucleic acid aptamers as novel class of therapeutics to mitigate Alzheimer's disease pathology. Curr Alzheimer Res. 2013;10(4):442–8.

144.   Kim S, Wark AW, Lee HJ. Femtomolar detection of tau proteins in undiluted plasma using surface plasmon resonance. Anal Chem. 2016;88(15):7793–9.

145.   Lee JH, Shin SK, Jiang Y, Choi WH, Hong C, Kim D-E, et al. Facilitated Tau degradation by USP14 aptamers *via* enhanced proteasome activity. Sci Rep. 2015;5:10757.

146.   Mashima T, Matsugami A, Nishikawa F, Nishikawa S, Katahira M. Unique quadruplex structure and interaction of an RNA aptamer against bovine prion protein. Nucleic Acids Res. 2009;37(18):6249–58.

Chapter 4 APP

4.1 Introduction

Mutations in the *APP* gene or copy number changes of the *APP* gene results in FAD in some cases (1, 2). Many patients with APP mutations have an onset of AD between the ages 45-60 years. The *APP* locus is encoded by Chromosome 21 (3-5). APP is a type-1 integral membrane glycoprotein containing the Aβ region, comprising of 28 amino acids that make up the ectodomain and 11-14 amino acids that make up the adjacent transmembrane domain (1). There have been 30 pathogenic mutations found in Exons 16 and 17 (Table 4.1) and occur around the Aβ cleavage sites affecting APP processing by secretases (2, 6). APP is cleaved by β and γ secretases to generate Aβ (1, 2). Down's syndrome is caused by chromosome 21 trisomy and individuals with Down's syndrome show overproduction of Aβ and present cognitive dysfunction similar to that seen in AD patients (1, 2, 6).

There is no treatment for FAD, and no AOs tested in clinical trials targeting *APP* for the treatment of FAD. There have been six mutations reported to date in exon 16 of the *APP* gene that is pathogenic and causes AD while there are 24 mutations reported to date in exon 17 of the *APP* gene that is pathogenic and cause AD and cerebral amyloid angiopathy (Table 4.1). Skipping of exon 17 has been shown to reduce Aβ production (7).

Table 4.1   Pathogenic mutations reported in Exon 17 of the APP gene that causes cerebral amyloid angiopathy or AD. Adapted from Alzforum Database (https://www.alzforum.org/mutations/app)(286)

Mutation	Exon	Type of Mutation	Disease
KM670/671NL	Exon16	Point, Double AAG&ATG to AAT & CTG	AD

Mutation	Exon	Type of Mutation	Disease
A673V	Exon 16	Point, Missense GCA to GTA	AD
D678H	Exon 16	Point, Missense GAC to CAC	AD
D678N	Exon 16	Point, Missense GAC to AAC	AD
E682K	Exon 16	Point, Missense GAA to AAA	AD
K687N	Exon 16	Point, Missense AAA to AAT	AD
A692G	Exon 17	Point, Missense GCA to GGA	AD
E693del	Exon 17	Deletion GAA to ---	AD
E693G	Exon 17	Point, Missense GAA to GGA	AD
E693K	Exon 17	Point, Missense GAA to AAA	Cerebral Amyloid Angiopathy
E693Q	Exon 17	Point Missense GAA to CAA	Hereditary Cerebral Hemorrhage with Amyloidosis of the Dutch type
D694N	Exon 17	Point, Missense GAT to AAT	AD, Cerebral Anyloid Angiopathy
L705V	Exon 17	Point, Missense CTC to GTC	Cerebral Amyloid Angiopathy
T714A	Exon 17	Point, Missense ACA to GCA	AD
T714I	Exon 17	Point, Missense ACA to ATA	AD
V715A	Exon 17	Point, Missense GTG to GCG	AD
V715M	Exon 17	Point, Missense GTG to ATG	AD
I716F	Exon 17	Point, Missense ATC to TTC	AD
I716M	Exon 17	Point, Missense ATC to ACC	AD
I716T	Exon 17	Point, Missense ATC to ACC	AD
I716V	Exon 17	Point, Missense ATC to GTC	AD
V717F	Exon 17	Point, Missense GTC to TTC	AD
V717G	Exon 17	Point, Missense GTC to GGC	AD
V717I	Exon 17	Point, Missense GTC to ATC	AD
V717L	Exon 17	Point, Missense GTC to CTC	AD
T719N	Exon 17	Point, Missense ACC to AAC	AD

Mutation	Exon	Type of Mutation	Disease
T719P	Exon 17	Point, Missense ACC to CCC	AD
M722K	Exon 17	Point, Missense ATG to AAG	AD
L723P	Exon 17	Point, Missense CTG to CCG	AD
K724N	Exon 17	Point, Missense AAG to AAC	AD

4.2 Aim

To develop splice-modulating AOs targeting exon 16 and 17 of APP to induce exon 16 and exon 17 skipping (to reduce APP mRNA or form a truncated APP without the deleterious mutations given in Table 4.1 and reduce production of amyloid beta) as a therapeutic strategy for FAD.

4.3 Methods

4.3.1 AO Design and Synthesis

The 2'-OMePS AOs (Table 4.2) were designed for exon 16 and exon 17 of APP (Exon map in Figure 4.1). The AOs were synthesised in-house using ABI ExpediteTM 8909 oligonucleotide synthesiser (Applied Biosystems) and AKTA Oligopilot 10 synthesiser (GE Healthcare Life Sciences) using standard phosphoramidite chemistry at 1 μmol scale. The synthesised oligonucleotides were deprotected by treatment with 1 mL Ammonium Hydroxide (Sigma Aldrich; Cat# 221228-500mL) overnight at 55 °C. The oligonucleotides were then purified and desalted using illustra NAP-10 columns (GE Healthcare; Cat#: 45-000-153) according to the manufacturer's protocol. AO2-PMO and AO8-PMO were purchased from Gene Tools.
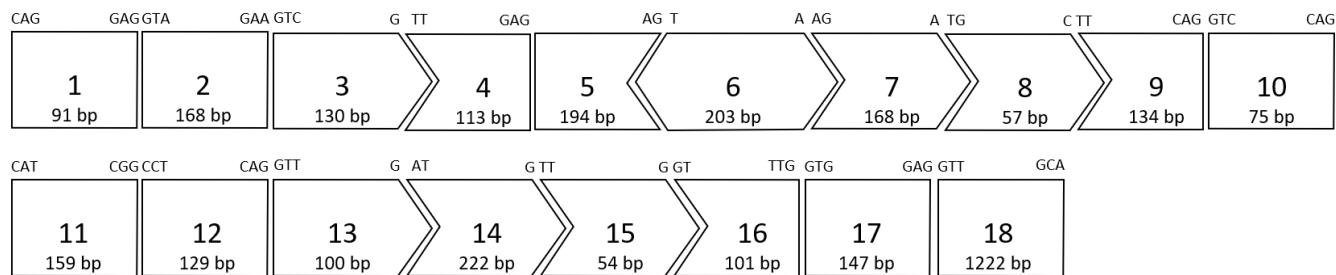
Figure 4.1   Exon map of APP showing the reading frame. The rectangles represent in-frame exons, whereas the arrows indicate codons that are disrupted by exon junctions. The codons at the start and end of each in-frame and out-of-frame exon are represented by the letters above the rectangles and arrows.

Table 4.2   List of 2'-OMePS AOs synthesised targeting exon 16 and 17 of the APP mRNA.

AO Number	AO name	Exon
AO1	APP 1E17A (-15+10)	Exon 17
AO2	APP 1E17A(+6+30)	Exon 17
AO3	APP 1E17A (+41+65)	Exon 17
AO4	APP 1E17A(+69+93)	Exon 17
AO5	APP 1E17A (+96+120)	Exon 17
AO6	APP 1E17A (+123+147)	Exon 17
AO7	APP 1E17D(+7-18)	Exon 17
AO8	APP 1E17A(+60+85)	Exon 17
AO9	APP 1E17A(+71+95)	Exon 17
AO10	APP 1E17A(+98+122)	Exon 17
AO11	APP 1E16A(-5+20)	Exon 16
AO12	APP 1E16A(+39+63)	Exon 16
AO13	APP 1E16A(+41+65)	Exon 16
AO14	APP 1E16A(+56+80)	Exon 16
AO15	APP 1E16D(+22-4)	Exon 16

4.3.2 Cell culture and transfection

HEK293 cells were obtained from Cell Bank Australia (kindly provided by Associate Prof. Bruno Meloni) and the primary human fibroblasts from muscle biopsies were kindly provided by Prof. Sue Fletcher and Prof. Steve Wilton. Cells were grown and maintained in 10% Foetal Bovine Serum in Dulbecco's Modified Eagle's Medium (ThermoFisher Scientific; Cat#: 11995073) in a humidified atmosphere 37 °C incubator with 5% CO_2. Cells were maintained at 70-90% confluency and seeded in a plate or flask at densities shown in Table 4.3, 24 h before transfection. The HEK293 cells were plated in a plate or flask pre-treated with 50 µg/mL poly-D-lysine (Merck Millipore; Cat#: P7886-50mg).

Table 4.3   *The seeding density of HEK293 cells used for different assays.*

Assay	Plate or Flask?	HEK293 seeding density	Fibroblast seeding density
RNA Extraction	24 well plate	50,000 cells/well	15,000 cells/well
Western Blot	T25cm2 flask	625,000 cells/flask	
Nucleofection	24 well plate	100,000 cells/well	

Next, the cells were then transfected with 2'-OMePS AOs at 400 nM and 50 nM using Lipofectamine 3000 (ThermoFisher Scientific; Cat#: L3000015) transfection reagent according to the manufacturer's protocol. Cocktails of AOs were transfected at a total transfection concentration of 400 nM and 50 nM for an initial screen, where the individual AO concentration (at 200 nM and 25 nM) was half the total transfection concentration. The best performing AO cocktails were then transfected using the same protocol at the following concentrations: 400 nM, 200 nM, 100 nM, 50 nM and 25 nM. Twenty- four hours after transfection, the cells were collected for RNA extraction. For western blot, the cells were collected for RNA extraction and western blot, 24h, 48h and 3 days after AO treatment. The AO2-PMO and AO8-PMO were transfected into HEK293 cells at 100 µM and 250 µM total concentrations (individual PMO concentrations were 50 µM and 125 µM) by nucleofection. For each treatment, 5×10^5 cells were trypsinised, centrifuged and resuspended in the nucleofection master mix as per the manufacturer's protocol. The cells were then nucleofected with AO2-PMO and AO8-PMO using program CM- 130 on the 4D Nuclofector system X-unit (Lonza) using the SF Cell Line 4D-NucleofectorTM X Kit S (Lonza; Cat#: V4XC-2032) and seeded into five wells of the 24 well plate. Cells were collected at 24 h, 48 h, 3 day, 5 day and 7 day timepoints after the first transfection for RNA extraction.

4.3.3 RNA extraction and RT-PCR

RNA was extracted from transfected cells using ISOLATE II RNA Mini kit (Bioline; Cat#: BIO-52073) as per the manufacturer's protocol. The *APP* transcript was amplified using the following

primers (ordered from IDT): Forward primer: TTGAGCCTGTTGATGCCCG and Reverse primer: ACATGAAGCATCCCCCATCG to amplify the region exon 16- exon 18 of the *APP* transcript with SuperScript III One-Step RT-PCR kit (ThermoFisher Scientific; Cat# 12574026). The following RT-PCR conditions were used: 30 mins at 55°C, 2 mins at 94 °C, 23 rounds of 30 s at 94 °C, 1 min at 60 °C and 2 mins at 68°C. The products were then separated on a 2% agarose gel in Tris-acetate-EDTA buffer, stained with Red Safe (iNtRON Biotechnology; Cat# 21141) and destained with water before being image captured with the Fusion Fx gel documentation system (Vilber Lourmat, Marne La Valle, France). Densitometry was performed by Image J Software (9). An AO sequence that does not anneal to any human transcript, supplied by Genetools (Genetools Control, GTC) was used as a negative control.

4.3.4 Sequencing Analysis

To confirm specific exon-skipping, the full-length product band and the bands representing the exon-skipped product were band stabbed using a previously published procedure (10). The isolated products were amplified using AmpliTaq Gold® 360 DNA Polymerase Kit (Thermofisher Scientific, Cat# 4398823) and the same primer set described in the previous section under the following RT-PCR conditions: 6 mins at 94 °C, 23 cycles of 30 s at 94 °C, 1 min at 52 °C and 2 mins at 72 °C. The quality of PCR products was confirmed by 2% agarose gel electrophoresis and purified using the Diffinity Rapid Tip® (Sigma Aldrich, Cat #: D1947-96RXN). The products were sequenced using both the forward and reverse primer by the Australian Genome Research AGRF Facility, Western Australia.

4.3.5 Western Blot

Western Blot was performed on the proteins extracted from cells treated with the best performing AO cocktail to evaluate the effect of the AO cocktail on the APP protein in comparison to the

scrambled and untreated AOs. Cells were lysed in lysis buffer (100 µL/ sample) containing 12% SDS, 100 mM Tris-HCl, pH 6.8, 10% glycerol with loading buffer containing 1.875 µL bromophenol blue, 4.688 µL dithiothreitol and 1.5 µL protease inhibitor per 100 µL samples. Cell pellets were sonicated six times for 3 s pulses and denatured at 95°C for 5 mins before being snap-frozen on ice. Protein concentrations were determined to ensure equal loading on the protein gel that was then stained with coomassie blue. The proteins were separated on a 10% separating gel containing 400 mM Tris-HCL (pH8.8) and 0.1% SDS and a 5% stacking gel containing 130 mM Tris-HCL (pH6.8), 0.1% SDS and 0.004% bromophenol blue in Tris-glycine-SDS running buffer before being transferred to a 0.2 µm nitrocellulose membrane (Biorad; Cat# 162-0112) in Tris-glycine-methanol transfer buffer. The membranes were blocked in 5% skim milk Tris-buffered saline with 0.1% Tween for 1 h. The membrane was washed three times in Tris-buffered saline with 0.1% Tween for 20 mins each, and the membrane was incubated in primary antibody solution, 1:5000 anti-APPL (Abcam, Cat# ab180140) and 1:1000 anti-GAPDH (ThermoFisher Scientific, Cat# PA1-988) overnight at 4 °C. After washing the membrane three times in Tris-buffered saline with 0.1% Tween for 20 mins each, the membrane was incubated in the secondary antibody (1:5000 anti-rabbit HRP, Thermofisher Scientific, Cat# 31460) for 1 h at room temperature before washing three times in Tris-buffered saline with 0.1% Tween for 20 mins each. The antibodies were detected using the Clarity Western ECL detection kit (Biorad; Cat# 1705060) according to the manufacturer's protocol and visualised using the Fusion Fx gel documentation system (Vilber Lourmat, Marne La Valle, France).

4.4 Results

4.4.1 Developing splice-modulating AOs to induce skipping of APP exon 17.

Various 2'-O-Methyl (2'-OMe)-modified AO sequences on a phosphorothioate (2'-OMePS) backbone were designed to target exon 17 of the APP mRNA and synthesised in house (Table 4.2). All single AOs were initially screened for induction of exon-skipping by transfection at 400 nM and 50 nM (Appendix B, Figure B.1) concentrations, using Lipofectamine 3000 as per manufacturer's protocol, in HEK293 cells. Twenty-four hours after transfection, the cells were collected, and the total RNA was extracted before performing a reverse transcription-polymerase chain reaction (RT-PCR) to amplify the exon 16- exon 18 APP product. The RT-PCR products were separated on a 2% agarose gel and Image J software was used to perform densitometry on the gel images. All 10 AOs were re-screened in cocktails at 400 nM and 50 nM concentrations (individual AOs concentrations of 200 nM and 25 nM; only 2 AOs per cocktail was tested in this study) (Appendix B, Figure B.2). The most efficient AO cocktails targeting exon 17 (AO2+AO8, AO9+AO2, AO9+AO10, and AO10+AO2) were further evaluated at 400 nM, 200 nM, 100 nM, 50 nM and 25 nM concentrations.

4.4.1.1 Evaluation of the most efficient 2'-OMePS AO cocktails to induce exon-skipping of exon 17 of the APP transcript in HEK293 cells in vitro.

We systematically evaluated the most effective AO cocktails (AO2+AO8, AO9+AO1, AO9+AO2, AO9+AO10, AO10+AO1, AO10+AO2 and AO10+AO8) *in vitro* at 400 nM, 200 nM, 100 nM, 50 nM, and 25 nM concentrations. Cocktail of two AOs that included a combination of AO1, AO2, AO8, AO9, and AO10 induced *APP* exon 17 skipping, however, AO2 and AO8 were found to be the most effective (Figure 4.2).
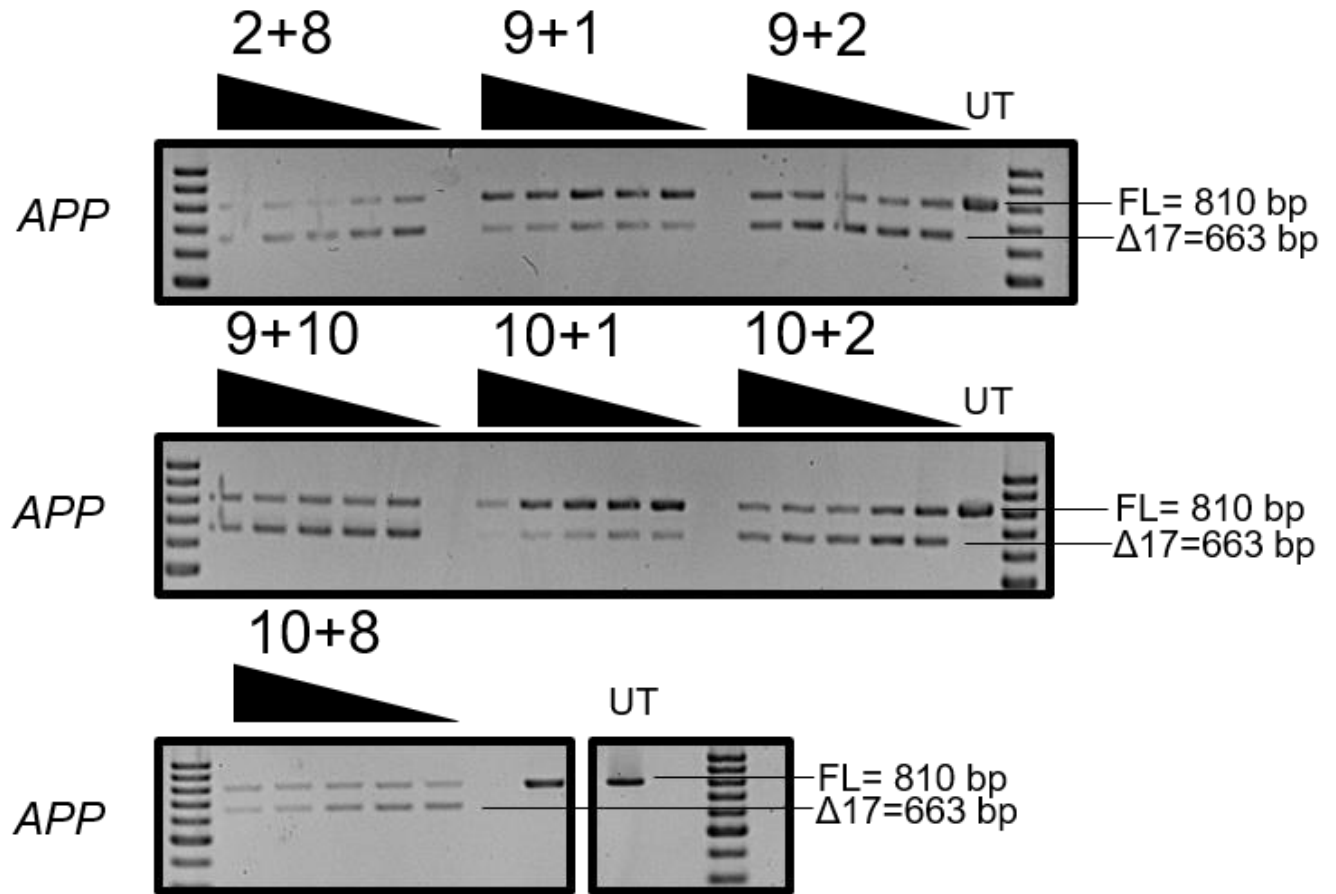
Figure 4.2   RT-PCR analysis of APP transcripts after treatment with the most effective 2'-OMePS AO cocktails (AO2+AO8, AO9+AO1, AO9+AO2, AO9+AO10, AO10+AO1, AO10+AO2 and AO10+AO8) targeting exon 17 at 400 nM, 200 nM, 100 nM, 50 nM and 25 nM in HEK293 cells. FL, full-length; UT, untreated; SCR, scrambled sequence. The gel images were cropped, however, the original images are shown in Figure B.3 (Appendix B).

4.4.1.2 Evaluation of the most efficient 2'-OMePS AO cocktail to induce exon 17 skipping.

We then evaluated the most effective exon 17 targeting AO cocktail, AO2+AO8 at lower concentrations (50 nM, 25 nM, 12.5 nM, 5 nM and 2.5 nM) to induce exon 17 skipping in HEK293 cells. The cocktail of AO2+AO8 induced dose-dependent exon 17 skipping of the *APP* transcript at the lower concentrations (Figure 4.3). The AO2+AO8 cocktail worked most efficiently at 100 nM concentration, and the skipped product was later confirmed by sequencing (Figure 4.3).

A. 2+8 (400-25 nM) 2+8 (50-2.5 nM) SCRUT

APP

FL= 810 bp
Δ17= 663 bp

B.

Sequencing from FL band

Exon 16   Exon 17

Sequencing from Δ17 band

Exon 16   Exon 18

470   480   490
G A C A G C G G C G T C A A C C T C C A C C A C

470   48   490
G A C A G C G G C G T C A A C C A A T T T T T G A T G

Exon 17 missing
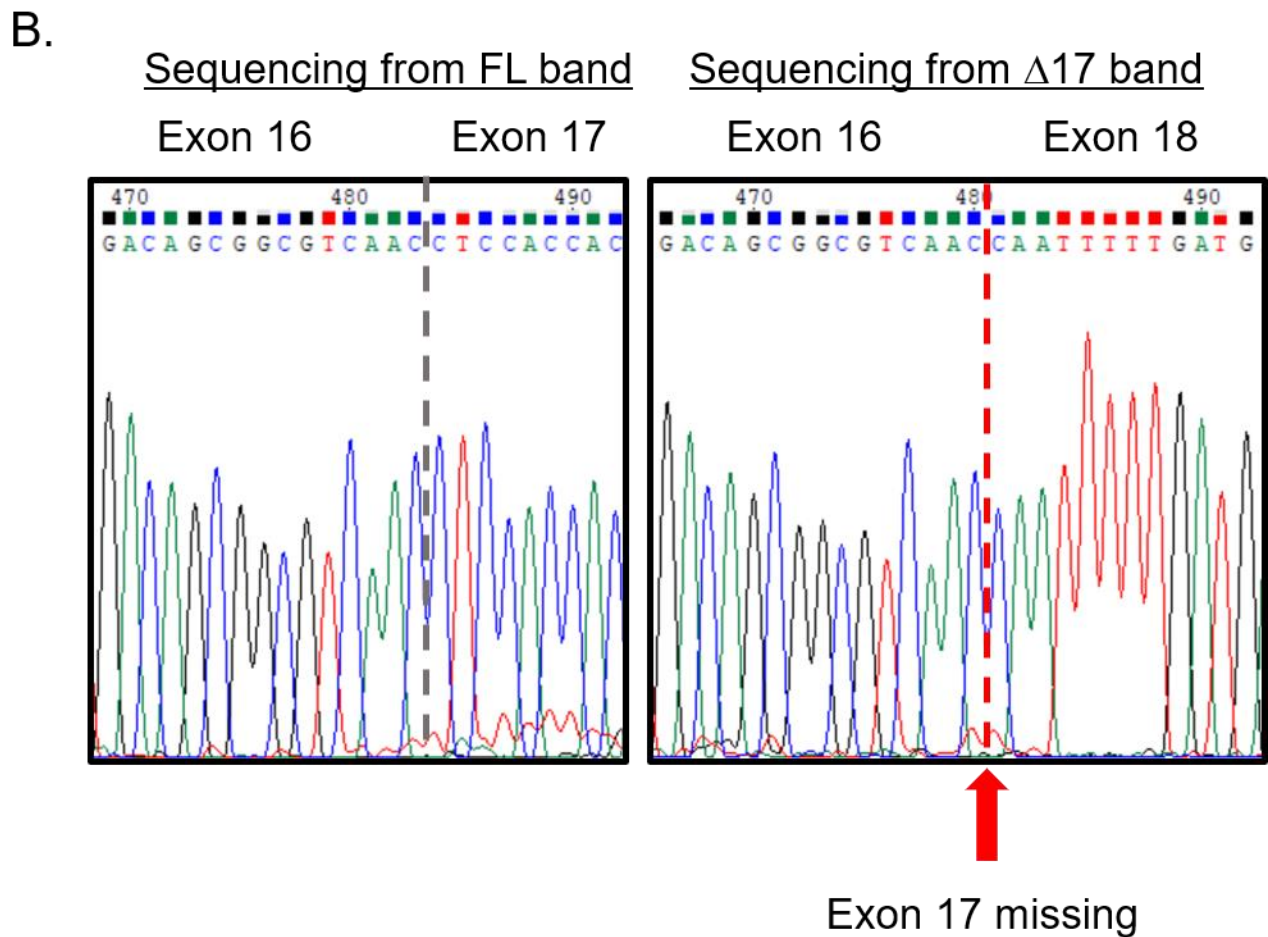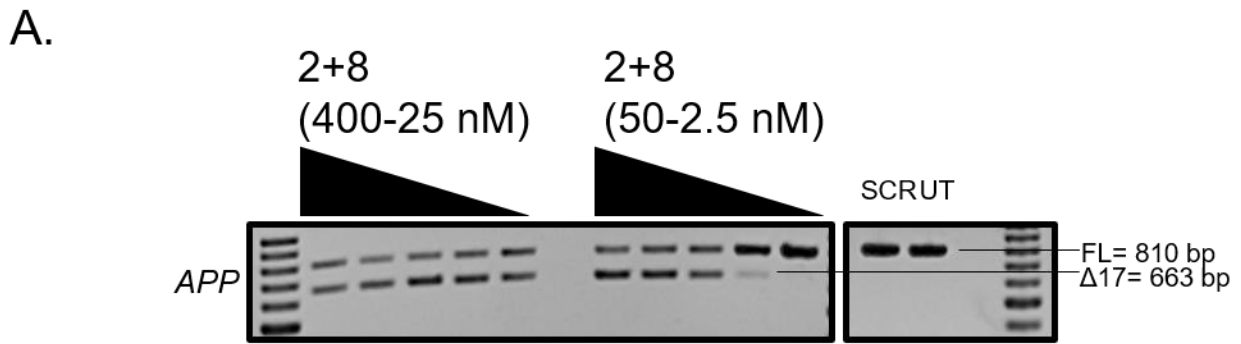
Figure 4.3   A. RT-PCR analysis of the APP transcript after treatment of HEK293 cells with the most effective 2'-OMePS AO cocktail, AO2+AO8, targeting exon 17 at two concentration ranges (range 1: 400 nM, 200 nM, 100 nM, 50 nM and 25 nM, range 2: 50 nM, 25 nM, 12.5 nM, 5 nM and 2.5 nM) in HEK293 cells. FL, full-length; UT, untreated; SCR, scrambled sequence. The gel images were cropped to highlight the APP specific products. The original images are shown in Figure B.4 (Appendix B). B. Sequencing data analysis of FL and Δ17 band.

4.4.1.3 Evaluation of the most efficient 2'-OMePS AO cocktail to induce exon-skipping in fibroblasts.

Although testing of AOs in mouse is important for further validation of the AOs to be clinically viable, testing of AOs in patient-derived cells may be equally important and more reliable at assessing whether the developed AOs can be effective in individual patients. Therefore, we assessed APP expression and exon-skipping efficiency of the AO2+AO8 cocktail in normal primary fibroblasts in the 50 nM, 25 nM, 12.5 nM, 5 nM and 2.5 nM concentrations (Figure 4.4). The AO cocktail also induced exon 17 skipping in fibroblasts but the efficiency was lower than in HEK293 cells.
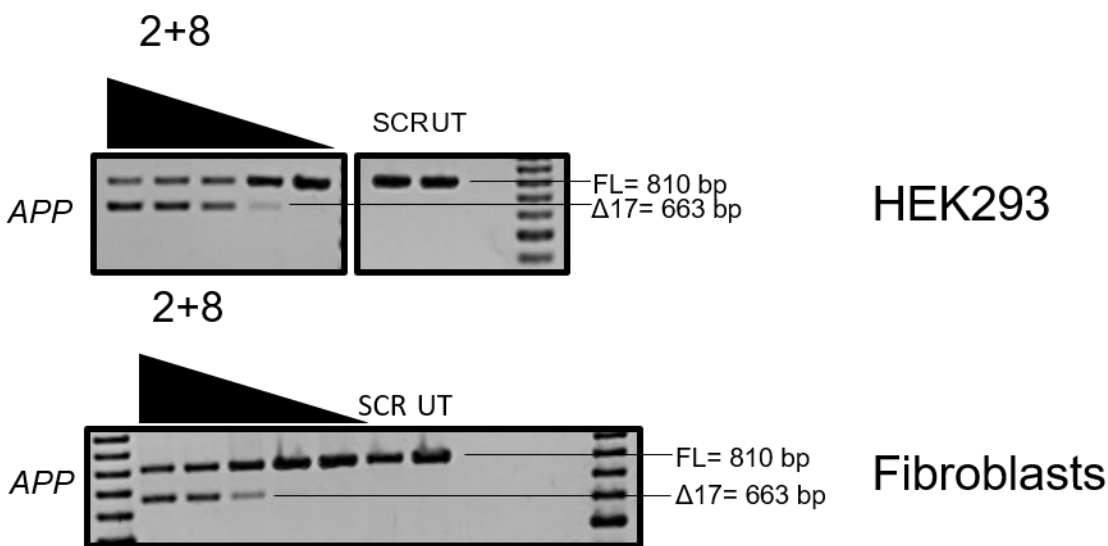
Figure 4.4   RT-PCR analysis of the APP transcript after treatment of HEK293 cells and healthy primary fibroblasts with the most effective 2'-OMePS AO cocktail, AO2+AO8, targeting exon 17 at 50 nM, 25 nM, 12.5 nM, 5 nM and 2.5 nM concentrations. FL, full-length; UT, untreated; SCR, scrambled sequence. The gel images were cropped, however the original images are shown in Figure B.5(Appendix B).

4.4.1.4 Evaluation of the most efficient 2'-OMePS AO cocktail as a PMO to induce exon-skipping.

To be clinically applicable, AOs need to be safe for use in humans. The PMO chemistry has been approved for clinical use demonstrating that PMO chemistry have an acceptable safety profile.

The AO sequences for AO2+AO8 were re-synthesised as PMOs and the ability of the cocktail to induce exon 17 skipping was evaluated in HEK293 cells (Figure 4.5). The AO2-PMO+AO8-PMO cocktail did not induce exon17 skipping.
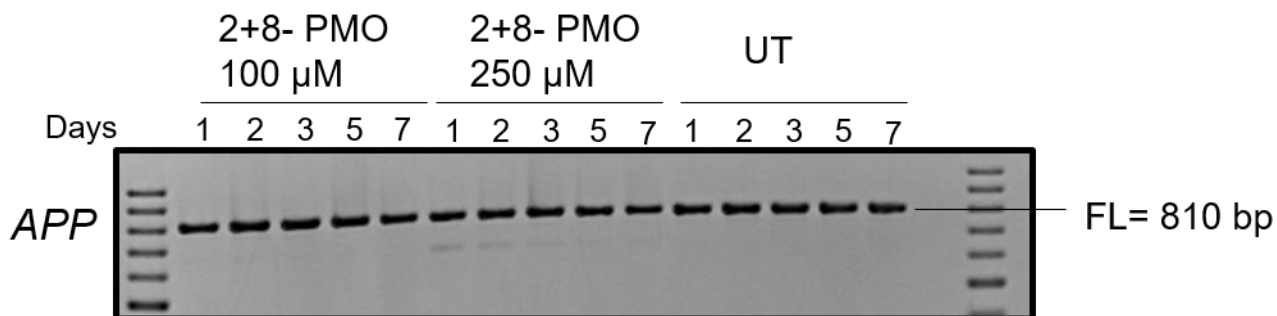
Figure 4.5   RT-PCR anlaysis of the APP transcript after treatment with the most effective AO sequences, AO2+AO8 as PMOs, targeting exon 17 (100 μM and 250 μM concentrations) in HEK293 cells after treatment for 1, 2, 3, 5 and 7 days. FL, full-length; UT, untreated; SCR, scrambled sequence. The gel images were cropped, however, the original images are shown in Figure B.6 (Appendix B).

4.4.1.5 Evaluation of APP protein downregulation.

The efficacy of the 2'-OMePS cocktail, AO2+AO8, to downregulate APP protein expression was evaluated by Western blotting in HEK293 cells after 24h, 48h and 3 days of AO treatment. Briefly, the AO2+AO8 cocktail (100 nM) treated HEK293 cells were incubated for 24h, 48h, and 3 days before the cell pellet was collected and lysed. The proteins were separated on a 10% separating gel and electroblotted onto a nitrocellulose membrane. The membrane was incubated with 1:5000 dilution of the anti-APP antibody overnight at 4°C, and 1:5000 anti-rabbit HRP secondary antibody for 1 h at room temperature. Western blot analysis showed that the APP protein was not downregulated after AO cocktail treatment although exon 17 skipping was evident at the same timepoints at the RNA level (Figure 4.6).
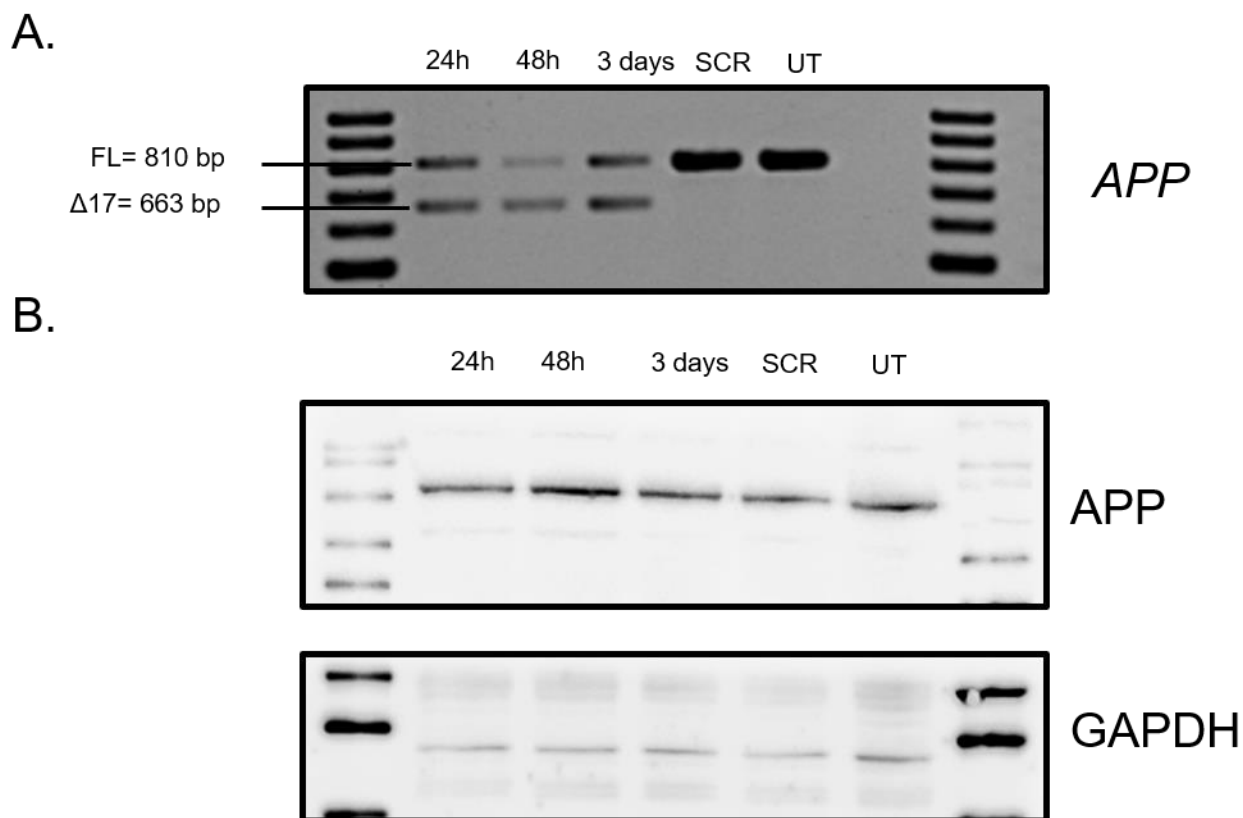
Figure 4.6   A. RT-PCR analysis of the APP transcript after treatment with the most effective AO sequences, AO2+AO8 targeting exon 17 at 100 nM concentration after cocktail treatment for 24 h, 48 h and 3 days in HEK293 cells. B. Western blot analysis of APP and GAPDH after treatment of HEK293 cells with AO2+AO8, at 100 nM for 24 h, 48 h and 3 days, FL, full-length; UT, untreated; SCR, scrambled sequence. The gel images were cropped to highlight the APP specific products. The original images are shown in Figure B.7 (Appendix B).

4.4.2 Developing splice-modulating AOs to induce exon 16 skipping of the APP transcript.

Following exon 17 studies, we designed and synthesised 2'-OMePS AOs in-house targeting Exon 16 of the *APP* mRNA (Table 4.2). All AOs were initially screened for exon-skipping at 400 nM and 50 nM (Figure 4.7) in HEK293 cells by incubating for 24 h using Lipofectamine 3000 as per manufacturer's protocol. Twenty-four hours after transfection, the cells were collected, and the total RNA was extracted before a reverse transcription-polymerase chain reaction (RT-PCR) was performed to amplify the exon 16- exon 18 region of the *APP* gene. The RT-PCR products were

separated on a 2% agarose gel by gel electrophoresis, and Image J software was used to perform densitometry on the gel image.

4.4.2.1 Evaluation of single AOs and AO cocktails for inducing skipping of APP exon 16 in HEK293 cells.

We systematically evaluated single AOs to induce exon 16 skipping in HEK293 cells at 400 nM and 50 nM concentrations (Figure 4.7). The results showed that AO12 and AO13 were able to induce low level of exon 16 skipping at 50 nM but not at 400 nM concentration. All exon 16 targeting AOs were then assessed as cocktails at 400 nM and 50 nM (individual AOs concentrations of 200 nM and 25 nM; only 2 AOs per cocktail was tested in this study) (Figure 4.8).
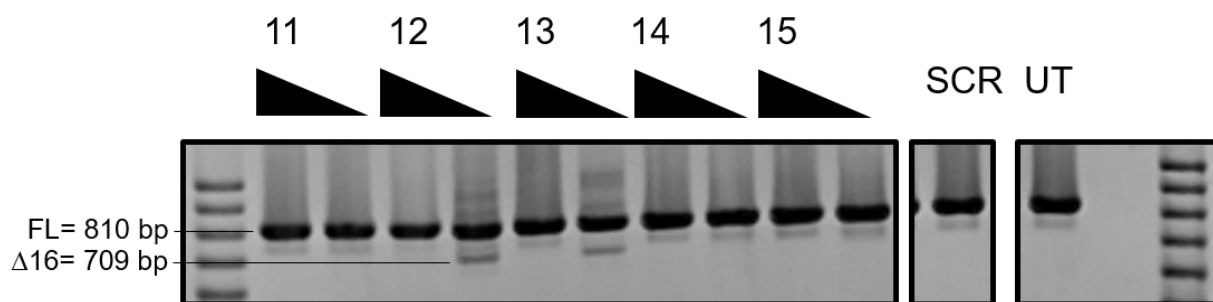
Figure 4.7   A screen of exon 16 AOs. RT-PCR analysis of the APP transcript after treatment with exon 16 2'-OMePS AOs, targeting exon 16 at 400 nM and 50 nM concentrations in HEK293 cells. FL, full-length; UT, untreated; SCR, scrambled sequence.

All exon 16 AO cocktails were able to induce exon 16 skipping. Similar to exon 17 AO cocktails, the AO cocktails were more efficient at induce exon-skipping at 50 nM concentration compared to its efficiency in inducing exon 16 skipping at 400 nM concentration. Therefore, the most effective AO sequences (AO11+AO12, AO11+AO13, AO11+AO14, AO12+AO13, AO12+AO14, AO12+AO15 and AO13+AO14) targeting exon 16 were further evaluated at 100 nM, 50 nM, 25 nM, and 12.5 nM concentrations.
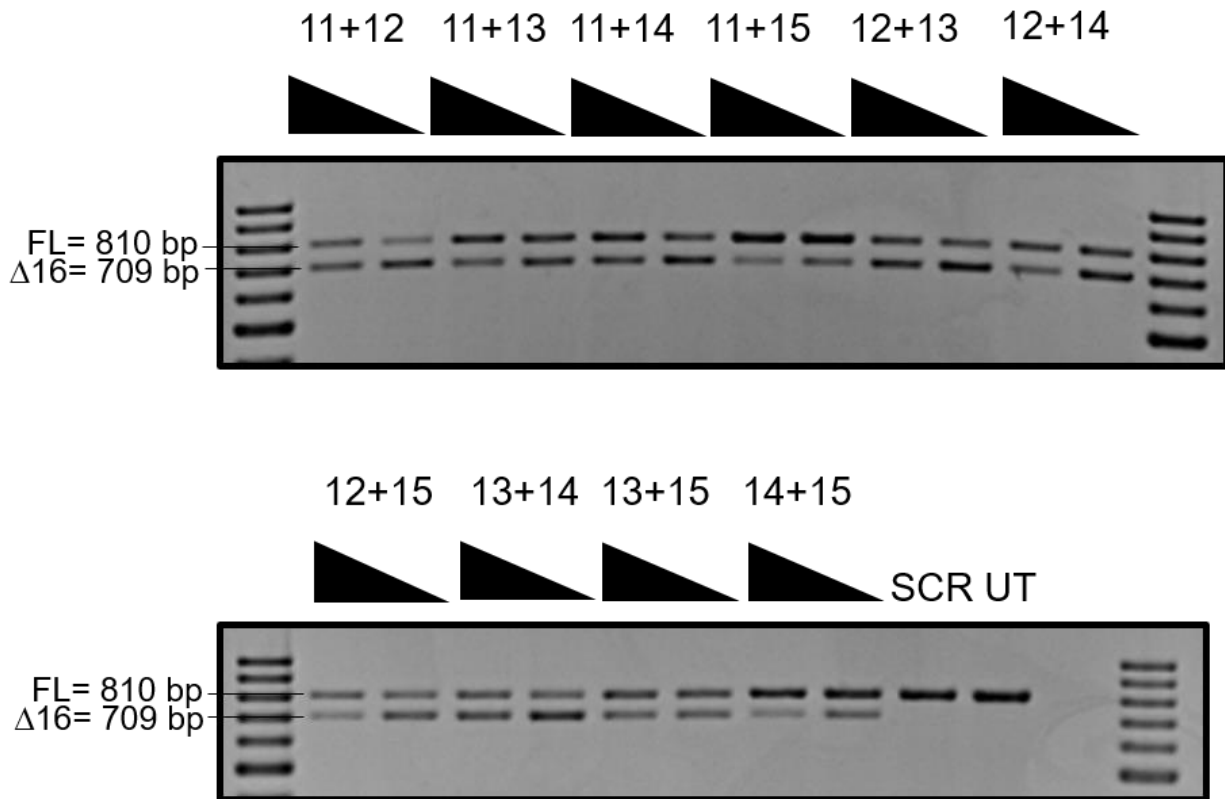
Figure 4.8   A screen of exon 16 AO cocktails. RT-PCR analysis of the APP transcript after treatment with exon 16 2'-OMePS AO cocktails, targeting exon 16 at 400 nM and 50 nM concentrations in HEK293 cells. FL, full-length; UT, untreated; SCR, scrambled sequence.

4.4.2.2 Evaluation of the most efficient 2'-OMePS AO cocktails to induce exon-skipping of exon 16 of the APP transcript in HEK293 cells in vitro.

The most efficient AO 16 sequences (AO11+AO12 and AO12+AO13) were further evaluated at 100 nM, 50 nM, 25 nM, and 12.5 nM concentrations in HEK293 cells (Figure 4.9). The AO sequences were most efficient at 50 nM concentration. The effect of these AO sequences on AOO protein levels need to be further evaluated by Western blot.
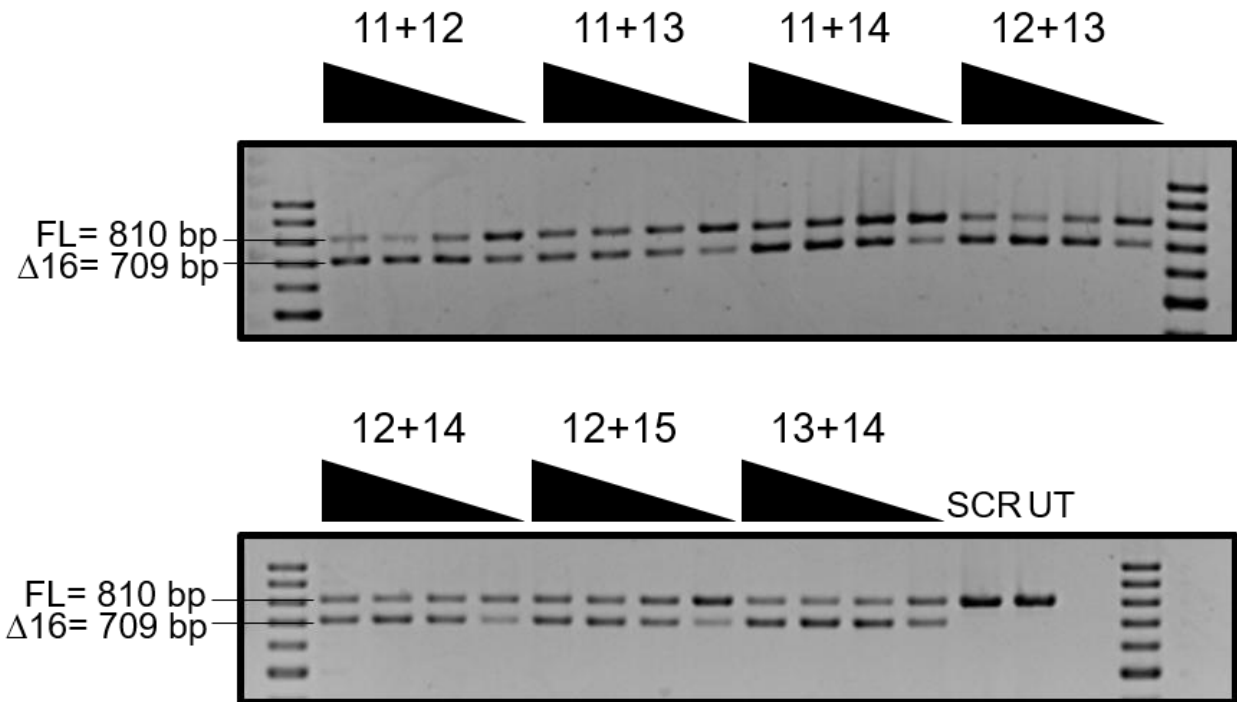
Figure 4.9   Most efficient exon 16 AO cocktails. RT-PCR analysis of the APP transcript after treatment with exon 16 2'-OMePS AO cocktails, targeting exon 16 at 100 nM, 50 nM, 25 nM and 12.5 nM concentrations in HEK293 cells. FL, full-length; UT, untreated; SCR, scrambled sequence.

4.5 Discussion

4.5.1 Developing splice-modulating AOs to induce exon 17 skipping of the *APP* transcript.

In this study, 10 different AOs targeting exon 17 were screened for the ability to induce exon 17 skipping; however, none of the AOs were effective. Previous studies demonstrated the application of a combination of ineffective or marginally effective individual AOs to induce efficient exon-skipping (11). Similarly, I screened cocktails of different combinations of two AOs to evaluate their ability to induce exon 17 skipping. Although it is unknown why cocktails of two individually ineffective AOs may work in synergy, I speculate that it could be due to the need to block a combination of splicing enhancer motifs. A cocktail of AOs may bind to two different regions of the exon and block a combination of splicing enhancer motifs that may be required for the

exclusion of an exon, not achieved by a single AO. Another reason for the better performance of a cocktail of AOs over a single AO to induce exon-skipping could be due to one AO annealing to its target and changing the secondary structure of the surrounding region that allows a second AO in the cocktail to bind to its target to block splicing motifs and induce exon-skipping. The target region of the mRNA may be otherwise inaccessible to a single AO. Although a previous study by Adams et al. (2007) demonstrated that the 2'-OMePS AOs and PMOs show similar exon skipping trends (11), this study shows that 2'-OMePS AOs do not always show a similar trend to PMOs. The 2'-OMePS cocktail of AO2 and AO8 induced exon 17 skipping; however, the same AO sequences as a PMO did not induce any exon-skipping. I speculate that this may be due to the conformational rigidity of the PMO structure in comparison to the 2'-OMePS chemistry that may restrict the accessibility of the PMOs to bind to their target and therefore behave differently to the cocktail of 2'-OMePS AOs (12-18). Although unlikely, the lack of activity of the PMO could also be due to an experimental issue with the electroporation of the PMO. To confirm that the PMO does not induce exon skipping compared to the 2'-OMePS cocktails, the 2'-OMePS cocktails would need to be electroporated similar to the PMOs to conclude if the lack of effect is real or due to an experimental issue with electroporation.

In comparison to my study using both 2'-OMePS sequences and PMO sequences, another recent report in 2018 used 2'-MOE AOs (7) to induce *APP* exon 17 skipping. Interestingly, single 2'-OMOE sequences were able to induce exon 17 skipping. In our study, 2'-OMePS sequences were not able to induce any exon 17 skipping, but, were able to induce efficient exon 17 skipping as cocktails. PMO sequences were not able to induce any exon 17 skipping even when used as cocktails. This study indicates that the chemistries of the AO sequences can determine its ability to induce exon-skipping as reported previously.

Adams et al. (2007) (11) also demonstrated that there might be species differences in the way that specific AO sequences perform between human and mouse cells, indicating that patient-derived cell lines may be more appropriate than mice in designing AO strategies to treat human disease. Although the cocktail of AO2 and AO8 induced exon 17 skipping in both HEK293 cells and primary fibroblasts, the cocktail was less efficient in primary fibroblasts compared to HEK293 cells. The AO2 and AO8 cocktail induced 50% exon-skipping in HEK293 cells at 12.5 nM concentration while in primary fibroblasts much lower exon 17 skipping, that may be due to reduced transfection efficiency in the primary fibroblasts compared to HEK293 cells. I have shown that the transfection efficiency using the same transfection reagent differs from cell to cell and the oligonucleotide efficacy is dependent on the transfection efficiency (19).

A previous study has shown that the 2'-OMePS AOs were initially very effective at splice altering the transcript but that 2'-OMePS AOs degrade rapidly and therefore are not effective long term or for analysing changes in gene expression at the protein level (20). The opposite was true for PMOs that were not as effective as 2'-OMe PS AOs at the mRNA level but the small effect it had was sufficient to have a significant effect on the protein level (20). As the PMO AO2+AO8 was not effective at the mRNA level, I assessed the effect of the cocktail of 2'-OMePS AOs, AO2 and AO8 on protein level and found that the 2'-OMePS AO cocktail had no effect. The quick degradation of the 2'-OMePS AOs may be one reason for the lack of effect of the AO cocktail on APP protein level. The other reason may be due to the short, 4 hour half-life of the APP protein *in vivo* that may mean that if an effect was detectable, this effect would have to be observed within 12 hours (21). However, both of the above suggestions may not explain the result, as exon-skipping at the mRNA level was observed at all time points. I can speculate that the mRNA levels do not correlate with the protein data in our study possibly due to change in the half-life of the protein or

the degradation rate of the protein to balance the reduction in protein synthesis (22). Protein levels are not only determined by the mRNA levels but are also determined by rate of protein synthesis and degradation, post-translational modifications and translational rate of the mRNA (22). It is also important to note that the *in vivo* half-life may differ from the half-life *in vitro*. However, the lack of AO effect on APP protein could be due to an issue with the antibody not recognising the APP protein. The validity of the antibody can be tested by use of a siRNA as a positive control to ensure that the antibody is picking up the APP protein.

A study by Chang *et al.* (2018) (7), were able to induce efficient APP exon 17 skipping. The current study indicates that there may be functional differences, due to the different chemistries in inducing exon-skipping that is target and/or sequence dependent. Furthermore, the study by Chang *et al.* (2018) (7) also showed that the 2'-OMOE sequence was efficient at inducing exon-skipping at the mRNA level as well as downregulate the protein. However, my study did not show downregulation of APP protein. I cannot compare our study with that of Chang *et al.* (2018) (7), as their study used different cells (HEK293 vs Down syndrome patient fibroblasts), different antibodies and used different chemistries (2'-OMePS vs 2'-OMOE). However, weather the lack of effect on the APP protein levels observed in my study is real or due to study design can be further validated by investigating the reasons for differences observed between the two studies.

4.5.2 Developing splice-modulating AOs to induce exon 16 skipping of the *APP* transcript.

Of the five AOs tested for inducing *APP* exon 16 skipping, only two AOs (AO12 and AO13) induced low level of exon 16 skipping (Figure 4.7) at 50 nM concentration but not at 400 nM concentration. This unexpected pattern of exon-skipping is similar to that resulting from AO cocktail treatment targeting exon 17 whereby the AO cocktail was more efficient at inducing exon

17 skipping at lower concentrations while at higher concentration, transcript knockdown was observed. As only low-level exon 16 skipping was observed, AO cocktails were evaluated at 400 nM and 50 nM concentrations (Figure 4.8). Again, at higher concentrations (400 nM), the AO cocktails induce lower levels of exon 16 skipping compared to those induced at lower concentrations (50 nM), where the AO cocktails were able to induce exon 16 skipping more efficiently. I therefore, further evaluated the most efficient exon 16 AO cocktails at lower concentrations (100 nM- 12.5 nM concentrations) (Figure 4.9). The AO cocktails 11+12 and 12+13 were the most efficient at inducing exon 16 skipping, particularly at 50 nM concentrations, with the skipping of the exon 16 dose-dependent at the lower concentrations. We speculate that similar to skipping of exon 17, the cocktails may be more efficient due to inaccessibility of the RNA to a single AO and a cocktail of two AOs may make the RNA more accessible to the efficient AO. The cocktails may also be more efficient due to the need to target multiple splicing motifs to induce efficient exon 16 skipping. Comparing all the AO cocktails that induced exon 16 skipping, the most efficient AO cocktails consisted of AO12 and AO13, that were also the AOs that induced detectable exon 16 skipping individually. This suggests that the regions that AO12 and AO13 target may be important regions for inducing exon 16 skipping. The AO cocktails 11+12 and 12+13 remain to be further evaluated as PMOs and in APP protein studies.

4.6 Conclusion

In conclusion, I have screened various AOs to induce *APP* exon 17 skipping and found no potential lead candidates. However, after testing various combinations of the AOs in cocktails, I identified a cocktail of AO2 and AO8 that could efficiently induce exon 17 skipping *in vitro* in HEK293 cells and primary fibroblasts. Of the two chemistries evaluated, the 2'-OMePS AOs cocktail was able to efficiently induce exon 17 skipping but the same sequences synthesised as a PMO were not

able to induce any exon 17 skipping. The 2'-OMePS cocktail of AO2 and AO8 did not downregulate APP protein. Further investigations are needed to explain the different effects of the same AO sequences as different chemistries. Understanding APP protein expression would help develop better treatment strategies for familial AD.

4.7 References

1.   Thinakaran G, Koo EH. Amyloid Precursor Protein Trafficking, Processing, and Function. J Biol Chem. 2008;283(44):29615-9.

2.   Tcw J, Goate AM. Genetics of β-Amyloid Precursor Protein in Alzheimer's Disease. Cold Spring Harbor Perspectives in Medicine. 2017;7(6):a024539.

3.   Wu L, Rosa-Neto P, Hsiung G-YR, Sadovnick AD, Masellis M, Black SE, et al. Early-Onset Familial Alzheimer's Disease (EOFAD). Canadian Journal of Neurological Sciences / Journal Canadien des Sciences Neurologiques. 2012;39(4):436-45.

4.   Shea Y-F, Chu L-W, Chan AO-K, Ha J, Li Y, Song Y-Q. A systematic review of familial Alzheimer's disease: Differences in presentation of clinical features among three mutated genes and potential ethnic differences. Journal of the Formosan Medical Association. 2016;115(2):67-75.

5.   Weggen S, Beher D. Molecular consequences of amyloid precursor protein and presenilin mutations causing autosomal-dominant Alzheimer's disease. Alzheimer's Research & Therapy. 2012;4(2):9.

6.   O'Brien RJ, Wong PC. Amyloid Precursor Protein Processing and Alzheimer's Disease. Annu Rev Neurosci. 2011;34(1):185-204.

7.   Chang JL, Hinrich AJ, Roman B, Norrbom M, Rigo F, Marr RA, et al. Targeting Amyloid-β Precursor Protein, APP, Splicing with Antisense Oligonucleotides Reduces Toxic Amyloid-β Production. Mol Ther. 2018;26(6):1539-51.

8.   Mutations APP: Alzforum; [Available from: https://www.alzforum.org/mutations/app.

9.   Schindelin J, Rueden CT, Hiner MC, Eliceiri KW. The ImageJ ecosystem: An open platform for biomedical image analysis. Mol Reprod Dev. 2015;82(7-8):518-29.

10.   Bjourson AJ, Cooper JE. Band-stab PCR: a simple technique for the purification of individual PCR products. Nucleic Acids Res. 1992;20(17):4675.

11.   Adams AM, Harding PL, Iversen PL, Coleman C, Fletcher S, Wilton SD. Antisense oligonucleotide induced exon skipping and the dystrophin gene transcript: cocktails and chemistries. BMC Molecular Biology. 2007;8(1):57.

12.   Chen S, Le B, Rahimizadeh K, Shaikh K, Mohal N, Veedu R. Synthesis of a morpholino nucleic acid (MNA)-uridine phosphoramidite, and exon skipping using MNA/2′-O-methyl mixmer antisense oligonucleotide. Molecules. 2016;21(11):1582.

13.   Chen S, Le BT, Chakravarthy M, Kosbar TR, Veedu RN. Systematic evaluation of 2′-Fluoro modified chimeric antisense oligonucleotide-mediated exon skipping in vitro. Sci Rep. 2019;9(1):6078.

14.   Le BT, Adams AM, Fletcher S, Wilton SD, Veedu RN. Rational design of short locked nucleic acid-modified 2′-O-methyl antisense oligonucleotides for efficient exon-skipping in vitro. Mol Ther Nucleic Acids. 2017;9:155-61.

15.   Le BT, Chen S, Abramov M, Herdewijn P, Veedu RN. Evaluation of anhydrohexitol nucleic acid, cyclohexenyl nucleic acid and d-altritol nucleic acid-modified 2′-O-methyl RNA

mixmer antisense oligonucleotides for exon skipping in vitro. ChemComm. 2016;52(92):13467-70.

16.   Le BT, Filichev VV, Veedu RN. Investigation of twisted intercalating nucleic acid (TINA)-modified antisense oligonucleotides for splice modulation by induced exon-skipping in vitro. RSC Adv. 2016;6(97):95169-72.

17.   Le BT, Hornum M, Sharma PK, Nielsen P, Veedu RN. Nucleobase-modified antisense oligonucleotides containing 5-(phenyltriazol)-2′-deoxyuridine nucleotides induce exon-skipping in vitro. RSC Adv. 2017;7(86):54542-5.

18.   Le BT, Murayama K, Shabanpoor F, Asanuma H, Veedu RN. Antisense oligonucleotide modified with serinol nucleic acid (SNA) induces exon skipping in mdx myotubes. RSC Adv. 2017;7(54):34049-52.

19.   Wang T, Larcher L, Ma L, Veedu R. Systematic Screening of Commonly Used Commercial Transfection Reagents towards Efficient Transfection of Single-Stranded Oligonucleotides. Molecules. 2018;23(10):2564.

20.   McClorey G, Moulton HM, Iversen PL, Fletcher S, Wilton SD. Antisense oligonucleotide-induced exon skipping restores dystrophin expression in vitro in a canine model of DMD. Gene Therapy. 2006;13(19):1373-81.

21.   Morales-Corraliza J, Mazzella MJ, Berger JD, Diaz NS, Choi JHK, Levy E, et al. In Vivo Turnover of Tau and APP Metabolites in the Brains of Wild-Type and Tg2576 Mice: Greater Stability of sAPP in the β-Amyloid Depositing Mice. PLoS ONE. 2009;4(9):e7134.

22.   Liu Y, Beyer A, Aebersold R. On the Dependency of Cellular Protein Levels on mRNA Abundance. Cell. 2016;165(3):535-50.

Chapter 5 BACE1

5.1 Introduction

Increased amyloid beta (Aβ)-42 peptide in the brain is one of the pathological hallmarks of Alzheimer's disease (AD) [1–3]. Aβ is produced by the processing of amyloid precursor protein (APP) by two secretases, a β-secretase, beta-site amyloid precursor protein cleaving enzyme 1 (BACE1) and a γ-secretase [4]. Since the APP is processed first by BACE1, a rate-limiting step, BACE1 is a good therapeutic target [5]. BACE is an aspartyl protease and a type I transmembrane protein that is highly expressed in the brain and pancreas [5]. Elevated BACE1 expression and activity have been reported in post-mortem brains and the cerebrospinal fluids (CSF) of AD patients [3,6]. BACE1 accumulation has also been observed around amyloid plaques in brains of AD mouse models and patients [7,8]. The *BACE1* gene is found on Chromosome 11 and includes nine exons. BACE1 has two aspartic protease active site motifs (DTGS and DSGT residues) in exons 2 and 6, respectively [5]. The *BACE1* pre-mRNA undergoes alternative splicing through the splice sites within exons 3 and 4 resulting in the production of protein isoforms that are 457 and 476 amino acids in length and expressed both in the brain and pancreas, respectively. However, the alternatively spliced variants of BACE1 have reduced β-secretase activity [5].

Although there have been no clinical trials on AOs targeting BACE1, six BACE1 inhibitors evaluated in clinical trials have failed due to liver toxicity in some cases and in others due to lack of an effect on cognitive decline [10]. Some early studies focused on AO development as research tools to better understand the role of BACE1 [10–13]; however, a systematic screening of steric blocking AO designs was not reported. It was speculated that BACE1 inhibitors may need to be

administered to presymptomatic patients at high risk of developing AD, and may only need to partially inhibit BACE1 activity to reduce Aβ load slightly over a long period to have a beneficial effect [14,15]. As BACE1 partial inhibition may help to reduce Aβ load to rescue patients from cognitive decline, the development of BACE1 inhibitors that cause partial BACE1 inhibition is required.

5.2 Aim

To systematically screen splice-modulating AOs targeting *BACE1* exons to devlop an AO that results in partial inhibition of BACE1.

5.3 Methods

5.3.1 AO Design and Synthesis

The 2'-OMethyl (2'-OMe)-modified AO sequences on a phosphorothioate (2'-OMePS) backbone were designed and synthesised in-house using an ABI Expedite^{TM} 8909 oligonucleotide synthesiser (Applied Biosystems) using standard phosphoramidite chemistry at the 1 µmol scale. The synthesised oligonucleotides were deprotected by treatment with 1 mL Ammonium Hydroxide (Sigma; Cat# 221228-500Ml) overnight at 55 °C. The oligonucleotides were then purified and desalted using illustra NAP-10 columns (GE Healthcare; Cat# 45-000-153) according to the manufacturer's protocol. The AO2-PMO was purchased from Gene Tools. High-performance liquid chromatography (HPLC from Shimadzu) analyses of the most efficient AOs are shown in Table C.5 (Appendix C).

5.3.2 Cell Culture and Transfection

HEK293 cells were obtained from Cell Bank Australia (kindly provided by Associate Prof. Bruno Meloni). Cells were grown and maintained in 10% Foetal Bovine Serum in Dulbecco's Modified Eagle's Medium (ThermoFisher Scientific; Cat# 11995073) in a humidified atmosphere 37 °C incubator with 5% CO2. Cells were maintained until 70-90% confluent and then seeded in a plate or flask pre-treated with 50 µg/mL poly-D-lysine (Merck Millipore; Cat# P7886-50mg) at densities shown in the Appendix C (Table C.1), 24 h before transfection.

Next, the cells were transfected with 2'-OMePS AOs using Lipofectamine 3000 (ThermoFisher Scientific; Cat# L3000015) transfection reagent according to the manufacturer's protocol at 400 nM and 200 nM for an initial screen. The best performing AOs were then transfected using the same protocol at the following concentrations: 600 nM, 400 nM, 200 nM, 100 nM, and 50 nM. Twenty- four hours after transfection, the cells were collected for RNA extraction or for analysis by Western Blot. The AO2-PMO (Gene Tools) was transfected into HEK293 cells at 100 µM and 250 µM concentrations by nucleofection. For each treatment, 5×10^5 cells were trypsinised, centrifuged, and resuspended in the nucleofection master mix as per the manufacturer's protocol. The cells were then nucleofected with AO2-PMO using program CM- 130 by 4D Nuclofector system X-unit (Lonza, Mt Waverly, VIC, Australia) using the SF Cell Line 4D-Nucleofector™ X Kit S (Lonza; Cat# V4XC-2032) and seeded into five wells of the 24-well plate. Cells were collected at the 24 h, 48 h, three-day, and five-day time points after the first transfection for RNA extraction.

5.3.3 RNA Extraction and RT-PCR

RNA was extracted from transfected cells using ISOLATE II RNA Mini kit (Bioline; Cat#: BIO-52073) as per the manufacturer's protocol. The *BACE1* transcripts were amplified using the primer

sets (Integrated DNA Technologies, Singapore) shown in the Appendix C (Table C.2) with SuperScript III One-Step RT-PCR kit (ThermoFisher Scientific; Cat# 12574026). The RT-PCR conditions for each primer set are given in Appendix C, Table C.4. Glyceraldehyde 3-phosphate dehydrogenase (*GAPDH*) expression was used as a loading control and the primer set (ordered from IDT), and RT-PCR conditions for *GAPDH* are given in Appendix C, Table C.3 and Table C.4, respectively. The products were then separated on a 2% agarose gel in Tris-acetate-EDTA buffer, stained with Red Safe (iNtRON Biotechnology; Cat# 21141) and destained with water before being visualised with the Fusion Fx gel documentation system (Vilber Lourmat). Densitometry was performed using BioD for image capture and the ImageJ software for data analysis [16]. The downregulation of specific RT-PCR products was determined by normalising the *BACE1* transcript levels to the loading control, *GAPDH*, and further normalised to the transcript levels from the untreated (UT) cells. The gene tools control AO sequences was used as a negative control (scrambled (SCR) sequence).

5.3.4 Western Blot

Western Blot was performed on the protein extracts obtained from cells treated with the best performing AO to evaluate the effect of the AO on BACE1 protein. Cells were lysed in lysis buffer (100 µL/ sample) containing 12% SDS, 100 mM Tris-HCl, pH 6.8, 10% glycerol and loading buffer containing 1.875 µL bromophenol blue, 4.688 µL dithiothreitol, and 1.5 µL protease inhibitor was added per 100 µL of samples. Cell pellets were sonicated six times for 3 s pulses and denatured at 95 °C for 5 mins before being snap-cooled on ice. Protein concentrations were validated by separation on a protein gel and stained with Coomassie blue to ensure equal loading. The proteins were then loaded onto a 5% stacking gel containing 130 mM Tris-HCL, pH 6.8, 0.1% SDS, and 0.004% Bromophenol blue and 10% separating gel containing 400 mM Tris-HCL,

pH 8.8, and 0.1% SDS, and run using a Tris-glycine-SDS running buffer before being electrotransferred to a 0.2 µm nitrocellulose membrane (Biorad; Cat# 162-0112) in a Tris-glycine-methanol transfer buffer. The membranes were blocked in 5% skim milk in Tris-buffered saline with 0.1% Tween for 1 h. The membrane was washed three times in Tris-buffered saline with 0.1% Tween for 20 mins each, and the membrane was incubated in primary antibodies overnight at 4 °C, 1:500 anti-BACE1 (Cell Signaling Technology, Cat# 5606) and 1:1000 anti-GAPDH (ThermoFisher Scientific, Cat# PA1-988). After washing the membrane three times in Tris-buffered saline with 0.1% Tween for 20 mins each, the membrane was incubated in the secondary antibody (1:5000 anti-rabbit horse radish peroxidase, Thermofisher Scientific, Cat# 31460) for 1 h at room temperature before washing three times in Tris-buffered saline with 0.1% Tween for 20 mins each. The antibodies were detected using a Clarity Western ECL detection kit (Biorad; Cat# 1705060) according to the manufacturer's protocol and visualised using chemiluminescence-based protocol on the Fusion Fx gel documentation system (Vilber Lourmat).

5.4 Results

Initially, various 2'-OMePS AOs, were synthesised in house targeting exons 2,3,4,6, and 8 of the *BACE1* gene transcript (exon map in Figure 5.1) to induce exon-skipping (Table 5.1). All AOs were initially screened for exon-skipping at 400 and 200 nM concentrations in HEK293 cells by incubating for 24 hrs using Lipofectamine 3000, Lipofectamine 2000, Lipofectin, and Lipofectamine RNAimax transfection reagents as per the manufacturer's protocol. Twenty-four hours after transfection, the cells were collected for total RNA extraction, and reverse transcription-polymerase chain reaction (RT-PCR) was performed to amplify the regions of interest. The RT-PCR products were separated by gel electrophoresis on a 2% agarose gel, and after image capture, the PCR products were quantified using ImageJ software. The *BACE1*

transcript knockdown was achieved at various levels using all AOs targeting exon 2 and 3 (Appendix C, Figure C.1). Skipping of exons 4, 6, and 8 was achieved at various levels with different AOs (AO9, AO11, AO12, AO13, AO15, AO17, AO18, and AO20) targeting *BACE1* exons 4,6 and 8 (Appendix C, Figure C.2). The most efficient AOs (AO2, AO5, AO6, AO12, and AO13) targeted exons 2, 3, and 4, were further evaluated systematically at two different series of concentration series including 600 nM, 400 nM, 200 nM, 100 nM, and 50 nM, and 100 nM, 50 nM, 25 nM, and 12.5 nM.
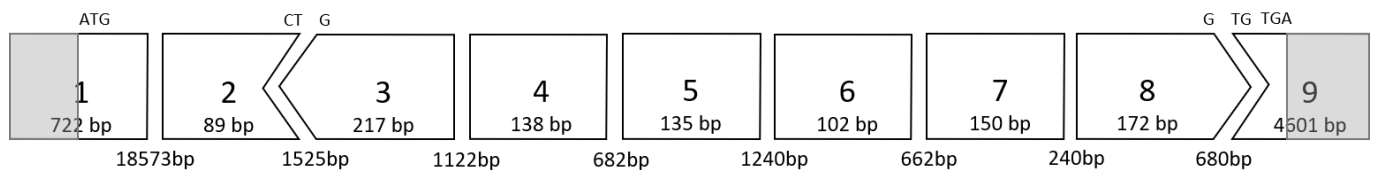
Figure 5.1   BACE1 exon map showing the size of the exons, introns and the reading frame. The rectangles represent in-frame exons, whereas the arrows indicate codons that are disrupted by exon junctions. The codons at the start and end of each in-frame and out-of-frame exon are represented by the letters above the rectangles and arrows.

.

Table 5.1   AO sequences targeting exons 2,3,4,6, and 8.

AO Coordinates		Target	Sequence(3'--> 5')	AO Number
BACE1	1E2A(+ 10 + 34)	Exon 2	AGTTACTGCTGCCTGTATCCACCAG	AO1
BACE1	1E2A(+ 38 + 62)	Exon 2	AAGGGGTGGGGGGCAGCACCCACTG	AO2
BACE1	1E2A(+ 65 + 89)	Exon 2	AGCTGCCTCTGGTAGTAGCGATGCA	AO3
BACE1	1E3A(+ 16 + 40)	Exon 3	CACATACACACCCTTCCGGAGGTCC	AO4
BACE1	1E3A(+ 41 + 65)	Exon 3	CTTCCCACTTGCCCTGGGTGTAGGG	AO5
BACE1	1E3A(+ 89 + 113)	Exon 3	TGACGTTGGGGCCATGGGGGATGCT	AO6
BACE1	1E3A(+ 141 + 165)	Exon 3	TTGATGAAGAACTTGTCTGATTCAG	AO7
BACE1	1E3A(+ 193 + 217)	Exon 3	CCTGGCAATCTCAGCATAGGCCAGC	AO8
BACE1	1E4A(+ 1 + 25)	Exon 4	AGAAAGGCTCCAGGGAGTCGTCAGG	AO9
BACE1	1E4A(+ 31 + 55)	Exon 4	GAACGTGGGTCTGCTTTACCAGAGA	AO10
BACE1	1E4A(+ 61 + 85)	Exon 4	CACCACAAAGCTGCAGGGAGAAGAG	AO11
BACE1	1E4A(+ 88 + 112)	Exon 4	CTTCAGACTGGTTGAGGGGGAAGCC	AO12
BACE1	1E4A(+ 114 + 138)	Exon 4	CATGCTCCCTCCGACAGAGGCCAGC	AO13
BACE1	1E6A(+ 4 + 28)	Exon 6	TGTCCACAATGCTCTTGTCATAGTT	AO14

148

AO Coordinates	Target	Sequence(3'--> 5')	AO Number
BACE1 1E6A(+ 36 + 60)	Exon 6	TTTCTTGGGCAAACGAAGGTTGGTG	AO15
BACE1 1E6A(+ 75 + 99)	Exon 6	GGAGGCTGCCTTGATGGATTTGACT	AO16
BACE1 1E8A(+ 6 + 30)	Exon 8	CTGCGGAAGGATGGTGATGCGGAAG	AO17
BACE1 1E8A(+ 33 + 57)	Exon 8	AAACTTGTAACAGTCGTCTTGGGAC	AO18
BACE1 1E8A(+ 63 + 87)	Exon 8	AACAGTGCCCGTGGATGACTGTGAG	AO19
BACE1 1E8A(+ 109 + 133)	Exon 8	CCCGATCAAAGACAACGTAGAAGCC	AO20
BACE1 1E8A(+ 148 + 172)	Exon 8	CATGGCAAGCGCTGACAGCAAAGCC	AO21

5.4.1 Evaluation of the Most Efficient 2'-OMePS AOs to Induce Exon-Skipping of the BACE1 Transcript in HEK293 Cells in vitro.

We then systematically evaluated the exon-skipping efficiency of the lead AOs (AO2, AO5, AO6, AO8, AO12, and AO13; Table 5.1) *in vitro,* initially at 600 nM, 400 nM, 200 nM, 100 nM, and 50 nM concentrations. The AOs targeting exons 2 and 3, AO2, AO5, AO6, and AO8 downregulated the *BACE1* transcript levels, and AO12 and AO13 that targeted Exon 4 were capable of inducing efficient exon-skipping *in vitro* (Figure 5.2). The AO2 and AO6 were found to be the most efficient at downregulating the *BACE1* transcript in a dose-dependent manner, while both AO12 and AO13 were very efficient in inducing exon 4 skipping of *BACE1* Variant A. Based on these results, the efficacy of AO2 and AO6 and AO12 and AO13 were also further tested at lower concentrations (100 nM, 50 nM, 25 nM, and 12.5 nM). Both AO2 and AO6 showed downregulation of the *BACE1* transcript in a dose-dependent manner (Figure 5.3); however, densitometry analysis revealed that AO2 and AO6 were the most efficient at 400 nM (Figure 5.4). Interestingly, although AO12 and AO13 induced exon-skipping, the dose-dependence was not as obvious (Figure 5.4); however, exon-skipping was observed even at 12.5 nM concentration. Both AO12 and AO13 were most efficient at inducing exon-skipping at 400 nM, but no concentration tested in this study could induce 100% exon-skipping. The most effective AOs were determined to be AO2 and AO6, both of which showed close to 100% downregulation of the *BACE1* transcript (Figure 5.4). Of the two

AOs, AO2 was used for further evaluation as it showed consistent dose-dependent downregulation of *BACE1* transcript at all concentrations without affecting the reference control transcript expression.
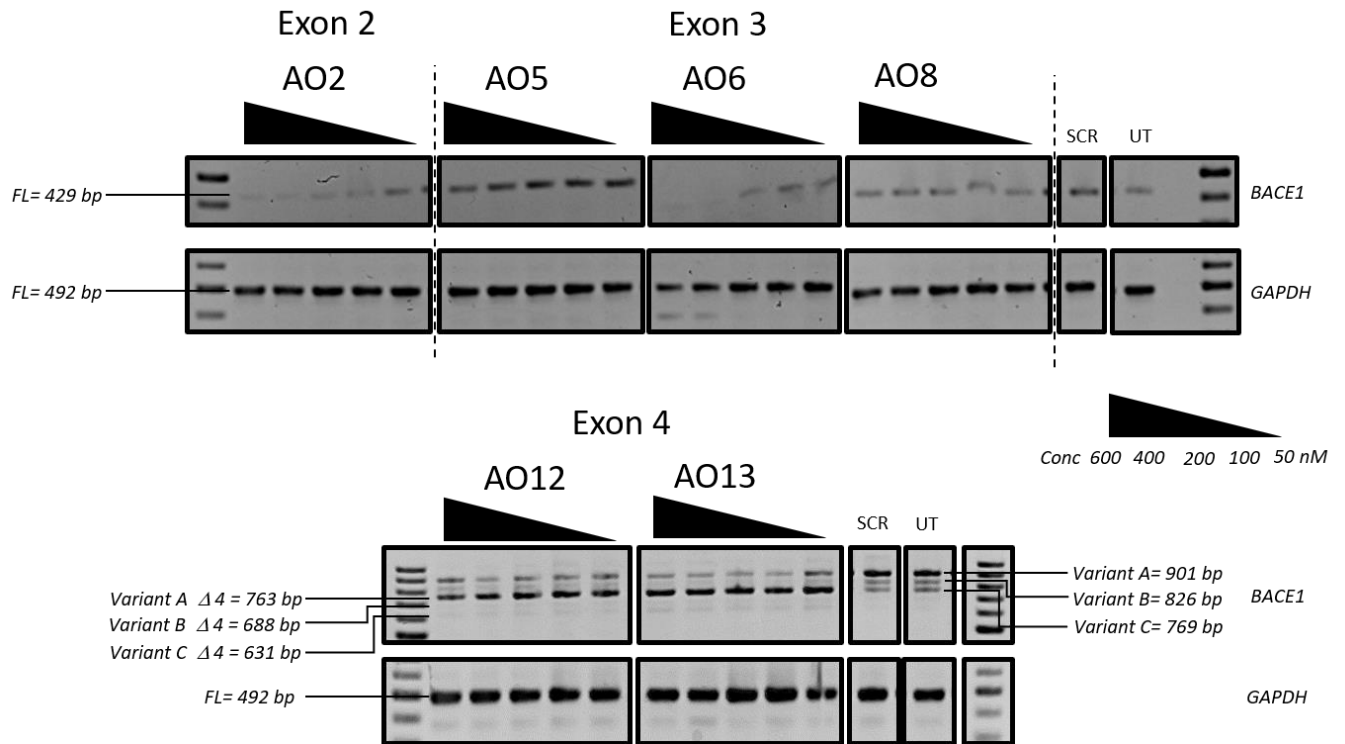
Figure 5.2   RT-PCR analysis of the BACE1 and GAPDH transcripts after treatment with the most effective 2'-O-MePS AOs (AO2, AO5, AO6, AO8, AO12, and AO13) targeting exons 2, 3, and 4 at 600 nM, 400 nM, 200 nM, 100 nM, and 50 nM concentrations in HEK293 cells. FL, full-length; UT, untreated; SCR, scrambled sequence; GAPDH was used as a house-keeping gene control. The gel images were cropped to highlight the BACE1-specific products and the corresponding house-keeping gene control GAPDH. The original images are shown in Figure C.3 (Appemdix B).
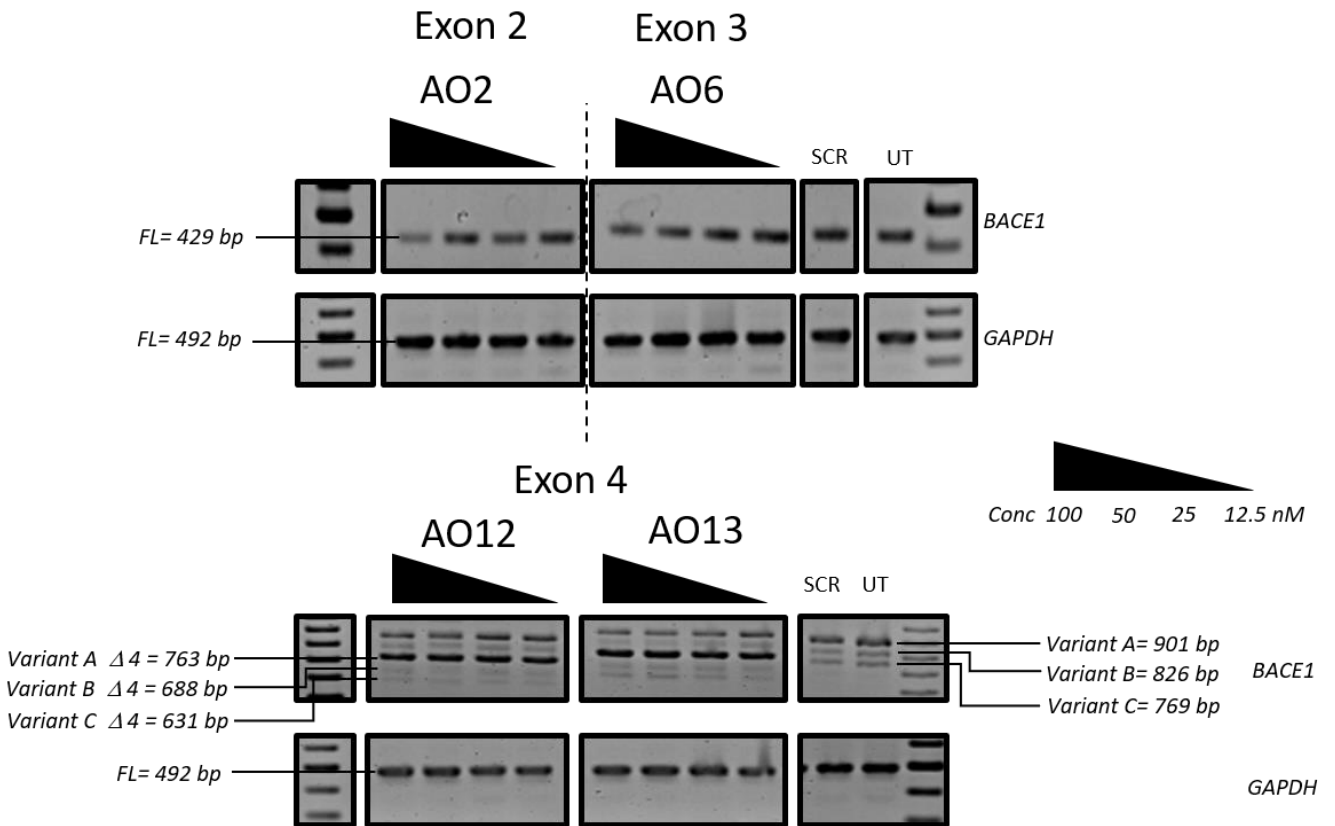
Figure 5.3　　　*RT-PCR analysis of the BACE1 and GAPDH transcripts after treatment of HEK293 cells with the most effective 2'-O-MePS AOs (AO2, AO6, AO12, and AO13) targeting BACE1 exons 2, 3, and 4 at 100 nM, 50 nM, 25 nM, and 12.5 nM concentrations. FL, full-length; UT, untreated; SCR, scrambled sequence; GAPDH was used as a loading control. The gel images were cropped to highlight the BACE1 specific products and the corresponding house-keeping gene control GAPDH. The original images are shown in Figure C.4 (Appendix C).*
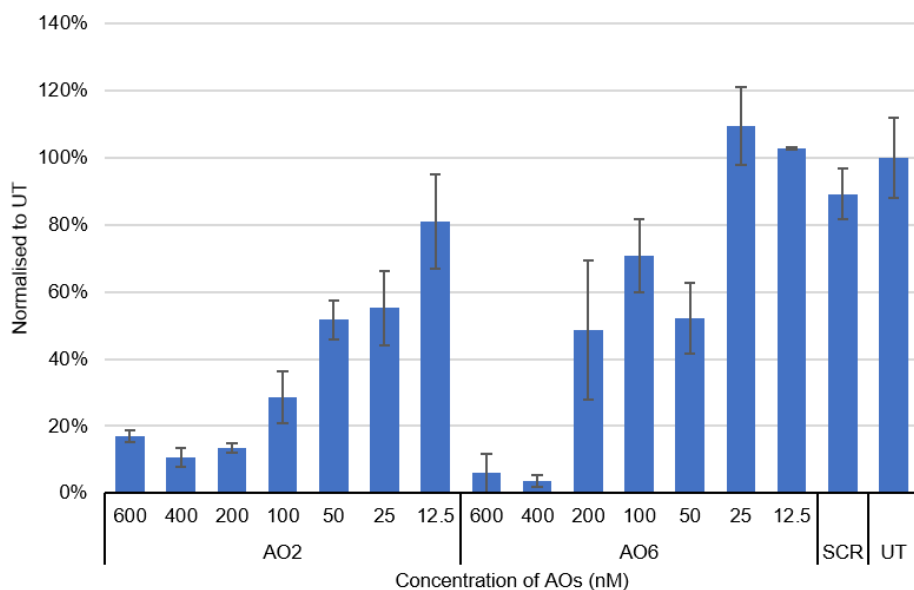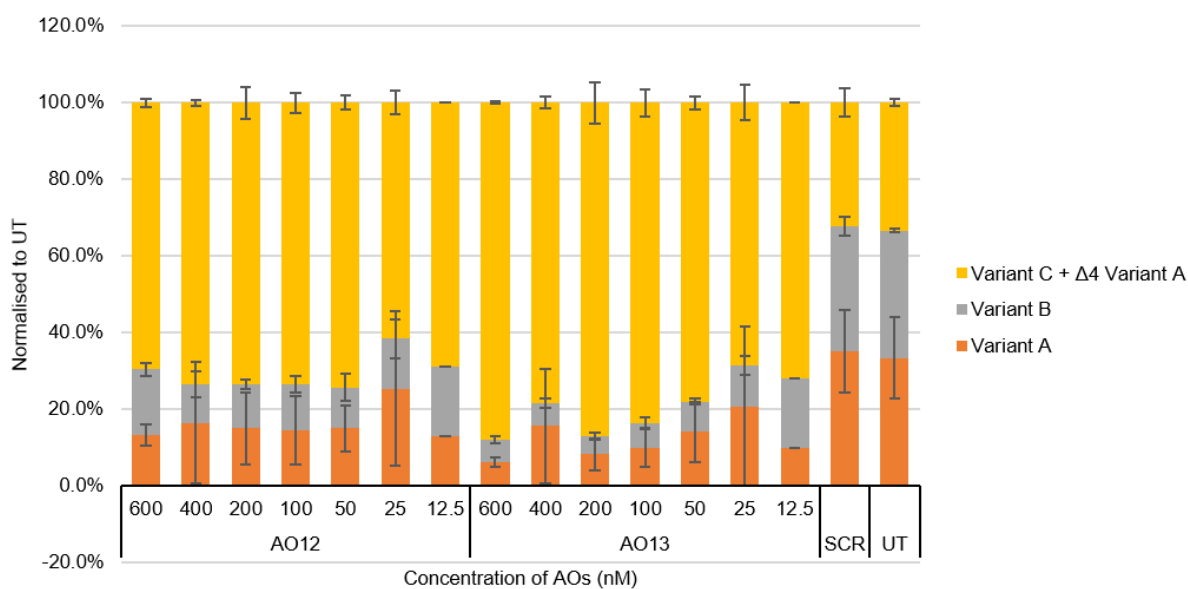
Figure 5.4   A. Densitometry analysis of RT-PCR products (three replicates) derived from HEK293 cells transfected with AO2 and AO6 B. Densitometry analysis of RT-PCR products (more than two replicates) derived from HEK293 cells transfected with AO12 and AO13. Concentrations of AOs used include 12.5 nM, 25 nM, 50 nM, 100 nM, 200 nM, 400 nM, and 600 nM. FL, full-length; UT, untreated; SCR, scrambled sequence.

5.4.2 Evaluation of the Most Efficient 2'-OMePS AO sequences prepared as PMOs to Induce Exon-Skipping of *BACE1* Transcript in HEK293 Cells *in vitro*.

For clinical application, it is important that the AOs are safe to use in humans. The PMO chemistry has demonstrated an excellent safety profile in humans at all doses tested. The most effective AO

sequence, AO2 was synthesised using the PMO chemistry (named AO2-PMO), and evaluated for potential downregulation of *BACE1* transcript levels in HEK293 cells at 100 µM and 250 µM concentrations. The cells were incubated with the AO2-PMO for 1, 2, 3, and 5 days (Figure 5.5). The results show that AO2-PMO treatment downregulated *BACE1* transcript at 100 µM and 250 µM concentrations at all time points assessed. However, *BACE1* downregulation was much less than that induced by AO2, the 2'-OMePS counterpart. The highest downregulation observed with AO2-PMO was around 60% after three days of incubation, whereas 89% reduction in *BACE1* levels was observed after one day of incubation with the 2'-OMePS AO of the same sequence.
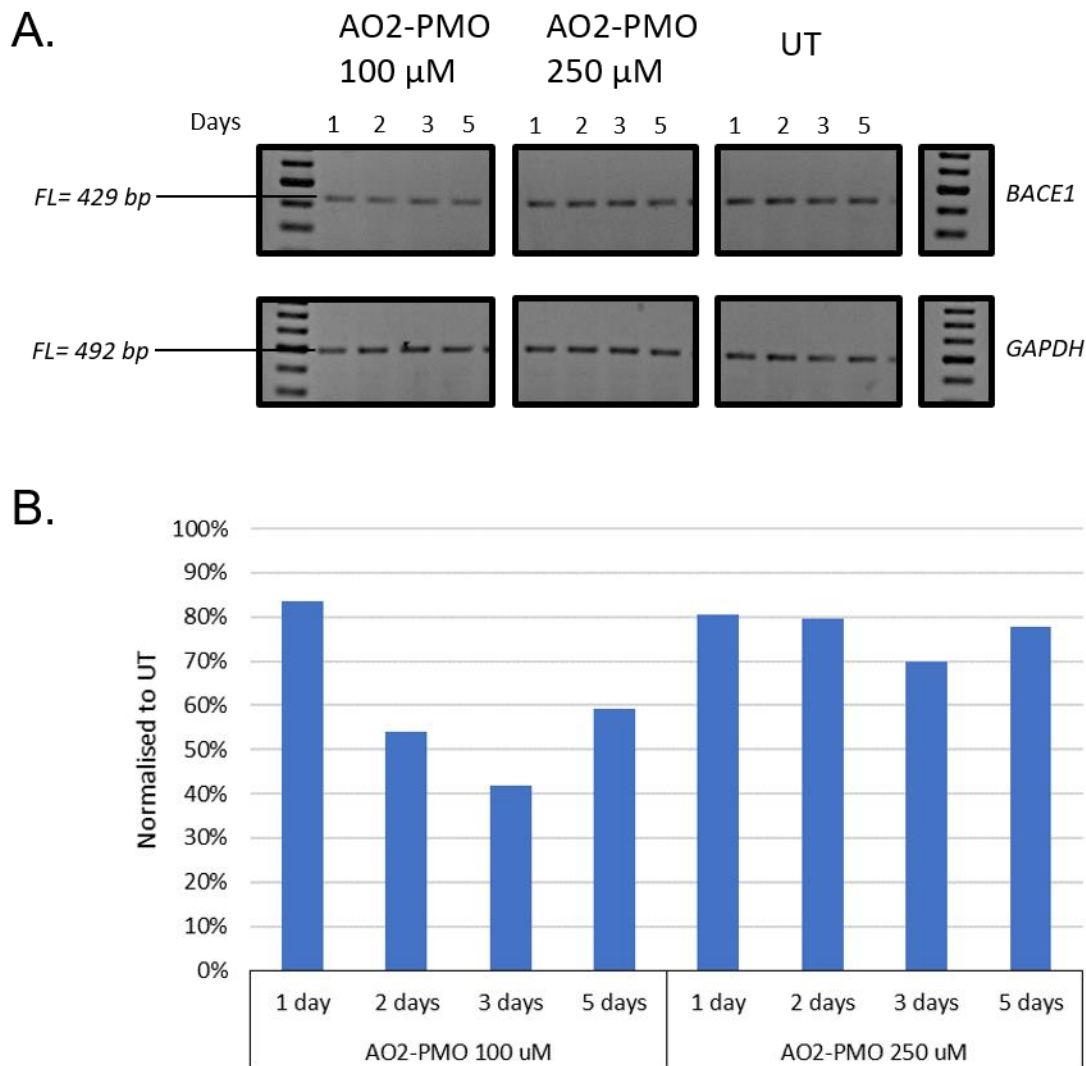
Figure 5.5   *(A). Representative RT-PCR analysis (of three replicates) of the BACE1 and GAPDH transcripts after treatment of HEK293 cells with AO2-PMO targeting exon 2 for 1, 2, 3, and 5 days at 100 μM and 250 μM. FL, full-length; UT, untreated; SCR, scrambled sequence; GAPDH was used as a loading control. The gel images were cropped , however the original images are shown in Figure C.5 (Appendix C). (B). Densitometry analysis of BACE1 transcript amplicons derived from transfected HEK293 cells.*

5.4.3 Evaluation of the Mechanism of Action of AO2.

As AO2 was found to be the most effective candidate showing dose-dependent downregulation of

the *BACE1* transcript, AO2 was further investigated for the mechanism of action. While AO2 was

designed to target the splicing enhancer region of *BACE1* exon 2 and induce exon 2 skipping,

exon-skipping was not observed as predicted, and we investigated the possible degradation of the

exon 2-skipped transcript by non-sense mediated decay. Other regions of the *BACE1* transcript

(exons 2–8, 3–8, and 4–9) were amplified, confirming reduced exon 1-4 transcript (Figure 5.6) and specifically reduced exon 1–2 transcript as the *BACE1* transcript was not downregulated from exons 3–9 (Figure 5.6). This is not indicative of exon 2 skipping and subsequent degradation of the skipped product by nonsense-mediated decay.
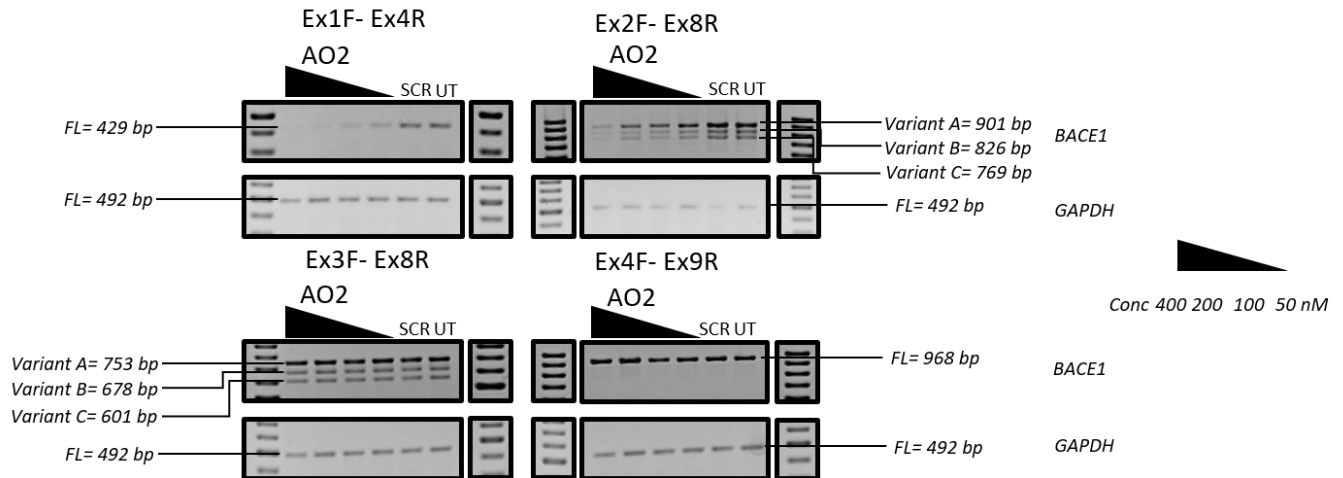
Figure 5.6   Representative RT-PCR analysis of the BACE1 and GAPDH transcripts (of three replicates) after treatment of HEK293 cells with AO2 targeting exons 2 at 400 nM, 200 nM, 100 nM, and 50 nM. Specific regions of the RNA were amplified using different primer sets. Exons 1–4 were amplified using primer set Ex1F-Ex4R, exons 2–8 were amplified using primer set Ex2F-Ex8R, exons 3–8 were amplified using primer set Ex3F-Ex8R, and exons 4–9 were amplified using primer set Ex4F-Ex9R. FL, full-length; UT, untreated; SCR, scrambled sequence; GAPDH was used as a loading control. The gel images were cropped to highlight the BACE1 specific products and the corresponding house-keeping gene control GAPDH. The original images are shown in Figure C.6 (Appendix C).

5.4.4 Evaluation of BACE1 Protein Downregulation.

The potential for of AO2 to downregulate BACE1 protein was evaluated y Western blotting of protein extracts from HEK293 cells, 24 h after transfection (Figure 5.7). Briefly, AO2 (400 nM) treated HEK293 cells were incubated for 24 h before collection. The cell pellet was collected and lysed with SDS lysis buffer. The proteins were separated on a 10% separating and 5% stacking gel and transferred onto a nitrocellulose membrane. The membrane was incubated with 1:500 dilution of the BACE1 antibody overnight at 4 °C, and 1:5000 anti-rabbit HRP secondary antibody for 1 h at room temperature. The total protein loading was evaluated using a loading control, GAPDH. The membrane was incubated with 1:1000 GAPDH antibody overnight at 4 °C, followed by

1:5000 anti-rabbit HRP secondary antibody. The antibodies were detected using the Clarity Western ECL detection kit (Biorad) and the chemiluminescence protocol on the Fusion Fx gel documentation system (Vilber Lourmat). The Western blot analysis showed that there was 45% downregulation of BACE1 in cells, 24 h after AO2 transfection.
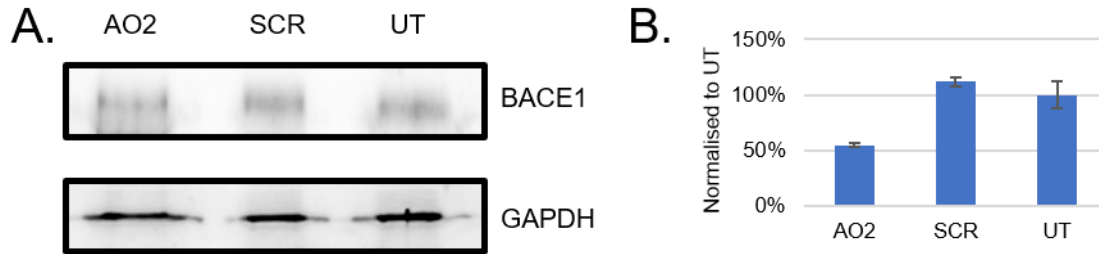
Figure 5.7   (A). Representative Western blot protein analysis of the BACE1 and GAPDH proteins, 24h after transfection with AO2, targeting exon 2, at 400 nM in HEK293 cells. FL, full-length; UT, untreated; SCR, scrambled sequence; GAPDH was used as a loading control. The gel images were cropped, however, the original images are shown in Figure C.7 (Appendix C). (B). Densitometry analysis of protein extracts from HEK293 cells, 24 h after AO transfection.

5.5 Discussion

A steric blocking AO that partially downregulates BACE1 protein expression has been developed in this study. Antisense oligonucleotides (AOs) were designed to target regions in exons 2, 3, and 8 to induce the respective exon-skipping by targeting the splicing factors binding sites to disrupt open reading frame, resulting in premature termination codons in exons 3, 4, and 9, respectively. Similarly, AOs were also designed to target regions in exons 4 and 6 to induce skipping of these exons that encode important functional domains required for β-secretase activity. All the AOs (AO1-8) targeting exons 2 and 3 of the *BACE1* transcript downregulated *BACE1* transcript to various degrees, of which AO2 and AO6 were found to be the most effective; however, these AOs did not show the predicted exon-skipping product. Notably, AOs (AO9, AO11, AO12, AO13, AO15, AO17, AO18, and AO20) targeting exons 4 and 6 induced exon-skipping as predicted, but

AO12 and AO13 targeting *BACE1* exon 4 were most effective at inducing the transcript product of 763 bp, missing exon 4.

This study used 2'-OMePS AOs for systematic screening of AO sequences to downregulate the *BACE1* transcript, with the lead AO sequence later evaluated as a PMO. Both 2'-OMePS and PMO chemistries have been well-established for the use *in vitro*, as well as *in vivo* for developing splice modulating therapeutics [24,25]. Negatively charged 2'-OMePS oligonucleotides are economical to synthesise and available commercially from several manufacturers. The PMO is a neutrally charged oligonucleotide; however, large scale production of PMO is challenging due to difficulties in its synthesis that is not compatible with standard phosphoramidite chemistry. Unlike 2'OMePS chemistry, the PMO chemistry also has shown an excellent safety profile and is used clinically. Therefore, while the 2'-OMePS chemistry is used for AO sequence screening purposes, the most effective AO sequences are later tested as PMOs. In our study, the best 2'-OMePS AO sequence (AO2) efficiently downregulated the *BACE1* transcript but, when this sequence was tested as a PMO, it was found to be less effective at inducing exon skipping and transcript downregulation. The AO2 sequence is a G-rich oligonucleotide sequence, and we speculate that the difference observed in the efficiency of the 2'-OMePS AO and the PMO AO may be due to the PMOs forming G-quadruplex structures, while the 2'-OMePS sequence does not, which may explain the lower efficiency of the same sequence with a PMO chemistry. However, although unlikely the lack of PMO effect may also be due to an experimental issue with electroporation of the PMO. To confirm if the lack of effect is real or due to an experimental issue, the 2'-OMeOS sequence would also have to be electroporated alongside the PMO.

The AOs in this study were designed to target selected exons for exclusion during pre-mRNA processing in order to reduce the expression of functional BACE1 protein. The lead AO candidate,

AO2, showed downregulation of *BACE1* mRNA, and we predicted that AO2-mediated *BACE1* mRNA downregulation might be due to nonsense-mediated decay, a result of reading frame disruption and induction of a premature stop codon [26]. Amplification of the isolated RNA after the treatment of the cells with AO2 showed that the downregulation of *BACE1* mRNA was evident only in the exon 1–exon 2 region, but showed unchanged expression levels in the regions between exons 3–9 indicating that AO2-mediated *BACE1* transcript downregulation may not be due to nonsense-mediated decay. We speculated that the potential reason for the downregulation of the exon 1–2 region might be due to a steric block imposed in this region that ultimately inhibits the translation. BACE1 protein analysis after AO2 treatment of HEK293 cells shows that there is a reduction in BACE1 level at 24 h (around 60% compared to UT). BACE1 has a half-life of over nine hours in cultured cells [5]; therefore, most of the inhibition is seen 24 h after AO2 treatment. Although we achieved close to 100% inhibition of the *BACE1* mRNA, we could not see a similar level of BACE1 protein inhibition (only 45% inhibition at the protein level). The partial inhibition may be due to the regulation of BACE1 protein levels by mechanisms both at the transcriptional, translational, and post-translational levels [27]. As studies have shown that 5'-UTR region of the BACE1 has a role in regulating the BACE1 protein levels [27], reducing *BACE1* mRNA may only have a small role in regulating BACE1 protein. The complete suppression of BACE1 may not be possible, but a partial reduction of BACE1 has been shown to improve amyloid neuropathology suggesting that a complete reduction of BACE1 is not required for beneficial effects [5,15,28]. Furthermore, BACE1 also has other substrates, and therefore, complete elimination of BACE1 may have deleterious effects [15,28]. The reduction of BACE1 protein levels observed in the study should result in reduced beta-secretase activity. The beta-secretase activity can be measured using the beta-secretase activity to further validate this study.

5.6 Conclusion

We have screened various AOs designed to induce *BACE1* splice modulation. One potential candidate named AO2 targeting exon 2, potentially by a steric blocking mechanism, was found to be the most efficient in inhibiting *BACE1* expression at the RNA and protein level in HEK293 cells. Of the two chemistries evaluated for this application, the 2'-OMePS chemistry was found to be far more efficient, compared with the PMO chemistry, yielding close to 90% *BACE1* transcript downregulation and resulted in 45% downregulation of the BACE1 protein. Although further validation of AO2 *in vivo* and its effect on Aβ production is required to ensure the applicability of this molecule in mitigating AD, we believe that partial inhibition of BACE1 protein levels achieved here could be used as a potential preventative strategy for people at high risk of developing AD.

5.7 References

1.   Näslund, J. Correlation between elevated levels of amyloid β-peptide in the brain and cognitive decline. JAMA 2000, 283, 1571–1577.

2.   Gandy, S. The role of cerebral amyloid β accumulation in common forms of alzheimer disease. J. Clin. Investig. 2005, 115, 1121–1129.

3.   Li, R.; Lindholm, K.; Yang, L.B.; Yue, X.; Citron, M.; Yan, R.; Beach, T.; Sue, L.; Sabbagh, M.; Cai, H.; et al. Amyloid peptide load is correlated with increased -secretase activity in sporadic alzheimer's disease patients. Proc. Natl. Acad. Sci. USA 2004, 101, 3632–3637.

4.   Selkoe, D.J. Alzheimer's disease: Genes, proteins, and therapy. Physiol. Rev. 2001, 81, 741–766.

5. Cole, S.L.; Vassar, R. The alzheimer's disease β-secretase enzyme, bace1. Mol. Neurodegener. 2007, 2, 22.

6. Yang, L.-B.; Lindholm, K.; Yan, R.; Citron, M.; Xia, W.; Yang, X.-L.; Beach, T.; Sue, L.; Wong, P.; Price, D.; et al. Elevated β-secretase expression and enzymatic activity detected in sporadic alzheimer disease. Nat. Med. 2003, 9, 3–4.

7. Zhao, J.; Fu, Y.; Yasvoina, M.; Shao, P.; Hitt, B.; O'Connor, T.; Logan, S.; Maus, E.; Citron, M.; Berry, R.; et al. β-site amyloid precursor protein cleaving enzyme 1 levels become elevated in neurons around amyloid plaques: Implications for alzheimer's disease pathogenesis. J. Neurosci. 2007, 27, 3639–3649.

8. Sadleir, K.R.; Kandalepas, P.C.; Buggia-Prévot, V.; Nicholson, D.A.; Thinakaran, G.; Vassar, R. Presynaptic dystrophic neurites surrounding amyloid plaques are sites of microtubule disruption, bace1 elevation, and increased aβ generation in alzheimer's disease. Acta Neuropathol. 2016, 132, 235–256.

9. Stein, C.A.; Castanotto, D. Fda-approved oligonucleotide therapies in 2017. Mol. Ther. 2017, 25, 1069–1075.

10. Panza, F.; Lozupone, M.; Solfrizzi, V.; Sardone, R.; Piccininni, C.; Dibello, V.; Stallone, R.; Giannelli, G.; Bellomo, A.; Greco, A.; et al. Bace inhibitors in clinical development for the treatment of alzheimer's disease. Expert Rev. Neurother. 2018, 18, 847–857.

11. Yan, R.; Bienkowski, M.J.; Shuck, M.E.; Miao, H.; Tory, M.C.; Pauley, A.M.; Brashler, J.R.; Stratman, N.C.; Mathews, W.R.; Buhl, A.E. Membrane-anchored aspartyl protease with alzheimer's disease β-secretase activity. Nature 1999, 402, 533–537.

12.   Vassar, R. β-secretase cleavage of alzheimer's amyloid precursor protein by the transmembrane aspartic protease bace. Science 1999, 286, 735–741.

13.   Mowrer, K.R.; Wolfe, M.S. Promotion of bace1 mrna alternative splicing reduces amyloid β-peptide production. J. Biol. Chem. 2008, 283, 18694–18701.

14.   Peters, F.; Salihoglu, H.; Rodrigues, E.; Herzog, E.; Blume, T.; Filser, S.; Dorostkar, M.; Shimshek, D.R.; Brose, N.; Neumann, U. Bace1 inhibition more effectively suppresses initiation than progression of β-amyloid pathology. Acta Neuropathol. 2018, 135, 695–710.

15.   Vassar, R. Implications for bace1 inhibitor clinical trials: Adult conditional bace1 knockout mice exhibit axonal organization defects in the hippocampus. J. Prev. Alzheimer's Dis. 2019, 6, 78–84.

16.   Schindelin, J.; Rueden, C.T.; Hiner, M.C.; Eliceiri, K.W. The imagej ecosystem: An open platform for biomedical image analysis. Mol. Reprod. Dev. 2015, 82, 518–529.

17.   Chen, S.; Le, B.; Rahimizadeh, K.; Shaikh, K.; Mohal, N.; Veedu, R. Synthesis of a morpholino nucleic acid (mna)-uridine phosphoramidite, and exon skipping using mna/2′-o-methyl mixmer antisense oligonucleotide. Molecules 2016, 21, 1582.

18.   Chen, S.; Le, B.T.; Chakravarthy, M.; Kosbar, T.R.; Veedu, R.N. Systematic evaluation of 2′-fluoro modified chimeric antisense oligonucleotide-mediated exon skipping in vitro. Sci. Rep. 2019, 9, 6078.

19.   Le, B.T.; Adams, A.M.; Fletcher, S.; Wilton, S.D.; Veedu, R.N. Rational design of short locked nucleic acid-modified 2′-o-methyl antisense oligonucleotides for efficient exon-skipping in vitro. Mol. Ther. Nucleic Acids 2017, 9, 155–161.

20.   Le, B.T.; Chen, S.; Abramov, M.; Herdewijn, P.; Veedu, R.N. Evaluation of anhydrohexitol nucleic acid, cyclohexenyl nucleic acid and d-altritol nucleic acid-modified 2′-o-methyl RNA mixmer antisense oligonucleotides for exon skipping in vitro. Chem. Commun. 2016, 52, 13467–13470.

21.   Le, B.T.; Filichev, V.V.; Veedu, R.N. Investigation of twisted intercalating nucleic acid (tina)-modified antisense oligonucleotides for splice modulation by induced exon-skipping in vitro. RSC Adv. 2016, 6, 95169–95172.

22.   Le, B.T.; Hornum, M.; Sharma, P.K.; Nielsen, P.; Veedu, R.N. Nucleobase-modified antisense oligonucleotides containing 5-(phenyltriazol)-2′-deoxyuridine nucleotides induce exon-skipping in vitro. RSC Adv. 2017, 7, 54542–54545.

23.   Le, B.T.; Murayama, K.; Shabanpoor, F.; Asanuma, H.; Veedu, R.N. Antisense oligonucleotide modified with serinol nucleic acid (sna) induces exon skipping in mdx myotubes. RSC Adv. 2017, 7, 34049–34052.

24.   Disterer, P.; Kryczka, A.; Liu, Y.; Badi, Y.E.; Wong, J.J.; Owen, J.S.; Khoo, B. Development of therapeutic splice-switching oligonucleotides. Hum. Gene Ther. 2014, 25, 587–598.

25.   Järver, P.; O'Donovan, L.; Gait, M.J. A chemical view of oligonucleotides for exon skipping and related drug applications. Nucleic Acid Ther. 2014, 24, 37–47.

26.   Chang, Y.-F.; Imam, J.S.; Wilkinson, M.F. The nonsense-mediated decay RNA surveillance pathway. Annu. Rev. Biochem. 2007, 76, 51–74.

27.	Roßner, S.; Sastre, M.; Bourne, K.; Lichtenthaler, S.F. Transcriptional and translational regulation of bace1 expression—Implications for alzheimer's disease. Prog. Neurobiol. 2006, 79, 95–111.

28.	Singer, O.; Marr, R.A.; Rockenstein, E.; Crews, L.; Coufal, N.G.; Gage, F.H.; Verma, I.M.; Masliah, E. Targeting bace1 with sirnas ameliorates alzheimer disease neuropathology in a transgenic model. Nat. Neurosci. 2005, 8, 1343–1349.

Chapter 6 MAPT

6.1 Introduction

The aggregation of the hyperphosphorylated tau protein encoded by the gene microtubule-associated protein tau (*MAPT*) leading to the formation of neurofibrillary tangles has been implicated in a variety of tauopathies including Alzheimer's disease (AD), frontotemporal dementia, Pick disease, argyrophilic grain disease, progressive supranuclear palsy and corticobasal degeneration (1), and tau levels are elevated in the cerebrospinal fluid (CSF) of AD patients. Although neurofibrillary tangles are a hallmark of AD, most of the drugs development initiatives target the Aβ pathway. However, with the failure of the drug molecules targeting the Aβ pathway, the focus is now shifting towards targeting hyperphosphorylated tau. One approach is the development of AOs against *MAPT* to reduce the production of hyperphosphorylated tau. A gapmer (RNase H mediated mRNA degradation), AO named $MAPT_{RX}$, developed by IONIS Pharmaceuticals is currently being tested in Phase II clinical trials (2). Another study evaluated PMO oligomers for downregulating tau expression in human neuroblastoma cells using splice modulation (3). Although tau is believed to be very important in stabilising microtubules and that neurodegeneration has been attributed to loss of this function, mouse models have shown that tau knockout is well tolerated and these mice show minor motor phenotypes that develop after 12-16 months (4). Furthermore, reducing tau levels in adult mice results in no behavioural or neuroanatomical abnormalities, indicating that there may be other microtubule-associated proteins that can compensate for the loss of tau in microtubule stabilisation (4, 5). In addition, the reduction

in tau monomers may result in depolymerisation of the paired helical filaments to maintain

equilibrium (5).
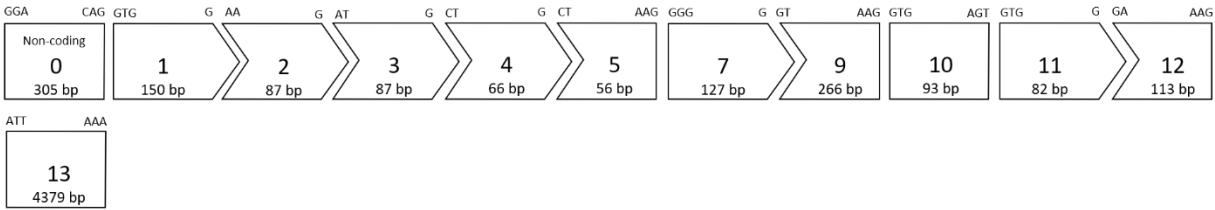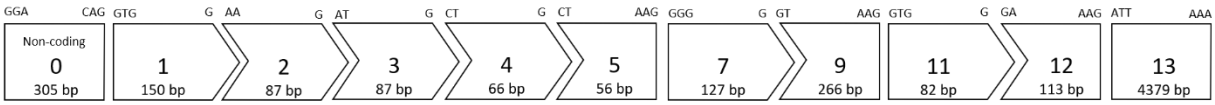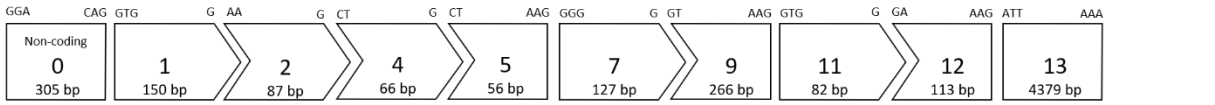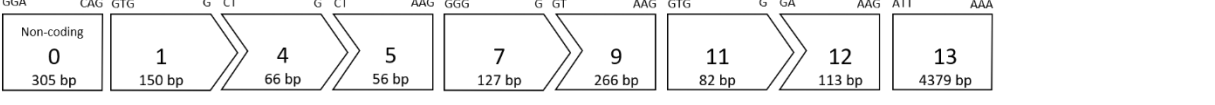
Figure 6.1   Exon map of MAPT isoforms found in the human brain showing the size of the exons and the reading frame. The rectangles represent in-frame exons, whereas the arrows indicate codons that are disrupted by exon junctions. The codons at the start and end of each in-frame and out-of-frame exon are represented by the letters above the rectangles and arrows.

6.2 Aim

To develop novel DNAzymes and 2'-O-Methyl PS RNA-modified splice-modulating AOs

targeting various *MAPT* exons for efficient downregulation of tau protein levels.

6.3 Methods

6.3.1 DNAzyme and antisense oligonucleotides

DNAzymes with stem-loop conformation were designed for the selected exons (sequences in Table D.3 and exon map shown in Figure 6.1) in line with our previous work on antimiRzymes (6), and the oligonucleotides were purchased from Integrated DNA Technologies (IDT, Singapore). The AOs (2'-OMePS AOs) were synthesised in-house on the AKTA Oligopilot 10 synthesiser (GE Healthcare Life Sciences) using standard phosphoramidite chemistry at 1 μmole scale (exon map shown in Figure 6.1 and AO names and their sequences are listed in Table D.6). The synthesised AOs were deprotected by treatment with 1 mL ammonium hydroxide (Sigma; Cat# 221228-500mL) overnight at 55°C and were purified by desalting using the illustra NAP-10 columns (GE Healthcare; Cat# 45-000-153) according to the manufacturer's protocol and verified by HPLC.

6.3.2 Cell culture and transfection of AOs and DNAzymes

Cell cultures media and supplements were purchased from (Life technologies, Australia) unless specified. The SH-SY5Y cells were obtained from Cell Bank Australia (Kindly provided by Prof. Sue Fletcher and Prof. Steve Wilton). The SH-SY5Y cells were propagated in Dulbecco's modified Eagle's F12 medium supplemented with 10% Fetal Bovine Serum (FBS) (Serana; Cat# FBS-AU-015) in a humidified atmosphere at 37°C incubator with 5% CO2. Cells were maintained until 70-90% confluent and then seeded onto plates or flasks for transfections. Transfections were performed in 24 well-plate formats seeded with approximately 70,000 cells/well for RNA transcript analysis. Transfections were also performed in T25cm^2 flasks seeded with approximately 875,000 cells for protein analysis. The cells were seeded one day before transfecting with the DNAzymes or 2'-OMe-PS AOs complexed with Lipofectamine 3000 transfection reagent

(ThermoFisher Scientific; Cat# L3000015) as per the manufacturer's protocol. Transfection were carried out for 24 hours before harvesting RNA for transcript analysis. For protein analysis, transfection was carried out 24 h, 48 h (re-transfected at 24h) and six days (re-transfected at 24 h, and 48 h) before collecting the cell pellet.

6.3.3 RT-PCR analysis of AOs and DNAzymes treatment

RNA was extracted using Bioline Isolate II RNA MiniPrep Kit (Bioline; Cat# BIO-52073) following the manufacturer's protocol. Total RNA (50 ng) was analysed using primer sets (purchased from IDT, Singapore) listed in Appendix D (Table D.1), Superscript III One-Step RT-PCR System (ThermoFisher Scientific; Cat# 12574026) and reaction conditions are given in the Appendix D (Table D.2). *GAPDH* was used as a housekeeping control and the primer set (purchased from IDT), and RT-PCR conditions for *GAPDH* are given in Appendix D (Table D.1 and Table D.2). The products were separated on a 2% agarose gel in Tris-acetate-EDTA buffer, stained with Red Safe (iNtRON Biotechnology; Cat# 21141) and destained with water before being visualised with Fusion Fx gel documentation system (Vilber Lourmat).

6.3.4 Densitometry analysis

Densitometry (measuring intensity after image capture) of the RT-PCR products on the gels was performed using Image J Software (7). The intensity of the *MAPT* product bands from different DNAzyme or AO treated samples was measured and normalised to the intensity of the corresponding *GAPDH* products before comparing that of the untreated samples. The percentage of *MAPT* transcript knockdown in SH-SY5Y cells was interpreted as the activity of DNAzyme or AO.

6.3.5 *In vitro* cleavage assay using DNAzymes

The cleavage efficiency of the DNAzymes *in vitro* was tested using an *in vitro* cleavage assay. 4.4 µL of 20 µM DNAzyme was incubated with an equi-molar concentration of FAM-conjugated *MAPT* RNA (5'-FAM-   UGUGGCUCAUUAGGCAACAUCCAUCAUAAACCAG-3') in 5 µL of buffer containing Mg^{2+} divalent cations (10 mM MgCl2) at 37°C. The reaction was stopped by adding 10 µL of formamide to 10 µL of the reaction mixture at 0, 30 mins, 60 mins and 2 h. Scrambled DNAzyme RNV563-SCR (AACATCCTCGTTGTAGCTAGCCTCATAAAC), RNV563-Mut1 (GTTTATGA<u>AA</u>CTAGCTACAACGAGGATGTT), and RNV563-Mut2 (GTTTATGAGGCTA<u>AA</u>TACAACGAGGATGTT) were used as negative controls, and the untreated (UT) samples did not have any DNAzyme added. The underlined bases are the mutated bases and the two double mutants RNV563-Mut1, and RNV 563-Mut2 were designed according to previous reports (8, 9). The reaction mixtures were separated on a 15% polyacrylamide gel containing 7M urea and run in a EDTA containing tris buffer for 50 mins at 13 W. The gel was visualised unstained and the image captured using the Fusion Fx gel documentation system (Vilber Lourmat).

6.3.6 Western Blot analysis

Western Blot was performed on the protein extracts from SH-SY5Y cells transfected with the lead AO candidate to evaluate the effect of the AO on the MAPT protein in comparison to the scrambled AO sequence. Cells were lysed in lysis buffer (100 µL/ sample) containing 12% SDS, 100 mM Tris-HCl, pH 6.8, 10% glycerol with loading buffer containing 1.875 µL bromophenol blue, 4.688 µL dithiothreitol and 1.5 µL protease inhibitor added per 100 µL of samples. Cell pellets were sonicated six times for 3 s pulses and denatured at 95°C for 5 mins before snap-cooling on ice. Protein concentrations were determined to ensure equal protein loading with Coomassie blue

staining. The samples were loaded onto a PAGE gel with 10% separating gel containing 400 mM Tris-HCL, pH8.8 and 0.1% SDS and 5% stacking gel containing 130 mM Tris-HCL, pH6.8, 0.1% SDS and 0.004% bromophenol blue in a Tris-glycine-SDS running buffer before being transferred to a 0.2 µm nitrocellulose membrane (Biorad; Cat# 162-0112) in a Tris-glycine-methanol transfer buffer. The membranes were blocked in 5% skim milk in Tris-buffered saline with 0.1% Tween for 1 h. The membrane was washed three times in Tris-buffered saline with 0.1% Tween for 20 mins each, and the membrane was incubated in primary antibodies overnight at 4 °C, 1:2000 anti-total tau (Abcam, Cat# ab76128) and 1:1000 anti-GAPDH (ThermoFisher Scientific, Cat# PA1-988). After washing the membrane three times in Tris-buffered saline with 0.1% Tween for 20 mins each, the membrane was incubated in the secondary antibody (1:5000 anti-rabbit HRP, Thermofisher Scientific, Cat# 31460) for 1 h at room temperature before washing three times in Tris-buffered saline with 0.1% Tween for 20 mins each. The antibodies were detected using a Clarity Western ECL detection kit (Biorad; Cat# 1705060) according to the manufacturer's protocol and visualised using the chemiluminescence protocol on the Fusion Fx gel documentation system (Vilber Lourmat).

6.4 Results

6.4.1 Design and screening of DNAzymes targeting *MAPT* mRNA

Arm-loop-arm type non-modified DNAzymes with the 10-23 catalytic motif were designed to target selected exons of the *MAPT* transcript (Table D.3; Appendix D). The sequences of the catalytic regions were pre-fixed according to previous reports (10, 11) and the arm regions were designed to be specific and complementary to the target *MAPT* mRNA sequences. Initially, the catalytic activities of all of the DNAzymes designed to target *MAPT* mRNA were screened in SH-

SY5Y neuroblastoma cells by transfecting at two different concentrations (400 nM and 50 nM) for 24 h. RNA was extracted from the cell lysate, and the integrity of the *MAPT* transcript was assessed by performing RT-PCR. Dose-dependent reduction of the full-length *MAPT* transcript was observed at various levels after treatment with RNV559, RNV561, RNV563, RNV569, RNV570, and RNV571 DNAzyme candidates (Figure D.1; Appendix D). The best *MAPT* transcript knockdown was induced by RNV559, RNV561, RNV563 and RNV569 DNAzymes at 400 nM. The catalytic activities of RNV559, RNV561, RNV563 and RNV569 were further validated against *MAPT* mRNA in SH-SY5Y cells at four different concentrations (50 nM, 100 nM, 200 nM, and 400 nM) (Figure 6.2). DNAzyme candidate RNV563 targeting exon 11 of the *MAPT* mRNA showed highest activity with 58% knockdown of *MAPT* followed by RNV561 (26%) (Figure 6.2; densitometry analysis in Appendix D, Table D.4).
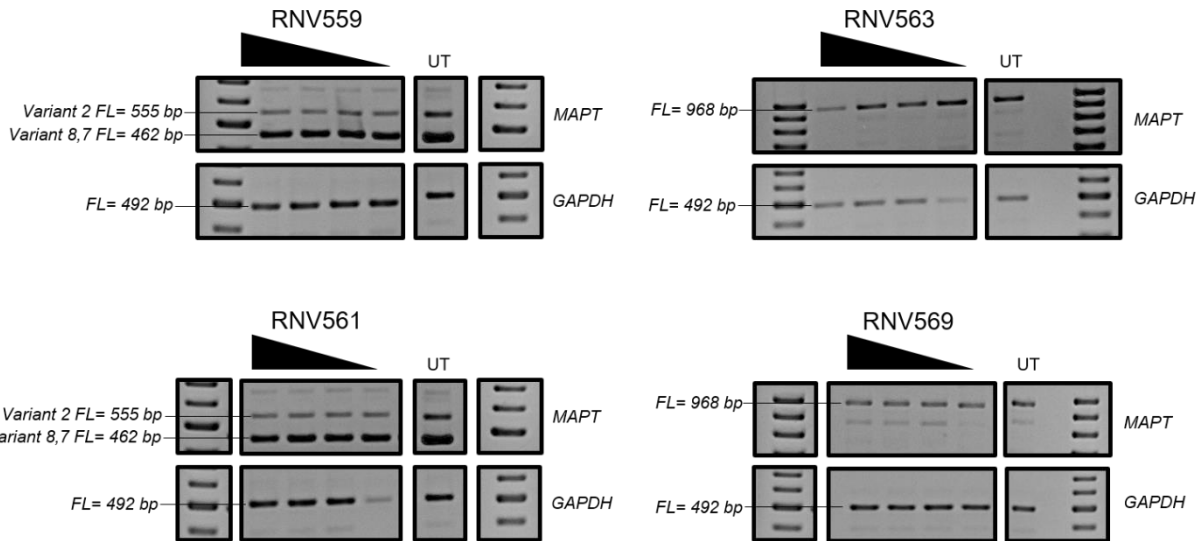
Figure 6.2   *Representative RT-PCR analysis of the MAPT and GAPDH transcripts (of three replicates) from SH-SY5Y cells after transfection with DNAzyme RNV559, RNV561, RNV563 and RNV569 at 400 nM, 200 nM, 100 nM and 50 nM concentrations. FL, full-length; UT, untreated; GAPDH was used as a loading control. The gel images were cropped, however, the original images are shown in Figure D.2 (Appendix D).*

6.4.2 Design and screening of second-generation DNAzymes targeting *MAPT* mRNA

Based on the initial screening outputs, the best performing DNAzyme RNV563 was selected for further modifications by systematically increasing and decreasing the binding arm lengths. Many studies have shown that modifying the length of the hybridisation arms on either side of the catalytic motif can increase the binding affinity and efficacy (12-14). In our study, the first generation of DNAzymes initially had eight nucleotides on one arm and seven on the other. Several studies showed that the optimal arm lengths vary from 7 to 10 nucleotides long. Therefore, the length of RNV563 was increased by one to three nucleotides at the end of both arms and named RNV610, RNV611 and RNV612 (Table 6.1), and then the activity of the modified DNAzymes was verified. Also, we decreased the arm-length of our first-generation DNAzyme RNV563 and verified the activity of the shorter DNAzymes by removing one and two nucleotides from both the ends (RNV608 and RNV609) (Table 6.1). The catalytic activities of these second-generation DNAzyme candidates were analysed in SH-SY5Y as described above. The transfections were repeated at least twice. Decreasing the length of the RNV563 completely abolished the DNAzyme activity of RNV608 (0%) and RNV609 (0%) even at 600 nM relative to the parent DNAzyme RNV563 (56%). Furthermore, increasing the length of the RNV563 also reduced the DNAzyme activity of RNV610 (11%), RNV611 (1%) and RNV612 (6%) (Figure D.3 and Table D.5). These results showed that increasing and decreasing the arm length abolished the DNAzyme RNV563 activity of the original RNV563 in SH-SY5Y cells.

Table 6.1   Second-generation DNAzymes derived from the first-generation parent DNAzyme RNV563 and their sequences.

Name	Sequence 5'→3'
RNV563	GTTTATGA GGCTAGCTACAACGA GGATGTT

Name	Sequence 5'→3'
RNV608	TTTATGA GGCTAGCTACAACGA GGATGT
RNV609	TTATGA GGCTAGCTACAACGA GGATG
RNV610	GGTTTATGA GGCTAGCTACAACGA GGATGTTG
RNV611	TGGTTTATGA GGCTAGCTACAACGA GGATGTTGC
RNV612	CTGGTTTATGA GGCTAGCTACAACGA GGATGTTGCC

6.4.3 *In vitro* cleavage of *MAPT* RNA template

To further verify and understand the catalytic activity of DNAzymes targeting the *MAPT* transcript, we performed the cleavage assay *in vitro* using a synthetic fluorescein dye (FAM)-labelled RNA target specific to the exon 11 region of the *MAPT* transcript. The experiments were performed by incubating DNAzymes RNV563, and their second-generation variants with FAM-labelled RNA template in the presence of divalent metal ions and the products were separated and analysed on a denaturing polyacrylamide gel. Briefly, 1.76 µM DNAzymes were incubated with 1.76 µM FAM-conjugated *MAPT* RNA in the presence of Mg^{2+} for 30 min, 60 min and 120 min at 37°C. The reactions were stopped by adding 10 µL of formamide solution. The products were then separated on a 15% denaturing polyacrylamide gel and visualised using the Fusion FX gel documentation system (Vilber Lourmat). The cleavage of the 34-mer full-length FAM-conjugated RNA target is expected to yield a 22 nucleotides long product. A scrambled (SCR) sequence and RNV563 mutants with different mutations (RNV563Mut1 and RNV563Mut2) within the catalytic region of RNV563 were used as negative controls in parallel, and an untreated (UT) sample with no DNAzyme was also included. DNAzymes RNV563, RNV610, RNV611 and RNV612 showed efficient cleavage of the *MAPT* RNA template *in vitro,* whereas the RNV608 and RNV609 with decreased arm lengths failed to yield any RNA cleavage (Figure 6.3). Notably, the *in vitro* cleavage rates of the DNAzymes with increased arm lengths, RNV610, RNV611 and RNV612 were faster

than that of their parent DNAzyme, RNV563. As expected, the scrambled control and the mutant

RNV563 did not show any cleavage (Figure 6.3).
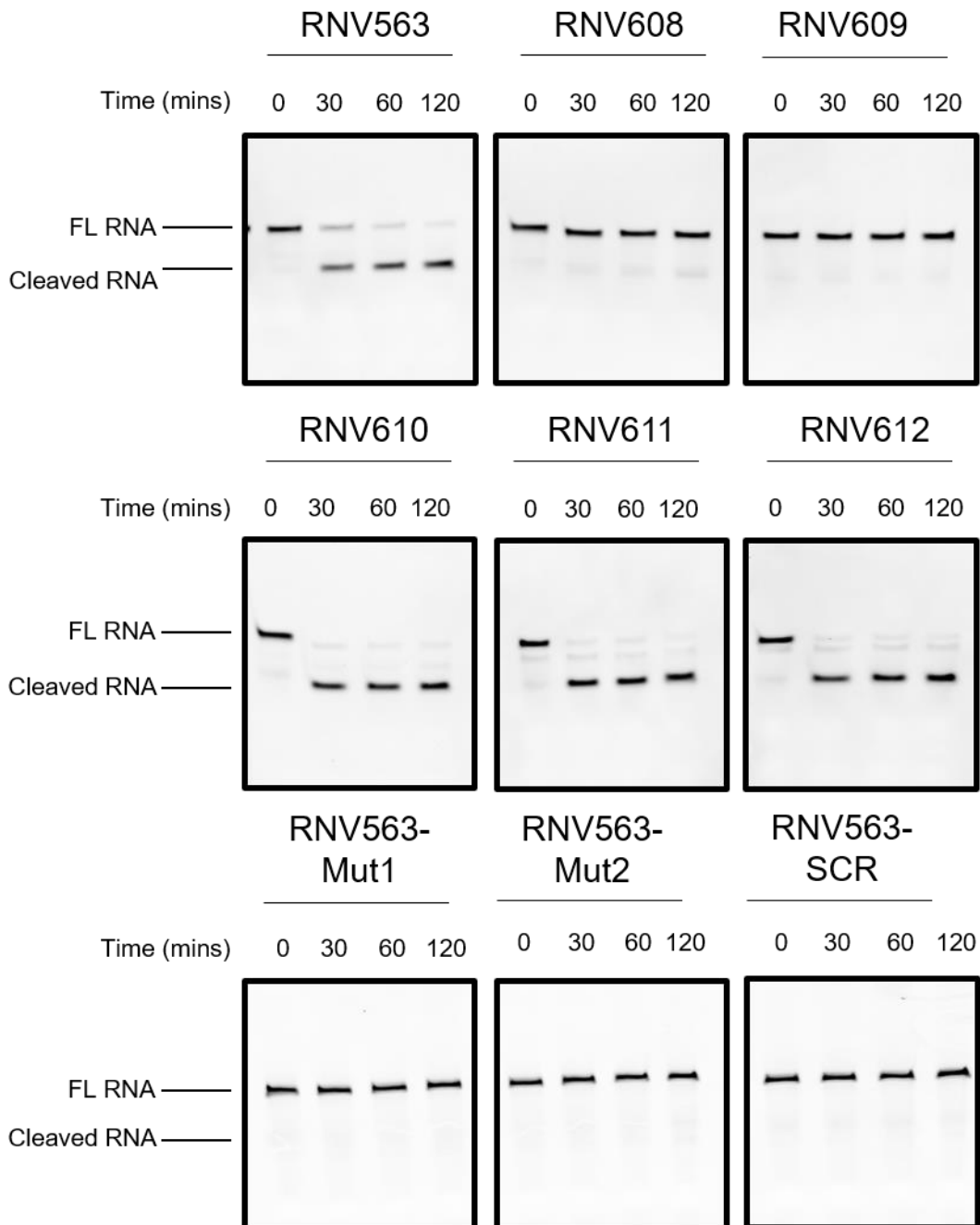
Figure 6.3   In vitro cleavage of the FAM-conjugated MAPT RNA template by RNV563 and its derivatives. FL RNA, full-length; FAM-conjugated RNA; cleaved RNA; the cleaved FAM-conjugated MAPT RNA (22 nucleotides long). The FAM- conjugated template RNA is a small region of the MAPT transcript complementary to the hybridisation arms of the DNAzymes. The gel images were cropped, however, the original images are shown in Figure D.4 (Appendix D).

6.4.4 Evaluation of splice modulating AOs to induce exon-skipping in the *MAPT* transcript.

Firstly, we evaluated the exon-skipping efficiency of all AOs targeting different exons (Table D.6) *in vitro* at two different concentrations (400 nM and 50 nM). The results demonstrated that AO4, AO5, AO6 and AO19 targeting exons 4, 5, and 19 resulted in exon-skipping and downregulation of the *MAPT* transcript *in vitro* (Figure D.5, Appendix D). The AO4, AO5, AO6, and AO19 were further validated at 400 nM, 200 nM, 100 nM and 50 nM (Figure 6.4; see Figure D.7 for densitometry analysis, Appendix D). The results showed that AO4 (94%), AO5 (88%), AO6 (92%) and AO19 (86%) all efficiently downregulated *MAPT* transcript levels (Figure 6.4) even at the lowest concentration (50 nM) tested. The AO4 (13%) and AO5 (24%) induced *MAPT* exon 4 skipping. The transfection of SH-SY5Y cells with AO6 resulted in *MAPT* exon 5 skipping (40%) at the 50 nM concentration (Figure 6.4). The AOs 4, 5, 6, and 19 were further tested at lower concentrations (50 nM, 25 nM, 12.5 nM and 6.25 nM) with *GAPDH* as a housekeeping control as they showed downregulation of the *MAPT* transcript at the higher concentrations (Figure 6.4; see Figure D.7 for densitometry analysis, Appendix D). Notably, AO4 (20%) and AO5 (32%) induced *MAPT* exon 4 skipping and were most efficient at 25 nM. In addition, AO4 (96%) and AO5 (77%) also resulted in dose-dependent downregulation of the *MAPT* transcript and were most efficient at 50 nM. Although AO19 downregulated the *MAPT* transcript, it failed to demonstrate dose-dependent inhibition. AO4 was further validated for inhibition of the expression of MAPT protein as it was found to be the most effective candidate at inhibiting *MAPT* transcript.
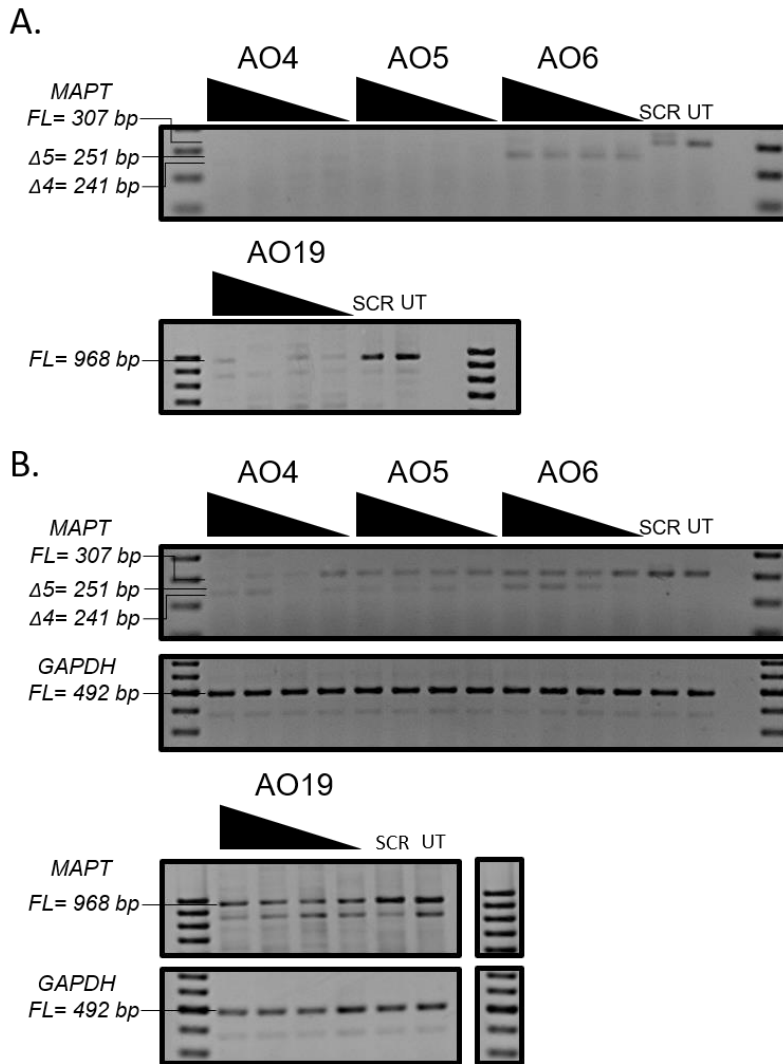
Figure 6.4   A. Representative RT-PCR analysis of the MAPT transcripts (from three replicates) from SH-SY5Y cells after treatment with AO4, AO5, AO6, and AO19 at 400 nM, 200 nM, 100 nM and 50 nM concentrations. B. Representative RT-PCR analysis of the MAPT and GAPDH transcripts from SH-SY5Y cells after treatment with AO4, AO5, AO6, and AO19 at 50 nM, 25 nM, 12.5 nM and 6.25 nM concentrations. AO4 and AO5 target exon 4, AO6 targets exon 5, and AO19 targets exon 12 of the MAPT transcript. FL, full-length; UT, untreated; SCR, scrambled sequence; GAPDH was used as a housekeeping control. The gel images were cropped, however, the original images are shown in Figure D.6 (Appendix D).

6.4.5 Evaluation of tau protein downregulation using AO4.

To further evaluate the ability of AO4 to inhibit MAPT, the total tau protein levels were evaluated

in SH-SY5Y cells 24 h, 48 h and six days after the transfection with AO4. Briefly, AO4 treated

SH-SY5Y cells were incubated for 24 h, 48 h, and 6 days before collection of the cells. The cell

pellet was collected and lysed, and the protein extracts were separated on a 10% separating gel and

transferred onto a nitrocellulose membrane. The membrane was incubated with 1:2000 dilution of the tau (total tau) antibody overnight at 4°. The results clearly demonstrated that there was downregulation of the *MAPT* gene transcript and tau protein in cells 24 h, 48 h and six days after AO4 treatment, however, the highest tau protein downregulation (70%) was seen six days after transfection (Figure 6.5; see Figure D.9 for densitometry analysis, Appendix D). A shorter protein product (around 48 kDa) can be observed in the 24 h and 48 h lanes.
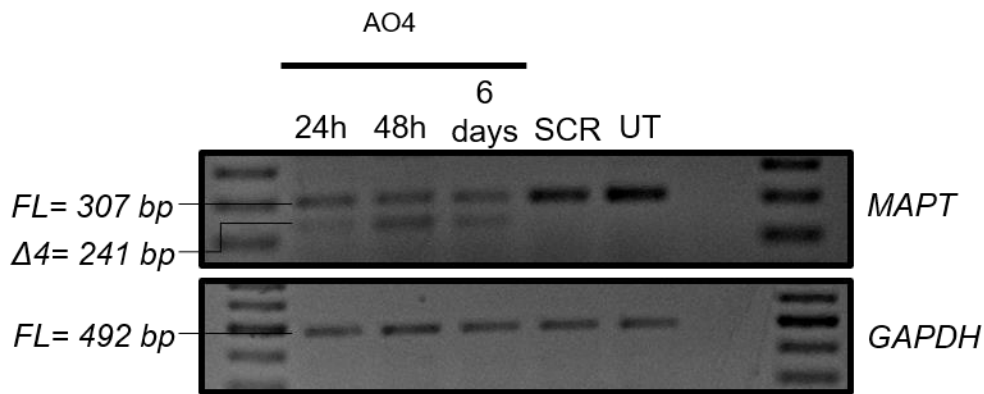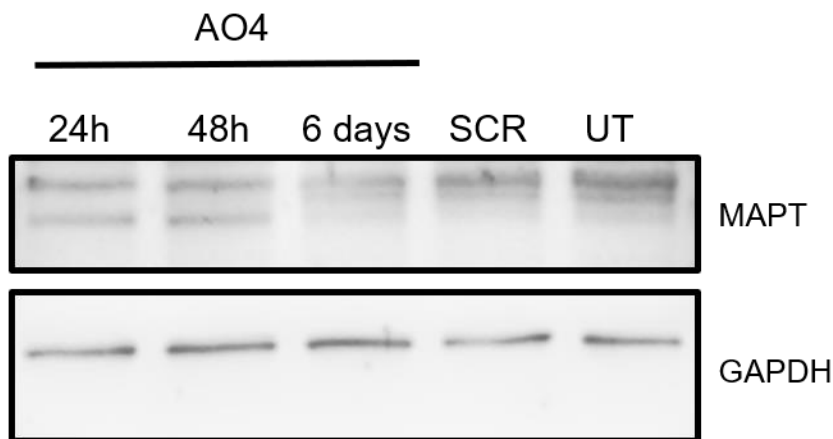
Figure 6.5   *A. Representative RT-PCR analysis of the MAPT transcripts (from three replicates) from SH-SY5Y cells after treatment with AO4 at 50 nM and incubation of the cells with AO for 24 h, 48 h and six days. B. Representative protein analysis of the MAPT and GAPDH from SH-SY5Y cells after treatment with AO4 at 50 nM and incubation of the cells with AO for 24 h, 48 h and six days. The top band in the MAPT western blot is the total tau while the shorter band may correspond to the exon-skipped tau protein. FL, full-length; UT, untreated; SCR, scrambled sequence; GAPDH was used as a housekeeping control. The gel images were cropped, however, the original images are shown in Figure D.8 (Appendix D).*

6.5 Discussion

Hyperphosphorylated tau neurofibrillary tangle formation is believed to be a pathological hallmark for various tauopathies, including AD. Although some early work focused on developing nucleic acid-based MAPT inhibitors, we revisited this target to develop of novel nucleic acid molecules for efficient tau inhibition. We screened various DNAzymes targeting different *MAPT* exons at two concentrations in SH-SY5Y cells (Figure D.1, Appendix D) and identified four candidates RNV559, RNV561, RNV563 and RNV569 that downregulated *MAPT* transcripts efficiently, by targeting exons 9, 11, and 13. Further systematic evaluation of the DNAzymes at 400 nM, 200 nM, 100 nM and 50 nM transfection concentrations identified RNV563 as the most efficient DNAzyme candidate. The variable efficiencies at downregulating *MAPT* transcripts were similar to those observed in previous studies including our work on DNAzymes targeting various regions of the ITGA4 mRNA (9), and others by Vester et al (2003) (12, 15) and Kurreck et al. (2002)(16). These studies have suggested that the DNAzyme's catalytic cleavage efficiency may vary due to its dependence on the RNA tertiary structure. The RNA tertiary structure affects the accessibility of the purine-pyrimidine cleavage sites to the DNAzyme and may differ between different regions of the mRNA, which may explain the differences observed in cleavage efficiencies.

The target binding arm of the DNAzyme is an important factor in determining cleavage efficiency. In our previously reported *ITGA4*-targeting DNAzyme RNV143, increasing the arm length did not have any significant effect on its cleavage efficiency (9). However, we tested the effect of increasing and decreasing the arm length of the most effective DNAzyme RNV563 on cleavage efficiency. Notably, increasing and decreasing the arm lengths significantly decreased the target cleavage efficiency in SH-SY5Y cells. In contrast, all candidates with increased arm lengths efficiently cleaved the corresponding shorter regions of *MAPT* synthetic RNA target *in vitro* in the

presence of divalent cation, although the candidates with decreased arm lengths failed to induce any cleavage. We speculate that this might be due to the structural variability of *MAPT* RNA in the cells compared to that of the shorter synthetic target.

We also identified an exon-skipping AO that efficiently downregulates the *MAPT* transcript in this study. The AOs were designed to target regions in exons 1,4,5,7, 9, and 12. Exon 1 contains the initiation codon, and skipping of exons 5,7,9 and 12 would induce a frameshift and generate a premature stop codon (in exon 13,9,10/11, and 12 respectively). Inducing exon 4 skipping does not change the reading frame; however, the exon encodes a structurally important domain (17). Furthermore, two amino acids, serine 113 and threonine 123 that are phosphorylated in AD are found within exon 4, supporting the importance of exon 4 skipping as a therapeutic strategy for AD (18, 19). Antisense oligonucleotides (AOs) were designed to target these regions and block the binding of splicing factors. The AOs that targeted regions in exon 4 (AO4 and AO5) and exon 5 (AO6) induced exon-skipping but also induced downregulation of the *MAPT* transcript simultaneously. The AO that targeted exon 12 (AO19) resulted in downregulation of the *MAPT* transcript but the effect was not dose-dependent. Although the mechanism for the *MAPT* downregulation using AO4, AO5 and AO6 needs to be further evaluated, we speculate that this may be due to steric bulkiness imposed by the AOs blocking translation.

The most effective AO candidate AO4 targeting exon 4, was highly efficient in downregulating the *MAPT* transcript compared to the lead DNAzyme candidate RNV563 which was only effective at higher concentrations (58% knockdown at 400 nM), whereas AO4 was very effective even at concentration as low as 6.25 nM (>60% knockdown). AO4 was therefore further validated by assessing the tau protein in AO4 transfected SH-SY5Y cells. Tau levels were reduced at the 24 h and 48 h timepoints, an effect that lasted at least 3 days after transfection with AO. Tau has a

relatively long half-life of about 12-14 h (20), explaining why the inhibition is seen at 24 h and 48 h after AO4 treatment. A shorter protein product was observed at 24 h and 48 h that was around 48 kDa (around 6-7 kDa shorter than the full-length product). The shorter protein product does not correspond to the exon-skipped band as the exon-skipped product should only be 2-3 kDa smaller than the full-length product. However, it may correspond to the exon-skipped product if the larger difference in size may be attributed to the loss of post-translational modifications in addition to the amino acids skipped from the full-length product.

6.6 Conclusions

In summary, we have successfully developed an arm-loop-arm type DNAzyme, RNV563 with 10-23 catalytic motif that cleaves the *MAPT* transcript both *in vitro* and in SH-SY5Y cells, identified by screening different DNAzyme targeting various exons of the *MAPT* gene transcript. We have also identified a 2'-OMePS AO (AO4) that induces efficient exon 4 skipping and downregulates *MAPT* transcript through RNase H activation in SH-SY5Y cells at concentrations as low as 6.25 nM, and downregulated tau protein by more than 70%. We believe that our findings will contribute towards tau targeting drug development, and help to improve the knowledge in the field.

6.7 References:

1.   Rademakers R, Cruts M, Van Broeckhoven C. The role of tau (MAPT) in frontotemporal dementia and related tauopathies. Human Mutation. 2004;24(4):277–95.

2.   Cummings J, Lee G, Ritter A, Sabbagh M, Zhong K. Alzheimer's disease drug development pipeline: 2019. Alzheimer's & Dementia: Translational Research & Clinical Interventions. 2019;5:272-93.

3.   Sud R, Geller ET, Schellenberg GD. Antisense-mediated exon skipping decreases tau protein expression: a potential therapy for tauopathies. Mol Ther Nucleic Acids. 2014;3(7):e180.

4.   Devos SL, Miller RL, Schoch KM, Holmes BB, Kebodeaux CS, Wegener AJ, et al. Tau reduction prevents neuronal loss and reverses pathological tau deposition and seeding in mice with tauopathy. Science Translational Medicine. 2017;9(374):eaag0481.

5.   Congdon EE, Sigurdsson EM. Tau-targeting therapies for Alzheimer disease. Nat Rev Neurol. 2018;14(7):399.

6.   Larcher LM, Wang T, Veedu RN. Development of Novel antimiRzymes for Targeted Inhibition of miR-21 Expression in Solid Cancer Cells. Molecules. 2019;24(13):2489.

7.   Schindelin J, Rueden CT, Hiner MC, Eliceiri KW. The ImageJ ecosystem: An open platform for biomedical image analysis. Mol Reprod Dev. 2015;82(7-8):518-29.

8.   Wang F, Saran R, Liu J. Tandem DNAzymes for mRNA cleavage: Choice of enzyme, metal ions and the antisense effect. Bioorganic Med Chem Lett. 2015;25(7):1460-3.

9.   Chakravarthy M, Aung-Htut MT, Le BT, Veedu RN. Novel Chemically-modified DNAzyme targeting Integrin alpha-4 RNA transcript as a potential molecule to reduce inflammation in multiple sclerosis. Sci Rep. 2017;7(1):1613.

10.   Santoro SW, Joyce GF. A general purpose RNA-cleaving DNA enzyme. Proc Natl Acad Sci. 1997;94(9):4262-6.

11.   Haseloff J, Gerlach WL. Simple RNA enzymes with new and highly specific endoribonuclease activities. Nature. 1988;334(6183):585.

12.   Vester B, Hansen LH, Lundberg LB, Babu BR, Sørensen MD, Wengel J, et al. Locked nucleoside analogues expand the potential of DNAzymes to cleave structured RNA targets. BMC molecular biology. 2006;7(1):1.

13.   Santoro SW, Joyce GF. Mechanism and utility of an RNA-cleaving DNA enzyme. Biochemistry-Us. 1998;37(38):13330-42.

14.   Ackermann JM, Kanugula S, Pegg AE. DNAzyme-mediated silencing of ornithine decarboxylase. Biochemistry-Us. 2005;44(6):2143-52.

15.   Vester B, Lundberg LB, Sørensen M, Babu B, Douthwaite S, Wengel J. Improved RNA cleavage by LNAzyme derivatives of DNAzymes. Portland Press Limited; 2004.

16.   Kurreck J, Bieber B, Jahnel R, Erdmann VA. Comparative study of DNA enzymes and ribozymes against the same full-length messenger RNA of the vanilloid receptor subtype I. J Biol Chem. 2002;277(9):7099-107.

17.   Wu X-L, Piña-Crespo J, Zhang Y-W, Chen X-C, Xu H-X. Tau-mediated neurodegeneration and potential implications in diagnosis and treatment of Alzheimer's disease. Chinese medical journal. 2017;130(24):2978.

18.   Šimić G, Babić Leko M, Wray S, Harrington C, Delalle I, Jovanov-Milošević N, et al. Tau protein hyperphosphorylation and aggregation in Alzheimer's disease and other tauopathies, and possible neuroprotective strategies. Biomolecules. 2016;6(1):6.

19.   Alavi Naini SM, Soussi-Yanicostas N. Tau hyperphosphorylation and oxidative stress, a critical vicious circle in neurodegenerative tauopathies? Oxidative medicine and cellular longevity. 2015;2015.

20.   David DC, Layfield R, Serpell L, Narain Y, Goedert M, Spillantini MG. Proteasomal degradation of tau protein. J Neurochem. 2002;83(1):176-85.

Final Remarks and Conclusions

Recent clinical success has demonstrated the potential of nucleic acid-based technologies as therapeutic molecules for various diseases. RNA and protein targets implicated in the pathology of various diseases can be manipulated by using synthetic nucleic acid-based therapeutic and diagnostic strategies. Nucleic acid technologies have several advantages over antibodies, including low production cost, freedom to incorporate chemically modifications and little or no immunogenicity. This thesis aimed to design and evaluate DNAzymes and splice modulating AOs to identify novel therapeutic molecules as research tools for tackling neurological diseases, in particular, for MS and AD.

I have designed DNAzymes to downregulate *ITGA4* RNA transcript towards tackling inflammation in MS. RNV143, a DNAzyme targeting exon 9 of *ITGA4* was found to be the most efficient at downregulating *ITGA4* RNA. RNV143 modified with an inverted thymidine, was found to be very stable against nuclease degradation. Modifying the DNAzyme 143 by increasing its arm lengths by one, two or three nucleotides at each ends did not really increase the cleavage efficiency of the parent DNAzyme RNV143. Further validation of this DNAzyme at the protein level against its clinically approved antibody counterpart, Natalizumab is required to evaluate the clinical benefits for further development.

I have also designed and synthesised AOs and DNAzymes for AD against *APP*, *BACE1* and *MAPT* RNA targets that are implicated in AD pathologies. We identified a cocktail of two AOs that could induce exon 16 and exon 17 skipping of *APP* as a treatment strategy for FAD; however, the AO cocktail targeting exon 17 was not able to downregulate APP protein levels. Furthermore, I have

identified a BACE1 AO (AO2) that could efficiently downregulate *BACE1* at the mRNA and protein level and the effect of this AO candidate on the Aβ levels needs to be validated.

I designed DNAzymes and AOs that can efficiently downregulate *MAPT* at the mRNA level. The most efficient DNAzyme and AO at downregulating *MAPT* mRNA were RNV563 targeting exon 13, and AO4 targeting exon 4 respectively. AO4 was found to be more efficient compared to the DNAzyme at lower concentrations and also downregulated MAPT at the protein level. The effect of AO4 on the formation of neurofibrillary tangles needs to be further validated for clinical viability.

The best candidates that have been identified in my projects need to be further tested for off-target effects through RNA sequencing. The best candidates that have been identified in this thesis are DNA sequences and 2'OMePS sequences and therefore are not suitable for clinical use in their current chemistries. The DNAzymes identified for ITGA4 and MAPT are DNA sequences and the best sequences identified had no chemical modifications and therefore are easily degraded by nucleases and are not clinically viable in their current form. An inverted thymidine chemical modification was introduced to the DNAzymes, however this reduced the efficacy of the parent DNAzyme and the PS modification abolished the DNAzyme activity completely. Therefore, for the DNAzymes to have potential clinically, other chemistries not tested in these studies need to be explored to find the best chemistry that does not affect the efficacy but increases nuclease resistance. Similarly, the AOs identified for the BACE1 and MAPT project were 2'-OMePS sequences which are toxic and cannot be used clinically. The PMO modified sequences were not effective and therefore, other chemistries that are clinically safe to use need to be tested including 2'-OMOE modifications. The sequences identified for the BACE1 and MAPT projects need to be delivered to the brain to be effective clinically and therefore conjugation strategies to different

molecules that allow the AOs to cross the BBB need to be explored and tested. For the DNAzymes and AOs identified in this thesis, the AOs effect in functional assays need to be validated. The DNAzyme candidate and AOs identified against MAPT needs to be further validated on its effect on the formation of neurofibrillary tangles while the AOs identified against BACE1 needs to be validated on its effect on the BACE1 activity as well as its effect on amyloid beta production.

In conclusion, this thesis has identified novel DNAzymes and AOs against validated targets implicated in MS and AD. Currently used antibody-based therapeutic strategies for MS have many side effects, which can be limited by the application of nucleic acid therapeutic technologies. However, there is no cure for AD, and most of the current therapeutic strategies only treat the symptoms for temporary benefits. I hope that the DNAzymes and AOs targeting ITGA4, APP, BACE1 and MAPT presented in this work may be beneficial towards developing therapies for MS and AD or used as research tools to improve our knowledge on tackling these diseases. .

Appendix A Supplementary   data   for

Chapter 2

A.1 Results
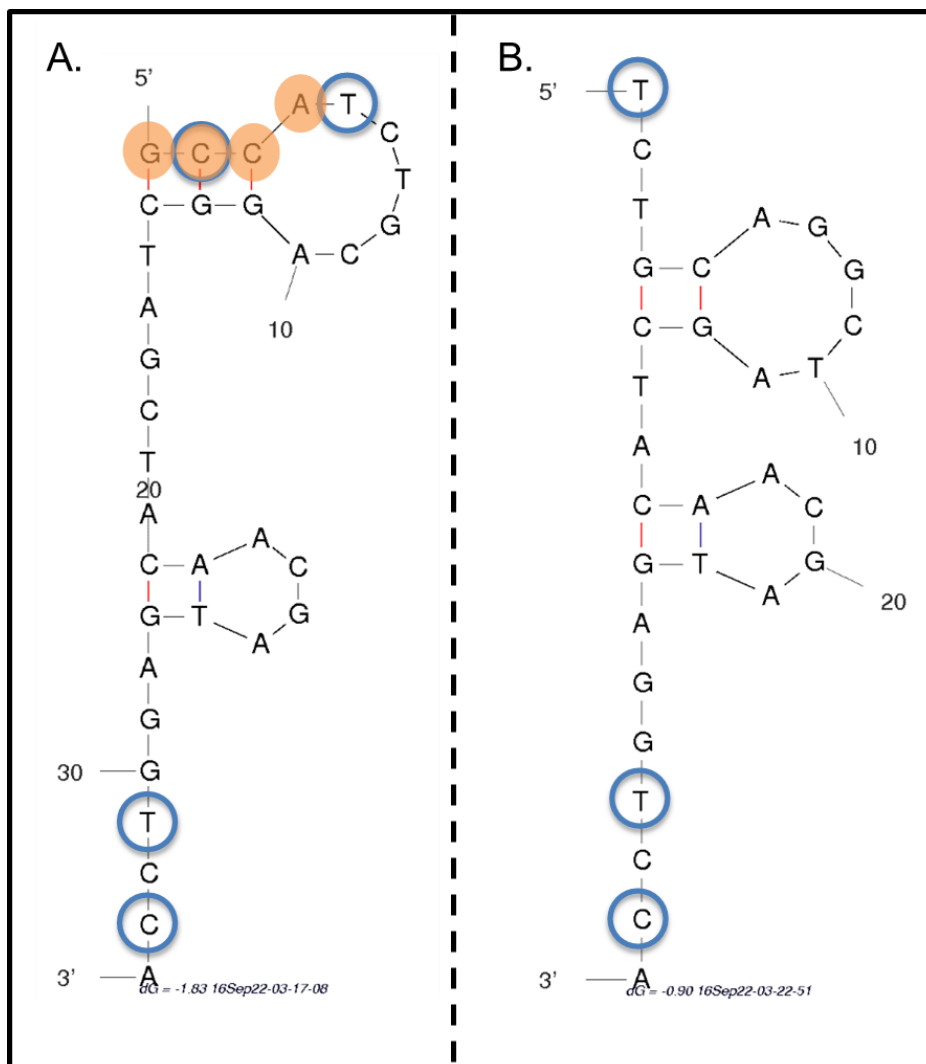
Figure A.1   The structure of the DNAzyme RNV183 (A) and LNA-3 predicted by mfold (B).1 183 was modified to develop LNA-3 by truncation of four residues at the 5' end (highlighted in orange) and modification of bases as LNA (blue circles).
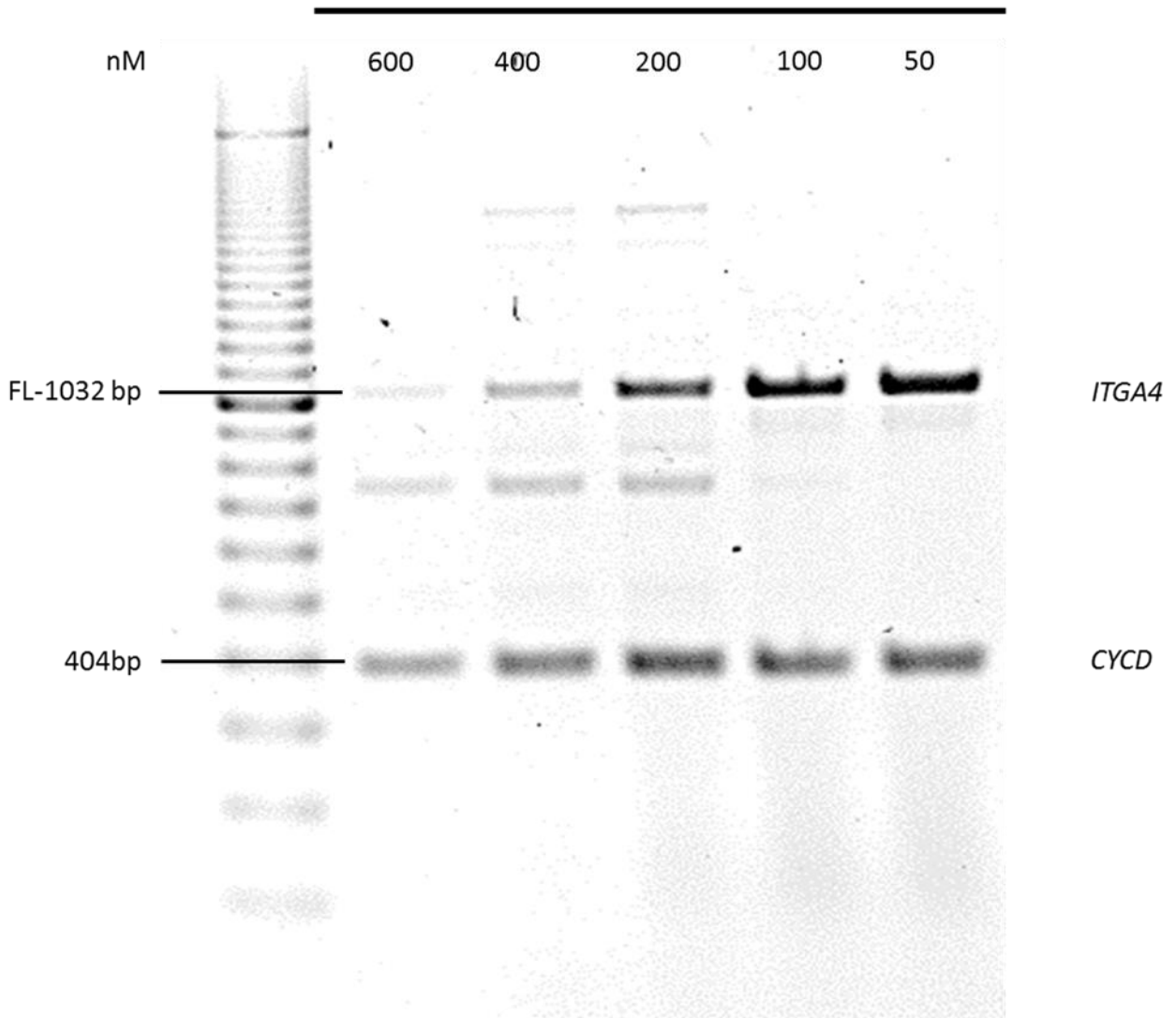
Figure A.2   The RT-PCR products after treatment with RNV143 is shown here. FL, full-length; CYCD was used as a loading control. [The gel in this figure is the original gel representing the gel in Figure 2.3 of the article. The cropped gel has been shown in Figure 2.3 due to non-specific bands that exist and other unimportant samples that exist between the desired samples.]
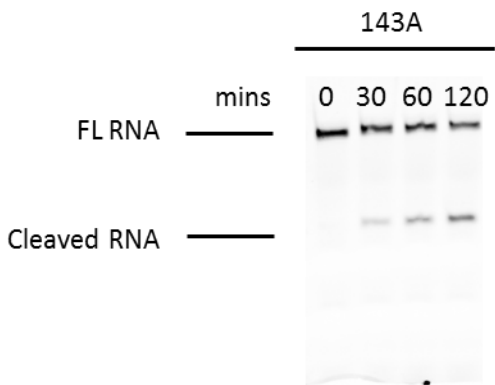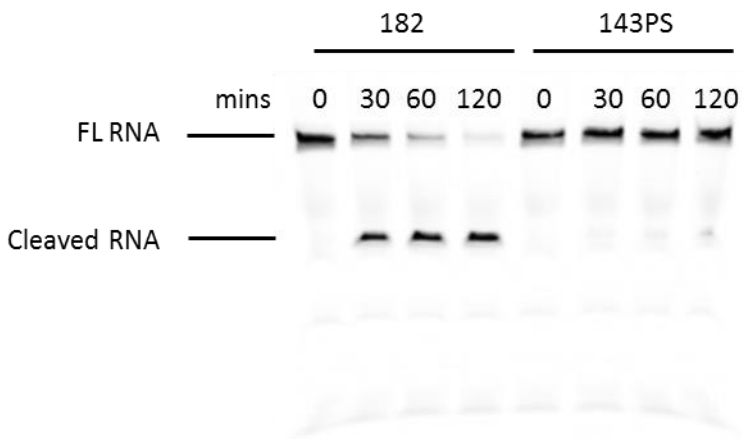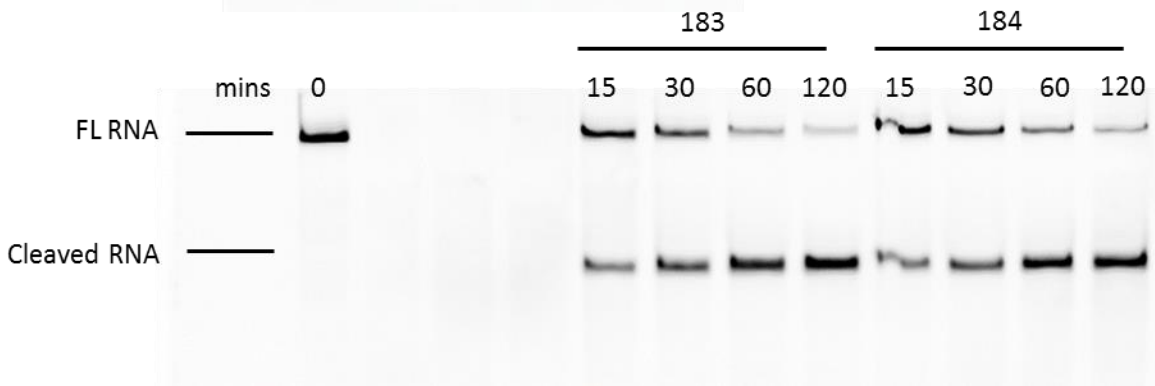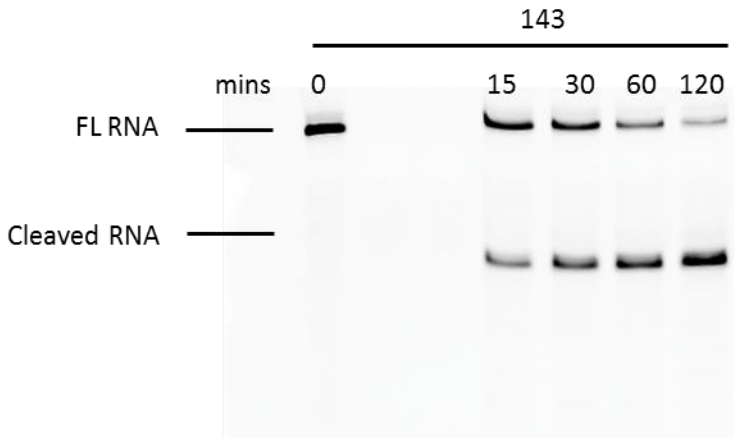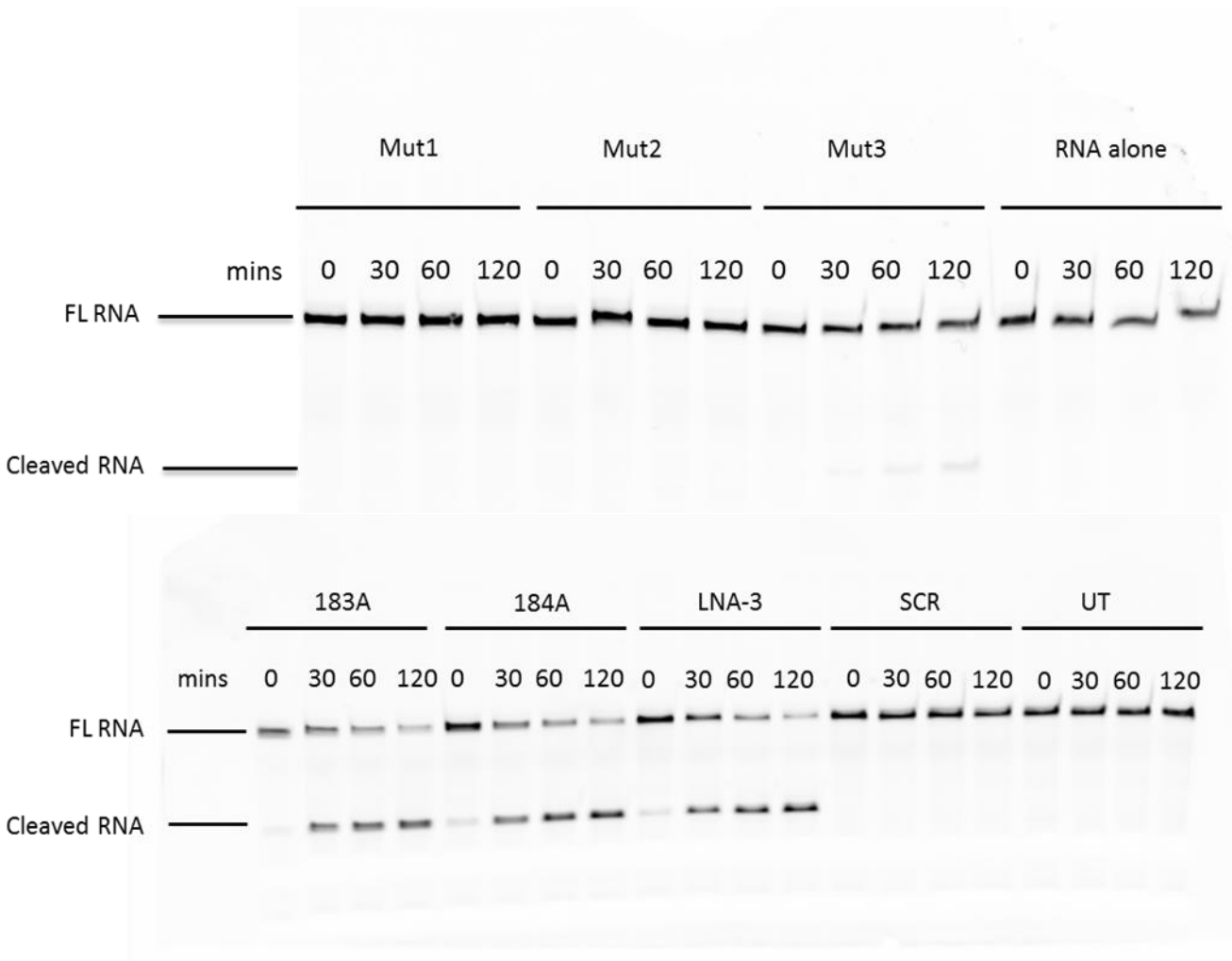
Figure A.3   *In vitro cleavage of the FAM-conjugated ITGA4 RNA template composed of exon 9 region (34 nucleotides) by RNV143 and its derivatives. FL RNA, full-length FAM-conjugated RNA; cleaved RNA, the cleaved FAM-conjugated ITGA4 RNA (18 nucleotides long). The FAM-conjugated template RNA is a small region of the ITGA4 transcript complementary to the hybridization arms of the DNAzymes of interest. [The gels in this figure are the original gels representing the gels in Figure 2.5. For DNAzymes 143, 183 and 184 there are 5 time points (0, 15, 30, 60 and 120 mins) in the original gels but these were cropped to include only 4 time points (0, 30, 60 and 120 mins with timepoint 15 mins excluded) in the article to ensure consistency with the data for the other DNAzymes. The order of the gels here are not the same as that represented in Figure 2.5 of the article and different experiments were run on different gel and therefore the data for each DNAzyme was cropped and arranged in the order seen in Figure 2.5 of the article.]*
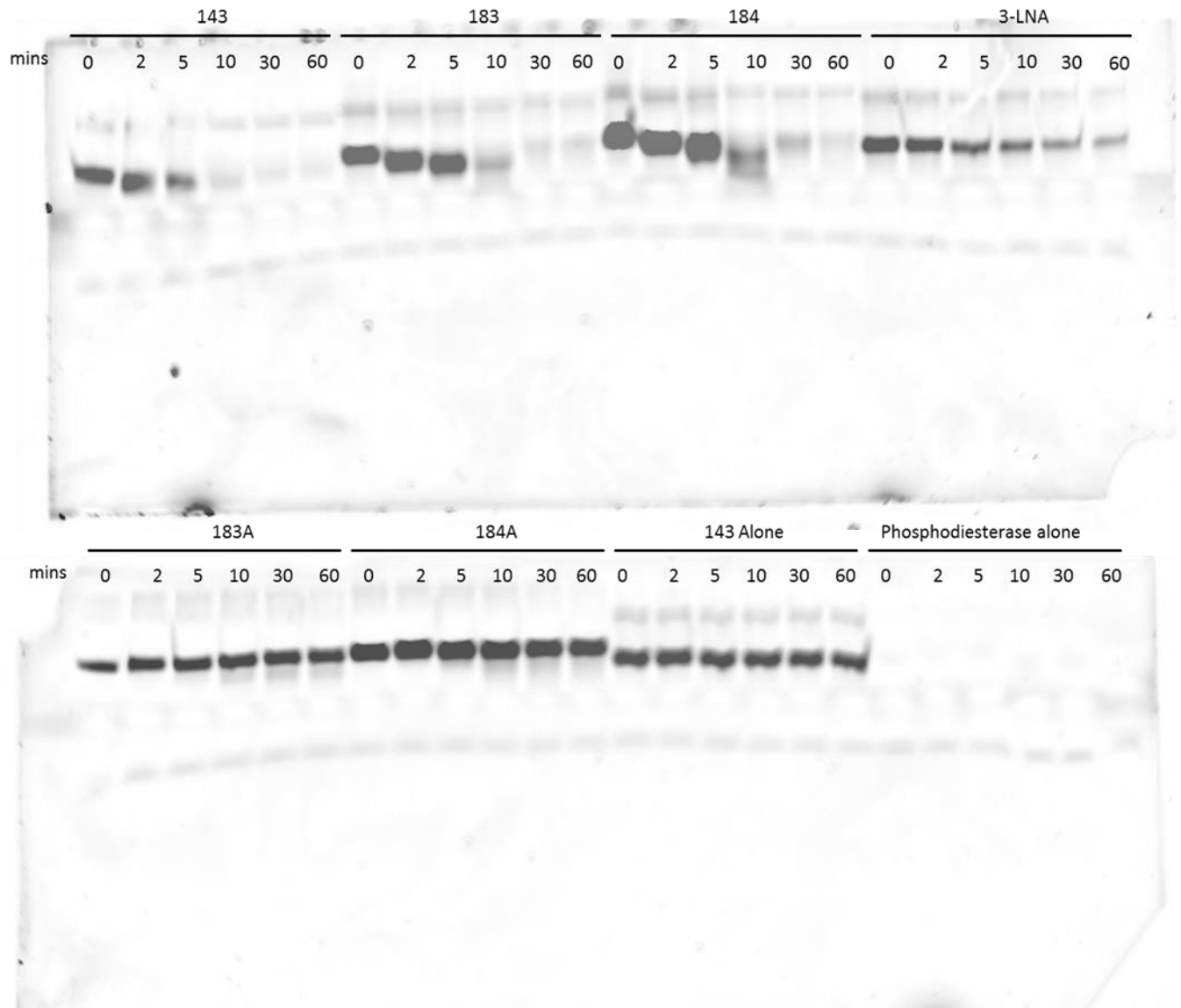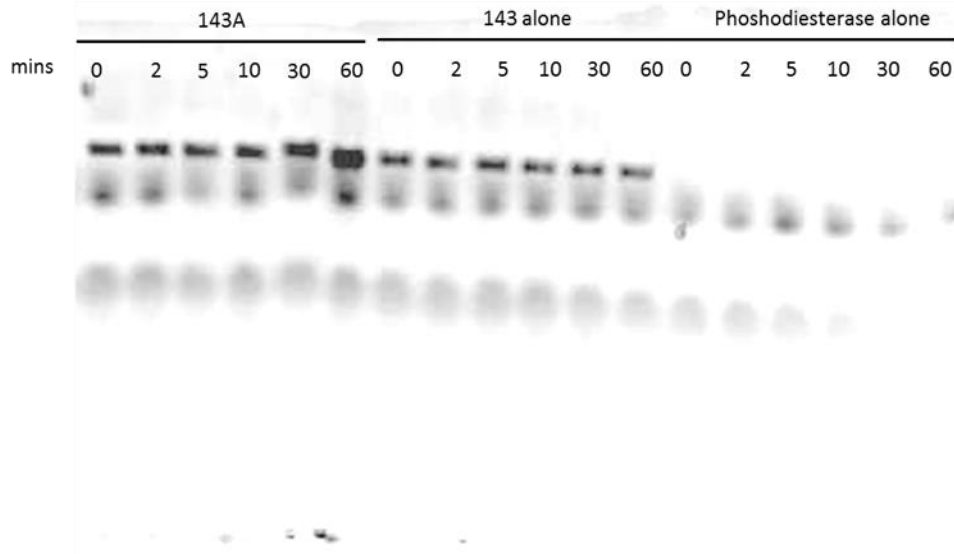
Figure A.4 Phosphodiesterase degradation analysis of DNAzymes that showed high efficiency in the cleavage of ITGA4 RNA in vitro and knockdown of ITGA4 RNA in fibroblasts. [The gels in this figure are the original gels representing the gels in Figure 2.6. The order of the gels here are not the same as that represented in Figure 2.6 and different experiments were run on different gels and therefore the data for each DNAzyme was cropped and arranged in the order seen in Figure 2.6.]

143 alone 143 143A 143PS

Time 0 30 60 2h 4h 6h 0 30 60 2h 4h 6h 0 30 60 2h 4h 6h 0 30 60 2h 4h 6h

Protein trapped in well

DNAzymes degraded by human serum are represented by the distinct band disappearing and a smear appearing

182 183 183A

Time 0 30 60 2h 4h 6h 0 30 60 2h 4h 6h 0 30 60 2h 4h 6h

Protein trapped in well

DNAzymes degraded by human serum are represented by the distinct band disappearing and a smear appearing

Figure A.5   Human serum degradation analysis of DNAzymes that showed high efficiency in the cleavage of ITGA4 RNA in vitro and knockdown of ITGA4 RNA in fibroblasts.

A.2 References

1.   M. Zuker, Nucleic Acids Res, 2003, 31, 3406-3415.

Appendix B Supplementary   data   for

Chapter 4

B.1 Results
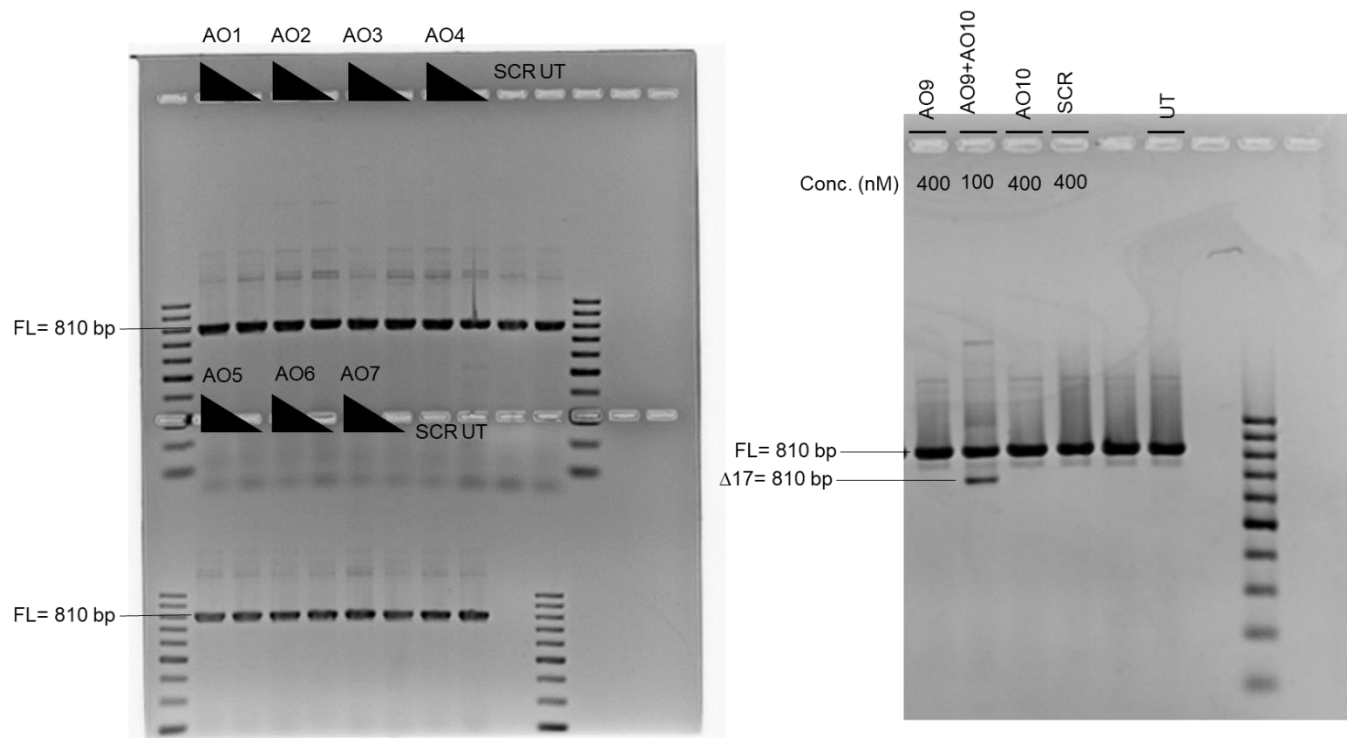
Figure B.1   Representative RT-PCR products of the APP transcript from HEK293 cells after treatment with AOs at 400 nM, and 50 nM concentrations. The RT-PCR products after treatment with AO1, AO2, AO3, AO4, AO5, AO6, AO7, AO9, and AO10 are shown here. FL, full-length; UT, untreated; SCR, scrambled sequence.

Conc. (nM)

1+2 1+3 1+4 1+5 1+6 1+7 2+3 2+4 2+5 2+6

50   400

FL= 810 bp
Δ17= 810 bp

2+7 3+4 3+5 SCR UT

FL= 810 bp

Δ17= 810 bp

FL= 810 bp

FL= 810 bp

3
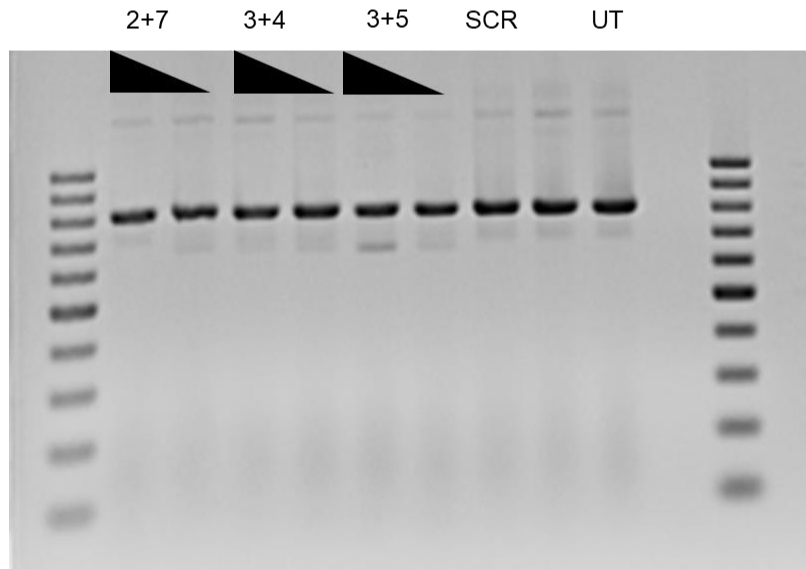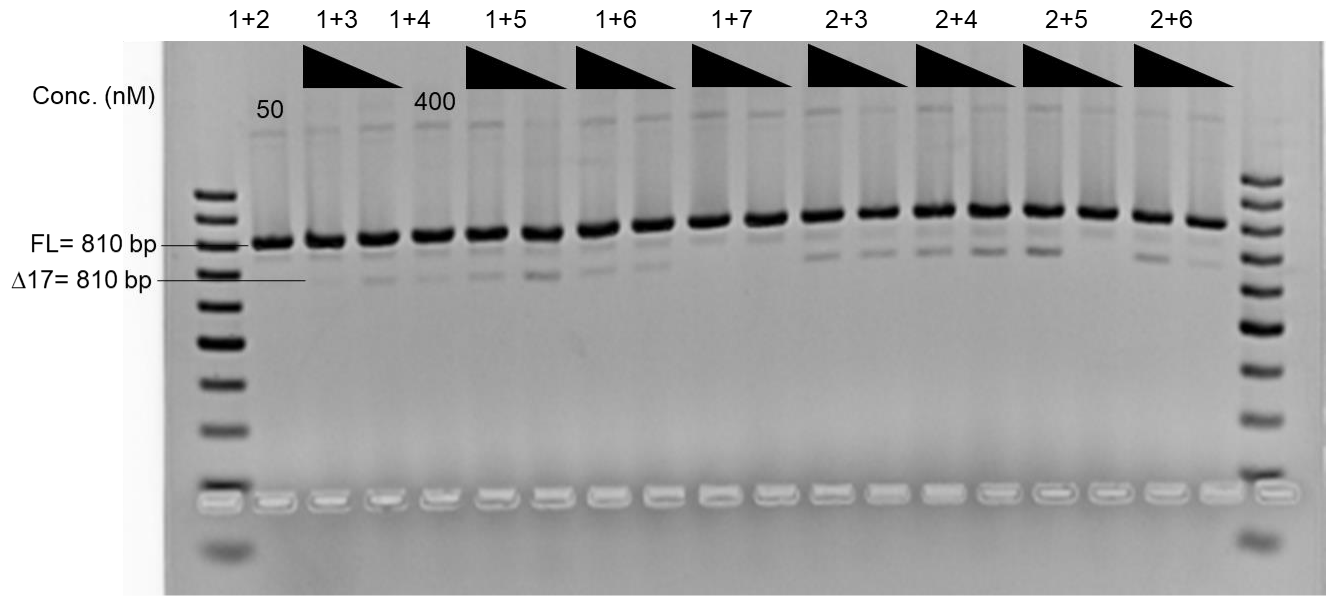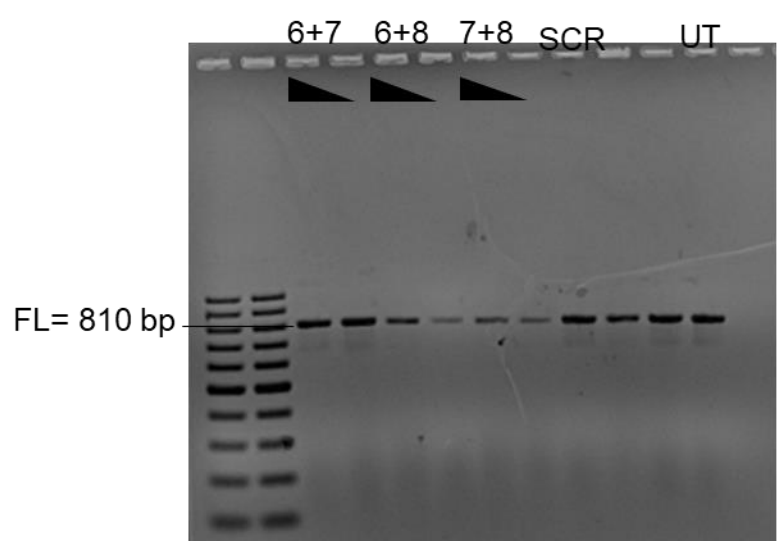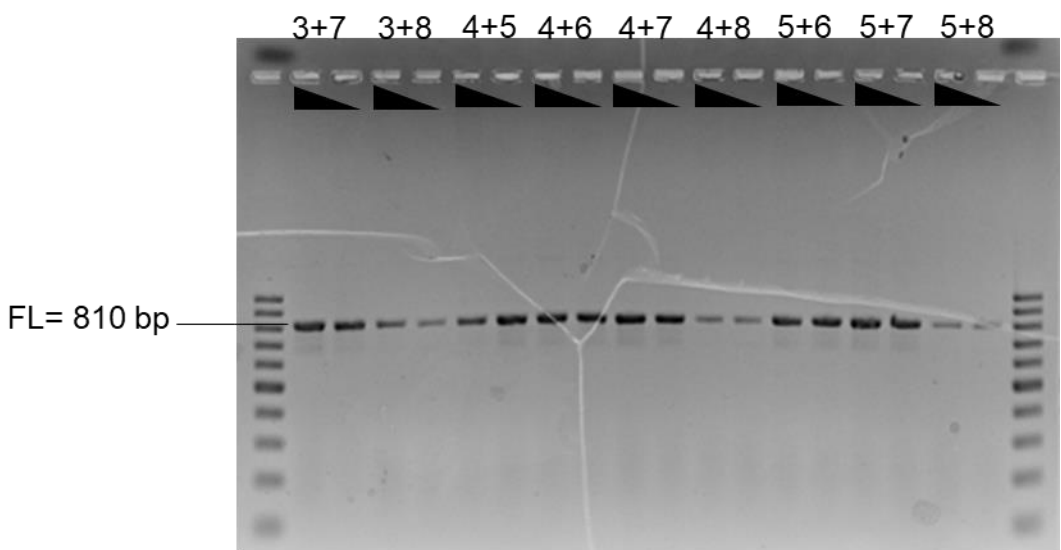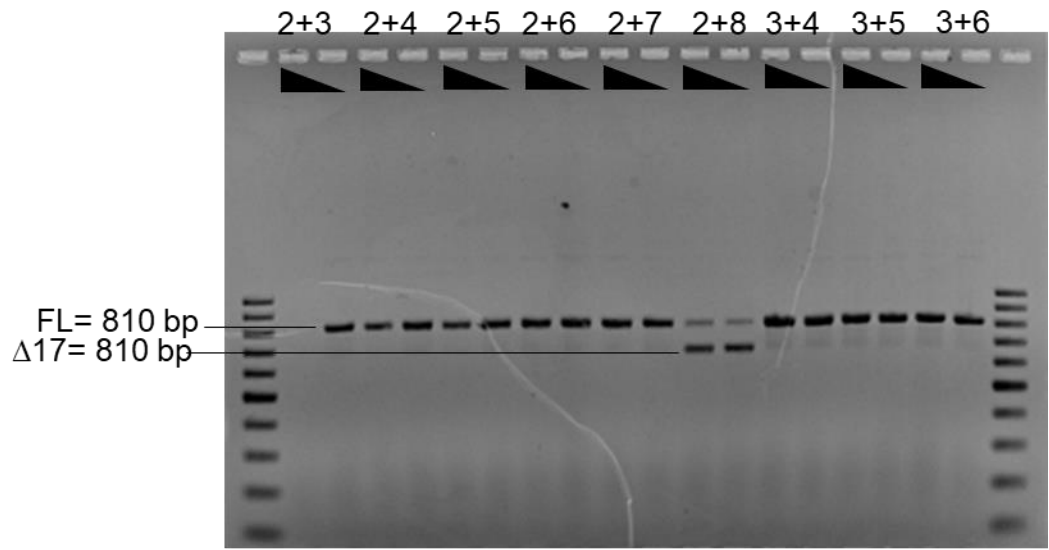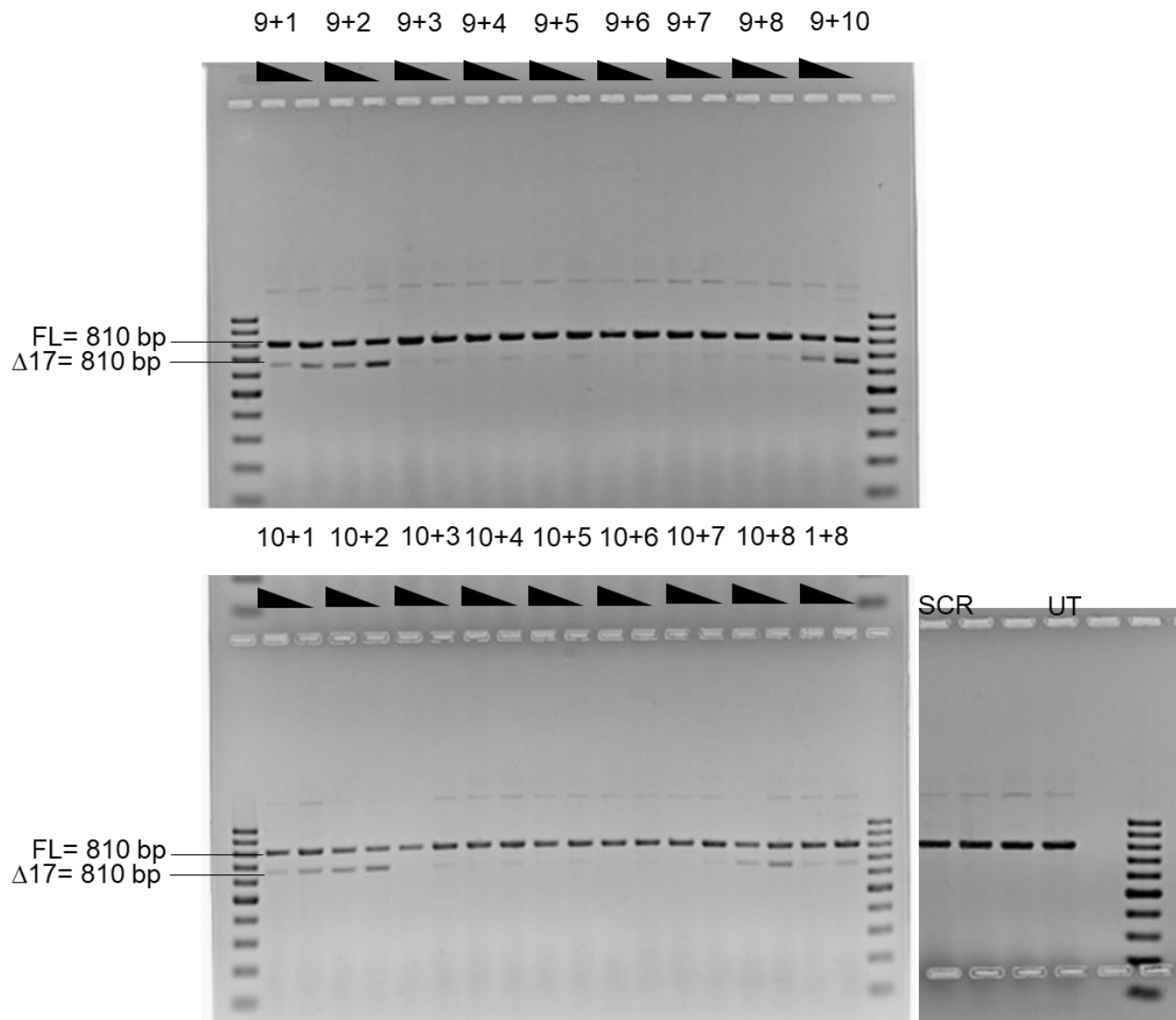
Figure B.2   Representative RT-PCR products of the APP transcript from HEK293 cells after treatment with AO cocktails at 400 nM, and 50 nM concentrations. The RT-PCR products after treatment with all combinations of AOs 1-10 as cocktails of two AOs are shown here. FL, full-length; UT, untreated; SCR, scrambled sequence.
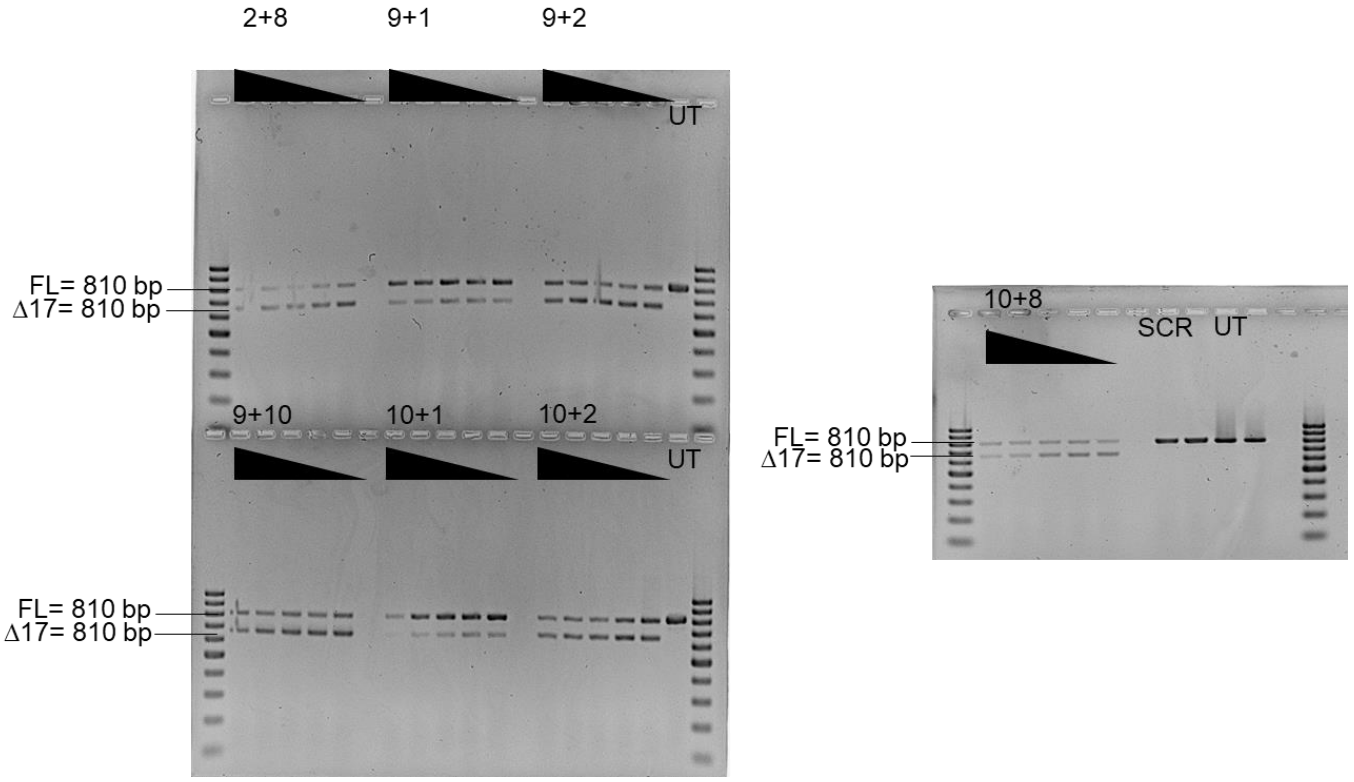
Figure B.3   RT-PCR products of the APP transcript after treatment with the best working 2'-OMePS AO cocktails (AO2+AO8, AO9+AO1, AO9+AO2, AO9+AO10, AO10+AO1, AO10+AO2 and AO10+AO8) targeting exon 17 at 400 nM, 200 nM, 100 nM, 50 nM and 25 nM in HEK293 cells. FL, full-length; UT, untreated; SCR, scrambled sequence. [The gel in this figure is the original gel representing the gel in Figure 4.2. The cropped gel has been shown in Figure 4.2 of the article due to unwanted spaces and unimportant samples that exist on the gel.]
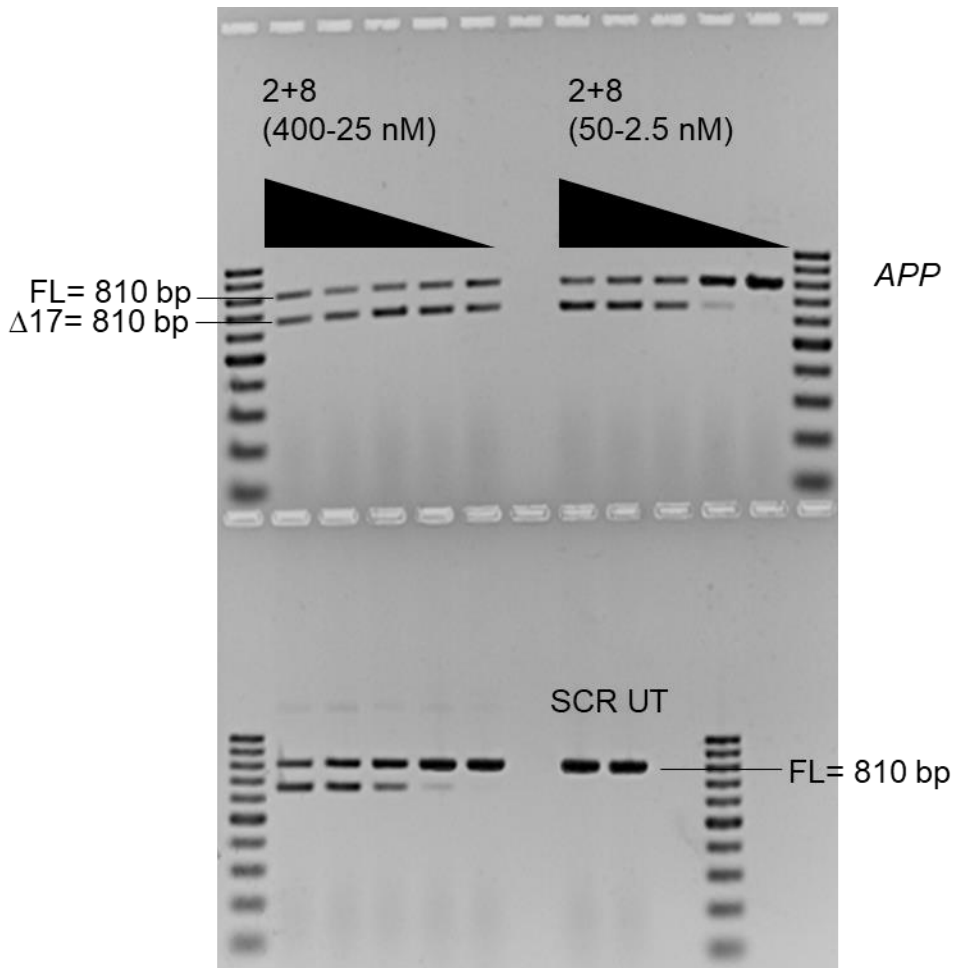
Figure B.4   RT-PCR products of the APP transcript after treatment with the best working 2'-OMePS AO cocktail, AO2+AO8, targeting exon 17 at two concentration ranges (range 1: 400 nM, 200 nM, 100 nM, 50 nM and 25 nM, range 2: 50 nM, 25 nM, 12.5 nM, 5 nM and 2.5 nM) in HEK293 cells. FL, full-length; UT, untreated; SCR, scrambled sequence. [The gel in this figure is the original gel representing the gel in Figure 4.3. The cropped gel has been shown in Figure 4.3 of the article due to unwanted spaces and unimportant samples that exist on the gel.]
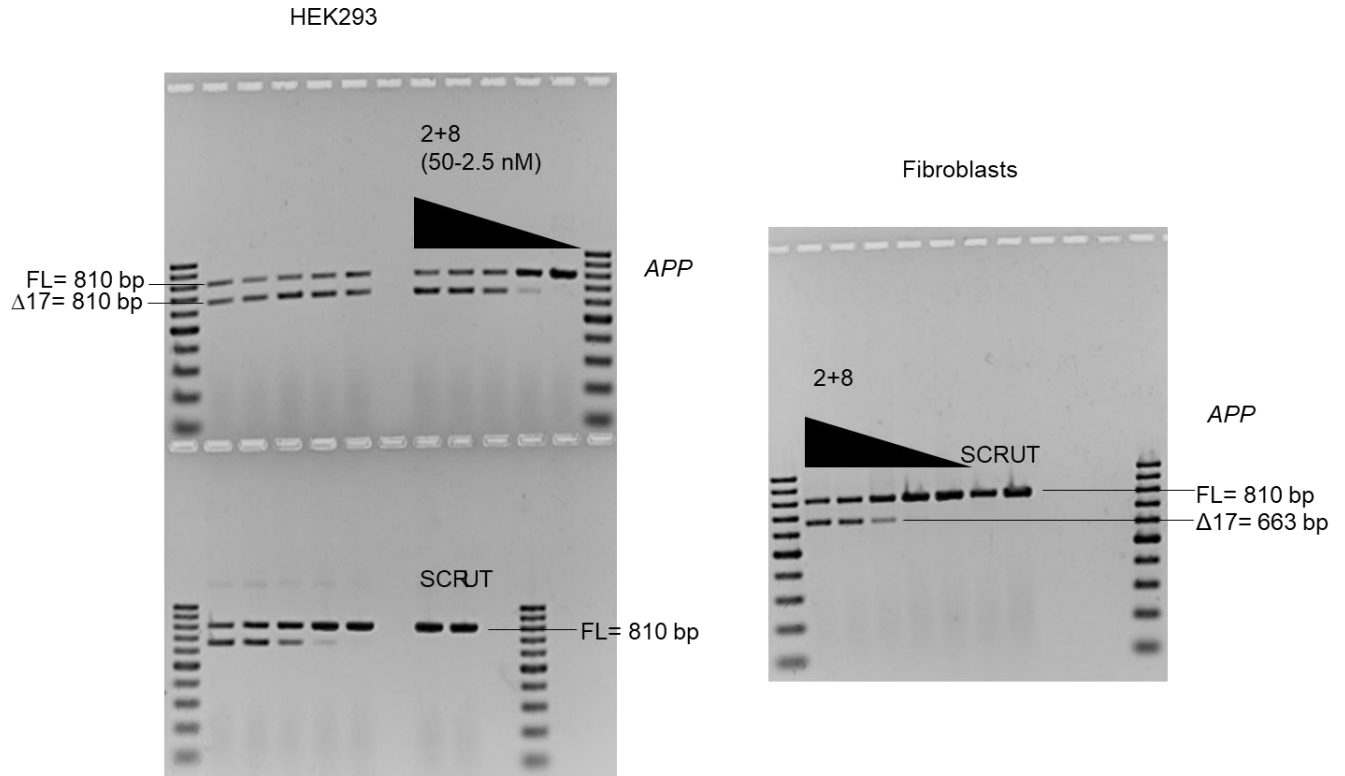
Figure B.5   RT-PCR products of the APP transcript after treatment with the best working 2'-OMePS AO cocktail, AO2+AO8, targeting exon 17 at 50 nM, 25 nM, 12.5 nM, 5 nM and 2.5 nM concentrations in HEK293 cells and normal primary fibroblasts. FL, full-length; UT, untreated; SCR, scrambled sequence. The gel images were cropped to highlight the APP specific products. [The gel in this figure is the original gel representing the gel in Figure 4.4. The cropped gel has been shown in Figure 4.4 due to unwanted spaces and unimportant samples that exist on the gel.]
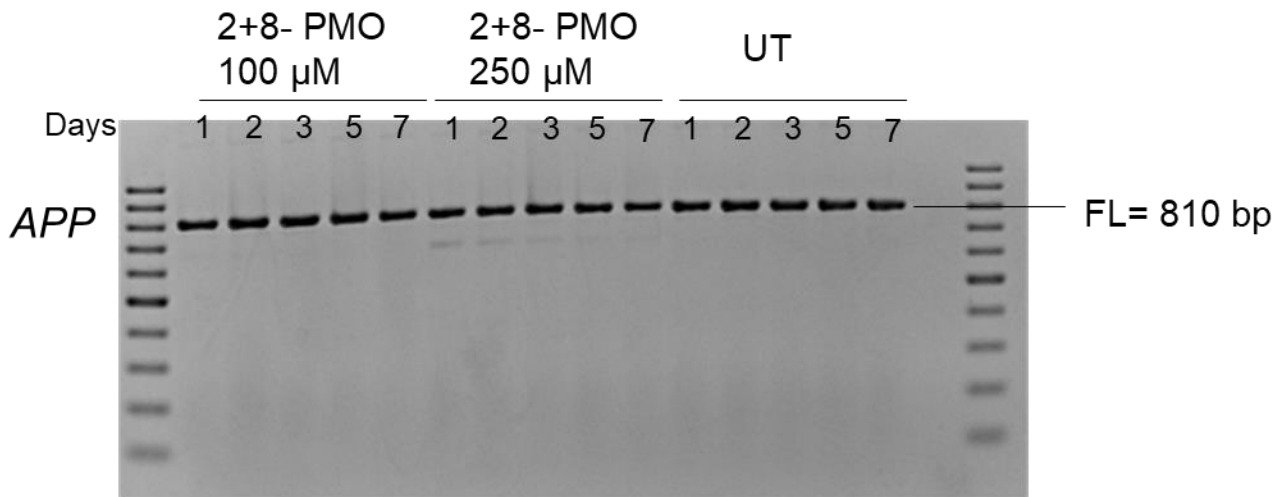
Figure B.6   RT-PCR products of the APP transcript after treatment with the best working AO cocktail, AO2+AO8 with a PMO chemistry, targeting exon 17 at 100 μM and 250 μM concentrations in HEK293 cells after cocktail treatment for 1, 2, 3, 5 and 7 days. FL, full-length; UT, untreated; SCR, scrambled sequence. [The gel in this figure is the original gel representing the gel in Figure 4.5. The cropped gel has been shown in Figure 4.5 due to unwanted spaces and unimportant samples that exist on the gel.]

7
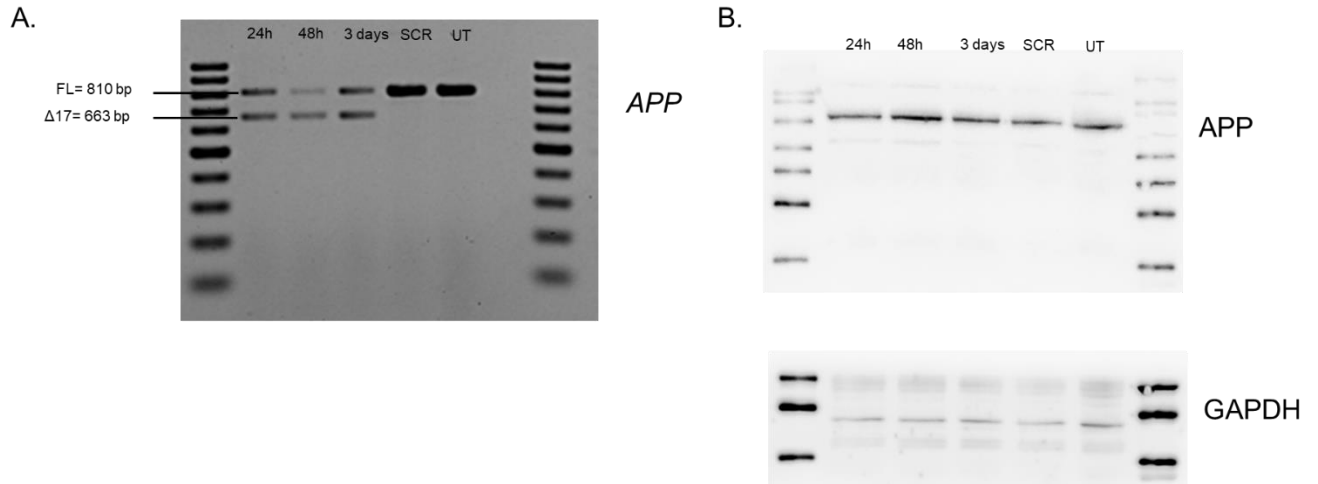
Figure B.7   A. RT-PCR products of the APP transcript after treatment with the best working AO cocktail, AO2+AO8 targeting exon 17 at 100 nM concentration after cocktail treatment for 24 h, 48 h and 3 days in HEK293 cells. B. Western blot protein analysis of the APP and GAPDH proteins after treatment for 24 h, 48 h and 3 days of AO cocktail, AO2+AO8, at 100 nM in HEK293 cells. FL, full-length; UT, untreated; SCR, scrambled sequence. [The gel in this figure is the original gel representing the gel in Figure 4.6. The cropped gel has been shown in Figure 4.6 due to unwanted spaces and unimportant samples that exist on the gel.]

Appendix C   Supplementary   data   for

Chapter 5

C.1 Methods

Table C.1   *The seeding density of HEK293 cells used for different assays.*

Assay	Plate or Flask?	Seeding density
RNA Extraction	24 well plate	50,000 cells/well
Western Blot	T25cm^2 flask	625,000 cells/flask
Nucleofection	24 well plate	100,000 cells/well

Table C.2   *The primer sets used to amplify BACE1 transcript.*

Primer sets	Primer pairs	Primer Sequences	Expected size
Primer Set 1	BACE1_Ex1Fa BACE1_Ex4R	5' GACAACCTGAGGGGCAAGTC 3' 5' AACGTGGGTCTGCTTTACCA 3'	429 bp
Primer Set 2	BACE1_Ex2F BACE1_Ex8R	5' ACCAAAGTGAACCACGGAGG 3' 5' TCTGGTAAAGCAGACCCACG 3'	968 bp
Primer Set 3	BACE1_4F BACE1_Ex9R	5' GGCAGCAGTAACTTTGCAGT 3' 5' CCATAACAGTGCCCGTGGAT 3'	Variant A= 901 bp Variant B= 826 bp Variant C= 769 bp
Primer Set 4	BACE1_Ex3F BACE1_Ex8R	5' ACCTGGTAAGCATCCCCCAT 3' 5' TCTGGTAAAGCAGACCCACG 3'	Variant A= 753 bp Variant B= 678 bp Variant C= 601 bp

Table C.3   *The primer sets used to amplify GAPDH transcript.*

GAPDH Primer set	Primer pairs	Primer Sequences	Expected product length
Primer Set 1	GAPDH For GAPDH Rev	5' GGACTCATGACCACAGTCCATGC 3' 5' TTACTCCTTGGAGGCCATGTGGG 3'	492 bp

Table C.4   The PCR conditions for each primer set

Primer pairs			PCR Conditions		
BACE1 Primer set (25 ng each)	Temperature 55°C 94°C		Time 30 min 2 min		
BACE1_Ex1Fa	94°C		30 s	30 cycles	
BACE1_Ex4R	58°C		1 min		
	68°C		2 min		
BACE1 Primer set (25 ng each)	Temperature 55°C 94°C		Time 30 min 2 min		
BACE1_Ex2F	94°C		30 s	30 cycles	
BACE1_Ex8R	55°C		1 min		
	68°C		2 min		
BACE1 Primer set (25 ng each)	Temperature 55°C 94°C		Time 30 min 2 min		
BACE1_4F	94°C		30 s	28 cycles	
BACE1_Ex9R	60°C		1 min		
	68°C		2 min		
BACE1 Primer set (25 ng each)	Temperature 55°C 94°C		Time 30 min 2 min		
BACE1_3F	94°C		30 s	30 cycles	
BACE1_Ex8R	60°C		1 min		
	68°C		2 min		
GAPDH Primer set (12.5 ng each)	Temperature 55°C		Time 30 min		
GAPDH For	94°C		2 min		
GAPDH Rev	94°C		30 s	18 cycles	
	60°C		1 min		
	68°C		2 min		

Table C.5   The HPLC analysis of the most efficient AOs (AO2, AO5, AO6, AO8, AO12, and AO13). All the AO samples were run on a Ion-Exchange HPLC using (1M NaClO4, 25mM Tris-HCl pH 8 and water) as mobile phase.

Sample code	IE-HPLC chromatogram
AO2	

Sample code	IE-HPLC chromatogram
AO5	
AO6	
AO8	
AO12	

Sample code	IE-HPLC chromatogram
AO13	

Datafile Name:4209-A013.lcd
Sample Name:4209
Sample ID:4209

mV
4209-A013.lcd Detector A 260nm

C.2 Results

Exon 2   Exon 3

AO1   AO2   AO3   AO5   AO6   AO7

UT

FL= 429 bp

BACE1

FL=404 bp
Δ7= 350 bp

SMN

200   100   50 nM

L3K
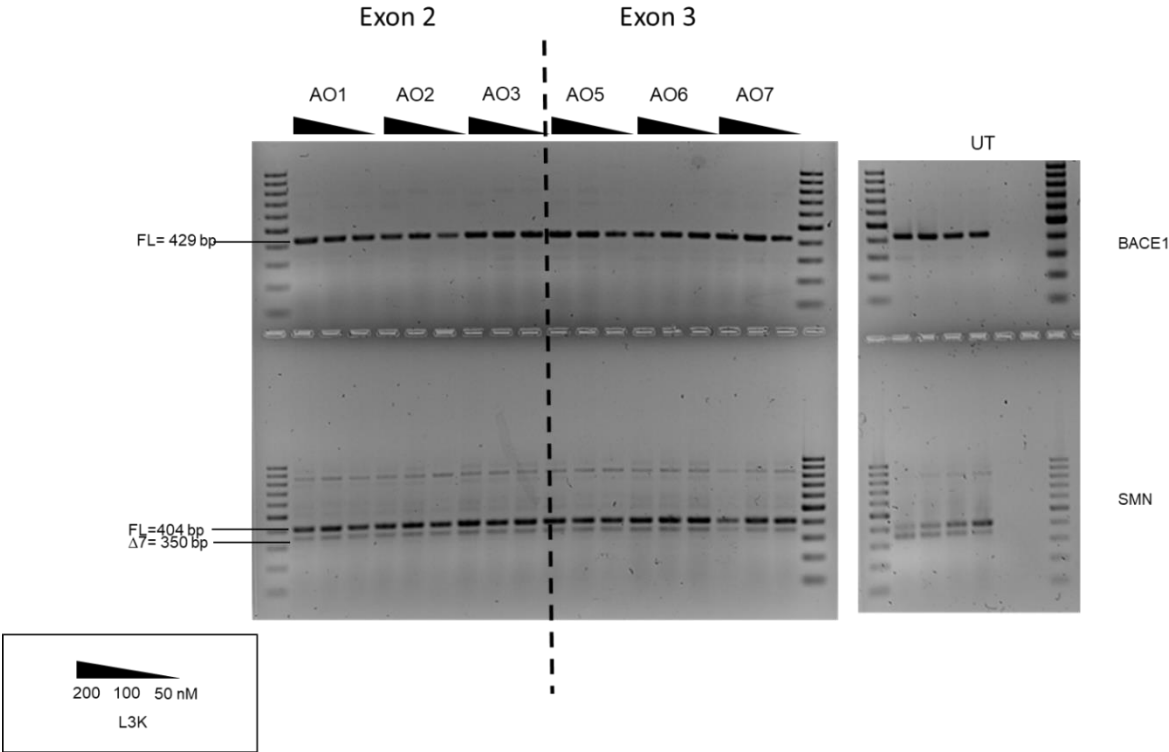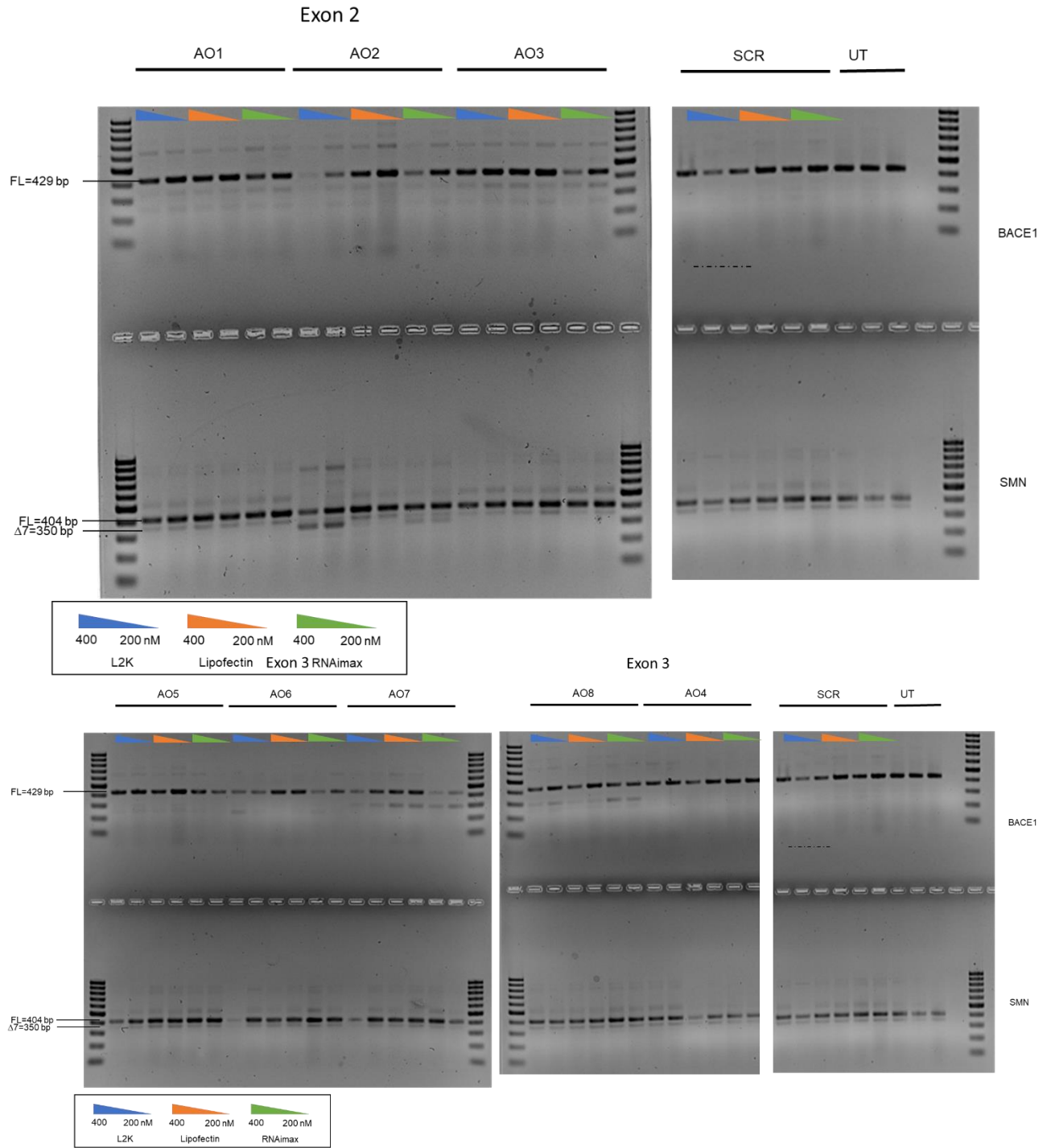
Figure C.1 The RT-PCR products after treatment with AO1, AO2, AO3, AO4, AO5, AO6, AO7, and AO8. The AOs were treated using a variety of transfection reagents including Lipofectamine 3000, Lipofectamine 2000, Lipofectamine RNAimax, and Lipofectin according to the manufacturer's protocol. FL, full-length; SMN was used as a loading control; SCR, Scrambled or Gene tools control was used as a control.

Exon 4

AO10 AO11 AO12 AO13

AO9

SCR UT

200 200 400400
nM nM nM nM

BACE1

Variant A Δ4 = 763 bp
Variant B Δ4 = 688 bp
Variant C Δ4 = 631 bp

Variant A= 901 bp
Variant B= 826 bp
Variant C= 769 bp

GAPDH

FL= 492 bp

FL= 492 bp

	400	200 nM	400	200 nM
	L2K		L3K	

Exon 6

AO15 AO16 AO14

SCR UT

200 200 400 400
nM nM nM nM

BACE1

Variant A Δ6 = 799 bp
Variant B Δ6= 724 bp
Variant C Δ6 = 667 bp

Variant A= 901 bp
Variant B= 826 bp
Variant C= 769 bp

GAPDH

FL= 492 bp

FL= 492 bp

	400	200 nM	400	200 nM
	L2K		L3K	

7
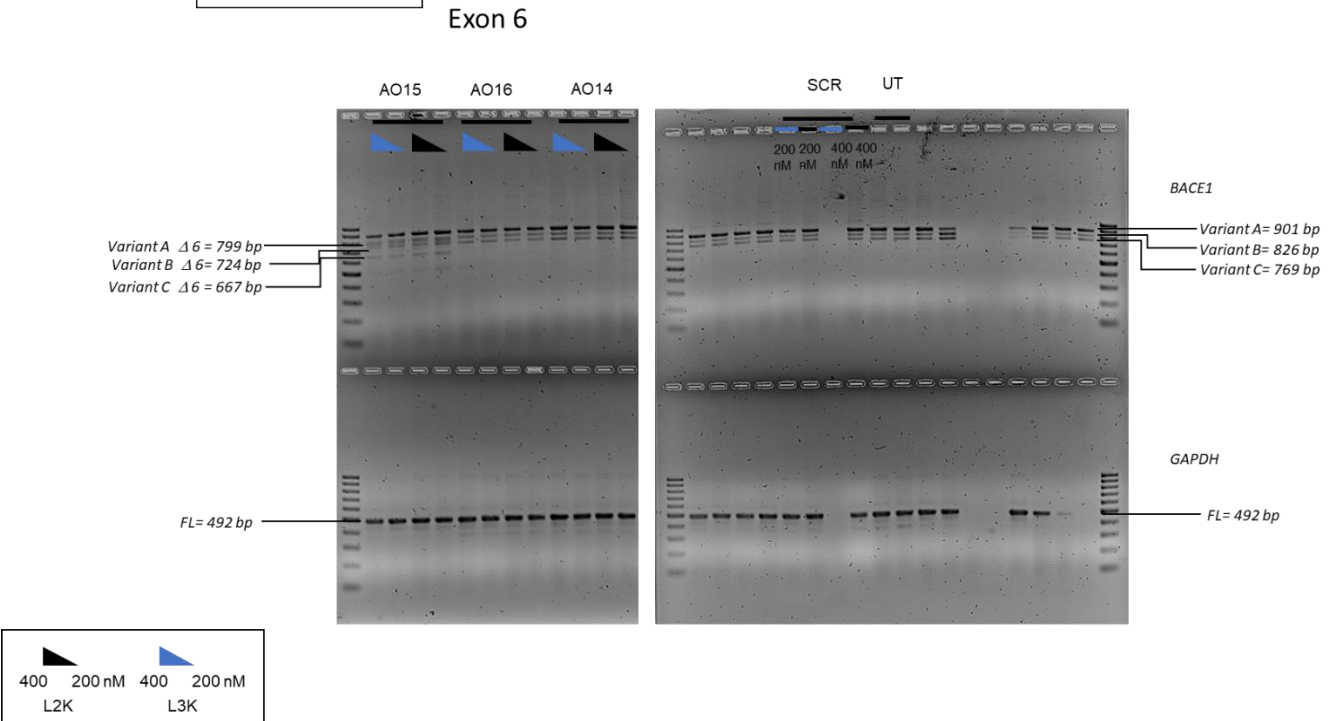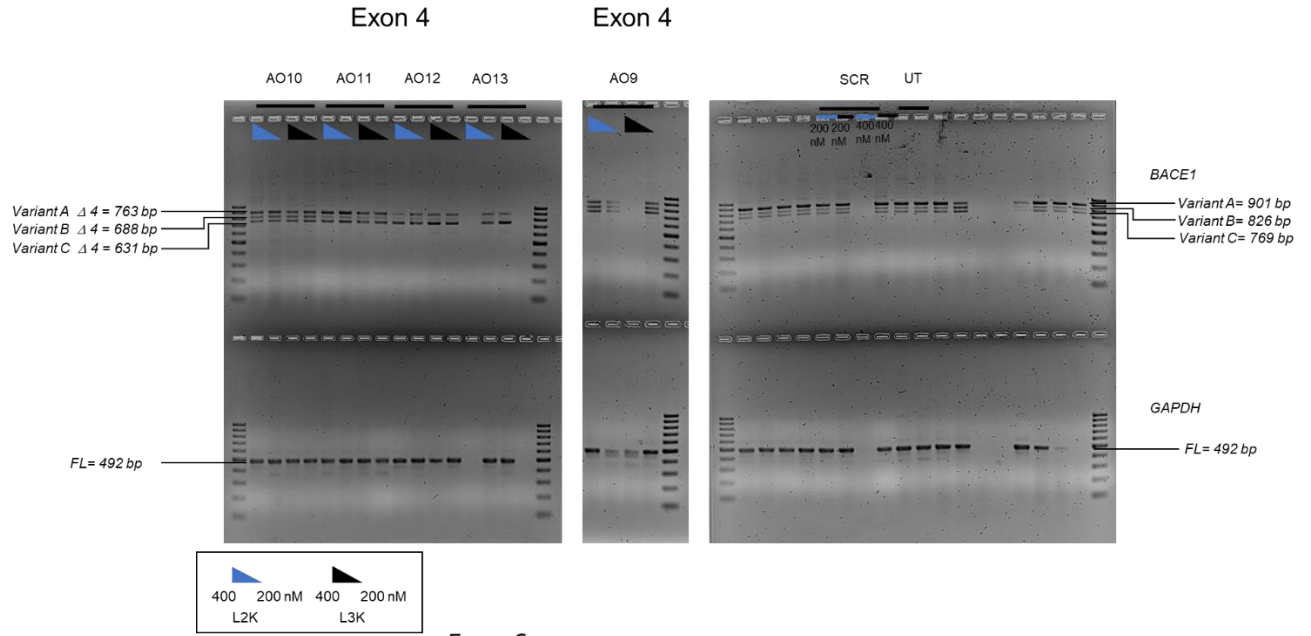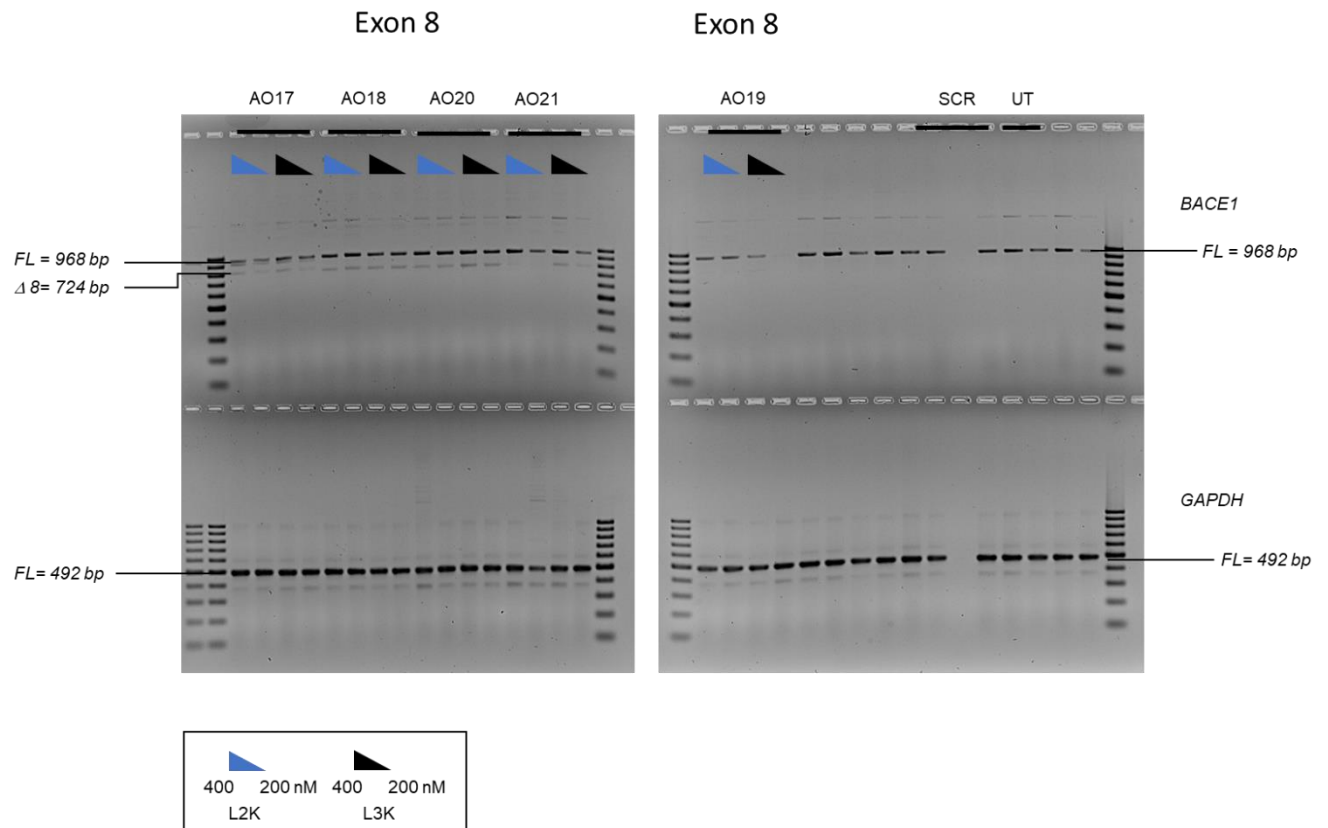
Figure C.2   The RT-PCR products after treatment with AO9, AO10, AO11, AO12, AO13, AO14, AO15, AO16, AO17, AO18, AO19, AO20 and AO21. The AOs were treated using a variety of transfection reagents including Lipofectamine 3000 and Lipofectamine 2000 according to the manufacturer's protocol. FL, full-length; GAPDH was used as a loading control; SCR, Scrambled or Gene tools control was used as a control.
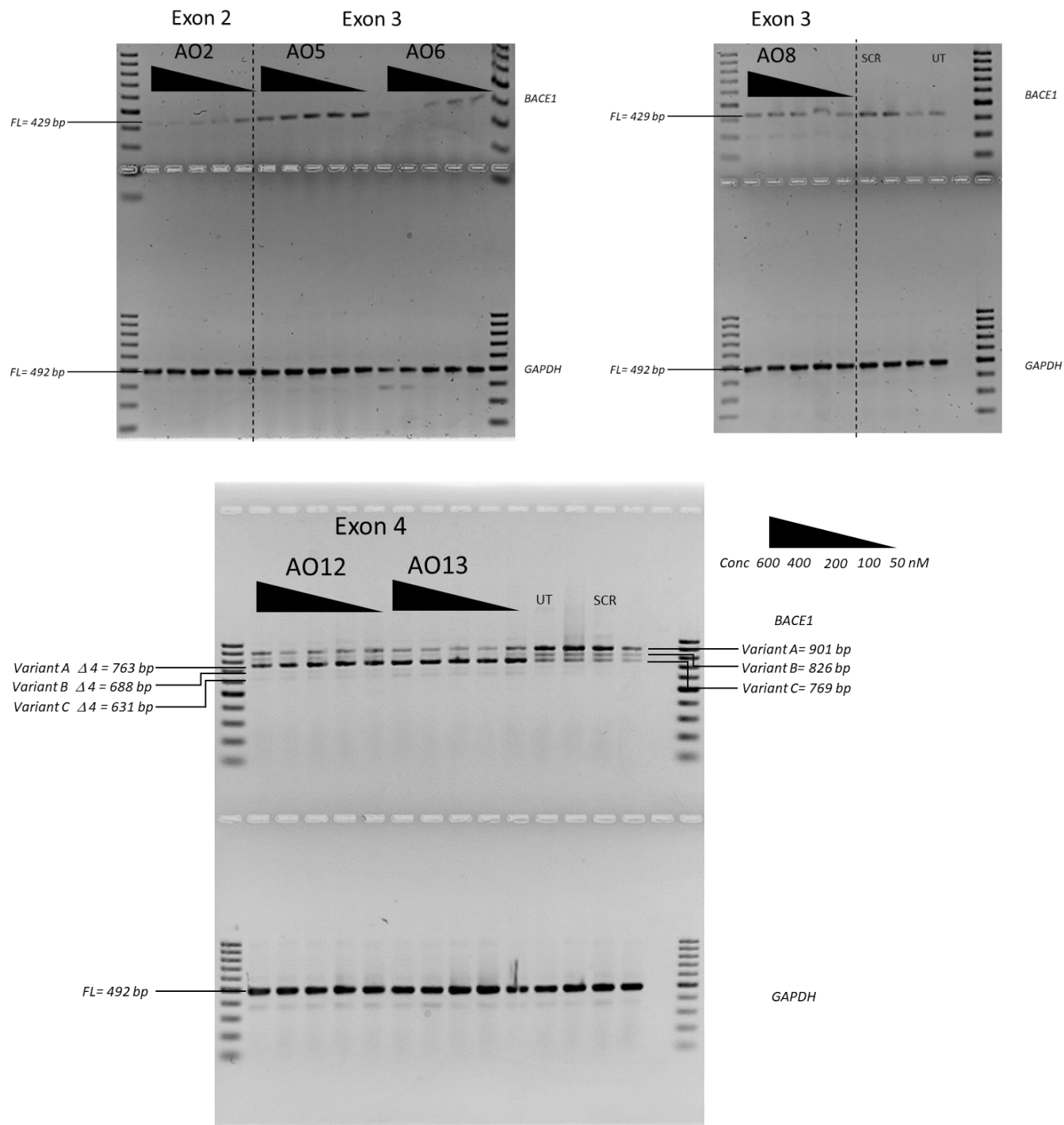
Figure C.3   The RT-PCR products after treatment with AO2, AO5, AO6, AO8, AO12 and AO13. FL, full-length; GAPDH was used as a loading control; SCR, Scrambled or Gene tools control was used as a control. [The gel in this figure is the original gel representing the gel in Figure 5.2. The cropped gel has been shown in Figure 5.2 due to other unimportant samples that exist between the desired samples.]
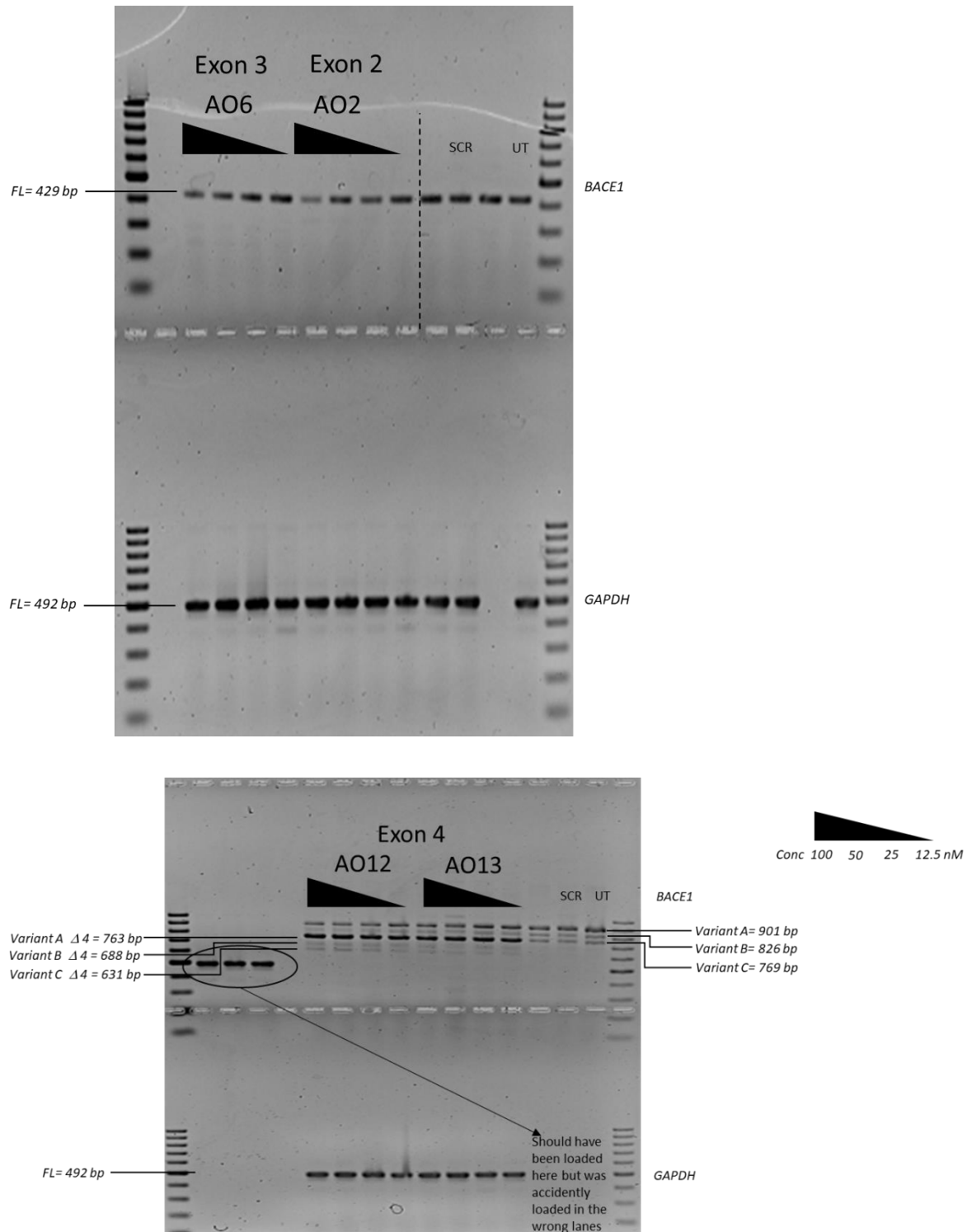
Figure C.4   The RT-PCR products after treatment with AO2, AO6, AO12, and AO13. FL, full-length; GAPDH was used as a loading control; SCR, Scrambled or Gene tools control was used as a control. [The gel in this figure is the original gel representing the gel in Figure 5.3. The cropped gel has been shown in Figure 5.3 due to other unimportant samples that exist between the desired samples and the samples loaded in the wrong wells.]
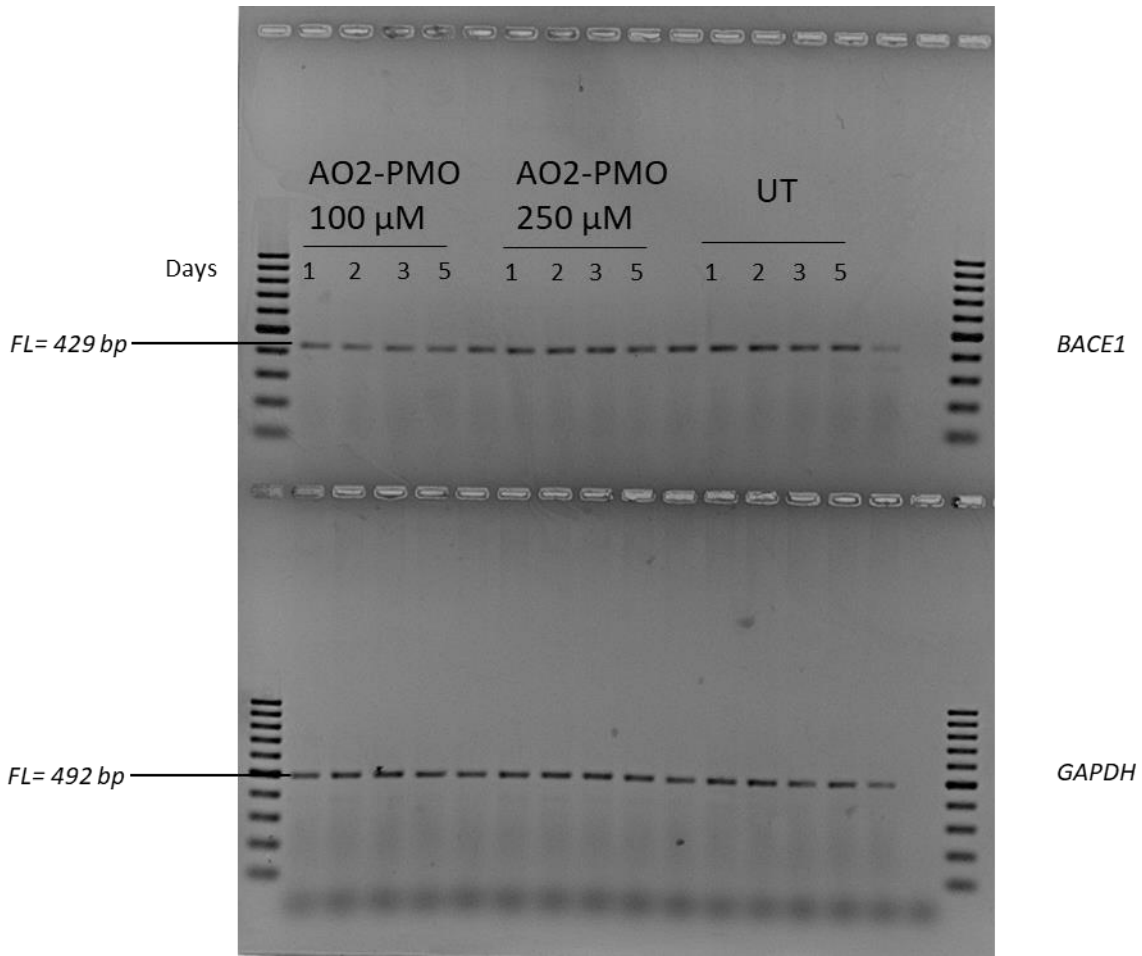
Figure C.5   The RT-PCR products after treatment with AO2-PMO. FL, full-length; GAPDH was used as a loading control SCR, Scrambled or Gene tools control was used as a control. [The gel in this figure is the original gel representing the gel in Figure 5.5. The cropped gel has been shown in Figure 5.5 due to other unimportant samples that exist between the desired samples.]
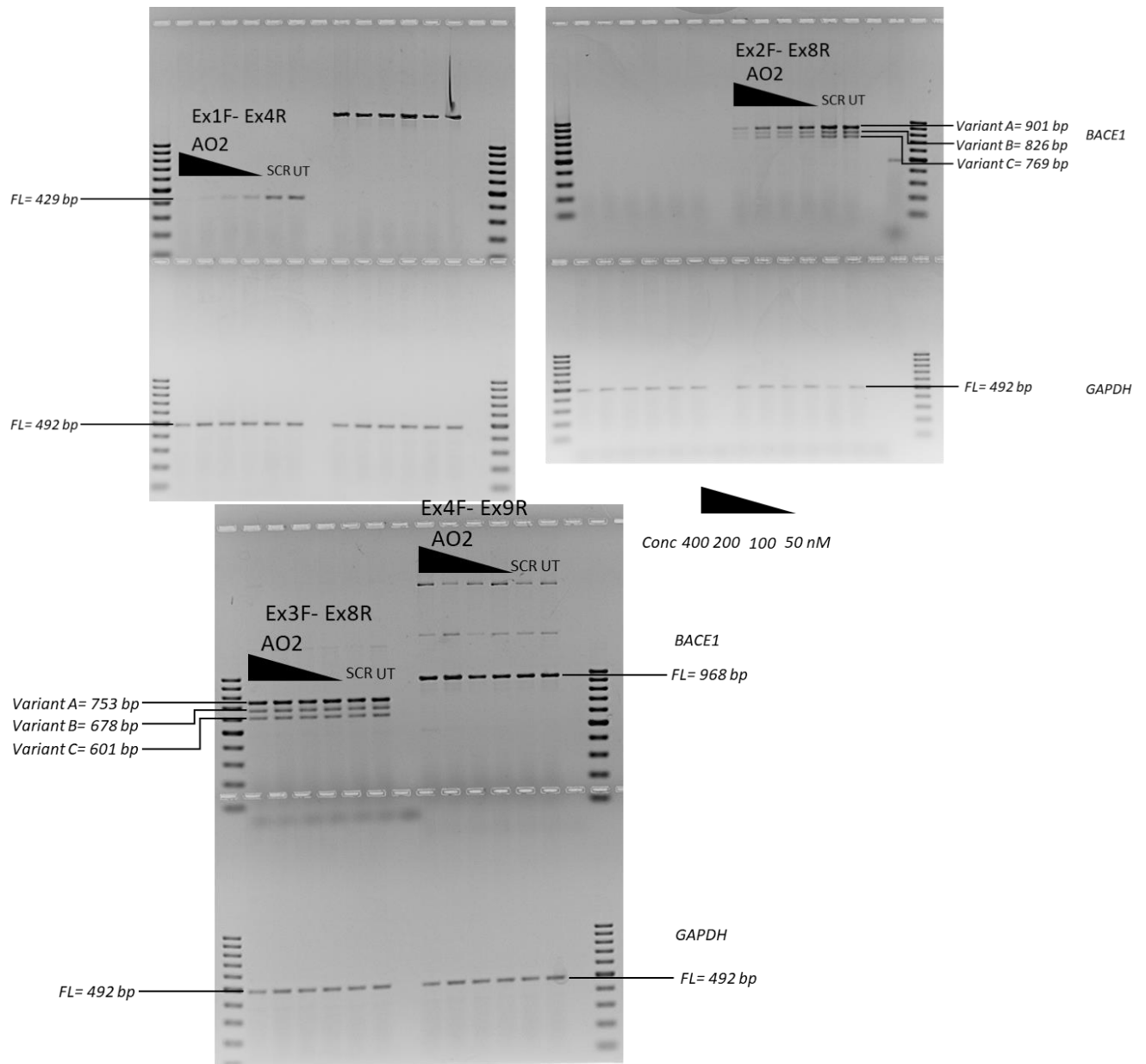
Figure C.6   The RT-PCR products after AO2 treatment amplified using different primer sets. FL, full-length; GAPDH was used as a loading control; SCR, Scrambled or Gene tools control was used as a control. [The gel in this figure is the original gel representing the gel in Figure 5.6. The cropped gel has been shown in Figure 5.6 due to other unimportant samples that exist between the desired samples and nonspecific bands that exist.]
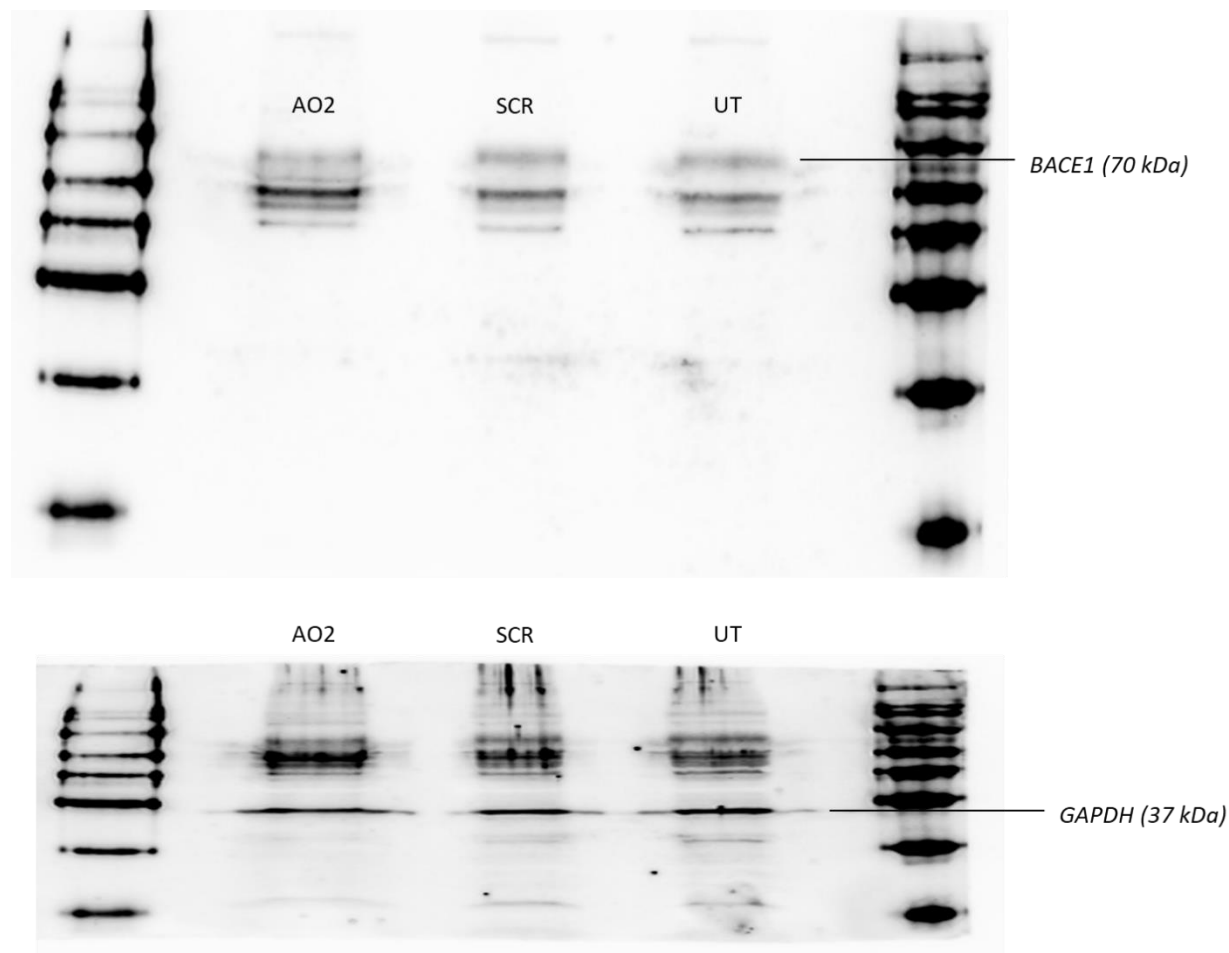
Figure C.7   The western blot membranes after AO2 treatment incubated with anti-BACE1 antibody (top membrane) and anti-GAPDH antibody (bottom membrane). GAPDH was used as a loading control; SCR, Scrambled or Gene tools control was used as a control. [The membrane in this figure is the original membrane representing the membrane in Figure 5.7. The cropped membrane has been shown in Figure 5.7 due to other nonspecific bands that exist.]

Appendix D   Supplementary data for Chapter 6

D.1 Methods

Table D.1   List of primers used, their sequences and the expected product lengths

Primer Set	Primer pairs	Primer Sequences	Expected product length
MAPT Primer Set 1	MAPT6_Ex1Fa	5' TCCTCGCCTCTGTCGACTAT 3'	Variant 2/8= 340 bp
	MAPT6_Ex4R	5' TCCTTCTGGGATCTCCGTGT 3'	
MAPT Primer Set 2	MAPT6_Ex4F	5' GTGACAGCACCCTTAGTGGA 3'	Variant 2/3/5= 968 bp
	MAPT6_Ex9R	5' GCGGGGTTTTTGCTGGAATC 3'	
MAPT Primer Set 3	MAPT6_Ex7F	5' AAGACGGGACTGGAAGCGAT 3'	Varian 2/3/5= 555 bp
	MAPT6_Ex13R	5' TGCTCAGGTCAACTGGTTTGT 3'	Variant 4/7/8= 462 bp
MAPT Primer Set 4	MAPT6_Ex12F	5' TTAGCAACGTCCAGTCCAAGT 3'	Variant 2/8= 307 bp
	MAPT6_Ex15Ra	5' AGGTTGACATCGTCTGCCTG 3'	
GAPDH Primer set	GAPDH For	5' GGACTCATGACCACAGTCCATGC 3'	492 bp
	GAPDH Rev	5' TTACTCCTTGGAGGCCATGTGGG 3'	

Table D.2   The PCR conditions for each primer set.

Primer Set	PCR Conditions		
MAPT Primer Set 1 (50 ng each)	Temperature	Time	
	55°C	30 min	
	94°C	2 min	
	94°C	30 s	28 cycles
	55°C	1 min	
	68°C	2 min	

MAPT Primer Set 3 & 4 (50 ng each)	Temperature	Time	
	55°C	30 min	
	94°C	2 min	
	94°C	30 s	
	60°C	1 min	34 cycles
	68°C	2 min	
MAPT Primer Set 2 & 3 (50 ng each)	Temperature	Time	
	55°C	30 min	
	94°C	2 min	
	94°C	30 s	
	60°C	1 min	30 cycles
	68°C	2 min	
GAPDH Primer set (12.5 ng each)	Temperature	Time	
	55°C	30 min	
	94°C	2 min	
	94°C	30 s	16 cycles

D.2 Results

Table D.3   List of first-generation DNAzymes and their sequences. Red nucleotides represent nucleotides in the catalytic loop. Blue nucleotides represent the cleavage site.

Name	Sequence	Target
RNV547	ATCTTCCA GGCTAGCTACAACGA CACTTCG	Exon 1
RNV548	CAGCGTGA GGCTAGCTACAACGA CTTCCAT	Exon 1
RNV549	CCCCCTGA GGCTAGCTACAACGA CTTTCCT	Exon 1
RNV550	TTGGTGCA GGCTAGCTACAACGA GGTGTAG	Exon 1
RNV551	TCCTCAGA GGCTAGCTACAACGA CCGTCCT	Exon 2
RNV552	TCTTAGCA GGCTAGCTACAACGA CAGAGGT	Exon 2
RNV553	CTCCCTCA GGCTAGCTACAACGA CCACTAA	Exon 3
RNV554	TTCTGGGA GGCTAGCTACAACGA CTCCGTG	Exon 3
RNV555	GTCTCCAA GGCTAGCTACAACGA GCCTGCT	Exon 3
RNV556	TTTTGTCA GGCTAGCTACAACGA CGCTTCC	Exon 5
RNV557	TGTGGCGA GGCTAGCTACAACGA CTTCGTT	Exon 7
RNV558	TGCTGGAA GGCTAGCTACAACGA CCTGGTG	Exon 7
RNV559	TCCCCTGA GGCTAGCTACAACGA TTTGGAG	Exon 9
RNV560	CCGCTGCGA GGCTAGCTACAACGA CCCCTGA	Exon 9
RNV561	ACTTGACA GGCTAGCTACAACGA TCTTCAG	Exon 9
RNV562	TTG CCTAA GGCTAGCTACAACGA GAGCCAC	Exon 11
RNV563	GTTTATGA GGCTAGCTACAACGA GGATGTT	Exon 11
RNV564	CTGGTTTA GGCTAGCTACAACGA GATGGAT	Exon 11
RNV565	TTCTCAGA GGCTAGCTACAACGA TTTACTT	Exon 12
RNV566	GGACCCAA GGCTAGCTACAACGA CTTCGAC	Exon 12
RNV567	GGGTGATA GGCTAGCTACAACGA TGTCCAG	Exon 12

Name	Sequence	Target
RNV568	GTGGGTGA GGCTAGCTACAACGA ATTGTCC	Exon 12
RNV569	GTACACGA GGCTAGCTACAACGA CTCCGCC	Exon 13
RNV570	TGCTGAGA GGCTAGCTACAACGA GCCGTGG	Exon 13
RNV571	AGGAGACA GGCTAGCTACAACGA TGCTGAG	Exon 13
RNV572	CATGTCGA GGCTAGCTACAACGA GCTGCCG	Exon 13
RNV573	GTCTACCA GGCTAGCTACAACGA GTCGATG	Exon 13
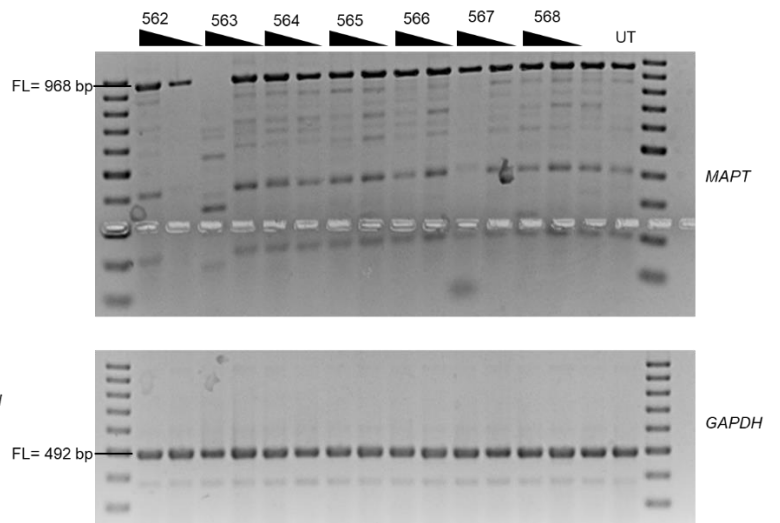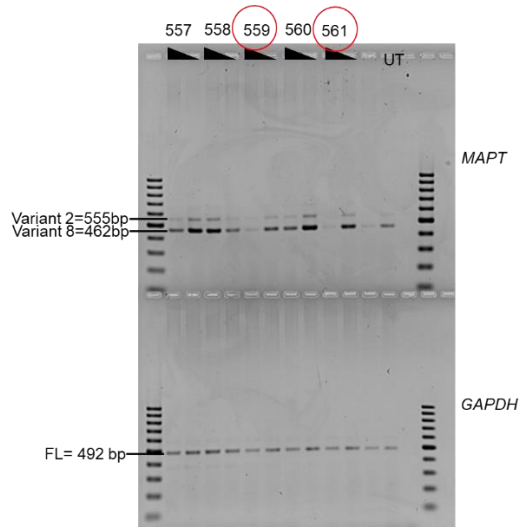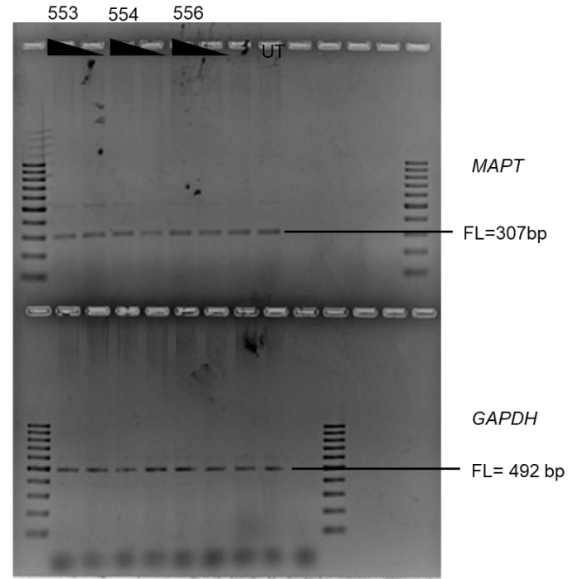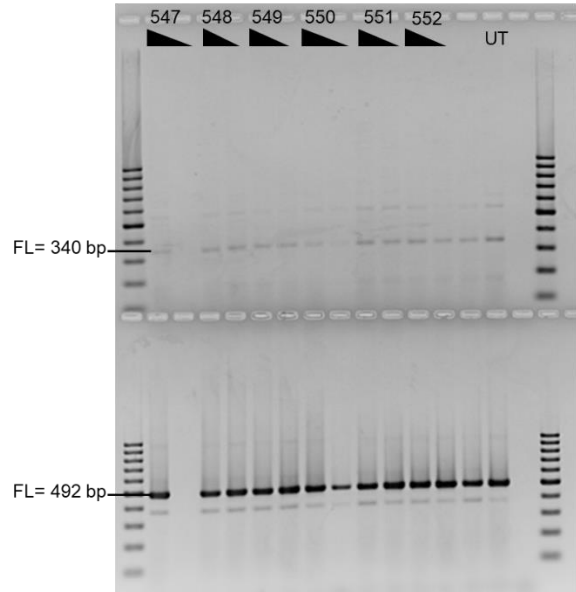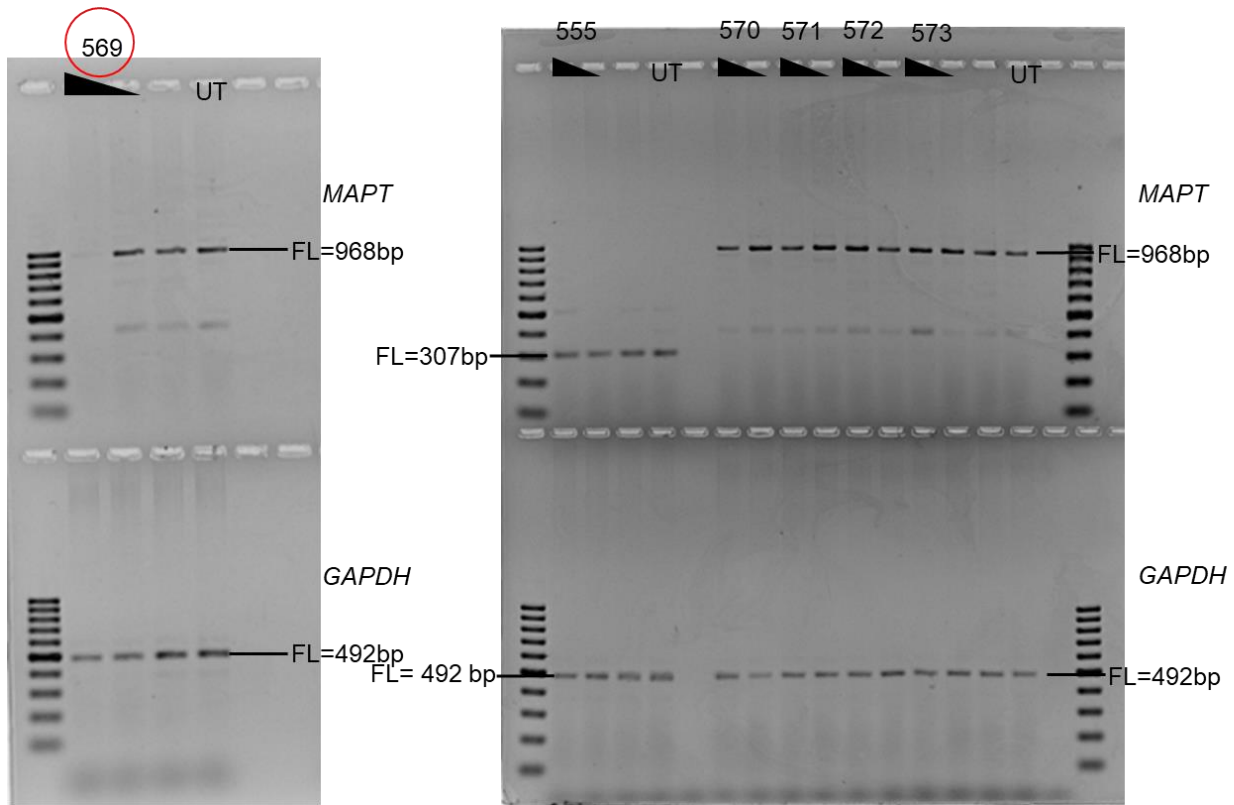
Figure D.1   Representative RT-PCR products of the MAPT and GAPDH transcripts from SH-SY5Y cells after treatment with DNAzyme at 400 nM, and 50 nM concentrations. The RT-PCR products after treatment with RNV547, RNV548, RNV549, RNV550, RNV551, RNV552, RNV553, RNV554, RNV555, RNV556, RNV557, RNV558, RNV559, RNV560, RNV561, RNV562, RNV563, RNV564, RNV565, RNV566, RNV567, RNV568, RNV569, RNV570, RNV571, RNV572 and RNV573 are shown here. FL, full-length; UT, untreated; GAPDH was used as a loading control.
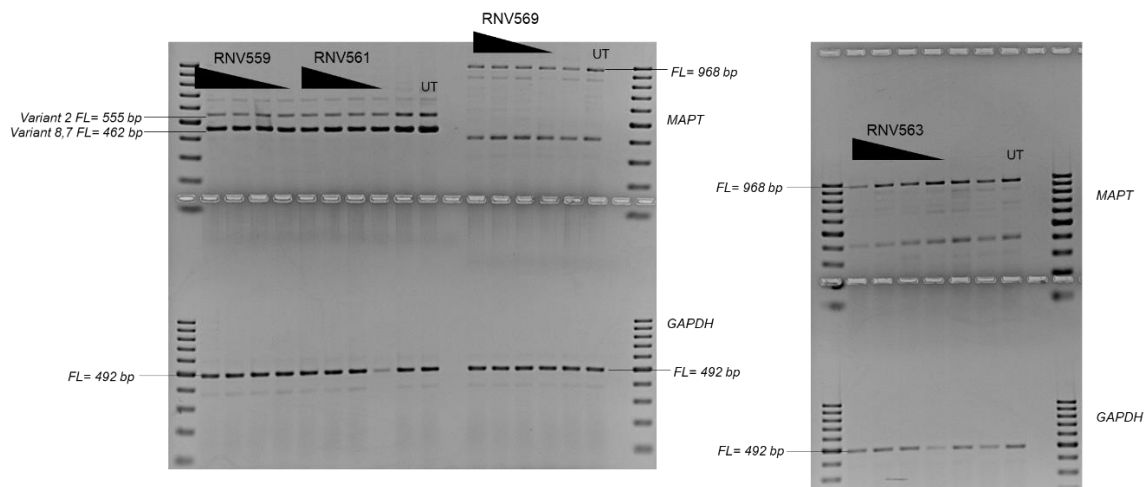
Figure D.2   Representative RT-PCR products of the MAPT and GAPDH transcripts from SH-SY5Y cells after treatment with DNAzyme at 400 nM, 200 nM, 100 nM and 50 nM concentrations. The RT-PCR products after treatment with RNV559, RNV561, RNV563 and RNV563 are shown here. FL, full-length; UT, untreated; GAPDH was used as a loading control. [The gel in this figure is the original gel representing the gel in Figure 6.2. The cropped gel has been shown in Figure 6.2 due to other unimportant samples that exist between the desired samples.]

Table D.4   The average activity of 1st generation DNAzymes (at 400 nM concentration) in SH-SY5Y cells (knockdown of MAPT transcript).

Name	Average Activity of DNAzyme in SH-SY5Y cells
559	0%
561	26%
563	58%
569	0%
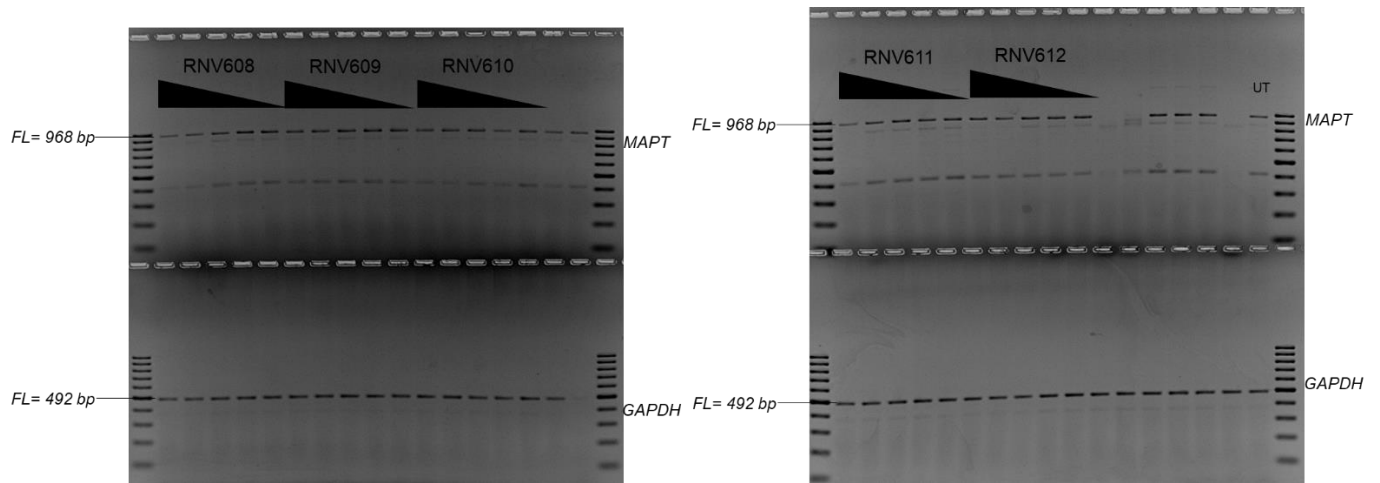
Figure D.3   Representative RT-PCR products of the MAPT and GAPDH transcripts from SH-SY5Y cells after treatment with DNAzyme at 400 nM, 200 nM, 100 nM and 50 nM concentrations. The RT-PCR products after treatment with RNV608, RNV609, RNV610, 611 and RNV612 are shown here. FL, full-length; UT, untreated; GAPDH was used as a loading control.

Table D.5   The average activity of 2nd generation DNAzymes (at 400 nM concentration) in SH-SY5Y cells (knockdown of MAPT transcript).

Name	Average Activity of DNAzymes in SH-SY5Y cells
608	0%
609	0%
610	15%
611	0%
612	2%
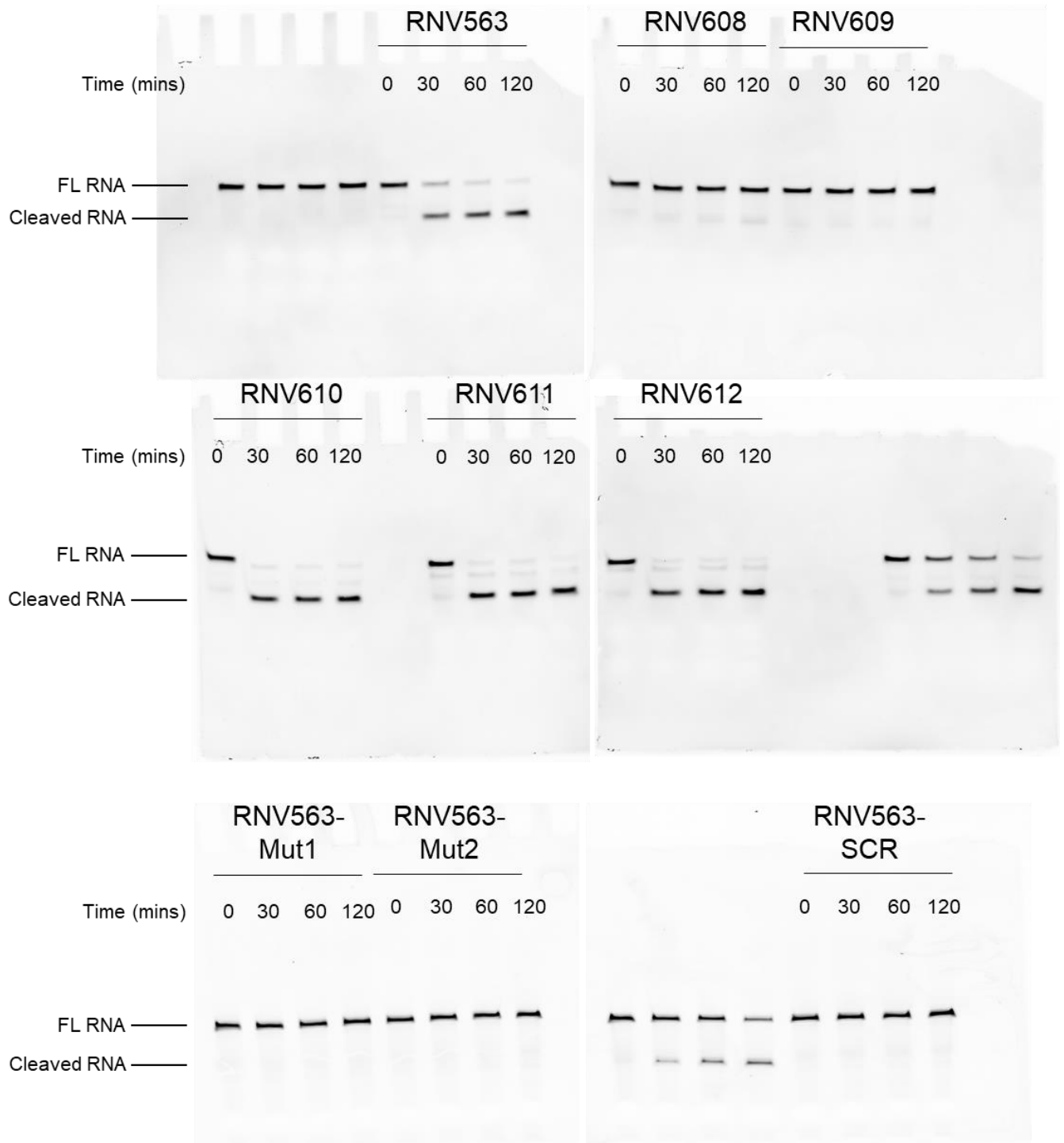
Figure D.4   In vitro cleavage of the FAM-conjugated MAPT RNA template composed of exon 11 region (34 nucleotides) by RNV563 and its derivatives. FL RNA, full-length; FAM-conjugated RNA; cleaved RNA; the cleaved FAM-conjugated MAPT RNA (22 nucleotides long). The FAM- conjugated template RNA is a small region of the MAPT transcript complementary to the hybridisation arms of the DNAzymes of interest. [The gel in this figure is the original gel representing the gel in Figure 6.3. The cropped gel has been shown in Figure 6.3 due to other unimportant samples or unwanted spaces that exist between the desired samples.]

Table D.6   *List of 2'-OMePS AOs and their sequences. In the sequences, capital letters denote bases from the exon regions, and small letters denote bases from the intronic region.*

AO Number	AO Name	AO Sequence	Target
AO1	MAPT E1A(+11+35)	TCCATCACTTCGAACTCCTGGCGGG	Exon 1
AO2	MAPT E1A(+41+65)	TCCCCCAACCCGTACGTCCCAGCGT	Exon 1
AO3	MAPT E1A(+91+115)	TGTCACCCTCTTGGTCTTGGTGCAT	Exon 1
AO4	MAPT E4A(+1+25)	GTGTCTCCAATGCCTGCTTCTTCAG	Exon 4
AO5	MAPT E4A(+26+50)	AGCAGCTTCGTCTTCCAGGCTGGGG	Exon 4
AO6	MAPT E5A(+16+40)	TCGCTTCCAGTCCCGTCTTTGCTTT	Exon 5
AO7	MAPT E5D(+3-22)	ctccgtggcatcgtcagcttacCTT	Exon 5
AO8	MAPT E7A(+26+50)	GGAGGGGCTGCTCCCCGCGGTGTGG	Exon 7
AO9	MAPT E7A(+46+70)	TGGCCTGGCCCTTCTGGCCTGGAGG	Exon 7
AO10	MAPT E7A(+71+95)	GTTTTTGCTGGAATCCTGGTGGCGT	Exon 7
AO11	MAPT E7A(+97+121)	TGGGTGGTGTCTTTGGAGCGGGCGG	Exon 7
AO12	MAPT E7D(+5-20)	caagagaacgttcttcttacCAGAG	Exon 7
AO13	MAPT E9A(+1+25)	CGATCCCCTGATTTTGGAGGTTCAC	Exon 9
AO14	MAPT E9A(+111+135)	TACGGACCACTGCCACCTTCTTGGG	Exon 9
AO15	MAPT E9A(+159+183)	GGGCTGTCTGCAGGCGGCTCTTGGC	Exon 9
AO16	MAPT E9A(+196+220)	TTGGACTTGACATTCTTCAGGTCTG	Exon 9
AO17	MAPT E9A(+226+250)	TGGTGCTTCAGGTTCTCAGTGGAGC	Exon 9
AO18	MAPT E9D(+21-4)	tcacCTTCCCGCCTCCCGGCTGGTG	Exon 9
AO19	MAPT E12A(-5+20)	TACTTCCACCTGGCCACCTCctaga	Exon 12
AO20	MAPT E12A(+ 21+45)	CCTTGAAGTCAAGCTTCTCAGATTT	Exon 12
AO21	MAPT E12A(+46+70)	GACCCAATCTTCGACTGGACTCTGT	Exon 12
AO22	MAPT E12A(+81+95)	AGGGACGTGGGTGATATTGTCCAGG	Exon 12
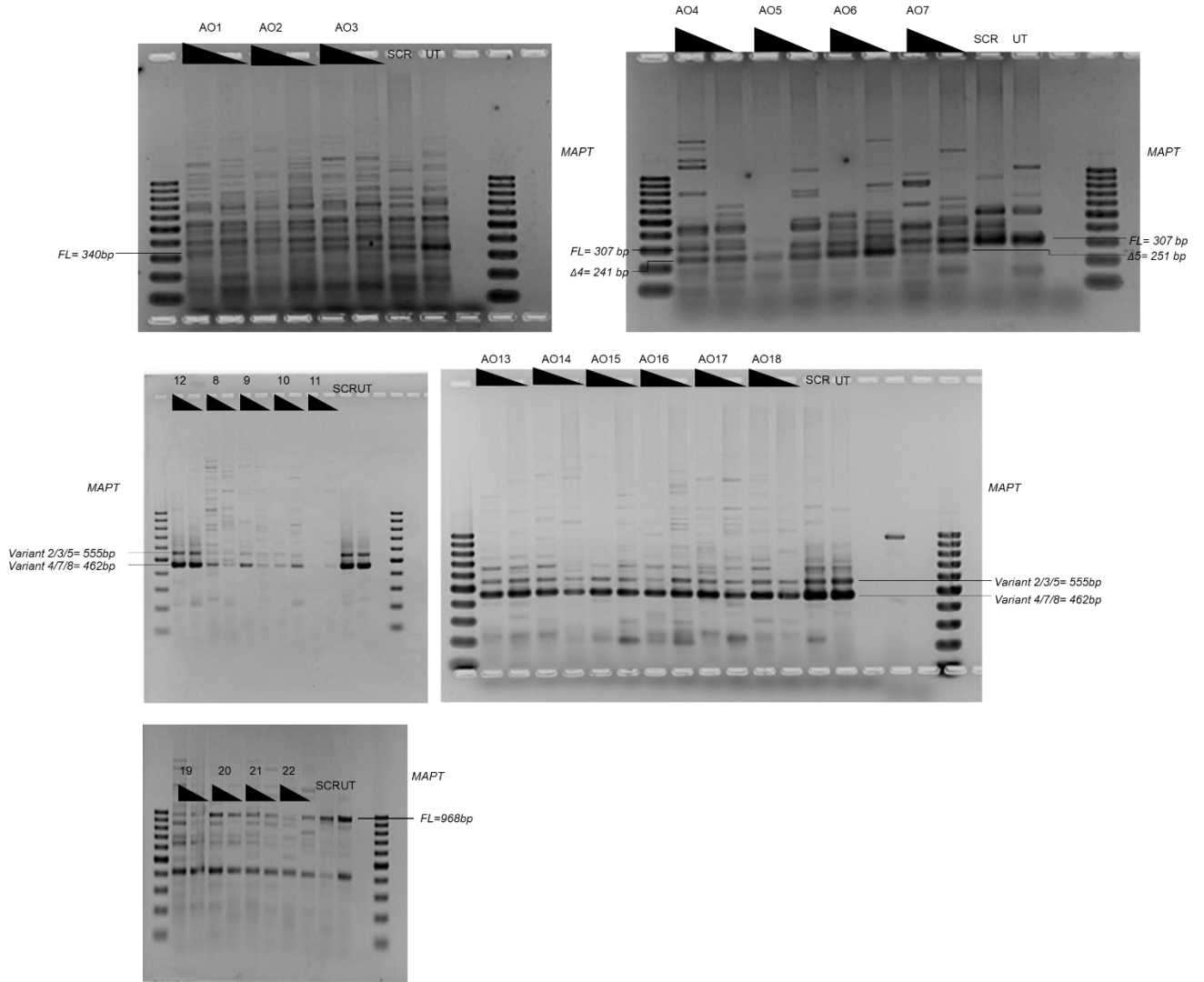
Figure D.5   Representative RT-PCR products of the MAPT transcripts from SH-SY5Y cells after treatment with splice-modulating AOs at 400 nM, and 50 nM concentrations. The RT-PCR products after treatment with AOs 1-22 are shown here. FL, full-length; UT, untreated; SCR, scrambled sequence.
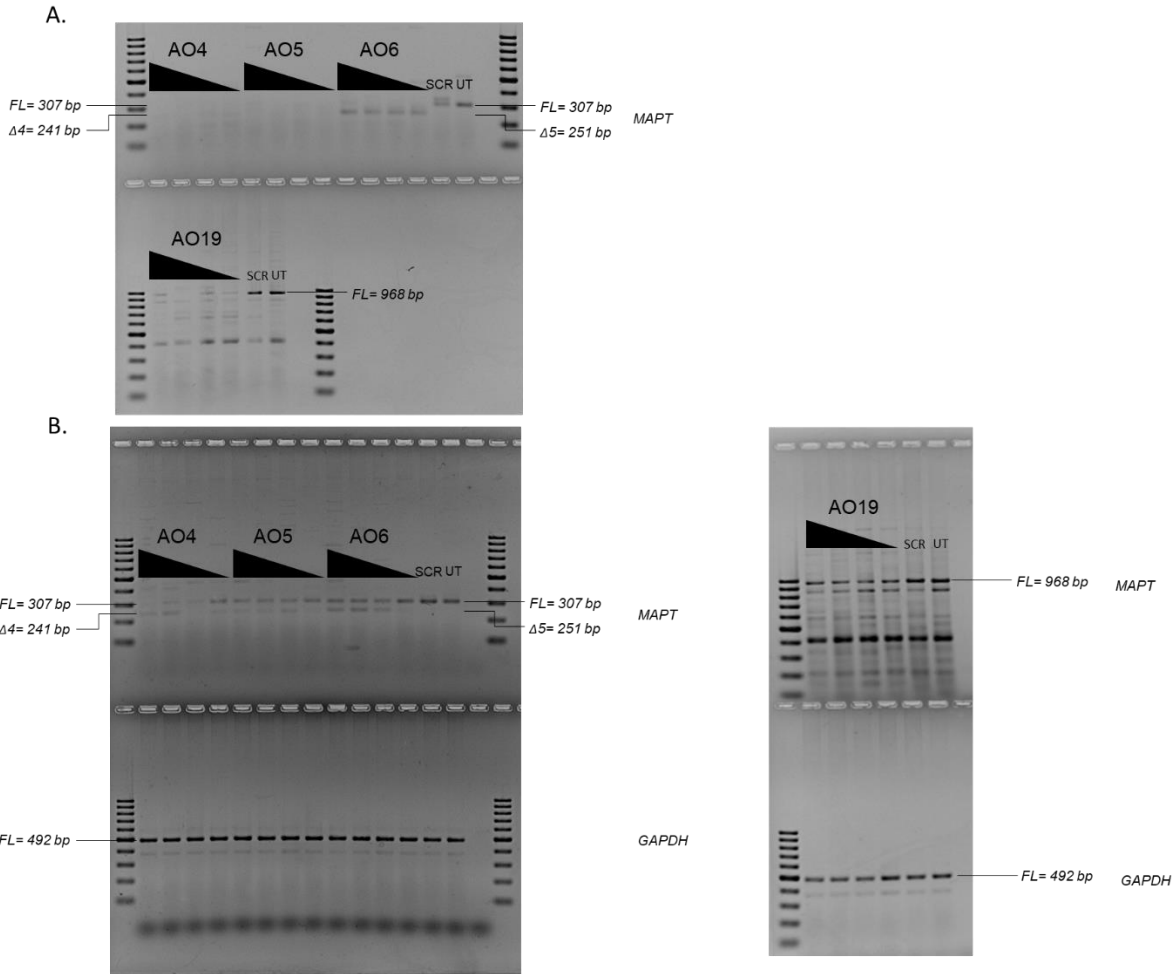
Figure D.6   A. Representative RT-PCR products of the MAPT transcripts from SH-SY5Y cells after treatment with AO4, AO5, AO6, and AO19 at 400 nM, 200 nM, 100 nM and 50 nM concentrations. B. Representative RT-PCR products of the MAPT and GAPDH transcripts from SH-SY5Y cells after treatment with AO4, AO5, AO6, and AO19 at 50 nM, 25 nM, 12.5 nM and 6.25 nM concentrations. AO4 targets exon 4, AO5 and AO6 target exon 5, and AO19 targets exon 12 of the MAPT transcript. FL, full-length; UT, untreated; SCR, scrambled sequence; GAPDH was used as a loading control. [The gel in this figure is the original gel representing the gel in Figure 6.4. The cropped gel has been shown in Figure 6.4 due to unwanted spaces that exist on the gel.]

A.
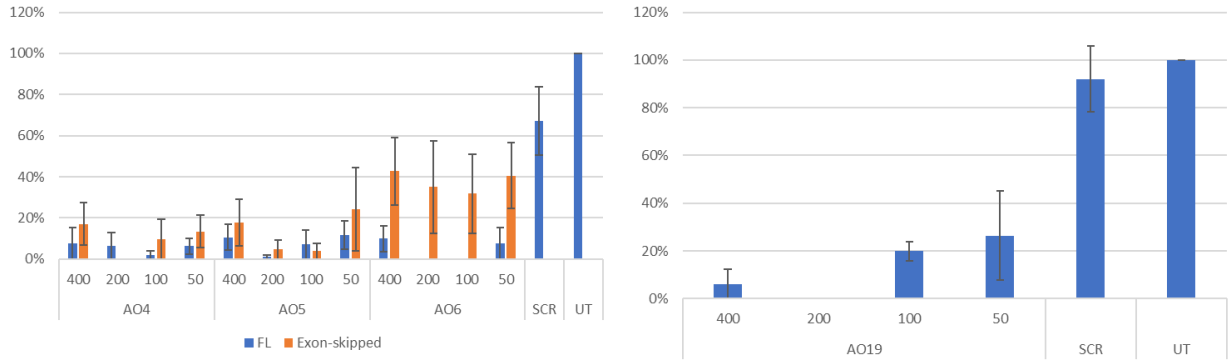
B.
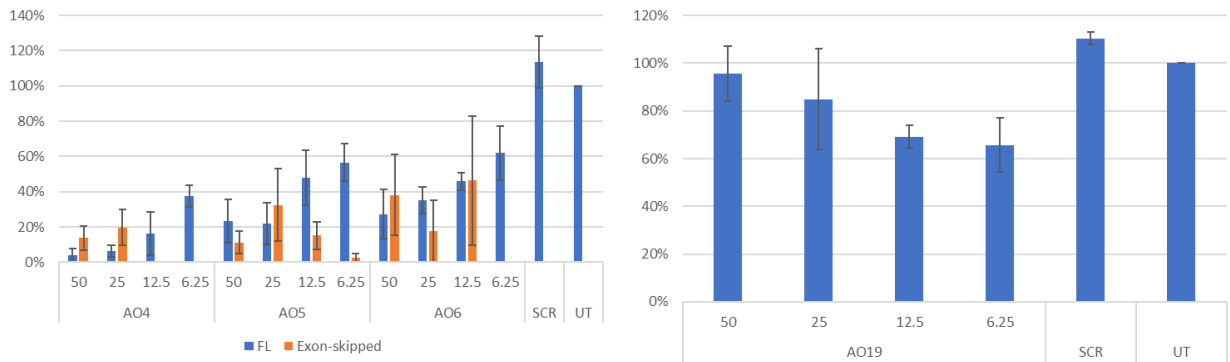
Figure D.7   Densitometry analysis of RT-PCR products (more than two replicates) using AO4, AO6, AO7 and AO19 showed downregulation and exon-skipping of MAPT transcript in SH-SY5Y cells in vitro. Concentrations of AOs used include 400 nM, 200 nM, 100 nM and 50 nM. B. Densitometry analysis of RT-PCR products (more than 2 replicates) using AO4, AO6, AO7 and AO19 showed downregulation and exon-skipping of MAPT transcript in SH-SY5Y cells in vitro. Concentrations of AOs used include 50 nM, 25 nM, 12.5 nM and 6.25 nM.
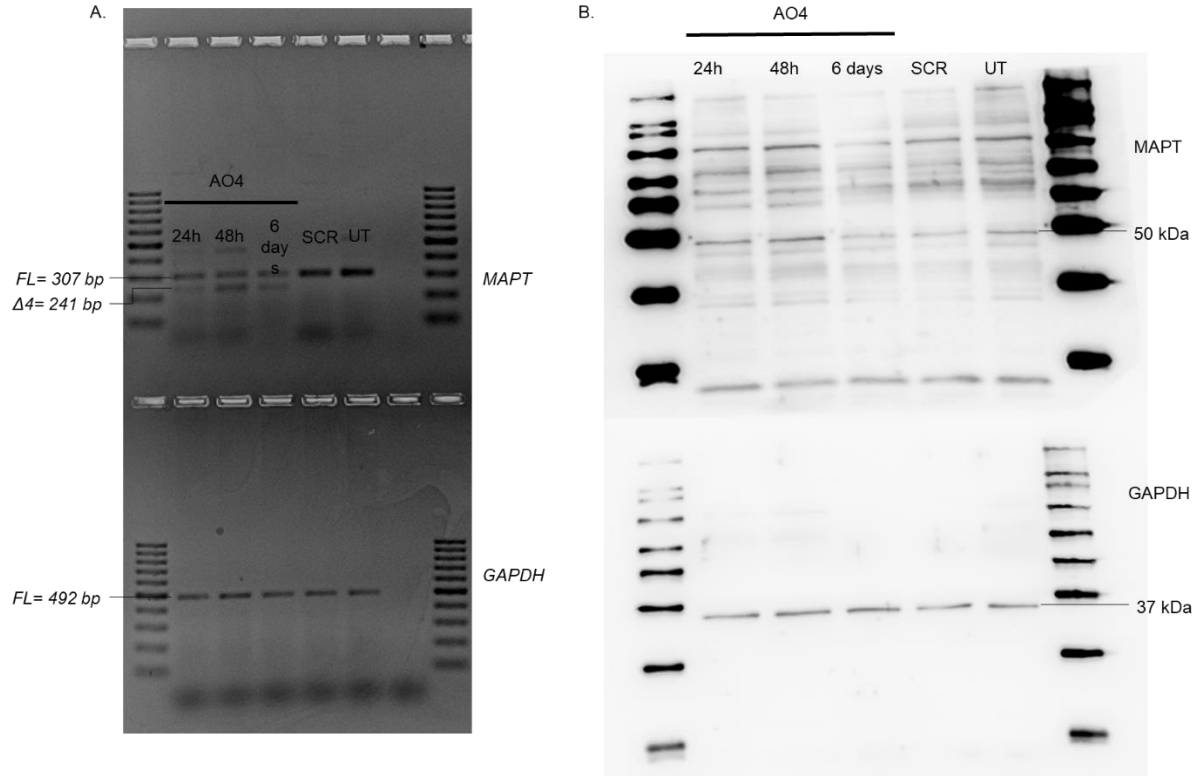
Figure D.8   A. Representative RT-PCR products of the MAPT transcripts from SH-SY5Y cells after treatment with AO4 50 nM concentration and incubation of AO for 24 h, 48 h and six days. AO4 targets exon 4 of the MAPT transcript. B. Representative protein products of the MAPT and GAPDH transcripts from SH-SY5Y cells after treatment with AO4 at 50 nM concentrations and incubation of AO for 24 h, 48 h and six days. AO4 targets exon 4 of the MAPT transcript. FL, full-length; UT, untreated; SCR, scrambled sequence; GAPDH was used as a loading control. [The gel in this figure is the original gel representing the gel in Figure 6.5. The cropped gel has been shown in Figure 6.5 due to unwanted spaces, other unimportant samples, and non-specific bands that exist on the gel and membrane.]
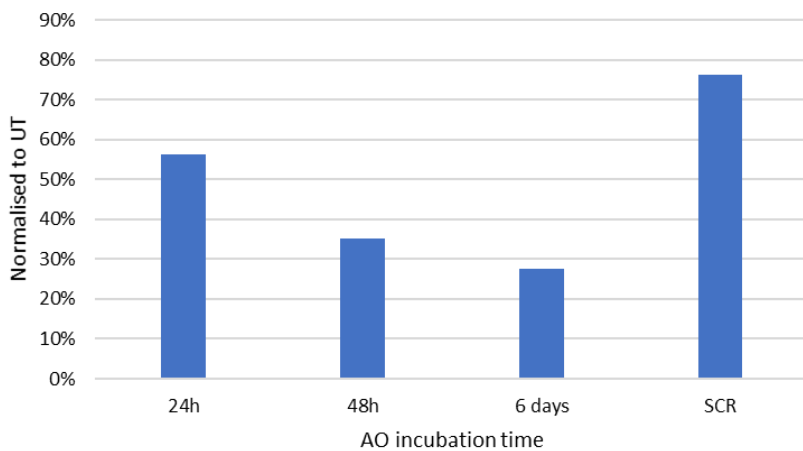
Figure D.9   Densitometry analysis of the western blot shown in Figure 6.5 and Appendix B, Figure D.8

Appendix E   Publications

First Author and first co-author publications.

Publications from this thesis are listed in chronological order.
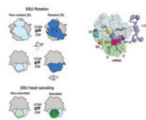
In vitro evolution of chemically-modified nucleic acid aptamers: Pros and cons, and comprehensive selection strategies

Farhana Lipi, Suxiang Chen, Madhuri Chakravarthy, Shilpa Rakesh & Rakesh N. Veedu

Taylor & Francis
Taylor & Francis Group

REVIEW

𝗔 OPEN ACCESS

In vitro evolution of chemically-modified nucleic acid aptamers: Pros and cons, and comprehensive selection strategies

Farhana Lipi [iD][a], Suxiang Chen[a,b], Madhuri Chakravarthy[a,b], Shilpa Rakesh[a], and Rakesh N. Veedu[a,b]

[a]Western Australian Neuroscience Research Institute, Perth, Australia; [b]Centre for Comparative Genomics, Murdoch University, Perth, Australia

ABSTRACT
Nucleic acid aptamers are single-stranded DNA or RNA oligonucleotide sequences that bind to a specific target molecule with high affinity and specificity through their ability to adopt 3-dimensional structure in solution. Aptamers have huge potential as targeted therapeutics, diagnostics, delivery agents and as biosensors. However, aptamers composed of natural nucleotide monomers are quickly degraded *in vivo* and show poor pharmacodynamic properties. To overcome this, chemically-modified nucleic acid aptamers are developed by incorporating modified nucleotides after or during the selection process by Systematic Evolution of Ligands by EXponential enrichment (SELEX). This review will discuss the development of chemically-modified aptamers and provide the pros and cons, and new insights on *in vitro* aptamer selection strategies by using chemically-modified nucleic acid libraries.

Abbreviations: SELEX, Systematic Evolution of Ligands by EXponential enrichment; US FDA, United States Food and Drug Administration; AMD, Age-related macular degeneration; VEGF, Vascular endothelial growth factor protein, 2′-NH$_2$, 2′-Amino; 2′-OH, 2′-Hydroxyl; K$_d$, Equilibrium dissociation constant; 2′-OMe, 2′-O-Methyl; Bfgf, Basic fibroblast growth factor; 2′-F, 2′-Fluoro; PSMA, Prostate specific membrane antigen; IFN-γ, Interferon-gamma; KGF, Keratinocyte growth factor; 4′-S, 4′-Thio; 2′-FANA, 2′-Fluoroarabino nucleic acid; HNA, 1,5-Anhydro hexitol nucleic acid; TAR, transactivation responsive element; TNA, Threose nucleic acid; LNA, Locked nucleic acid; SOMAmers, Slow Off-rate Modified Aptamers

Introduction

Nucleic acid aptamer technology has attracted considerable attention in recent years in light of their widespread applications in therapeutic development, targeted drug delivery, biosensing and accurate molecular imaging. Aptamers are short single-stranded DNA or RNA oligonucleotides with unique 3-dimensional shape that can bind to their specific target with very high affinity and specificity.[1-5] Aptamers are generally developed from a large pool of oligonucleotide libraries containing approximately 10^{14} members by a reiterative process referred to as SELEX which involves selection, separation and enrichment steps (Fig. 1).[6,7] Till now, antibodies have been widely used for target specific molecular recognition.[8] However, compared to antibody-based technologies, aptamers may possess a number of advantages including easy laboratory production *in vitro* effectively eliminating the use of live animals, no batch to batch variation, low or no immunogenicity, freedom to introduce multiple chemistries during synthesis without losing the affinity and specificity, small size that allows faster tissue penetration, ability to reverse target binding interactions using its complementary antidote sequence, significantly longer shelf-life and low cost. In 2004, an aptamer drug Macugen (Pegaptanib Sodium) was approved by United States Food and Drug Administration (US FDA) for the treatment of neovascular age-related macular degeneration (AMD) by targeting

vascular endothelial growth factor protein 165 (VEGF$_{165}$).[9,10] Currently, a number of aptamer-based therapeutic candidates are in preclinical development and in different stages of clinical trials.[11]

Typically, aptamers are developed with naturally occurring nucleotides. However, aptamers composed of natural nucleotide monomers are not suitable for theranostic applications as they possess very poor resistance to enzymatic degradation and show decreased binding affinity, rendering poor pharmacokinetic properties. To circumvent these shortcomings, aptamers containing chemically-modified nucleotide analogs with high stability against nucleases are normally used. Early examples of modified aptamers were primarily produced by post-SELEX-based approach. In this process, the aptamers were first isolated using natural RNA or DNA random sequences by SELEX method and then modified as per demand on affinity, stability and functionality. For this purpose, appropriate chemically-modified nucleotides are systematically incorporated into an existing DNA/RNA aptamer during solid-phase oligonucleotide synthesis. Generally, a web-based secondary structure prediction algorithm (e.g. mfold,[12] RNAfold[13]) is used as a tool to assist with the positioning of chemically-modified nucleotides and to truncate the overall size of the selected aptamers during chemical synthesis. Such chemically-fabricated

Figure 1. Schematic illustration of the SELEX and post-SELEX methods for developing aptamers.

aptamer variants are then tested for binding affinity, and the best candidates are used for further analysis and downstream applications *in vitro* and *in vivo*. Evolution of chemically-modified aptamers would be a far more powerful approach to develop modified aptamers as this could generate aptamers with unique structures and with even shorter libraries.

Evolution of chemically-modified aptamers

A large repertoire of chemically-modified nucleotide analogs with remarkable biophysical properties have been developed in recent years and a few papers have reviewed the use of these chemically-modified nucleotides in the generation of aptamers and nucleic acids with enzymatic activity including DNAzymes and ribozymes.[14-18] But, their applicability in *de novo* evolution of aptamers via SELEX methodologies are rather impeded by poor or lack of enzymatic recognition capabilities. Conventional selection methodologies involve multiple enzymatic steps that are required to amplify and regenerate chemically-modified nucleotide-containing libraries. Some sugar-modified nucleotides are reported to tolerate few commercially available DNA or RNA polymerases,[19] making them promising candidates for aptamer selection. However, it is worth mentioning that the level of enzymatic recognition capabilities of the reported modified nucleotides varies depending on the specific chemical modification. Still, the substrate properties of a number of other promising analogs have not been reported which might be due to the lack of enzymatic recognition. One option is to evolve an enzyme specific to the modified nucleotide, and there are reports of successful aptamer selection using engineered enzymes for chemically-modified nucleotides.[20,21] An overview of possible strategies that can be applied for selecting chemically-modified aptamers are outlined below (Fig. 2).

Generation of chemically-modified libraries and selection strategies

Starting oligonucleotide libraries containing the desired chemically-modified nucleotide or a combination of different modifications can be chemically synthesized using an oligonucleotide synthesizer via standard phosphoramidite chemistry. Another approach could be to synthesize normal DNA library which subsequently can be converted to a chemically-modified library by following enzymatic protocols involving PCR and/or *in vitro* transcription reactions with modified nucleotide triphosphates using the specific polymerase which could also be used in subsequent amplification/regeneration steps of multiple selection rounds. Synthetic chemically-modified libraries can be constructed by incorporating the modified nucleotides in the randomized region or in the primer-binding region.

Library with modified random region

Modified nucleotides can be incorporated as mixmers together with natural nucleotide monomers or as fully modified in the random region to furnish a chemically-modified oligonucleotide library for aptamer selection. However, the libraries containing fully modified random region with all four modified nucleotide bases may be limited to use in one-step aptamer selection-based methodologies. This is mainly because the selected aptamer candidates are regenerated using triphosphate derivatives of the corresponding modified nucleotides, but during an enzymatic synthesis process, the primer-binding region will also be modified with the same modified nucleotides contrary to the starting library design. In SELEX to allow maximum base variations of the chemically-modified nucleotides (good substrates of specific enzymes) in the random region, the nucleotide bases can be mixed with one, two or three modified
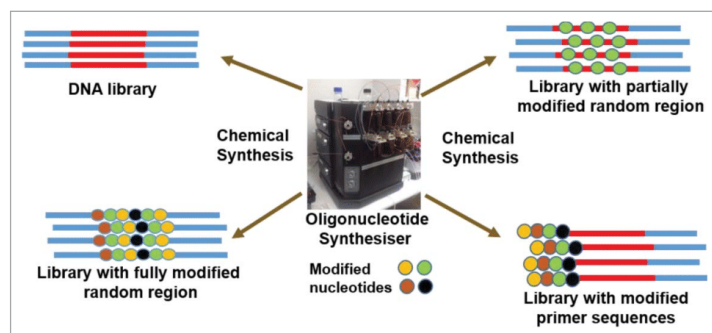
Figure 2. The construction of oligonucleotide libraries for developing chemically modified libraries.

nucleotide bases of the same or different nucleotide analogs in combination with the natural counterparts. But, depending on the number of modified nucleotide bases in the randomized region, the primer-binding region needs to be adjusted with the base composition of unmodified nucleotides. In this approach, where nucleotide mixmers are randomized, it is difficult to locate the positioning of modified nucleotide analogs, and if the library is constructed with successive stretch of modified nucleotides it may be hard for the polymerases to regenerate these particular sequences for subsequent selection rounds.

Another design approach could be to fix the positioning of modified nucleotides in the random region, which will assist to keep track of the positioning of modified nucleotides after sequencing. But, this could limit the pool diversity to some extent, however, it is worthwhile to perform selection since some chemical modifications could generate unique shapes and enhance target binding affinity. It is best to limit up to two fixed modifications that could be incorporated individually at different positions or as a mixture at the same positions allowing two nucleotide variations. Again, the primer-binding region needs to be constructed only with the unmodified natural nucleotide bases (avoiding similar base counterparts of the chemically-modified nucleotides) to regenerate the selected aptamer candidates for use in the subsequent selection rounds. During the sequence alignment after sequencing, only those candidates that maintain the initial library design need to be considered for further analysis and chemical synthesis.

Library with modified primer-binding region

For some modified nucleotide analogs that offer potential biophysical properties, enzymatic recognition may be difficult limiting their application in aptamer selection using conventional SELEX method. But, such modifications can still be used in aptamer selection using a library with one of the primer-binding regions containing the desired chemically-modified nucleotides, and the other region with all four natural nucleotide monomers. This will essentially eliminate the need of an enzymatic recognition of modified nucleotides as a synthetic primer sequence with the chemical modifications can be used during the enrichment steps. But, the protocol may be limited to

DNA-based oligonucleotides. This approach may not fit very well in line to the concept of aptamer selection where it is speculated that the randomized region would promote the formation of target-binding motifs due to high sequence variability. But, one cannot ignore the fact that a part of the primer-binding region also plays a role in the folding pattern of the binding aptamers in majority of the cases. On this ground, aptamer selection using a library with chemically-modified primer-binding regions can be well justified, and can be used as an alternate approach. This method has been successfully applied for generating LNA-modified aptamers.[22,23]

∞-aptamer library

Aptamer selections can also be performed using a library containing infinite range (∞) of modified nucleotides with non-natural structural chemistries of the nucleobase, sugar and phosphate backbone. Libraries containing infinite nucleotides could come with diverse range of chemistries bearing positive charges, hydrophobic groups, phosphorothioates, amino acids etc. that could improve and enhance the target binding interactions and nuclease resistance. Such libraries are mainly suitable for one-step selection protocols.[24-27] ∞-nucleotides can be best positioned in the randomized regions. During synthesis, ∞-nucleotides of all four bases can also be mixed with their natural counterparts.

Aptamer selection using sugar-modified nucleotides

Modifications of sugars will result in libraries with a greater functional diversity and can form stable aptamers with unique shapes. Sugar modifications could allow screening of ligands that bind with greater affinity to their targets than their unmodified counterparts. These unnatural modifications are less likely to be recognized by nucleases, making them more stable in serum. Most frequently, chemical modifications are introduced at the 2′-position of the nucleotide for increased nuclease resistance, and binding affinity. The SELEX evolution of various sugar- modified nucleotide (Fig. 3) containing aptamers against different targets, their binding affinities and stabilities are described below. Table 1 shows an overview of sugar-modified aptamer development in recent years.

5
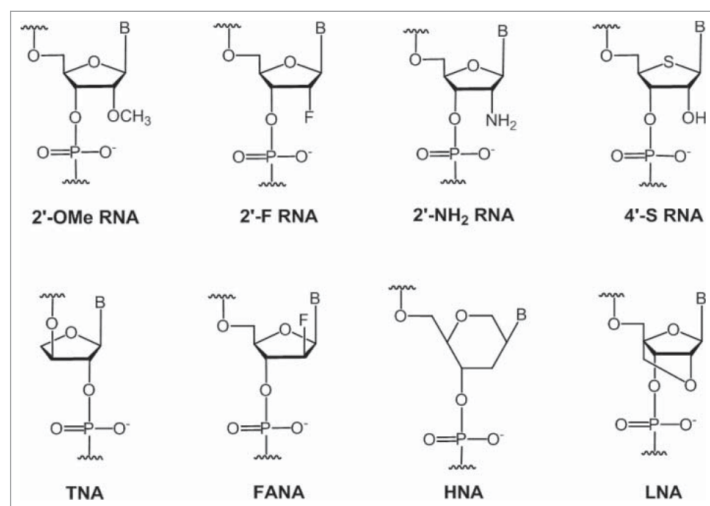
Figure 3. Structures of various sugar-modified nucleotides used in aptamer selection by SELEX methodologies.

2′-Amino (2′-NH₂) modified aptamers

Aptamers have been selected from libraries where the 2′-hydroxyl (2′-OH) group of the pyrimidine is replaced by a NH_2 group. A modified aptamer was screened from a 2′-NH_2-modified RNA library involving 2′-NH_2-UTP and 2′-NH_2-CTP replacing unmodified UTP and CTP during enrichment steps, specific to the human neutrophil elastase using nitrocellulose filter binding assay.[28] The selected aptamers showed high affinity to the target with the equilibrium dissociation constant (K_d) in the range of 7–30 nM which is much lower than that of the unmodified RNA aptamer ($K_d > 1$ μM).[28] These aptamers were found to be very selective to human neutrophil elastase.[28] These modified RNA aptamers also improved nuclease resistance, with an extended half-life (20 h and 9 h in serum and urine respectively) than the unmodified aptamer (degraded in less than 8 and 5 mins in serum and urine respectively).[28] Another 2′-NH_2-pyrimidine-modified RNA aptamer was developed against VPF/VEGF by SELEX process.[29] The affinity was measured through nitrocellulose filter binding assay and one aptamer NX-178 had a K_d of 2.4 nM, with an increased half-life in urine (17 h).[29] Interestingly the introduction of a 2′-O-Methyl (2′-OMe) nucleotide post-SELEX further increased the binding affinity to $K_d = 0.14$ nM and half-life in urine to 31 h.[29] This study suggests that the affinity and nuclease resistance of the RNA modified aptamers developed by SELEX methodology can be further improved by post-SELEX modification. In another study, *Beaudry et al.* developed a 2′-NH_2 pyrimidine-modified ribozyme which was identified by affinity column-based SELEX.[30] The selected aptamer had a half-life of 16 h in human serum, whereas the unmodified counterpart degraded in serum in just 5 mins.[30] *Jellinek et al.* developed a different 2′-NH_2 pyrimidine-modified RNA aptamer, selected through nitrocellulose membrane filter binding assay specific to basic fibroblast growth factor (bFGF).[31] The identified aptamer m21A bound to bFGF with high binding affinity

($K_d = 0.35$ nM).[31] The stability of this aptamer in serum is 100 fold higher than the natural RNA aptamer.[31] In another study, *Bugaut et al.* used an interesting methodology whereby SELEX and dynamic combinatorial chemistry were combined to select conjugated RNA aptamers against MiniTAR by magnetic bead immobilisation using a 2′-NH_2- modified RNA library. The resulting conjugated aptamers developed bound to MiniTAR with high affinity ($K_d = $ 26–47 nM).[32]

2′-fluoro (2′-F) modified aptamers

Ruckman et al. developed an RNA aptamer specific to VEGF$_{165}$ isoform by nitrocellulose filter binding assay using 2′-F modified RNA libraries.[33] Most of the selected 2′-F RNA aptamers had affinities for VEGF$_{165}$ in the pM range (aptamer with the lowest affinities had a K_d value of 2 pM).[33] This candidate aptamer after further chemical modifications has been approved by the US FDA for the treatment of AMD. *Lupold et al.* developed another 2′-F modified RNA aptamer A10, targeting prostate specific membrane antigen (PSMA), cell surface receptors expressed on prostate cancer cells by SELEX using magnetic bead separation-based method.[34] The aptamer A10 bound to PSMA with a K_d of 11.9 nM in LNCaP cells.[34] This was later used to link siRNA to form aptamer-siRNA chimeras that allowed targeted delivery of siRNA to cells expressing PSMA wherein the siRNA reduced the expression of two survival genes, Polo-like kinase 1 and B-cell lymphoma 2.[34,35] In another study, *Biesecker et al.* developed another aptamer against human complement C5 component using 2′-F pyrimidine-modified RNA libraries by nitrocellulose membrane filter binding assay.[36] The aptamers generated had K_d of between 20–40 nM and this was further improved by a second biased SELEX experiment where the generated aptamers had a K_d of 2–5 nM.[36] The aptamers generated were able to bind to human complement C5 component with high affinity and were able to inhibit its activity in human

6

Table 1. Aptamers selected from sugar-modified DNA/RNA libraries and the binding affinity of aptamers to their targets.

Modified nucleotide	Target	Selection Method	Polymerases Used	Binding Affinity (K_d)	Ref.
2′-NH$_2$	Human neutrophil elastase	Nitrocellulose membrane filter binding	T7 RNA polymerase	7–25 nM	28
	VPF/VEGF	Nitrocellulose membrane filter binding	Y639F T7 RNA Polymerase	2.4 nM	29
	mRNAs	Affinity column	T7 RNA polymerase	No K_d ($K_{cat} = 0.04$ min^{-1})	30
	bFGF	Nitrocellulose membrane filter binding	Y639F T7 RNA Polymerase	Apparent $K_d = 0.35$ nM	31
	KGF	Nitrocellulose membrane filter binding	Y639F T7 RNA Polymerase	0.4 nM	41
	IFN-γ	Nitrocellulose membrane filter binding	Y639F T7 RNA Polymerase	1.8 nM	40
	MiniTAR	Magnetic bead immobilisation	DNA polymerase	26–47 nM	32
2′-F	VEGF$_{165}$	Nitrocellulose membrane filter binding	T7 RNA Polymerase	2 pM	33
	PSMA	Magnetic bead immobilisation	Y639F T7 RNA Polymerase	No K_d (IC$_{50}$ = 27 nM) K_i = 11.9 nM	34, 35
	Human complement C5 component	Nitrocellulose membrane filter binding	T7 RNA polymerase	2–5 nM	36
	KGF	Nitrocellulose membrane filter binding	Y639F T7 RNA Polymerase	14F K_d = 0.3–3 pM	41
	Factor IX	Nitrocellulose membrane filter binding	AMV Reverse Transcriptase	K_d = 0.64 nM (9.3)	37,38
	Factor IXa			K_d = 364 pM (Clone 9D-6)	
	IFN-γ	Nitrocellulose membrane filter binding	Y639F T7 RNA Polymerase	106 nM	40
	IFN-γ	Nitrocellulose membrane filter binding	Y639F T7 RNA Polymerase	6.8 nM	40
	Cancer Antigen 125	Magnetic bead immobilisation	Y639F T7 RNA Polymerase	CA125.1 K_d = 4.13 nM	39
2′-OMe	VEGF	Electrophoretic mobility shift assay	Y639F/H784A/K378R T7 RNA Polymerase	2 nM	42
	Interleukin-23 and thrombin	Nitrocellulose membrane filter binding	Y639F/H784A/K378R T7 RNA Polymerase	Clone A5 K_d = 8.4 nM Clone B4 K_d = 26 nM	43
	Tissue factor pathway inhibitor	Nitrocellulose membrane filter binding	Not Specified	ARC17480 K_d = 2.8 nM ARC19499 IC$_{50}$ = 17.9 nM	44
4′-S	Human thrombin	Nitrocellulose membrane filter binding	T7 RNA polymerase	4.7 nM	50
2′-FANA	HIV-1 reverse transcriptase	Electrophoretic mobility shift assay	Taq polymerase	4 pM	51
HNA	TAR	Magnetic bead immobilisation	Pol6G12	28–67 nM	52
	HIV Hen egg lysozyme	Magnetic bead immobilisation	Pol6G12	HNA11 K_d = 107 nM HNA19 K_d = 141 nM	52
TNA	Human thrombin	Capillary electrophoresis	Therminator DNA polymerase	200–900 nM	53
BNA/LNA	Human thrombin	Capillary electrophoresis	an enzyme mix of KOD Dash and KOD mutant DNA polymerases	0.26–27 nM	23,70
	CD73	Affinity column	KOD XL	3.7 nM	22
Spiegelmers	D-adenosine	Affinity column	T7 polymerase	1.7 μM	71
	L-arginine	Affinity column	T7 polymerase	Bound to L-arginine with K_d = 129 μM	72
	HIV-1 Tat protein			Bound to HIV-1 tat protein with K_d=26 μM	
	D-vasopressin	Electrophoretic mobility shift assay	T7 polymerase	0.9 μM	73
	D-staphylococcal enterotoxin B	Electrophoretic mobility shift assay	Taq DNA polymerase	200 nM	74
	Nociceptin/ orphanin FQ	Affinity column	T7 polymerase	L-NOX2149 K_d = 0.3 μM L-NOX2137 K_d = 0.7 μM	77
	D-gonadotropin-releasing hormone	Affinity column	T7 polymerase	L-S42 K_d = 45 nM L-A10 K_d not specified (IC$_{50}$ = 200 nM)	78
	Ghrelin	Electrophoretic mobility shift assay	T7 polymerase	44.4 nM	79,80
	Calcitonin gene-related peptide	Affinity column	T7 polymerase	Apparent K_d = 2.5 nM	75
	Substance P	Affinity column	T7 polymerase	40 nM	76

serum with high stability.[36] *Rusconi et al.* developed 2′-F modified aptamers for Factor II, Factor VII, Factor IX and Factor X through nitrocellulose membrane filter binding assay.[37,38] By this approach a RNA aptamer was identified against Factor IXa with the highest affinity (K_d of 0.64 nM), and was a potent anticoagulant.[38] Another aptamer generated against Factor IX had a K_d of 364 pM.[37] *Lamberti et al.* developed an aptamer against Cancer Antigen 125 by magnetic bead immobilisation using a 2′-F

modified RNA library.[39] Of the two RNA aptamers isolated, CA125.1 had a K_d of 4.15 nM and can be developed further for use as a diagnostic tool.[39]

Comparison of 2′-F and 2′-NH$_2$ modifications

Various studies indicate that both 2′-F and 2′-NH$_2$ modifications increase the nuclease resistance and binding affinity of

aptamers toward their targets. There are a few studies comparing the two modifications to validate which modification was more powerful. *Kubik et al.* reported an aptamer that bound to interferon-gamma (IFN-γ) which was screened from RNA libraries modified at the 2′-position of pyrimidine nucleotides with F, NH$_2$, or a mixture of F and NH$_2$ (2′-F/NH$_2$) groups using nitrocellulose filter binding assay.[40] The binding affinity of the modified aptamers to IFN-γ differed depending on the sugar modifications.[40] 2′-NH$_2$ modified aptamers had the highest binding affinity to IFN-γ with a K$_d$ of 1.8 nM, whereas the 2′-F modified aptamers with the highest binding affinity had a K$_d$ of 6.8 nM and the aptamers containing 2′-F/NH$_2$ mixture had a K$_d$ of 106 nM.[40] The half-lives of these aptamers were measured through their stability in human serum, where 2′-NH$_2$ modified aptamer had a half-life of 80 h, 2′-F modified aptamers had a half-life of 6 h and the mixed 2′F/NH$_2$ modified aptamers had a half-life of 48 h.[40] However, all three were more nuclease-resistant than the unmodified aptamer which had a half-life of 20 s in human serum.[40] 2′-NH$_2$ modified aptamers seemed to confer the highest binding affinity to IFN-γ and nuclease resistance in human serum.[40] 2′-NH$_2$ aptamer also inhibited IFN-γ binding to its receptor on A549 human lung carcinoma cells with an ID$_{50}$ of 10 nM.[40] Another study by *Pagratis et al.* suggested that 2′-F modified aptamers improved the binding affinity compared to the 2′-NH$_2$ modified aptamers.[41] In this study, aptamers have been selected successfully from libraries containing 2′-NH$_2$ and 2′-F modified pyrimidines by nitrocellulose filter binding assay and compared the affinities of the two different aptamer variants to keratinocyte growth factor (KGF).[41] The best 2′-F modified aptamer 14F bound to KGF with a higher affinity (K$_d$ = 0.3–3 pM) than the best 2′-NH$_2$ modified aptamer (K$_d$ = 0.4 nM).[41] 2′-F modified aptamers (6F and 14F) inhibited KGF binding to their receptor in PC3 cells with a K$_i$ of 100 and 200 pM respectively and had a much higher inhibitory activity than the 2′-NH$_2$ modified variants, 14N and 29N (K$_i$ = 1.4 nM).[41] Although if 2′-F or 2′-NH$_2$ modification is more powerful is arguable the use of 2′-NH$_2$ modifications result in problems in solid-phase synthesis and the ribose sugar adopting an unfavorable conformation which has resulted in the reduced use of 2′-NH$_2$.

2′-OMe modifications:

2′-OMe modification involves the replacement of the 2′-OH group of the nucleotide with a methoxy group. 2′-OMe is a common sugar modification that has been used post-SELEX to generate aptamers with high nuclease resistance. *Burmeister et al.* developed an aptamer against VEGF from oligonucleotide libraries modified with 2′-OMe adenine and guanines by electrophoretic mobility shift assay.[42] The selected aptamer candidate, ARC245 had a K$_d$ of 2 nM, however this is lower than Macugen, the FDA approved aptamer drug targeting VEGF (K$_d$ = 50 pM).[42] ARC245 showed inhibition of VEGF binding to VEGF receptor in 293 cells at 10 nM concentrations and was also highly stable in serum for up to 96 h.[42] *Burmeister et al.* also screened aptamers comprising 2′-OMe pyrimidines by the SELEX process to multiple protein targets including thrombin and interleukin-23, using proteins immobilized on a 96-well plate and nitrocellulose filter binding assay.[43] The identified

aptamers targeting interleukin-23 had a K$_d$ of 8.4 nM while the aptamer targeting thrombin had a K$_d$ of 26 nM.[43] *Waters et al.* developed 2′-OMe modified aptamers, ARC19499 and ARC17480 against tissue factor pathway inhibitor by nitrocellulose filter binding using a 2′-OMe modified library.[44] ARC17480 bound to the tissue factor pathway inhibitor with a K$_d$ of 2.8 nM, however as ARC19499 was not viable in experiments requiring radiolabelling a competition-binding experiment showed that ARC19499 competed with radiolabelled ARC17480 with an IC$_{50}$ of 17.9 nM.[44] 2′-OMe incorporation into libraries and using these modified libraries for SELEX is hard due to lack of enzymes that are capable of recognizing these 2′-OMe modified bases. However, recently polymersases have been evolved that accept 2′-OMe modified triphosphates which would allow generation of additional 2′-OMe modified aptamers.[21,45-49]

4′-Thio (4′-S) modifications

4′-S modifications had a sulfur atom at the 4′-position of the sugar moiety. *Kato et al.* developed a 4′-S modified RNA aptamer that bound to human α-thrombin by nitrocellulose filter binding assay.[50] In the presence of RNase, the stability of the aptamer candidate, thioRNA59, had a half-life of 1174 mins and was stable even after 12 h of incubation, which was 50 times greater than that of the corresponding natural RNA (completely degraded in the presence of RNase A in 3 h), and it also showed high binding affinity to thrombin with a K$_d$ of 4.7 nM.[50]

2′-fluoroarabino nucleic acid (2′-FANA) modified aptamers

Very recently, *Alves Ferreira-Bravo et al.* reported a 2′-FANA aptamer to human immunodeficiency virus-1 (HIV-1) reverse transcriptase.[51] This 2′-FANA aptamer was isolated from a 2′-FANA modified DNA pool through SELEX using electrophoretic mobility shift assay.[51] The developed 2′-FANA modified DNA aptamer, FA$_1$ had a K$_d$ value of 4 pM and showed greater resistance to nucleases.[51]

1,5-anhydro hexitol nucleic acid (HNA) modified aptamers

Pinheiro et al. developed HNA aptamers against HIV-1 transactivation responsive element (TAR) and hen egg lysozyme through SELEX using magnetic bead-based separation.[52] HNA aptamer, T5-S8-7 bound to TAR with high specificity and had a K$_d$ of 28–67 nM.[52] HNA aptamers that bound specifically to hen egg lysozyme had a K$_d$ of 107 to 141 nM as determined by surface plasmon resonance.[52]

Threose nucleic acid (TNA) modified aptamers

Yu et al. selected a TNA modified aptamer against thrombin using affinity column and capillary electrophoresis.[53,54] TNA backbone is nuclease-resistant as TNA remained undigested even after 72 h of incubation with a pure nuclease unlike DNA and RNA which exhibit half-lives of 30 mins and less than 10s respectively.[54] The developed TNA aptamers to thrombin had a K$_d$ in the range of 200–900 nM.[53] A new manganese-

8

independent TNA polymerase was evolved using droplet-based optical polymerase sorting which can be used in TNA aptamer selection protocol.[55]

Locked nucleic acid (LNA) modified aptamers

In LNA, the sugar ring is locked by a $2'O$, $4'C$ methylene linkage and is conformationally restricted adopting a C3'-endo conformation.[56-61] Toward the development of LNA-modified aptamers, *Veedu et al.* and others have extensively investigated the enzymatic recognition capabilities of LNA-nucleotides.[58-68] DNA aptamers containing LNA (BNA/LNA) nucleotides were developed against human thrombin using capillary electrophoresis SELEX. BNA/LNA-modified nucleotides were introduced in the primer-binding region of the library, and after selection the selected candidates were enriched by PCR using the LNA-modified primer sequence to regenerate the selected aptamer candidates using KOD polymerase.[23,69] Many aptamers showed K_d values in the low nanomolar range.[23,70] In another study, *Elle et al.* generated LNA-modified aptamers against CD73 immobilized on anti-His tag plates.[22] A LNA-modified DNA aptamer NAC6772 showed high binding affinity to CD73 through surface plasmon resonance experiment with a K_d of 3.54 nM and inhibited the CD73 activity by 85%.[22]

Spiegelmers

Spiegelmers are mirror images of the natural aptamers in which the D-ribose (the natural ribose) are replaced with the unnatural L-ribose. Spiegelmers prevent enzymatic degradation as the chiral form of the nucleic acid (the L-form) is unnatural and is not recognized by nucleases. However, the L-form of the nucleic acid like their D-form natural counter parts can bind to the target with high affinity and will not trigger the immune response. Similar to the other sugar modifications described above, spiegelmers can be enriched by T7 RNA polymerases. *Klussmann et al.* generated one of the first spiegelmers through SELEX against the naturally occurring D-adenosine.[71] The high affinity L-RNA aptamers against D-adenosine were isolated through affinity column and had a K_d of 1.7 μM which was comparable to the affinity displayed by the D-RNA aptamers.[71] *Nolte et al.* reported another spiegelmer that bound to L-arginine that could also bind to a short peptide that contains an arginine-rich region in HIV-1 Tat protein.[72] The aptamer, L-R16c was isolated through affinity column based SELEX.[72] L-R16c bound to L-arginine with a K_d of 129 μM and to the Tat protein with a K_d of 26 μM.[72] L-R16c was very stable in serum and did not degrade even after 60 h of incubation.[72] In another study, spiegelmers were selected against D-vasopressin and D-staphylococcal enterotoxin B through SELEX using electrophoretic mobility shift assay.[73] The L-DNA aptamers targeting D-vasopressin showed no degradation with exo- and endonucleases and showed high binding affinity for D-vasopressin with a K_d of 0.9 μM.[73] The corresponding D-aptamer degraded in 10 s while the L-aptamer showed no degradation even after 10 days incubation with exo- and endonucleases and 7 days in serum.[73] A DNA spiegelmer targeting D-staphylococcal enterotoxin B, B12b10 had a K_d of 200 nM.[74] *Vater et al.* isolated a

RNA spiegelmer against migraine associated calcitonin gene-related peptide through SELEX using affinity columns.[75] The developed RNA spiegelmer STAR-F12 bound to calcitonin gene-related peptide with a K_d of 2.5 nM and inhibits its activity.[75] In another study, a RNA spiegelmer targeting Substance P was generated through SELEX using affinity column.[76] The developed L-RNA aptamer, SUP-A-004, which was further truncated and the resulting spiegelmer bound to Substance P with a K_d of 40 nM.[76] SUP-A-004 inhibited L-substance P mediated Ca^{2+} release in AR42J pancreatic cells.[76] *Faulhammer et al.*, in another study reported the development of L-RNA aptamers NOX2149 and NOX2137 against Nociceptin/orphanin FQ through SELEX using affinity column.[77] The L-NOX2149 and L-NOX2137 bound to the nociception/orphanin FQ with a K_d of 0.3 μM and 0.7 μM respectively which were similar to the binding affinity to their D-aptamer counterparts.[77] However L-aptamers had the advantage of being more stable in serum.[77] In another study, L-DNA/RNA aptamers that bind to D-gonadotropin-releasing hormone with high affinity and specificity were isolated out of L-RNA and DNA libraries through SELEX using affinity column.[78] The L-DNA aptamer, S42 bound to gonadotropin-releasing hormone with a K_d of 45 nM which is similar to that of the D-DNA aptamer and the IC_{50} was 50 nM.[78] The D-RNA aptamer, A10 bound with K_d of 55 nM, however the K_d of L-RNA aptamer could not be obtained.[78] Both the DNA and RNA spiegelmers bound to gonadotropin-releasing hormones and inhibited their binding to their receptor in Chinese hamster ovary cells and there was no immune response produced in zimmermann rabbits.[78] *Helming et al.* reported L-RNA aptamers targeting ghrelin through SELEX using electrophoretic mobility shift assay.[79,80] L-NOX-B11, a L-RNA aptamer was isolated and bound to ghrelin with high affinity with a K_d of 44.4 nM.[80] L-NOX-B11 inhibited ghrelin from binding to its receptor with an IC_{50} value of 5 nM in Chinese hamster ovary cells.[79,80] NOXXON Pharma have developed many spiegelmers against various targets and a few of the spiegelmers are in various stages of the preclinical and clinical trials, two of which are described in a recent review by *Sundaram et al.* NOX-A12 is a spiegelmer that bound to and inhibits stroma cell-derived factor-1.[81] After completion of Phase I and Phase IIa trials of NOX-A12, Phase 3 trials have been planned for multiple myeloma.[81] Also, Phase 2b/3 trials have been planned for the same candidate against glioblastoma.[81] Phase 2a clinical trials have been completed for another spiegelmer, NOX-E36, targeting monocyte chemoattractant- protein 1.[81] Several other candidates are currently in different stages of clinical investigation.[82] NOX-D20 is another spiegelmer that binds to anaphylatoxin C5a with picomolar affinity and is being considered for preclinical and clinical development.[83] *Wang et al.* has described the generation of a chemically-synthesized D-amino acid polymerase that is capable of recognizing and catalyzing transcription and polymerisation of an L-DNA template.[84] This polymerase could result in generation of new speigelmers in the future.[84]

Aptamer selection using modified nucleotide bases

Incorporating chemical modification to the nucleotide bases could increase the stability and target-binding affinity of

aptamers. A number of researchers have succeeded in generating aptamers with base-modified nucleotides (Fig. 4), some of which are in preclinical stages. Various base modifications are incorporated into the nucleic acid library and in many cases have been able to be amplified using family B-DNA polymerases.[85] Table 2 provides a summary of base-modified aptamer development. There is also a new method called click-SELEX which is used to generate base-modified libraries by replacing the thymidines with C5-ethynyl-2′-deoxyuridine which is then further modified through click reaction with copper(I)-catalyzed alkyne-azide cycloaddition.[86-91] The library is then used in selection experiments to evolve modified aptamers.[86-91] This is a powerful method that allows generation of modified aptamers with new chemical modifications without problems caused by lack of enzymatic recognition as seen with the addition of a cluster of oligomannose glycans.[86-91] This will allow targeting of many molecules and epitopes that is currently not possible with standard SELEX.[86-91] Addition of new nucleotides and/or unnatural base pairs to the libraries and using these libraries for aptamer selection allows generation of modified
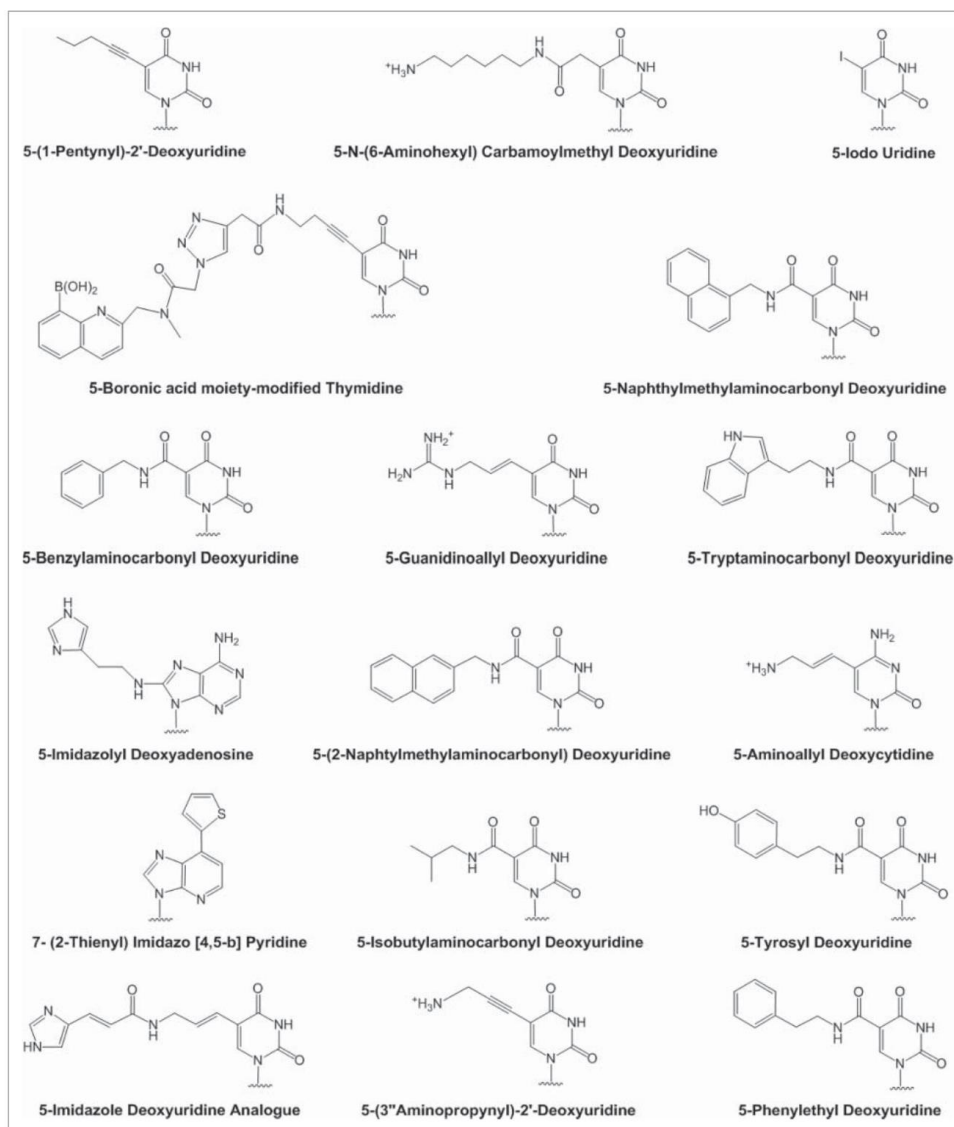
Figure 4. Structures of various base-modified nucleotides used in aptamer selection by SELEX methodologies.

Table 2. Aptamers selected from base-modified DNA/RNA libraries and the binding affinity of aptamers to their targets.

Modified nucleotide	Target	Selection Method	Polymerases Used	Binding affinity (K_d)	Ref.
5-pentynyl-dU	Human thrombin	Affinity column	Vent DNA Polymerase	400 nM	96
5-N-(6-aminohexyl) carbamoylmethyl-dU	Thalidomide (T5N and T5-IB)	Streptavidin-sepharose gel	*KOD Dash DNA polymerase*	T5N K_d= 113 μM T5-1B K_d= 133 μM	100
5-boronic acid-dT	Fibrinogen	Magnetic bead immobilisation	Taq DNA Polymerase	3–30 nM	102
5-iodouridine	HIV-1 Rev protein.	Nitrocellulose membrane filter binding	T7 RNA polymerase	0.8 nM	97
5-(3'-aminopropynyl)-2'-dU	ATP (Sequence 409)	Capillary electrophoresis	Vent DNA polymerase	6 nM	98
5-benzylaminocarbonyl dU	Plasminogen Activator Inhibitor	Magnetic bead immobilisation	*KOD DNA Polymerase*	$\leq$30 nM	107
5-isobutylaminocarbonyl –dU 5-tryptaminocarbonyl -dU 5-naphthylmethylaminocarbonyl-dU	Human mobility group -1 Fractalkine Human protein targets			$\leq$30 nM $\leq$30 nM $\leq$30 nM	
5-(3-aminoallyl)-dC 5-guanidinoallyl-dU, 5-imidazolyl-dA	RNA	Magnetic bead immobilisation	Vent (exo -) DNA Polymerase	K_d not specified (DNAzyme12–91 K_{obs} = 0.06 min^{-1} DNAzyme 16.2–11 K_{cat}= 1.4–1.5 min^{-1})	106
7-(2-thienyl)imidazo[4,5-b]pyridine	VEGF$_{165}$ IFN-γ	Magnetic bead immobilisation	Accu Prime Pfx DNA Polymerase	0.65 pM 0.038 nM	105
5-tyrosyl-dU	Clostridium difficile binary toxins A and B	Magnetic bead immobilisation	KOD EX DNA polymerase	1.4 nM (Toxin A) 0.31 nM (Toxin B)	109
5-(2-naphthylmethylaminocarbonyl)-dU				9.2 nM (Toxin A) 0.25 nM (Toxin B)	
5-phenylethyl-dU				13.1 nM (Toxin A) 0.27 nM (Toxin B)	
5-benzylaminocarbonyl-dU 5-naphthylmethylaminocarbonyl-dU 5-tryptaminocarbonyl-dU				5 nM (Toxin B) 0.43 nM (Toxin B) 1.7 nM (Toxin A) 0.45 nM (Toxin B)	
5-carboxamide-modified-dU	Tumor necrosis factor receptor super family member 9 (6_a and 6_d)	Magnetic bead immobilisation	Deep Vent and KOD XL DNA Polymerases	6_a K_d= 6 nM 6_d K_d= 4 nM	103
5-imidazole-dU analog	RNA	Affinity column	DNA Polymerase	K_d not specified (DNAzyme 16.2–11 K_{cat}= 1.4–1.5 min^{-1}	104

aptamers with greater sequence and functional diversity.[92-95] *Zhang et al.* has shown that addition of new nucleotides Z and P allowed generation of sequences that had better binding affinity to the target molecule indicating that new nucleotides are viable in the library and can show higher binding affinity than natural bases in some cases.[92]

Uridine modifications

Latham et al. developed a modified aptamer containing 5-(1-pentynyl)-2'-deoxyuridine against thrombin by affinity column.[96] The affinity of the selected aptamer pool was 400 nM.[96] This was one of the first examples of using a base-modified nucleic acid library for screening aptamers. In another study, *Jensen et al.* developed RNA aptamers from a random RNA library containing photoreactive chromophore 5-iodouridine using crosslinking SELEX.[97] The selected RNA aptamers bound and also cross-linked to the target with UV irradiation.[97] These modified aptamers had high affinity with a K_d of 0.8 nM.[97] *Battersby et al.* isolated another base-modified aptamer containing 5-aminopropynyl-deoxyuridine against ATP by electrophoretic mobility shift assay.[98,99] One of the selected aptamer candidate, 409 was found to bind ATP with higher affinity (K_d = 6 μM) than their unmodified counterparts.[98,99] *Shoji et al.* reported another base-modified aptamer with 5'-N-6-NH$_2$-hexyl carbamoylmethyl dU.[100,101] The modified library was used to screen aptamers against thalidomide using streptavidin-sepharose

gel.[100] Surface plasmon resonance showed that the selected base-modified aptamer T5N and T51B had a K_d of 113 μM and 133 μM respectively.[100] *Li et al.* selected an aptamer containing boronic acid-modified thymidine against fibrinogen using magnetic bead immobilization-based SELEX.[102] The resulting modified aptamers bound to fibrinogen with high affinity compared to that of the unmodified aptamers (K_d = 3–30 nM compared to K_d = 450 nM).[102] *Vaught et al.* selected a DNA aptamer against tumor necrosis factor receptor super family 9 from a library possessing 5-amide-modified deoxyuridine via a magnetic bead-based SELEX method.[103] Six 5-position modified 2'-dUTP derivatives were used.[103] Two of the modified DNA aptamers developed showed high affinity (K_d = 6 nM and 4 nM respectively) compared to an unmodified RNA aptamer that has been previously reported (K_d = 40 nM).[103]

Imidazole modifications

Aptamers can also act as DNA enzymes which are catalytic nucleic acids and modified libraries have been used to select such aptamers. *Santoro et al.* developed a modified DNAzyme aptamer via affinity column from a modified library containing C5-imidazole-functionalised dU.[104] The isolated DNAzyme was one of the smallest nucleic acid enzymes, which showed multiple turnovers in the presence of millimolar concentrations of Zn^{2+}, and a catalytic rate of 1.4–1.5 min^{-1} for cleavage.[104] *Kimoto et al.* reported the selection of 7-(2-thienyl)imidazole
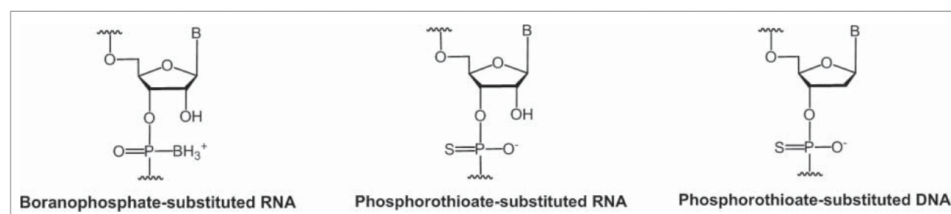
Figure 5. Structures of various phosphate-modified nucleotides used in aptamer selection by SELEX methodologies.

[4,5-*b*]pyridine modified DNA aptamers against $VEGF_{165}$ and IFN-γ by magnetic bead-based SELEX.[105] The isolated DNA aptamers bound to $VEGF_{165}$ and IFN-γ with 100 fold higher affinity than their natural counterparts with K_d values of 0.64 pM and 0.038 nM respectively.[105] *Hollenstein et al.* reported the development of Dz12–91, a modified DNAzyme containing imidazole, ammonium and guanidinium groups. Dz12–91 was isolated through SELEX using magnetic streptavidin particles and cleaves all RNA sequence independently of M^{2+} with a K_{obs} of 0.06 min^{-1}.[106]

Slow off-rate modified aptamers (SOMAmers)

Another class of aptamers with improved binding properties through base-modifications that result in slow dissociation rates called SOMAmers. There are many SOMAmer modifications that are used to generate aptamers to difficult protein targets.[107] The affinities of the SOMAmers are consistently in the nanomolar range to their targets and show high nuclease resistance.[107] Various proteins have been used as targets to generate SOMAmers.[107,108] In many SOMAmers, the modifications are introduced at the 5-position of the uridine nucleotide.[107] *Gold et al.* described the development of SOMAmers against more than 800 targets using multiplex SOMAmer affinity assay system from base-modified libraries including 5-benzylaminocarbonyl, 5-naphthylmethylaminocarbonyl, 5-tryptaminocarbonyl, 5-isobutylaminocarbonyl, 5-tyrosyl, 5-phenylethyl, and 5-guanidinoallyl.[107,109] *Ochsner et al.* reported development of SOMAmers against toxins A, B and binary toxins using 5-benzylaminocarbonyl, 5-naphthylmethylaminocarbonyl, 5-tryptaminocarbonyl, 5-phenylethyl-1-aminocarbonyl, 5-tyrosylaminocarbonyl or 5-(2-naphthylmethyl)aminocarbonyl-modified uridine containing library using magnetic bead-based SELEX.[109] Most of the modified aptamers bound to the toxin A and B with high binding affinity with the K_d in the nanomolar range.[109] For example, the selected 5-tryptaminocarbonyl dU modified aptamer showed a K_d of 1.7 nM to Toxin A and 0.45 nM for Toxin B.[109]

Aptamer selection using phosphate modified nucleotides

A few phosphate-modified aptamers (Fig. 5) were reported as substrates of T7 RNA polymerase that could accept the triphosphate analogs of the modified phosphate moiety, mainly phosphorothioate and boranophosphates. Table 3 provides a summary of base-modified aptamer development.

Phosphorothioate modifications

Through nitrocellulose membrane filter binding, phosphothioate-modifed RNA aptamer 11–20 was isolated that bound to bFGF with a K_d of 1.8 nM which was similar to the K_d of all RNA aptamers ($K_d = 0.19$ nM and 0.49 nM).[110] K_d of another bFGF aptamer containing 2'-NH_2 pyrimidines was 0.35 nM, which was also comparable to the unmodified RNA aptamers.[110] These aptamers also bound to other bFGF members in the family, but not to the unrelated targets and were therefore "semi-specific" for the FGF family members.[110] Another phosphorothioate DNA aptamer was selected against nuclear factor for human interleukin 6 which was nuclease-resistant to DNase 1 enzyme at the point of modifications.[111,112] This modified DNA aptamer was selected through nitrocellulose filter binding from a library with thiophosphate backbone substitution at the thymidine positions and the modified aptamer was found to bind with stoichemistry of two protein dimers/duplex unlike the unmodified aptamer which bound with one protein dimer/duplex stoichemistry.[112] The binding constant (K_{obs}) measured by fluorescence anisotropy was 2 nM

Table 3. Aptamers selected from phosphate-modified DNA/RNA libraries and the binding affinity of aptamers to their targets.

Modified nucleotide	Target	Selection Method	Polymerases Used	Binding affinity (K_d)	Ref.
Boranophosphate-5'-(α-P-borano)-G 5'-(α-P-borano)-U	ATP	Affinity column	T7 RNA Polymerase	Not Specified	113
Phosphorothioate-modified DNA	bFGF	Nitrocellulose membrane filter binding	Taq polymerase	1.8 nM	110
Phosphorothioate-dA	Nuclear factor for human Interleukin6	Nitrocellulose membrane filter binding	Taq DNA Polymerase	K_d not specified ($K_{obs} = 2$ nM)	112
Phosphorothioate-dA	Human Nuclear factor-kappa B RelA (p65)	Nitrocellulose membrane filter binding	Taq DNA Polymerase	4.8 nM	111
	Human Nuclear Factor-kappa B RelA (p50)			0.8 nM	

12

for a 66-mer.[112] Another phosphorothioate aptamer was selected against Nuclear Factor kappa B proteins Rel A (p65) and p50 and the selected aptamer had a K_d value of 4.8 nM and 0.8 nM respectively, which was comparable to the unmodified aptamer ($K_d = 4.77$ nM).[111]

Boranophosphate modification

Boronated nucleotide analog modifications of guanosine ($5'(\alpha$-P-borano)triphosphate) for GTP and uridine ($5'(\alpha$-P-borano) triphosphate) for UTP were also introduced into general libraries to select modified aptamers that bind ATP through affinity matrix containing C8-linked ATP agarose.[113] Each of the 2 modifications were tolerated in the backbone alone, however both modifications in one backbone were not tolerated.[113]

Conclusions and future perspectives

Aptamers are nucleic acid ligands that are generally developed through SELEX and bind to their targets with high affinity and specificity. Aptamers can be used therapeutically, diagnostically, as molecular beacons or as DNAzymes in various diseases. Macugen is a therapeutic aptamer approved by the US FDA for the treatment of AMD. One of the major disadvantages of aptamers composed of natural nucleotides is their rapid degradation *in vivo*. To overcome this obstacle, chemically-modified aptamers have been developed through SELEX using modified-oligonucleotide libraries. There are many potential chemically-modified nucleotides with excellent properties, however many of them cannot be used in the SELEX processes to develop aptamers mainly because of their very limited enzymatic recognition capabilities which are required for enrichment steps. As reviewed here, it is very promising to see the development of chemically-modified aptamers using several sugar, base and phosphate-modified nucleotides. It is also very encouraging to note the development of novel engineered polymerases capable of recognizing a specific modified nucleotide. Recent developments in one-step-based selection methodologies further offer tremendous hope for developing aptamers containing modified aptamers with limited enzymatic recognition capabilities.

Disclosure of potential conflicts of interest

No potential conflicts of interest were disclosed.

Acknowledgment

ORCID

Farhana Lipi http://orcid.org/0000-0002-0467-6409

References

1. Keefe AD, Pai S, Ellington A. Aptamers as therapeutics. Nat Rev Drug Discov 2010; 9:537-50; PMID:20592747; http://dx.doi.org/10.1038/nrd3141
2. Nimjee SM, Rusconi CP, Sullenger BA. Aptamers: an emerging class of therapeutics. Annu Rev Med 2005; 56:555-83; PMID:15660527; http://dx.doi.org/10.1146/annurev.med.56.062904.144915
3. Famulok M, Hartig JS, Mayer G. Functional aptamers and aptazymes in biotechnology, diagnostics, and therapy. Chem Rev 2007; 107:3715-43; PMID:17715981; http://dx.doi.org/10.1021/cr0306743
4. Veedu RN. Editorial (Thematic Issue: Medicinal Chemistry of Aptamers). Curr Top Med Chem 2015; 15:1065; PMID:25866280; http://dx.doi.org/10.2174/156802661566615041316 1707
5. Jayasena SD. Aptamers: an emerging class of molecules that rival antibodies in diagnostics. Clin Chem 1999; 45:1628-50; PMID:10471678
6. Stoltenburg R, Reinemann C, Strehlitz B. SELEX—a (r) evolutionary method to generate high-affinity nucleic acid ligands. Biomol Eng 2007; 24:381-403; PMID:17627883; http://dx.doi.org/10.1016/j.bioeng.2007.06.001
7. Gopinath SCB. Methods developed for SELEX. Anal Bioanal Chem 2007; 387:171-82; PMID:17072603; http://dx.doi.org/10.1007/s00216-006-0826-2
8. Demarest SJ, Glaser SM. Antibody therapeutics, antibody engineering, and the merits of protein stability. Curr Opin Drug Discov Devel 2008; 11:675-87; PMID:18729019
9. Ng EWM, Shima DT, Calias P, Cunningham ET, Guyer DR, Adamis AP. Pegaptanib, a targeted anti-VEGF aptamer for ocular vascular disease. Nat Rev Drug Discov 2006; 5:123-32; PMID:16518379; http://dx.doi.org/10.1038/nrd1955
10. Group MDRS. A phase II randomized double-masked trial of pegaptanib, an anti–vascular endothelial growth factor aptamer, for diabetic macular edema. Ophthalmology 2005; 112:1747-57; PMID:16154196; http://dx.doi.org/10.1016/j.ophtha.2005.06.007
11. Kanwar JR, Roy K, Maremanda NG, Subramanian K, Veedu RN, Bawa R, Kanwar RK. Nucleic acid-based aptamers: applications, development and clinical trials. Curr Med Chem 2015; 22:2539-57; PMID:25723512; http://dx.doi.org/10.2174/0929867322666150227144909
12. Zuker M. Mfold web server for nucleic acid folding and hybridization prediction. Nucleic Acids Res 2003; 31:3406-15; PMID:12824337; http://dx.doi.org/10.1093/nar/gkg595
13. Hofacker IL. Vienna RNA secondary structure server. Nucleic Acids Res 2003; 31:3429-31; PMID:12824340; http://dx.doi.org/10.1093/nar/gkg599
14. Diafa S, Hollenstein M. Generation of aptamers with an expanded chemical repertoire. Molecules 2015; 20:16643-71; PMID:26389865; http://dx.doi.org/10.3390/molecules200916643
15. Dellafiore MA, Montserrat JM, Iribarren AM. Modified Nucleoside Triphosphates for In-vitro Selection Techniques. Front Chem 2016; 4:18; PMID:27200340; http://dx.doi.org/10.3389/fchem.2016.00018
16. Kong D, Yeung W, Hili R. Generation of Synthetic Copolymer Libraries by Combinatorial Assembly on Nucleic Acid Templates. ACS Comb Sci 2016; 18:355-70; PMID:27275512; http://dx.doi.org/10.1021/acscombsci.6b00059
17. Lapa SA, Chudinov AV, Timofeev EN. The toolbox for modified aptamers. Mol Biotechnol 2016; 58:79-92; PMID:26607475; http://dx.doi.org/10.1007/s12033-015-9907-9
18. Rohloff JC, Gelinas AD, Jarvis TC, Ochsner UA, Schneider DJ, Gold L, Janjic N. Nucleic acid ligands with protein-like side chains: modified aptamers and their use as diagnostic and therapeutic agents. Mol Ther Nucleic Acids 2014; 3:e201; PMID:25291143; http://dx.doi.org/10.1038/mtna.2014.49
19. Lauridsen LH, Rothnagel JA, Veedu RN. Enzymatic recognition of $2'$−modified ribonucleoside $5'$−triphosphates: Towards the evolution of versatile aptamers. ChemBioChem 2012; 13:19-25; PMID:22162282; http://dx.doi.org/10.1002/cbic.201100648
20. Loakes D, Holliger P. Polymerase engineering: towards the encoded synthesis of unnatural biopolymers. Chem Commun 2009:4619-31; PMID:19641798; http://dx.doi.org/10.1039/b903307f

21. Aschenbrenner J, Marx A. Direct and site-specific quantification of RNA 2′-O-methylation by PCR with an engineered DNA polymerase. Nucleic Acids Res 2016; 44:3495-502; PMID:27016740; http://dx.doi.org/10.1093/nar/gkw200

22. Elle IC, Karlsen KK, Terp MG, Larsen N, Nielsen R, Derbyshire N, Mandrup S, Ditzel HJ, Wengel J. Selection of LNA-containing DNA aptamers against recombinant human CD73. Mol Biosyst 2015; 11:1260-70; PMID:25720604; http://dx.doi.org/10.1039/C5MB00045A

23. Kasahara Y, Irisawa Y, Ozaki H, Obika S, Kuwahara M. 2′, 4′-BNA/LNA aptamers: CE-SELEX using a DNA-based library of full-length 2′-O, 4′-C-methylene-bridged/linked bicyclic ribonucleotides. Bioorg Med Chem Lett 2013; 23:1288-92; PMID:23374873; http://dx.doi.org/10.1016/j.bmcl.2012.12.093

24. Lauridsen LH, Shamaileh HA, Edwards SL, Taran E, Veedu RN. Rapid one-step selection method for generating nucleic acid aptamers: Development of a DNA aptamer against α-bungarotoxin. PLoS One 2012; 7:e41702; PMID:22860007; http://dx.doi.org/10.1371/journal.pone.0041702

25. Nitsche A, Kurth A, Dunkhorst A, Pänke O, Sielaff H, Junge W, Muth D, Scheller F, Stöcklein W, Dahmen C et al. One-step selection of Vaccinia virus-binding DNA aptamers by MonoLEX. BMC Biotechnol 2007; 7(1):48; PMID:17199888; http://dx.doi.org/10.1186/1472-6750-7-48

26. Peng L, Stephens BJ, Bonin K, Cubicciotti R, Guthold M. A combined atomic force/fluorescence microscopy technique to select aptamers in a single cycle from a small pool of random oligonucleotides. Microsc Res Tech 2007; 70:372-81; PMID:17262788; http://dx.doi.org/10.1002/jemt.20421

27. Fan M, McBurnett SR, Andrews CJ, Allman AM, Bruno JG, Kiel JL. Aptamer selection express: a novel method for rapid single-step selection and sensing of aptamers. J Biomol Tech 2008; 19:311; PMID:19183794

28. Lin Y, Qiu Q, Gill SC, Jayasena SD. Modified RNA sequence pools for in vitro selection. Nucleic Acids Res 1994; 22:5229-34; PMID:7529404; http://dx.doi.org/10.1093/nar/22.24.5229

29. Green LS, Jellinek D, Bell C, Beebe LA, Feistner BD, Gill SC, Jucker FM, Janjić N. Nuclease-resistant nucleic acid ligands to vascular permeability factor/vascular endothelial growth factor. Chem Biol 1995; 2:683-95; PMID:9383475; http://dx.doi.org/10.1016/1074-5521(95)90032-2

30. Beaudry A, DeFoe J, Zinnen S, Burgin A, Beigelman L. In vitro selection of a novel nuclease-resistant RNA phosphodiesterase. Chem Biol 2000; 7:323-34; PMID:10801472; http://dx.doi.org/10.1016/S1074-5521(00)00110-1

31. Jellinek D, Green LS, Bell C, Lynott CK, Gill N, Vargeese C, Kirschenheuter G, McGee DP, Abesinghe P. Potent 2′-amino-2′-deoxypyrimidine RNA inhibitors of basic fibroblast growth factor. Biochemistry 1995; 34:11363-72; PMID:7547864; http://dx.doi.org/10.1021/bi00036a009

32. Bugaut A, Toulmé J-J, Rayner B. SELEX and dynamic combinatorial chemistry interplay for the selection of conjugated RNA aptamers. Org Biomol Chem 2006; 4:4082-8; PMID:17312962; http://dx.doi.org/10.1039/b610890c

33. Ruckman J, Green LS, Beeson J, Waugh S, Gillette WL, Henninger DD, Claesson-Welsh L, Janjic N. 2′-Fluoropyrimidine RNA-based aptamers to the 165-amino acid form of vascular endothelial growth factor (VEGF165). Inhibition of receptor binding and VEGF-induced vascular permeability through interactions requiring the exon 7-encoded domain. J Biol Chem 1998; 273:20556-67; PMID:9685413; http://dx.doi.org/10.1074/jbc.273.32.20556

34. Lupold SE, Hicke BJ, Lin Y, Coffey DS. Identification and characterization of nuclease-stabilized RNA molecules that bind human prostate cancer cells via the prostate-specific membrane antigen. Cancer Res 2002; 62:4029-33; PMID:12124337; http://dx.doi.org/10.1158/0008-5472.can-12-2152

35. McNamara JO, Andrechek ER, Wang Y, Viles KD, Rempel RE, Gilboa E, Sullenger BA, Giangrande PH. Cell type–specific delivery of siRNAs with aptamer-siRNA chimeras. Nat Biotechnol 2006; 24:1005-15; PMID:16823371; http://dx.doi.org/10.1038/nbt1223

36. Biesecker G, Dihel L, Enney K, Bendele RA. Derivation of RNA aptamer inhibitors of human complement C5. Immunopharmacology 1999; 42:219-30; PMID:10408383; http://dx.doi.org/10.1016/S0162-3109(99)00020-X

37. Layzer JM, Sullenger BA. Simultaneous generation of aptamers to multiple gamma-carboxyglutamic acid proteins from a focused aptamer library using DeSELEX and convergent selection. Oligonucleotides 2007; 17:1-11; PMID:17461758; http://dx.doi.org/10.1089/oli.2006.0059

38. Rusconi CP, Scardino E, Layzer J, Pitoc GA, Ortel TL, Monroe D, Sullenger BA. RNA aptamers as reversible antagonists of coagulation factor IXa. Nature 2002; 419:90-4; PMID:12214238; http://dx.doi.org/10.1038/nature00963

39. Lamberti I, Scarano S, Esposito CL, Antoccia A, Antonini G, Tanzarella C, De Franciscis V, Minunni M. In vitro selection of RNA aptamers against CA125 tumor marker in ovarian cancer and its study by optical biosensing. Methods 2016; 97:58-68; PMID:26542762; http://dx.doi.org/10.1016/j.ymeth.2015.10.022

40. Kubik MF, Bell C, Fitzwater T, Watson SR, Tasset DM. Isolation and characterization of 2′-fluoro-, 2′-amino-, and 2′-fluoro-/amino-modified RNA ligands to human IFN-gamma that inhibit receptor binding. J Immunol 1997; 159:259-67; PMID:9200462

41. Pagratis NC, Bell C, Chang Y-F, Jennings S, Fitzwater T, Jellinek D, Dang C. Potent 2′-amino-, and 2′-fluoro-2′-deoxyribonucleotide RNA inhibitors of keratinocyte growth factor. Nat Biotechnol 1997; 15:68-73; PMID:9035109; http://dx.doi.org/10.1038/nbt0197-68

42. Burmeister PE, Lewis SD, Silva RF, Preiss JR, Horwitz LR, Pendergrast PS, McCauley TG, Kurz JC, Epstein DM, Wilson C. Direct in vitro selection of a 2′-O-methyl aptamer to VEGF. Chem Biol 2005; 12:25-33; PMID:15664512; http://dx.doi.org/10.1016/j.chembiol.2004.10.017

43. Burmeister PE, Wang C, Killough JR, Lewis SD, Horwitz LR, Ferguson A, Thompson KM, Pendergrast PS, McCauley TG, Kurz M. 2-Deoxy purine, 2-O-methyl pyrimidine (dRmY) aptamers as candidate therapeutics. Oligonucleotides 2006; 16:337-51; PMID:17155909; http://dx.doi.org/10.1089/oli.2006.16.337

44. Waters EK, Genga RM, Schwartz MC, Nelson JA, Schaub RG, Olson KA, Kurz JC, McGinness KE. Aptamer ARC19499 mediates a procoagulant hemostatic effect by inhibiting tissue factor pathway inhibitor. Blood 2011; 117:5514-22; PMID:21389323; http://dx.doi.org/10.1182/blood-2010-10-311936

45. Chelliserrykattil J, Ellington A. Evolution of a T7 RNA polymerase variant that transcribes 2′-O-methyl RNA. Nat Biotechnol 2004; 22:1155-60; PMID:15300257; http://dx.doi.org/10.1038/nbt1001

46. Fa M, Radeghieri A, Henry AA, Romesberg FE. Expanding the substrate repertoire of a DNA polymerase by directed evolution. J Am Chem Soc 2004; 126:1748-54; PMID:14871106; http://dx.doi.org/10.1021/ja038525p

47. Siegmund V, Santner T, Micura R, Marx A. Screening mutant libraries of T7 RNA polymerase for candidates with increased acceptance of 2′-modified nucleotides. Chem Commun 2012; 48:9870-2; PMID:22932771; http://dx.doi.org/10.1039/c2cc35028a

48. Padilla R, Sousa R. A Y639F/H784A T7 RNA polymerase double mutant displays superior properties for synthesizing RNAs with non-−canonical NTPs. Nucleic Acids Res 2002; 30:e138-e; PMID:12490729; http://dx.doi.org/10.1093/nar/gnf138

49. Wu Y, Sefah K, Liu H, Wang R, Tan W. DNA aptamer–micelle as an efficient detection/delivery vehicle toward cancer cells. Proc Natl Acad Sci 2010; 107:5-10; PMID:20080797; http://dx.doi.org/10.1073/pnas.0909611107

50. Kato Y, Minakawa N, Komatsu Y, Kamiya H, Ogawa N, Harashima H, Matsuda A. New NTP analogs: the synthesis of 4′-thioUTP and 4′-thioCTP and their utility for SELEX. Nucleic Acids Res 2005; 33:2942-51; PMID:15914669; http://dx.doi.org/10.1093/nar/gki578

51. Ferreira-Bravo IA, Cozens C, Holliger P, DeStefano JJ. Selection of 2′-deoxy-2′-fluoroarabinonucleotide (FANA) aptamers that bind HIV-1 reverse transcriptase with picomolar affinity. Nucleic Acids Res 2015; 43:9587-99; PMID:26476448; http://dx.doi.org/10.1093/nar/gkv1057

14

52. Pinheiro VB, Taylor AI, Cozens C, Abramov M, Renders M, Zhang S, Chaput JC, Wengel J, Peak-Chew S-Y, McLaughlin SH. Synthetic genetic polymers capable of heredity and evolution. Science 2012; 336:341-4; PMID:22517858; http://dx.doi.org/10.1126/science.1217622

53. Yu H, Zhang S, Chaput JC. Darwinian evolution of an alternative genetic system provides support for TNA as an RNA progenitor. Nat Chem 2012; 4:183-7; PMID:22354431; http://dx.doi.org/10.1038/nchem.1241

54. Yu H, Zhang S, Dunn MR, Chaput JC. An efficient and faithful in vitro replication system for threose nucleic acid. J Am Chem Soc 2013; 135:3583-91; PMID:23432469; http://dx.doi.org/10.1021/ja3118703

55. Larsen AC, Dunn MR, Hatch A, Sau SP, Youngbull C, Chaput JC. A general strategy for expanding polymerase function by droplet microfluidics. Nat Commun 2016; 7:11235; PMID:27044725; http://dx.doi.org/10.1038/ncomms11235

56. Veedu RN, Vester B, Wengel J. In vitro incorporation of LNA nucleotides. Nucleosides Nucleotides Nucleic Acids 2007; 26:1207-10; PMID:18058567; http://dx.doi.org/10.1080/15257770701527844

57. Veedu RN, Vester B, Wengel J. Novel applications of locked nucleic acids. Nucleic Acids Symp Ser: Oxford Univ Press, 2007; 51(1):29-30; PMID:18029570; http://dx.doi.org/10.1093/nass/nrm015

58. Veedu RN, Vester B, Wengel J. Enzymatic incorporation of LNA nucleotides into DNA strands. ChemBioChem 2007; 8:490-2; PMID:17315250; http://dx.doi.org/10.1002/cbic.200600501

59. Veedu RN, Vester B, Wengel J. Polymerase chain reaction and transcription using locked nucleic acid nucleotide triphosphates. J Am Chem Soc 2008; 130:8124-5; PMID:18533656; http://dx.doi.org/10.1021/ja801389n

60. Veedu RN, Vester B, Wengel J. Efficient enzymatic synthesis of LNA-modified DNA duplexes using KOD DNA polymerase. Org Biomol Chem 2009; 7:1404-9; PMID:19300826; http://dx.doi.org/10.1039/b819946a

61. Veedu RN, Wengel J. Locked nucleic acid nucleoside triphosphates and polymerases: on the way towards evolution of LNA aptamers. Mol Biosyst 2009; 5:787-92; PMID:19603111; http://dx.doi.org/10.1039/b905513b

62. Veedu RN, Wengel J. Locked nucleic acids: promising nucleic acid analogs for therapeutic applications. Chem Biodivers 2010; 7:536-42; PMID:20232325; http://dx.doi.org/10.1002/cbdv.200900343

63. Veedu RN, Wengel J. Locked nucleic acid as a novel class of therapeutic agents. RNA Biol 2009; 6:321-3; PMID:19458498; http://dx.doi.org/10.4161/rna.6.3.8807

64. Crouzier L, Dubois C, Edwards SL, Lauridsen LH, Wengel J, Veedu RN. Efficient reverse transcription using locked nucleic acid nucleotides towards the evolution of nuclease resistant RNA aptamers. PLoS One 2012; 7:e35990; PMID:22558297; http://dx.doi.org/10.1371/journal.pone.0035990

65. Højland T, Veedu RN, Vester B, Wengel J. Enzymatic synthesis of DNA strands containing α-L-LNA (α-L-configured locked nucleic acid) thymine nucleotides. Artif DNA PNA XNA 2012; 3:14-21; PMID:22679529; http://dx.doi.org/10.4161/adna.19272

66. Johannsen MW, Veedu RN, Madsen AS, Wengel J. Enzymatic polymerisation involving 2′-amino-LNA nucleotides. Bioorg Med Chem Lett 2012; 22:3522-6; PMID:22503454; http://dx.doi.org/10.1016/j.bmcl.2012.03.073

67. Veedu RN, Vester B, Wengel J. Polymerase directed incorporation studies of LNA-G nucleoside 5′-triphosphate and primer extension involving all four LNA nucleotides. New J Chem 2010; 34:877-9; http://dx.doi.org/10.1039/b9nj00628a

68. Wheeler M, Chardon A, Goubet A, Morihiro K, Tsan SY, Edwards SL, Kodama T, Obika S, Veedu RN. Synthesis of selenomethylene-locked nucleic acid (SeLNA)-modified oligonucleotides by polymerases. Chem Commun 2012; 48:11020-2; PMID:23042489; http://dx.doi.org/10.1039/c2cc36464f

69. Kuwahara M, Obika S, Nagashima J-i, Ohta Y, Suto Y, Ozaki H, Sawai H, Imanishi T. Systematic analysis of enzymatic DNA polymerization using oligo-DNA templates and triphosphate analogs involving 2′, 4′-bridged nucleosides. Nucleic Acids Res 2008; 36:4257-65; PMID:18583360; http://dx.doi.org/10.1093/nar/gkn404

70. Kasahara Y, Irisawa Y, Fujita H, Yahara A, Ozaki H, Obika S, Kuwahara M. Capillary electrophoresis–systematic evolution of ligands by exponential enrichment selection of base- and sugar-modified DNA aptamers: target binding dominated by 2′-O, 4′-C-methylene-bridged/locked nucleic acid primer. Anal Chem 2013; 85:4961-7; PMID:23662585; http://dx.doi.org/10.1021/ac400058z

71. Klussmann S, Nolte A, Bald R, Erdmann VA, Fürste JP. Mirror-image RNA that binds D-adenosine. Nat Biotechnol 1996; 14:1112-5; PMID:9631061; http://dx.doi.org/10.1038/nbt0996-1112

72. Nolte A, Klussmann S, Bald R, Erdmann VA, Fürste JP. Mirror-design of L-oligonucleotide ligands binding to L-arginine. Nat Biotechnol 1996; 14:1116-9; PMID:9631062; http://dx.doi.org/10.1038/nbt0996-1116

73. Williams KP, Liu X-H, Schumacher TNM, Lin HY, Ausiello DA, Kim PS, Bartel DP. Bioactive and nuclease-resistant L-DNA ligand of vasopressin. Proc Natl Acad Sci 1997; 94:11285-90; PMID:9326601; http://dx.doi.org/10.1073/pnas.94.21.11285

74. Purschke WG, Radtke F, Kleinjung F, Klussmann S. A DNA Spiegelmer to staphylococcal enterotoxin B. Nucleic Acids Res 2003; 31:3027-32; PMID:12799428; http://dx.doi.org/10.1093/nar/gkg413

75. Vater A, Jarosch F, Buchner K, Klussmann S. Short bioactive Spiegelmers to migraine−associated calcitonin gene−related peptide rapidly identified by a novel approach: Tailored−SELEX. Nucleic Acids Res 2003; 31:e130-e; PMID:14576330; http://dx.doi.org/10.1093/nar/gng130

76. Eulberg D, Buchner K, Maasch C, Klussmann S. Development of an automated in vitro selection protocol to obtain RNA-based aptamers: identification of a biostable substance P antagonist. Nucleic Acids Res 2005; 33:e45-e; PMID:15745995; http://dx.doi.org/10.1093/nar/gni044

77. Faulhammer D, Eschgaller B, Stark S, Burgstaller P, Englberger W, Erfurth J, Kleinjung F, Rupp J, Vulcu SD, Schroder W. Biostable aptamers with antagonistic properties to the neuropeptide nociceptin/orphanin FQ. RNA 2004; 10:516-27; PMID:14970396; http://dx.doi.org/10.1261/rna.5186504

78. Leva S, Lichte A, Burmeister J, Muhn P, Jahnke B, Fesser D, Erfurth J, Burgstaller P, Klussmann S. GnRH binding RNA and DNA Spiegelmers: a novel approach toward GnRH antagonism. Chem Biol 2002; 9:351-9; PMID:11927260; http://dx.doi.org/10.1016/S1074-5521(02)00111-4

79. Jarosch F, Buchner K, Klussmann S. In vitro selection using a dual RNA library that allows primerless selection. Nucleic Acids Res 2006; 34:e86-e; PMID:16855281; http://dx.doi.org/10.1093/nar/gkl463

80. Helmling S, Maasch C, Eulberg D, Buchner K, Schröder W, Lange C, Vonhoff S, Wlotzka B, Tschöp MH, Rosewicz S. Inhibition of ghrelin action in vitro and in vivo by an RNA-Spiegelmer. Proc Natl Acad Sci U S A 2004; 101:13174-9; PMID:15329412; http://dx.doi.org/10.1073/pnas.0404175101

81. Sundaram P, Kurniawan H, Byrne ME, Wower J. Therapeutic RNA aptamers in clinical trials. Eur J Pharm Sci 2013; 48:259-71; PMID:23142634; http://dx.doi.org/10.1016/j.ejps.2012.10.014

82. 2016 NPA. NOXXON Pharma AG 2016.

83. Yatime L, Maasch C, Hoehlig K, Klussmann S, Andersen GR, Vater A. Structural basis for the targeting of complement anaphylatoxin C5a using a mixed L-RNA/L-DNA aptamer. Nat Commun 2015; 6:6481; PMID:25901944; http://dx.doi.org/10.1038/ncomms7481

84. Wang Z, Xu W, Liu L, Zhu TF. A synthetic molecular system capable of mirror-image genetic replication and transcription. Nat Chem 2016; 8:698-704; PMID:27325097; http://dx.doi.org/10.1038/nchem.2517

85. Kuwahara M, Nagashima J-i, Hasegawa M, Tamura T, Kitagata R, Hanawa K, Hososhima S-i, Kasamatsu T, Ozaki H, Sawai H. Systematic characterization of 2′-deoxynucleoside-5′-triphosphate analogs as substrates for DNA polymerases by polymerase chain reaction and kinetic studies on enzymatic production of modified DNA. Nucleic Acids Res 2006; 34:5383-94; PMID:17012278; http://dx.doi.org/10.1093/nar/gkl637

86. MacPherson IS, Temme JS, Habeshian S, Felczak K, Pankiewicz K, Hedstrom L, Krauss IJ. Multivalent glycocluster design through

15

directed evolution. Angew Chem Int Ed 2011; 50:11238-42; PMID:22191092; http://dx.doi.org/10.1002/anie.201105555

87. Temme JS, MacPherson IS, DeCourcey JF, Krauss IJ. High temperature SELMA: Evolution of DNA-supported oligomannose clusters which are tightly recognized by HIV bnAb 2G12. J Am Chem Soc 2014; 136:1726-9; PMID:24446826; http://dx.doi.org/10.1021/ja411212q

88. Tolle F, Brändle GM, Matzner D, Mayer G. A Versatile approach towards nucleobase−modified aptamers. Angew Chem Int Ed 2015; 54:10971-4; PMID:26224087; http://dx.doi.org/10.1002/anie.201503652

89. Horiya S, MacPherson IS, Krauss IJ. Recent strategies targeting HIV glycans in vaccine design. Nat Chem Biol 2014; 10:990-9; PMID:25393493; http://dx.doi.org/10.1038/nchembio.1685

90. Temme JS, Drzyzga MG, MacPherson IS, Krauss IJ. Directed Evolution of 2G12−Targeted Nonamannose Glycoclusters by SELMA. Chem Eur J 2013; 19:17291-5; PMID:24227340; http://dx.doi.org/10.1002/chem.201303848

91. Veedu R, Burri H, Kumar P, Sharma P, Hrdlicka P, Vester B, Wengel J. Polymerase-directed synthesis of C5-ethynyl locked nucleic acids. Bioorg Med Chem Lett 2010; 20:6565-8; PMID:20932755; http://dx.doi.org/10.1016/j.bmcl.2010.09.044

92. Zhang L, Yang Z, Sefah K, Bradley KM, Hoshika S, Kim M-J, Kim H-J, Zhu G, Jiménez E, Cansiz S. Evolution of functional six-nucleotide DNA. J Am Chem Soc 2015; 137:6734-7; PMID:25966323; http://dx.doi.org/10.1021/jacs.5b02251

93. Thyer R, Ellefson J. Synthetic biology: New letters for life's alphabet. Nature 2014; 509:291-2; PMID:24805244; http://dx.doi.org/10.1038/nature13335

94. Sefah K, Yang Z, Bradley KM, Hoshika S, Jiménez E, Zhang L, Zhu G, Shanker S, Yu F, Turek D. In vitro selection with artificial expanded genetic information systems. Proc Natl Acad Sci 2014; 111:1449-54; PMID:24379378; http://dx.doi.org/10.1073/pnas.1311778111

95. Georgiadis MM, Singh I, Kellett WF, Hoshika S, Benner SA, Richards NG. Structural basis for a six nucleotide genetic alphabet. J Am Chem Soc 2015; 137:6947-55; PMID:25961938; http://dx.doi.org/10.1021/jacs.5b03482

96. Latham JA, Johnson R, Toole JJ. The application of a modified nucleotide in aptamer selection: novel thrombin aptamers containing-(1-pentynyl)-2′-deoxyuridine. Nucleic Acids Res 1994; 22:2817-22; PMID:7519769; http://dx.doi.org/10.1093/nar/22.14.2817

97. Jensen KB, Atkinson BL, Willis MC, Koch TH, Gold L. Using in vitro selection to direct the covalent attachment of human immunodeficiency virus type 1 Rev protein to high-affinity RNA ligands. Proc Natl Acad Sci 1995; 92:12220-4; PMID:8618873; http://dx.doi.org/10.1073/pnas.92.26.12220

98. Battersby TR, Ang DN, Burgstaller P, Jurczyk SC, Bowser MT, Buchanan DD, Kennedy RT, Benner SA. Quantitative analysis of receptors for adenosine nucleotides obtained via in vitro selection from a library incorporating a cationic nucleotide analog. J Am Chem Soc 1999; 121:9781-9; PMID:11543572; http://dx.doi.org/10.1021/ja9816436

99. Vaish NK, Larralde R, Fraley AW, Szostak JW, McLaughlin LW. A novel, modification-dependent ATP-binding aptamer selected from an RNA library incorporating a cationic functionality. Biochemistry 2003; 42:8842-51; PMID:12873145; http://dx.doi.org/10.1021/bi027354i

100. Shoji A, Kuwahara M, Ozaki H, Sawai H. Modified DNA aptamer that binds the (R)-isomer of a thalidomide derivative with high enantioselectivity. J Am Chem Soc 2007; 129:1456-64; PMID:17263432; http://dx.doi.org/10.1021/ja067098n

101. Imaizumi Y, Kasahara Y, Fujita H, Kitadume S, Ozaki H, Endoh T, Kuwahara M, Sugimoto N. Efficacy of base-modification on target binding of small molecule DNA aptamers. J Am Chem Soc 2013; 135:9412-9; PMID:23734784; http://dx.doi.org/10.1021/ja4012222

102. Li M, Lin N, Huang Z, Du L, Altier C, Fang H, Wang B. Selecting aptamers for a glycoprotein through the incorporation of the boronic acid moiety. J Am Chem Soc 2008; 130:12636-8; PMID:18763762; http://dx.doi.org/10.1021/ja801510d

103. Vaught JD, Bock C, Carter J, Fitzwater T, Otis M, Schneider D, Rolando J, Waugh S, Wilcox SK, Eaton BE. Expanding the chemistry of DNA for in vitro selection. J Am Chem Soc 2010; 132:4141-51; PMID:20201573; http://dx.doi.org/10.1021/ja908035g

104. Santoro SW, Joyce GF, Sakthivel K, Gramatikova S, Barbas CF. RNA cleavage by a DNA enzyme with extended chemical functionality. J Am Chem Soc 2000; 122:2433-9; PMID:11543272; http://dx.doi.org/10.1021/ja993688s

105. Kimoto M, Yamashige R, Matsunaga K-i, Yokoyama S, Hirao I. Generation of high-affinity DNA aptamers using an expanded genetic alphabet. Nat Biotechnol 2013; 31:453-7; PMID:23563318; http://dx.doi.org/10.1038/nbt.2556

106. Hollenstein M, Hipolito CJ, Lam CH, Perrin DM. Toward the combinatorial selection of chemically modified DNAzyme RNase A mimics active against all-RNA substrates. ACS Comb Sci 2013; 15:174-82; PMID:23485334; http://dx.doi.org/10.1021/co3001378

107. Gold L, Ayers D, Bertino J, Bock C, Bock A, Brody EN, Carter J, Dalby AB, Eaton BE, Fitzwater T. Aptamer-based multiplexed proteomic technology for biomarker discovery. PLoS One 2010; 5:e15004; PMID:21165148; http://dx.doi.org/10.1371/journal.pone.0015004

108. Davies DR, Gelinas AD, Zhang C, Rohloff JC, Carter JD, O'Connell D, Waugh SM, Wolk SK, Mayfield WS, Burgin AB. Unique motifs and hydrophobic interactions shape the binding of modified DNA ligands to protein targets. Proc Natl Acad Sci 2012; 109:19971-6; PMID:23139410; http://dx.doi.org/10.1073/pnas.1213933109

109. Ochsner UA, Katilius E, Janjic N. Detection of Clostridium difficile toxins A, B and binary toxin with slow off-rate modified aptamers. Diagn Microbiol Infect Dis 2013; 76:278-85; PMID:23680240; http://dx.doi.org/10.1016/j.diagmicrobio.2013.03.029

110. Jhaveri S, Olwin B, Ellington AD. In vitro selection of phosphorothiolated aptamers. Bioorg Med Chem Lett 1998; 8:2285-90; PMID:9873529; http://dx.doi.org/10.1016/S0960-894X(98)00414-4

111. King DJ, Bassett SE, Li X, Fennewald SA, Herzog NK, Luxon BA, Shope R, Gorenstein DG. Combinatorial selection and binding of phosphorothioate aptamers targeting human NF-κB RelA (p65) and p50. Biochemistry 2002; 41:9696-706; PMID:12135392; http://dx.doi.org/10.1021/bi020220k

112. King DJ, Ventura DA, Brasier AR, Gorenstein DG. Novel combinatorial selection of phosphorothioate oligonucleotide aptamers. Biochemistry 1998; 37:16489-93; PMID:9843415; http://dx.doi.org/10.1021/bi981780f

113. Lato SM, Ozerova NDS, He K, Sergueeva Z, Shaw BR, Burke DH. Boron-containing aptamers to ATP. Nucleic Acids Res 2002; 30:1401-7; PMID:11884639; http://dx.doi.org/10.1093/nar/30.6.1401

16

SCIENTIFIC REPORTS

Novel Chemically-modified DNAzyme targeting Integrin alpha-4 RNA transcript as a potential molecule to reduce inflammation in multiple sclerosis

Madhuri Chakravarthy[1,2], May T. Aung-Htut[1,2], Bao T. Le[1,2] & Rakesh N. Veedu[1,2]

Integrin alpha-4 (ITGA4) is a validated therapeutic target for multiple sclerosis (MS) and Natalizumab, an antibody targeting ITGA4 is currently approved for treating MS. However, there are severe side effects related to this therapy. In this study, we report the development of a novel DNAzyme that can efficiently cleave the *ITGA4* transcript. We designed a range of DNAzyme candidates across various exons of *ITGA4*. RNV143, a 30mer arm-loop-arm type DNAzyme efficiently cleaved 84% of the *ITGA4* mRNA in human primary fibroblasts. RNV143 was then systematically modified by increasing the arm lengths on both sides of the DNAzymes by one, two and three nucleotides each, and incorporating chemical modifications such as inverted-dT, phosphorothioate backbone and LNA-nucleotides. Increasing the arm length of DNAzyme RNV143 did not improve the efficiency however, an inverted-dT modification provided the most resistance to $3' \rightarrow 5'$ exonuclease compared to other modifications tested. Our results show that RNV143A could be a potential therapeutic nucleic acid drug molecule towards the treatment for MS.

Nucleic acid-based therapeutic technologies have gained significant interest for developing therapies targeting RNA molecules[1]. So far, four oligonucleotide drugs have been approved by the United States Food and Drug Administration for clinical use[2–5]. Vitravene, Kynamro and Eteplirsen are antisense oligonucleotides approved for the treatment of cytomegaloviral retinitis, familial hypercholestrolemia and Duchenne muscular dystrophy respectively, while a nucleic acid aptamer candidate Macugen was approved for age-related macular degeneration[2–5]. DNAzymes are another unique class of synthetic catalytic oligonucleotides that can play various roles including gene silencing and as biosensing molecules for diagnostic applications[6]. DNAzymes anneal to complementary RNA substrates through Watson-Crick base pairing rules and cleaves the phosphodiester bond mainly at purine-pyrimidine or less frequently at purine-purine junction in the presence of divalent metal ions (e.g. Mg^{2+}, Ca^{2+}, Pb^{2+})[7–9]. DNAzymes possess enzyme-like characteristic and the catalytic activity is dependent on divalent metal ions as cofactors[7]. The simple structure of DNAzyme includes two binding arms for specific target mRNA binding, and a catalytic core in between the binding arms to catalyse the cleavage of the target mRNA (Fig. 1A). One big advantage of DNAzymes over RNase-H dependent antisense oligonucleotides is that it can recognize and cleave the target mRNA without RNase-H recruitment and the process is reiterative (Fig. 1A).

Inflammation in the central nervous system is one of the major problems of chronic neurodegenerative disease such as multiple sclerosis (MS)[10]. ITGA4 is a validated therapeutic target for MS since a humanized monoclonal antibody, natalizumab, against ITGA4 is successful in delaying the disease progression[11]. The drug interferes with the interaction between ITGA4 and vascular cell adhesion molecule-1 and prevents immune cells from crossing the blood brain barrier and attacking the central nervous system[11]. Patients treated with natalizumab over several years have reduced or are free of annual relapses, however, there are significant limitations associated

[1]Centre for Comparative Genomics, Discovery Way, Murdoch University, Perth, WA, 6150, Australia. [2]Perron Institute for Neurological and Translational Science, Nedlands, WA, 6009, Australia. Madhuri Chakravarthy and May T. Aung-Htut contributed equally to this work. Correspondence and requests for materials should be addressed to R.N.V. (email: R.Veedu@murdoch.edu.au)

17
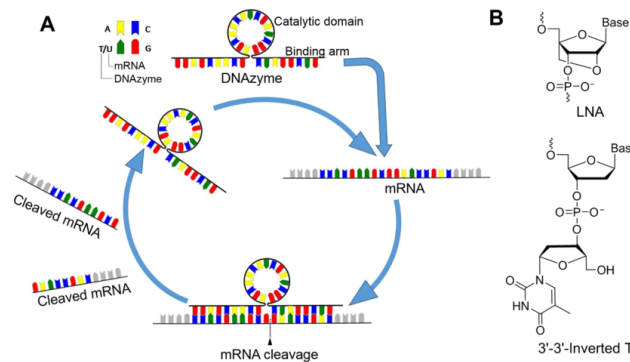
Figure 1. (**A**) Schematic illustration of DNAzyme-based mRNA cleavage, and (**B**) structural representations of LNA and inverted thymidine monomers.

with natalizumab such as an increased risk of progressive multifocal leukoencephalopathy and development of side effects including serum sickness, generation of anti-drug antibodies and other adverse effects as discussed in recent reviews[12, 13]. Herein, we report the development of novel DNAzymes that can efficiently cleave *ITGA4* mRNA transcript as potential therapeutics to reduce ITGA4 activity in MS.

Results

Design and screening of first-generation DNAzymes targeting *ITGA4* mRNA.   Two groups of DNAzymes, one with 10–23 catayltic motif (hammerhead) and the other with 8–17 catalytic motif (arm-loop) (Fig. 2A) were designed to target various exons of the *ITGA4* transcript. The sequences of the catalytic regions were pre-fixed according to previous reports[14, 15] and the arm regions were designed to be specific and complementary to the *ITGA4* mRNA sequences (Fig. 2B). The catalytic activities of these DNAzymes against *ITGA4* mRNA were screened in human primary fibroblasts by transfecting DNAzymes at different concentrations (600 nM, 400 nM, 200 nM, 100 nM and 50 nM) for 24 h. RNA was extracted from the cell lysate and the integrity of *ITGA4* transcript was assessed by performing RT-PCR. Scrambled sequence (SCR) was used as a negative control to account for the non-specific effects.

Dose-dependent reduction of the full-length *ITGA4* transcript was observed for all DNAzymes treated samples. The best *ITGA4* transcript knockdown was observed at 600 nM and therefore, the efficiency of each DNAzyme was calculated as a percentage of *ITGA4* transcript knockdown at 600 nM after normalising to the house keeping gene transcript cyclin D (*CYCD*) and described as the activity in fibroblasts (Fig. 2B). DNAzyme candidate RNV143 targeting the exon 9 of the *ITGA4* mRNA showed highest efficacy with 84% knockdown of *ITGA4* (gel shown in Fig. 2C) followed by RNV148 (71% although this was not statistically significant) and RNV145 (68%) (Fig. 2B).

Design and screening of second-generation DNAzymes targeting *ITGA4* mRNA.   Based on the initial screen, the best performing DNAzyme RNV143 was selected for further modifications. Many studies have shown that increasing the hybridisation arms on either side of the catalytic motif can increase the binding affinity and efficacy[16–18]. In our study, the first generation of DNAzymes initially had 8 nucleotides on one arm and 7 on the other. Several studies showed that the optimal arm lengths vary from 7 to 10 nucleotides long[16–21]. Therefore, the length of RNV143 was systematically increased at the end of both arms, and then the efficacy of the modified DNAzymes was verified. One, two and three nucleotides were added to both arms of RNV143 and named RNV182, RNV183 and RNV184 respectively (Fig. 3). The catalytic activities of these second generation DNAzyme candidates were analysed in human primary fibroblasts as described above. The transfections were repeated at least twice. Notably, a decrease in activities were observed for RNV182 (57%) and RNV183 (74%) at 600 nM compared to the parent DNAzyme RNV143 (84%) (Fig. 3). RNV184 with additional six nucleotides (three on each ends) was the only candidate that showed similar activity to the parent RNV143, with 89% knockdown of *ITGA4* mRNA. These results showed that increasing the arm length did not dramatically improve the efficacy of DNAzyme RNV143 in fibroblasts.

Next, we explored the improvement of nuclease stability of the DNAzymes since the natural nucleotide monomers are rapidly degraded *in vivo*. First, we introduced phosphorothioate (PS) linkages to the arm regions of RNV143 to improve nuclease resistance and named RNV143PS. However, RNV143PS failed to cleave *ITGA4* RNA when transfected into the human fibroblasts. Only 10% of the *ITGA4* transcript was degraded when treated with RNV143PS while nearly 29% of the *ITGA4* transcript was non-specifically knocked down by the scrambled control (Fig. 3). Then we introduced another chemical modification, an 'inverted dT' (Fig. 1B) at the 3′ end of RNV143, RNV183 and RNV184, the DNAzymes with high activities, and the new generation DNAzymes were named RNV143A, RNV183A and RNV184A respectively. RNV143A, RNV183A and RNV184A slightly improved the activities of DNAzymes (89%, 76% and 92% respectively; Fig. 3).
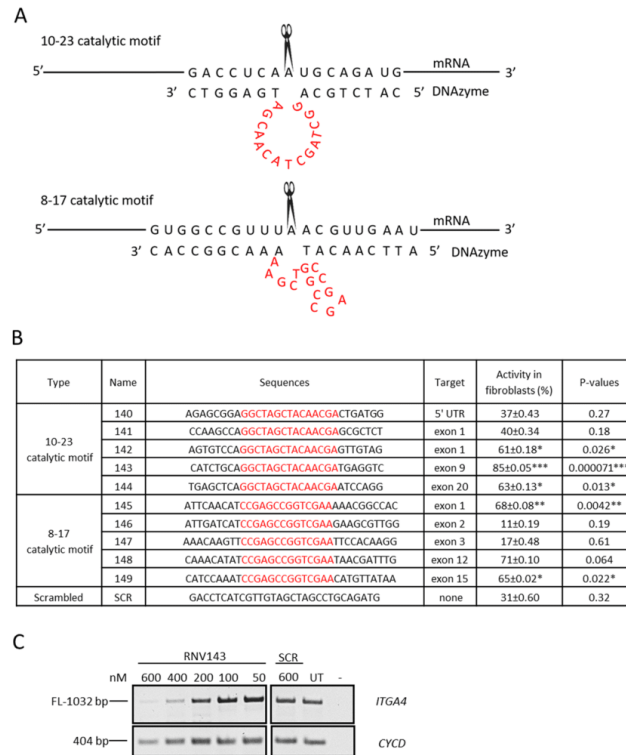
Figure 2. (**A**) Schematic illustration of the 10–23 and 8–17 catalytic motifs of DNAzymes. (**B**) Table for the activities of first-generation DNAzymes targeting *ITGA4* mRNA that is directly correlated with the percentages of *ITGA4* mRNA knockdown (See Materials and Methods for detailed procedures); The catalytic motifs are shown in red, the arm regions are in black, and the sequences are from $5' \rightarrow 3'$. p-values were calculated for the activity in fibroblasts which was normalised to the UT using student t-test and *Indicates p-value < 0.05, **Indicates p-value < 0.005 and ***Indicates p-value < 0.0005. p-values have been rounded to 2 s.f. (**C**) Representative RT-PCR products of the *ITGA4* and *CycD* transcripts from normal human primary fibroblasts after treatment with DNAzyme at different concentrations. The RT-PCR products after treatment with RNV143 are shown here. FL, full-length; UT, untreated; SCR, scrambled sequence; *CYCD* was used as a loading control. The gel images were cropped to highlight the *ITGA4* specific products and the corresponding house-keeping gene control *CYCD*. The original images are shown in Figure S2 (Supplementary Information).

Figure 3. Second-generation DNAzymes derived from RNV143, targeting the *ITGA4* mRNA. The activity of DNAzymes directly correlated with the percentage of *ITGA4* mRNA knockdown. Activities of DNAzymes were calculated as described in Materials and Methods. The catalytic motifs are shown in red, the arm regions are in black and the residues modified with LNA are in blue. The sequences are from $5' \rightarrow 3'$.

19

Figure 4. *In vitro* cleavage of the FAM-conjugated *ITGA4* RNA template composed of exon 9 region (34 nucleotides) by RNV143 and its derivatives. FL RNA, full length; FAM-conjugated RNA; cleaved RNA; the cleaved FAM-conjugated *ITGA4* RNA (18 nucleotides long). The FAM- conjugated template RNA is a small region of the *ITGA4* transcript complementary to the hybridisation arms of the DNAzymes of interest. The gel images were cropped for better overview. The original images are shown in Figure S3 (Supplementary Information). The table shows the cleavage rate in %/min which was calculated as described in Materials and Methods section.

We also investigated the potential use of locked nucleic acid (LNA) nucleotides in DNAzymes. Two LNA nucleotides were incorporated to both arms of RNV183 at positions 2, 5 and 31, 35. However, RNV183 with 4 LNA modifications was not effective (did not cleave *ITGA4*) when tested in cells (data not shown). We believe that this may be due to the formation of secondary structures caused by LNAs within the arms of the DNAzymes that could potentially affect the catalytic motif (sequence of the LNA modified RNV183 and the mfold[22] predicted structures are shown in Supplementary Material, Figure S1). To limit this secondary structure formation, we truncated the LNA modified RNV183 by four nucleotides from the 5′ end to generate RNVLNA-3 (Fig. 3) with one LNA nucleotide on the truncated arm and two LNA nucleotides on the other non-truncated arm. This truncation is predicted to limit the secondary structure formation, and promote its ability to bind to the *ITGA4* mRNA. Transfection with RNVLNA-3 showed 58% knockdown of *ITGA4* transcript indicating that the truncation helped to improve the activity, although the efficacy of *ITGA4* knockdown was not efficient (Fig. 3).

***In vitro* cleavage of *ITGA4* RNA template.**   To further verify the catalytic activity of DNAzyme towards the target region of *ITGA4* transcript, we performed the cleavage efficacy *in vitro* using a synthetic fluorescein dye (FAM)-labelled RNA target composed of exon 9 region of the *ITGA4* transcript. The experiments were performed by incubating DNAzymes with FAM-labelled RNA template in the presence of divalent metal ions and the products were separated and analysed on polyacrylamide gels. Briefly, 1.76 μM DNAzymes were incubated with 1.76 μM FAM-conjugated *ITGA4* RNA in the presence of Mg^{2+} divalent cations for 30 min, 60 min and 120 min at 37 °C. The reactions were stopped by adding 10 μL of formamide solution. The products were then separated on a 15% denaturing polyacrylamide gel and visualised using Fusion FX Vilber Lourmat imager. The cleaved products of the 34mer full length FAM-conjugated RNA was expected to be 18 nucleotides. A scrambled (SCR) sequence and RNV143 mutants with different mutations within the catalytic region of RNV143 were used as negative controls in parallel and an untreated (UT) sample with no DNAzyme was also included.

Although variable efficiencies were observed for these DNAzymes in fibroblasts, RNV143, RNV182, RNV183 and RNV184 showed similar cleavage efficiency *in vitro* (around 0.7%/min) (Fig. 4). In general, the *in vitro* cleavage rates of the modified DNAzymes were slower than that of their parent oligonucleotides. Notably, RNV143PS showed very low cleavage efficiency with small percentage of cleaved FAM-conjugated RNA appearing after 120 minutes of incubation. Similar results were observed for RNV143-Mut3 while the other mutant DNAzymes and the SCR sequence showed no cleavage (Fig. 4).

Nuclease stability analysis of DNAzymes.   High nuclease stability is paramount towards the clinical development of oligonucleotides. Towards this goal, we tested the stability of DNAzymes RNV143, RNV183, RNV184, RNVLNA-3, RNV143A, RNV183A, and RNV184A using snake venom phosphodiesterase, a harsh enzyme with very high 3′ → 5′ exonuclease activity. DNAzyme candidates were incubated with the enzyme at 37 °C and samples were collected at different time points (0, 30, 60 and 120 minutes) followed by the products analysis on 15% denaturing polyacrylamide gels. As expected the stability was increased by increasing the arm

20
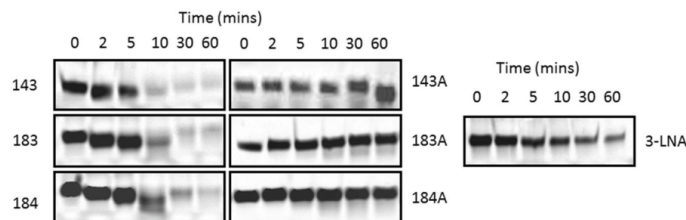
Figure 5. Phosphodiesterase degradation analysis of DNAzymes that showed high efficacy in the cleavage of *ITGA4* RNA *in vitro* and knockdown of *ITGA4* RNA in fibroblasts. The gel images were cropped for better overview. The original images are shown in Figure S4 (Supplementary Information).

lengths of the DNAzymes and RNV184 (36 nt long) was found to be the most stable compared to RNV183 and RNV143 (Fig. 5). RNVLNA-3 with LNA modifications (known for high nuclease stability[23, 24]) was more stable than RNV143, RNV183 and RNV184. A weak product band was visible even after 60 minutes of incubation. Remarkably, the DNAzymes with inverted dT nucleotide at 3′-end (RNV143A, RNV183A and RNV184A) showed highest stability with no significant degradation even after 1 hour incubation with phosphodiesterase (Fig. 5).

Discussion

We have successfully identified a DNAzyme that cleaves the *ITGA4* transcript both *in vitro* and in human primary fibroblasts by screening different DNAzyme constructs with 10–23 catalytic motif and 8–17 catalytic motif targeting different sites of *ITGA4* mRNA. The DNAzyme was not only capable of downregulating the *ITGA4* transcript *in vitro* and in human primary fibroblasts but also showed high resistance to exonuclease degradation. Our study thus provides a novel approach for downregulating *ITGA4* transcript that may have therapeutic potential towards the treatment of MS where ITGA4 is a validated target for tackling inflammation.

Cleavage by first generation DNAzymes with either 10–23 or 8–17 catalytic motif targeting five different cleavage sites of the *ITGA4* transcript showed variable cleavage efficiencies (Fig. 2B). The best cleavage efficiency was achieved with the 10–23 catalytic motif DNAzymes designed to cleave a site located in exon 9 of the *ITGA4* transcript. The variable target-cleaving efficiencies observed for different first generation DNAzymes targeting different regions of the *ITGA4* transcript could be due to the structure variations that might affect the accessibility of target sequences. This is consistent with previous observations by Vester *et al.*[17, 21, 25]. The cleavage efficiency of DNAzyme has been proposed to be dependent on the structural complexity of the RNA that is targeted[17, 26]. In a comparison between different substrate structures, Vester *et al.*, targeted three different cleavage sites of either a short (17 nucleotides) unstructured RNAs; or longer (58 nucleotides) RNAs with stable secondary structures; or longer (2904 nucleotides) RNAs with both stable secondary and tertiary structures[17, 26]. The results indicated that only one cleavage site out of three could be efficiently cleaved by the DNAzymes and the cleavage of the short unstructured RNAs were more efficient than the longer structured RNA[17, 26]. This implies that the accessibility of the purine-pyrimidine sites differs in different regions of the *ITGA4* (1032 bp long) transcript due to the formation of different secondary and tertiary structures in the transcript inside the cells, leading to differences in the ability of DNAzymes to cleave them.

The optimal arm length may vary for different DNAzymes and there is no evidence on whether the arms should be asymmetrical or symmetrical for optimal catalytic activity. In addition, the GC content may also have an effect on the catalytic efficiency[16, 18, 21, 27], but how it is affected is unclear[16, 18, 19]. In parallel, increasing the DNAzyme binding arm length would increase DNAzyme-target affinity as it enhances the heteroduplex stability[28], but it could also result in slower product release that would inhibit or decrease the rate of multiple turnovers. Therefore, longer binding arms may not always produce higher catalytic efficiency[14, 29]. Using the best candidate RNV143 from the first screen, we further tested the impact of DNAzyme arm lengths aiming for increased efficiency. However, the catalytic efficiency was decreased in most DNAzymes with longer arms. We speculate that increasing the arm length of the DNAzyme RNV143 could increase the binding affinity of DNAzymes to the target RNA but result in slower product release and turnover[26]. For DNAzymes to have therapeutic potential, it is desirable to have high turnover.

Although we have identified a DNAzyme with high cleavage efficiency, one of the disadvantages of unmodified DNAzymes, similar to antisense oligonucleotides, is their vulnerability to nucleases *in vivo* and therefore, nuclease resistance is a critical characteristic of their physical property[30]. The suitable solution to increase nuclease resistance is to introduce chemical modifications[30]. Several modifications have been successfully introduced into the oligonucleotides including sugar modifications such as LNA[21, 22], and inverted thymidine and backbone modification such as PS[30]. In line with this, we modified several of our efficient DNAzyme candidates, RNV143 and its two derivatives RNV183 and RNV184 with PS, LNA and inverted-dT. When modified with PS modification (RNV143PS), RNV143 resulted in decreased cleavage efficiency both *in vitro* (Fig. 4) and in human fibroblasts (Fig. 3). PS modification typically enhances the stability of the oligonucleotide against nucleases, however, they compromise the affinity to their target in some cases, which could result in decreased cleavage efficiency[30]. Similar results were also observed in another study that further support our observation that PS modification may not be ideal for developing efficient DNAzymes[19]. Although truncation and incorporation of LNA to the DNAzymes

21

increased resistance to nuclease (Fig. 5), the activity was decreased (Fig. 3). The reduction in the activity may be due to a combination of reduced size and slower DNAzyme dissociation from the mRNA target based on the high affinity of LNA nucleotides[19]. Among all modifications tested, incorporation of inverted dT (RNV143A, RNV183A and RNV184A) was found to be the best chemistry in this case, since it not only conferred nuclease resistance (Fig. 5) but also achieved high activity (89%, 76% and 92% respectively) (Fig. 3). The result is also consistent with a previous study performed by *Schubert et al*.[19]. Additionally, we have also performed a human serum degradation experiment to observe the stability of the DNAzymes in human serum (Figure S4 in Supplementary Material). RNV143, RNV182, RNV183 and RNV184 showed similar stability (degradation observed after 2 hours incubation) in human serum and as expected their modified counterparts RNV143A, RNV183A and RNV184A showed better stability (~26–50% DNAzymes remained after 6 h incubation). Interestingly, RNVLNA-3 conferred the best stability in human serum, however as discussed above, its activity in cells was decreased (Fig. 3).

We observed a discrepancy between the *ITGA4* knock down observed in fibroblasts and the *in vitro* cleavage for the same DNAzymes. Although variable efficiencies are observed for second generation DNAzymes in human primary fibroblasts (Fig. 3), the *in vitro* data does not reflect this (Fig. 4). It is expected that *cell-free* conditions are incomparable to the crowded *cell-culture* environment and the mRNA folding and accessibility of the template may significantly influence the success of experiments within the cells. It is also expected that the *ITGA4* RNA expressed in fibroblasts (1032 base pairs long) is much longer and can adopt complex secondary and tertiary structures while the synthetic short single stranded RNA (34 nucleotides long) used for the *in vitro* cleavage assay may not form any secondary or tertiary structures and therefore it is much easier for the DNAzyme to access and cleave. However, the DNAzymes that knocked down *ITGA4* transcript in fibroblasts also showed the ability to cleave the synthetic *ITGA4* transcript template *in vitro* and from this we may suggest that the *ITGA4* knock down observed in the fibroblast could be due to the DNAzymes-mediated cleavage of *ITGA4* transcript. Furthermore, we designed three RNV 143 mutants RNV143-Mut1, RNV143-Mut2 and RNV143-Mut3 to investigate the possibility of antisense effect rather than DNAzyme cleavage. RNV143-Mut1 and RNV 143-Mut2 are double mutants designed based on the paper by Wang *et al*. that suggested that these double mutants were critical for activity in the hammerhead and the stem loop respectively[31]. Both double mutants may be important for catalytic activity as they abolished the *in vitro* cleavage activity (Fig. 4). However, RNV143-Mut3 showed very small cleavage activity indicating that the nucleotide mutated may not be crucial for catalytic activity, supporting the previous study by Wang *et al*.[31]. These controls also suggest that the gene silencing effects seen in cells by RNV143 may be due to DNAzyme cleavage rather than the antisense effect. The cleavage rates of the DNAzymes observed here is about half of that reported by Schubert *et al*.[19]. However, we performed the *in vitro* cleavage reactions with equal molar ratio of the DNAzyme to substrate in the presence of 0.5 mM MgCl$_2$ while Schubert *et al*., performed the reactions with 10-fold excess of DNAzyme to substrate in 10 mM MgCl$_2$[19].

In conclusion, we identified DNAzymes that are capable of cleaving the *ITGA4* transcript in human primary fibroblasts. The DNAzyme candidate RNV143 targeting exon 9 of the *ITGA4* transcript showed 92% knock down of the *ITGA4* transcript and the catalytic ability of the DNAzyme was verified by *in vitro* cleavage assay. Furthermore, introducing a chemical modification such as an inverted dT at the 3′ end (RNV143A) significantly improved the stability while maintaining efficient catalytic activity. Although RNV143A needs further validations, based our current results, we firmly believe that the candidate could provide therapeutic benefits.

Methods

DNAzyme design and synthesis.   DNAzymes with either stem loop or hammer head conformation were designed for the selected exons (Fig. 2B) and the oligonucleotides were ordered from IDT. The LNA modified DNAzyme was made in-house by ABI Expedite 8909 nucleic acid synthesis system in 1 μM scale, deprotected by NH$_4$OH at 55 °C overnight and purified by NAP column (GE Health care).

Cell propagation and transfection.   Cell cultures media and supplements were purchased from (Life technologies, Australia) unless specified. Normal human fibroblasts were propagated in Dulbecco's modified Eagle's medium supplemented with GlutaMAX™ and 10% fetal bovine serum. Transfections were performed in 24 well-plate format with approximately 15,000 cells/well. The cells were seeded one day before transfecting with the DNAzymes complexed with Lipofectamine 3000® transfection reagent (Life Technologies, Australia) per the manufacturer's protocol. Transfection was carried out for 24 hours before harvesting RNA for transcript analysis. RNA was extracted using Direct-zol RNA MiniPrep Kit (Zymo Research, USA) following manufacturer's protocol.

RT-PCR assays.   50 ng of total RNA was analysed using a Superscript III One-Step RT-PCR System (Life technologies, Australia) and reaction conditions are as follows: 55 °C for 30 min, 94 °C for 2 min, 28 rounds of 94 °C for 30 sec, 55 °C for 30 sec and 68 °C for 1 min 30 sec. Exon 1–10 was amplified using primer pair 1F (5′-gagagcgcgctgctttaccagg-3′) and 10R (5′-gccatcattgtcaatgtcgcca-3′); exon 9–20 using primer pair 9F (5′-ggatcgtactttggagcttctg-3′) and 20R (5′-gcatgcactgtgatactgaggt-3′). The products were analysed on 2% agarose gels.

Image analysis of the gel from gel electrophoresis.   Densitometry (measuring the band intensity) of the bands was performed using Image J Software[32]. The band intensity of the *ITGA4* bands in different DNAzymes treated samples were measured and normalised to the band intensity of the corresponding *CYCD* bands before comparing to the band intensity of the untreated samples. The percentage of *ITGA4* transcript knockdown by DNAzymes in fibroblasts was expressed as activity of DNAzyme.

***In vitro* cleavage assay.**   4.4 μL of 20 μM DNAzyme was incubated with equal molar concentration of FAM-conjugated *ITGA4* RNA (5′-FAM-CUGUGCUGUGGACCUCAAUGCAGAUGGCUUCUCA-3′) in

22

$5\,\mu L$ of buffer containing Mg^{2+} divalent cations ($10\,mM$ $MgCl_2$) at $37\,°C$. The reaction was stopped by adding $10\,\mu L$ of formamide to $10\,\mu L$ of the reaction mixture at 0, 30 mins, 60 mins and 2 hours. Scrambled DNAzyme RNV174, RNV143-Mut1 (5′-CATCTGCAGGCTA**AA**TACAACGATGAG-3′), RNV143-Mut2 (5′-CATC TGCA**AA**CTAGCTACAACGATGAG-3′) and RNV143-Mut3 (5′-CATCTGCAGGCTAGC**A**ACAACGA TGAG-3′) were used as negative controls and the untreated samples did not have any DNAzyme. The mutated bases are in bold and the two double mutants RNV143-Mut1 and RNV 143-Mut2 were designed based on a previous paper[31] The reaction mixtures were separated on a 15% polyacrylamide gel/7 M urea for 50 mins at 13 W. The gel was visualised using the Fusion FX Vilber Lourmat Imager (Fisher Biotech).

Image Analysis of the gel from *in vitro* cleavage assay.   Densitometry (measuring the band intensity) of the bands was performed using Image J Software[32]. The band intensity of the full length RNA bands for different time points were measured and normalised to the combined band intensity of both cleaved and full length RNA bands for different time points and plotted on excel as the % of uncleaved RNA. The same analysis was repeated to calculate % of cleaved RNA. The slope of the curve was used to calculate the % cleaved per minute.

Phosphodiesterase assay. $5\,\mu M$ DNAzyme was incubated with 0.00001 U phosphodiesterase from *Crotalus adamanteurs* venom (Sigma Aldrich) at $37\,°C$. At different time points 0, 2 mins, 5 mins, 10 mins, 30 mins and 1 hour, $10\,\mu L$ of formamide was added to equal volume of the reaction mixture to stop the reaction. The reaction mixture was separated on a 20% polyacrylamide/7 M urea gel. The gel was stained with ethidium bromide for 10 minutes and destained in water for 10 minutes before visualizing under UV light using Bio-Rad Molecular Imager ChemiDoc XRS Imaging System.

Human serum degradation assay. $5\,\mu M$ DNAzyme was incubated in human serum at $37\,°C$. At different time points 0, 30 mins, 60 mins, 2 hours, 4 hours and 6 hours, $10\,\mu L$ of formamide was added to equal volume of the reaction mixture to stop the reaction. The reaction mixture was separated on a 15% polyacrylamide/7 M urea gel. The gel was stained with ethidium bromide for 10 minutes and destained in water for 10 minutes before visualizing under UV light using Bio-Rad Molecular Imager ChemiDoc XRS Imaging System. The images are shown in Figure S4 (Supplementary Information).

References

1. Burnett, J. C. & Rossi, J. J. RNA-based therapeutics: current progress and future prospects. *Chem Biol* **19**, 60–71, doi:10.1016/j. chembiol.2011.12.008 (2012).
2. Group, V. S. A randomized controlled clinical trial of intravitreous fomivirsen for treatment of newly diagnosed peripheral cytomegalovirus retinitis in patients with AIDS. *Am J Opthalmol* **133**, 467–474 (2002).
3. Crooke, S. T. & Geary, R. S. Clinical pharmacological properties of mipomersen (Kynamro), a second generation antisense inhibitor of apolipoprotein B. *Br J Clin Pharmacol* **76**, 269–276, doi:10.1111/j.1365-2125.2012.04469.x (2013).
4. Mendell, J. R. *et al*. Longitudinal effect of eteplirsen versus historical control on ambulation in Duchenne muscular dystrophy. *Ann Neurol* **79**, 257–271, doi:10.1002/ana.24555 (2016).
5. Group, M. D. R. S. Changes in retinal neovascularization after pegaptanib (Macugen) therapy in diabetic individuals. *Ophthalmology* **113**, 23–28, doi:10.1016/j.ophtha.2005.10.012 (2006).
6. Hollenstein, M. DNA catalysis: the chemical repertoire of DNAzymes. *Molecules* **20**, 20777–20804, doi:10.3390/molecules201119730 (2015).
7. Achenbach, J., Chiuman, W., Cruz, R. & Li, Y. DNAzymes: from creation *in vitro* to application *in vivo*. *Curr Pharm Biotechnol* **5**, 321–336, doi:10.2174/1389201043376751 (2004).
8. Zhou, W., Saran, R., Huang, P. J. J., Ding, J. & Liu, J. An Exceptionally Selective DNA Cooperatively Binding Two Ca2+ Ions. *ChemBioChem* (2017).
9. Torabi, S.-F. *et al*. *In vitro* selection of a sodium-specific DNAzyme and its application in intracellular sensing. *Proc Natl Acad Sci* **112**, 5903–5908, doi:10.1073/pnas.1420361112 (2015).
10. Hauser, S. L. & Oksenberg, J. R. The neurobiology of multiple sclerosis: genes, inflammation, and neurodegeneration. *Neuron* **52**, 61–76, doi:10.1016/j.neuron.2006.09.011 (2006).
11. Polman, C. H. *et al*. A randomized, placebo-controlled trial of natalizumab for relapsing multiple sclerosis. *N Engl J Med* **354**, 899–910, doi:10.1056/NEJMoa044397 (2006).
12. Hansel, T. T., Kropshofer, H., Singer, T., Mitchell, J. A. & George, A. J. The safety and side effects of monoclonal antibodies. *Nat Rev Drug Discov* **9**, 325–338, doi:10.1038/nrd3003 (2010).
13. Clifford, D. B. *et al*. Natalizumab-associated progressive multifocal leukoencephalopathy in patients with multiple sclerosis: lessons from 28 cases. *Lancet Neurol* **9**, 438–446, doi:10.1016/S1474-4422(10)70028-4 (2010).
14. Santoro, S. W. & Joyce, G. F. A general purpose RNA-cleaving DNA enzyme. *Proc Natl Acad Sci* **94**, 4262–4266, doi:10.1073/pnas.94.9.4262 (1997).
15. Haseloff, J. & Gerlach, W. L. Simple RNA enzymes with new and highly specific endoribonuclease activities. *Nature* **334**, 585–591, doi:10.1038/334585a0 (1988).
16. Ackermann, J. M., Kanugula, S. & Pegg, A. E. DNAzyme-mediated silencing of ornithine decarboxylase. *Biochemistry* **44**, 2143–2152, doi:10.1021/bi047918d (2005).
17. Vester, B. *et al*. Locked nucleoside analogues expand the potential of DNAzymes to cleave structured RNA targets. *BMC Mol Biol* **7**, 1, doi:10.1186/1471-2199-7-19 (2006).
18. Santoro, S. W. & Joyce, G. F. Mechanism and utility of an RNA-cleaving DNA enzyme. *Biochemistry* **37**, 13330–13342, doi:10.1021/bi9812221 (1998).
19. Schubert, S. *et al*. RNA cleaving '10–23'DNAzymes with enhanced stability and activity. *Nucleic Acids Res* **31**, 5982–5992, doi:10.1093/nar/gkg791 (2003).
20. Sun, L.-Q. *et al*. Suppression of smooth muscle cell proliferation by a c-myc RNA-cleaving deoxyribozyme. *J Biol Chem* **274**, 17236–17241, doi:10.1074/jbc.274.24.17236 (1999).
21. Kurreck, J., Bieber, B., Jahnel, R. & Erdmann, V. A. Comparative study of DNA enzymes and ribozymes against the same full-length messenger RNA of the vanilloid receptor subtype I. *J Biol Chem* **277**, 7099–7107, doi:10.1074/jbc.M107206200 (2002).
22. Zuker, M. Mfold web server for nucleic acid folding and hybridization prediction. *Nucleic Acids Res* **31**, 3406–3415, doi:10.1093/nar/gkg595 (2003).

23

23. Veedu, R. N. & Wengel, J. Locked nucleic acids: promising nucleic acid analogs for therapeutic applications. *Chem Biodivers* **7**, 536–542, doi:10.1002/cbdv.v7:3 (2010).
24. Veedu, R. N. & Wengel, J. Locked nucleic acid as a novel class of therapeutic agents. *RNA biology* **6**, 321–323, doi:10.4161/rna.6.3.8807 (2009).
25. Cairns, M. J., Hopkins, T. M., Witherington, C., Wang, L. & Sun, L.-Q. Target site selection for an RNA-cleaving catalytic DNA. *Nature Biotechnol* **17**, 480–486, doi:10.1038/8658 (1999).
26. Vester, B. *et al.* Improved RNA cleavage by LNAzyme derivatives of DNAzymes. *Biochem Soc Trans* **32**, 37–40, doi:10.1042/bst0320037 (2004).
27. Cairns, M. J., Hopkins, T. M., Witherington, C. & Sun, L.-Q. The influence of arm length asymmetry and base substitution on the activity of the 10–23 DNA enzyme. *Antisense Nucleic Acid Drug Dev* **10**, 323–332, doi:10.1089/oli.1.2000.10.323 (2000).
28. Cairns, M., Saravolac, E. & Sun, L. Catalytic DNA: a novel tool for gene suppression. *Curr Drug Targets* **3**, 269–279, doi:10.2174/1389450023347722 (2002).
29. Tsuchihashi, Z., Khosla, M. & Herschlag, D. Protein enhancement of hammerhead ribozyme catalysis. *Science* **262**, 99–102, doi:10.1126/science.7692597 (1993).
30. Chan, C. & Khachigian, L. DNAzymes and their therapeutic possibilities. *Intern Med* **39**, 249–251, doi:10.1111/j.1445-5994.2009.01799.x (2009).
31. Wang, F., Saran, R. & Liu, J. Tandem DNAzymes for mRNA cleavage: Choice of enzyme, metal ions and the antisense effect. *Bioorganic & medicinal chemistry letters* **25**, 1460–1463, doi:10.1016/j.bmcl.2015.02.032 (2015).
32. Schindelin, J., Rueden, C. T., Hiner, M. C. & Eliceiri, K. W. The ImageJ ecosystem: An open platform for biomedical image analysis. *Mol Reprod Dev* **82**, 518–529, doi:10.1002/mrd.22489 (2015).

Acknowledgements

Author Contributions

R.N.V. conceived the research; M.C., M.T.A. and B.T.L. performed the experiments; M.C., M.T.A and R.N.V. analysed the results and co-wrote the manuscript and all authors reviewed the manuscript.

Additional Information

Supplementary information accompanies this paper at doi:10.1038/s41598-017-01559-w

Competing Interests: The authors declare that they have no competing interests.

Publisher's note: Springer Nature remains neutral with regard to jurisdictional claims in published maps and institutional affiliations.

24

Review

Nucleic Acid-Based Theranostics for Tackling Alzheimer's Disease

Madhuri Chakravarthy[1, 2], Suxiang Chen[1, 2], Peter R. Dodd[3], Rakesh N. Veedu[1, 2, 3]✉

1. Centre for Comparative Genomics, Murdoch University, Murdoch, Perth, Australia 6150;
2. Perron Institute for Neurological and Translational Science, QEII Medical Centre, Nedlands, Perth, Australia 6005;
3. School of Chemistry and Molecular Biosciences, The University of Queensland, St Lucia, Brisbane, Australia 4072.

✉ Corresponding author: Rakesh N. Veedu, PhD. Centre for Comparative Genomics, Murdoch University, Building 390 Discovery Drive, Perth, Western Australia, Australia 6150. Email: R.Veedu@murdoch.edu.au

Abstract

Nucleic acid-based technologies have received significant interest in recent years as novel theranostic strategies for various diseases. The approval by the United States Food and Drug Administration (FDA) of Nusinersen, an antisense oligonucleotide drug, for the treatment of spinal muscular dystrophy highlights the potential of nucleic acids to treat neurological diseases, including Alzheimer's disease (AD). AD is a devastating neurodegenerative disease characterized by progressive impairment of cognitive function and behavior. It is the most common form of dementia; it affects more than 20% of people over 65 years of age and leads to death 7–15 years after diagnosis. Intervention with novel agents addressing the underlying molecular causes is critical. Here we provide a comprehensive review on recent developments in nucleic acid-based theranostic strategies to diagnose and treat AD.

Key words: nucleic acids; Alzheimer's disease; amyloid beta peptides; tau peptide; chemically modified oligonucleotides; nucleic acid therapeutics.

Introduction

Nucleic acid-based technologies typically use synthetic oligonucleotides 8–50 nucleotides in length, most of which bind to RNA through Watson-Crick base pairing to alter the expression of the targeted RNA and protein. Novel chemical modifications and conjugation strategies have been developed to improve pharmacokinetics and tissue-specific delivery. Vitravene, Kynamro, Nusinersen and Eteplirsen are antisense oligonucleotides (AOs) approved by the FDA to treat cytomegalovirus retinitis, familial hypercholesterolemia, spinal muscular atrophy, and Duchenne muscular dystrophy respectively [1-3]. The nucleic acid aptamer drug Macugen was approved for age-related macular degeneration [4]. These successful clinical translations demonstrate the potential of nucleic acid-based technologies and provide scope for developing novel therapeutics for AD. AD is the most common form of dementia; it accounts for 70% of cases with that diagnosis. Globally there are ~47 million current cases; 7.7 million new cases are added each year [5]. AD is characterized by a progressive loss of memory and cognitive function [6]. Patients eventually need 24-hour care that places emotional and economic burdens on the community. There is no cure for AD, nor any treatment that addresses its underlying molecular cause [5]. Current treatments use cholinesterase inhibitors [7] and *N*-methyl-D-aspartate receptor (NMDA) antagonists [8] that improve cognitive function and reduce symptoms temporarily but do not stop the progression of the disease. The current approach to diagnosis relies on a combination of cognitive and clinical assessment, genetic profiling, and magnetic resonance imaging to measure anatomical changes in the brain [9], but confirmation relies on post-mortem neuropathological assessment

and misdiagnosis is common [6]. Two hallmarks of the disease are extracellular amyloid-β (Aβ) plaques (mainly an agglomeration of Aβ peptides) and intracellular neurofibrillary tangles (hyperphosphorylated tau peptides). In this review we focus on the potential of nucleic acid therapeutic, diagnostic, and research strategies that target both Aβ and tau pathologies to help diagnose and treat AD.

Amyloid β (Aβ) hypothesis

The Aβ hypothesis states that there is an imbalance of toxic Aβ peptide production and clearance [10-12]. The main Aβ species, $Aβ_{1-40}$ and $Aβ_{1-42}$, can aggregate to form fibrils and plaques [10-12]. $Aβ_{1-40}$ and $Aβ_{1-42}$ are produced by the aberrant splicing of amyloid precursor protein (APP) by β-site APP cleaving enzyme 1 (BACE1) and γ-secretase (Figure 1) [11-15]. Mutations in the APP and Presenilin genes (*PSEN1* codes for the catalytic subunits of γ-secretase) increase $Aβ_{1-42}$ levels [10-12, 14, 16-18] and lead to early-onset familial AD. Down syndrome cases have an extra copy of chromosome 23, and hence of the *APP* gene, and develop Aβ plaques early in adulthood [19]. Oligomers of Aβ promote synaptic loss, neuronal dysfunction, and cell death [20, 21]. $Aβ_{1-42}$ inhibits the maintenance of hippocampal long-term potentiation, resulting in altered memory function [10, 22] and reduced synaptic neurotransmission through NMDA receptor-mediated signaling [10, 22, 23]. Aβ toxicity has also been implicated in inflammation [11], oxidative stress [11, 24], cholinergic transmission [23], glucose metabolism [25, 26], and cholesterol metabolism [27].

Tau hypothesis

Microtubule-associated protein tau (tau), predominantly expressed in neuronal axons, is involved in microtubule assembly and stability. Tau is regulated by phosphorylation [28, 29]. Hyperphosphorylation decreases the ability of tau to bind to microtubules, leading to reduced trafficking, destabilization of microtubules, and synaptic loss [29, 30] (Figure 2). Abnormal tau can aggregate into paired helical filaments to form neurofibrillary tangles [31] in the cytosol and sequester normal tau to inhibit microtubule assembly [29]. Alternatively, tau aggregation may be a protective mechanism to stop hyperphosphorylated tau sequestering normal tau and inhibit microtubule assembly [29]. Tau hyperphosphorylation is detrimental in various neurodegenerative diseases termed "tauopathies" [28, 32]. Hyperphosphorylation of tau correlates with neurodegeneration and cognitive decline [29, 32]. Other post-translational modifications of tau, including abnormal glycosylation and reduced β-linked acylation of N-acetylglucosamine, increase hyperphosphorylation [29, 33]. Inhibition of the ubiquitin-proteasome system may also increase the aggregation of hyperphosphorylated tau [31].

Other hypothesis of AD

Drugs currently approved by the FDA for the treatment of AD are Donepezil, Rivastigmine, Galantamine and Memantine (Table 1) [34-37]. These agents enhance cholinergic and glutamatergic neurotransmission and improve cognitive function temporarily. However, they do not slow the progression of the disease. Oxidative stress [38], inflammation [39], insulin impairment [40, 41] and abnormal cholesterol metabolism [27] may also play roles (Table 1), but will not be considered in depth here.
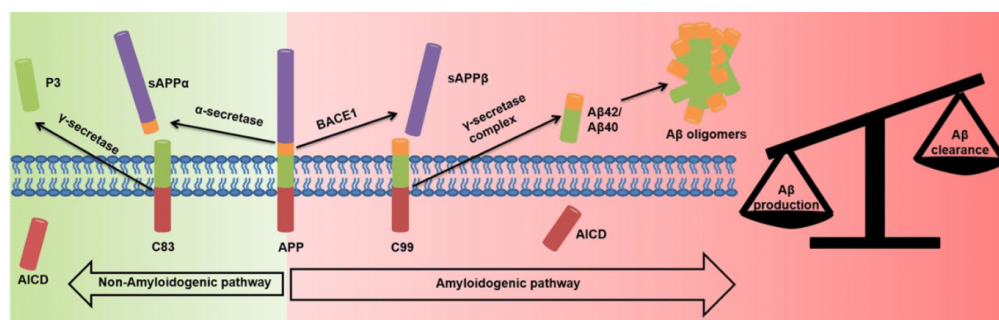
Figure 1. Non-amyloidogenic and amyloidogenic pathways in AD neurons. In the amyloidogenic pathway the APP is aberrantly spliced by BACE1 and γ-secretase to overproduce toxic Aβ species.
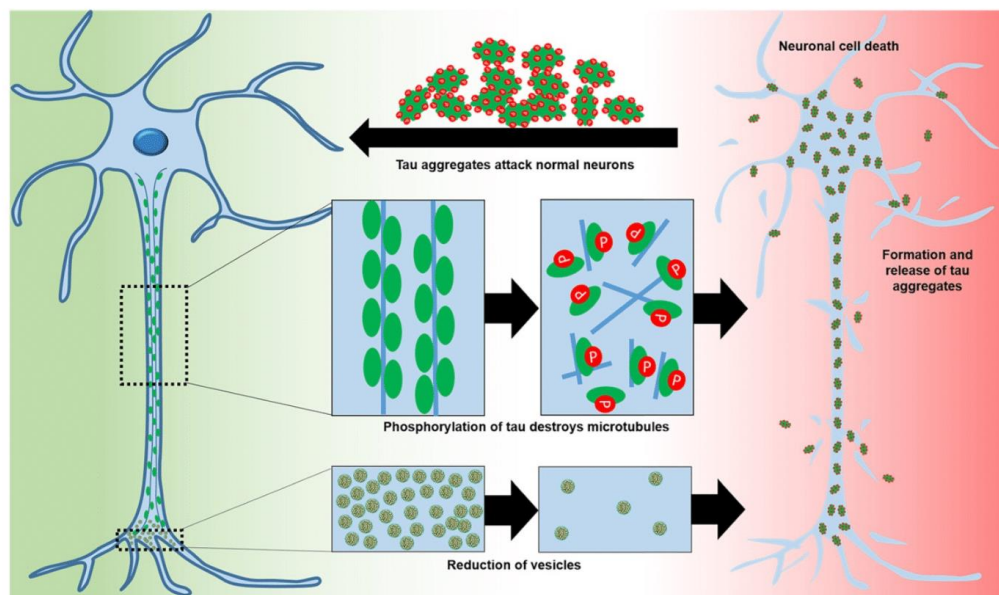
Figure 2. The roles of tau in normal neurons and of hyperphosphorylation in AD neurons that lead to neuronal toxicity.

Table 1. Therapeutic molecules in clinical trials, their targets, and trial outcomes.

Drug molecule	Role/ Target	Trial stage	Results	References
Donepezil (Pfizer)	Cholinesterase inhibitor	FDA approved- Although they improve the symptoms temporarily these drugs do not stop the progression of the disease.		[34-37]
Rivastigmine (Novartis)	Cholinesterase inhibitor			
Galantamine (Jansen-Cilag)	Cholinesterase inhibitor			
Memantine (Lundbeck)	NMDA receptor antagonist			
Tramiprosate	Aβ aggregation inhibitor	Phase III	No significant benefit. May promote abnormal tau aggregation	[47-49]
Colostrinin	Aβ aggregation inhibitor	Phase III	Modest improvements not sustained	[50-52]
Scyllo-inositol	Stabilizes Aβ aggregates and inhibits toxicity	Phase II	No statistically significant effect. Reduced Aβ in cerebrospinal fluid	[53]
Aβ vaccination	Aβ aggregation inhibitor	Phase II	Halted because patients developed meningo-encephalitis	[54]
Bapineuzumab	Aβ aggregation inhibitor	Phase III	End points not significantly different	[55]
Solanezumab	Aβ aggregation inhibitor	Phase III	End points not significantly improved	[56]
Anti-amyloid Ab	Aβ aggregation inhibitor	Phase III	No positive primary outcome	[57]
Other mAbs	Aβ aggregation inhibitor	Various	No positive outcome	[42, 58, 59]
Tarenflurbil	γ-secretase inhibitor	Phase III	No significant improvement	[60-62]
LY450139 (Eli Lilly)	γ-secretase inhibitor	Phase III	Discontinued: no Aβ$_{40/42}$ reduction	[63]
BMS-708163 (B-M Squibb)	γ-secretase inhibitor	Phase II	Terminated due to lack of favorable pharmacodynamics	[42, 64]
Verubecestat	BACE1 inhibitor	Phase III	Currently running	[65]
Rogiglitazone	BACE1 inhibitor and Type 2 diabetes drug	Phase III	No positive outcome	[66]
Pioglitaozone	BACE1 inhibitor and Type 2 diabetes drug	Phase III	No positive outcome	[66]
Methyl thionium chloride	Tau aggregation inhibitor	Phase II	Significantly improved cognitive function	[67, 68]
Tideglusib	GSK3β	Phase IIb	No positive outcome	[68, 69]
Davunetide	Microtubule stabilizer	Phase III	No significant improvement	[30]
Antioxidants	ROS	Phase III	No positive outcome	[42, 70]
Anti-inflammatories	Inflammation	Phase III	No significant improvement	[25, 39, 59, 71-73]
Intranasal insulin	Insulin impairment	Pilot	Improvement in patients without APOE-ε4 allele	[40, 74]
Other anti-diabetics	Insulin impairment	Phase III	Currently running	
Statins	Cholesterol metabolism	Phase III	Preliminary results positive; mechanism unknown.	[27, 75]

Current therapeutic molecules and clinical trials for the treatment of AD

Many disease-modifying therapeutics show positive outcomes in animal models but disappointing results in clinical trials (for drug candidates and ongoing trials see Table 1). Current strategies have been comprehensively reviewed [42]. Poor outcomes might have arisen because each agent is targeting a single pathway, whereas AD is a complex disease and it may be important to aim at multiple targets [43, 44]. Success in developing a suitable therapeutic approach is challenging because the pathogenesis of AD is unknown [45]. Trials might be affected by factors such as genetics, metabolism, and diet [46], but there is clearly a need to develop novel therapeutics for this disease.

Nucleic-acid based molecules for tackling AD

Unlike conventional small-molecule drugs, nucleic acid-based therapeutic agents such as AOs, small-interfering RNAs (siRNAs), microRNA moieties that target oligonucleotides (antimiRs and miRNA mimics), and DNAzymes/ribozymes can regulate the expression of key proteins by selectively targeting their mRNAs. The outcome is mRNA cleavage, repair, or steric blockade (Figure 3). The class of modified nucleic acids called aptamers can target proteins and inhibit their function (Figure 3). Nucleic acid-based strategies could be an effective alternative to drug development for AD because they can target a range of pathological features.
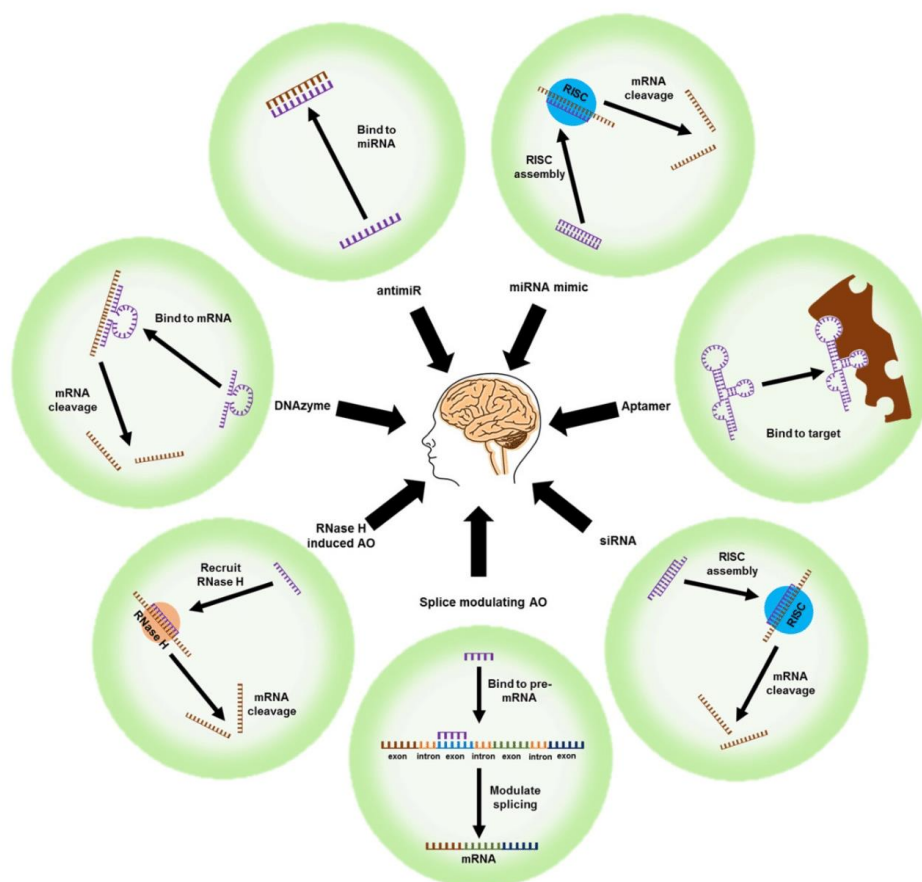
Figure 3. Nucleic acid-based therapeutic strategies. mRNA: messenger RNA; RNase H: ribonuclease H; siRNA: small interfering RNA; RISC: RNA inducing silencing complex; AO: antisense oligonucleotide; antimiR: anti-microRNA; miRNA mimic: microRNA mimic
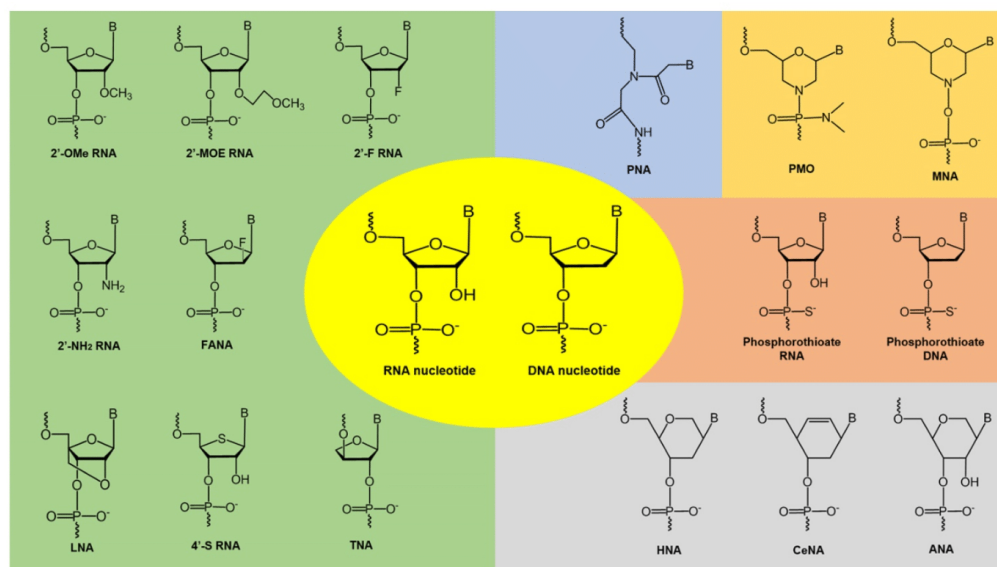
Figure 4. Examples of chemically-modified nucleotide analogues. 2'-OMe: 2'-*O*-methyl; 2'-MOE:2'-*O*-methoxyethyl; 2'-F: 2'-fluoro; 2'-NH₂: 2'-amino; FANA: fluoroarabinonucleotide; LNA: locked nucleic acid; TNA: threose nucleic acid; PNA: peptide nucleic acid; PMO: phosphorodiamidate morpholino oligomer; MNA: morpholino nucleic acid; HNA: hexitol nucleic acid; CeNA: cyclohexenyl nucleic acid; ANA: anhydrohexitol nucleic acid

Improving the stability and efficacy of nucleic acid-based therapeutics

Therapeutic oligonucleotides composed of naturally occurring nucleotides are rapidly degraded *in vivo*, which makes them unsuitable for drug development. To improve their pharmacokinetic properties, chemically modified nucleotide analogues with high resistance to nucleases are normally used. A number of analogues have been developed by modifying the base or sugar moieties, or the inter-nucleotide linkages (see Figure 4) [76-78]. Phosphorothioate DNA [79], 2'-*O*-methyl (2′-OMe) RNA [80], 2'-fluoro (2′-F) RNA [81], 2'-*O*-methoxyethyl (2′-MOE) RNA [82], and phosphorodiamidate morpholino (PMO) [83] analogues have been successfully utilized in FDA-approved oligonucleotide drugs. Analogues such as locked nucleic acids (LNA) [84, 85], peptide nucleic acids (PNA) [86], tricyclo-DNA (tcDNA) [87], and cyclohexenyl nucleic acids (CeNA) [88] also show excellent biophysical properties and offer further scope for novel oligonucleotide development. These chemistries can be used to construct fully modified or mixmer oligonucleotides. Aptamers can be modified during the selection or post-selection stages to improve their affinity and bioavailability [77]. Another challenge in the clinical utilization of unmodified oligonucleotides is rapid renal clearance from the blood due to their small size that falls under the renal filtration threshold. To increase their bioavailability, oligonucleotides can be conjugated with polyethylene glycol (PEG) to increase their size, which could also improve their resistance to nucleases [89]. Several PEGylated drugs have been approved by the FDA for clinical use [89, 90]. Other strategies include conjugating the oligonucleotides to albumin, which has a size of around 7 nm and shows reduced renal clearance and can therefore increase the circulation half-life of the oligonucleotides. Phosphorothioate modified oligonucleotides also showed reduced renal clearance by binding to plasma proteins like albumin to avoid glomerular filtration [91]. Another strategy is the synthesis of neutral siRNA (masking the negative charge on the phosphate backbone). Neutral siRNA showed reduced renal clearance [92].

Recent progress in modified nucleic acids for AD

Antisense oligonucleotides

A classical nucleic acid approach to controlling the expression of proteins is to use AOs, short single-stranded synthetic oligonucleotides, which can precisely target an mRNA transcript to regulate the

expression of the protein it codes for. Antisense mechanisms include RNase H recruitment and cleavage of mRNA, modulation of splicing in pre-mRNA, and steric blockade of either mature or pre-mRNAs (Figure 3). RNase H-mediated cleavage involves designing a short DNA oligonucleotide that binds to the target mRNA to form a RNA-DNA duplex [93]. The duplex is recognized and cleaved by endogenous RNase H. AOs that modulate pre-mRNA splicing can be used to repair defective RNA and eliminate disease-associated splice variants [94]. Many pre-mRNA transcripts are alternatively spliced to produce different mRNA, and hence protein, variants [94].

APP

Many groups have designed AOs that target APP to reduce APP expression. An early study by Allinquant *et al.* [95] developed AOs that successfully blocked rat APP synthesis. Administration of the AOs showed that APP played a role in axonal and dendritic growth, and thus in neuronal differentiation [95]. ISIS Pharmaceuticals (now Ionis Pharma) have patented (US 2003/0232435 A1) 78 gapmer AOs with 2'-MOE wings and central DNA region. The AOs target various regions of APP mRNA and inhibit 39–82% of APP protein expression [96].

Kumar and colleagues [97] developed phosphorothioated DNA AOs against sequences that correspond to the Aβ region of APP (17-42 amino acids). Administration of the AOs led to improved cognitive function in senescence-accelerated mouse-prone 8 (SAMP8) mice. SAMP8 mice have a natural mutation that leads to APP over-expression, impaired Aβ removal, and loss of memory with increasing age. The AOs that target the mid-Aβ region reduced APP levels by 43–68% in the amygdala, septum and hippocampus [97]. The mice showed improvement in acquisition and retention in the footshock avoidance paradigm, which reversed their deficits in learning and memory [97]. AOs that target the sequences that correspond to the region of APP coding for the first 17–30 amino acids of Aβ were the subject of intellectual property protection [98]. Banks and colleagues [99] showed that a radioactively tagged phosphorothioate DNA AO targeting the Aβ region of APP could transit the blood-brain barrier (BBB) of mice to enter the cerebrospinal fluid. When a 100-fold higher dose of the AO was injected into the brain by intracerebroventricular injection it reversed the learning and memory deficits in SAMP8 mice, possibly through reduced oxidative stress. Poon *et al.* [100] used proteomics to show that lower Aβ levels result in reduced oxidative stress in brain.

Opazo *et al.* [101] transfected the AOs described by Kumar and colleagues [97] into the CTb cell line, a neuronal line from mice that overexpresses APP, and the CNh cell line from normal mice. The AOs resulted in APP knockdown in CTb cells by 36%, 40% and 50% compared with normal CNh cells after 24 h, 48 h and 72 h respectively [101]. By 72 h after AO transfection, choline uptake was similar to that in CNh cells and there was increased choline release in response to glutamate, nicotine and KCl depolarization, which reached similar levels to those observed in CNh cells. The CTb cells come from a Down syndrome mouse model, which show some learning deficits and cholinergic dysfunction that are similar to those found in AD [102]. Similarly, Rojas *et al.* [103] showed that APP overexpression reduced the expression and retrograde transport of nerve growth factor. This reduced nicotine-induced stimulation of $\alpha_3\beta_2$ nicotinic acetylcholine receptor and in consequence lowered intracellular Ca^{2+} responses in CTb cells. The effects of APP overexpression were restored close to normal by treatment with AOs targeting APP expression.

Chauhan and colleagues [104] designed gapmer AOs with 2'-OMe and DNA nucleotides on a phosphorothioate backbone that target the β-secretase cleavage site of APP and found that they reduced brain Aβ_{40} and Aβ_{42} levels in a mouse model of AD. The AOs were delivered intracerebroventricularly and showed rapid uptake and retention for 30 minutes. They efficiently crossed cell membranes into the nuclear and cytoplasmic compartments of neuronal and non-neuronal cells. Chauhan and Siegel [105] designed two additional AOs targeting the β- and γ-secretase site of APP in the Tg2576 mouse model that expresses APP. The AO targeting the mutated β-secretase site increased soluble APPα by 43% and decreased soluble Aβ_{40} and Aβ_{42} levels by 39%, whereas the AO targeting the γ-secretase site had no effect. The AO targeting β-secretase also inhibited acetylcholinesterase activity, increasing acetylcholine by five-fold in cortex compared with controls.

Erickson *et al.* [106] peripherally administered an APP AO to SAMP8 mice. This resulted in a 30% increase in APP levels but no change in soluble Aβ levels. The treated mice showed improved memory. They also showed [107] that AO-mediated APP knockdown in Tg2576 mouse brains reduced cytokine expression and improved learning and memory. Attenuating APP overexpression may improve learning and memory by reducing inflammation (also implicated in AD pathology).

BACE1

Yan *et al.* [108] developed two AOs that target β-secretase aspartyl protease and found that they

reduced the release of $A\beta_{40}$ and $A\beta_{42}$ by 50–80%. Vassar and colleagues [109] also used AOs that target β-secretase to reduce $A\beta_{40}$ and $A\beta_{42}$ production by around 30%. These studies showed that β-secretase is important for the production of $A\beta_{40}$ and $A\beta_{42}$ and highlighted BACE1 as an important target for AD. Wolfe *et al.* [110] designed splice-modulating AOs to target BACE1, since alternatively spliced transcript variants at exons 2 and 3 do not show β-secretase activity. The AOs reduced Aβ production significantly in cells without altering total BACE1 mRNA.

Presenilin 1 (PSEN1)

Refolo *et al.* [111] found that AOs targeting PSEN1 in a human cell line reduced PSEN1 holoprotein by 80% 12 days after treatment and by 90% after 14 days. This was correlated with a two-fold increase in $A\beta_{42}$ levels. Grilli *et al.* [112] found that hippocampal primary neurons overexpressing mutant PSEN1 were vulnerable to excitotoxic and hypoxia-hypoglycemic damage and increased cell death. They designed two phosphorothioate AOs targeting PSEN1 in wild type mice. In contrast to Refolo *et al.* [111] they found that lower PSEN1 expression reduced cell death and provided neuroprotection [112]. Fiorini *et al.* [113] administered AOs targeting PSEN1 to aged SAMP8 mice and found they reduced brain oxidative stress biomarkers. In the T-maze foot shock avoidance and novel object recognition tests the mice showed a reversal of learning and memory deficits.

Tau

Caceres *et al.* [114] showed that an AO targeting the 5' end of the tau gene, in the region before the start codon, showed strong inhibition of neurite elongation in primary rat neurons. Immunoblotting revealed that the tau protein level was reduced in AO-treated mice but not in control mice. The effect of AO treatment on cognition needs to be assessed. DeVos *et al.* [115] screened 80 AOs targeting tau and selected the three that showed the best knockdown of tau to test *in vivo*. The latter reduced tau mRNA levels by more than 75%. The best AO was selected for further testing in mice; it lowered brain tau mRNA and protein significantly in a dose-dependent manner. Behavioral impacts and neurotoxicity were not measured. Kalbfuss *et al.* [116] developed splice-modulating AOs modified with 2'-OMe nucleotides to target the tau exon 10 splice junctions to reduce exon 10 inclusion. Exclusion of exon 10 increases the ratio of tau proteins lacking the microtubule-binding domain. In consequence, the microtubule cytoskeleton becomes destabilized as observed in frontotemporal dementia

and parkinsonism.

Peacey *et al.* [117] designed bipartite AOs that bound to the hairpin structure at the boundary between exon 10 and intron 10 of tau to inhibit exon 10 splicing, reversing the effect of disease-causing mutations in cells. Liu *et al.* [118] developed a small-molecule (mitoxantrone) conjugated to a bipartite AO that binds to the tau RNA hairpin structure. The conjugate also inhibited exon 10 splicing in cell-free conditions more effectively than mitoxantrone or the bipartite AO alone, but induced cytotoxicity. The same group used a PNA-modified bipartite AO conjugated to mitoxantrone that inhibited tau splicing but was also cytotoxic [110].

Sud *et al.* [119] developed PMO AOs to modulate the splicing of tau and tau expression. The AOs were designed to target sequences at the donor and acceptor splice sites, the splicing branch points, and splicing enhancers and inhibitors to induce exon skipping. Exons 0, 1, 4, 5, 7, 9, and 10 were targeted. Exons 1, 4, 5, 7, and 9 are found in all 6 isoforms of tau while exon 10 is present in only three of the six isoforms. Of the 31 AOs tested, AO E1.4 targeting the splice donor site at the exon 1 – intron 1 junction reduced tau mRNA expression by 50%. The other AOs effective in this region were a combination of AOs that targeted the splice donor and acceptor sites and the start codon. AO E5.3 targeted the splice donor site at the exon 5 –intron 5 junction and reduced total tau mRNA expression by 29–46%. It also reduced tau protein level by 58–62%. The resulting transcript was missing exons 4 to exon 7 using the normal splice sites. AO E7.7 targeted the splice donor site on exon 7; it reduced tau mRNA expression by 30% and tau protein levels by 67%. E5.3 injected into mice *in vivo* produced lower tau mRNA levels than in non-injected regions.

GSK-β

Farr *et al.* [120] showed that a phosphorothioated AO that targets GSK-3β decreased GSK-3β protein levels in the cortex of SAMP8 mice. There were improvements in learning and memory, reduced oxidative stress, increased levels of the antioxidant transcription factor nuclear factor erythroid-2 related factor 2, and decreased tau phosphorylation.

Acetylcholinesterase (AChE)

Fu *et al.* [121] found that AOs against human AChE mRNA reduced AChE activity in an AD mouse model after 8 h; the effect lasted till 42 h. Lower enzymic activity was accompanied by improvement on behavioral tasks, which showed increased memory retention and improved water maze performance (shorter swimming time).

Apolipoprotein E receptor 2 (ApoER2)

ApoER2 may be a primary risk factor for late-onset AD [122, 123]. Dysregulation of ApoER2 splicing may result in impaired synaptic homeostasis. Cerebral injection of mice with AOs targeting the adjacent introns enhanced exon 19 inclusion, an effect that persisted for up to 6 months [123]. The mice showed improvement in Aβ-induced cognitive defects. It was postulated that the AOs bind to the splicing factor SRF1 to reduce its expression and increase the inclusion of exon 19, thereby increasing the level of the active form of ApoER2 to enhance NMDA receptor phosphorylation.

siRNA

These are short synthetic double stranded RNA oligonucleotides that target complementary mRNA and silence gene expression through the assembly of the RNA-induced silencing complex (RISC) (Figure 3) [93, 124]. Chemical modifications can be introduced into the siRNA to increase its stability against nucleases and increase its selectivity for the target (Figure 4).

APP

Miller and colleagues [125] found that siRNAs against the Swedish mutant in APP that causes a familial form of AD silenced the expression of mutant alleles. The siRNAs were designed to ensure that they bound specifically to the mutant alleles and not the wild-type. The mutation was placed in the central region of the siRNA duplex to achieve high silencing efficiency.

BACE1

McSwiggen and colleagues [126] patented 325 siRNAs that target BACE (NCBI ID: NM_012104). The patent covers sequences with various chemically modified siRNAs that include 2'-deoxy, 2'-F and 2'-OMe pyrimidine and purine nucleotides, phosphorothioate internucleotide linkages and inverted deoxyabasic caps. Four of the siRNAs reduced BACE expression by 40–90% at 25 nM concentration, but there was no data on whether this altered $A\beta_{40}$ and $A\beta_{42}$ expression. Basi *et al*. [127] made a siRNA that reduced the BACE1 mRNA level by 50% and BACE protein level by more than 90%. It decreased the secretion of Aβ peptide without affecting BACE2 expression, indicating specificity for BACE1. Kao *et al*. [128] also designed siRNAs, where two of the siRNAs reduced BACE1 mRNA by more than 90% and Aβ production by 36–41%. Pretreatment of neurons with the siRNA increased neuroprotection against hydrogen peroxide-induced oxidative stress. Modarresi *et al.* [129] injected LNA-modified siRNAs

targeting BACE1 antisense transcripts into the third ventricle of Tg-19959 mice to downregulate BACE1 and BACE1 antisense transcripts, which led to lower BACE1 protein levels and less Aβ production and aggregation in the brain. Notably, Cai *et al*. [130] showed that siRNAs targeting BACE1 inhibited it in mice and increased choroidal neovascularization: BACE1 is also expressed in the neural retina and in *in vitro* and *in vivo* angiogenesis. Although BACE1 inhibition may be therapeutically beneficial in AD, it may contribute to retinal pathologies and exacerbate conditions such as age-related macular degeneration.

Heterogeneous nuclear ribonucleoprotein H

A G-rich region in exon 3 of BACE1 may form a G-quadruplex structure and recruit a splicing regulator, heterogeneous nuclear ribonucleoprotein H, that regulates splicing to increase generation of the BACE1 501 isoform. Fisette *et al*. [131] reported that siRNA and short hairpin RNA candidates that target heterogeneous nuclear ribonucleoprotein H reduced its expression and thereby decreased BACE1 501 isoform levels and Aβ production.

AntimiRs and miRNA mimics

miRNAs are short non-coding RNAs that regulate protein expression post-transcriptionally. miRNA mimics can modulate RNA and protein expression by acting like their endogenous miRNA counterparts. AntimiRs can modulate RNA and protein expression by inhibiting endogenous miRNA similar to AOs (Figure 3). miRNAs silence gene expression by translational repression and/or mRNA degradation [132, 133]. miRNAs are first transcribed by RNA polymerases II or III to form long primary miRNA with a 5′ CAP and a poly(A) tail [133-135]. These are then processed in the nucleus into short 70-nucleotide hairpin structures called precursor miRNAs (pre-miRNA) by the microprocessor complex [133-135]. The pre-miRNAs are exported to the cytoplasm by Exportin 5 and processed by Dicer into double-stranded miRNA duplexes, which are approximately 22 nucleotides long [133-135].

BACE1

An endogenous non-coding BACE1 antisense transcript stabilizes the BACE1 transcript and may upregulate BACE1 in AD cases. BACE1 antisense binds to BACE1 at the miR-485-5p binding site and suppresses BACE1 expression. Faghihi *et al*. [136] found that LNA-antimiRs that target miR-485-5p decreased miRNA-induced suppression of BACE1 and increased BACE1 antisense expression. Hebért *et al*. [137] showed that miR-29a/b-1 cluster was significantly reduced in sporadic AD patients and correlated with increased BACE1 expression and Aβ

generation, and therefore may be potential targets for miRNA mimics as a therapeutic strategy for AD.

Tau

Mi34a reduces endogenous tau expression at both the mRNA and protein level in M17D cells by binding to the 3' UTR region of tau [110], whereas miR-34c levels are elevated in the hippocampus of AD patients and mouse AD models [138]. Wolfe *et al.* [110] used LNA antimiRs to inhibit miR-34a, -34b and -34c and found increased tau expression. Zovolis *et al.* [138] found that an antimiR that targets miR-34c rescued learning in mouse models.

Acetyl-CoA acyl transferase

Acetyl-CoA acyl transferase has a role in lipid metabolism that has been implicated in the pathogenesis of AD. Murphy *et al.* [139] inhibited Acetyl-CoA acyl transferase using an artificial miRNA to reduce Aβ plaque burden and improve cognition in a mouse model of AD. The miRNA also reduced full-length human APP levels.

Brain-derived neurotropic factor

Brain-derived neurotropic factor regulates synaptic plasticity and memory and is decreased in AD brains [140-142], while miR-206 suppresses brain-derived neurotropic factor levels and memory function in AD mice [143]. Lee *et al.* [143] injected an anti-miR candidate AM-206 that targets miR-206 into the third ventricle of Tg2576 mice. It increased brain levels of brain-derived neurotropic factor, enhanced hippocampal synaptic density, neurogenesis, and memory. Intranasally administered AM-206 also reached the brain and had similar effects to the injected AM-206.

DNAzymes/Ribozymes as therapeutic candidates for AD

A target RNA can be cleaved to reduce its expression using catalytic oligonucleotides such as DNAzymes and ribozymes [144]. The arms of these enzymes hybridise with the target RNA and cleave their targets through the catalytic loop in the middle. DNAzymes and ribozymes cleave the phosphodiester bond at the purine-pyrimidine or purine-purine junction (Figure 3).

BACE1

Nawrot *et al.* [145] designed RNA-cleaving hammerhead ribozymes that downregulated BACE1 mRNA expression by more than 90% in HEK293 and SH-SY5Y cells and reduced $A\beta_{40}$ and $A\beta_{42}$ production by more than 80%. They also showed that a DNAzyme with the 10–23 catalytic loop reduced BACE mRNA expression by 70%. However, whether the reduced BACE mRNA expression leads to reduced Aβ production is unknown and requires validation.

Nucleic acid aptamers

Aptamers are short single stranded RNA or DNA oligonucleotides with unique three-dimensional structure that bind to targets with high affinity and specificity. Aptamers can be developed against a variety of targets ranging from small molecules to complex proteins over whole cells. Aptamers can be used for therapeutic, diagnostic (biosensors and molecular imaging), and targeted drug delivery applications. They are typically selected from large DNA and RNA oligonucleotide libraries through a process called Systematic Evolution of Ligands by EXponential enrichment (SELEX) [146, 147].

Aβ

Ylera *et al.* [148] were the first to report novel RNA aptamers that bound to $A\beta_{1-40}$ fibrils with high affinity (29–48 nM). Bunka *et al.* [149] made aptamers against amyloid-like fibrils from β_2-microglobulin. They bound to the target with high affinity, but also bound to other amyloid fibrils including, but not confined to, those found in dialysis-related amyloidosis patients. Rahimi *et al.* [150] also developed RNA aptamers against Aβ fibrils, but these also interacted with other amyloidogenic proteins by binding to a common β-sheet motif. They bound to fibrils with ≥15-fold higher sensitivity than thioflavin-T, suggesting that aptamers might be diagnostic tools for AD. Takahashi *et al.* [151] isolated two RNA aptamers, N2 and E2, that bound to monomeric $A\beta_{40}$ with dissociation constants of 21.6 and 10.9 µM respectively. Though the affinities were quite low for clinical use, enzyme-linked immunosorbent assay (ELISA) showed that they could inhibit Aβ aggregation efficiently. When conjugated to AuNP gold nanoparticles, N2 and E2 bound to both Aβ monomers and oligomers. Mathew *et al.* [152] showed that the N2 aptamer conjugated to curcumin-polymer nanoparticles enhanced binding to, and disaggregated, amyloid plaques, which were then cleared by phagocytosis. The study targeted peripheral amyloid as peripheral organs may also generate amyloid proteins, which have also been implicated in AD. Targeting peripheral amyloid is easier due to the challenges in the brain delivery of aptamers.

Farrar *et al.* [153] developed a fluorescently tagged aptamer that bound to Aβ oligomers in both AD and transgenic mouse brain tissue. The aptamer may be useful for Aβ imaging, which has diagnostic implications. Similarly, Babu and colleagues [154]

developed an aptamer complexed with ruthenium that binds to, and inhibits the formation of, Aβ oligomers. The aptamer-ruthenium interaction increases luminescence intensity, which is reduced when the aptamer binds to Aβ monomer or oligomers.

BACE1

Rentmeister *et al.* [155] made an RNA aptamer that binds to the short cytoplasmic tail of BACE1. It is a good research tool to investigate the biological function of the cytoplasmic tail without interfering with BACE1 transport and localization. Liang *et al.* [156] developed two DNA aptamers, A1 and A4, that bind to the extracellular domain of BACE1 with high affinity (K_d 15–69 nM) and specificity. They have similar affinities to the anti-BACE1 antibody. *In vitro*, APP Swedish mutant cells treated with A1 showed lower $A\beta_{40}$ and $A\beta_{42}$ levels than control cells. sAPPβ expression decreased with A1 treatment compared with untreated controls.

Tau

Kim *et al.* [157] used recombinant his-tagged tau40 to select aptamers from an RNA library through SELEX. 12 rounds of selection produced a tau-1 aptamer, which represented ~76% of identified aptamers, that reduced the levels of oligomeric tau (by ~94%) *in vitro* in a dose-dependent manner. However, it could not de-oligomerize pre-existing tau oligomers and had no effect on tau degradation. The aptamer bound to tau protein and inhibited its oligomerization, unlike control aptamers. Primary neurons treated with tau-1 aptamer showed less cytotoxicity than controls but no difference in membrane integrity or viability; there was little effect on normal tau function. Primary rat cortical neurons administered tau oligomers and treated with tau-1 aptamers showed significantly less oligomeric tau phosphorylation at Ser199/202 but there was no effect on monomeric tau. Extracellular tau oligomers also stress neighboring neurons. Administration of tau oligomers leads to severe neurotoxicity, which was reduced by tau-1 aptamer treatment. Tau-1 aptamers can prevent or reverse cytotoxicity mediated by tau oligomerization both in a non-neuronal cell line and in primary rat cortical neurons. Unfortunately, the tau-1 aptamers isolated by Kim *et al.* bound only to one of the six isoforms of tau. Therefore, the effects of tau-1 aptamers observed in mice may not translate clinically, because six isoforms are prone to aggregation and implicated in neurodegeneration. To be successful clinically, the aptamers must be able to cross the BBB and the neuronal cell membrane, and disaggregate the neurofibrillary tangles after binding

[158]. Kim *et al.* [159] reported a DNA aptamer-antibody sandwiched to the tau-381 isoform that detected tau in human plasma at femtomolar concentrations by surface plasmon resonance.

The ubiquitin-proteasome system

Lee *et al.* [160] developed an aptamer against USP14, an enzyme that delays protein degradation by the ubiquitin-proteasome system. Recombinant USP14 was incubated with a random RNA library for SELEX. Three aptamers, USP14-1, USP14-2 and USP-14-3, were identified, all of which bound to USP14 with high affinity. USP14-3 showed the strongest inhibition of deubiquitination, which may be due to its ability to bind both USP14 and UCH37. UCH37 is a protein that also slows protein degradation in the proteasome. The aptamers have yet to be tested in mice for their effect on tau oligomerization and degeneration.

Prion protein

Mashima *et al.* [161] isolated aptamers against bovine prion protein by SELEX that may have therapeutic potential in prion diseases and AD. Aβ oligomers bind to the prion protein to block long-term potentiation. Thus, prion protein may mediate Aβ oligomer-induced synaptic dysfunction.

Brain delivery of nucleic acid molecules

Receptor-mediated endocytosis or nanoparticle conjugation strategies

The barrier for any successful drug to treat neurological diseases is its failure to cross the BBB. Various approaches have been made to overcome this issue, and in many instances the drug can be conjugated with other molecules to improve brain delivery. Lipophilic molecules under 500 Da can cross the BBB by simple diffusion. Therapeutic nucleic acids are typically too large to cross the BBB, although nanotechnology is now starting to overcome this problem. This was the subject of a comprehensive review by Kanwar *et al.* [162]. Nucleic acids can be transported through the BBB by receptor-mediate endocytosis when conjugated to molecules such as transferrin, insulin, leptin, and insulin-like growth factor 1: these bind to their receptors on the BBB, which allows them to cross the BBB. Many studies have used nucleic acids conjugated to molecules that target the transferrin receptor. Transferrin-conjugated nanoparticles, or nanoparticles conjugated to transferrin receptor antibodies, can transport drugs across the BBB [163, 164]. An aptamer that targeted the mouse transferrin receptor allowed a lysosomal enzyme to enter cells via endocytosis; this can be applied to drug transport [165]. Two aptamers that

bound to epithelial cell adhesion molecule and transferrin receptor were fused together; the product could bind to cancer cells expressing the epithelial cell adhesion molecule after crossing the BBB by transferrin-receptor targeting [166].

Cell-penetrating peptide-based delivery systems

The use of cell-penetrating peptide-based delivery systems is another approach for transporting nucleic acids across the BBB. These systems generally contain between 8 and 30 amino acids. Fluorescein isothiocyanate-labeled cell-penetrating peptides were conjugated to a morpholino AO targeting the mutant *ataxia telangiectasia* gene and were able to cross the BBB [167]. Heitz *et al.* [168] reviewed the development of cell-penetrating peptides.

Intracerebroventricular infusion

Nucleic acids can also be introduced directly into the cerebrospinal fluid by intracerebroventricular infusion. The advantage of this over the use of targeting molecules is that the drugs are delivered at therapeutic concentrations quickly. However, intracerebroventricular infusions are highly invasive and rely on diffusion of the drugs throughout the ventricular system. The drugs can then enter the blood stream, because the cerebrospinal fluid turns over every 4–5 hours [169]. Pardridge *et al.* [169] described the advantages and disadvantages of different drug delivery methods to the brain. Intranasal methods are non-invasive and can deliver nucleic acids directly to the brain. They have been used successfully to deliver insulin to AD patients [170]. Various molecules delivered intranasally have improved cognitive function in a mouse model of AD and in clinical trials, as summarized in the review by Hanson *et al.* [171]. Many reviews describe how nose-to-brain delivery occurs, the different drugs that have been successfully delivered this way, and its potential for treating neurodegenerative diseases such as AD [172, 173].

Conclusions and Future Perspectives

Nucleic acid-based approaches offer great promise for developing novel therapeutics for AD, a complex neurodegenerative disease with several pathological features. Confounds include genetic factors, metabolic disorders including high cholesterol levels, insulin resistance due to impaired glucose metabolism, and dysfunction in various molecular pathways. Existing therapies only treat AD symptoms, not the underlying molecular causes. Although many drug molecules have shown success in cell and animal models, this effect often cannot be replicated in human trials. There is an unmet need for

better theranostic strategies. The drug Nusinersen, recently approved by the FDA for spinal muscular atrophy, shows that nucleic acids have potential for the treatment of neurological diseases, including AD. Their efficacy in targeting several pathways that underlie AD highlights their potential to be developed as novel therapeutics for AD.

Abbreviations

FDA: Food and Drug Administration; AD: Alzheimer's disease; AO: antisense oligonucleotides; NMDA: N-methyl-D- aspartate receptor; Aβ: amyloid β; APP: amyloid precursor protein; BACE1: β-site amyloid precursor protein cleaving enzyme 1; PSEN: Presenilin; tau: microtubule associated protein; siRNA: small interfering RNA; antimiR: anti-microRNA; 2′-OMe: 2′-O-methyl; 2′-MOE: 2′-O-methoxyethyl; 2′-F: 2′-fluoro; LNA: locked nucleic acids; PNA: peptide nucleic acids; PMO: phosphorodiamidate morpholino; tcDNA: tricyclo-DNA; CeNA: cyclohexenyl nucleic acid; PEG: polyethylene glycol; mRNA: messenger RNA; SAMP8: senescence- accelerated mouse-prone 8; BBB: blood brain barrier; AChE: acetylcholinesterase; ApoER2: Apolipoprotein E receptor 2; RISC: RNA induced silencing complex; SELEX: systemic evolution of ligands by exponential enrichment.

Acknowledgements

Competing Interests

The authors have declared that no competing interest exists.

References

1. Mendell JR, Goemans N, Lowes LP, Alfano LN, Berry K, Shao J, et al. Longitudinal effect of eteplirsen versus historical control on ambulation in Duchenne muscular dystrophy. Ann Neurol. 2016; 79: 257–271.
2. Crooke ST, Geary RS. Clinical pharmacological properties of mipomersen (Kynamro), a second generation antisense inhibitor of apolipoprotein B. Br J Clin Pharmacol. 2013; 76: 269–276.
3. Vitravene Study Group. A randomized controlled clinical trial of intravitreous fomivirsen for treatment of newly diagnosed peripheral cytomegalovirus retinitis in patients with AIDS. Am J Ophthalmol. 2002; 133: 467–474.
4. Macugen Diabetic Retinopathy Study Group. A phase II randomized double-masked trial of pegaptanib, an anti-vascular endothelial growth factor aptamer, for diabetic macular edema. Ophthalmology. 2005; 112: 1747–1757.
5. Prince M, Comas-Herrera A, Knapp M, Guerchet M, Karagiannidou M. World Alzheimer Report 2016: Improving healthcare for people living with dementia. In: Rees G, editor. World Alzheimer Report. London, UK: London School of Economics and Political Sciences; 2016:140.
6. [No authors listed]. Alzheimers Association Update. Alzheimers Dement (Amst). 2015; 11: 104–105.
7. Birks JS. Cholinesterase inhibitors for Alzheimer's disease. Cochrane Database Syst Rev. 2006.
8. Olivares D, Deshpande VK, Shi Y, Lahiri DK, Greig NH, Rogers JT, et al. *N*-methyl D-aspartate (NMDA) receptor antagonists and memantine

treatment for Alzheimer's disease, vascular dementia and Parkinson's disease. Curr Alzheimer Res. 2012; 9: 746–758.

9. Robinson SW, Fernandes M, Husi H. Current advances in systems and integrative biology. Comput Struct Biotechnol J. 2014; 11: 35–46.

10. Haass C, Selkoe DJ. Soluble protein oligomers in neurodegeneration: lessons from the Alzheimer's amyloid β-peptide. Nat Rev Mol Cell Biol. 2007; 8: 101–112.

11. Selkoe DJ. Alzheimer's disease: genes, proteins, and therapy. Physiol Rev. 2001; 81: 741–766.

12. Blennow K, de Leon MJ, Zetterberg H. Alzheimer's disease. The Lancet. 2006; 368: 387–403.

13. Haass C, Selkoe DJ. Cellular processing of beta-amyloid precursor protein and the genesis of amyloid β-peptide. Cell. 1993; 75: 1039–1042.

14. Selkoe DJ. Translating cell biology into therapeutic advances in Alzheimer's disease. Nature. 1999; 399: A23–A31.

15. Wilquet V, De Strooper B. Amyloid-β precursor protein processing in neurodegeneration. Curr Opin Neurol. 2004; 14: 582–588.

16. Selkoe DJ. Normal and abnormal biology of the β-amyloid precursor protein. Annu Rev Neurosci. 1994; 17: 489–517.

17. Tanzi RE, Bertram L. Twenty years of the Alzheimer's disease amyloid hypothesis: a genetic perspective. Cell. 2005; 120: 545–555.

18. Hardy JA, Higgins GA. Alzheimer's disease: the amyloid cascade hypothesis. Science. 1992; 256: 184-185.

19. Lahiri DK, Farlow MR, Greig NH, Sambamurti K. Current drug targets for Alzheimer's disease treatment. Drug Dev Res. 2002; 56: 267–281.

20. Palop JJ, Mucke L. Amyloid-β-induced neuronal dysfunction in Alzheimer's disease: from synapses toward neural networks. Nat Neurosci. 2010; 13: 812–818.

21. Sindi IA, Tannenberg RK, Dodd PR. Role for the neurexin-neuroligin complex in Alzheimer's disease. Neurobiol Aging. 2014; 35: 746–756.

22. Ondrejcak T, Klyubin I, Hu N-W, Barry AE, Cullen WK, Rowan MJ. Alzheimer's disease amyloid β-protein and synaptic function. Neuromolecular Med. 2010; 12: 13–26.

23. Danysz W, Parsons CG. Alzheimer's disease, β-amyloid, glutamate, NMDA receptors and memantine–searching for the connections. Br J Pharmacol. 2012; 167: 324–352.

24. Scheltens P, Feldman H. Treatment of Alzheimer's disease; current status and new perspectives. Lancet Neurol. 2003; 2: 539–547.

25. Ferreira ST, Clarke JR, Bomfim TR, De Felice FG. Inflammation, defective insulin signaling, and neuronal dysfunction in Alzheimer's disease. Alzheimers Dement (Amst). 2014; 10: S76–S83.

26. Hoyer S. Glucose metabolism and insulin receptor signal transduction in Alzheimer disease. Eur J Pharmacol. 2004; 490: 115–125.

27. Maulik M, Westaway D, Jhamandas J, Kar S. Role of cholesterol in APP metabolism and its significance in Alzheimer's disease pathogenesis. Mol Neurobiol. 2013; 47: 37–63.

28. Lee VM, Goedert M, Trojanowski JQ. Neurodegenerative tauopathies. Annu Rev Neurosci. 2001; 24: 1121–1159.

29. Iqbal K, Alonso AdC, Chen S, Chohan MO, El-Akkad E, Gong C-X, et al. Tau pathology in Alzheimer disease and other tauopathies. Biochim Biophys Acta Mol Bas Dis. 2005; 1739: 198–210.

30. Medina M, Avila J. New perspectives on the role of tau in Alzheimer's disease. Implications for therapy. Biochem Pharmacol. 2014; 88: 540–547.

31. Hernandez F, Avila J. Tauopathies. Cell Mol Life Sci. 2007; 64: 2219–2233.

32. Brandt R, Hundelt M, Shahani N. Tau alteration and neuronal degeneration in tauopathies: mechanisms and models. Biochim Biophys Acta Mol Bas Dis. 2005; 1739: 331–354.

33. Hart GW, Slawson C, Ramirez-Correa G, Lagerlof O. Cross talk between *O*-GlcNAcylation and phosphorylation: roles in signaling, transcription, and chronic disease. Annu Rev Biochem. 2011; 80: 825–858.

34. Feldman H, Gauthier S, Hecker J, Vellas B, Emir B, Mastey V, et al. Efficacy of donepezil on maintenance of activities of daily living in patients with moderate to severe Alzheimer's disease and the effect on caregiver burden. J Am Geriatr Soc. 2003; 51: 737–744.

35. McKeith I, Del Ser T, Spano P, Emre M, Wesnes K, Anand R, et al. Efficacy of rivastigmine in dementia with Lewy bodies: a randomised, double-blind, placebo-controlled international study. The Lancet. 2000; 356: 2031–2036.

36. Raskind M, Peskind E, Wessel T, Yuan W, Galantamine USA Study Group. Galantamine in AD A 6-month randomized, placebo-controlled trial with a 6-month extension. Neurology. 2000; 54: 2261–2268.

37. Tariot PN, Farlow MR, Grossberg GT, Graham SM, McDonald S, Gergel I, et al. Memantine treatment in patients with moderate to severe Alzheimer disease already receiving donepezil: a randomized controlled trial. JAMA. 2004; 291: 317–324.

38. Wang X, Wang W, Li L, Perry G, Lee H-g, Zhu X. Oxidative stress and mitochondrial dysfunction in Alzheimer's disease. Biochim Biophys Acta Mol Bas Dis. 2014; 1842: 1240–1247.

39. Pimplikar SW. Neuroinflammation in Alzheimer's disease: from pathogenesis to a therapeutic target. J Clin Immunol. 2014; 34: 64–69.

40. Freiherr J, Hallschmid M, Frey II WH, Brünner YF, Chapman CD, Hölscher C, et al. Intranasal insulin as a treatment for Alzheimer's disease: a review of basic research and clinical evidence. CNS Drugs. 2013; 27: 505–514.

41. Ribarič S. The rationale for insulin therapy in Alzheimer's disease. Molecules. 2016; 21: E689.

42. Galimberti D, Scarpini E. Progress in Alzheimer's disease. J Neurol. 2012; 259: 201–211.

43. Mangialasche F, Solomon A, Winblad B, Mecocci P, Kivipelto M. Alzheimer's disease: clinical trials and drug development. Lancet Neurol. 2010; 9: 702–716.

44. Karran E. Current status of vaccination therapies in Alzheimer's disease. J Neurochem. 2012; 123: 647–651.

45. St George-Hyslop PH, Morris JC. Will anti-amyloid therapies work for Alzheimer's disease? The Lancet. 2008; 372: 180–182.

46. Ballard C, Gauthier S, Corbett A, Brayne C, Aarsland D, Jones E. Alzheimer's disease. The Lancet. 2011; 377: 1019–1031.

47. Santa-Maria I, Hernández F, Del Rio J, Moreno FJ, Avila J. Tramiprosate, a drug of potential interest for the treatment of Alzheimer's disease, promotes an abnormal aggregation of tau. Mol Neurodegener. 2007; 2: 17.

48. Aisen PS, Saumier D, Briand R, Laurin J, Gervais F, Tremblay P, et al. A Phase II study targeting amyloid-beta with 3APS in mild-to-moderate Alzheimer disease. Neurology. 2006; 67: 1757–1763.

49. Gervais F, Chalifour R, Garceau D, Kong X, Laurin J, McLaughlin R, et al. Glycosaminoglycan mimetics: a therapeutic approach to cerebral amyloid angiopathy. Amyloid. 2001; 8 Suppl 1: 28–35.

50. Bilikiewicz A, Gaus W. Colostrinin (a naturally occurring, proline-rich, polypeptide mixture) in the treatment of Alzheimer's disease. J Alzheimers Dis. 2004; 6: 17–26.

51. Leszek J, Inglot AD, Janusz M, Lisowski J, Krukowska K, Georgiades JA. Colostrinin: a proline-rich polypeptide (PRP) complex isolated from ovine colostrum for treatment of Alzheimer's disease. A double-blind, placebo-controlled study. Archivum Immunologiæ et Therapiæ Experimentalis. 1999; 47: 377–385.

52. Popik P, Bobula B, Janusz M, Lisowski J, Vetulani J. Colostrinin, a polypeptide isolated from early milk, facilitates learning and memory in rats. Pharmacol Biochem Behav. 1999; 64: 183–189.

53. Townsend KP, Praticò D. Novel therapeutic opportunities for Alzheimer's disease: focus on nonsteroidal anti-inflammatory drugs. FASEB J. 2005; 19: 1592–1601.

54. Gilman S, Koller M, Black RS, Jenkins L, Griffith SG, Fox NC, et al. Clinical effects of Aβ immunization (AN1792) in patients with AD in an interrupted trial. Neurology. 2005; 64: 1553–1562.

55. Salloway S, Sperling R, Fox NC, Blennow K, Klunk W, Raskind M, et al. Two phase 3 trials of bapineuzumab in mild-to-moderate Alzheimer's disease. N Engl J Med. 2014; 370: 322–333.

56. Doody RS, Thomas RG, Farlow M, Iwatsubo T, Vellas B, Joffe S, et al. Phase 3 trials of solanezumab for mild-to-moderate Alzheimer's disease. N Engl J Med. 2014; 370: 311–321.

57. Relkin N. Clinical trials of intravenous immunoglobulin for Alzheimer's disease. J Clin Immunol. 2014; 34: 74–79.

58. Moreth J, Mavoungou C, Schindowski K. Passive anti-amyloid immunotherapy in Alzheimer's disease: What are the most promising targets? Immunity and Ageing. 2013; 10: 18.

59. McGeer PL, McGeer EG. The amyloid cascade-inflammatory hypothesis of Alzheimer disease: implications for therapy. Acta Neuropathol. 2013; 126: 479–497.

60. Kukar T, Prescott S, Eriksen JL, Holloway V, Murphy MP, Koo EH, et al. Chronic administration of R-flurbiprofen attenuates learning impairments in transgenic amyloid precursor protein mice. BMC Neurosci. 2007; 8: 54.

61. Galasko DR, Graff-Radford N, May S, Hendrix S, Cottrell BA, Sagi SA, et al. Safety, tolerability, pharmacokinetics, and Aβ levels after short-term administration of R-flurbiprofen in healthy elderly individuals. Alzheimer Disease and Associated Disorders. 2007; 21: 292–299.

62. Wilcock GK, Black SE, Hendrix SB, Zavitz KH, Swabb EA, Laughlin MA, et al. Efficacy and safety of tarenflurbil in mild to moderate Alzheimer's disease: a randomised phase II trial. The Lancet Neurology. 2008; 7: 483–493.

63. Siemers ER, Quinn JF, Kaye J, Farlow MR, Porsteinsson A, Tariot P, et al. Effects of a γ-secretase inhibitor in a randomized study of patients with Alzheimer disease. Neurology. 2006; 66: 602–604.

64. Coric V, Salloway S, van Dyck C, Kerselaers W, Kaplita S, Curtis C, et al. A phase II study of the γ-secretase inhibitor avagacestat (BMS-708163) in predementia Alzheimer's disease. Alzheimers Dement (Amst). 2013; 9: P283.

65. Kennedy ME, Stamford AW, Chen X, Cox K, Cumming JN, Dockendorf MF, et al. The BACE1 inhibitor verubecestat (MK-8931) reduces CNS β-amyloid in animal models and in Alzheimer's disease patients. Science Translational Medicine. 2016; 8: 363ra150.

66. Miller BW, Willett KC, Desilets AR. Rosiglitazone and pioglitazone for the treatment of Alzheimer's disease. Ann Pharmacother. 2011; 45: 1416–1424.

67. Wischik CM, Edwards PC, Lai RY, Roth M, Harrington CR. Selective inhibition of Alzheimer disease-like tau aggregation by phenothiazines. Proc Natl Acad Sci USA. 1996; 93: 11213–11218.

68. Martinez A, Gil C, Perez DI. Glycogen synthase kinase 3 inhibitors in the next horizon for Alzheimer's disease treatment. Int J Alzheimers Dis. 2011; 2011: 280502.

69. Lovestone S, Boada M, Dubois B, Hüll M, Rinne JO, Huppertz H-J, et al. A phase II trial of tideglusib in Alzheimer's disease. J Alzheimers Dis. 2015; 45: 75–88.

70. Mecocci P, Polidori MC. Antioxidant clinical trials in mild cognitive impairment and Alzheimer's disease. Biochim Biophys Acta Mol Bas Dis. 2012; 1822: 631–638.

71. Ray B, Lahiri DK. Neuroinflammation in Alzheimer's disease: different molecular targets and potential therapeutic agents including curcumin. Curr Opin Pharmacol. 2009; 9: 434–444.

72. Wyss-Coray T. Inflammation in Alzheimer disease: driving force, bystander or beneficial response? Nat Med. 2006; 12: 1005–1015.

73. Heneka MT, Carson MJ, El Khoury J, Landreth GE, Brosseron F, Feinstein DL, et al. Neuroinflammation in Alzheimer's disease. Lancet Neurol. 2015; 14: 388–405.

74. Yarchoan M, Arnold SE. Repurposing diabetes drugs for brain insulin resistance in Alzheimer disease. Diabetes. 2014; 63: 2253–2261.

75. Casserly I, Topol EJ. Convergence of atherosclerosis and Alzheimer's disease: inflammation, cholesterol, and misfolded proteins. The Lancet. 2004; 363: 1139–1146.

76. De Mesmaeker A, Haener R, Martin P, Moser HE. Antisense oligonucleotides. Acc Chem Res. 1995; 28: 366–374.

77. Lipi F, Chen S, Chakravarthy M, Rakesh S, Veedu RN. *In vitro* evolution of chemically-modified nucleic acid aptamers: pros and cons, and comprehensive selection strategies. RNA Biol. 2016; 13: 1232-1245.

78. Chan JH, Lim S, Wong W. Antisense oligonucleotides: from design to therapeutic application. Clin Exp Pharmacol Physiol. 2006; 33: 533–540.

79. Vu H, Hirschbein BL. Internucleotide phosphite sulfurization with tetraethylthiuram disulfide. Phosphorothioate oligonucleotide synthesis via phosphoramidite chemistry. Tetrahedron Lett. 1991; 32: 3005-3008.

80. Majlessi M, Nelson NC, Becker MM. Advantages of 2′-O-methyl oligoribonucleotide probes for detecting RNA targets. Nucleic Acids Res. 1998; 26: 2224-2229.

81. Kawasaki AM, Casper MD, Freier SM, Lesnik EA, Zounes MC, Cummins LL, et al. Uniformly modified 2'-deoxy-2'-fluoro-phosphorothioate oligonucleotides as nuclease-resistant antisense compounds with high affinity and specificity for RNA targets. J Med Chem. 1993; 36: 831-841.

82. Geary RS, Watanabe TA, Truong L, Freier S, Lesnik EA, Sioufi NB, et al. Pharmacokinetic properties of 2′-O-(2-methoxyethyl)-modified oligonucleotide analogs in rats. J Pharmacol Exp Ther. 2001; 296: 890-897.

83. Summerton J, WELLER D. Morpholino antisense oligomers: design, preparation, and properties. Antisense Nucleic Acid Drug Dev. 1997; 7: 187-195.

84. Veedu RN, Wengel J. Locked nucleic acids: promising nucleic acid analogs for therapeutic applications. Chem Biodivers. 2010; 7: 536-542.

85. Veedu RN, Wengel J. Locked nucleic acid as a novel class of therapeutic agents. RNA Biol. 2009; 6: 321-323.

86. Hyrup B, Nielsen PE. Peptide nucleic acids (PNA): synthesis, properties and potential applications. Bioorg Med Chem. 1996; 4: 5-23.

87. Renneberg D, Leumann CJ. Watson− Crick base-pairing properties of tricyclo-DNA. J Am Chem Soc. 2002; 124: 5993-6002.

88. Wang J, Verbeure B, Luyten I, Lescrinier E, Froeyen M, Hendrix C, et al. Cyclohexene nucleic acids (CeNA): serum stable oligonucleotides that activate RNase H and increase duplex stability with complementary RNA. J Am Chem Soc. 2000; 122: 8595-8602.

89. Ikeda Y, Nagasaki Y. Impacts of PEGylation on the gene and oligonucleotide delivery system. J Appl Polym Sci. 2014; 131.

90. Knop K, Hoogenboom R, Fischer D, Schubert US. Poly (ethylene glycol) in drug delivery: pros and cons as well as potential alternatives. Angew Chem Int Ed. 2010; 49: 6288-6308.

91. White PJ, Anastasopoulos F, Pouton CW, Boyd BJ. Overcoming biological barriers to in vivo efficacy of antisense oligonucleotides. Expert Rev Mol Med. 2009; 11.

92. Juliano RL. The delivery of therapeutic oligonucleotides. Nucleic Acids Res. 2016; 44: 6518-6548.

93. Bennett CF, Swayze EE. RNA targeting therapeutics: molecular mechanisms of antisense oligonucleotides as a therapeutic platform. Annu Rev Pharmacol Toxicol. 2010; 50: 259–293.

94. Kole R, Krainer AR, Altman S. RNA therapeutics: beyond RNA interference and antisense oligonucleotides. Nat Rev Drug Discov. 2012; 11: 125–140.

95. Allinquant B, Hantraye P, Mailleux P, Moya K, Bouillot C, Prochiantz A. Downregulation of amyloid precursor protein inhibits neurite outgrowth *in vitro*. J Cell Biol. 1995; 128: 919–927.

96. Dobie K. Antisense modulation of amyloid β protein precursor expression. US: Scios Inc., Fremont, CA (US); 2007.

97. Kumar VB, Farr SA, Flood JF, Kamlesh V, Franko M, Banks WA, et al. Site-directed antisense oligonucleotide decreases the expression of amyloid precursor protein and reverses deficits in learning and memory in aged SAMP8 mice. Peptides. 2000; 21: 1769–1775.

98. Kumar VB. Antisense modulation of amyloid β protein expression. US: St. Louis University, St. Louis, MO (US); 2001.

99. Banks WA, Farr SA, Butt W, Kumar VB, Franko MW, Morley JE. Delivery across the blood-brain barrier of antisense directed against amyloid β: reversal of learning and memory deficits in mice overexpressing amyloid precursor protein. J Pharmacol Exp Ther. 2001; 297: 1113–1121.

100. Poon HF, Farr SA, Banks WA, Pierce WM, Klein JB, Morley JE, et al. Proteomic identification of less oxidized brain proteins in aged senescence-accelerated mice following administration of antisense oligonucleotide directed at the Aβ region of amyloid precursor protein. Brain Res Mol Brain Res. 2005; 138: 8–16.

101. Opazo P, Saud K, de Saint Pierre M, Cárdenas AM, Allen DD, Segura-Aguilar J, et al. Knockdown of amyloid precursor protein normalizes cholinergic

102. Saud K, Arriagada C, Cárdenas AM, Shimahara T, Allen DD, Caviedes R, et al. Neuronal dysfunction in Down syndrome: contribution of neuronal models in cell culture. Journal of Physiology, Paris. 2006; 99: 201–210.

103. Rojas G, Cárdenas AM, Fernández-Olivares P, Shimahara T, Segura-Aguilar J, Caviedes R, et al. Effect of the knockdown of amyloid precursor protein on intracellular calcium increases in a neuronal cell line derived from the cerebral cortex of a trisomy 16 mouse. Exp Neurol. 2008; 209: 234–242.

104. Chauhan NB. Trafficking of intracerebroventricularly injected antisense oligonucleotides in the mouse brain. Antisense Nucleic Acid Drug Dev. 2002; 12: 353–357.

105. Chauhan NB, Siegel GJ. Antisense inhibition at the β-secretase-site of β-amyloid precursor protein reduces cerebral amyloid and acetyl cholinesterase activity in Tg2576. Neuroscience. 2007; 146: 143–151.

106. Erickson MA, Niehoff ML, Farr SA, Morley JE, Dillman LA, Lynch KM, et al. Peripheral administration of antisense oligonucleotides targeting the amyloid-β protein precursor reverses AβPP and LRP-1 overexpression in the aged SAMP8 mouse brain. J Alzheimers Dis. 2012; 28: 951–960.

107. Erickson M, Farr S, Niehoff M, Morley J, Banks W. Antisense directed against the amyloid precursor protein reduces cytokine expression in the brain and improves learning and memory in the Tg2576 mouse model of Alzheimer's disease. Brain Behav Immun. 2012; 26: S27.

108. Yan R, Bienkowski MJ, Shuck ME, Miao H, Tory MC, Pauley AM, et al. Membrane-anchored aspartyl protease with Alzheimer's disease β-secretase activity. Nature. 1999; 402: 533–537.

109. Vassar R, Bennett BD, Babu-Khan S, Kahn S, Mendiaz EA, Denis P, et al. β-Secretase cleavage of Alzheimer's amyloid precursor protein by the transmembrane aspartic protease BACE. Science. 1999; 286: 735–741.

110. Wolfe MS. Targeting mRNA for Alzheimer's and related dementias. Scientifica. 2014; 2014: 1-13.

111. Refolo LM, Eckman C, Prada CM, Yager D, Sambamurti K, Mehta N, et al. Antisense-induced reduction of Presenilin 1 expression selectively increases the production of amyloid β 42 in transfected cells. J Neurochem. 1999; 73: 2383–2388.

112. Grilli M, Diodato E, Lozza G, Brusa R, Casarini M, Uberti D, et al. Presenilin-1 regulates the neuronal threshold to excitotoxicity both physiologically and pathologically. Proc Natl Acad Sci USA. 2000; 97: 12822–12827.

113. Fiorini A, Sultana R, Förster S, Perluigi M, Cenini G, Cini C, et al. Antisense directed against PS-1 gene decreases brain oxidative markers in aged senescence accelerated mice (SAMP8) and reverses learning and memory impairment: a proteomics study. Free Radic Biol Med. 2013; 65: 1–14.

114. Caceres A, Kosik KS. Inhibition of neurite polarity by tau antisense oligonucleotides in primary cerebellar neurons. Nature. 1990; 343: 461–463.

115. DeVos SL, Goncharoff DK, Chen G, Kebodeaux CS, Yamada K, Stewart FR, et al. Antisense reduction of tau in adult mice protects against seizures. J Neurosci. 2013; 33: 12887–12897.

116. Kalbfuss B, Mabon SA, Misteli T. Correction of alternative splicing of tau in frontotemporal dementia and parkinsonism linked to chromosome 17. J Biol Chem. 2001; 276: 42986–42993.

117. Peacey E, Rodriguez L, Liu Y, Wolfe MS. Targeting a pre-mRNA structure with bipartite antisense molecules modulates tau alternative splicing. Nucleic Acids Res. 2012; 40: 9836-9849.

118. Liu Y, Rodriguez L, Wolfe MS. Template-directed synthesis of a small molecule-antisense conjugate targeting an mRNA structure. Bioorg Chem. 2014; 54: 7–11.

119. Sud R, Geller ET, Schellenberg GD. Antisense-mediated exon skipping decreases tau protein expression: a potential therapy for tauopathies. Mol Ther Nucleic Acids. 2014; 3: e180.

120. Farr SA, Ripley JL, Sultana R, Zhang Z, Niehoff ML, Platt TL, et al. Antisense oligonucleotide against GSK-3β in brain of SAMP8 mice improves learning and memory and decreases oxidative stress: Involvement of transcription factor Nrf2 and implications for Alzheimer disease. Free Radic Biol Med. 2014; 67: 387–395.

121. Fu A-L, Zhang X-M, Sun M-J. Antisense inhibition of acetylcholinesterase gene expression for treating cognition deficit in Alzheimer's disease model mice. Brain Res. 2005; 1066: 10–15.

122. Wasser CR, Herz J. Splicing therapeutics for Alzheimer's disease. EMBO Mol Med. 2016; 8: 308–310.

123. Hinrich AJ, Jodelka FM, Chang JL, Brutman D, Bruno AM, Briggs CA, et al. Therapeutic correction of ApoER2 splicing in Alzheimer's disease mice using antisense oligonucleotides. EMBO Mol Med. 2016; 8: 328–345.

124. Hannon GJ. RNA interference. Nature. 2002; 418: 244–251.

125. Miller VM, Gouvion CM, Davidson BL, Paulson HL. Targeting Alzheimer's disease genes with RNA interference: an efficient strategy for silencing mutant alleles. Nucleic Acids Res. 2004; 32: 661–668.

126. McSwiggen J. RNA interference mediated treatment of Alzheimer's disease using short interfering RNA. Terpstra, Anita, J.; McDonnell Boehnen Hulbert & Berghoff, Suite 3200, 300 South Wacker Drive, Chicago, IL 60606 (US); 2002.

127. Basi G, Frigon N, Barbour R, Doan T, Gordon G, McConlogue L, et al. Antagonistic effects of β-site amyloid precursor protein-cleaving enzymes 1 and 2 on β-amyloid peptide production in cells. J Biol Chem. 2003; 278: 31512–31520.

128. Kao S-C, Krichevsky AM, Kosik KS, Tsai L-H. BACE1 suppression by RNA interference in primary cortical neurons. J Biol Chem. 2004; 279: 1942–1949.

129. Modarresi F, Faghihi MA, Patel NS, Sahagan BG, Wahlestedt C, Lopez-Toledano MA. Knockdown of BACE1-AS nonprotein-coding transcript modulates β-amyloid-related hippocampal neurogenesis. Int J Alzheimers Dis. 2011; 2011: 929042.

130. Cai J, Qi X, Kociok N, Skosyrski S, Emilio A, Ruan Q, et al. β-Secretase (BACE1) inhibition causes retinal pathology by vascular dysregulation and accumulation of age pigment. EMBO Mol Med. 2012; 4: 980–991.

131. Fisette JF, Montagna DR, Mihailescu MR, Wolfe MS. AG-Rich element forms a G-quadruplex and regulates BACE1 mRNA alternative splicing. J Neurochem. 2012; 121: 763–773.

132. Jonas S, Izaurralde E. Towards a molecular understanding of microRNA-mediated gene silencing. Nat Rev Genet. 2015; 16: 421-433.

133. Ha M, Kim VN. Regulation of microRNA biogenesis. Nat Rev Mol Cell Biol. 2014; 15: 509-524.

134. He L, Hannon GJ. MicroRNAs: small RNAs with a big role in gene regulation. Nat Rev Genet. 2004; 5: 522-531.

135. Stenvang J, Petri A, Lindow M, Obad S, Kauppinen S. Inhibition of microRNA function by antimiR oligonucleotides. Silence. 2012; 3: 1.

136. Faghihi MA, Zhang M, Huang J, Modarresi F, Van der Brug MP, Nalls MA, et al. Evidence for natural antisense transcript-mediated inhibition of microRNA function. Genome Biol. 2010; 11: R56.

137. Hébert SS, Horré K, Nicolaï L, Papadopoulou AS, Mandemakers W, Silahtaroglu AN, et al. Loss of microRNA cluster miR-29a/b-1 in sporadic Alzheimer's disease correlates with increased BACE1/β-secretase expression. Proc Natl Acad Sci. 2008; 105: 6415-6420.

138. Zovoilis A, Agbemenyah HY, Agis-Balboa RC, Stilling RM, Edbauer D, Rao P, et al. microRNA-34c is a novel target to treat dementias. EMBO J. 2011; 30: 4299–4308.

139. Murphy SR, Chang CC, Dogbevia G, Bryleva EY, Bowen Z, Hasan MT, et al. ACAT1 knockdown gene therapy decreases amyloid-β in a mouse model of Alzheimer's disease. Mol Ther. 2013; 21: 1497–1506.

140. Zuccato C, Cattaneo E. Brain-derived neurotrophic factor in neurodegenerative diseases. Nat Rev Neurol. 2009; 5: 311-322.

141. Peng S, Wuu J, Mufson EJ, Fahnestock M. Precursor form of brain-derived neurotrophic factor and mature brain-derived neurotrophic factor are decreased in the pre-clinical stages of Alzheimer's disease. J Neurochem. 2005; 93: 1412–1421.

142. Phillips HS, Hains JM, Armanini M, Laramee GR, Johnson SA, Winslow JW. BDNF mRNA is decreased in the hippocampus of individuals with Alzheimer's disease. Neuron. 1991; 7: 695–702.

143. Lee ST, Chu K, Jung KH, Kim JH, Huh JY, Yoon H, et al. miR-206 regulates brain-derived neurotrophic factor in Alzheimer disease model. Ann Neurol. 2012; 72: 269–277.

144. Achenbach J, Chiuman W, Cruz R, Li Y. DNAzymes: from creation in vitro to application in vivo. Curr Pharm Biotechnol. 2004; 5: 321–336.

145. Nawrot B. Targeting BACE with small inhibitory nucleic acids — a future for Alzheimer's disease therapy? Acta Biochim Pol. 2004; 51: 431–444.

146. Gopinath SCB. Methods developed for SELEX. Anal Bioanal Chem. 2007; 387: 171–182.

147. Stoltenburg R, Reinemann C, Strehlitz B. SELEX — a (r) evolutionary method to generate high-affinity nucleic acid ligands. Biomol Eng. 2007; 24: 381–403.

148. Ylera F, Lurz R, Erdmann VA, Fürste JP. Selection of RNA aptamers to the Alzheimer's disease amyloid peptide. Biochem Biophys Res Commun. 2002; 290: 1583–1588.

149. Bunka DH, Mantle BJ, Morten IJ, Tennent GA, Radford SE, Stockley PG. Production and characterization of RNA aptamers specific for amyloid fibril epitopes. J Biol Chem. 2007; 282: 34500–34509.

150. Rahimi F, Murakami K, Summers JL, Chen C-HB, Bitan G. RNA aptamers generated against oligomeric Aβ40 recognize common amyloid aptatopes with low specificity but high sensitivity. PLoS One. 2009; 4: e7694.

151. Takahashi T, Tada K, Mihara H. RNA aptamers selected against amyloid β-peptide (Aβ) inhibit the aggregation of Aβ. Mol Biosyst. 2009; 5: 986–991.

152. Mathew A, Aravind A, Brahatheeswaran D, Fukuda T, Nagaoka Y, Hasumura T, et al. Amyloid-binding aptamer conjugated curcumin–PLGA nanoparticle for potential use in Alzheimer's disease. Bionanoscience. 2012; 2: 83–93.

153. Farrar CT, William CM, Hudry E, Hashimoto T, Hyman BT. RNA aptamer probes as optical imaging agents for the detection of amyloid plaques. PLoS One. 2014; 9: e89901.

154. Babu E, Mareeswaran PM, Sathish V, Singaravadivel S, Rajagopal S. Sensing and inhibition of amyloid-β based on the simple luminescent aptamer–ruthenium complex system. Talanta. 2015; 134: 348–353.

155. Rentmeister A, Bill A, Wahle T, Walter J, Famulok M. RNA aptamers selectively modulate protein recruitment to the cytoplasmic domain of β-secretase BACE1 in vitro. RNA. 2006; 12: 1650–1660.

156. Liang H, Shi Y, Kou Z, Peng Y, Chen W, Li X, et al. Inhibition of BACE1 Activity by a DNA Aptamer in an Alzheimer's Disease Cell Model. PLoS One. 2015; 10: e0140733.

157. Kim JH, Kim E, Choi WH, Lee J, Lee JH, Lee H, et al. Inhibitory RNA aptamers of tau oligomerization and their neuroprotective roles against proteotoxic stress. Mol Pharm. 2016; 13: 2039–2048.

158. Tannenberg RK, Lauridsen LH, Kanwar JR, Dodd PR, Veedu RN. Nucleic acid aptamers as novel class of therapeutics to mitigate Alzheimer's disease pathology. Curr Alzheimer Res. 2013; 10: 442–448.

159. Kim S, Wark AW, Lee HJ. Femtomolar detection of tau proteins in undiluted plasma using surface plasmon resonance. Anal Chem. 2016; 88: 7793–7799.

160. Lee JH, Shin SK, Jiang Y, Choi WH, Hong C, Kim D-E, et al. Facilitated Tau degradation by USP14 aptamers *via* enhanced proteasome activity. Sci Rep. 2015; 5: 10757.

161. Mashima T, Matsugami A, Nishikawa F, Nishikawa S, Katahira M. Unique quadruplex structure and interaction of an RNA aptamer against bovine prion protein. Nucleic Acids Res. 2009; 37: 6249–6258.

162. Kanwar JR, Sun X, Punj V, Sriramoju B, Mohan RR, Zhou SF, et al. Nanoparticles in the treatment and diagnosis of neurological disorders: untamed dragon with fire power to heal. Nanomedicine : Nanotechnology, Biology, and Medicine. 2012; 8: 399–414.

163. Ulbrich K, Hekmatara T, Herbert E, Kreuter J. Transferrin- and transferrin-receptor-antibody-modified nanoparticles enable drug delivery across the blood–brain barrier (BBB). Eur J Pharm Biopharm. 2009; 71: 251–256.

164. Gan CW, Feng SS. Transferrin-conjugated nanoparticles of poly(lactide)-D-alpha-tocopheryl polyethylene glycol succinate diblock copolymer for targeted drug delivery across the blood-brain barrier. Biomaterials. 2010; 31: 7748–7757.

165. Chen CH, Dellamaggiore KR, Ouellette CP, Sedano CD, Lizadjohry M, Chernis GA, et al. Aptamer-based endocytosis of a lysosomal enzyme. Proc Natl Acad Sci USA. 2008; 105: 15908–15913.

166. Macdonald J, Henri J, Goodman L, Xiang D, Duan W, Shigdar S. Development of a bifunctional aptamer targeting the transferrin receptor and epithelial cell adhesion molecule (EpCAM) for the treatment of brain cancer metastases. ACS Chem Neurosci. 2017; 8: 777–784.

167. Du L, Kayali R, Bertoni C, Fike F, Hu H, Iversen PL, et al. Arginine-rich cell-penetrating peptide dramatically enhances AMO-mediated ATM aberrant splicing correction and enables delivery to brain and cerebellum. Hum Mol Genet. 2011; 20: 3151–3160.

168. Heitz F, Morris MC, Divita G. Twenty years of cell-penetrating peptides: from molecular mechanisms to therapeutics. Br J Pharmacol. 2009; 157: 195–206.

169. Pardridge WM. Drug targeting to the brain. Pharm Res. 2007; 24: 1733–1744.

170. Claxton A, Baker LD, Wilkinson CW, Trittschuh EH, Chapman D, Watson GS, et al. Sex and ApoE genotype differences in treatment response to two doses of intranasal insulin in adults with mild cognitive impairment or Alzheimer's disease. J Alzheimers Dis. 2013; 35: 789–797.

171. Hanson LR, Frey WH, 2nd. Intranasal delivery bypasses the blood-brain barrier to target therapeutic agents to the central nervous system and treat neurodegenerative disease. BMC Neurosci. 2008; 9 Suppl 3: S5.

172. Dhuria SV, Hanson LR, Frey WH, 2nd. Intranasal delivery to the central nervous system: mechanisms and experimental considerations. J Pharm Sci. 2010; 99: 1654–1673.

173. Lochhead JJ, Thorne RG. Intranasal delivery of biologics to the central nervous system. Adv Drug Deliv Rev. 2012; 64: 614–628.

Author Biography

Madhuri Chakravarthy obtained her Bachelor's (2011) in Biomedical Science and Master's (2014) in Biomedical Science from the University of Auckland, New Zealand. She is currently a PhD student under the supervision of Dr. Rakesh N. Veedu at the Murdoch University, Western Australia. Her research is centered on developing novel nucleic acid technologies to tackle neurological diseases.

Suxiang Chen received his Bachelor degree of Agriculture in 2010 in South China Agricultural University. He then obtained his Master degree in Biotechnology (Advanced) and a second Master degree in Technology and Innovation Management from the University of Queensland in 2013 and 2014 respectively. Later, he worked in Darui Biotechonology Co. Ltd and Gene Denovo Biotechnology Co. Ltd in Guangzhou, China as a core technician and technical support team

member respectively. Since 2016, he has been pursuing a PhD degree at Murdoch University under the supervision of Dr. Rakesh N. Veedu. His current research focuses include the development of novel RNA targeting therapies for tackling Duchenne muscular dystrophy and Type-2 Diabetes.

A/Prof. Peter R. Dodd obtained his PhD from Imperial College, University of London, and is currently the Director of Queensland Brain Bank at the School of Chemistry and Molecular Biosciences, The University of Queensland, Brisbane, Australia. His lab uses human autopsy tissues to study amino acid neurotransmission, and has developed protocols to prepare good-quality mRNA, miRNA, and proteins for mapping and quantification. His lab studied phenotype-genotype interactions in alcoholics and dementia cases, partitioned by sex and comorbid disease, with key findings including altered expression of GABA receptors in alcoholics without comorbid disease and of glutamate receptors in cirrhotic alcoholics, and altered expression of glutamate transporters and receptors in Alzheimer disease. Prof. Dodd's group was the first to use microarrays to study the human brain transcriptome. Overall, his lab researches the pathogenesis of human neurological diseases.

Rakesh N. Veedu is currently leading the precision nucleic acid theranostics group at Murdoch University and Perron Institute for Neurological and Translational Science. He obtained his PhD in synthetic organic chemistry in 2006 from The University of Queensland, Australia under the supervision of Prof. Curt Wentrup after completing his MSc from Griffith University, Australia. He then continued his postdoctoral career under the supervision of Prof. Jesper Wengel at the Nucleic Acid Center, University of Southern Denmark in the field of nucleic acid chemical biology. Later in 2009, he was appointed as a Research Associate Professor within the Nucleic Acid Center. He then returned to The University of Queensland in mid-2010 and established his independent research career in Functional Nucleic Acid Theranostics Development. His current research is focused on developing novel precision nucleic acid theranostics for tackling solid cancers, neurological diseases including Alzheimer's disease and infectious diseases using nucleic acid aptamers, antisense oligonucleotides, siRNA, antimiRs, molecular beacons and DNAzymes.

Development of Cell-Specific Aptamers: Recent Advances and Insight into the Selection Procedures

Kamal Rahimizadeh [1], Hadi AlShamaileh [1], Milena Fratini [1], Madhuri Chakravarthy [1,2], Michelle Stephen [1], Sarah Shigdar [3] and Rakesh N. Veedu [1,2,*]

[1]   Centre for comparative Genomics, Murdoch University, Perth 6150, Australia;
     rahimizadeh.kamal@gmail.com (K.R.); h.alshamaileh@murdoch.edu.au (H.A.);
     milena.fratini@murdoch.edu.au (M.F.); m.chakravarthy@murdoch.edu.au (M.C.);
     mish.96@live.com.au (M.S.)
[2]   Perron Institute for Neurological and Translational Science, Perth 6005, Australia
[3]   School of Medicine, Deakin University, Waurn Ponds, Geelong 3216, Australia; sarah.shigdar@deakin.edu.au
*   Correspondence: r.veedu@murdoch.edu.au; Tel.: +61-8-9360-2803

Abstract: Systematic evolution of ligands by exponential enrichment (SELEX) is an established procedure for developing short single-stranded nucleic acid ligands called aptamers against a target of choice. This approach has also been used for developing aptamers specific to whole cells named Cell-SELEX. Aptamers selected by Cell-SELEX have the potential to act as cell specific therapeutics, cell specific markers or cell specific drug delivery and imaging agents. However, aptamer development is a laborious and time-consuming process which is often challenging due to the requirement of frequent optimization of various steps involved in Cell-SELEX procedures. This review provides an insight into various procedures for selection, aptamer enrichment, regeneration and aptamer-binding analysis, in addition to a very recent update on all aptamers selected by Cell-SELEX procedures.

Keywords: aptamers; Cell-SELEX; aptamer enrichment; ssDNA; binding assays

---

1. Introduction

Aptamers are short single-stranded DNA or RNA oligonucleotides that bind to specific targets through three-dimensional structural conformation and with a collection of other forces such as hydrogen bonding, stacking of aromatic rings and Van der Waals interactions [1,2]. This binding of the aptamers to their targets is typically highly sensitive, with binding affinities in the low nanomolar to picomolar ranges [2]. Aptamer length can vary, but usually ranges between 25 and 90 nucleotide bases, and the smallest known aptamer is 12 bases long [1]. Aptamers are conventionally developed by a process referred to as systematic evolution of ligands by exponential enrichment (SELEX) [3–5]. In 2012, our group also reported a one-step selection methodology for rapid aptamer selection [6]. The modifiable nature of the starting oligonucleotide libraries increases the number of aptamer structural variants and increases the possibility of successful binding to the target [5,7]. Additionally, through the introduction of appropriate functional groups, both DNA and RNA aptamers can be made more stable with increased half-life in vitro and in vivo [5,7,8]. The modification and synthesis of aptamers is easily achieved by solid-phase oligonucleotide synthesis [9], and this simplicity and effectiveness of oligonucleotide synthesis is attractive to meet diagnostic/therapeutic challenges towards the treatment of various diseases [10]. Before aptamers became a treatment option, antibodies, proteins and peptides were used for targeted therapy [2]. However, the use of antibodies may involve costly development procedures [10], as they are produced by a complex process that requires the use of animals, cells or other in vivo conditions which often results in batch to batch product variation

in different yields, and also require frequent optimization [11]. In contrast, aptamers are chemically synthesized, and therefore, can be produced in consistent yields with no product variation [12]. Furthermore, facile modification of the aptamer endows these aptamers with preferable properties such as fast penetration into cells, lack of immunogenicity, reduced side effects and freedom to introduce multiple chemistries and contrast agents without losing its affinities and specificities to the target [1]. These properties are ideal for aptamers to be used as a tool for targeted therapy, drug delivery and molecular imaging [2,9,13]. Typically, tissue-specific delivery of drug molecules including nucleic acid drugs is very challenging, however, the application of aptamers could be an excellent alternative to circumvent this limitation. Although the use of Cell-surface receptor targeting aptamers could achieve tissue-specific drug delivery to a great extent, development of Cell-specific aptamers may be a better choice. In this review, we highlight the recent advances in the development of Cell-specific aptamers, and provide a comprehensive insight into the selection procedures.

2. Cell Specific Aptamer Development by Cell-SELEX

Aptamers selected by conventional SELEX involve the use of a large oligonucleotide library of approximately 10^{15} unique sequences that undergo a series of selection cycles against a specific target of choice [14]. Several rounds of binding, partitioning and amplification are repeated until a pool of high affinity aptamers are enriched [15]. Theoretically, aptamers can be developed against a wide range of targets including peptides, proteins, viruses and whole cells, of which aptamers can bind to intra- or extracellular sites [1,9]. Cell-SELEX follows the similar approach as the traditional SELEX, but uses live cells as the aptamer selection target. A major advantage of Cell-SELEX is the conservation of the native conformation of proteins, as opposed with traditional SELEX that uses mainly the recombinant proteins as targets [1].

3. Selection

A general SELEX process involves repetitive series of selection cycles starting with the incubation of the target cell with a random sequence single strand oligonucleotides library (Figure 1). Each of the random sequences form unique three-dimensional structures, and the sequences that bind to the target cells are recovered for enrichment and regeneration for subsequent selection cycles, leading to the enrichment of aptamers that bind to the target cells with high affinity and specificity [1]. The enriched library is sequenced to identify the individual bound aptamers.

Consistent cell culture maintenance is critical for Cell-SELEX success, such as consistent confluency across all selection cycles, passage number and growth conditions [16]. Prolonged cell growth or poor culture conditions can influence cell morphology and protein expression and therefore can lead to decreased efficiency of Cell-SELEX [16,17]. Furthermore, to eliminate non-specific binding of oligonucleotides, it is important to block the target cells with tRNA, salmon sperm DNA or Poly (I:C) prior to incubation with the randomized oligonucleotide library [8]. Cell-SELEX can be performed on both adherent and suspension culture. It is important to note that trypsin treatment can strip the cell surface markers and therefore the cells need to be recovered by incubation with the culture media for at least 2 h. Furthermore, if using adherent cells as a cell suspension for aptamer development, the cells should be shaken gently to prevent adhesion of cells [16,17]. Cell-SELEX is performed within the range of 4–37 °C, and increasing selection temperature and extended time increases the possibility of aptamers internalization into cells [17], which is desirable for some aptamer applications.

41
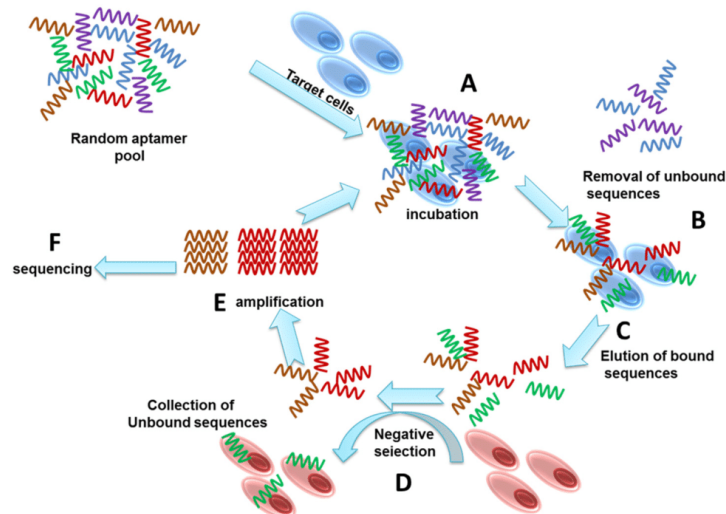
Figure 1. Schematic illustration showing the steps involved in Cell-SELEX. **A**. Incubation of cells with an aptamer library; **B**. Isolating bound sequences from unbound sequences; **C**. Elution of bound sequences; **D**. Negative selection to remove non-specific sequences; **E**. Amplification of target specific sequences; **F**. Sequencing of the selected aptamer pool.

4. Enrichment and Amplification

After each selection cycle, aptamer sequences within the oligonucleotide pool are enriched due to the continuous amplification of high affinity aptamers. However, the amplification of selected aptamers requires optimization to enhance yield without amplifying non-specific sequences due to mispriming. The number of amplification cycles can be optimized by analyzing the PCR products at different amplification cycles by gel electrophoresis. Excessive cycles would result in the amplification of non-specific products, whilst fewer cycles may result in insufficient yields [18]. The number of PCR amplification cycles that results in a band with the highest density without non-specific bands and the lowest amount of smear possible is considered the optimal number of PCR cycles. The optimized amplification cycles number can be used to amplify the aptamer sequences at a larger scale with at least 1 mL of total PCR reaction volume. The PCR product is used to regenerate the library pool for subsequent aptamer selection cycles either by RNA transcription if developing RNA aptamers, or DNA strand separation if developing DNA aptamers [17]. The separation of DNA strands requires a more intricate procedure compared to RNA transcription. In the following section, we focus on four common methodologies used for ssDNA preparation. Although these methods are effective in regenerating ssDNA libraries in SELEX, it is highly recommended to verify the quality of ssDNA with gel electrophoresis.

5. Regeneration of Selected Aptamers

5.1. Asymmetric PCR

Asymmetric PCR is a simple method for ssDNA preparation in which PCR amplification is carried out with different ratios of primers to preferentially amplify the aptamer sequences without its complementary strand [19–21]. In principle, the selected aptamers are amplified into dsDNA during the early PCR amplification cycles. However, the higher amounts of primers that extends the aptamer sequence leads to enrichment of the desired ssDNA [19]. It is important to note that unlike traditional

PCR amplification, asymmetric PCR does not exhibit exponential amplification, but rather a linear amplification after depletion of one of the primers. Therefore, it is imperative to optimize the primer ratios and cycle numbers to maximize ssDNA generation. In a case-specific manner, various ratios of primers need to be tested to find the optimum ratio for each SELEX experiment, which is clearly indicated by the highly diverse ratios used in previous Cell-SELEX experiments. Such ratios that displayed efficient ssDNA generation ranged between 15:1 for 20 amplification cycles for Tabarzad et al. [22] and 20:1 for 10–20 amplification cycles for Citartan et al. [19]. Each of these ratios required their own optimization procedure with varying ranges of ratios and different amplification cycle numbers. Indeed, in the case with Tabarzad et al., a small ratio difference between the primers could result in higher yield of dsDNA than ssDNA, while higher ratios (20:1) could lead to higher length sequences due of product-product or product-primer annealing [22]. However, the same ratio (20:1) used by Citartan et al. was found to be optimum for their ssDNA generation. In addition to primer ratio optimization, the number of PCR amplification cycles also contributes to the efficiency of ssDNA generation. Tabarzad et al. [22] stated that it is imperative to determine the highest optimal amplification cycles that guarantees high ssDNA yield and purity without amplification of non-specific products due to opportunistic mispairing. While the amplification parameters established by Citartan et al. and Tabarzad et al. are similar (10–20 amplification cycles), there were successful studies that used much higher amplification cycles for asymmetric PCR up to 30 to 45 cycles with a single primer [19]. Following asymmetric PCR amplification, it is highly recommended to purify the PCR product with gel extraction to eliminate extra primers and any traces of non-specific amplification. Other types of Asymmetric PCR are currently being tested. One such type is the linear-after-the exponential (LATE) PCR in which the length and sequence of the primers can be modified so that the melting temperature of the limiting primer is the same or more than the temperature of the excess primer. This is a promising method for future SELEX experiments [23].

5.2. Electrophoresis-Based Separation of DNA Strands

A highly effective method includes the denaturation of the double stranded DNA with urea-containing denaturing polyacrylamide gel electrophoresis (PAGE) [24]. The urea breaks the hydrogen bonds between the two strands, which can be separated on a denaturing PAGE if both strands are of unequal sizes. The enriched aptamer sequences can be identified with UV or blue light transilluminator and subsequently extracted and purified [25,26]. The blue light transilluminator is generally favored over UV for its safety and non-damaging DNA property. Complementary DNA strands usually have equal lengths which would migrate through the denaturing PAGE at equal paces. However, there are various strategies that mitigate this issue. Walder et al. [27] amplified the enriched aptamer sequences with chemically synthesized primers containing ribose residue at the 5′ and 3′ ends. After amplification with the modified primer, the ribose residue can be broken with the ribonuclease enzyme, releasing two separate strands of different lengths and allowing the separation of the aptamer sequence with denaturing PAGE. Separation of complementary strands can also be achieved with linking the aptamer sequence strand with a poly A or T tail with a polyethylene glycol spacer in between, which inhibits DNA polymerization of the complementary to the tail sequence and results in size differences between the strands separable by denaturing PAGE. Alternatively, Keefe et al. [25] added a pH susceptible base on the 3′ end of one of the primers primer, which can be digested with alkaline treatment and creates two different lengths of DNA strands. After separating the aptamer sequence from its complementary strand by denaturing PAGE, the aptamer sequence can be identified and extracted from the gel. While this method is both time-consuming and labor-intensive, it remains a very efficient method for the preparation of ssDNA library for aptamer selection.

5.3. Magnetic Beads Separation

Magnetic beads exhibit magnetic properties and congregate when exposed to a magnetic field, which allows for the rapid separation of molecules from a mixture. The amplified aptamer library (dsDNA) are immobilized on streptavidin coated magnetic beads, generally through biotin-streptavidin interaction, allowing for the separation of the DNA strands by increasing the temperature or alkaline treatment (Figure 2). Once immobilized and de-stranded, the immobilized strand is separated from its complementary strand by exposing the magnetic beads to a magnetic field, followed by multiple washings with the recommended buffer. This method has been used in successful Cell-SELEX [28,29]. However, a significant disadvantage is the release the biotin-labeled primer along with the desired ssDNA in the strand separation step, which could overestimate the amount of ssDNA and interfere with aptamer binding to the target molecule. It is therefore recommended to determine the purity of the ssDNA with denaturing gel electrophoresis or mass spectrometry [28].
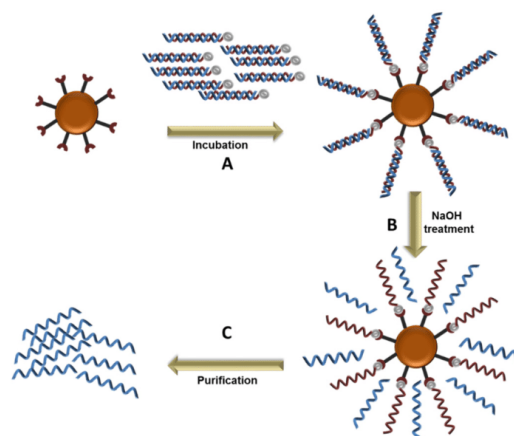
Figure 2. DNA strand separation using magnetic beads. **A**. Immobilization of the double stranded sequences on the magnetic beads; **B**. Denaturation of the double stranded DNA by NaOH treatment; **C**. Purification of the unbound sequences.

5.4. Lambda Exonuclease Digestion

Lambda exonuclease digests phosphorylated DNA strand from 5′ to 3′ end, leaving the non-phosphorylated ssDNA strand intact [30]. Lambda exonuclease is less active on ssDNA and non-phosphorylated dsDNA and inactive on nicked or gapped DNA, making it an efficient method for ssDNA regeneration for aptamer development [31] (Figure 3). However, extended exposure of ssDNA to lambda exonuclease, even if not phosphorylated, can lead to digestion. Furthermore, low concentration of the lambda exonuclease can be insufficient while high concentration can non-specifically digest DNA [30]. Therefore, it is critical to identify the ideal period of incubation of DNA with lambda exonuclease through a time course analysis [32]. A major disadvantage to lambda exonuclease is the high cost of the enzyme for aptamer development. In addition, after the synthesis has finished, it has to remove not only the phosphate group but also the blocking group which protects the phosphate group. An incomplete digestion of the phosphorylated aptamer leads to accumulation of dsDNA [30].

The ssDNA product from lambda exonuclease digestion requires purification from traces of digested oligonucleotides and the lambda exonuclease enzyme prior to Cell-SELEX progression. Purification can be achieved with phenol chloroform isoamyl alcohol removal followed by ethanol precipitation. However, this process may risk considerable loss of ssDNA yield [31]. Alternatively, the ssDNA can be purified with denaturing PAGE. Regardless of the purification method used, it remains a critical step to run the ssDNA with a denaturing PAGE to confirm the size, yield and digestion efficiency. Purification of ssDNA prevents contamination of digested oligonucleotides and the lambda exonuclease enzyme into the aptamer development process.
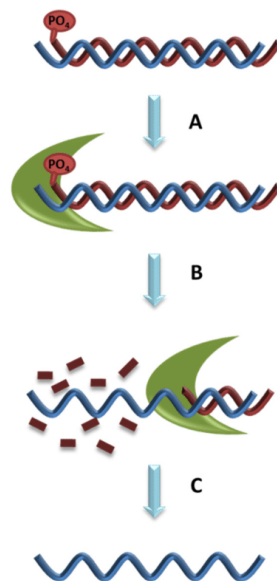
Figure 3. Generation of ssDNA with lambda exonuclease. **A**. Adding enzyme to dsDNA which has a phosphate group; **B**. Incubate enzyme with dsDNA; **C**. Extract and purify the ssDNA.

6. Aptamer Binding Evaluation

Binding assays serve as the first step of confirming the binding efficiency of the newly selected aptamers. It is recommended to perform the binding assays at various stages of the aptamer development process to confirm target-binding enrichment. There are already a number of established binding assays for confirming Cell-specific aptamer binding, such as flow cytometry, fluorescence or confocal microscopy, and enzyme-linked assay. While these methods are different in principle, they share similar steps in binding affinity and specificity determination. Firstly, initial binding affinity tests should be carried out in a similar environment used in the aptamer development process, such as temperature, buffer composition and incubation time. Secondly, it is recommended to block the cells with non-specific oligonucleotide sequences (tRNA, poly I:C, salmon sperm DNA) to block non-specific aptamer binding, which is critical in determining binding specificity. Thirdly, binding affinity can be determined by incubating the target cells with increasing concentrations of the aptamer (generally between 10 and 500 nM), which can be plotted on a non-linear regression curve to determine the dissociation constant (K_d) of the aptamer. Determination of K_d also requires a blank treatment (cells without aptamer treatment, or incubated with the random sequence oligonucleotide library used at the start of Cell-SELEX) to subtract the background noise from the other treatments.

If using fluorescence labels, it is recommended to use amber tubes or microplates designed for fluorescence-based assays to minimize photo bleaching. Finally, it is highly recommended to use positive controls, such as aptamers or antibodies that are known to bind to their targets to confirm the efficacy of the binding assay being used.

6.1. Flow Cytometry

Flow cytometry is a laser-based method capable of characterizing physical and chemical properties of molecules with high reproducibility and accuracy [33]. Therefore, it has become one of the most common methods in characterizing aptamer binding affinities by passing a stream of single cell suspension through a detection apparatus in single file to detect tagged cells within a population. Indeed, several studies used flow cytometry to demonstrate the binding characteristics of their selected aptamers against a wide variety of cells, including CD133-expressing HEK293T cells [34], acute myeloid leukemia [35], lymphoma [36], *Campylobacter jejuni* [37] and small cell lung cancer [38]. It is necessary to avoid cell clumps with efficient trypsinization and filtration with cell strainers. If trypsinization was a necessary step, the cells need to be incubated with serum-free media for approximately 2 h to recover its cell surface markers.

6.2. Enzyme-Linked Assays

Similar to traditional enzyme-linked immunosorbent assays (ELISA) used for specific substance detection, aptamers can be incorporated into enzyme-linked assays to determine their binding affinities, and was first reported in 1996 by Drolet [39] as a highly sensitive and quantitative tool for aptamer binding assay. Furthermore, enzyme-linked assays were also developed specifically for confirming aptamer binding affinities developed by Cell-SELEX, and can be applied to study binding affinities to whole cells, cell lysates, or cell excretions/lysates. Several aptamers developed against microorganisms, such as *Trypanosoma cruzi* excreted secreted antigens (TESA) [40], and human cells, such as U88 glioma cells expressing epidermal growth factor receptor variant III [41], or tumor cells expressing tenascin-C [42] were confirmed through enzyme-linked assays.

6.3. Fluorescence and Confocal Microscopy

Although not semi-quantitative, confocal and fluorescence microscopy are among the most popular tools to screen aptamer binding to cells, and can also visually demonstrate the specificity of aptamers towards their targeted cells. While fluorescence and confocal microscopy are similar in principle in the excitation and emission of fluorescence signals, confocal microscopy offers the ability for depth field control, reduction of background and the ability to take serial optical sections. Indeed, aptamer binding affinity and specificity were confirmed with fluorescence and confocal microscopy on human cells, including SK-BR3 expressing human epidermal growth factor receptor-2 (Her-2) [43], HEK cells expressing TrKB [44], leukemia cells [45], HepG2 [46], pancreatic cancer stem cells [47] and HPV-associated cervical cancer cells [48]. In addition to human cells, aptamers developed against microorganisms were also confirmed by fluorescence and confocal microscopy on microorganisms, including *Campylobacter jejuni* [37], trypanosomes [49] and salmonellosis [50]. Both live and stained cells can be used for fluorescence or confocal microscopy, and fluorescence signaling can be achieved by directly adding a fluorescence label to the aptamer, or indirectly by targeting a specific tag on the aptamer with a fluorescently labeled antibody.

6.4. Radioactive Scintillation Counting

Scintillation counting offers high sensitivity detection of radiolabeled samples, making it a powerful tool for the detection of aptamer binding reactions to their target cells. For accurate measurements of aptamer binding affinities, separation of aptamer-bound targets from non-binding aptamers is essential and can be achieved by filtration or centrifugation. Aptamer binding assays using scintillation counting was applied to ^{32}P-labelled aptamers specific to IVB pili encoded by

Salmonella enterica serovar Typhi *pil* operon and required filtration of the binding reaction through a nitrocellulose filter, followed by scintillation counting of the nitrocellulose filter [51]. Similarly, aptamers developed for African trypanosomes [49], MCF-7 [52] and differentiated PC12 cells [53] were confirmed by washing away unbound cells and the binding affinity was determined with scintillation counting.

7. Aptamers Developed by Cell-SELEX

Traditional SELEX develops aptamers targeting homogeneous molecules, which offers a higher rate of success in selecting high affinity aptamers. However, in biological systems, the use of recombinant proteins as targets away from their native environment risks altering their structural conformation and stability. Native structural conformation is an essential component for aptamer selection intended for therapeutic purposes, and therefore the use of Cell-SELEX is generally favoured as it retains the aptamer selection targets in their natural environment. Although the aptamer targets in Cell-SELEX uses cells in a heterogeneous solution, such as growth media with serum, it remains a highly achievable process as evident by the many Cell-SELEX experiments performed in last few years that resulted in Cell-specific aptamers with high affinity and specificity (Table 1).

Table 1. Summary of different Cell-SELEX experiments performed in the last few years.

Aptamer	Method	Target Cell	Kd (nM)	Reference
RNA	Cell-SELEX	HER-2-overexpressing breast cancer	94.6	[43]
DNA	Cell-SELEX	Acute myeloid leukemia cells	5.4 ± 1.6	[35]
RNA	Cell-SELEX	Mouse embryonic stem cells	-	[54]
DNA	Cell-SELEX	Human hepatocarcinoma	19–450	[55]
RNA	Cell-SELEX	AC133-epitope of CD133 expressed on HEK293T cells	33.85–145	[34]
DNA	Cell-SELEX	Over-expressing epidermal growth factor receptor variant III on human glioblastoma	≤ 100	[56]
DNA	on-chip Cell-SELEX	Different histologically classified ovarian cancer cells	1.3	[57]
DNA	Cell-SELEX	Epidermal growth factor receptor variant III on Glioblastoma	3.37 ± 0.98	[58]
DNA	Cell-SELEX	Metastatic colorectal cell	8.1 ± 0.9	[59]
DNA	Cell-SELEX	Prostate cancer cells	73.59 ± 11.01	[60]
RNA	Cell-SELEX	Annexin A2	10.5 ± 4.6	[61]
DNA	Cell-SELEX By flow cytometry	3T3-L1 adipocytes cells	33.1 ± 2.9	[62]
RNA	Cell-SELEX	PC3-prostate cancer cell	71.57 ± 12.96	[63]
DNA	Cell-SELEX	Human hepatoma cells HepG2	64–349	[64]
DNA	On-chip Cell-SELEX	Colorectal cancer cells	12.3	[65]
DNA	Cell-SELEX	Hepatocellular carcinoma	9.4 ± 2.0	[66]
DNA	Cell internalization SELEX	MCF10CA1h human breast ductal carcinoma		[67]
DNA	Cell-SELEX	Nasopharyngeal carcinoma cell lines	11.93 ± 1.40	[68]
DNA	Cell-SELEX	Renal cell carcinoma (768-O)	9.4 ± 2.0	[69]
DNA	Cell-SELEX	Metastatic colorectal carcinoma LOVO cells	167.3 ± 30.2	[70]

8. Aptamers Developed Against Cell-Specific Markers

Not all cell-specific aptamers are developed by Cell-SELEX, but can also be developed by traditional SELEX against specific intra- or extra-cellular markers. Aptamers generated against cell markers with traditional SELEX vastly outnumbers aptamers generated by Cell-SELEX. Only a few cell-specific aptamers are presented in this section as more detailed reviews are available [71,72]. Determining the binding affinity aptamers that were developed against a surface cell marker can be

achieved with fluorescence/confocal microscopy and flow cytometry, such as the aptamers developed against the Epithelial cell adhesion molecule [73] and CD44 [74]. To determine the binding affinity of aptamers that bind to intracellular targets, it is necessary to lyse the cells to release the aptamers for detection. Furthermore, aptamers released from cell lysis can be immobilized either on plates or magnetic beads to enable enzyme-linked binding assays [39,40,75]. Alternatively, quantitative PCR (qPCR) can be used to detect aptamers in cell lysates by primer-extension [43]. However, it is limited to long sequence aptamers as primers can span between 18 and 22 nt. In addition, surface plasmon resonance (SPR) is an efficient light-based method that can detect aptamer binding via changes in light refraction. Aptamers binding to tenascin-C, a protein found on tumor cells, was detected by passing tenascin-C extracted from tumor cells through a flow cell containing the immobilized aptamers [42].

9. Conclusions

The development of cell-specific aptamers carries significant diagnostic and therapeutic potential. Their small size allows for efficient tissue penetration, ease of chemical modification permits longer systemic circulation and high binding affinities allows for rapid molecular detection. However, Cell-SELEX often carries more complications than traditional SELEX that uses pure forms of targets. Unlike the use of purified targets, it is more difficult to direct aptamer binding towards specific parts of the target cell, which may result in the development of non-specific aptamers. The definitive strategy to alleviate the issue of enriching non-specific binding aptamers is the use of a different, but similar, cell line as the negative control selection, one that shares the majority of the target cells' markers but not the actual aptamer target molecule. In tumor Cell-SELEX, neighboring healthy cells that surround the targeted tumor cells can also serve in negative control selection. Optimized methods for aptamer library regeneration and binding assays play a significant part for the success of Cell-SELEX. Indeed, efficient regeneration and purification of RNA or ssDNA pool is a critical step for aptamer selection as oligonucleotide fragments and dsDNA can nonspecifically bind to cell surfaces and lead to enrichment. Moreover, enrichment of non-specific binding oligonucleotides can potentially give false positive results in non-optimized binding assays. By efficiently regenerating the enriched aptamer pool, non-specific binding can be eliminated from the selection process, and high affinity aptamers are preferentially selected. The DNA strand separation methods described in this review are efficient in regenerating the ssDNA pool for DNA aptamer development, and it is highly recommended to confirm the ssDNA product with gel electrophoresis to confirm the purity and yield. Furthermore, it is critical to use a binding assay method that is compatible with the cell target, such as flow cytometry that scans individual cells in a single-file stream, fluorescence and confocal microscopy for visual aptamer binding confirmation, and scintillation counting for high sensitivity assays. In addition, enzyme-linked assays and qPCR assays allow for the detection of internalized aptamers by analyzing cell lysates or excreted products. Cell-SELEX is a powerful tool, and its successful implementation leads to the development of high affinity aptamers with diagnostic and therapeutic potential, as well as the identification of new cellular markers that advances cell biology research.

Conflicts of Interest: The authors declare no conflict of interest.

References

1. Fang, X.; Tan, W. Aptamers generated from cell-selex for molecular medicine: A chemical biology approach. *Acc. Chem. Res.* **2009**, *43*, 48–57. [CrossRef] [PubMed]
2. Orava, E.W.; Cicmil, N.; Gariépy, J. Delivering cargoes into cancer cells using DNA aptamers targeting internalized surface portals. *Biochim. Biophys. Acta* **2010**, *1798*, 2190–2200. [CrossRef] [PubMed]
3. Gopinath, S.C.B. Methods developed for selex. *Anal. Bioanal. Chem.* **2007**, *387*, 171–182. [CrossRef] [PubMed]

4.　Stoltenburg, R.; Reinemann, C.; Strehlitz, B. Selex—A (r) evolutionary method to generate high-affinity nucleic acid ligands. *Biomol. Eng.* **2007**, *24*, 381–403. [CrossRef] [PubMed]

5.　Lipi, F.; Chen, S.; Chakravarthy, M.; Rakesh, S.; Veedu, R.N. In vitro evolution of chemically-modified nucleic acid aptamers: Pros and cons, and comprehensive selection strategies. *RNA Biol.* **2016**, *13*, 1232–1245. [CrossRef] [PubMed]

6.　Lauridsen, L.H.; Shamaileh, H.A.; Edwards, S.L.; Taran, E.; Veedu, R.N. Rapid one-step selection method for generating nucleic acid aptamers: Development of a DNA aptamer against α-bungarotoxin. *PLoS ONE* **2012**, *7*, e41702. [CrossRef] [PubMed]

7.　Gopinath, S.C.B.; Lakshmipriya, T.; Chen, Y.; Arshad, M.M.; Kerishnan, J.P.; Ruslinda, A.; Al-Douri, Y.; Voon, C.; Hashim, U. Cell-targeting aptamers act as intracellular delivery vehicles. *Appl. Microbiol. Biotechnol.* **2016**, *100*, 6955–6969. [CrossRef] [PubMed]

8.　Thiel, W.H.; Thiel, K.W.; Flenker, K.S.; Bair, T.; Dupuy, A.J.; McNamara, J.O.; Miller, F.J.; Giangrande, P.H. Cell-internalization selex: Method for identifying cell-internalizing rna aptamers for delivering sirnas to target cells. *RNA Interf. Chall. Ther. Oppor.* **2015**, *1218*, 187–199. [CrossRef]

9.　Meyer, C.; Hahn, U.; Rentmeister, A. Cell-specific aptamers as emerging therapeutics. *J. Nucleic Acids* **2011**, *2011*, 904750. [CrossRef] [PubMed]

10.　Chen, Z.; Ali, Z.; Li, S.; Liu, B.; He, N. Aptamers generated from cell-systematic evolution of ligands through exponential enrichment and their applications. *J. Nanosci. Nanotechnol.* **2016**, *16*, 9346–9358. [CrossRef]

11.　Kunert, R.; Reinhart, D. Advances in recombinant antibody manufacturing. *Appl. Microbiol. Biotechnol.* **2016**, *100*, 3451–3461. [CrossRef] [PubMed]

12.　Jayasena, S.D. Aptamers: An emerging class of molecules that rival antibodies in diagnostics. *Clin. Chem.* **1999**, *45*, 1628–1650. [PubMed]

13.　Veedu, R.N. *Aptamers: Tools for Nanotherapy and Molecular Imaging*; CRC Press: Boca Raton, FL, USA, 2017.

14.　Teng, J.; Yuan, F.; Ye, Y.; Zheng, L.; Yao, L.; Xue, F.; Chen, W.; Li, B. Aptamer-based technologies in foodborne pathogen detection. *Front. Microbiol.* **2016**, *7*, 1426. [CrossRef] [PubMed]

15.　Chen, M.; Yu, Y.; Jiang, F.; Zhou, J.; Li, Y.; Liang, C.; Dang, L.; Lu, A.; Zhang, G. Development of cell-selex technology and its application in cancer diagnosis and therapy. *Int. J. Mol. Sci.* **2016**, *17*, 2079. [CrossRef] [PubMed]

16.　Raddatz, M.S.L.; Dolf, A.; Endl, E.; Knolle, P.; Famulok, M.; Mayer, G. Enrichment of cell-targeting and population-specific aptamers by fluorescence-activated cell sorting. *Angew. Chem. Int. Ed. Engl.* **2008**, *47*, 5190–5193. [CrossRef] [PubMed]

17.　Sefah, K.; Shangguan, D.; Xiong, X.; O'donoghue, M.B.; Tan, W. Development of DNA aptamers using cell-selex. *Nat. Protoc.* **2010**, *5*, 1169–1185. [CrossRef] [PubMed]

18.　Tolle, F.; Wilke, J.; Wengel, J.; Mayer, G. By-product formation in repetitive PCR amplification of DNA libraries during selex. *PLoS ONE* **2014**, *9*, e114693. [CrossRef] [PubMed]

19.　Citartan, M.; Tang, T.-H.; Tan, S.-C.; Hoe, C.-H.; Saini, R.; Tominaga, J.; Gopinath, S.C. Asymmetric PCR for good quality ssDNA generation towards DNA aptamer production. *Songklanakarin J. Sci. Technol.* **2012**, *34*, 125.

20.　Poddar, S. Symmetric vs asymmetric PCR and molecular beacon probe in the detection of a target gene of adenovirus. *Mol. Cell. Probes* **2000**, *14*, 25–32. [CrossRef] [PubMed]

21.　Gyllensten, U.B.; Erlich, H.A. Generation of single-stranded DNA by the polymerase chain reaction and its application to direct sequencing of the HLA-DQA locus. *Proc. Natl. Acad. Sci. USA* **1988**, *85*, 7652–7656. [CrossRef] [PubMed]

22.　Tabarzad, M.; Kazemi, B.; Vahidi, H.; Aboofazeli, R.; Shahhosseini, S.; Nafissi-Varcheh, N. Challenges to design and develop of DNA aptamers for protein targets. I. Optimization of asymmetric PCR for generation of a single stranded DNA library. *Iran. J. Pharm. Res.* **2014**, *13*, 133. [PubMed]

23.　Sanchez, J.A.; Pierce, K.E.; Rice, J.E.; Wangh, L.J. Linear-after-the-exponential (late)–PCR: An advanced method of asymmetric PCR and its uses in quantitative real-time analysis. *Proc. Natl. Acad. Sci. USA* **2004**, *101*, 1933–1938. [CrossRef] [PubMed]

24.　Summer, H.; Grämer, R.; Dröge, P. Denaturing urea polyacrylamide gel electrophoresis (urea page). *JoVE J. Vis. Exp.* **2009**, *32*, e1485. [CrossRef] [PubMed]

25.　Keefe, A.D.; Pai, S.; Ellington, A. Aptamers as therapeutics. *Nat. Rev. Drug Discov.* **2010**, *9*, 537–550. [CrossRef] [PubMed]

26. Hempelmann, E.; Wilson, R.J.M. Detection of glucose-6-phosphate dehydrogenase in malarial parasites. *Mol. Biochem. Parasitol.* **1981**, *2*, 197–204. [CrossRef]

27. Walder, R.Y.; Hayes, J.R.; Walder, J.A. Use of PCR primers containing a 3′terminal ribose residuce to prevent cross-contamination of amplified sequences. *Nucleic Acids Res.* **1993**, *21*, 4339–4343. [CrossRef] [PubMed]

28. Paul, A.; Avci-Adali, M.; Ziemer, G.; Wendel, H.P. Streptavidin-coated magnetic beads for DNA strand separation implicate a multitude of problems during cell-selex. *Oligonucleotides* **2009**, *19*, 243–254. [CrossRef] [PubMed]

29. DeGrasse, J.A. A single-stranded DNA aptamer that selectively binds to staphylococcus aureus enterotoxin b. *PLoS ONE* **2012**, *7*, e33410. [CrossRef] [PubMed]

30. Citartan, M.; Tang, T.-H.; Tan, S.-C.; Gopinath, S.C. Conditions optimized for the preparation of single-stranded DNA (ssDNA) employing lambda exonuclease digestion in generating DNA aptamer. *World J. Microbiol. Biotechnol.* **2011**, *27*, 1167–1173. [CrossRef]

31. Avci-Adali, M.; Paul, A.; Wilhelm, N.; Ziemer, G.; Wendel, H.P. Upgrading selex technology by using lambda exonuclease digestion for single-stranded DNA generation. *Molecules* **2009**, *15*, 1–11. [CrossRef] [PubMed]

32. Oh, S.S.; Ahmad, K.M.; Cho, M.; Kim, S.; Xiao, Y.; Soh, H.T. Improving aptamer selection efficiency through volume dilution, magnetic concentration, and continuous washing in microfluidic channels. *Anal. Chem.* **2011**, *83*, 6883–6889. [CrossRef] [PubMed]

33. Tan, S.Y.; Acquah, C.; Sidhu, A.; Ongkudon, C.M.; Yon, L.; Danquah, M.K. Selex modifications and bioanalytical techniques for aptamer–target binding characterization. *Crit. Rev. Anal. Chem.* **2016**, *46*, 521–537. [CrossRef] [PubMed]

34. Shigdar, S.; Qiao, L.; Zhou, S.-F.; Xiang, D.; Wang, T.; Li, Y.; Lim, L.Y.; Kong, L.; Li, L.; Duan, W. Rna aptamers targeting cancer stem cell marker cd133. *Cancer Lett.* **2013**, *330*, 84–95. [CrossRef] [PubMed]

35. Sefah, K.; Tang, Z.; Shangguan, D.; Chen, H.; Lopez-Colon, D.; Li, Y.; Parekh, P.; Martin, J.; Meng, L.; Phillips, J. Molecular recognition of acute myeloid leukemia using aptamers. *Leukemia* **2009**, *23*, 235–244. [CrossRef] [PubMed]

36. Tang, Z.; Shangguan, D.; Wang, K.; Shi, H.; Sefah, K.; Mallikratchy, P.; Chen, H.W.; Li, Y.; Tan, W. Selection of aptamers for molecular recognition and characterization of cancer cells. *Anal. Chem.* **2007**, *79*, 4900–4907. [CrossRef] [PubMed]

37. Dwivedi, H.P.; Smiley, R.D.; Jaykus, L.-A. Selection and characterization of DNA aptamers with binding selectivity to campylobacter jejuni using whole-cell selex. *Appl. Microbiol. Biotechnol.* **2010**, *87*, 2323–2334. [CrossRef] [PubMed]

38. Kunii, T.; Ogura, S.-I.; Mie, M.; Kobatake, E. Selection of DNA aptamers recognizing small cell lung cancer using living cell-selex. *Analyst* **2011**, *136*, 1310–1312. [CrossRef] [PubMed]

39. Drolet, D.W.; Moon-McDermott, L.; Romig, T.S. An enzyme-linked oligonucleotide assay. *Nat. Biotechnol* **1996**, *14*, 1021–1025. [CrossRef] [PubMed]

40. Nagarkatti, R.; de Araujo, F.F.; Gupta, C.; Debrabant, A. Aptamer based, non-PCR, non-serological detection of chagas disease biomarkers in *Trypanosoma cruzi* infected mice. *PLoS Negl. Trop. Dis.* **2014**, *8*, e2650. [CrossRef] [PubMed]

41. Tan, Y.; Liang, H.; Wu, X.; Gao, Y.; Zhang, X. Cell-ELA-based determination of binding affinity of DNA aptamer against U87-EGFRvIII cell. *Sheng Wu Gong Cheng Xue Bao* **2013**, *29*, 664–671. [PubMed]

42. Daniels, D.A.; Chen, H.; Hicke, B.J.; Swiderek, K.M.; Gold, L. A tenascin-C aptamer identified by tumor cell SELEX: Systematic evolution of ligands by exponential enrichment. *Proc. Natl. Acad. Sci. USA* **2003**, *100*, 15416–15421. [CrossRef] [PubMed]

43. Kang, H.S.; Huh, Y.M.; Kim, S.; Lee, D.-K. Isolation of RNA aptamers targeting HER-2-overexpressing breast cancer cells using cell-SELEX. *Bull. Korean Chem. Soc.* **2009**, *30*, 1827–1831. [CrossRef]

44. Huang, Y.Z.; Hernandez, F.J.; Gu, B.; Stockdale, K.R.; Nanapaneni, K.; Scheetz, T.E.; Behlke, M.A.; Peek, A.S.; Bair, T.; Giangrande, P.H. RNA aptamer-based functional ligands of the neurotrophin receptor, trkb. *Mol. Pharmacol.* **2012**, *82*, 623–635. [CrossRef] [PubMed]

45. Shangguan, D.; Li, Y.; Tang, Z.; Cao, Z.C.; Chen, H.W.; Mallikaratchy, P.; Sefah, K.; Yang, C.J.; Tan, W. Aptamers evolved from live cells as effective molecular probes for cancer study. *Proc. Natl. Acad. Sci. USA* **2006**, *103*, 11838–11843. [CrossRef] [PubMed]

46. Huang, R.; Chen, Z.; Liu, M.; Deng, Y.; Li, S.; He, N. The aptamers generated from HepG2 cells. *Sci. China Chem.* **2017**, *60*. [CrossRef]

47. Kim, Y.J.; Lee, H.S.; Jung, D.E.; Kim, J.M.; Song, S.Y. The DNA aptamer binds stemness-enriched cancer cells in pancreatic cancer. *J. Mol. Recognit.* **2016**, *30*, e2591. [CrossRef] [PubMed]

48. Graham, J.C.; Zarbl, H. Use of cell-SELEX to generate DNA aptamers as molecular probes of HPV-associated cervical cancer cells. *PLoS ONE* **2012**, *7*, e36103. [CrossRef] [PubMed]

49. Goringer, H.; Adler, A.; Forster, N.; Homann, M. Post-SELEX chemical optimization of a trypanosome-specific RNA aptamer. *Comb. Chem. High Throughput Screen.* **2008**, *11*, 16–23. [CrossRef]

50. Pathania, P.; Sharma, A.; Kumar, B.; Rishi, P.; Suri, C.R. Selective identification of specific aptamers for the detection of non-typhoidal salmonellosis in an apta-impedimetric sensing format. *Microchim. Acta* **2017**, *184*, 1499–1508. [CrossRef]

51. Pan, Q.; Zhang, X.-L.; Wu, H.-Y.; He, P.-W.; Wang, F.; Zhang, M.-S.; Hu, J.-M.; Xia, B.; Wu, J. Aptamers that preferentially bind type IVB pili and inhibit human monocytic-cell invasion by *Salmonella enterica* serovar typhi. *Antimicrob. Agents Chemother.* **2005**, *49*, 4052–4060. [CrossRef] [PubMed]

52. Quang, N.N.; Miodek, A.; Cibiel, A.; Ducongé, F. Selection of aptamers against whole living cells: From cell-selex to identification of biomarkers. *Synth. Antib. Methods Protoc.* **2017**, 253–272. [CrossRef]

53. Wang, C.; Zhang, M.; Yang, G.; Zhang, D.; Ding, H.; Wang, H.; Fan, M.; Shen, B.; Shao, N. Single-stranded DNA aptamers that bind differentiated but not parental cells: Subtractive systematic evolution of ligands by exponential enrichment. *J. Biotechnol.* **2003**, *102*, 15–22. [CrossRef]

54. Gao, H.; Qian, J.; Cao, S.; Yang, Z.; Pang, Z.; Pan, S.; Fan, L.; Xi, Z.; Jiang, X.; Zhang, Q. Precise glioma targeting of and penetration by aptamer and peptide dual-functioned nanoparticles. *Biomaterials* **2012**, *33*, 5115–5123. [CrossRef] [PubMed]

55. Ninomiya, K.; Kaneda, K.; Kawashima, S.; Miyachi, Y.; Ogino, C.; Shimizu, N. Cell-SELEX based selection and characterization of DNA aptamer recognizing human hepatocarcinoma. *Bioorg. Med. Chem. Lett.* **2013**, *23*, 1797–1802. [CrossRef] [PubMed]

56. Tan, Y.; Shi, Y.-S.; Wu, X.-D.; Liang, H.-Y.; Gao, Y.-B.; Li, S.-J.; Zhang, X.-M.; Wang, F.; Gao, T.-M. DNA aptamers that target human glioblastoma multiforme cells overexpressing epidermal growth factor receptor variant III in vitro. *Acta Pharmacol. Sin.* **2013**, *34*, 1491. [CrossRef] [PubMed]

57. Hung, L.-Y.; Wang, C.-H.; Hsu, K.-F.; Chou, C.-Y.; Lee, G.-B. An on-chip cell-SELEX process for automatic selection of high-affinity aptamers specific to different histologically classified ovarian cancer cells. *Lab Chip* **2014**, *14*, 4017–4028. [CrossRef] [PubMed]

58. Wu, X.; Liang, H.; Tan, Y.; Yuan, C.; Li, S.; Li, X.; Li, G.; Shi, Y.; Zhang, X. Cell-SELEX aptamer for highly specific radionuclide molecular imaging of glioblastoma in vivo. *PLoS ONE* **2014**, *9*, e90752. [CrossRef] [PubMed]

59. Li, W.-M.; Bing, T.; Wei, J.-Y.; Chen, Z.-Z.; Shangguan, D.-H.; Fang, J. Cell-SELEX-based selection of aptamers that recognize distinct targets on metastatic colorectal cancer cells. *Biomaterials* **2014**, *35*, 6998–7007. [CrossRef] [PubMed]

60. Wang, Y.; Luo, Y.; Bing, T.; Chen, Z.; Lu, M.; Zhang, N.; Shangguan, D.; Gao, X. DNA aptamer evolved by cell-selex for recognition of prostate cancer. *PLoS ONE* **2014**, *9*, e100243. [CrossRef] [PubMed]

61. Cibiel, A.; Quang, N.N.; Gombert, K.; Thézé, B.; Garofalakis, A.; Ducongé, F. From ugly duckling to swan: Unexpected identification from cell-SELEX of an anti-Annexin A2 aptamer targeting tumors. *PLoS ONE* **2014**, *9*, e87002. [CrossRef] [PubMed]

62. Kim, E.Y.; Kim, J.W.; Kim, W.K.; Han, B.S.; Park, S.G.; Chung, B.H.; Lee, S.C.; Bae, K.-H. Selection of aptamers for mature white adipocytes by cell SELEX using flow cytometry. *PLoS ONE* **2014**, *9*, e97747. [CrossRef] [PubMed]

63. Souza, A.G.; Marangoni, K.; Fujimura, P.T.; Alves, P.T.; Silva, M.J.; Bastos, V.A.F.; Goulart, L.R.; Goulart, V.A. 3D cell-SELEX: Development of RNA aptamers as molecular probes for PC-3 tumor cell line. *Exp. Cell Res.* **2016**, *341*, 147–156. [CrossRef] [PubMed]

64. Xu, J.; Teng, I.-T.; Zhang, L.; Delgado, S.; Champanhac, C.; Cansiz, S.; Wu, C.; Shan, H.; Tan, W. Molecular recognition of human liver cancer cells using DNA aptamers generated via cell-SELEX. *PLoS ONE* **2015**, *10*, e0125863. [CrossRef] [PubMed]

65. Hung, L.-Y.; Wang, C.-H.; Che, Y.-J.; Fu, C.-Y.; Chang, H.-Y.; Wang, K.; Lee, G.-B. Screening of aptamers specific to colorectal cancer cells and stem cells by utilizing on-chip cell-SELEX. *Sci. Rep.* **2015**, *5*, 10326. [CrossRef] [PubMed]

66. Rong, Y.; Chen, H.; Zhou, X.-F.; Yin, C.-Q.; Wang, B.-C.; Peng, C.-W.; Liu, S.-P.; Wang, F.-B. Identification of an aptamer through whole cell-SELEX for targeting high metastatic liver cancers. *Oncotarget* **2016**, *7*, 8282. [CrossRef] [PubMed]

67. Chandrasekaran, R.; Lee, A.S.W.; Yap, L.W.; Jans, D.A.; Wagstaff, K.M.; Cheng, W. Tumor cell-specific photothermal killing by SELEX-derived DNA aptamer-targeted gold nanorods. *Nanoscale* **2016**, *8*, 187–196. [CrossRef] [PubMed]

68. Jia, W.; Ren, C.; Wang, L.; Zhu, B.; Jia, W.; Gao, M.; Zeng, F.; Zeng, L.; Xia, X.; Zhang, X. Cd109 is identified as a potential nasopharyngeal carcinoma biomarker using aptamer selected by cell-SELEX. *Oncotarget* **2016**, *7*, 55328. [CrossRef] [PubMed]

69. Wang, J.; Zhang, Y.; Chen, Y.; Hong, S.; Sun, Y.; Sun, N.; Pei, R. In vitro selection of DNA aptamers against renal cell carcinoma using living cell-SELEX. *Talanta* **2017**, *175*, 235–242. [CrossRef] [PubMed]

70. Yuan, B.; Jiang, X.; Chen, Y.; Guo, Q.; Wang, K.; Meng, X.; Huang, Z.; Wen, X. Metastatic cancer cell and tissue-specific fluorescence imaging using a new DNA aptamer developed by cell-SELEX. *Talanta* **2017**, *170*, 56–62. [CrossRef] [PubMed]

71. Mercier, M.-C.; Dontenwill, M.; Choulier, L. Selection of nucleic acid aptamers targeting tumor cell-surface protein biomarkers. *Cancers* **2017**, *9*, 69. [CrossRef] [PubMed]

72. Wang, J.; Li, G. Aptamers against cell surface receptors: Selection, modification and application. *Curr. Med. Chem.* **2011**, *18*, 4107–4116. [CrossRef] [PubMed]

73. Shigdar, S.; Lin, J.; Yu, Y.; Pastuovic, M.; Wei, M.; Duan, W. Rna aptamer against a cancer stem cell marker epithelial cell adhesion molecule. *Cancer Sci.* **2011**, *102*, 991–998. [CrossRef] [PubMed]

74. Alvarez-Erviti, L.; Seow, Y.; Yin, H.; Betts, C.; Lakhal, S.; Wood, M.J. Delivery of siRNA to the mouse brain by systemic injection of targeted exosomes. *Nat. Biotechnol.* **2011**, *29*, 341–345. [CrossRef] [PubMed]

75. McNamara, J.O.; Kolonias, D.; Pastor, F.; Mittler, R.S.; Chen, L.; Giangrande, P.H.; Sullenger, B.; Gilboa, E. Multivalent 4–1BB binding aptamers costimulate CD8+ T cells and inhibit tumor growth in mice. *J. Clin. Investig.* **2008**, *118*, 376–386. [CrossRef] [PubMed]

Sample Availability: Not Available.

Check for updates

Development of DNA aptamers targeting low-molecular-weight amyloid-β peptide aggregates *in vitro*†

Madhuri Chakravarthy, [ID] [ab] Hadi AlShamaileh,[ac] He Huang,[c] Rudi K. Tannenberg,[c] Suxiang Chen,[abc] Simon Worrall,[c] Peter R. Dodd [ID] [c] and Rakesh N. Veedu [ID] *[abc]

We have developed a novel functional nucleic acid aptamer to amyloid-β peptide 1–40 ($A\beta_{1-40}$) and investigated its potential to detect Aβ peptide fragments in neuropathologically confirmed Alzheimer brain hippocampus tissues samples. Our results demonstrate that the aptamer candidate RNV95 could detect tetrameric/pentameric low-molecular-weight Aβ aggregates in autopsy hippocampal tissue from two neuropathologically confirmed Alzheimer disease cases. Although these are preliminary observations, detailed investigations are under way. This is the first demonstration of aptamer-Aβ binding in Alzheimer brain tissues.

Synthetic functional nucleic acids have attracted considerable attention in recent years; they show great potential as therapeutics for various diseases.[1] Aptamers are prominent class of synthetic short single-stranded DNA or RNA oligonucleotide sequences that can bind to their targets with very high affinity and specificity because of their ability to adopt three-dimensional structures in solution.[2–7] Aptamers are normally developed from a large pool ($\sim 10^{15}$ members) of randomised oligonucleotide sequences by an *in vitro* reiterative selection process called Systematic Evolution of Ligands by EXponential enrichment (SELEX).[8,9] We recently reported a rapid one-step selection methodology for developing nucleic acid aptamers.[10] Aptamers (often termed 'chemical antibodies') are ideal for applications in drug delivery[11] and therapeutics development (*e.g.*, blocking target receptors; mediating delivery of a therapeutic agent), biosensing (*e.g.*, labelling and detection) and nanotechnology (*e.g.*, anchoring and nano-sensors). An aptamer-based drug, Macugen (Pegaptanib Sodium), has been approved

by the United States Food and Drug Association for clinical use in the treatment of age-related macular degeneration.[12]

Aptamers can potentially target the pathogenic components of Alzheimer's disease (AD).[6,13–16] AD is characterised by progressive impairment of cognitive function and behaviour. It affects more than 20% of people aged 65 or older and leads to death on average nine years after diagnosis.[17] The neuropathological hallmarks of AD are extracellular amyloid-β (Aβ) plaques[18] and intracellular neurofibrillary tangles (NFTs)[19] that accumulate in specific brain areas. Amyloid plaques are mainly composed of aggregates of Aβ peptide 40 to 42 amino acids in length ($A\beta_{1-40}$ and $A\beta_{1-42}$). Previous reports on aptamers developed against the $A\beta_{1-40}$ peptide showed that it is difficult to select peptide-specific aptamers against monomeric $A\beta_{1-40}$ due to its high tendency to form Aβ aggregates in solution, even under strict experimental conditions that aim to limit the aggregation.[20–22] Herein, for the first time, we describe the development of novel nucleic acid aptamers that can detect low-molecular-weight aggregates in brain tissues from confirmed AD cases.

First, we conducted *in vitro* selection (Fig. 1) experiments to isolate novel DNA aptamers targeting $A\beta_{1-40}$ (see ESI† for detailed experimental protocols). An 81mer DNA oligonucleotide library containing 40mer randomised regions flanked by 20 and 21 nucleotide primer-binding regions was used in magnetic bead-based affinity selection protocols. Biotinylated $A\beta_{1-40}$ peptide monomers were immobilised onto streptavidin-coated magnetic beads (Dynabeads®). Prior to immobilisation, $A\beta_{1-40}$ peptide was dissolved in 1,1,1,3,3,3-hexafluoro-2-propanol (HFIP) and sonicated to prevent rapid aggregation. Ten rounds of selection consisted of incubating the ssDNA library with bead-immobilized $A\beta_{1-40}$ peptides, separation of the bound aptamer candidate sequences from the unbound, and amplification and regeneration of the target-bound aptamer candidates. Before target incubation, the library was denatured at 95 °C in selection buffer and slowly cooled to enhance folding to adopt the most stable structure. In the first round of selection, 1 nmol of the library was used; which was then reduced to 100 pmol in

a Centre for Comparative Genomics, Murdoch University, Perth, 6150, Australia.
  E-mail: R.Veedu@murdoch.edu.au
b Perron Institute for Neurological and Translational Science, Perth, 6150, Australia
c School of Chemistry and Molecular Biosciences, The University of Queensland,
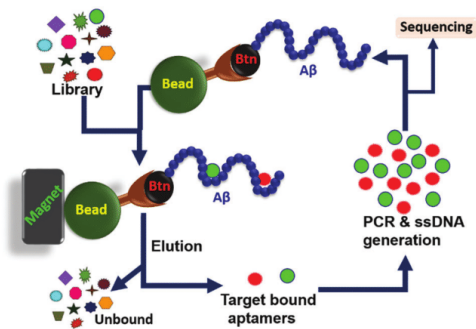 *Brisbane, 4072, Australia*

Fig. 1   Magnetic-bead assisted selection procedure for developing DNA aptamers against Aβ$_{1-40}$ peptide. Btn, biotin.

subsequent selection cycles. The stringency of aptamer selection was improved in each cycle by increasing the washing after incubation, and by reducing the amounts of bead-immobilized Aβ$_{1-40}$ peptides. To avoid non-specific binding, counter-selection steps were performed in rounds 2, 4, 6, 8 and after 10 using the selected candidate sequences of the previous round against magnetic beads and adding heparin to limit charge-based interactions.

The amplified DNA products from the 10th round of selection, after counter-selection with magnetic beads, was then cloned and sequenced. The sequence data were analysed, and the sequences with the most number of repeats (Table S3, ESI†) aligned to the initial sequence design were considered for further evaluation. To limit the number of candidates, the primer-binding regions of the shortlisted candidates were truncated and the structure of each aptamer candidate was predicted using Mfold, a web-based DNA or RNA folding algorithm.[23] The structure of one candidate, RNV95, had the lowest energy and formed a very stable stem-loop conformation (Fig. 2A). The candidates were then chemically synthesised with or without a biotin tag at the 5′ end. The stem-loop structure of synthesised RNV95 was also supported by CD spectroscopy (Fig. 2B).

To investigate the efficacy of aptamers in binding to Aβ peptides in clinical samples, we used autopsy hippocampal tissue from two neuropathologically confirmed AD cases (AD1
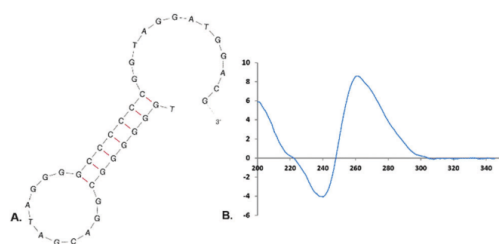

Fig. 2   Structural prediction of the aptamer candidate RNV95. (A) Computational prediction of the stem-loop structure of RNV95 by Mfold DNA Folding algorithm; (B) circular dichroism (CD) spectrum of RNV95.

and AD2; Queensland Brian Bank, University of Queensland). To verify the binding specificity of RNV95 we also collected two non-AD normal control samples (NC1 and NC2). The hippocampal tissue was homogenised in Tris buffer to test the efficacy of aptamers in detecting Aβ aggregates. To assess Aβ binding, western blot analysis was performed in which the gel was probed with biotinylated aptamers followed by Alexa Fluor 680-conjugated streptavidin. After washing, the images were captured on an Odyssey scanner system (Licor). An anti-Aβ monoclonal antibody (anti-Aβ$_{1-16}$), selective for human Aβ, was used in parallel as positive control.

Western blot analysis showed a prominent low-molecular-weight band at ∼15 kDa with both RNV95 and anti-Aβ monoclonal antibody (see ESI† for detailed experimental protocols; Fig. 3A and C). Bands of this size correspond to a tetrameric and/or pentameric aggregate of Aβ. It is noteworthy that RNV95 showed significantly higher intensities in detecting this band than the anti-Aβ antibody, which only showed weak bands at this molecular weight. Both RNV95 and anti-Aβ antibody also detected a high-molecular-weight aggregate between 75 and 100 kDa in low yields, and another product at 150 kDa in reasonably high yield (Fig. 3A and C). RNV95 did not show the ∼15 kDa band corresponding tetrameric/pentameric Aβ aggregates in healthy control brain tissue samples (NC1 and NC2, Fig. 3A and C) which is indicative of the binding specificity of RNV95 to AD. These results indicate that RNV95 could be a better alternative to the characterised monoclonal anti-Aβ antibody to detect low-molecular-weight aggregates of Aβ in AD brain tissue by western blot.
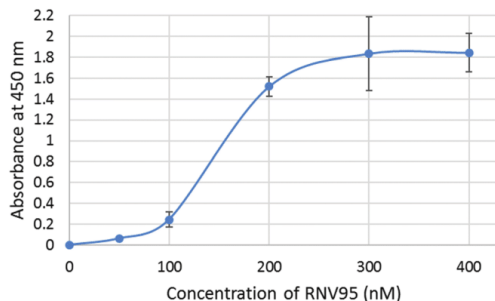
We then assessed the binding affinity of RNV95 and anti-Aβ monoclonal antibody for Aβ aggregates at different concentrations of the AD1 homogenate (Fig. 3B). RNV95 detected the ∼15 kDa band corresponding to the tetrameric/pentameric aggregate in 30 µg of the tissue homogenate, whereas the anti-Aβ monoclonal antibody showed the band only in 50 µg aliquots in low yield (Fig. S1, ESI†). Both the aptamer and the antibody also detected a product at ∼150 kDa. The results were consistent with the previous western blot as in Fig. 3A.

To further confirm the binding affinity of the aptamer for Aβ peptide aggregates, we performed an enzyme-linked oligonucleotide assay (ELONA). First, the oligomeric Aβ was prepared as per the protocol described by Tsukakoshi et al.[25] (see ESI† for detailed protocol). A 100 µL sample of Aβ oligomer was then immobilized onto 96-well microtiter plate wells and incubated at 37 °C for 2 h, followed by blocking with 4% skim milk in TBS–T buffer. Biotin-labelled RNV95 was added and the incubation continued for 2 h, followed by washing and incubation with anti-biotin antibody conjugated to HRP for 1 h. After washing, 100 µL of the TMB substrate was added and the incubation continued for 45 min, followed by the addition of stop solution (0.5 M sulfuric acid). Chemiluminescence was measured at 450 nm using a FLUOstar Omega Microplate Reader (BMG Biotech). The results clearly demonstrated high binding affinity of RNV95 for Aβ peptide aggregates across 50–400 nM concentrations (Fig. 4). Note that when monomeric Aβ peptide was used, binding was only apparent at concentrations above 10 µM of RNV95.
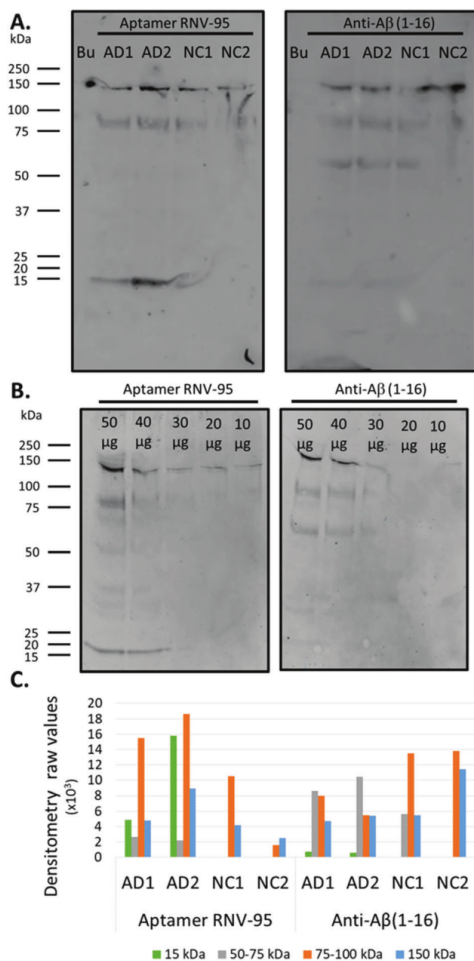
Fig. 3 Binding analysis of aptamers to Aβ peptides in human brain tissues. (A) Western blot analysis of the aptamer RNV95 and anti-Aβ monoclonal antibody-detected Aβ aggregates in two controls (NC1 and NC) and two AD (AD1 and AD2) brain samples; Bu = loading buffer control. (B) Binding analysis of aptamers to Aβ peptides in different amounts of whole AD brain homogenates. (C) Densitometry analysis of (A) using Image J software.[24]

Fig. 4 Binding analysis of RNV95 to Aβ peptide aggregates. ELONA-binding assay using different concentrations of RNV95 (0, 50, 100, 200, 300 and 400 nM) to oligomeric Aβ peptide.

Conflicts of interest

There are no conflicts to declare.

References

1 K. E. Lundin, O. Gissberg and C. E. Smith, Hum. Gene Ther., 2015, 26, 475–485.
2 M. Famulok, J. S. Hartig and G. Mayer, Chem. Rev., 2007, 107, 3715–3743.
3 A. D. Keefe, S. Pai and A. Ellington, Nat. Rev. Drug Discovery, 2010, 9, 537–550.
4 F. Lipi, S. Chen, M. Chakravarthy, S. Rakesh and R. N. Veedu, RNA Biol., 2016, 13, 1232–1245.
5 K. Rahimizadeh, H. AlShamaileh, M. Fratini, M. Chakravarthy, M. Stephen, S. Shigdar and R. N. Veedu, Molecules, 2017, 22, 2070.
6 R. N. Veedu, Aptamers: Tools for Nanotherapy and Molecular Imaging, CRC Press, 2017.
7 R. N. Veedu, Curr. Top. Med. Chem., 2015, 15, 1065.
8 R. Stoltenburg, C. Reinemann and B. Strehlitz, Biomol. Eng., 2007, 24, 381–403.
9 S. C. B. Gopinath, Anal. Bioanal. Chem., 2007, 387, 171–182.
10 L. H. Lauridsen, H. A. Shamaileh, S. L. Edwards, E. Taran and R. N. Veedu, PLoS One, 2012, 7, e41702.
11 L. J. Aaldering, H. Tayeb, S. Krishnan, S. Fletcher, S. D. Wilton and R. N. Veedu, RNA Biol., 2015, 12, 412–425.
12 E. W. Ng, D. T. Shima, P. Calias, E. T. Cunningham Jr, D. R. Guyer and A. P. Adamis, Nat. Rev. Drug Discovery, 2006, 5, 123.
13 T. Simao, A. Ng, D. Fatehi, S. Corluka, A. Abulrob and M. Zourob, J. Biomed. Nanotechnol., 2015, 11, 2264–2274.
14 H. Liang, Y. Shi, Z. Kou, Y. Peng, W. Chen, X. Li, S. Li, Y. Wang, F. Wang and X. Zhang, PLoS One, 2015, 10, e0140733.
15 R. K. Tannenberg, L. H. Lauridsen, J. R. Kanwar, P. R. Dodd and R. N. Veedu, Curr. Alzheimer Res., 2013, 10, 442–448.
16 B. Sriramoju, R. Kanwar, R. N. Veedu and J. R. Kanwar, Curr. Top. Med. Chem., 2015, 15, 1115–1124.
17 H. W. Querfurth and F. M. Laferla, N. Engl. J. Med., 2010, 362, 1844–1845.
18 M. P. Murphy and H. LeVine III, J. Alzheimer's Dis., 2010, 19, 311–323.

In summary, we have developed a 39-nucleotide DNA aptamer, RNV95, to Aβ peptide. Western blot analysis indicated that RNV95 had the capability to bind to tetrameric and/or pentameric Aβ peptide aggregates in neuropathologically confirmed AD brain tissue. Current aptamers developed specifically for Aβ peptides show affinity to synthetic Aβ fibrils and plaques. Although further characterisation, particularly in situ, needs to be done, the evidence presented here strongly supports the proposition that RNV95 could be applied to wide range of affinity assays to detect Aβ.

55

19 L. I. Binder, A. L. Guillozet-Bongaarts, F. Garcia-Sierra and R. W. Berry, *Biochim. Biophys. Acta*, 2005, **1739**, 216–223.

20 F. Rahimi, K. Murakami, J. L. Summers, C.-H. B. Chen and G. Bitan, *PLoS One*, 2009, **4**, e7694.

21 F. Ylera, R. Lurz, V. A. Erdmann and J. P. Fürste, *Biochem. Biophys. Res. Commun.*, 2002, **290**, 1583–1588.

22 T. Takahashi, K. Tada and H. Mihara, *Mol. BioSyst.*, 2009, **5**, 986–991.

23 M. Zuker, *Nucleic Acids Res.*, 2003, **31**, 3406–3415.

24 J. Schindelin, C. T. Rueden, M. C. Hiner and K. W. Eliceiri, *Mol. Reprod. Dev.*, 2015, **82**, 518–529.

25 K. Tsukakoshi, K. Abe, K. Sode and K. Ikebukuro, *Anal. Chem.*, 2012, **84**, 5542–5547.

SCIENTIFIC REPORTS

OPEN

Systematic evaluation of 2′-Fluoro modified chimeric antisense oligonucleotide-mediated exon skipping *in vitro*

Suxiang Chen[1,2], Bao T. Le[1,2], Madhuri Chakravarthy[1,2], Tamer R. Kosbar [2] & Rakesh N. Veedu[1,2]

Antisense oligonucleotide (AO)-mediated splice modulation has been established as a therapeutic approach for tackling genetic diseases. Recently, Exondys51, a drug that aims to correct splicing defects in the dystrophin gene was approved by the US Food and Drug Administration (FDA) for the treatment of Duchenne muscular dystrophy (DMD). However, Exondys51 has relied on phosphorodiamidate morpholino oligomer (PMO) chemistry which poses challenges in the cost of production and compatibility with conventional oligonucleotide synthesis procedures. One approach to overcome this problem is to construct the AO with alternative nucleic acid chemistries using solid-phase oligonucleotide synthesis via standard phosphoramidite chemistry. 2′-Fluoro (2′-F) is a potent RNA analogue that possesses high RNA binding affinity and resistance to nuclease degradation with good safety profile, and an approved drug Macugen containing 2′-F-modified pyrimidines was approved for the treatment of age-related macular degeneration (AMD). In the present study, we investigated the scope of 2′-F nucleotides to construct mixmer and gapmer exon skipping AOs with either 2′-*O*-methyl (2′-*O*Me) or locked nucleic acid (LNA) nucleotides on a phosphorothioate (PS) backbone, and evaluated their efficacy in inducing exon-skipping in *mdx* mouse myotubes *in vitro*. Our results showed that all AOs containing 2′-F nucleotides induced efficient exon-23 skipping, with LNA/2′-F chimeras achieving better efficiency than the AOs without LNA modification. In addition, LNA/2′-F chimeric AOs demonstrated higher exonuclease stability and lower cytotoxicity than the 2′-*O*Me/2′-F chimeras. Overall, our findings certainly expand the scope of constructing 2′-F modified AOs in splice modulation by incorporating 2′-*O*Me and LNA modifications.

Nucleic acid therapeutics has attracted tremendous attention in recent years with a number of successful clinical translations for various diseases[1]. To date, the US Food and Drug Administration (FDA) has approved six oligonucleotide-based therapeutic molecules including one aptamer (Macugen) for the treatment of age-related macular degeneration (AMD), four antisense oligonucleotides (AOs) (Vitravene, Kynamro, Exondys51, and Spinraza) for the treatment of cytomegalovirus retinitis, familial hypercholesterolemia, Duchenne muscular dystrophy (DMD), and spinal muscular atrophy (SMA), respectively[2–4] and one siRNA drug (Onpattro) for the treatment of amyloidosis. Unlike other protein-targeting therapeutic approaches, AOs can alter the pathological hallmark of the disease at the RNA level via different intracellular mechanisms (RNase-H-mediated degradation, imposing steric block to block translation or to modulate splicing)[1,5]. However, oligonucleotides composed of naturally occurring nucleotide monomers (deoxyribonucleotide or ribonucleotide) are easily degraded by nucleases and possess poor target binding affinity[5], thus, they are not suitable for drug development. To overcome these limitations, chemically-modified nucleic acid analogues, mainly of sugar and phosphate backbone modifications, have been utilized in developing therapeutic oligonucleotides. So far, prominent chemical modifications that have been granted approval for clinical usage include phosphorothioate (PS)[6], used in Vitravene, Kynamro, and Spinraza; 2′-*O*-methyl (2′-*O*Me)[7–11], used in Macugen and Onpattro; 2′-Fluoro (2′-F)[7–11], used in Macugen;

[1]Centre for Molecular Medicine and Innovative Therapeutics, Murdoch University, Perth, 6150, Australia. [2]Perron Institute for Neurological and Translational Science, Perth, 6150, Australia. Correspondence and requests for materials should be addressed to R.N.V. (email: R.Veedu@murdoch.edu.au)
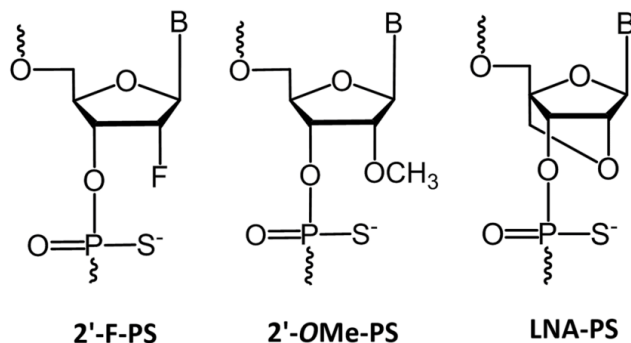
Figure 1. Structural representations of 2′-F, 2′-OMe, and LNA monomers on a PS backbone.

2′-O-methoxyethyl (2′-OMOE)[12], used in Kynamro and Spinraza; and phosphorodiamidate morpholino (PMO)[13], used in Exondys51. Of these, 2′-OMe and PMO have been explored extensively for AO-mediated splice modulation. In addition, several other analogues such as locked nucleic acid (LNA)[14–16], unlocked nucleic acid (UNA)[17], peptide nucleic acid (PNA)[18], serinol nucleic acid (SNA)[19], tricyclo DNA (tcDNA)[20], twisted intercalating nucleic acid (TINA)[21], anhydrohexitol nucleic acid (HNA)[22], cyclohexenyl nucleic acid (CeNA)[22], D-altritol nucleic acid (ANA)[22] and morpholino nucleic acid (MNA)[23] have also been investigated in splice modulation. Recently, nucleobase-modified AOs containing 2-thioribothymidine[24], and 5-(phenyltriazol)-2′-deoxyuridine[25] nucleotides have been reported to induce exon skipping in DMD model systems.

DMD is a severe and fatal muscle wasting genetic disorder mainly affecting newborn boys[26–28]. DMD is caused by one or more mutations in the dystrophin gene that ablate the expression of functional dystrophin proteins required for protecting muscle fibers from eccentric contraction and movement[29,30]. Recently, AO-mediated exon skipping has been established as one of the most promising therapeutic strategy for treating DMD[28,31–36]. Skipping the mutation containing exons can restore the dystrophin reading frame and rescue the production of the truncated but partially functional dystrophin protein. PMO and 2′-OMe-PS-modified AOs have been investigated in phase-3 clinical trials for DMD[27,28,32–38]. In 2016, the PMO-based AO drug (Exondys51) has been granted accelerated approval by the US FDA[3]. In contrast, the 2′-OMe-PS-based candidate (drisapersen) was rejected mainly due to safety issues and lack of efficacy[39]. Although PMO-modified oligonucleotides showed excellent safety profile, it is not compatible with standard oligonucleotide synthesis chemistries in order to synthesise as mixmers with other well-known nucleotide analogues and large-scale production of PMOs is challenging due to distinctive synthesis procedure. Therefore, it is necessary to evaluate alternative nucleic acid chemistries that can be used for AO drug development.

Towards this, Kawasaki *et al.* introduced 2′-F as an attractive ribonucleotide analogue for constructing AO. In fact, 2′-F-PS (Fig. 1) AOs showed higher target binding affinity, and nuclease stability[8]. Previous studies have also revealed its enhanced capability of inducing exon skipping *in vitro* compared to 2′-OMe-PS (Fig. 1) AOs[8–11], which may be due to the recruitment of interleukin enhancer binding factors 2 and 3 (ILF2/3) by 2′-F AO/pre-mRNA duplex which may result in improved steric block efficiency[9–11]. However, 2′-F-modified AOs did not reach clinical evaluation and the scope of 2′-F-modified AOs needs to be improved by novel design approaches. LNA (Fig. 1) is another prominent RNA analogue that has been successfully investigated in recent studies to induce exon skipping in the dystrophin gene transcript[16,40]. In this study, for the first time, we herein report the design, synthesis and evaluation of 2′-F-modified exon skipping AOs to induce exon-23 skipping in DMD mouse myotubes *in vitro*.

Results

In the present study, we used a previously reported fully modified 2′-OMe-PS 18-mer AO sequence, DmdE23D (+1–17) which was designed to induce exon-23 skipping in mouse *Dmd* transcript[16], as a positive control (Table 1). Based on this AO, we systematically designed and synthesised a fully modified 2′-F AO on a PS backbone, three 2′-OMe/2′-F-PS chimeric AOs, and three LNA/2′-F-PS chimeric AOs which include a gapmer and two mixmer designs (Table 1). Two-step systematic evaluation was performed *in vitro* in mouse myotubes differentiated from H-2K^b-tsA58 (H2K) *mdx* myoblasts. Initial evaluation was conducted for all AOs at 12.5 nM, 25 nM, and 50 nM concentrations while secondary evaluation was performed at lower concentrations (2.5 nM, 5 nM, and 12.5 nM) for chimeric AOs. In general, *H2K mdx* myoblasts were plated on 24-well plates and incubated for 24 h for differentiation. The differentiated myotubes were then transfected with different concentrations of the above-mentioned AOs by Lipofectin transfection reagent using a ratio of 2:1 (Lipofectin: AO). Twenty-four hours after transfection, cells were collected followed by total cellular RNA extraction, and reverse transcription polymerase chain reaction (RT-PCR) to amplify the dystrophin transcripts across exons 20–26 as reported previously[41]. Next, 2% agarose gel electrophoresis and densitometry (using Image J software) were performed to quantify the PCR products. The actual percentages of full length (901 bp), exon-23 skipping (688 bp), and exon-22/23 dual skipping (542 bp) products are presented based on the total amount of the dystrophin transcripts. Systematic exon skipping evaluation was performed in duplicates.

58

| AO name	Sequence, $5' \to 3'$ direction
Fully 2′-OMe-PS	**GCCAAACCUCGGCUUACC**
Fully 2′-F-PS	G^{F}C^{F}C^{F}A^{F}A^{F}A^{F}C^{F}C^{F}U^{F}C^{F}G^{F}G^{F}C^{F}U^{F}U^{F}A^{F}C^{F}C^F
2′-OMe/2′-F-PS gapmer	**GC**C^{F}A^{F}A^{F}A^{F}C^{F}C^{F}U^{F}C^{F}G^{F}G^{F}C^{F}U^{F}U^{F}A^F**CC**
2′-OMe/2′-F-PS mixmer 1	**G**C^{F}C^{F}A^{F}A^{F}A^F**CC**U^{F}C^{F}G^F**GC**U^{F}U^{F}A^{F}C^F**C**
2′-OMe/2′-F-PS mixmer 2	G^{F}C^{F}C^{F}A^{F}A^{F}A^{F}C^{F}C^F**U**C^{F}G^F**GC**U^{F}U^F**UA**^{F}C^F**C**
LNA/2′-F-PS gapmer	***G**^{L}**C**^{L}C^{F}A^{F}A^{F}A^{F}C^{F}C^{F}U^{F}C^{F}G^{F}G^{F}C^{F}U^{F}U^{F}A^F**C**^{L}**C**^{L}
LNA/2′-F-PS mixmer 1	***G**^{L}C^{F}C^{F}A^{F}A^{F}A^F**C**^{L}C^{F}U^{F}C^{F}G^F**G**^{L}C^{F}U^{F}U^{F}A^{F}C^F**C**^{L}
LNA/2′-F-PS mixmer 2	G^{F}C^{F}C^{F}A^{F}A^{F}A^{F}C^{F}C^F***T**^{L}C^{F}G^F**G**^{L}C^{F}U^F***T**^{L}A^{F}C^F**C**^{L}

Table 1. List of AO names and sequences used in this study. 2′-OMe nucleotides are represented in underlined and bold letters; 2′-F nucleotides are represented in black letters with superscript F; LNA nucleotides are represented in underlined and bold-italic letters with superscript L. All AOs possess PS backbone.

Evaluation of 2′-F modified AOs to induce exon skipping in dystrophin transcript in H2K *mdx* mouse myotubes *in vitro* at 12.5 nM, 25 nM, and 50 nM concentrations.   Firstly, we evaluated the exon skipping efficiency of all AOs (Table 1) *in vitro* at three different concentrations (12.5 nM, 25 nM, and 50 nM). The results demonstrated that all AOs are capable of inducing efficient exon skipping at various levels (Figs 2 and 3). In line with previous report[16], the 2′-OMe-PS control AO induced efficient exon-23 skipping by yielding the skipped product of 688 bp at all concentrations (43% at 12.5 nM, 47% at 25 nM, and 51% at 50 nM; Fig. 3A). Interestingly, the fully modified 2′-F-PS AO showed higher exon-23 skipping at 12.5 nM (50%) compared to the control AO (43%), but the efficiency reduced to 44% at 25 nM and remained 51% at 50 nM, respectively. But, 2′-F-PS AOs showed the undesired exon-22/23 dual skipping product of 542 bp in higher yield at 25 nM (35%) compared to 2′-OMe-PS AO (27%) (Fig. 3A).

All mixmer and gapmer AOs achieved the highest exon-23 skipping at 25 nM or 50 nM (Fig. 3B,C). Markedly, the LNA/2′-F-PS mixmer 2 yielded the highest exon-23 skipping product (63%) (Fig. 3C) compared to all other AOs (42–53%) at 50 nM concentration (Fig. 3). Surprisingly, a significant drop in exon-23 skipping product was observed after transfection with 12.5 nM of the 2′-OMe/2′-F-PS gapmer, which induced only 26% (Fig. 3B) of skipping while other AOs achieved 43–56% of skipping at this concentration (Fig. 3). Direct comparison between the 2′-OMe/2′-F-PS and the corresponding LNA/2′-F-PS gapmer and mixmer AOs indicated that the LNA/2′-F-PS AOs achieved higher exon-23 skipping efficiency at various concentrations. For instance, at 25 nM concentration, exon-23 skipping induced by LNA/2′-F gapmer (58%) was higher than 2′-OMe/2′-F gapmer (42%), LNA/2′-F mixmer 1 (54%) was higher than 2′-OMe/2′-F mixmer 1 (46%), and LNA/2′-F mixmer 2 (51%) was higher than 2′-OMe/2′-F mixmer 2 (50%). Furthermore, at all concentrations, each type of LNA/2′-F mixmers (mixmer 1: 31% at 12.5 nM, 35% at 25 nM; mixmer 2: 19% at 12.5 nM, 27% at 25 nM, 22% at 50 nM) induced the less undesired exon-22/23 dual skipping than its corresponding 2′-OMe/2′-F mixmers (mixmer 1: 39% at 12.5 nM, 37% at 25 nM; mixmer 2: 37% at 12.5 nM, 36% at 25 nM, 40% at 50 nM) except mixmer 1 AOs at 50 nM (LNA/2′-F mixmer 1: 46%; 2′-OMe/2′-F mixmer 1: 39%).

Evaluation of chimeric AOs to induce exon skipping in dystrophin transcript in H2K *mdx* mouse myotubes *in vitro* at 2.5 nM, 5 nM, and 12.5 nM concentrations.   To further explore the ability of the 2′-F modified chimeric AOs in inducing exon skipping, we transfected all chimeric AOs (2′-OMe/2′-F-PS chimeras and LNA/2′-F-PS chimeras) (Table 1) at lower concentrations (2.5 nM, 5 nM, and 12.5 nM) together with 2′-OMe-PS control. In general, all AOs yielded efficient exon-23 skipped products in a dose-dependent manner, except the 2′-OMe/2′-F gapmer (Figs 4 and 5). Furthermore, all 2′-F modified chimeras achieved higher exon-23 skipping efficiency than the 2′-OMe-PS control at all concentrations except 2′-OMe/2′-F gapmer at 12.5 nM (2′-OMe/2′-F gapmer: 20%; 2′-OMe-PS control: 33%) (Fig. 5). Notably, at 12.5 nM, LNA/2′-F-PS gapmer achieved the highest exon-23 skipping level (51%) (Fig. 5C) in comparison to all other chimeric AOs (20–48%) (Fig. 5B,C). It was also noted that LNA/2′-F chimeric AOs achieved higher or comparable exon-23 skipping efficiency compared with its corresponding 2′-OMe/2′-F chimeric AO at all concentrations except LNA/2′-F mixmer 2 at 2.5 nM (LNA/2′-F mixmer 2: 18%; 2′-OMe/2′-F mixmer 2: 24%) (Fig. 5B,C). The percentage of exon-23 skipping induced by LNA/2′-F gapmer (33% at 2.5 nM, 40% at 5 nM, 51% at 12.5 nM) was higher than 2′-OMe/2′-F gapmer (14% at 2.5 nM, 26% at 5 nM, 20% at 12.5 nM); LNA/2′-F mixmer 1 (33% at 2.5 nM, 40% at 5 nM, 48% at 12.5 nM) was higher than 2′-OMe/2′-F mixmer 1 (31% at 2.5 nM, 34% at 5 nM, 39% at 12.5 nM); and LNA/2′-F mixmer 2 (32% at 5 nM, 44% at 12.5 nM) was higher than or equivalent to 2′-OMe/2′-F mixmer 2 (32% at 5 nM, 41% at 12.5 nM). In addition, at all concentrations (2.5 nM, 5 nM, 12.5 nM), LNA/2′-F mixmers (mixmer 1: 15%, 18%, 27%; mixmer 2: 16%, 13%, 22%) induced less undesired exon-22/23 dual skipping than their corresponding 2′-OMe/2′-F mixmer (mixmer 1: 23%, 29%, 35%; mixmer 2: 29%, 33%, 34%) (Fig. 5B,C). Interestingly, exon-22/23 dual skipping was not visible in the case of 2′-OMe/2′-F-PS gapmer at 2.5 nM and 5 nM (Figs 4B and 5B).

To further evaluate the optimal design of the AO, we compared the exon skipping efficiency between the gapmer and two mixmer chimeric AOs. The results demonstrated that at all concentrations (2.5 nM, 5 nM, 12.5 nM), the 2′-OMe/2′-F mixmer chimeras achieved higher exon-23 skipping efficiency than the 2′-OMe/2′-F gapmer chimeras (Figs 4B and 5B), however, the LNA/2′-F gapmer induced higher or comparable exon-23 skipping compared with the LNA/2′-F mixmers. That is, exon-23 skipping induced by 2′-OMe/2′-F mixmers (mixmer 1: 31% at 2.5 nM, 34% at 5 nM, 39% at 12.5 nM; mixmer 2: 24% at 2.5 nM, 32% at 5 nM, 41% at 12.5 nM) was higher than 2′-OMe/2′-F gapmer (14% at 2.5 nM, 26% at 5 nM, 20% at 12.5 nM) (Fig. 5B); while exon-23 skipping induced by

59
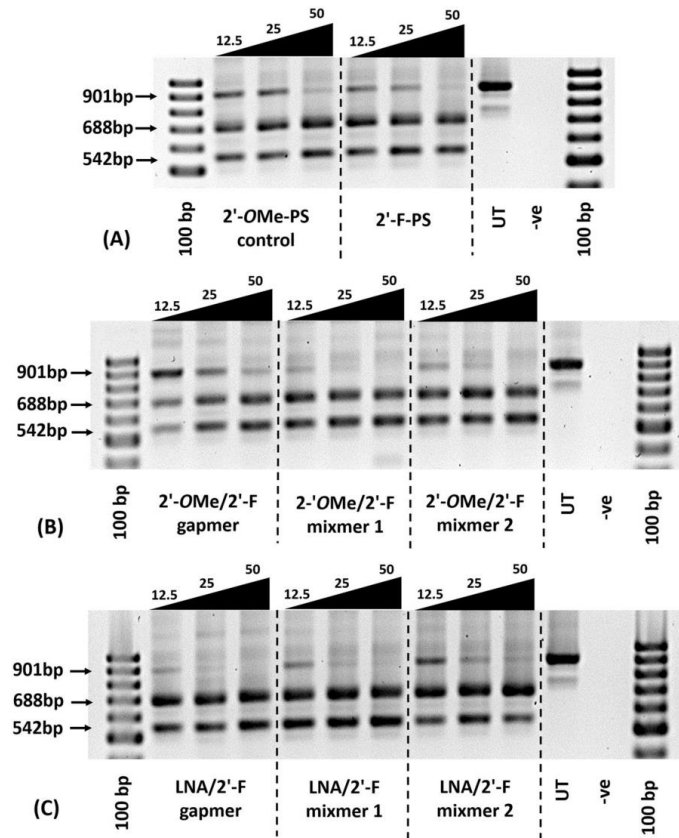
Figure 2. Agarose gel analysis of RT-PCR products showed exon-23 and exon-22/23 dual skipping in *mdx* mouse myotubes *in vitro*. Concentrations of AOs used include 12.5 nM, 25 nM, and 50 nM. (**A**) Fully modified 2′-*O*Me-PS control AO and fully modified 2′-F-PS AO; the original gel image is shown in Fig. S1 (A2) (Supplementary Information). (**B**) 2′-*O*Me modified 2′-F-PS AO chimeras including 2′-*O*Me/2′-F-PS gapmer, 2′-*O*Me/2′-F-PS mixmer 1, and 2′-*O*Me/2′-F-PS mixmer 2; the original gel image is shown in Fig. S1(B2) (Supplementary Information). (**C**) LNA modified 2′-F-PS AO chimeras including LNA/2′-F-PS gapmer, LNA/2′-F-PS mixmer 1, and LNA/2′-F-PS mixmer 2; the original gel image is shown in Fig. S1(C2) (Supplementary Information). The corresponding densitometry data of the gel images are shown in Fig. S1(A1, B1 and C1) (Supplementary Information).

LNA/2′-F gapmer (33% at 2.5 nM, 40% at 5 nM, 51% at 12.5 nM) was higher than or comparable to the LNA/2′-F mixmers (mixmer 1: 33% at 2.5 nM, 40% at 5 nM, 48% at 12.5 nM; mixmer 2: 18% at 2.5 nM, 32% at 5 nM, 44% at 12.5 nM) (Fig. 5C). On the other hand, LNA/2′-F mixmers induced less unwanted exon-22/23 dual skipping than LNA/2′-F gapmer. Therefore, exon-22/23 skipping induced by LNA/2′-F mixmers (mixmer 1: 15% at 2.5 nM, 18% at 5 nM, 27% at 12.5 nM; mixmer 2: 16% at 2.5 nM, 13% at 5 nM, 22% at 12.5 nM) was lower than LNA/2′-F gapmer (21% at 2.5 nM, 27% at 5 nM, 28% at 12.5 nM) (Fig. 5C).

Evaluation of *in vitro* cytotoxicity of the 2′-F modified AOs. Safety is crucial for any clinically relevant therapeutic drug. Therefore, we performed the cytotoxicity evaluation for all 2′-F modified AOs by conducting WST-1 reagent-based cell viability assay. Briefly, mouse myoblasts were seeded and differentiated into myotubes, followed by transfecting with the AOs (50 nM and 12.5 nM) as described previously. The untreated (UT) groups were not transfected by any AO but only incubated with Lipofectin reagent instead. The cells were then incubated with WST-1 reagent at a ratio of 1:10 (v/v) at 37 °C, 5% CO_2 for 4 h. Cytotoxicity was determined by measuring the absorbance at 450 nm. In general, all 2′-F modified AOs did not show any significant cytotoxicity in comparison to the fully 2′-*O*Me-PS control (Fig. 6). Notably, at 12.5 nM, LNA modified 2′-F chimeras showed higher viability than 2′-*O*Me modified 2′-F chimeras. On the other hand, 2′-*O*Me/2′-F-PS mixmer 2

60
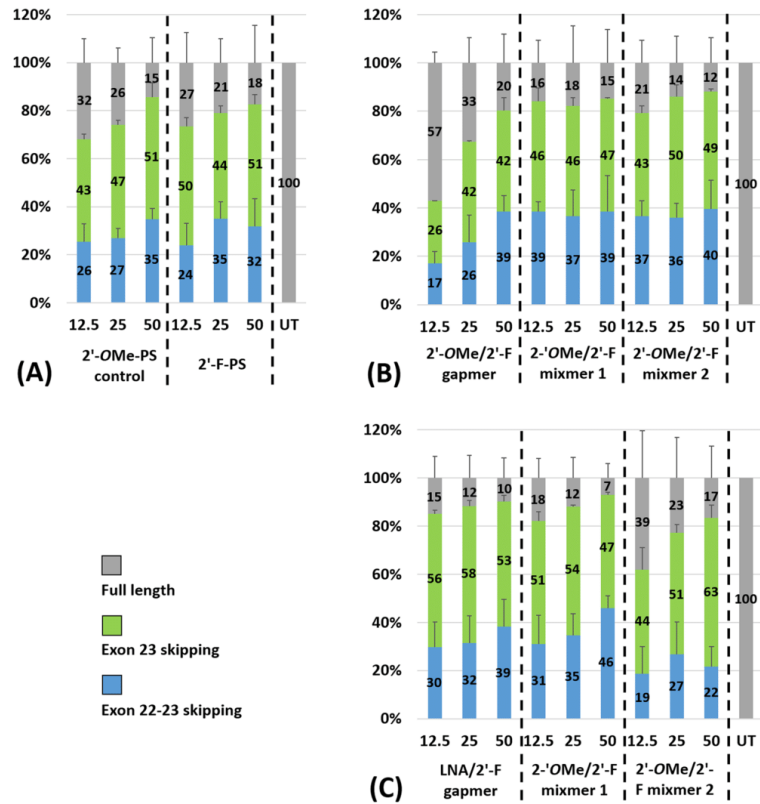
Figure 3. Densitometry analysis of RT-PCR products (in duplicates) showed exon-23 and exon-22/23 dual skipping in *mdx* mouse myotubes *in vitro*. Concentrations of AOs used include 12.5 nM, 25 nM, and 50 nM. (**A**) Fully modified 2′-OMe-PS control AO and fully modified 2′-F-PS AO; (**B**) 2′-OMe modified 2′-F-PS AO chimeras including 2′-OMe/2′-F-PS gapmer, 2′-OMe/2′-F-PS mixmer 1, and 2′-OMe/2′-F-PS mixmer 2; (**C**) LNA modified 2′-F-PS AO chimeras including LNA/2′-F-PS gapmer, LNA/2′-F-PS mixmer 1, and LNA/2′-F-PS mixmer 2. The gel images and their corresponding densitometry data of each repetition are shown in Figs S1 and S3 (Supplementary Information).

demonstrated less viability than the other AOs at both concentrations, which may be due to the positioning of the 2′-OMe nucleotides as the 2′-OMe/2′-F-PS mixmer 1 achieved higher cell viability at both concentrations (Fig. 6).

Evaluation of *in vitro* nuclease stability of the 2′-F modified AOs. To gain more insight into the AO stability, we then performed the nuclease degradation assay of all the 2′-F modified AOs in comparison to the fully 2′-OMe-PS control. In short, AOs were incubated with Phosphodiesterase I from Crotalus adamanteus venom which possesses very high exonuclease activity, at 37 °C for various incubation periods including 0, 1, 2, 4, and 6 h. Samples were collected at the desired timepoints and quenched with formamide loading buffer, followed by denaturation at 95 °C for 5 min. Next, 20% denaturing polyacrymide gel analysis was performed and the results were analysed by gel imaging. All 2′-F modified AOs demonstrated high stability under the applied conditions compared to the fully 2′-OMe-PS control (Fig. 7). Not surprisingly, all the LNA/2′-F-PS chimeras showed higher nuclease resistance than the other AOs without LNA modification (Fig. 7). In addition, the gapmer chimeras showed higher stability than the mixmer chimeras.

Discussion

Therapeutic potential of AOs was first demonstrated by Zamecnik *et al.* in 1978[42]. Stemming from this initial work, AOs have been extensively explored as a potential gene-targeting approach for the treatment of various genetic diseases. In line with this, splice-switching AOs have been developed, firstly by Dominski *et al.* in 1993, and later became promising therapies towards tackling genetic diseases caused by mutations such as DMD and SMA[43]. Along this line, chemically-modified nucleic acid analogues play a crucial role in the successful clinical
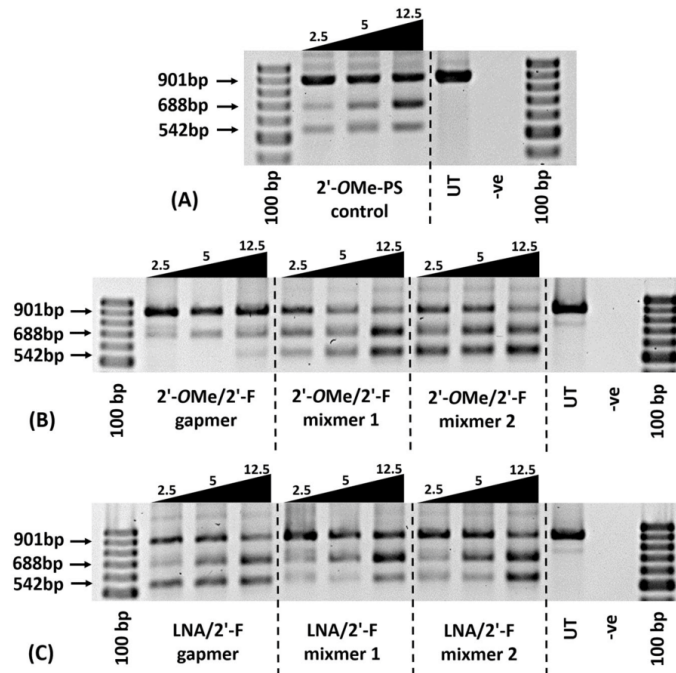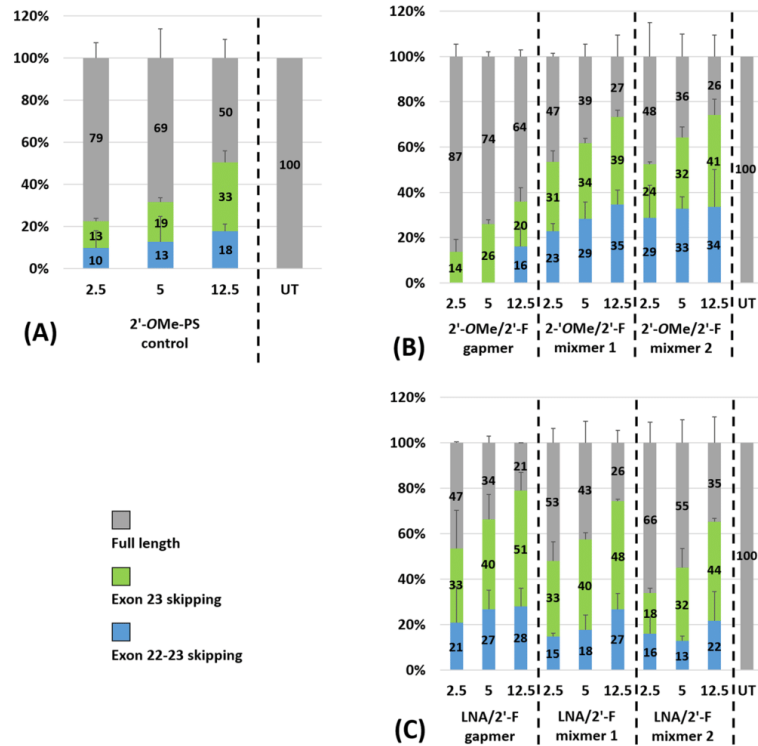
Figure 4. Agarose gel analysis of the RT-PCR products showed exon-23 and exon-22/23 dual skipping in *mdx* mouse myotubes *in vitro*. Concentrations of AOs used include 2.5 nM, 5 nM, and 12.5 nM. (**A**) Fully modified 2′-*O*Me-PS control AO; the original gel image is shown in Fig. S2(A2) (Supplementary Information). (**B**) 2′-*O*Me modified 2′-F-PS AO chimeras including 2′-*O*Me/2′-F-PS gapmer, 2′-*O*Me/2′-F-PS mixmer 1, and 2′-*O*Me/2′-F-PS mixmer 2; the original gel image is shown in Fig. S2(B2) (Supplementary Information). (**C**) LNA modified 2′-F-PS AO chimeras including LNA/2′-F-PS gapmer, LNA/2′-F-PS mixmer 1, and LNA/2′-F-PS mixmer 2; the original gel image is shown in Fig. S2(C2) (Supplementary Information). The corresponding densitometry data of the gel images are shown in Fig. S2(A1,B1,C1) (Supplementary Information).

translation of any AO-based drug, given the PMO-based Exondys51 was granted conditional approval in 2016, while the 2′-*O*Me-PS-based drisapersen was rejected in the same year due to lack of efficacy and life-threatening side effects. Although a PMO-based AO is relatively non-toxic, PMO chemistry has its disadvantages due to limitation of large-scale synthesis and lack of compatibility with other chemistries. Towards exploring chemically modified AOs targeting DMD, Aartsma-Rus and colleagues evaluated AOs constructed by fully modified 2′-F-PS and LNA-PS[10,11,44], while our group has investigated LNA, HNA, CeNA, ANA, and MNA monomers[16,22,23].

The first attempt to study 2′-F modified AO was reported in 1993 when Kawasaki *et al.* found that 2′-F modification enhanced the AO's target binding affinity to their complementary RNA compared to 2′-*O*Me modified AO, and showed excellent nuclease stability[8]. Two decades later, Rigo and colleagues discovered a unique property of the 2′-F modified AO/target pre-mRNA duplex that is able to recruit the ILF2/3 proteins, resulting in exon-7 skipping of *SMN2* mRNA in a SMA model system[9]. Based on this finding, Aartsma-Rus and coworkers compared the exon skipping capability of the fully 2′-F-PS and fully 2′-*O*Me-PS AOs in targeting DMD, and showed that 2′-F-PS AO induced higher human exon-53 and mouse exon-23 skipping *in vitro*[10,11], which was not surprising as 2′-F modification has many advantages as proven by Kawasaki *et al.*[8] and Rigo *et al.*[9], however, 2′-F-PS AO was less efficient than 2′-*O*Me-PS *in vivo* and indicated toxicity in mice[11]. Thus, their results did not support clinical use of 2′-F-PS AOs[11].

In an attempt to improve the therapeutic potential of 2′-F modified AO, we incorporated 2′-*O*Me-PS and LNA-PS nucleotides into an 18 mer 2′-F-PS AO sequence that contained either four 2′-*O*Me or LNA nucleotides designed to target exon-23 of *mdx* mouse myotubes (Table 1). The efficacies of the AOs were first evaluated at higher (12.5 nM, 25 nM, 50 nM), and then lower concentrations (2.5 nM, 5 nM, 12.5 nM); in addition to performing cytotoxicity and nuclease stability analysis.

Fully modified 2′-F-PS AO induced higher exon-23 skipping than the fully modified 2′-*O*Me-PS control at 12.5 nM, and both of them indicated similar exon-23 skipping efficiency on higher concentrations (25 nM, 50 nM), in line with Aartsma-Rus *et al.*[12] finding that 2′-F-PS AO induced minimal increase of exon-23 skipping

62

www.nature.com/scientificreports/

Figure 5. Agarose gel and densitometry analysis of the RT-PCR products (in duplicates) showed exon-23 and exon-22/23 dual skipping in *mdx* mouse myotubes *in vitro*. Concentrations of AOs used include 2.5 nM, 5 nM, and 12.5 nM. (A) Fully modified 2′-*O*Me-PS control AO; (B) 2′-*O*Me modified 2′-F-PS AO chimeras including 2′-*O*Me/2′-F-PS gapmer, 2′-*O*Me/2′-F-PS mixmer 1, and 2′-*O*Me/2′-F-PS mixmer 2; (C) LNA modified 2′-F-PS AO chimeras including LNA/2′-F-PS gapmer, LNA/2′-F-PS mixmer 1, and LNA/2′-F-PS mixmer 2. The gel images and their corresponding densitometry data of each repetition are shown in Figs S2 and S4 (Supplementary Information).
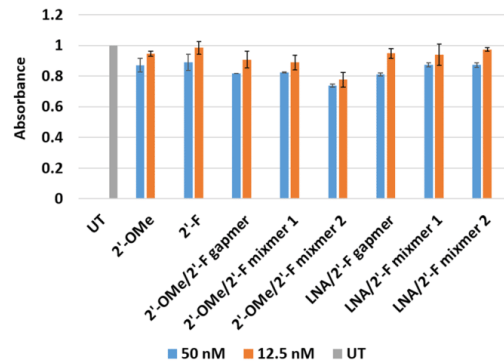
Figure 6. Cell viability assay (in duplicates) of 2′-F modified AOs. The original data of absorbance is shown in Table S1 (Supplementary Information).

SCIENTIFIC **REPORTS** | *(2019) 9:6078* | https://doi.org/10.1038/s41598-019-42523-0   7

63
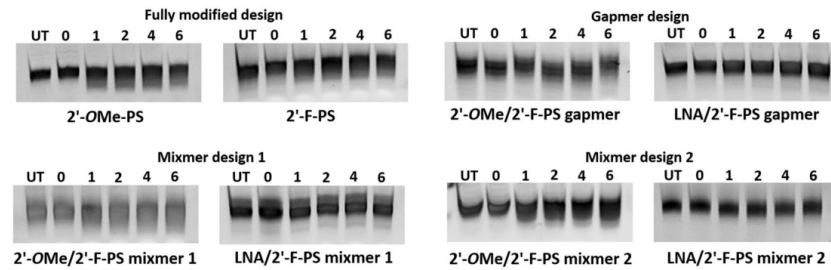
Figure 7. Nuclease stability analysis of 2′-F modified AOs. The original gel images are shown in Fig. S5 (Supplementary Information).

when compared to 2′-OMe-PS AO *in vitro*. In general, chimeric 2′-F-PS AOs induced efficient exon-23 skipping. Each of the LNA/2′-F-PS chimeras achieved higher or comparable exon-23 skipping in comparison to their corresponding 2′-OMe/2′-F-PS counterparts (LNA/2′-F-PS gapmer > 2′-OMe/2′-F-PS gapmer, LNA/2′-F-PS mixmer 1 ≥ 2′-OMe/2′-F-PS mixmer 1, LNA/2′-F-PS mixmer 2 > 2′-OMe/2′-F-PS mixmer 2), indicating that LNA modification may possess better exon-23 skipping capability than 2′-OMe on a 2′-F-PS platform. Notably, at 50 nM, LNA/2′-OMe/2′-F-PS mixmer 2 achieved the highest exon-23 skipping over other AOs, and, 2′-OMe/2′-F-PS gapmer induced the least exon-23 skipping compared to the others at 12.5, 25, and 50 nM, suggesting that the positioning of LNA or 2′-OMe analogues also affects exon skipping efficiency. Interestingly, at 12.5 and 25 nM concentrations, the LNA/2′-F mixmers induced less undesired exon-22/23 dual skipping than their corresponding 2′-OMe/2′-F mixmers, suggesting that LNA/2′-F mixmers may be a better tool for exon skipping application compared to 2′-OMe/2′-F mixmers.

At lower concentrations (2.5 nM, 5 nM, 12.5 nM), all 2′-OMe/2′-F mixmer AOs showed higher exon-23 skipping than their gapmer counterpart at all three concentrations, while LNA/2′-F gapmer AO showed higher or comparable exon-23 skipping in comparison to its mixmer counterparts. This further suggests that the positioning of 2′-OMe or LNA nucleotides on a 2′-F-PS platform affects exon skipping efficiency. On the other hand, each of the LNA/2′-F-PS chimeras achieved higher or comparable exon-23 skipping compared with their corresponding 2′-OMe/2′-F-PS counterparts at 5 nM and 12.5 nM (LNA/2′-F-PS gapmer > 2′-OMe/2′-F-PS gapmer, LNA/2′-F-PS mixmer 1 > 2′-OMe/2′-F-PS mixmer 1, LNA/2′-F-PS mixmer 2 ≥ 2′-OMe/2′-F-PS mixmer 2), which is consistent with previous experiments, and confirmed that LNA modification can result in higher exon-23 skipping than 2′-OMe on a 2′-F-PS platform. Furthermore, similar to the observation at higher concentrations (12.5 nM, 25 nM, 50 nM), the LNA/2′-F mixmers induced less exon-22/23 dual skipping than its corresponding 2′-OMe/2′-F mixmers at all concentrations, which further confirmed that LNA/2′-F mixmers may be more preferable than 2′-OMe/2′-F mixmers in exon skipping application.

In addition, cell viability assay performed to assess the cytotoxicity of the AOs showed that all 2′-F modified chimeric AOs achieved comparable cytotoxicity profiles in comparison to their fully 2′-OMe-PS control and the fully modified 2′-F-PS AO. Notably, the LNA/2′-F-PS chimeras showed better safety profile than the 2′-OMe/2′-F-PS chimeras, and the 2′-OMe/2′-F-PS mixmer 2 appeared to be the most toxic AO compared to others. This suggests that nucleotide positioning can be important in optimizing AO toxicity, although further evaluation in *in vivo* models are required. Nuclease stability assay demonstrated that fully 2′-F-PS AO and 2′-OMe/2′-F-PS chimeras possess similar stability as their fully 2′-OMe-PS control *in vitro*. Not surprisingly, LNA/2′-F-PS chimeras were more stable than the other AOs without LNA modification.

In conclusion, 2′-F-PS modified AOs induce higher *Dmd* exon-23 skipping efficiency than fully 2′-OMe-PS AO. Introduction of LNA nucleotides into 2′-F-PS sequence further improved exon-23 skipping efficiency, while not compromising cell viability and nuclease stability, in comparison to the 2′-OMe/2′-F-PS chimeras. In addition, mixmer designs of 2′-OMe/2′-F chimeras achieved higher efficiency of exon-23 skipping than their gapmer counterpart, while gapmer design of LNA/2′-F chimeras achieved higher efficiency of exon-23 skipping than their mixmer counterparts. Collectively, our findings expand the scope of utilizing 2′-F modified AOs in splice modulation application by constructing 2′-OMe and LNA-modified 2′-F-PS chimeras. Specifically, we suggest that development of LNA modified 2′-F-PS mixmer or gapmer chimeric AOs, may present a promising therapeutic strategy for DMD.

Methods

Design and synthesis of chemically modified AOs. All AOs (Table 1) were synthesised in-house on an Expedite™ 8909 oligonucleotide synthesiser (Applied Biosystems) via standard phosphoramidite chemistry at 1 μmol scale. Deprotection was performed by incubating the crude oligonucleotides with ammonium hydroxide (Sigma; cat#: 221228-500 ml) at 55 °C overnight, followed by desalting through illustra NAP-10 columns (GE Healthcare; cat#: 45-000-153). All synthesis reagents were purchased from Merck Millipore.

Cell culture and transfection. *H-2K^b*-tsA58 (H2K) *mdx* mouse myoblasts were cultured and differentiated as described previously[41,45,46]. Briefly, when 60–80% confluent, myoblast cultures were treated with trypsin (ThermoFisher Scientific; cat#: 15400054) and seeded on a 24-well plate at a density of 2×10^4 cells/well. The

64

plates were pre-treated with 50 μg/mL poly-D-lysine (Merck Millipore; cat#: P7886-50mg), followed by 100 μg/mL Matrigel (Corning Life Science; cat#: FAL354234). Myoblasts were differentiated into myotubes in Dulbecco's Modified Eagle Medium (DMEM) (ThermoFisher Scientific; cat#: 11885084) containing 5% horse serum (ThermoFisher Scientific; cat#: 16050122) by incubating at 37 °C, 5% CO$_2$ for 24 h. AOs were complexed with Lipofectin transfection reagent (ThermoFisher Scientific; cat#: 18292011) at the ratio of 2:1 (v:w) (Lipofectin:AO) and used in a final transfection volume of 500 μL/well in a 24-well plate as per the manufacturer's instructions.

RNA isolation and reverse transcription polymerase chain reaction (RT-PCR). Total RNA was extracted from transfected mouse myotubes using Direct-zol™ RNA MiniPrep Plus with TRI Reagent® (Zymo Research, supplied through Integrated Sciences; cat#: R2052) as per the manufacturer's instructions. The dystrophin transcripts were then analysed by RT-PCR using SuperScript™ III Reverse Transcriptase III (ThermoFisher Scientific; cat#: 12574026) across exons-20 to 26 as described previously[38]. PCR products were separated on a 2% agarose gel in Tris–acetate–EDTA buffer and the images were captured on a Fusion Fx gel documentation system (Vilber Lourmat). Densitometry was performed by Image J software[47]. To quantify the actual exon skipping efficacy induced by AOs, the amount of full length (901 bp), exon-23 skipping (688 bp), and exon-22/23 dual skipping (542 bp) products are expressed as percentages of total dystrophin transcript products.

***In vitro* cytotoxicity analysis of AOs.** Myoblasts were seeded, allowed to differentiate to myotubes, and transfected with AOs at 50 and 12.5 nM as described previously. 24 h after transfection, cytotoxicity was determined by a colorimetric assay using WST-1 reagent (2-(4-iodophenyl)-3-(4-nitro-phenyl)-5-(2,4-disulfophenyl)-2*H*-tetrazolium) (Sigma; cat#: ab65473). Briefly, WST-1 solution was added at a ratio of 1:10 (v/v) per well and incubated for 4 h at 37 °C, 5% CO$_2$. The absorbance was then measured in a microplate reader (FLUOstar Omega, BMG Labtech) at 450 nm.

***In vitro* nuclease stability analysis of AOs.** Stability of all the AOs (Table 1) against 3′ end to 5′ end exonuclease degradation was evaluated using 0.08 units/reaction of Phosphodiesterase I from Crotalus adamanteus venom (Sigma; cat#: P3134-100MG) in a buffer of 10 mM Tris-HCL, 100 mM NaCl, and 15 mM MgCl$_2$ in a final volume of 45 μL. Briefly, samples were incubated at 37 °C and 7.5 μL of reaction aliquots were removed at different time points (0, 1, 2, 4, and 6 h) and an equal volume of 80% formamide containing bromophenol blue and xylene cyanol gel tracking dyes was then added, followed by heating for 5 min at 95 °C. Next, the products were separated on a 20% denaturing polyacrylamide gel. Quantitation was performed on a Fusion Fx gel documentation system (Vilber Lourmat).

References
1. Lundin, K. E., Gissberg, O. & Smith, C. I. Oligonucleotide therapies: the past and the present. *Hum Gene Ther* **26**, 475–485 (2015).
2. Sharma, V. K., Sharma, R. K. & Singh, S. K. Antisense oligonucleotide: modifications and clinical trials. *Med Chem Commun* **5**, 1454–1471 (2014).
3. Syed, Y. Y. Eteplirsen: first global approval. *Drugs* **76**, 1699–1704 (2016).
4. Corey, D. R. Nusinersen, an antisense oligonucleotide drug for spinal muscular atrophy. *Nat Neurosi* **20**, 497–499 (2017).
5. Dias, N. & Stein, C. A. Antisense oligonucleotides: basic concepts and mechanisms. *Mol Cancer Ther* **1**, 347–355 (2002).
6. Eckstein, F. Phosphorothioate oligodeoxynucleotides: what is their origin and what is unique about them? *Nucleic Acid Drug Dev* **10**, 117–121 (2000).
7. Majlessi, M., Nelson, N. C. & Becker, M. M. Advantages of 2′-O-methyl oligoribonucleotide probes for detecting RNA targets. *Nucleic Acids Res* **26**, 2224–2229 (1998).
8. Kawasaki, A. M. *et al.* Uniformly modified 2′-deoxy-2′-fluoro-phosphorothioate oligonucleotides as nuclease-resistant antisense compounds with high affinity and specificity for RNA targets. *J Med Chem* **36**, 831–841 (1993).
9. Rigo, F. *et al.* Synthetic oligonucleotides recruit ILF2/3 to RNA transcripts to modulate splicing. *Nat Chem Biol* **8**, 555–561 (2012).
10. Jirka, S. M. G. *et al.* Evaluation of exon skipping activity of 2′-deoxy-2′-fluoro antisense oligonucleotides for Duchenne muscular dystrophy. *Abstracts / Neuromuscul Disord* **24**, 791–924. G.P.109 (2014).
11. Jirka, S. M. G. *et al.* Evaluation of 2′-deoxy-2′-fluoro antisense oligonucleotides for exon skipping in Duchenne muscular dystrophy. *Mol Ther Nucleic Acids* **4**, e265 (2015).
12. Geary, R. S. *et al.* Pharmacokinetic properties of 2′-O-(2-methoxyethyl)-modified oligonucleotide analogs in rats. *J Pharmacol Exp Ther* **296**, 890–897 (2001).
13. Summerton, J. & Weller, D. Morpholino antisense oligomers: design, preparation, and properties. *Antisense Nucleic Acid Drug Dev* **7**, 187–195 (1997).
14. Veedu, R. N. & Wengel, J. Locked nucleic acids: promising nucleic acid analogs for therapeutic applications. *Chem Biodivers* **7**, 536–542 (2010).
15. Veedu, R. N. & Wengel, J. Locked nucleic acid as a novel class of therapeutic agents. *RNA Biol* **6**, 321–323 (2009).
16. Le, B. T. *et al.* Rational design of short locked nucleic acid-modified 2′-O-methyl antisense oligonucleotides for efficient exon-skipping *in vitro*. *Mol Ther Nucleic Acids* **9**, 155–161 (2017).
17. Langkjaer, N., Pasternak, A. & Wengel, J. UNA (unlocked nucleic acid): a flexible RNA mimic that allows engineering of nucleic acid duplex stability. *Bioorg Med Chem* **17**, 5420–5425 (2009).
18. Hyrup, B. & Nielsen, P. E. Peptide nucleic acids (PNA): synthesis, properties and potential applications. *Bioorg Med Chem* **4**, 5–23 (1996).
19. Le, B. T. *et al.* Antisense oligonucleotide modified with serinol nucleic acid (SNA) induces exon skipping in mdx myotubes. *RSC Adv* **7**, 34049–34052 (2017).
20. Renneberg, D. & Leumann, C. J. Watson−crick base-pairing properties of tricyclo-DNA. *J Am Chem Soc* **124**, 5993–6002 (2002).
21. Le, B. T., Filichev, V. V. & Veedu, R. N. Investigation of twisted intercalating nucleic acid (TINA)-modified antisense oligonucleotides for splice modulation by induced exon-skipping *in vitro*. *RSC Adv* **6**, 95169–95172 (2016).
22. Le, B. T. *et al.* Evaluation of anhydrohexitol nucleic acid, cyclohexenyl nucleic acid and D-altritol nucleic acid-modified 2′-O-methyl RNA mixmer antisense oligonucleotides for exon skipping *in vitro*. *Chem Commun* **52**, 13467–13470 (2016).
23. Chen, S. *et al.* Synthesis of a morpholino nucleic acid (MNA)-uridine phosphoramidite, and exon skipping using MNA/2′-O-methyl mixmer antisense oligonucleotide. *Molecules.* **21**, 1582 (2016).
24. Masaki, Y. *et al.* Enhancement of exon skipping in mdx52 mice by 2′-O-methyl-2-thioribothymidine incorporation into phosphorothioate oligonucleotides. *Med Chem Commun* **6**, 630-633 (2015).

25. Le, B. T. *et al*. Nucleobase-modified antisense oligonucleotides containing 5-(phenyltriazol)-2′-deoxyuridine nucleotides induce exon-skipping *in vitro*. *RSC Adv* **7**, 54542–54545 (2017).
26. Mercuri, E. & Muntoni, F. Muscular dystrophies. *Lancet* **381**, 845–860 (2013).
27. Le, B. T. *et al*. Antisense oligonucleotide development for the treatment of muscular dystrophies. Expert Opin Orphan. *Drugs* **4**, 139–152 (2016).
28. Wilton, S. D., Veedu, R. N. & Fletcher, S. The emperor′s new dystrophin: finding sense in the noise. *Trends Mol Med* **21**, 417–426 (2015).
29. Davies, K. E. & Nowak, K. J. Molecular mechanisms of muscular dystrophies: old and new players. *Nat Rev Mol Cell Biol* **7**, 762–773 (2006).
30. Arechavala-Gomeza, V. *et al*. Antisense oligonucleotide-mediated exon skipping for Duchenne muscular dystrophy: progress and challenges. *Curr Gene Ther* **12**, 152–160 (2012).
31. Mitrpant, C., Fletcher, S. & Wilton, S. D. Personalised genetic intervention for Duchenne muscular dystrophy: antisense oligomers and exon skipping. *Curr Mol Pharmacol* **2**, 110–121 (2009).
32. Fairclough, R. J., Wood, M. J. & Davies, K. E. Therapy for Duchenne muscular dystrophy: renewed optimism from genetic approaches. *Nat Rev Genet* **14**, 373–378 (2013).
33. Mendell, J. R. *et al*. Eteplirsen for the treatment of Duchenne muscular dystrophy. *Ann Neurol* **74**, 637–647 (2013).
34. Kole, R. & Krieg, A. M. Exon skipping therapy for Duchenne muscular dystrophy. *Adv Drug Deliv Rev* **87**, 104–107 (2015).
35. Fletcher, S. *et al*. Translational development of splice-modifying antisense oligomers. *Expert Opin Biol Ther* **17**, 15–30 (2017).
36. Fletcher, S. *et al*. Targeted exon skipping to address "leaky" mutations in the dystrophin gene. *Mol Ther Nucleic Acids* **1**, e48 (2012).
37. Govoni, A. *et al*. Ongoing therapeutic trials and outcome measures for Duchenne muscular dystrophy. *Cell Mol Life Sci* **70**, 4585–4602 (2013).
38. Miceli, M. C. & Nelson, S. F. The case for eteplirsen: paving the way for precision medicine. *Mol Genet Metab* **118**, 70–71 (2016).
39. GSK and Prosensa Announce Primary Endpoint Not Met in Phase III Study of Drisapersen in Patients With Duchenne Muscular Dystrophy. Available online, https://globenewswire.com/news-release/2013/09/20/574726/10049265/en/GSK-and-Prosensa-Announce-Primary-Endpoint-Not-Met-in-Phase-III-Study-of-Drisapersen-in-Patients-With-Duchenne-MuscularDystrophy.html (accessed on 20 July 2018).
40. Shimo, T. *et al*. Design and evaluation of locked nucleic acid-based splice-switching oligonucleotides *in vitro*. *Nucleic Acids Res* **42**, 8174–8187 (2014).
41. Mann, C. J. *et al*. Antisense-induced exon skipping and synthesis of dystrophin in the mdx mouse. *Proc Natl Acad Sci USA* **98**, 42–47 (2001).
42. Zamecnik, P. C. & Stephenson, M. L. Inhibition of Rous sarcoma virus replication and cell transformation by a specific oligodeoxynucleotide. *Proc Natl Acad Sci USA* **75**, 280–284 (1978).
43. Dominski, Z. & Kole, R. Restoration of correct splicing in thalassemic pre-mRNA by antisense oligonucleotides. *Proc Natl Acad Sci USA* **90**, 8673–8677 (1993).
44. Aartsma-Rus, A. *et al*. Comparative analysis of antisense oligonucleotide analogs for targeted DMD exon 46 skipping in muscle cells. *Gene ther* **11**, 1391–1398 (2004).
45. Bulfield, G. *et al*. X chromosome-linked muscular dystrophy (mdx) in the mouse. *Proc. Natl Acad Sci USA* **81**, 1189–1192 (1984).
46. Rando, T. A. & Blau, H. M. Primary mouse myoblast purification, characterization, and transplantation for cell-mediated gene therapy. *J Cell Biol* **125**, 1275–1287 (1994).
47. Schneider, C. A., Rasband, W. S. & Eliceiri, K. W. NIH Image to ImageJ: 25 years of image analysis. *Nat Methods* **9**, 671–675 (2012).

Acknowledgements

Author Contributions

S.C. performed the experiments and co-wrote the manuscript. R.N.V. conceived the idea, initiated the research, co-wrote the manuscript. B.T.L., M.C., and T.R.K. performed the experiments, and all authors proof read and corrected the manuscript.

Additional Information

Supplementary information accompanies this paper at https://doi.org/10.1038/s41598-019-42523-0.

Competing Interests: The authors declare no competing interests.

Publisher's note: Springer Nature remains neutral with regard to jurisdictional claims in published maps and institutional affiliations.

BACE1 Inhibition Using 2'-OMePS Steric Blocking Antisense Oligonucleotides

Madhuri Chakravarthy [1,2] and **Rakesh N Veedu** [1,2,*]

1   Centre for Molecular Medicine and Innovative Therapeutics, Murdoch University, Perth 6150, Australia;
    M.Chakravarthy@murdoch.edu.au
2   Perron Institute for Neurological and Translational Science, Perth 6150, Australia
*   Correspondence: R.Veedu@murdoch.edu.au

Abstract: Amyloid beta-peptide is produced by the cleavage of amyloid precursor protein by two secretases, a β-secretase, beta-site amyloid precursor protein cleaving enzyme 1 (BACE1) and a γ-secretase. It has been hypothesised that partial inhibition of BACE1 in individuals with a high risk of developing Alzheimer's disease may be beneficial in preventing cognitive decline. In this study, we report the development of a novel antisense oligonucleotide (AO) that could efficiently downregulate the *BACE1* transcript and partially inhibit BACE1 protein. We designed and synthesised a range of 2'-OMethyl-modified antisense oligonucleotides with a phosphorothioate backbone across various exons of the *BACE1* transcript, of which AO2, targeting exon 2, efficiently downregulated *BACE1* RNA expression by 90%. The sequence of AO2 was later synthesised with a phosphorodiamidate morpholino chemistry, which was found to be not as efficient at downregulating *BACE1* expression as the 2'-OMethyl antisense oligonucleotides with a phosphorothioate backbone variant. AO2 also reduced BACE1 protein levels by 45%. In line with our results, we firmly believe that AO2 could be used as a potential preventative therapeutic strategy for Alzheimer's disease.

Keywords: chemically-modified oligonucleotides; antisense oligonucleotides; Alzheimer's disease

---

1. Introduction

Amyloid beta (Aβ)-42 peptide elevation in the brain is one of the pathological hallmarks of Alzheimer's disease (AD) [1–3]. Aβ is produced by the cleavage of amyloid precursor protein by two secretases, a β-secretase, beta-site amyloid precursor protein cleaving enzyme 1 (BACE1) and a γ-secretase [4]. Since the amyloid precursor protein is cleaved first by BACE1, a rate-limiting step, BACE1 is a good therapeutic target [5]. BACE is an aspartyl protease and a type I transmembrane protein that is highly expressed in the brain and pancreas [5]. Elevated BACE1 expression and activity have been reported in post-mortem brains and the cerebrospinal fluids of AD patients [3,6]. BACE1 accumulation has also been observed around amyloid plaques in brains of AD mouse models and patients [7,8]. The *BACE1* gene is found on Chromosome 11 and includes nine exons. BACE1 has two aspartic protease active site motifs (DTGS and DSGT residues) in exons 2 and 6, respectively [5]. The *BACE1* pre-mRNA undergoes alternative splicing through the splice sites within exon 3 and exon 4 resulting in the production of protein isoforms that are 457 and 476 amino acids in length and expressed both in the brain and pancreas, respectively. However, the alternatively spliced variants of BACE1 have reduced β-secretase activity [5].

In recent years, antisense oligonucleotides (AOs) have shown great potential in developing therapies against various diseases. There have been six AOs that have been approved for clinical use for the treatment of various diseases including formivirsen, mipomersen, eteplirsen, nusinersen, inotersen, and volanesorsen. In particular, the approval of nusinersen was important as it demonstrated the potential of AOs for treating neurological diseases [9]. Although there have been no clinical trials

on AOs targeting BACE1, six BACE1 inhibitors entered previously into clinical trials have failed due to liver toxicity in some cases and in others due to lack of improvement in cognitive decline [10]. Some early studies focused on AO development as research tools to better understand the role of BACE1 [10–13]; however, a systematic screening of steric blocking AO designs is not available. It was speculated that BACE1 inhibitors may need to be administered in the presymptomatic stages to patients at high-risk of developing AD, and may only need to partially inhibit BACE1 activity for reducing Aβ load slightly over a long period to have a beneficial effect [14,15]. As BACE1 partial inhibition may help in reducing Aβ load to rescue patients from cognitive decline, the development of BACE1 inhibitors that cause partial BACE1 inhibition is required. In this study, we systematically screened splice-modulating AOs targeting *BACE1* exons to identify an AO that results in partial inhibition of BACE1.

2. Materials and Methods

2.1. AO Design and Synthesis

The 2′-OMethyl (2′-OMe)-modified AO sequences on a phosphorothioate (2′-OMePS) backbone were designed and synthesised in-house using ABI Expedite^{TM} 8909 oligonucleotide synthesiser (Applied Biosystems, Foster City, CA, USA) using standard phosphoramidite chemistry at 1 μmol scale. The synthesised oligonucleotides were deprotected by treatment with 1 mL Ammonium Hydroxide (Sigma; Cat# 221228-500Ml, Castle Hill, NSW, Australia overnight at 55 °C. The oligonucleotides were then purified and desalted using illustra NAP-10 columns (GE Healthcare; Cat# 45-000-153, Springfield, QLD, Australia) according to the manufacturer's protocol. AO2-PMO was purchased from Gene Tools. The high performance liquid chromatography (HPLC from Shimadzu, Sydney, NSW, Australia) analysis of the most efficient AOs are given in Table S5 (Supplementary Information).

2.2. Cell Culture and Transfection

HEK293 cells were obtained from Cell Bank Australia (kindly provided by Associate Prof. Bruno Meloni). Cells were grown and maintained in 10% Foetal Bovine Serum in Dulbecco's Modified Eagle's Medium (ThermoFisher Scientific; Cat# 11995073, Riverstone, NSW, Australia) in a humidified atmosphere 37 °C incubator with 5% CO_2. Cells were maintained at 70–90% confluency and seeded in a plate or flask pre-treated with 50 μg/mL poly-D-lysine (Merck Millipore; Cat# P7886-50 mg, Bayswater, VIC, Australia) at densities shown in the Supplementary Information (Table S1), 24 h before transfection.

Next, the cells were transfected with 2′-OMePS AOs using Lipofectamine 3000 (ThermoFisher Scientific; Cat# L3000015, Riverstone, NSW, Australia) transfection reagent according to the manufacturer's protocol at 400 nM and 200 nM for an initial screen. The best performing AOs were then transfected using the same protocol at the following concentrations: 600 nM, 400 nM, 200 nM, 100 nM, and 50 nM. Twenty- four hours after transfection, the cells were collected for RNA extraction or Western Blot. The AO2-PMO (Gene Tools, Philomath, Oregon, USA) was transfected into HEK293 cells at 100 μM and 250 μM concentrations by nucleofection method using SF Nucleofection kit (Lonza, Mt Waverley, VIC, Australia). For each treatment, 5×10^5 cells were trypsinised, centrifuged, and resuspended in the nucleofection master mix as per the manufacturer's protocol. The cells were then nucleofected with AO2-PMO using program CM- 130 by 4D Nuclofector system X-unit (Lonza Mt Waverley, VIC, Australia) using the SF Cell Line 4D-Nucleofector^{TM} X Kit S (Lonza; Cat# V4XC-2032, Mt Waverley, VIC, Australia) and seeded into five wells of the 24-well plate. Cells were collected at the 24 h, 48 h, three-day, and five-day time points after the first transfection for RNA extraction.

2.3. RNA Extraction and RT-PCR

RNA was extracted from transfected cells using ISOLATE II RNA Mini kit (Bioline; Cat#: BIO-52073,Eveleigh, NSW, Australia) as per the manufacturer's protocol. The *BACE1* transcripts were

amplified using the primer sets (ordered from Integrated DNA Technologies, Singapore) shown in the Supplementary Information (Table S2) with SuperScript III One-Step RT-PCR kit (ThermoFisher Scientific; Cat# 12574026, Riverstone, NSW, Australia). The RT-PCR conditions for each primer set are given in the Supplementary Information (Table S4). Glyceraldehyde 3-phosphate dehydrogenase (*GAPDH*) was used as a loading control and the primer set (ordered from IDT), and RT-PCR conditions for *GAPDH* are given in the Supplementary Information (Tables S3 and S4), respectively. The products were then separated on a 2% agarose gel in Tris-acetate-EDTA buffer, stained with Red Safe (iNtRON Biotechnology; Cat# 21141, Burlington, MA, USA) and destained with water before being visualised with the Fusion Fx gel documentation system (Vilber Lourmat, Marne-la-Vallée, France). Densitometry was performed by the ImageJ Software [16]. The downregulation of products was determined by normalising the *BACE1* transcript levels to the loading control, *GAPDH*, and further normalised to the transcript levels from the untreated (UT) cells. A gene tool control was used as a scrambled (SCR) sequence.

2.4. Western Blot

Western Blot was performed on the best performing AO to evaluate the effect of the AO on the inhibition of the BACE1 protein in comparison to the scrambled (SCR) and untreated (UT) samples. Cells were lysed in lysis buffer (100 μL/ sample) containing 12% SDS, 100 mM Tris-HCl, pH 6.8, 10% glycerol with loading buffer containing 1.875 μL bromophenol blue, 4.688 μL dithiothreitol, and 1.5 μL protease inhibitor per 100 μL samples. Cell pellets were sonicated six times for 3 s pulses and denatured at 95 °C for 5 mins before snap-frozen on ice. Protein concentrations were determined to ensure equal loading by a protein gel with Coomassie blue staining. The proteins were separated on a 10% separating gel containing 400 mM Tris-HCL, pH 8.8, and 0.1% SDS, and 5% stacking gel containing 130 mM Tris-HCL, pH 6.8, 0.1% SDS, and 0.004% Bromophenol blue in a Tris-glycine-SDS running buffer before being transferred to a 0.2 μm nitrocellulose membrane (Biorad; Cat# 162-0112) in a Tris-glycine-methanol transfer buffer. The membranes were blocked in 5% skim milk Tris-buffered saline with 0.1% Tween for 1 h. The membrane was washed three times in Tris-buffered saline with 0.1% Tween for 20 mins each, and the membrane was incubated in primary antibodies overnight at 4 °C, 1:500 anti-BACE1 (Cell Signaling Technology, Cat# 5606, Danvers, MA, USA) and 1:1000 anti-GAPDH (ThermoFisher Scientific, Cat# PA1-988, Riverstone, NSW, Australia). After washing the membrane three times in Tris-buffered saline with 0.1% Tween for 20 mins each, the membrane was incubated in the secondary antibody (1:5000 anti-rabbit horse radish peroxidase, Thermofisher Scientific, Cat# 31460, Riverstone, NSW, Australia) for 1 h at room temperature before washing three times in Tris-buffered saline with 0.1% Tween for 20 mins each. The antibodies were detected using a Clarity Western ECL detection kit (Biorad; Cat# 1705060, Riverstone, NSW, Australia) according to the manufacturer's protocol and visualised using chemiluminescence-based protocol on the Fusion Fx gel documentation system (Vilber Lourmat, Marne-la-Vallée, France).

3. Results

First, various 2'-OMePS AOs, in line with our previous work on Duchene muscular dystrophy [17–23], were designed and synthesised in house targeting exons (Figure 1) 2,3,4,6, and 8 of the *BACE1* gene to induce exon-skipping in the human *BACE1* transcript (Table 1). All AOs were initially screened for exon-skipping at 400 and 200 nM concentrations in HEK293 cells by incubating for 24 h using Lipofectamine 3000, Lipofectamine 2000, Lipofectin, and Lipofectamine RNAimax transfection reagents as per the manufacturer's protocol. Twenty-four hours after transfection, the cells were collected before the total RNA was extracted, and reverse transcription-polymerase chain reaction (RT-PCR) was performed to amplify the regions of interest. The RT-PCR products were separated by gel electrophoresis on a 2% agarose gel, and the PCR products were quantified using ImageJ software. The results showed that *BACE1* transcript knockdown was achieved at various levels with all AOs targeting exon 2 and 3 (Supplementary Information Figure S1). Exon-skipping of exons 4,6, and 8 was

achieved at various levels with different AOs (AO9, AO11, AO12, AO13, AO15, AO17, AO18, and AO20) targeting *BACE1* exons 4,6 and 8 (Supplementary Information Figure S2). The most efficient AOs (AO2, AO5, AO6, AO12, and AO13) targeted exons 2, 3, and 4, which were further evaluated systematically at two different series of concentration sets including 600 nM, 400 nM, 200 nM, 100 nM, and 50 nM, and 100 nM, 50 nM, 25 nM, and 12.5 nM.
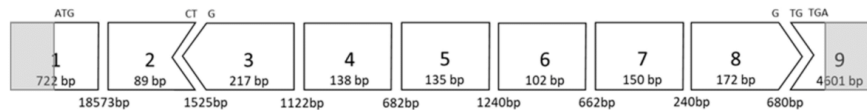
Figure 1. BACE1 exon map showing the size of the exons, as well as the intron size.

Table 1. AO sequences targeting exons 2,3,4,6, and 8.

| AO Coordinates	Target	Sequence(3'–> 5')	AO Number
BACE1 1E2A(+ 10 + 34)	Exon 2	AGTTACTGCTGCCTGTATCCACCAG	AO1
BACE1 1E2A(+ 38 + 62)	Exon 2	AAGGGGTGGGGGGCAGCACCCACTG	AO2
BACE1 1E2A(+ 65 + 89)	Exon 2	AGCTGCCTCTGGTAGTAGCGATGCA	AO3
BACE1 1E3A(+ 16 + 40)	Exon 3	CACATACACACCCTTCCGGAGGTCC	AO4
BACE1 1E3A(+ 41 + 65)	Exon 3	CTTCCCACTTGCCCTGGGTGTAGGG	AO5
BACE1 1E3A(+ 89 + 113)	Exon 3	TGACGTTGGGGCCATGGGGGATGCT	AO6
BACE1 1E3A(+ 141 + 165)	Exon 3	TTGATGAAGAACTTGTCTGATTCAG	AO7
BACE1 1E3A(+ 193 + 217)	Exon 3	CCTGGCAATCTCAGCATAGGCCAGC	AO8
BACE1 1E4A(+ 1 + 25)	Exon 4	AGAAAGGCTCCAGGGAGTCGTCAGG	AO9
BACE1 1E4A(+ 31 + 55)	Exon 4	GAACGTGGGTCTGCTTTACCAGAGA	AO10
BACE1 1E4A(+ 61 + 85)	Exon 4	CACCACAAAGCTGCAGGGAGAAGAG	AO11
BACE1 1E4A(+ 88 + 112)	Exon 4	CTTCAGACTGGTTGAGGGGGAAGCC	AO12
BACE1 1E4A(+ 114 + 138)	Exon 4	CATGCTCCCTCCGACAGAGGCCAGC	AO13
BACE1 1E6A(+ 4 + 28)	Exon 6	TGTCCACAATGCTCTTGTCATAGTT	AO14
BACE1 1E6A(+ 36 + 60)	Exon 6	TTTCTTGGGCAAACGAAGGTTGGTG	AO15
BACE1 1E6A(+ 75 + 99)	Exon 6	GGAGGCTGCCTTGATGGATTTGACT	AO16
BACE1 1E8A(+ 6 + 30)	Exon 8	CTGCGGAAGGATGGTGATGCGGAAG	AO17
BACE1 1E8A(+ 33 + 57)	Exon 8	AAACTTGTAACAGTCGTCTTGGGAC	AO18
BACE1 1E8A(+ 63 + 87)	Exon 8	AACAGTGCCCGTGGATGACTGTGAG	AO19
BACE1 1E8A(+ 109 + 133)	Exon 8	CCCGATCAAAGACAACGTAGAAGCC	AO20
BACE1 1E8A(+ 148 + 172)	Exon 8	CATGGCAAGCGCTGACAGCAAAGCC	AO21

3.1. Evaluation of the Most Efficient 2'-OMePS AOs to Induce Exon-Skipping of the BACE1 Transcript in HEK293 Cells In Vitro

We then systematically evaluated the exon-skipping efficiency of efficient AOs (AO2, AO5, AO6, AO8, AO12, and AO13; Table 1) in vitro initially at 600 nM, 400 nM, 200 nM, 100 nM, and 50 nM concentrations. The results demonstrated that AO2, AO5, AO6, and AO8 targeting exons 2 and 3 downregulated the *BACE1* transcript levels, and AO12 and AO13 that targeted Exon 4 were capable of inducing efficient exon-skipping in vitro (Figure 2). AO2 and AO6 were found to be the most efficient at downregulating the *BACE1* transcript levels in a dose-dependent manner while both AO12 and AO13 showed very high efficiency to induce exon 4 skipping of *BACE1* Variant A. Based on this, the efficacy of AO2 and AO6 and AO12 and AO13 were also further tested at lower concentrations (100 nM, 50 nM, 25 nM, and 12.5 nM). Both AO2 and AO6 showed downregulation of the *BACE1* transcript in a dose-dependent manner (Figure 3); however, densitometry analysis revealed that AO2 and AO6 were found to be the most efficient at 400 nM (Figure 4). Interestingly, although AO12 and AO13 induced exon-skipping, the dose-dependence was not as obvious (Figure 4); however, exon-skipping was observed even at 12.5 nM concentration. AO12 and AO13 were most efficient at inducing exon-skipping at 400 nM, but no concentration tested in this study could induce 100% exon-skipping. The best working AOs were determined to be AO2 and AO6, both of which showed close to 100% downregulation (Figure 4). Of the two AOs, AO2 was used for further evaluation as it

showed consistent dose-dependent downregulation of *BACE1* transcript at all concentrations without affecting the loading control expression.
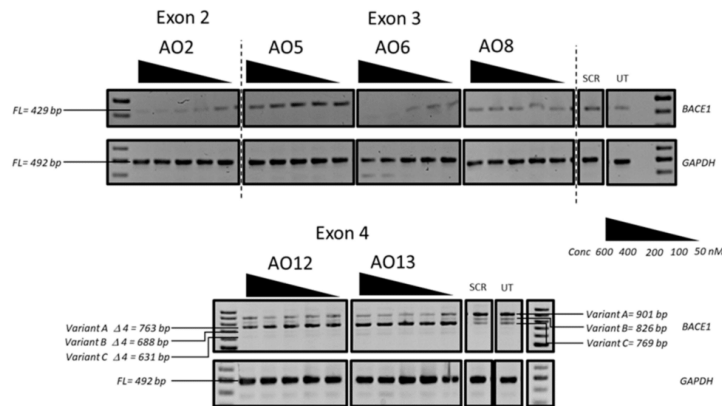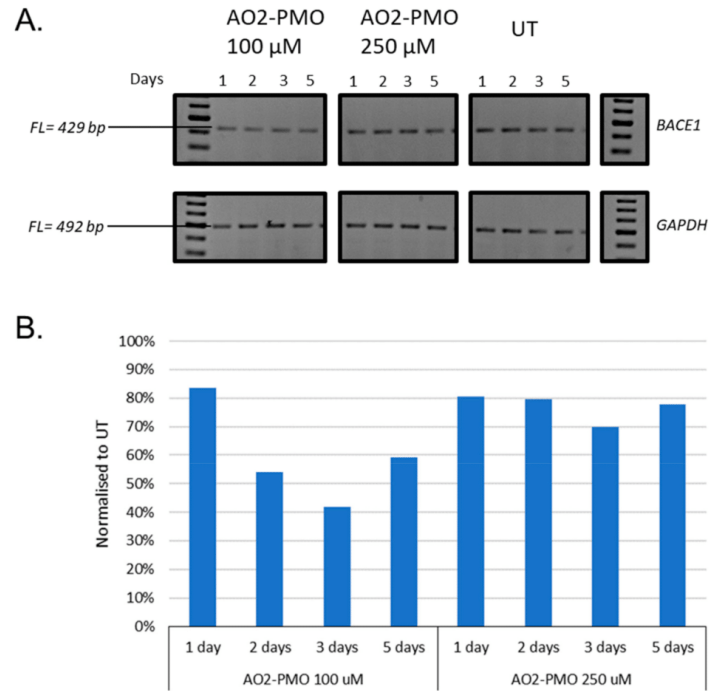

Figure 2. RT-PCR analysis of the *BACE1* and *GAPDH* transcripts after treatment with the best working 2'-O-MePS AOs (AO2, AO5, AO6, AO8, AO12, and AO13) targeting exons 2, 3, and 4 at 600 nM, 400 nM, 200 nM, 100 nM, and 50 nM concentrations in HEK293 cells. FL, full-length; UT, untreated; SCR, scrambled sequence; *GAPDH* was used as a loading control. The gel images were cropped to highlight the *BACE1*-specific products and the corresponding house-keeping gene control *GAPDH*. The original images are shown in Figure S3 (Supplementary Information).
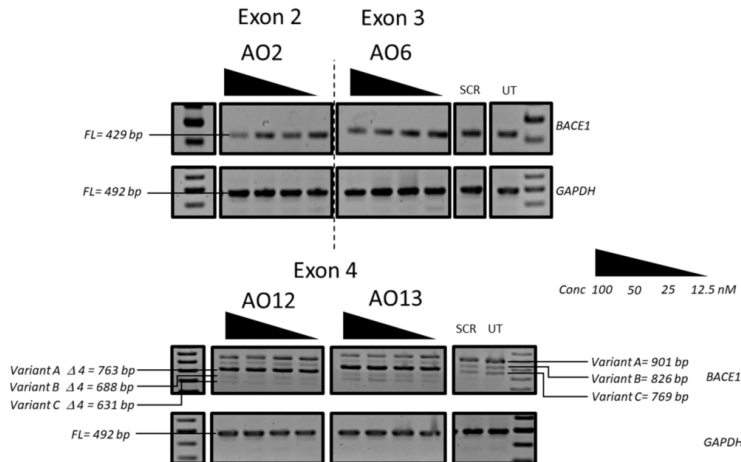
Figure 3. RT-PCR analysis of the *BACE1* and *GAPDH* transcripts after treatment with the best working 2'-O-MePS AOs (AO2, AO6, AO12, and AO13) targeting exons 2, 3, and 4 at 100 nM, 50 nM, 25 nM, and 12.5 nM concentrations in HEK293 cells. FL, full-length; UT, untreated; SCR, scrambled sequence; *GAPDH* was used as a loading control. The gel images were cropped to highlight the *BACE1* specific products and the corresponding house-keeping gene control *GAPDH*. The original images are shown in Figure S4 (Supplementary Information).
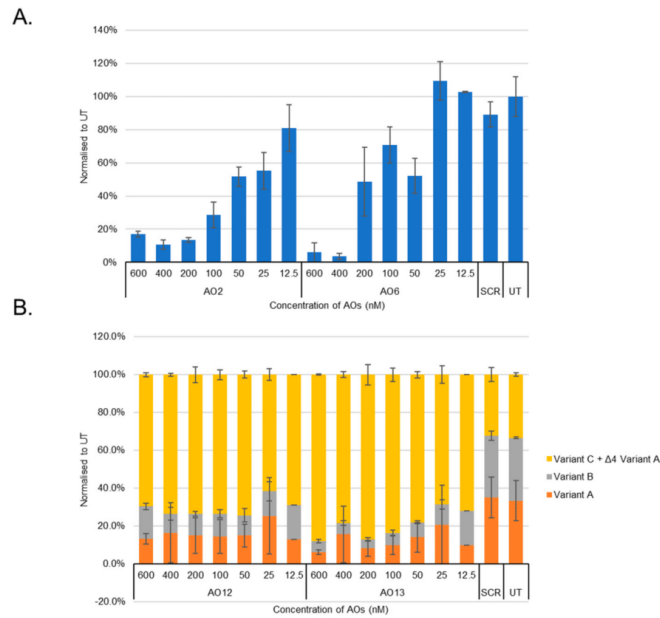
Figure 4. (**A**) Densitometry analysis of RT-PCR products (more than two replicates) using AO2 and AO6 showed downregulation of *BACE1* transcript in HEK293 cells in vitro. (**B**) Densitometry analysis of RT-PCR products (more than two replicates) using AO12 and AO13 showed exon-skipping of exon 4 of the *BACE1* variant A transcript in HEK293 cells in vitro. Concentrations of AOs used include 12.5 nM, 25 nM, 50 nM, 100 nM, 200 nM, 400 nM, and 600 nM. FL, full-length; UT, untreated; SCR, scrambled sequence.

3.2. Evaluation of the Most Efficient 2'-OMePS AOs as a PMO to Induce Exon-Skipping of BACE1 Transcript in HEK293 Cells In Vitro

To be clinically viable, it is important that the AOs are safe to use in humans. Towards this, PMO chemistry demonstrated excellent safety profiles in humans at very high doses. Towards this, the best working AO sequence AO2 was re-synthesised with a PMO chemistry, and called AO2-PMO, and evaluated its potential to downregulate *BACE1* transcript levels in HEK293 cells at 100 µM and 250 µM concentrations. The cells were incubated with the AO2-PMO for different time points, including 1, 2, 3, and 5 days (Figure 5). The results showed that AO2-PMO treatment downregulated *BACE1* transcript at 100 µM and 250 µM concentrations at all time points. However, BACE1 downregulation levels were much lower compared with AO2. The highest downregulation observed with AO2-PMO was around 60% after three days of incubation, whereas 89% reduction in BACE1 levels was observed after one day of incubation with the 2'-OMePS AO.

Figure 5. (**A**) Representative RT-PCR analysis of the *BACE1* and *GAPDH* transcripts after treatment with AO2-PMO targeting exon 2 for 1, 2, 3, and 5 days at 100 μM and 250 μM inHEK293 cells. FL, full-length; UT, untreated; SCR, scrambled sequence; *GAPDH* was used as a loading control. The gel images were cropped to highlight the *BACE1* specific products and the corresponding house-keeping gene control *GAPDH*. The original images are shown in Figure S5 (Supplementary Information). (**B**) Densitometry analysis of *BACE1* transcript downregulation in HEK293 cells in vitro.

3.3. Evaluation of the Mechanism of Action of AO2

As AO2 was found to be the most efficient candidate that showed dose-dependent downregulation of the *BACE1* transcript, AO2 was further investigated for the mechanism of action. AO2 was designed to target the splicing enhancer region of *BACE1* exon 2 towards inducing exon 2 skipping. However, exon-skipping was not observed as predicted, and we investigated the possible degradation of the exon 2 skipped transcript by non-sense mediated decay by amplifying the other regions (exons 2–8, 3–8, and 4–9) of the AO2 treated RNA. The *BACE1* transcript was downregulated in the exon 1–exon 4 region (Figure 6) and specifically between exons 1–2 as the *BACE1* transcript was not downregulated in the exons 3–9 regions, when amplified using a variety of primers (Figure 6), which is not indicative of exon 2 skipping and subsequent degradation of the skipped product by nonsense-mediated decay.
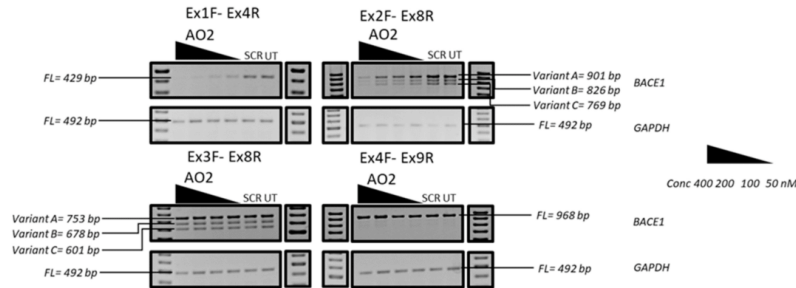
Figure 6. Representative RT-PCR analysis of the *BACE1* and *GAPDH* transcripts after treatment with AO2 targeting exons 2 at 400 nM, 200 nM, 100 nM, and 50 nM in HEK293 cells. Specific regions of the RNA were amplified by different primer sets. Exons 1–4 were amplified using primer set Ex1F-Ex4R, exons 2–8 were amplified using primer set Ex2F-Ex8R, exons 3–8 were amplified using primer set Ex3F-Ex8R, and exons 4–9 were amplified using primer set Ex4F-Ex9R. FL, full-length; UT, untreated; SCR, scrambled sequence; *GAPDH* was used as a loading control. The gel images were cropped to highlight the *BACE1* specific products and the corresponding house-keeping gene control *GAPDH*. The original images are shown in Figure S6 (Supplementary Information).

3.4. Evaluation of BACE1 Protein Downregulation

The efficacy of AO2 to downregulate BACE1 protein level was evaluated in HEK293 cells after 24 h of treatment by Western blotting (Figure 7). Briefly, AO2 (400 nM) treated HEK293 cells were incubated for 24 h before collection. The cell pellet was later collected and lysed with SDS lysis buffer. The proteins were separated on a 10% separating and 5% stacking gel and transferred onto a nitrocellulose membrane. The membrane was incubated with 1:500 dilution of the BACE1 antibody overnight at 4 °C, and 1:5000 anti-rabbit HRP secondary antibody for 1 h at room temperature. The total protein loading was evaluated using a loading control, GAPDH. The membrane was incubated with 1:1000 GAPDH antibody overnight at 4 °C and 1:5000 anti-rabbit HRP secondary antibody. The antibodies were detected using a Clarity Western ECL detection kit (Biorad) using a chemiluminescence-based protocol on the Fusion Fx gel documentation system (Vilber Lourmat). The results of the Western blot analysis showed that there was 45% BACE1 protein downregulation in cells 24 h after AO2 treatment.
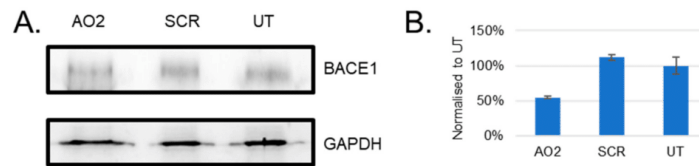
Figure 7. (**A**) Representative Western blot protein analysis of the BACE1 and GAPDH proteins after 24 h treatment with AO2 targeting exon 2 at 400 nM in HEK293 cells. FL, full-length; UT, untreated; SCR, scrambled sequence; GAPDH was used as a loading control. The gel images were cropped to highlight the BACE1 protein and the corresponding house-keeping protein control GAPDH. The original images are shown in Figure S7 (Supplementary Information). (**B**) Densitometry analysis of protein products showed downregulation of BACE1 protein in HEK293 cells in vitro.

4. Discussion

A steric blocking AO that downregulates BACE1 protein expression partially has been developed in this study. AOs were designed to target regions in exons 2, 3, and 8 to induce the respective exon-skipping by blocking the binding of splicing factors which will generate a premature stop codon in the subsequent exons (in exons 3, 4, and 9). Similarly, AOs were also designed to target regions

in exons 4 and 6 to induce skipping of these exons with important functional domains which are required for β-secretase activity. All of the AOs (AO1-8) targeting exons 2 and 3 of the *BACE1* transcript downregulated *BACE1* transcript at various efficiencies, of which AO2 and AO6 were found to be the most efficient; however, these AOs did not show the expected product of exon-skipping as predicted. Notably, AOs (AO9, AO11, AO12, AO13, AO15, AO17, AO18, and AO20) targeting exons 4 and 6 induced exon-skipping of the *BACE1* transcript as predicted, but AO12 and AO13 targeting exon 4 were found to be the best at inducing the exon-skipped product of 763 bp.

This study used 2'-OMePS AOs for systematic screening, but the most efficient AO was later tested as a PMO. 2'-OMePS and PMO chemistries have been well-established for the use in vitro, as well as in vivo for developing splice modulating AOs [24,25]. Negatively charged 2'-OMePS oligonucleotides are cheap to synthesise and available commercially from several manufacturers. The PMO is a neutrally charged oligonucleotide; however, large scale production of PMO is challenging due to difficulties in synthesis which is not compatible with standard phosphoramidite chemistry. Unlike 2'OMePS chemistry, the PMO chemistry also has shown an excellent safety profile and is used clinically. Therefore, although 2'-OMePS chemistry is used for screening purposes, the most efficient AOs are later tested with a PMO chemistry. In our study, the best 2'-OMePS AO (AO2) efficiently downregulated the *BACE1* transcript but, when this sequence was tested as a PMO, it was found to be less efficient. The AO2 sequence is a G-rich oligonucleotide sequence. Therefore, we speculate that the difference observed in the efficiency of the 2'-OMePS AO and the PMO AO may be due to the PMOs forming G-quadruplex structures, while the 2'-OMePS sequence does not, which may explain the lower efficiency of the same sequence with a PMO chemistry.

The AOs in this study were designed to target and skip exons with important functional domains by inducing premature stop codons to inhibit the expression of functional BACE1 protein. However, the most efficient AO candidate, AO2, showed downregulation of *BACE1* mRNA. We predicted that AO2-mediated *BACE1* mRNA downregulation might be due to nonsense-mediated decay, a mechanism proposed for mRNA degradation by the induction of a premature stop codon [26]. Amplification of the isolated RNA after the treatment with AO2 showed that the downregulation of *BACE1* mRNA was seen only in the exon 1–exon 2 region, but showed normal expression in the regions between exons 3–9 indicating that AO2-mediated *BACE1* transcript downregulation may not be through nonsense-mediated decay. We speculated that the potential reason for the downregulation of the exon 1–2 region might be due to a steric block imposed in this region that ultimately inhibits the translation. BACE1 protein analysis after AO2 treatment of HEK293 cells shows that there is a reduction in BACE1 level at 24 h (around 60% compared to UT). BACE1 has a half-life of over nine hours in cultured cells [5]; therefore, most of the inhibition is seen 24 h after AO2 treatment. Although we achieved close to 100% inhibition of the *BACE1* mRNA, we could not see a similar level of BACE1 protein inhibition (only 45% inhibition at protein level). This may be due to the regulation of BACE1 protein levels by mechanisms both at the transcriptional, translational, and post-translational levels [27]. As studies have shown that 5'-UTR region of the BACE1 has a role in regulating the BACE1 protein levels [27], reducing *BACE1* mRNA may only have a small role in regulating BACE1 protein level. The complete suppression of BACE1 may not be possible, but a partial reduction of BACE1 has been shown to improve amyloid neuropathology suggesting that a complete reduction of BACE1 is not required for beneficial effects [5,15,28]. Furthermore, BACE1 also has other substrates, and therefore, complete elimination of BACE1 may have deleterious effects [15,28].

5. Conclusions

We have screened various AOs designed to induce *BACE1* splice modulation. One potential candidate named AO2 targeting exon 2, potentially by steric blocking mechanism, was found to be the most efficient in inhibiting BACE1 expression at the RNA and protein level in HEK293 cells. Of the two chemistries evaluated, the 2'-OMePS chemistry was found to be far more efficient compared with the PMO chemistry, yielding close to 90% *BACE1* transcript downregulation and resulted in 45%

downregulation of the BACE1 protein. Although further validation of AO2 in vivo and its effect on Aβ production is required to ensure the applicability of this molecule towards the clinical benefits in mitigating AD, we believe that partial inhibition of BACE1 protein levels achieved in this work could be used as a potential preventative strategy for people at high-risk of developing AD.

References

1. Näslund, J. Correlation between elevated levels of amyloid β-peptide in the brain and cognitive decline. *JAMA* **2000**, *283*, 1571–1577. [CrossRef] [PubMed]
2. Gandy, S. The role of cerebral amyloid β accumulation in common forms of alzheimer disease. *J. Clin. Investig.* **2005**, *115*, 1121–1129. [PubMed]
3. Li, R.; Lindholm, K.; Yang, L.B.; Yue, X.; Citron, M.; Yan, R.; Beach, T.; Sue, L.; Sabbagh, M.; Cai, H.; et al. Amyloid peptide load is correlated with increased -secretase activity in sporadic alzheimer's disease patients. *Proc. Natl. Acad. Sci. USA* **2004**, *101*, 3632–3637. [CrossRef] [PubMed]
4. Selkoe, D.J. Alzheimer's disease: Genes, proteins, and therapy. *Physiol. Rev.* **2001**, *81*, 741–766. [CrossRef]
5. Cole, S.L.; Vassar, R. The alzheimer's disease β-secretase enzyme, bace1. *Mol. Neurodegener.* **2007**, *2*, 22. [CrossRef] [PubMed]
6. Yang, L.-B.; Lindholm, K.; Yan, R.; Citron, M.; Xia, W.; Yang, X.-L.; Beach, T.; Sue, L.; Wong, P.; Price, D.; et al. Elevated β-secretase expression and enzymatic activity detected in sporadic alzheimer disease. *Nat. Med.* **2003**, *9*, 3–4. [CrossRef]
7. Zhao, J.; Fu, Y.; Yasvoina, M.; Shao, P.; Hitt, B.; O'Connor, T.; Logan, S.; Maus, E.; Citron, M.; Berry, R.; et al. β-site amyloid precursor protein cleaving enzyme 1 levels become elevated in neurons around amyloid plaques: Implications for alzheimer's disease pathogenesis. *J. Neurosci.* **2007**, *27*, 3639–3649. [CrossRef]
8. Sadleir, K.R.; Kandalepas, P.C.; Buggia-Prévot, V.; Nicholson, D.A.; Thinakaran, G.; Vassar, R. Presynaptic dystrophic neurites surrounding amyloid plaques are sites of microtubule disruption, bace1 elevation, and increased aβ generation in alzheimer's disease. *Acta Neuropathol.* **2016**, *132*, 235–256. [CrossRef]
9. Stein, C.A.; Castanotto, D. Fda-approved oligonucleotide therapies in 2017. *Mol. Ther.* **2017**, *25*, 1069–1075. [CrossRef]
10. Panza, F.; Lozupone, M.; Solfrizzi, V.; Sardone, R.; Piccininni, C.; Dibello, V.; Stallone, R.; Giannelli, G.; Bellomo, A.; Greco, A.; et al. Bace inhibitors in clinical development for the treatment of alzheimer's disease. *Expert Rev. Neurother.* **2018**, *18*, 847–857. [CrossRef]

11. Yan, R.; Bienkowski, M.J.; Shuck, M.E.; Miao, H.; Tory, M.C.; Pauley, A.M.; Brashler, J.R.; Stratman, N.C.; Mathews, W.R.; Buhl, A.E. Membrane-anchored aspartyl protease with alzheimer's disease β-secretase activity. *Nature* **1999**, *402*, 533–537. [CrossRef]

12. Vassar, R. β-secretase cleavage of alzheimer's amyloid precursor protein by the transmembrane aspartic protease bace. *Science* **1999**, *286*, 735–741. [CrossRef]

13. Mowrer, K.R.; Wolfe, M.S. Promotion of bace1 mrna alternative splicing reduces amyloid β-peptide production. *J. Biol. Chem.* **2008**, *283*, 18694–18701. [CrossRef]

14. Peters, F.; Salihoglu, H.; Rodrigues, E.; Herzog, E.; Blume, T.; Filser, S.; Dorostkar, M.; Shimshek, D.R.; Brose, N.; Neumann, U. Bace1 inhibition more effectively suppresses initiation than progression of β-amyloid pathology. *Acta Neuropathol.* **2018**, *135*, 695–710. [CrossRef]

15. Vassar, R. Implications for bace1 inhibitor clinical trials: Adult conditional bace1 knockout mice exhibit axonal organization defects in the hippocampus. *J. Prev. Alzheimer's Dis.* **2019**, *6*, 78–84.

16. Schindelin, J.; Rueden, C.T.; Hiner, M.C.; Eliceiri, K.W. The imagej ecosystem: An open platform for biomedical image analysis. *Mol. Reprod. Dev.* **2015**, *82*, 518–529. [CrossRef]

17. Chen, S.; Le, B.; Rahimizadeh, K.; Shaikh, K.; Mohal, N.; Veedu, R. Synthesis of a morpholino nucleic acid (mna)-uridine phosphoramidite, and exon skipping using mna/2′-o-methyl mixmer antisense oligonucleotide. *Molecules* **2016**, *21*, 1582. [CrossRef]

18. Chen, S.; Le, B.T.; Chakravarthy, M.; Kosbar, T.R.; Veedu, R.N. Systematic evaluation of 2′-fluoro modified chimeric antisense oligonucleotide-mediated exon skipping in vitro. *Sci. Rep.* **2019**, *9*, 6078. [CrossRef] [PubMed]

19. Le, B.T.; Adams, A.M.; Fletcher, S.; Wilton, S.D.; Veedu, R.N. Rational design of short locked nucleic acid-modified 2′-o-methyl antisense oligonucleotides for efficient exon-skipping in vitro. *Mol. Ther. Nucleic Acids* **2017**, *9*, 155–161. [CrossRef] [PubMed]

20. Le, B.T.; Chen, S.; Abramov, M.; Herdewijn, P.; Veedu, R.N. Evaluation of anhydrohexitol nucleic acid, cyclohexenyl nucleic acid and d-altritol nucleic acid-modified 2′-o-methyl RNA mixmer antisense oligonucleotides for exon skipping in vitro. *Chem. Commun.* **2016**, *52*, 13467–13470. [CrossRef] [PubMed]

21. Le, B.T.; Filichev, V.V.; Veedu, R.N. Investigation of twisted intercalating nucleic acid (tina)-modified antisense oligonucleotides for splice modulation by induced exon-skipping in vitro. *RSC Adv.* **2016**, *6*, 95169–95172. [CrossRef]

22. Le, B.T.; Hornum, M.; Sharma, P.K.; Nielsen, P.; Veedu, R.N. Nucleobase-modified antisense oligonucleotides containing 5-(phenyltriazol)-2′-deoxyuridine nucleotides induce exon-skipping in vitro. *RSC Adv.* **2017**, *7*, 54542–54545. [CrossRef]

23. Le, B.T.; Murayama, K.; Shabanpoor, F.; Asanuma, H.; Veedu, R.N. Antisense oligonucleotide modified with serinol nucleic acid (sna) induces exon skipping in mdx myotubes. *RSC Adv.* **2017**, *7*, 34049–34052. [CrossRef]

24. Disterer, P.; Kryczka, A.; Liu, Y.; Badi, Y.E.; Wong, J.J.; Owen, J.S.; Khoo, B. Development of therapeutic splice-switching oligonucleotides. *Hum. Gene Ther.* **2014**, *25*, 587–598. [CrossRef] [PubMed]

25. Järver, P.; O'Donovan, L.; Gait, M.J. A chemical view of oligonucleotides for exon skipping and related drug applications. *Nucleic Acid Ther.* **2014**, *24*, 37–47. [CrossRef] [PubMed]

26. Chang, Y.-F.; Imam, J.S.; Wilkinson, M.F. The nonsense-mediated decay RNA surveillance pathway. *Annu. Rev. Biochem.* **2007**, *76*, 51–74. [CrossRef] [PubMed]

27. Roßner, S.; Sastre, M.; Bourne, K.; Lichtenthaler, S.F. Transcriptional and translational regulation of bace1 expression—Implications for alzheimer's disease. *Prog. Neurobiol.* **2006**, *79*, 95–111. [CrossRef]

28. Singer, O.; Marr, R.A.; Rockenstein, E.; Crews, L.; Coufal, N.G.; Gage, F.H.; Verma, I.M.; Masliah, E. Targeting bace1 with sirnas ameliorates alzheimer disease neuropathology in a transgenic model. *Nat. Neurosci.* **2005**, *8*, 1343–1349. [CrossRef]